NASA CR-121237
FR-5654

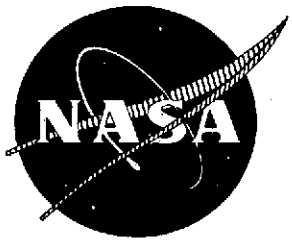

ADVANCED SPACE ENGINE PRELIMINARY DESIGN FINAL REPORT

by J. P. B. Cuffe and R. E. Bradie

PRATT & WHITNEY AIRCRAFT
DIVISION OF UNITED AIRCRAFT CORPORATION
FLORIDA RESEARCH AND DEVELOPMENT CENTER

Prepared for
NATIONAL AERONAUTICS AND SPACE ADMINISTRATION

NASA Lewis Research Center
Contract NAS3-16750

1. Report No.	2. Government Accession No.	3. Recipient's Catalog No.
NASA CR-121237		

4. Title and Subtitle	5. Report Date
Advanced Space Engine Preliminary Design	December 1973
	6. Performing Organization Code

7. Author(s)	8. Performing Organization Report No.
J. P. B. Cuffe and R. E. Bradie	FR-5654
	10. Work Unit No.

9. Performing Organization Name and Address	11. Contract or Grant No.
Pratt & Whitney Aircraft Florida Research and Development Center West Palm Beach, Florida 33402	NAS3-16750
	13. Type of Report and Period Covered
12. Sponsoring Agency Name and Address	Contractor Report
National Aeronautics and Space Administration Washington, D. C. 20546	14. Sponsoring Agency Code

15. Supplementary Notes

Project Manager, D. D. Scheer, Chemical Propulsion Division,
NASA Lewis Research Center, Cleveland, Ohio

16. Abstract

A preliminary design was completed for an O_2/H_2, 89 kN (20,000 lb) thrust staged combustion rocket engine that has a single-bell nozzle with an overall expansion ratio of 400:1. The engine has a "best estimate" vacuum specific impulse of 4623.8 N-s/kg (471.5 sec) at full thrust and mixture ratio = 6.0. The engine employs gear-driven, low pressure pumps to provide low NPSH capability while individual turbine-driven, high-speed main pumps provide the system pressures required for high-chamber pressure operation. The engine design dry weight for the fixed-nozzle configuration is 206.9 kg (456.3 lb). Engine overall length is 234 cm (92.1 in.). The extendible nozzle version has a stowed length of 141.5 cm (55.7 in.).

The tank head idle mode of operation is used for engine thermal conditioning and settling of the main tank propellants. Operation at an intermediate thrust level (pumped idle) of 4% is accomplished using the expander cycle (unlit preburner). The engine is capable of supplying GO_2 and GH_2 for vehicle tank pressurization during pumped-idle and full-thrust operation.

Critical technology items in the development of the engine have been defined. Development program plans and their costs for development, production, operation, and flight support of the ASE were established for minimum cost and minimum time programs.

17. Key Words (Suggested by Author(s))	18. Distribution Statement
Rocket Propulsion Rocket Engines Space Propulsion Hydrogen-Oxygen Engines	Unclassified - Unlimited

19. Security Classif. (of this report)	20. Security Classif. (of this page)	21. No. of Pages	22. Price*
Unclassified	Unclassified	409	

* For sale by the National Technical Information Service, Springfield, Virginia 22151

CONTENTS

CONTENTS (Continued)

ILLUSTRATIONS

ILLUSTRATIONS (Continued)

ILLUSTRATIONS (Continued)

ILLUSTRATIONS (Continued)

ILLUSTRATIONS (Continued)

ILLUSTRATIONS (Continued)

ILLUSTRATIONS (Continued)

ILLUSTRATIONS (Continued)

ILLUSTRATIONS (Continued)

ILLUSTRATIONS (Continued)

TABLES

TABLES (Continued)

TABLES (Continued)

SECTION I
SUMMARY

A. GENERAL

The preliminary design of an 89 kN (20,000-lb) thrust, O_2/H_2 staged combustion cycle, 400:1 bell nozzle research engine, the Advanced Space Engine (ASE), was performed under NASA/LeRC Contract No. NAS3-16750. Critical technology items in the development of the ASE were identified. An ASE transient digital computer deck and User's Manual were delivered to the NASA/LeRC. Four alternate program plans and their costs for the ASE were established and delivered to the NASA in an informal report. In addition, the impact on weight and cost of changing the ASE fixed bell nozzle to a retractable nozzle and making the engine/vehicle interfaces compatible with the RL10A-3-3 engine installation was assessed. An ASE study program summary chart is presented in figure 1.

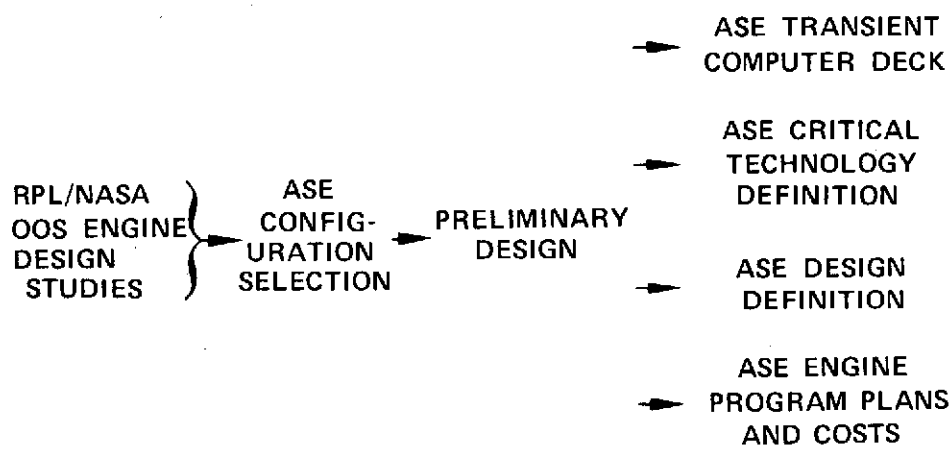

Figure 1. ASE Preliminary Design Program Summary FD 65404A

B. ASE PRELIMINARY DESIGN

In the initial phase of the ASE study, the evaluation and selection of major configuration details and operating modes/capabilities was made. The selections as well as the choices are presented in figure 2. The ASE engine basic configuration and operating conditions are presented in table I. The component arrangement for the baseline, fixed position nozzle engine configuration that evolved from the study is shown in figure 3. The ASE "best estimate" vacuum specific impulse is 4623.8 N-s/kg (471.5 sec) at rated thrust and an engine mixture ratio of 6.0 when operated at its nominal chamber pressure of 1324 N/cm^2 (1920 psia). At the nominal operating point (100% thrust, MR = 6.0), the engine is capable of delivering 0.0608 kg/s (0.134 lb/sec) of GO_2 and 0.0154 kg/sec (0.034 lb/sec) of GH_2 at 235°K (423°R) and 266°K (478°R), respectively, for vehicle tank pressurization.

The ASE fixed nozzle configuration (baseline engine) has a design dry weight of 206.9 kg (456.3 lb) and a target dry weight of 178.3 kg (393.3 lb). Overall

length of the engine is 234 cm (92.1 in.) and the maximum diameter is 135 cm (53.2 in.). The two-position nozzle configuration weighs approximately 30.8 kg (68 lb) more than the baseline engine, but has a stowed length of only 141.5 cm (55.7 in.) and slightly improved specific impulse, ~11.8 N-s/kg (1.2 sec). A summary of characteristics of the two ASE configurations is presented in table II.

The engine is operated in the tank head idle (THI) mode to thermally condition the engine and to settle the main tank propellants. At THI, with nominal pressures and saturated propellant conditions at the engine inlets and thermally conditioned pumps, the engine operates at a mixture ratio of 1.5:1 and produces a thrust of 244.7 N (55 lb). Vacuum specific impulse is 3939.3 N-s/kg (401.7 sec). During the acceleration to pumped idle (PI) and the initial portion of the operation at PI propellants are supplied to the engine at saturated liquid conditions. The engine is operated in PI at a power level sufficient to provide autogenous pressurization of the vehicle main tanks to produce the NPSH levels required for rated thrust operation. Operating as an expander cycle (unlit preburner) in pumped idle, the engine is capable of producing 4% of rated thrust at MR = 3.5 and it has a vacuum specific impulse of 4413 N-s/kg (450 sec). A summary of engine vacuum specific impulse as a function of mixture ratio is presented in figure 4.

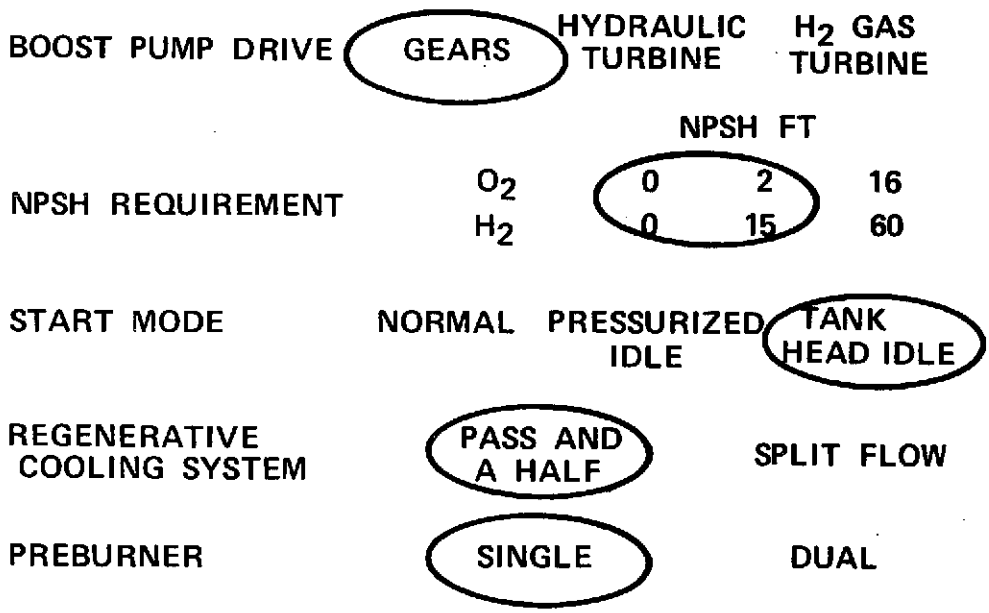

Figure 2. Configuration Selected for ASE FD 65406

Table I. Baseline ASE Configuration and Operating Conditions (Fixed Nozzle Configuration)

Propellants:	
Fuel	Liquid Hydrogen
Oxidizer	Liquid Oxygen
Vacuum Thrust:	89 kN (20,000 lb)
Vacuum Thrust Throttling Capability:	None
Vacuum Specific Impulse (MR = 6.0):	4624 N-s/k (471.5 sec)
Engine Mixture Ratio:	6.0 ± 0.5
Chamber Pressure (MR = 6.0):	1324 N/cm^2 (1920 psia)
Drive Cycle:	Staged Combustion
Envelope (Cold):	
Length (maximum)	234 cm (92.1 in.)
Diameter (maximum)	135 cm (53.2 in.)
Engine System Dry Weight:	207 kg (456.3 lb)
Nozzle Type:	Fixed Bell
Nozzle Expansion Ratio:	400:1
Propellant Inlet Temperatures:	
Hydrogen Range:	20.3°K (36.5°R) to 22.2°K (40°R)
Oxygen Range:	90°K (162°R) to 95.6°K (172°R)
NPSH at Pump Inlet at Full Thrust	
Hydrogen	45 N-m/kg (15 ft)
Oxygen	6 N-m/kg (2 ft)
Engine Temperature at Normal Prestart: Range:	111.1°K (200°R) to 311.1°K (560°R)
Service Life Between Overhauls:	300 Thermal cycles or 10 hours accumulated run time
Service Free Life:	60 Thermal cycles or 2 hours accumulated run time
Maximum Single Run Duration:	2000 seconds
Maximum Time Between Firings During Mission:	14 days
Minimum Time Between Firings During Mission:	1 minute
Maximum Storage Time in Orbit (Dry):	52 weeks

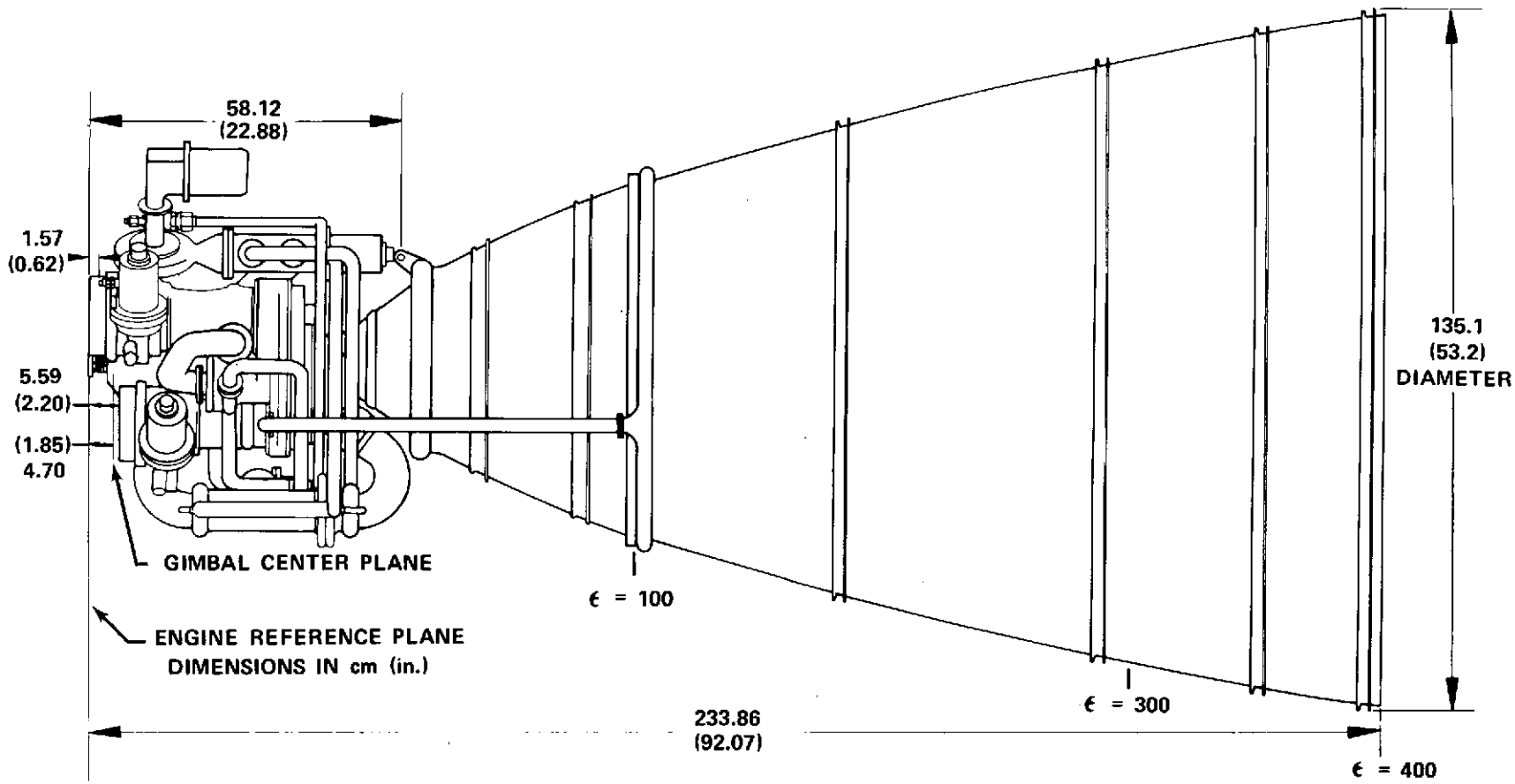

Figure 3. Advanced Space Engine Installation

FD 68858B

Table II. ASE Characteristics

	Configuration	
	2 Position Nozzle	Fixed Nozzle
Thrust, N (lb)	89,000 (20,000)	89,000 (20,000)
Mixture Ratio	6.0	6.0
Chamber Pressure, N/cm^2 (psia)	1,324 (1,920)	1,324 (1,920)
Expansion Ratio	200/400	400
Length, cm (in.)	141.5/233.9 (55.7/92.1)	233.9 (92.1)
Exit Diameter, cm (in.)	92.7/135.1 (36.5/53.2)	135.1 (53.2)
Dry Weight (Target), kg (lb)	202.8 (447)	178.3 (393)
Best Estimate Vacuum Specific Impulse, N-s/kg (sec)	4635.6 (472.7)	4623.8 (471.5)
NPSH Required, N-m/kg (ft) O_2	6 (2)	6 (2)
H_2	45 (15)	45 (15)

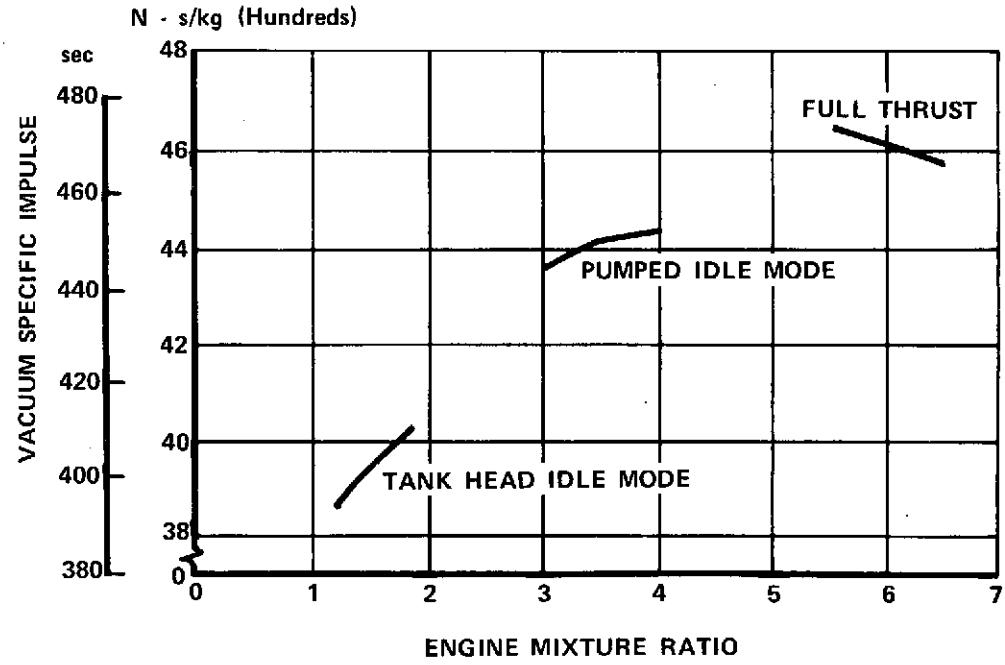

Figure 4. Advanced Space Engine "Best Estimate" Vacuum Specific Impulse FD 71595

C. PROGRAM PLANS

Four alternate program plans for the development and production of the ASE were established. The engine development program plans include development costs, production operations and support costs as well as production engine costs. The impact on costs for the changes required to equip the ASE with a retractable nozzle and to make the engine/vehicle interfaces compatible with the RL10A-3-3 engine installation was also assessed. RL10A-3-3 engine interface compatibility was effected by repositioning the oxidizer turbopump assembly, including the gearbox and the fuel and oxidizer boost pumps, and relocating affected plumbing lines and valves. Program Plans I and II for minimum cost and minimum time development programs for the ASE, respectively, are incorporated in the Final Report as Section V.

D. CRITICAL TECHNOLOGY

Critical technology items in the development of the ASE were identified. The critical technology areas are broadly categorized into the following groups: (1) performance, (2) materials, (3) components, (4) subassemblies, and (5) component integration and control.

These categories include:

1. Verification of specific impulse levels for high chamber pressure, high expansion ratio nozzles with high regenerative enthalpy levels

2. Establishment of low cycle fatigue (LCF) properties of candidate materials for thrust chambers

3. Oxygen seal development

4. High DN hydrogen cooled bearings

5. Integration and control of powerhead and main chamber operation for mainstage and pumped idle modes

SECTION II
INTRODUCTION

A high-performance propulsion system is required for a reusable vehicle to perform future Air Force and NASA space maneuvering missions. A reusable vehicle is essential to complement the Space Shuttle, whose capabilities limit it to operation in low earth orbit. The space maneuvering vehicle will be carried in the Space Shuttle's Orbiter stage payload bay and deployed after the Orbiter is in orbit. Gross weight and volume of this tug vehicle are, therefore, restricted, being defined by the Space Shuttle Orbiter payload capability of 29,470 kg (65,000 lb) and the cylindrical payload bay, which is to be 18.3 m (60 ft) long and 4.6 m (15 ft) in diameter. A typical mission for the Space Tug is to transfer a 1361 kg (3000-lb) payload from the Shuttle, in a 185.2 km (100 nmi) earth orbit, to synchronous equatorial orbit and return to the Shuttle. This mission requires the Space Tug's main engine to be operated for six to ten burns and impart a total velocity increment of 8,717 m/s (28,600 ft/sec). The requirement for multiple space restarts emphasizes the need for reliable and predictable transient operation, preferably without the requirements for high pump inlet NPSH conditions. To obtain the required 8,717 m/s (28,600 ft/sec) velocity increment from a single stage vehicle clearly places a premium on high performance. Previous engine system studies for space maneuvering missions have shown that a staged combustion cycle, bell nozzle engine offers the highest performance potential; therefore, it was selected for this study.

The purpose of the Advanced Space Engine (ASE) Preliminary Design Study was to synthesize the design of an 89 kN (20,000 lb) thrust staged combustion H_2/O_2 research engine that has a single bell nozzle with an expansion ratio of 400:1. The design incorporates the best features of each of the propulsion systems resulting from the three Orbit-to-Orbit Shuttle Engine Design studies funded by AF/RPL (Contracts F04611-71-C-0040, F04611-71-C-0039, and F04611-67-C-0116). The resultant preliminary engine design focused on the component technology work needed to provide a firm base for a research engine. The research engine is to allow studies of component interactions and engine dynamics before beginning any effort on a development engine.

A digital computer program, which is a mathematical model used for simulating the ASE engine chilldown and transient operation, and a User's Manual were delivered to the NASA/LeRC for use in studying engine dynamics.

In support of current cryogenic Space Tug vehicle studies, four alternative engine development program plans, and their costs, were established for the development, production, operation and flight support of the ASE. These program plans were published in FR-5689, Volumes I and II, dated 30 April 1973, and delivered to the NASA-LeRC.

SECTION III
CONFIGURATION AND OPERATIONAL MODE SELECTION

A. GENERAL

Engine studies by three propulsion contractors for space maneuvering systems were conducted under Air Force/RPL Contracts F04611-71-C-0040, F04611-71-C-0039 and F04611-67-C-0116. In these studies, parametric data in the 35.6 kN (8000 lb) to 222.4 kN (50,000 lb) thrust range were generated and preliminary designs were produced for 111 kN (25,000 lb) and 44.5 kN (10,000 lb) thrust engines. While all three contractors selected the staged combustion cycle for their engine preliminary designs, there were significant differences in engine configuration details in regard to:

- Boost pump drive method
- Regenerative cooling scheme
- Preburner configuration.

Also as a result of these engine studies and various vehicle studies, the advanced features considered attractive included:

- Low net positive suction head (NPSH) capability
- Idle mode operation

As a consequence, the initial ASE task was to define the configuration details of the 89 kN (20,000 lb) thrust engine and to select the operating modes and capabilities. The various options considered are summarized below:

1. Boost Pump Drive Methods
   a. Gears
   b. Hydraulic Turbine
   c. Hydrogen Gas Turbines
2. Throttling Requirement
   a. No throttling
   b. 6:1 throttling
3. Net Positive Suction Head (NPSH) Levels

	NPSH, N-m/kg (ft)					
LO_2	0	(0)	6	(2)	48	(16)
LH_2	0	(0)	45	(15)	180	(60)

4. Start Mode Requirement

   a. Normal start from zero to full thrust assuming propellants are settled, engine is thermally conditioned, and NPSH levels are as given in item 3 above.

   b. Pressurized-idle start.

   c. Tank-head-idle start.

5. Regenerative Cooling Schemes

   a. Pass-and-a-half

   b. Split

6. Preburner Configuration

   a. Single Preburner

   b. Dual Preburners separately supplying combustion products to each turbopump.

Three of the six configuration decisions that were to be made were primarily operation-oriented: throttling, NPSH capability and start mode. The other three were configuration-oriented: number of preburners, boost pump drive method and thrust chamber regenerative cooling scheme. The latter two configuration decisions were closely related since the selection of the boost pump drive method could impact the chamber cooling scheme selection. That is, if the GH_2 turbine drive were selected the logical choice would be a split flow regenerative cooling scheme.

The recommended P&WA™ selections were as follows:

Configuration

- Geared boost pump drive system
- Pass-and-a-half regeneratively cooled thrust chamber
- Single preburner

Operational Modes

- Fixed thrust
- Net positive suction head (NPSH) at rated thrust: 45 N-m/kg (15-ft) LH_2 and 6 N-m/kg (2-ft) LO_2.

The initial selection of the configuration and operating modes for the ASE involved evaluation of the 111 kN (25,000-lb) thrust Orbit-to-Orbit Shuttle Engine preliminary designs of the three propulsion system contractors as presented in their final reports. (References 1, 2 and 3.) The evaluations were carried out in the following manner:

1. Tabulations, comparing the three different designs.

2. Tabulations, comparing the design criteria used by each contractor where applicable.

3. Evaluation of the effects of the different criteria (if any) upon the contractor design decisions.

4. Comparison of the three designs, and identification of both the good and bad features including the influence of item 3.

5. Recommendation of design features that should be considered for the ASE, while accounting for differences in engine requirements and design criteria.

The evaluation tasks were broken down into the following

1. Design of engine assembly and major subassemblies

2. Engine cycle selection (steady-state operation)

3. Engine cycle selection (transient operation)

4. Ignition system, valves, and controls

5. Engine vacuum specific impulse.

The individual configuration decisions are discussed in the following paragraphs; the configuration oriented selections are discussed first and the operationally oriented selections follow.

B. BOOST PUMP DRIVE METHODS

1. General

In the evaluation of the three boost pump drive methods, the major factors considered were (1) start transient characteristics, (2) weight, (3) vehicle/engine interface flexibility, and (4) control requirements. The geared boost pump drive system was selected for the ASE primarily because of its better start transient characteristics and reduced control system requirements and risk.

2. Start Transient Characteristics

a. General

The boost pump drive method has a significant impact on engine transient operation. The engine cannot accelerate and decelerate properly unless sufficient NPSH is supplied to the main pumps. With low vehicle tank NPSH, the NPSH required by high speed main pumps must be supplied by the boost pumps. This condition requires that the boost pump acceleration coincide with main pump acceleration or that sufficient NPSH margin must be provided by the boost pumps to compensate for lags in boost pump acceleration. Rocketdyne, Aerojet, and P&WA proposed three configurations that differ in transient characteristics. P&WA proposed boost pumps that were geared from the high pressure oxidizer turbopump shaft. Rocketdyne proposed boost pumps that were gas turbine-driven using the hydrogen tapped off from a split flow thrust chamber regenerative cooling jacket scheme. Aerojet proposed hydraulic turbine drives that were located between the high speed inducer and first pump stage of its respective propellant system. The scope of the ASE program did not permit the development of a dynamic simulation of each contractor's engine in complete

detail. Only the P&WA 111 kN (25K) configuration was simulated but it was programed with options to investigate gas and hydraulic turbine boost pump drive systems. The Aerojet and Rocketdyne turbine designs were modified to fit the P&WA cycle and a comparative transient investigation was conducted. Polar moments of inertia for the turbomachinery were calculated from reported information. The simulations were run on the computer through a typical normal start mode transient to determine the starting characteristics for each of the boost pump drive systems. The resultant start transients for the three drive systems are shown in figures 5 through 9.

b. Gear Drive

The gear-driven configuration is the ideal dynamic system, particularly when driven by the oxidizer turbine. The oxidizer turbopump has the design characteristic of accelerating faster than the fuel turbopump (when used in a single preburner system). Thus in the gear drive system, the oxidizer boost pump is perfectly matched with the oxidizer main pump and the fuel boost pump will lead the fuel main pump during transients thereby assuring adequate NPSH for both main pumps. This characteristic is shown in figures 5 through 9, which also show that the gear-driven boost pump system accelerates faster than the other two systems during the early portion of the transient. During the latter portion of the transient, the GH_2 turbine-driven boost pumps provide more NPSH margin to the main pumps than does the gear system.

A problem in the original OOS design of the P&WA gear-driven boost pump system was identified. The seal packages used in the oxidizer main and boost pumps have an excessively high breakaway torque requirement that results in an unacceptable transient. Since seal package design is a problem common to all drive systems and not a function of the boost pump drive concept, it was not considered as a factor in the comparisons and evaluations. A breakaway torque of zero was used for all transient characteristic comparisons. The turbine drive systems are more sensitive to the torque level than the gear drive system as cited in paragraph B6, which discusses turbopump seal design.

c. GH_2 Turbine Drive

The Rocketdyne turbines derived their power from the expansion of hydrogen that had been heated as a result of being used as a coolant for a portion of the regeneratively cooled thrust chamber nozzle. This configuration, to result in acceptable transients, requires sufficient hydrogen flow at a high enough temperature to supply the required energy to the turbines. The latter condition will normally occur at start from the heat sink provided by the high initial temperature of the thrust chamber cooling jacket. The first condition requires pressure from the main fuel pump. Thus, the relative acceleration between the boost pumps and main pumps depends on the combination of these two conditions. Figures 5 through 9 indicate that generally acceptable transients can be obtained with gas-driven turbines. A small period of cavitation, as shown in figure 7 for the main fuel pump, may be eliminated by adjusting the start schedule for the fuel valve. No attempt was made to optimize the start schedules for the three configurations. In the P&WA Space Shuttle Main Engine (SSME) program, acceptable start transients were simulated for GH_2 turbine-driven boost pumps.

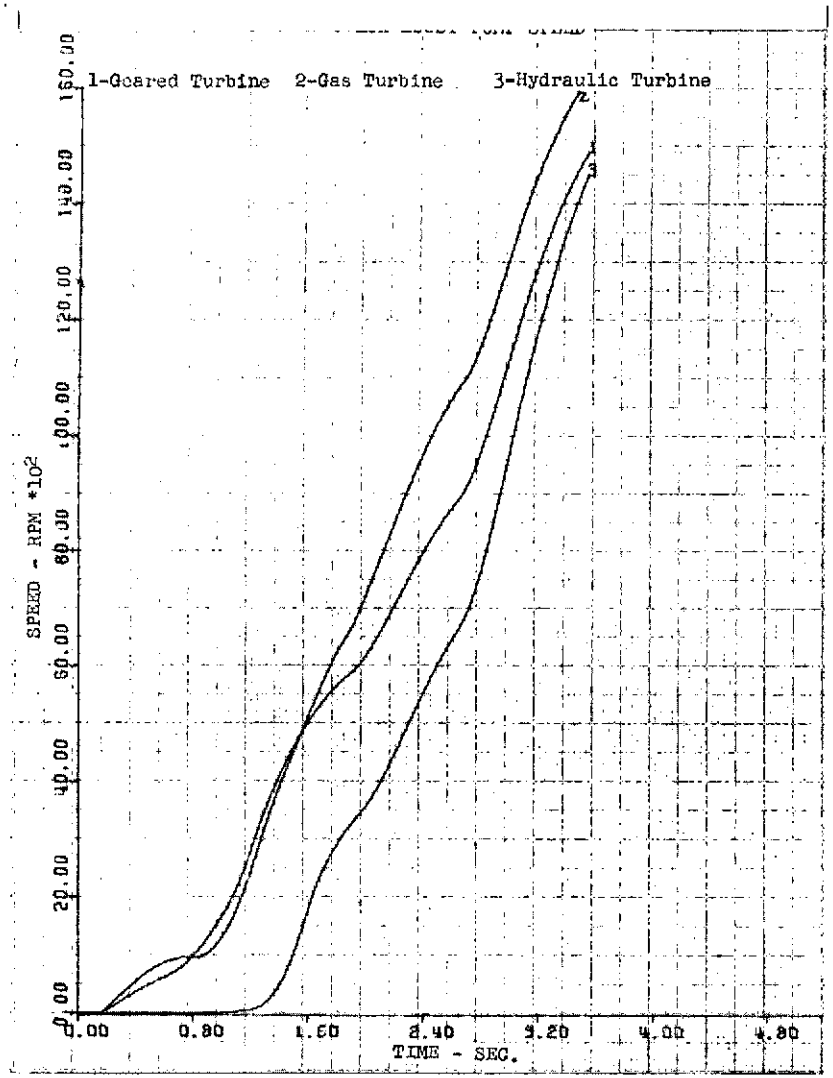

Figure 5. Start Transient Simulation, Normal Start: LO_2 Boost Pump Speed

DF 96311

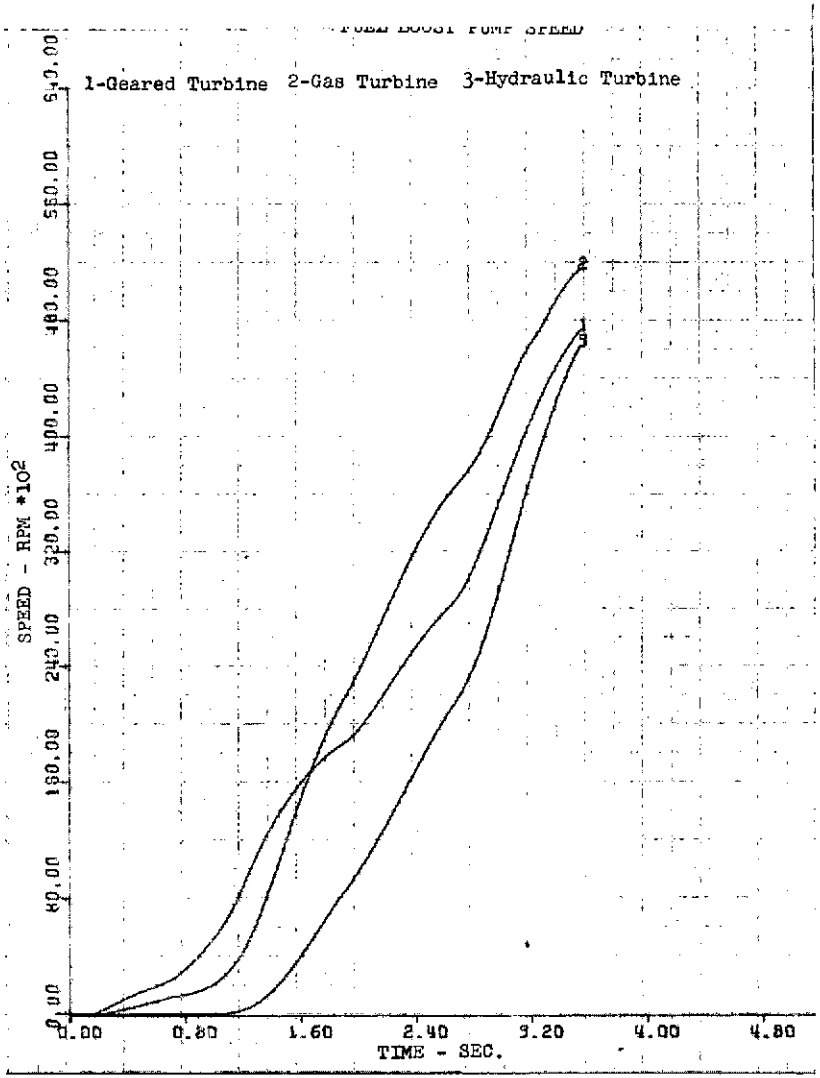

Figure 6. Start Transient Simulation Normal Start: Fuel Boost Pump Speed

DF 96312

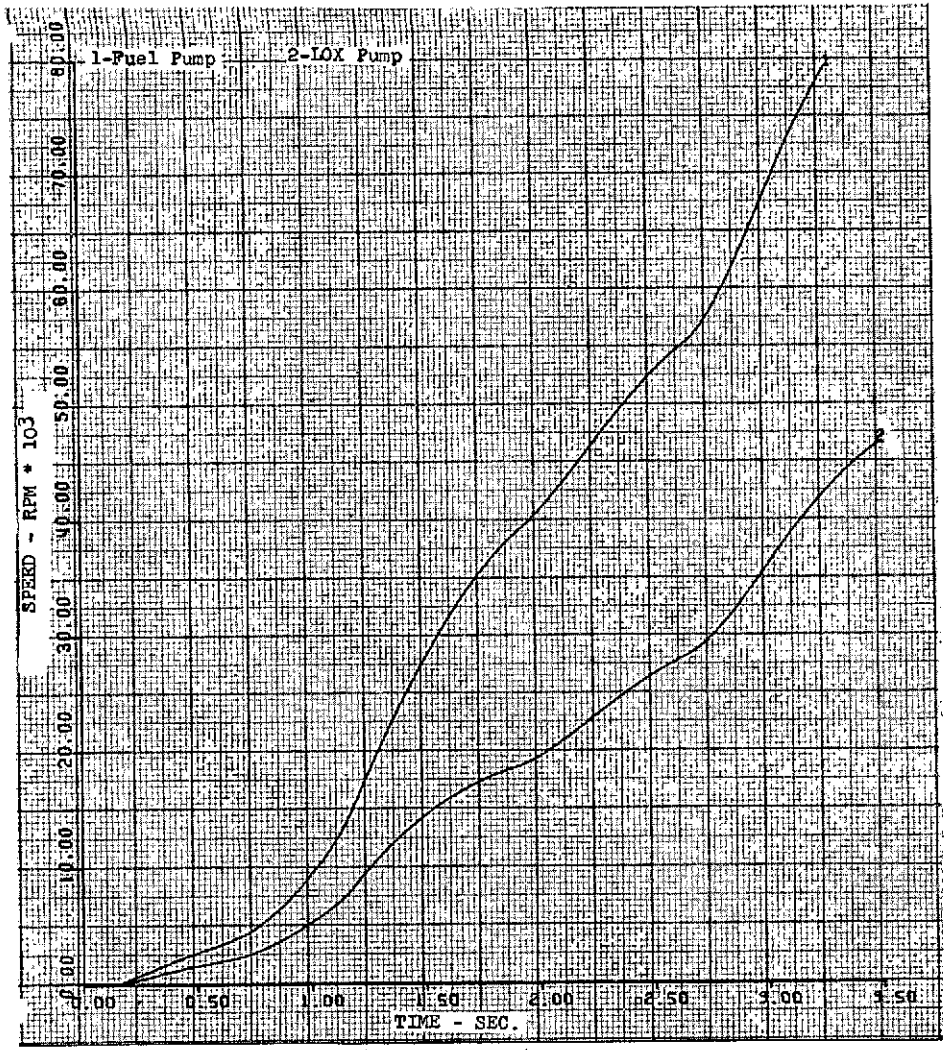

Figure 7. Start Transient Simulation
Normal Start: 1st Stage
Main Pump Speed

DF 96313

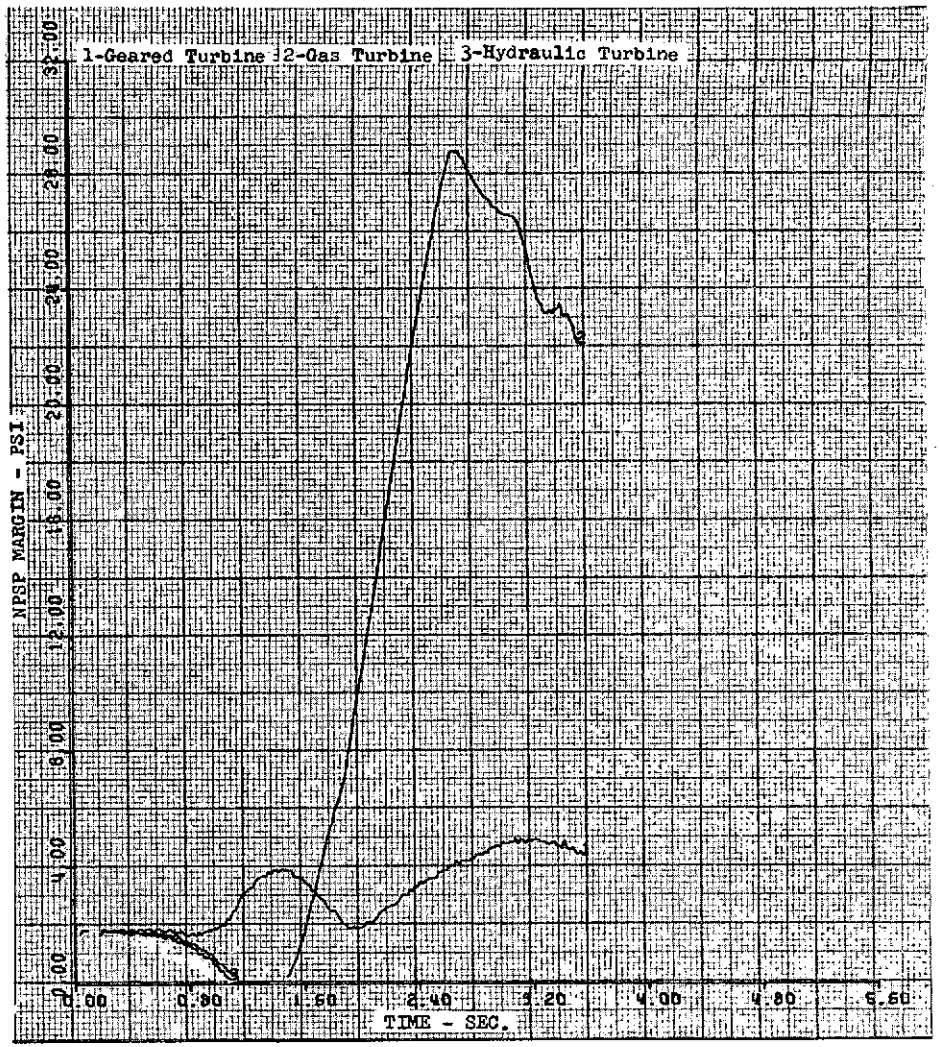

Figure 8. Start Transient Simulation
Normal Start: 1st Stage
Main Fuel Pump NPSP Margin

DF 96314

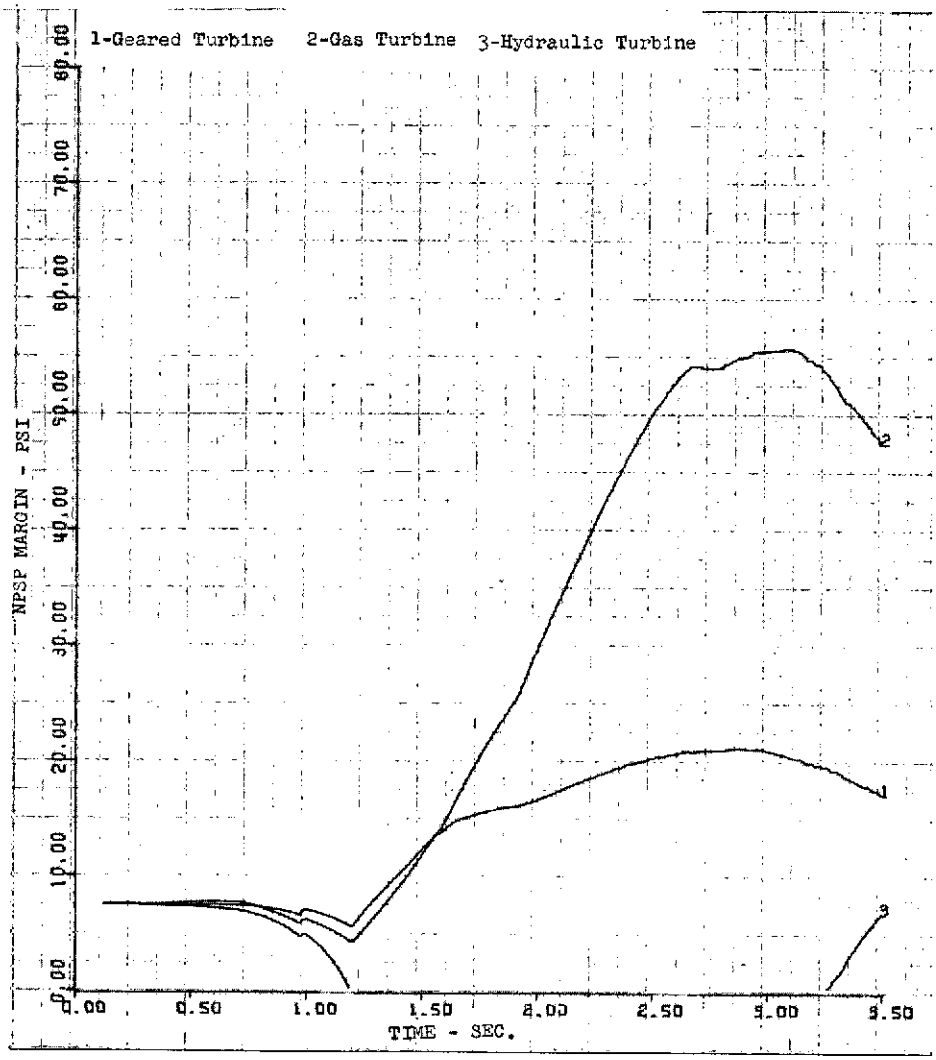

Figure 9. Start Transient Simulation, Normal Start: 1st Stage Main LO_2 Pump NPSP Margin DF 96315

d. Hydraulic Turbine Drive

The hydraulic turbine is one that receives its energy potential from the propellant pumped by the main pump inducer. Since there is little thermal energy in the cold propellants, the energy must come from the pressure rise generated by the main pump. This condition creates an inherent lag in the acceleration of the boost pumps relative to their main pumps. The study of the start transient of the hydraulic turbine boost pump drive system indicated that the main pumps reached 30-40% of their operating speeds before the boost pumps reached a speed that produced a pressure rise. The characteristics of this transient are shown in figures 5 through 9. The main pump as simulated showed operation with possible cavitation throughout most of the transient. The solution to this problem is to significantly slow the start transient.

3. Weight

A weight comparison was made of the boost pump systems selected by the three contractors. The gear-driven boost pump system is inherently heavier than the other types of drives and is also more weight sensitive to changes in design NPSH levels. The hydraulic turbine drive is the lightest in weight and least sensitive to design NPSH changes. However, the weight differences between a GH_2 turbine drive system and a geared system are not sufficient to result in significant engine weight differentials.

4. Vehicle/Engine Interface Flexibility

The GH_2 turbine drive system affords the maximum degree of flexibility of propellant inlet location of all the candidate systems, and the Aerojet integral hydraulic drive turbine concept, although it provides the most compact system, is the least flexible. The geared boost pump drive system is reasonably flexible; however, the fuel and oxidizer boost pumps must remain relatively fixed in their relation to each other. In general, the propellant inlets can be located both axially and radially wherever desired with all the candidate boost pump drive systems; however, long length and multiple bends in the lines between engine inlets and the boost pump inlets reduce boost pump suction capability and should be avoided.

5. Control and System Complexity

Of the three candidate boost pump drive systems, the hydraulic turbine drive proposed by Aerojet, which is integral with the main pump, is the simplest system and requires no controls.

In the gear drive system with both the oxidizer and fuel boost pumps driven from the high pressure oxidizer turbopumps shaft, only the main fuel pump speed must be controlled. On the other hand, the GH_2 turbine drive system may require independent control of the two individual turbines used to drive the fuel and oxidizer boost pumps. Control of boost pump speed is necessary to ensure adequate NPSH for the main pumps during rated thrust as well as transient operation in an actual engine system. It may be possible, however, to overdesign the boost pump pressure rise capabilities so that the need for drive turbine controls would be obviated.

The use of the GH_2 turbine drive impacts the selection of the type of thrust chamber regenerative cooling scheme. The more complex split flow cooling scheme is required for the gas turbine system if cycle chamber pressure capability is not to be compromised, while either of the two candidate schemes could be used with a geared boost pump drive system without affecting chamber pressure. (See paragraph D for a comparison of thrust chamber regenerative cooling schemes.)

The gears for the gear-driven boost pump drive system can be operated with pitch line velocities and Hertz stresses that are of the same level as that demonstrated on the RL10. Therefore, only a test program, in contrast to a development program, would be required to demonstrate the required 10-hr life for the ASE.

Significant potential problem areas for the GH_2 turbine drive system are the turbines themselves. In the ASE application, the turbines must be designed to operate with low pressure ratios (1.2:1 or less), low admission arcs ($\leq 10\%$), and with blade heights on the order of 5.08 mm (0.2 in.). With this combination of design requirements, the predictability of turbine performance is poor and the two turbines may require a substantial development effort. Thus, the GH_2 turbine drive system is considered to have a relatively high degree of risk.

A hydraulic turbine drive system that is separate from the main pump (independent main pump and hydraulic turbine shafts) would be similar in control requirements to the GH_2 turbine drive and would also lose the packaging simplicity of the Aerojet OOS drive concept.

6. Turbopump Seal Design

The design of the turbopump seal packages affects start transient acceleration characteristics because it determines the turbine torque required to overcome seal friction when starting the engine. A summary of the seal designs selected by the three contractors is shown in table III. The rubbing face seal used in the P&WA OOS oxidizer turbopump design is similar to those used in the RL10 turbopump assembly. RL10 experience shows that the static friction of these seals varies between 2.26 and 7.9 N-m (20 and 70 in.-lb). However, the staged combustion cycle has the capability of generating 1.36 to 2.72 N-m (12 to 24 in.-lb) of zero speed turbine torque at start under the typical ASE low inlet pressure conditions for a normal start. Therefore, rubbing face seals cannot be used in the design of the P&WA turbopump. The liftoff seals proposed by Aerojet are estimated to require 1.36 N-m (12 in.-lb) of torque or less and should result in an acceptable design. There is insufficient information to evaluate the static friction and breakaway torque required for the floating ring seals of the Rocketdyne design.

Table III. Summary of Seal Designs Selected by P&WA™, Rocketdyne, and Aerojet

Description	P&WA	Rocketdyne	Aerojet
Boost Pump Drive	Gear Driven	GH_2 Turbines	Hydraulic Turbines
Turbopump Seals			
Boost pump	Rubbing Face	Floating ring	None
Main pump	Liftoff (Fuel) Rubbing (Oxidizer)	Floating ring	Liftoff

The GH_2 and hydraulic turbine boost pump drive systems are particularly sensitive to breakaway torque requirements. The turbine drives are dependent on low pressure ratio (ΔP) energy potential because of their location in the engine system. Small changes or differences in pressure ratio (or ΔP) at low pressure ratios produce large changes in available power. Therefore, small reductions in the initial pressure ratio (ΔP) available at the time turbopump rotation is to be initiated may result in failure of the rotors to break away because of insufficient energy potential. On the other hand, the geared boost

pumps are driven by a high pressure ratio turbine that is less sensitive power-wise to pressure ratio changes.

C. PREBURNER CONFIGURATION

1. General

Of the three OOS engine designs, only one (Rocketdyne) incorporated dual preburners. The deletion of the 6:1 throttling requirement for the ASE (see paragraph G) reduces any cycle advantage inherent in the dual preburner configuration. The added complexity, weight, and risk of the dual preburner configuration do not justify its use in the ASE; therefore, a single preburner was selected. A discussion of single and dual preburner configurations follows.

2. Single Preburner

The single preburner arrangement is one in which a single preburner supplies combustion gases to both main turbines arranged in parallel. P&WA proposed this system with an oxidizer lead ignition while Aerojet proposed a single preburner with a fuel lead ignition. Satisfactory ignition can be accomplished with either propellant lead. The primary advantage of the single preburner is that only one ignition (in addition to main chamber ignition) is required at start and only one burner must be controlled at main stage, thus eliminating the failure mode of additional components and the complexity of maintaining power management control with two preburners. The primary disadvantage of a single preburner is the lack of independent control of energy supplied to the two main turbopumps. This arrangement limits the flexibility in the design of the main turbopumps since they must be dynamically matched (rotating inertias). Even with these limitations, the oxidizer pump has a tendency to accelerate faster than the fuel pump. The oxidizer flow must be restricted by the valves to prevent overtemperature of the preburner and turbines, thus driving the oxidizer pump toward cavitation. This condition forces the engine to start through a "window" between overtemperature and cavitation. Analytical studies have indicated that starts can be successfully made if the pumps are dynamically matched.

3. Dual Preburner

Rocketdyne proposed a dual preburner arrangement in which each of the two preburners produced fuel-rich combustion products and expanded them in the turbines supplying power to the respective main pumps. The primary advantages of a dual preburner system are the independent control of the two turbopumps which eliminates the "window" through which the single preburner must start, and operational flexibility when wide mixture ratio range capability at rated thrust or deep throttling is required. Because fixed thrust operation was baselined for the ASE with a limited mixture ratio range capability (MR = 6.0 ± 0.5), the flexibility advantage of dual preburners is partially lost for the ASE application.

The disadvantages of the dual arrangement are that two burners in addition to the main chamber must be ignited instead of one, and the increased complexity of power management control. A further disadvantage of a dual preburner system is the possibility of problems in achieving simultaneous ignition in the two preburners. Delayed ignition in one preburner could cause the preburner that lit first to unlight. Relighting of the preburner at higher than desired pressure levels might result in a detonation that could produce hardware failure.

D. REGENERATIVE COOLING SCHEME

For an engine with geared boost pumps, the system chosen for the ASE, the selection of a cooling scheme is largely a matter of designer choice. The pass-and-a-half scheme was selected because we consider it an inherently lower risk concept, and the split-flow scheme has no particular advantage. The two candiate regenerative chamber cooling schemes are compared below.

The two regenerative cooling schemes which were studied for ASE are the pass-and-a-half and the split-flow configurations shown in figure 10. In the pass-and-a-half scheme selected by Aerojet and P&WA, all of the available coolant (hydrogen) is used to cool the regenerative section of the thrust chamber in a series flowpath, whereas in the split-flow scheme selected by Rocketdyne the available coolant is split into two parallel flowpaths, each of which cools a separate section of the thrust chamber. The split-flow scheme provides the energy source for a gas turbine-driven boost pump system and can also readily provide fuel tank pressurants. However, it may require positive control to provide the desired flow split. The pass-and-a-half scheme, on the other hand, is a simpler system with no flow split controls required.

Early in the evaluation of the split-flow heat exchanger, a possible failure mode resulting from positive feedback was identified. In this particular failure mode, anything that caused a change in the flow split to the two parallel heat exchanger flow sections would result in one section being overcooled and the other undercooled. Positive feedback could drive the flow split further apart, i.e., the undercooled section would receive less coolant and the overcooled section more coolant until chamber failure occurred. The study of this possible failure mode of the split-flow heat exchanger configuration suggests that the feedback effects are self-limiting. Whether this self-limiting effect is adequate to prevent thrust chamber failure or would cause a significant reduction in chamber life is dependent upon the engine's control system. There appeared to be no significant weight difference or coolant pressure loss/temperature rise characteristic for the candidate schemes.

E. START MODE

1. General

The tank head idle start mode was selected for ASE. This start mode was found to be practical in initial studies and is very attractive for an operational Space Tug. With a "dry" engine and the low inlet pressures desired for the Space Tug, tank head idle operation for approximately 3 min is required to achieve the necessary thermal conditioning of the low pressure and main pumps before initiating the pumped idle mode of operation. As discussions with Space Tug systems contractors and with the NASA/MSFC Space Tug office indicated that the length of this cooldown period does not represent a problem, no further investigation into the use of boost pumps as recirculation pumps was undertaken.

Operating the engine in an expander cycle mode for the pumped idle phase, produces about 5% of rated thrust. This mode of operation requires only low flow turndown ratios in the preburner oxidizer system, which would not be possible if conventional staged combustion operation were used for pumped idle.

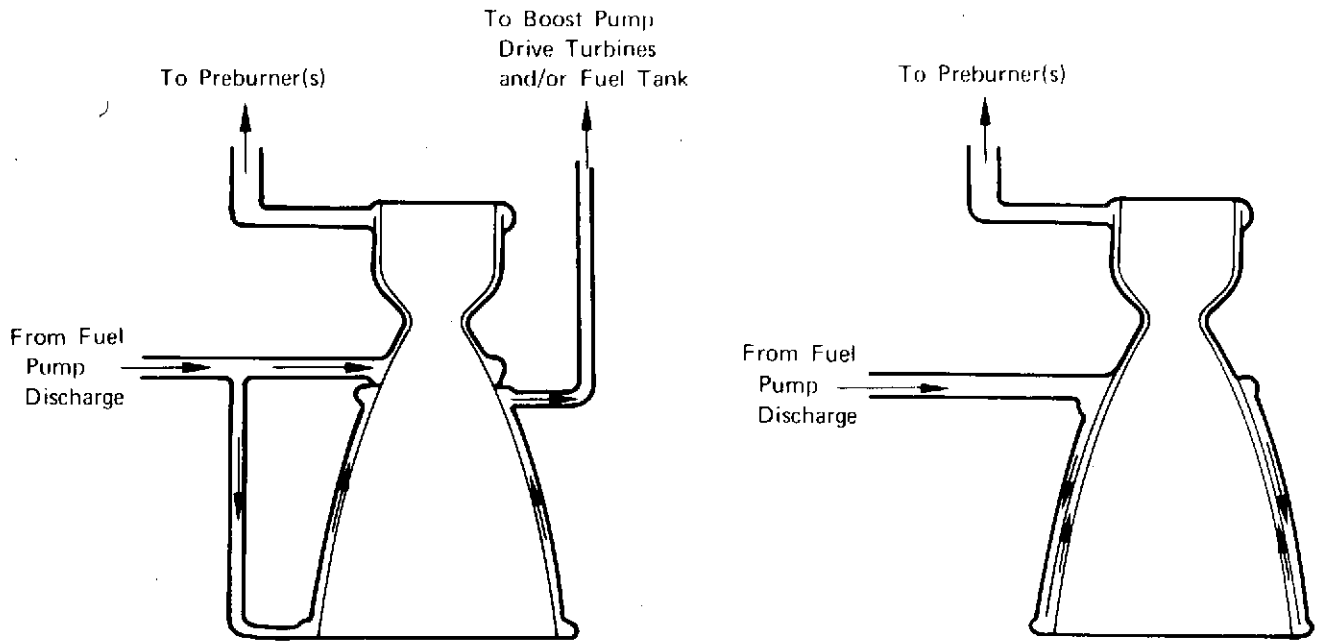

Figure 10. Thrust Chamber Regenerative Cooling Schemes

FD 61379

Therefore, full advantage of the relaxation in the engine's throttling requirement can be taken (fixed thrust operation was baselined for the ASE) by eliminating the need for large preburner oxidizer flow turndown and more sophisticated injector designs for all engine operating modes.

Helium purge requirements for the preburner oxidizer manifold are less than 0.023 kg (0.05 lb) per start for transition to full thrust. This purge, which is not required if the engine is only run in the pumped idle mode and then shut down (as for a low ΔV trim maneuver), would require only a small quantity of helium for a typical Space Tug mission and should therefore be acceptable.

The start modes that were considered for ASE operation were normal start, pressurized idle start and tank head idle (or pumped idle) start. The pressurized- and tank-head idle starts are illustrated in figures 11 and 12.

A normal start is one in which the engine accelerates from zero to full thrust upon receipt of an engine start signal. Prior to receiving the start command, the engine has been thermally conditioned and the available NPSH's are at the levels required for full thrust operation.

Pressurized idle start is a mode in which the tanks are prepressurized from an auxiliary source to provide the NPSH's required for full thrust operation prior to engine start. This start mode is intended to settle main tank propellants and thermally condition the engine. (Refer to figure 11.)

Tank head idle is a start mode in which propellants are supplied to the engine at saturated conditions. This operational mode is intended to settle main tank propellants and thermally condition the engine prior to transitioning to a pumped operational mode. Pumped-idle follows tank head idle operation, and is a mode in which the pumps are operated at a level sufficient to provide autogenous pressurization of the main propellant tanks.

A discussion of the various start modes follows.

2. Normal Start Mode

The normal start mode was used in the analysis of the boost pump drive systems. A normal start can be made safely with the GH_2 turbine and gear systems but not with the hydraulic turbine system. The engine acceleration from time of ignition to full thrust requires 3.5 to 4.0 sec as shown in figures 13 through 15. Valve schedules for the normal start are presented in figures 16 and 17.

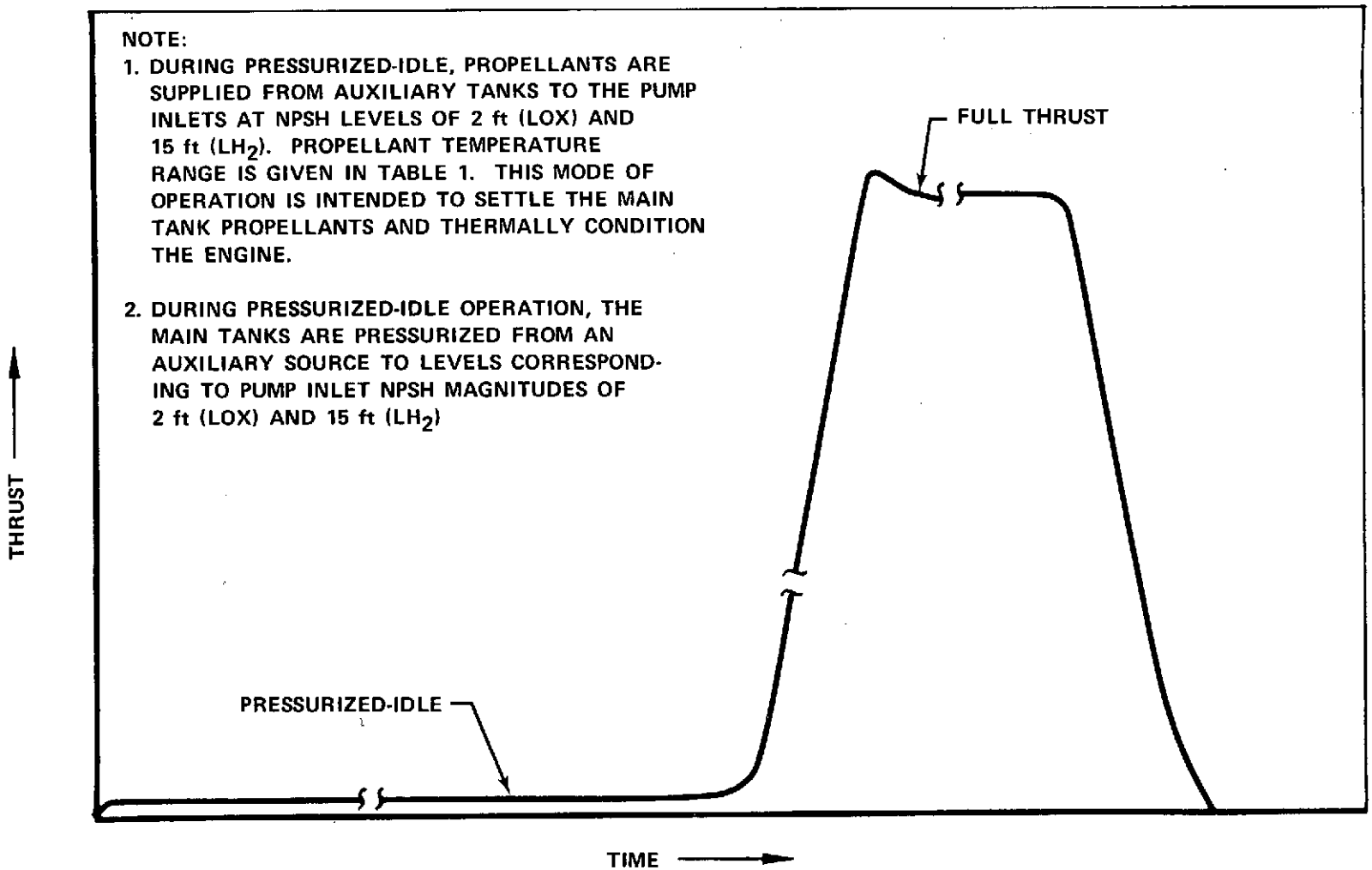

Figure 11. Pressurized Idle and Full Thrust Definitions

FD 72528

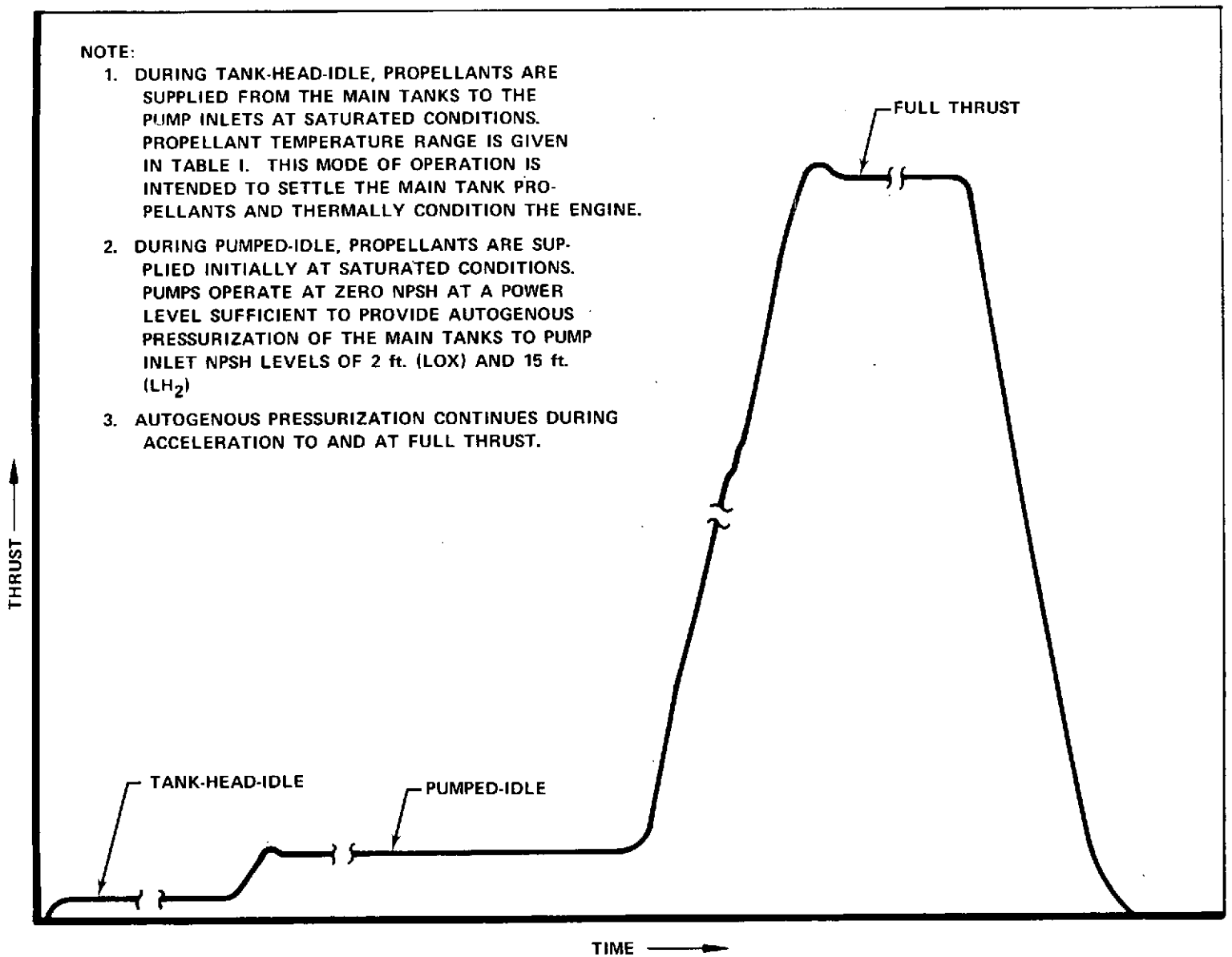

Figure 12. Tank Head Idle, Pumped Idle, and Full Thrust Definitions FD 68845

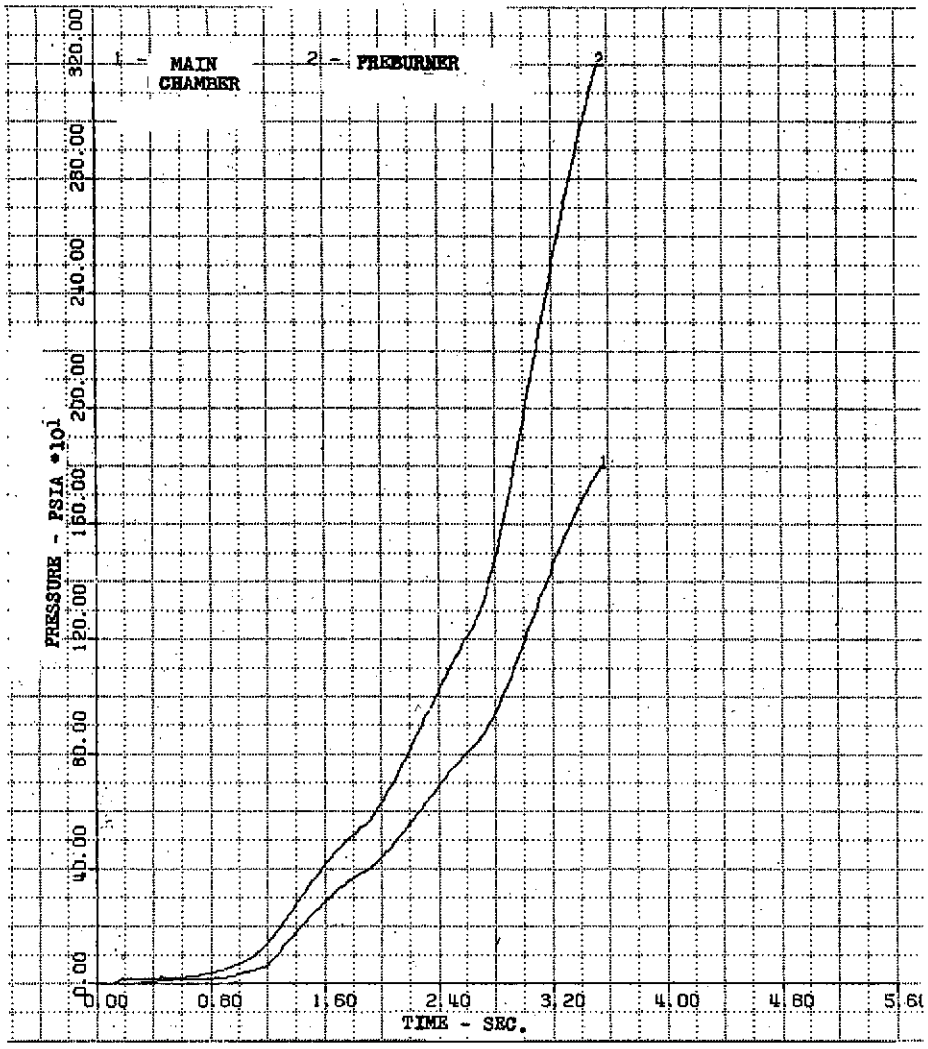

Figure 13. Start Transient Simulation Normal Start: Preburner and Main Chamber Pressure

DF 96316

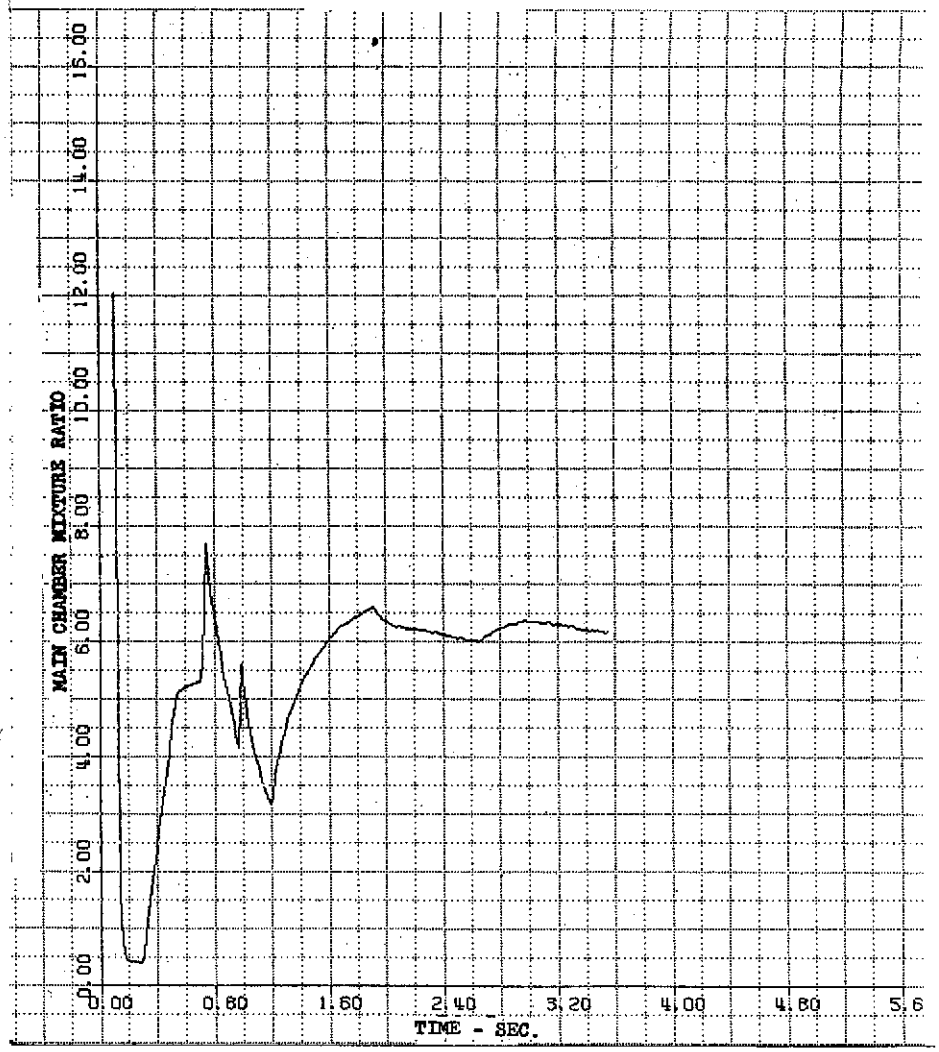

Figure 14. Start Transient Simulation Normal Start: Main Chamber Mixture Ratio

DF 96317

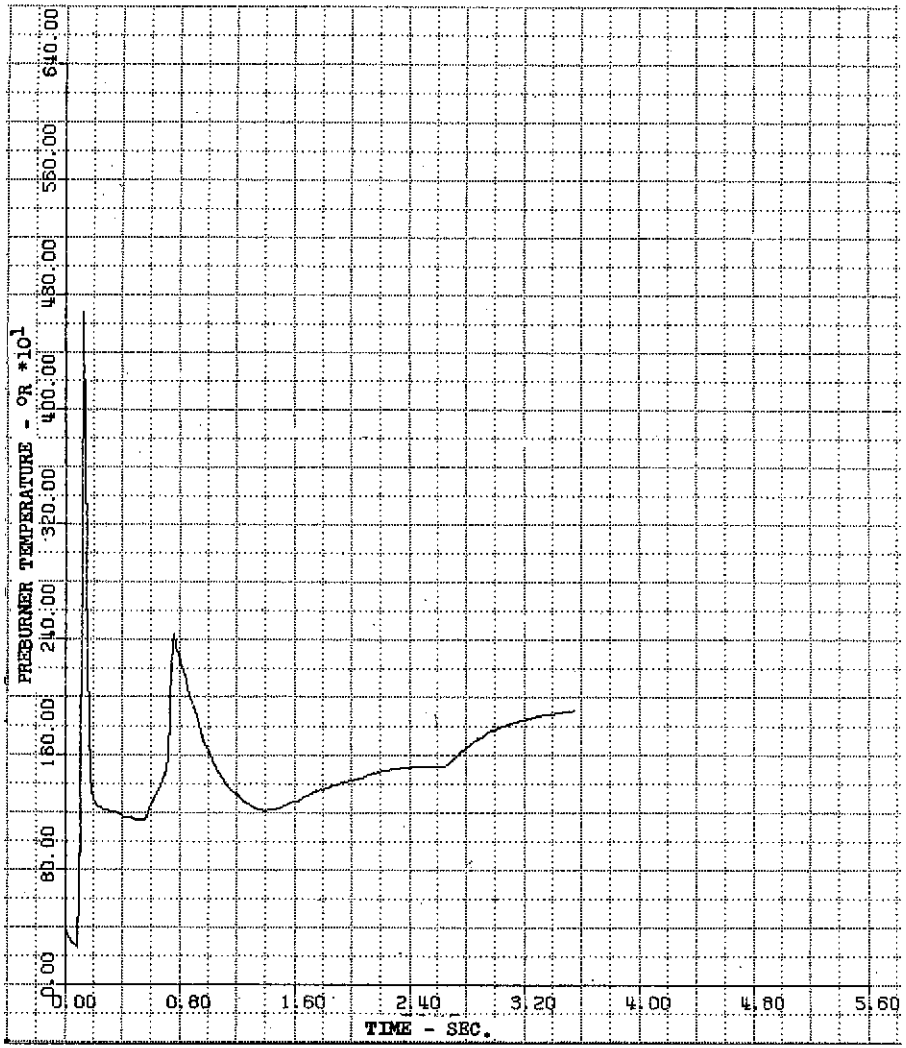

Figure 15. Start Transient Simulation Normal Start: Preburner Temperature

DF 96318

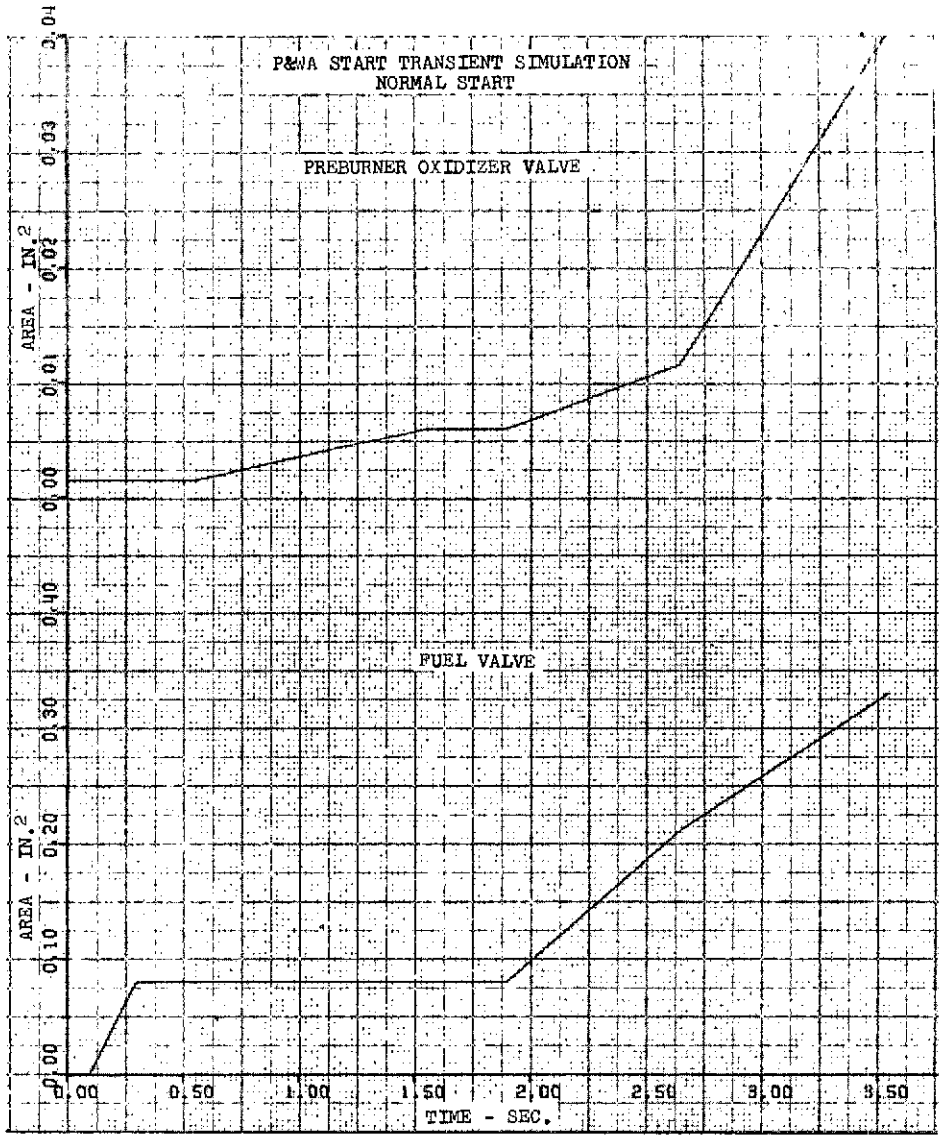

Figure 16. Start Transient Simulation Normal Start: Preburner Oxidizer Valve Area, Fuel Valve Area

DF 96319

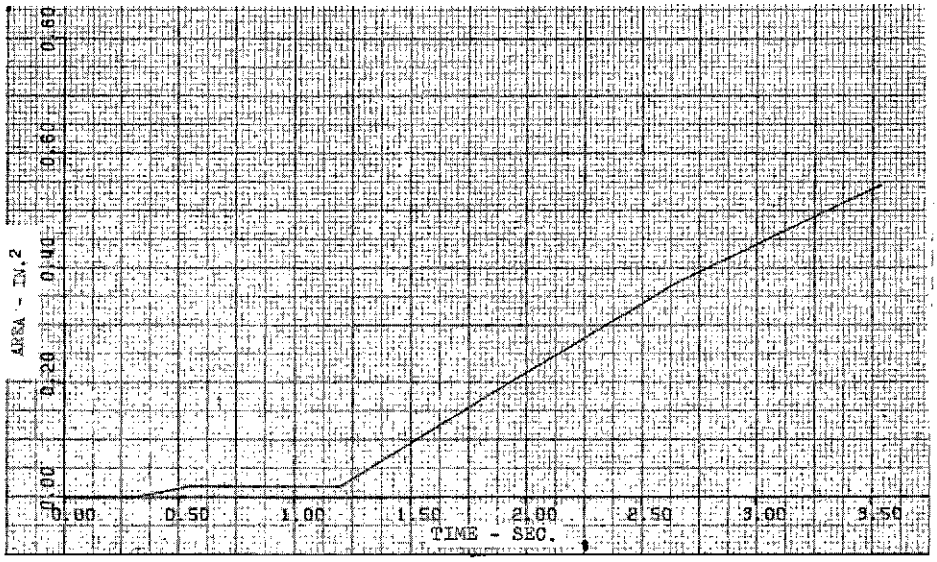

Figure 17. Start Transient Simulation, Normal Start: Main Chamber Oxidizer Valve Area DF 96320

3. Pressurized Start Mode

An OOS dynamic simulation was used to investigate the pressurized idle mode. The decision was made to run the engine with the expander cycle (preburner(s) unlit) based upon RL10 idle experience. The pumps were assumed to be at an ambient temperature of 222°K (400°R) with nominal NPSH's at the engine inlets at start. The main oxidizer valve was set to provide a short LO_2 lead and a mixture ratio of approximately 4.0 when fuel is introduced. The preburner oxidizer valve remains closed and the fuel valve is opened to its maximum position. While the engine is cooling down there is insufficient energy available to start turbopump rotation. The engine will operate at a chamber pressure of approximately 4.83-5.52 N/cm^2 (7-8 psia) and will take approximately 125 sec to cool down the fuel turbopump while consuming approximately 2.72 kg (6.0 lb) of fuel. The oxidizer turbopump is cooled down in approximately 50 sec while consuming 3.86 kg (8.5 lb) of propellant. The fuel side cooldown time can be shortened by bypassing fuel around the thrust chamber cooling jacket, directly to the preburner. Aerojet proposed to do this with the use of a thrust chamber cooling jacket bypass valve which closes when the engine starts to mainstage. Additional shortening of fuel and oxidizer cooldown time could be accomplished by using overboard vents in conjunction with idle mode.

4. Tank Head Idle Mode

The tank head idle mode is similar to pressurized idle except the propellants at the inlets are at saturation conditions. The same philosophy that was used for pressurized idle (i.e., expander mode operation, start sequence, etc.) was used. In tank head idle mode, the engine will operate at a chamber pressure of approximately 4.14-4.83 N/cm^2 (6-7 psia). The fuel pump will cool down in approximately 125-150 sec while consuming about 2.72 kg (6.0 lb) of fuel. The oxidizer-side will cool down in 50-60 sec while

consuming 14.1 kg (7.0 lb) of propellant. The same techniques that were recommended to decrease cooldown time for pressurized idle can be used with tank head idle.

5. Pumped Idle Mode

Pumped idle can follow either as an extension of pressurized idle or tank head idle. After the fuel turbopump has cooled down, fuel flow will have increased sufficiently to permit turbopump rotation on command. The engine while operating in the expander mode will become power limited and generate approximately 5% of rated thrust. The propellant utilization system can vary mixture ratio from 3.0 to 6.0. Only mixture ratio control is needed for idle mode operation and this can be accomplished with the main oxidizer valve. Coolant jacket discharge temperature would be monitored and would schedule main oxidizer valve position. To continue the acceleration to full thrust, the preburner oxidizer valve is opened, and the preburner is lit to provide additional turbine drive energy to the turbopumps.

F. NET POSITIVE SUCTION HEAD (NPSH) LEVELS

The required NPSH operating levels were selected from the following:

	NPSH, N-m/kg (ft)		
LO_2	0(0)	6(2)	48(16)
LH_2	0(0)	45(15)	180(60)

Orbit-to-Orbit Shuttle vehicle studies indicate that the engine operating NPSH level has an appreciable effect on vehicle gross weight. This sensitivity is shown in figure 18. Emphasis was, therefore, placed on providing zero LO_2 and LH_2 NPSH capability for pumped idle operation, and 6 N-m/kg (2 ft) LO_2 and 45 N-m/kg (15 ft) LH_2 NPSH capability for full thrust operation. The impact of increasing the full thrust NPSH levels to 48 N-m/kg (16 ft) for LO_2 and 180 N-m/kg (60 ft) for LH_2 was evaluated and found to result in an engine weight decrease of approximately 15.9 kg (35 lb) for the geared boost pump drive system. A smaller engine weight reduction would be realized if hydraulic or GH_2 turbine boost pump drive systems were used.

The engine weight reduction resulting from higher NPSH values does not include the added weight reduction resulting from decreased inlet (suction) valve and actuator sizes.

G. THROTTLING REQUIREMENT

The baseline mission for the ASE application, which consists of a trip with 1361 N (3000 lb) payload from low earth orbit (185 km (100 nmi) altitude, 0.511 rad (28.3 deg) inclination) to synchronous equatorial orbit and back, does not require continuous throttling capability nor do most of the applications for an advanced maneuvering propulsion system. Therefore, the ASE was to be designed as a fixed-thrust engine and the impact of providing 6:1 throttling was to be assessed.

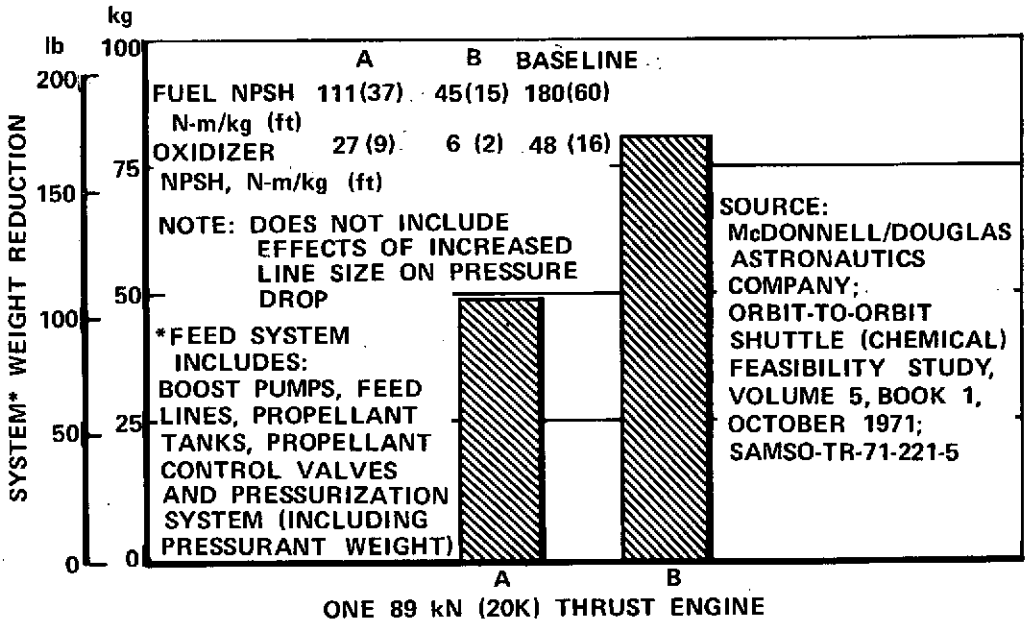

Figure 18. Effect of NPSH on System Weight FD 68870

Dual oxidizer elements in the preburner injector would replace the fixed thrust single-slot element configuration if the 6:1 throttling capability were to be provided. An increase in the main oxidizer injector pressure loss would also be necessary to ensure stable combustion for throttled operation. The overall impact of a 6:1 throttling capability was an increase in control and injector complexity with an attendant weight increase of 5 kg (11 lb), and because of increased main injector pressure losses, chamber pressure at full thrust would be reduced by approximately 34.5 N/cm^2 (50 psi).

SECTION IV
89,000 N (20,000 lb) THRUST ENGINE PRELIMINARY DESIGN

A. INTRODUCTION

The preliminary design of the experimental research Advanced Space Engine that resulted from this study program conforms to the configuration requirements and operating conditions specified in the contract, which are reproduced herein and designated table IV. Other engine requirements not defined by the contract were obtained from the Space Tug Definition Document, Reference 4. The turbine drive cycle (staged combustion) and thrust chamber nozzle type (400:1 expansion ratio, fixed-bell) were specified and the basic engine configuration (boost pump drive method, number of preburners, etc.) and operating modes were selected early in the program as reported in Section III. The engine system's work was directed primarily towards maximizing chamber pressure to provide a minimal engine envelope and reduced engine weight. Because the nozzle expansion ratio ($\epsilon = 400$) was specified, chamber pressure effects on engine specific impulse are of minor importance. The cycle work for tank head and pumped idle were concerned, in the main, with showing the feasibility of these operating modes and to determine potential problem areas. Optimization of pumped idle operation to provide the best combination of thrust level, specific impulse, and tank pressurization flowrate capability was beyond the scope of the contract. The following subsections present a description of the engine system, its operation, physical characteristics, and the subassembly/component designs.

B. ENGINE SYSTEM

1. General

The following paragraphs present a description of the propellant flowpaths and the engine system that evolved as a result of the cycle studies performed using the selected engine configuration. Engine steady-state operating characteristics are also presented herein for rated thrust, pumped, and tank head idle modes.

2. System Description

A simplified propellant flow schematic of the 89-kN (20,000-lb) thrust ASE engine is presented in figure 19. A brief description of the propellant paths at the engine nominal operating point (100% thrust and MR = 6.0) follows. Fuel (hydrogen) enters the engine through a ball-type inlet shutoff valve mounted on the inlet of a low pressure pump (boost pump) that is driven by gearing from the main oxidizer turbopump shaft. The low pressure pump operates at a rotational speed of 2,555 rad/s (24,400 rpm) to provide it with 45-N-m/kg (15-ft) NPSH capability. From the low pressure pump, fuel enters the first of two back-to-back shrouded impeller centrifugal stages. The impellers are mounted on a shaft driven by a single-stage, low-reaction, 56% admission turbine. The high pressure pump operates at the nominal speed of 9,740 rad/s (93,000 rpm).

Table IV. Engine Configuration and Operating Conditions (Contract NAS3-16750)

Propellants:	Liquid Hydrogen Liquid Oxygen
Vacuum Thrust:	20,000 lb
Vacuum Thrust Throttling Capability:	*
Vacuum Specific Impulse	*
Engine Mixture Ratio:	6.0 (nominal at full thrust) 5.5 - 6.5 (operating range at full thrust) *(1)
Chamber Pressure:	*(2)
Drive Cycle:	Staged Combustion
Envelope Restrictions: Length (max.) Diameter (max.)	 * *
Engine System Weight:	*
Nozzle Type:	Fixed Bell
Nozzle Expansion Ratio:	400:1
Propellant Inlet Temperatures: Hydrogen Oxygen	 Range: 36.5°R to 40°R Range: 162°R to 172°R
NPSP at Pump Inlet @ Full Thrust Hydrogen Oxygen	 * *
Engine Temperature at Normal Pre-start:	Range: 200°R to 560°R
Service Life Between Overhauls:	300 Thermal cycles or 10 hr accumulated run time. (3)
Service Free Life:	60 Thermal cycles or 2 hr accumulated run time.
Maximum Single Run Duration:	2000 sec
Maximum Time Between Firings During Mission:	14 days
Minimum Time Between Firings During Mission:	1 min
Maximum Storage Time in Orbit (Dry):	52 weeks

*To be determined or selected during contract.

(1) Engine mixture ratio at throttled, pressurized-idle, or tank-head-idle and pumped-idle conditions shall be selected during the contract and shall be at magnitudes which do not compromise the full thrust design.

(2) Maximum attainable within limits imposed by component performance and/or life.

(3) Thermal cycle defined as engine start (to any thrust level) and shutdown.

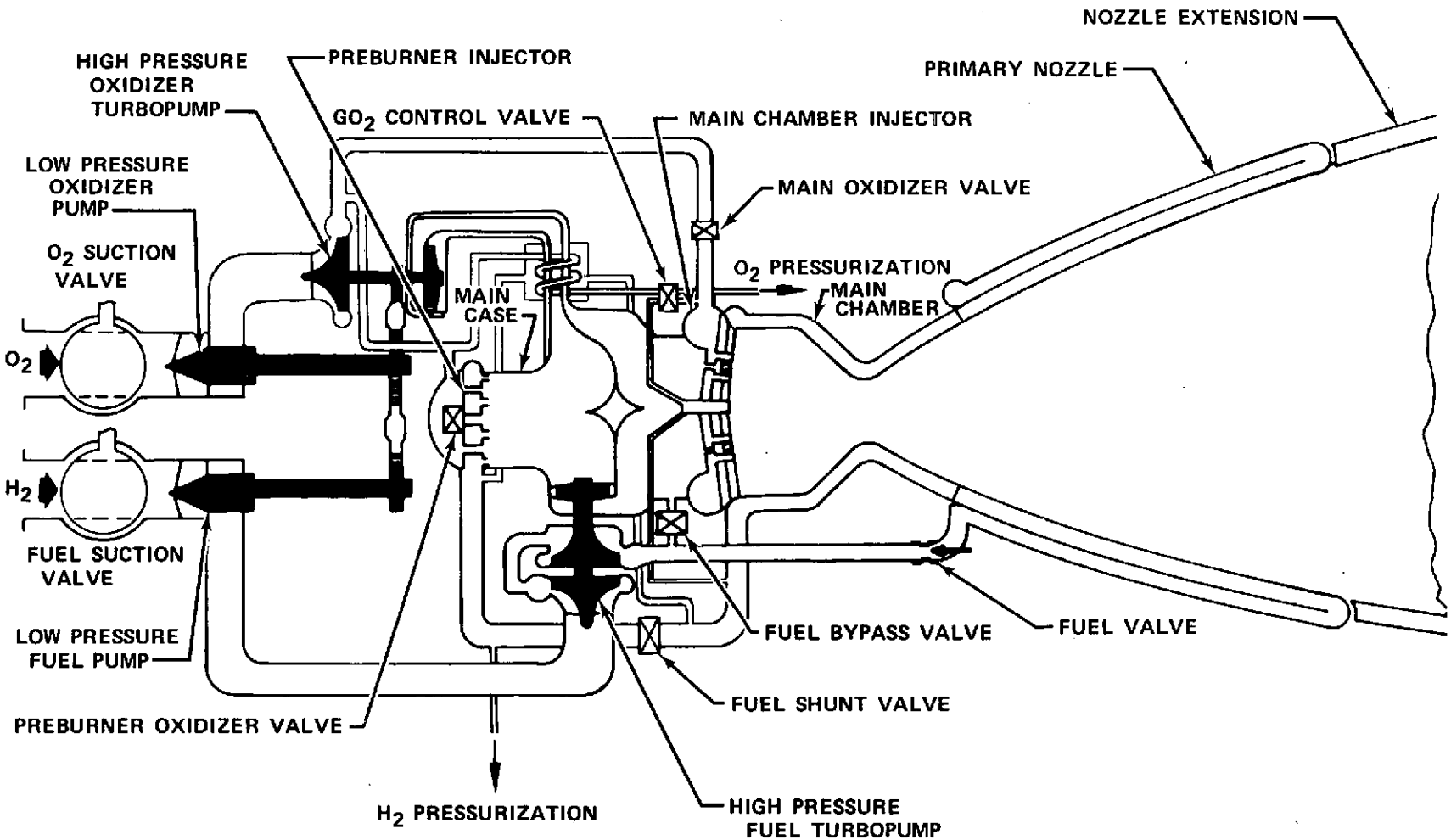

Figure 19. Advanced Space Engine System Schematic

FD 68849A

Approximately 83% of the fuel from the pump second stage is discharged through a cavitating venturi control valve to the thrust chamber regenerative cooling jacket. This control valve is used to schedule flow during transients, to prevent pressure fluctuations in the coolant jacket from affecting pump operation when in pumped idle mode, and to trim thrust and mixture ratio at engine rated thrust.

The chamber regenerative coolant (fuel) enters the pass-and-a-half tubular exhaust nozzle through an inlet manifold located at an area ratio of 25:1. Coolant flows from the inlet manifold into and through half of the tubes to the area ratio of 100:1, where a turnaround manifold routes it back (counter to the chamber combustion gas flow) through the remaining tubes to an area ratio of 6:1. At the area ratio of 6:1, the coolant enters and flows through a nontubular (copper alloy liner - electroformed nickel shell) short nozzle section and combustion chamber to the plane of the injector face. Flow is collected in a manifold, then a portion is split off in a parallel path through a GO_2 heat exchanger, is mixed with the main flow and is then injected into the preburner. The exhaust nozzle from the area ratio of 100:1 to the nozzle plane at $\epsilon = 400$, consists of a dump-cooled (fuel) nozzle skirt. When configured with a two-position nozzle for Space Tug application, the regenerative tubular section of the nozzle is lengthened and extended to an area ratio of 200:1.

The other 17% of the fuel from the pump 2nd-stage discharge is used to cool the turbopump bearings, gears, and various component housings. Part of this cooling flow passes through the gearbox and into the dump-cooled nozzle. The nozzle coolant flow is heated to a temperature of about 1000°K (1800°R) and expanded overboard through individual 3.5:1 area ratio nozzles located at the end of each of the coolant passages. The exiting coolant produces 623 N (140 lb) of thrust at a specific impulse level of 4266 N-s/kg (435 sec).

The fuel flowing into the preburner is injected through a fixed area fuel injector and is burned with a small portion of the oxidizer to produce combustion products at a design point temperature of 1140°K (2050°R). Ignition of the propellants in the preburner is accomplished with two spark igniters. The preburner produces the working fluid for the parallel turbines, which drive the fuel and oxidizer high pressure pumps. The preburner is mounted on a case that forms the fuel manifold for the main chamber injector (main case). The fuel turbopump is mounted in the same case and the preburner gases are routed to the fuel turbine through an internal duct. The duct also connects to an external line leading to the high pressure oxidizer turbopump turbine. The oxidizer line is a coaxial supply/return assembly with the return flow in the outer annulus discharging into the main case. (The oxidizer turbine line is an integral part of the GO_2 heat exchanger system, which is described in paragraph E, Engine Subassembly/ Component Design.) The fuel turbine drive gases discharge directly into the main case from the turbine exit, combine with the oxidizer turbine discharge flow, and then pass through the main chamber injector into the main combustion chamber.

Oxidizer enters the engine through an inlet valve similar to the fuel-side inlet valve. A low pressure oxidizer pump, geared from the main oxidizer turbopump and operating at a shaft speed of 628 rad/s (6000 rpm), provides engine capability for 6 N-m/kg (2-ft) NPSH operation. The discharge from the low pressure pump enters the single-stage, shrouded, centrifugal-type, high pressure pump driven at 5,760 rad/s (55,000 rpm) by a single-stage, low reaction, 26% admission turbine. All the oxidizer is pumped to the preburner injection pressure.

Approximately 13% of the LO_2 discharged from the high pressure oxidizer pump flows to the preburner injector through a control valve that regulates preburner gas temperatures to control engine thrust and mixture ratio.

The remainder of the oxidizer pump discharge flow (87%) is routed to the main burner injector through a control valve, which is also used for flow scheduling and engine trimming. The main burner oxidizer injector consists of fixed area, tangential entry elements arranged in radial spraybars.

The above valves are controlled by an electronic control unit (ECU), which receives electrical command signals from the vehicle. The control system is basically an open-loop system for valve scheduling with second-level, closed-loop logic for precision trimming and limit protection. Helium solenoid valves, sensors, etc., complete the control system.

A hydrogen-oxygen torch igniter is used to light the main burner. Fuel for the igniter is tapped off at the fuel valve, and gaseous oxidizer is supplied from the GO_2 heat exchanger/GO_2 control valve system.

Gaseous hydrogen for autogenous tank pressurization is tapped off from the fuel line to the preburner. The fuel pressurant, 0.015 kg/s (0.034 lb/sec), is supplied to the vehicle at a temperature of 266°K (487°R). The oxidizer tank pressurant is obtained from a GO_2 heat exchanger, which is an integral part of the oxidizer turbine flow coaxial supply/return line. The oxidizer pressurant flow of 0.061 kg/s (0.134 lb/sec) is supplied to the vehicle at a temperature of 235°K (423°R).

3. Cycle Optimization

The objective of the cycle optimization work was to define an engine system that would operate at the highest chamber pressure to maximize performance and to minimize the engine envelope providing the required total and thermal cycle life. Cycle optimization is a result of iterations between cycle studies and preliminary subassembly design. The iterative procedure is illustrated in figure 20. Cycle criteria used in the ASE study are presented in table V.

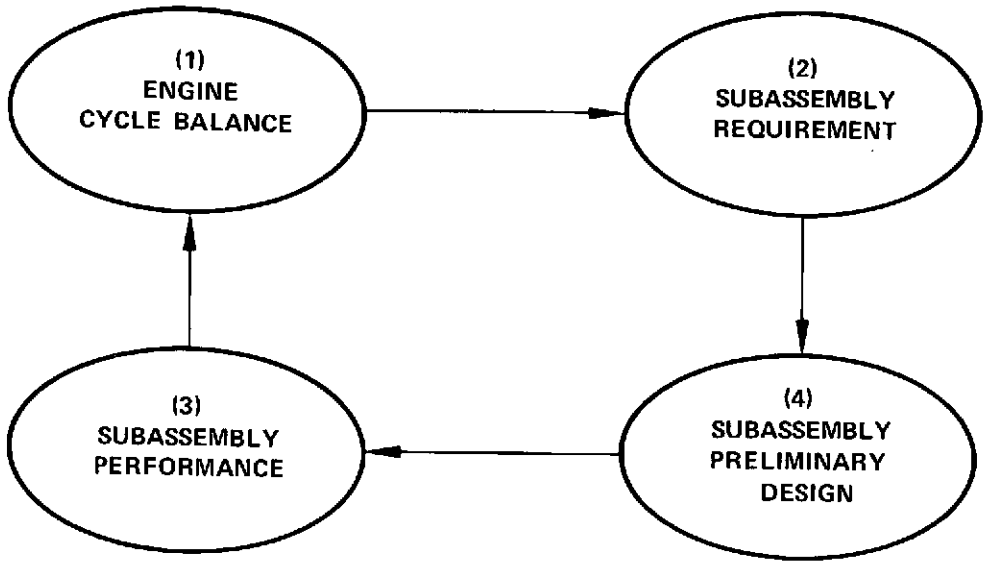

Figure 20. Design Study Logic Diagram FD 70530

Table V. Cycle Criteria and Groundrules for 89 kN (20,000-lb) Thrust ASE Preliminary Design

A. Engine Performance

1. Performance to be determined using JANNAF methodology (as one method) for minimum surface area nozzle contour, $\epsilon = 400$

B. Turbopump

1. Impellers:

- Shrouded: 701 m/s (2300 ft/sec) tip speed (Limit)

2. Pump and Turbine Efficiency To Be Determined by Design Analysis

3. Turbines:

- Inlet Temperature Uncooled: 1194°K (2150°R) (Limit)
- Design Stress (Limit)

  Blade Pull Stress Limit: 37,921 N/cm^2 (55,000 psi) for 10-hr creep 1% life at 1194°K (2150°R) for IN100 material

- Minimum Pressure Ratio: 1.1:1 (Limit)
- Minimum Blade Height: 0.76 cm (0.30 in.) (Limit)
- Minimum Vane Angle: 261.8 mrad (15 deg) (Limit)

C. Pressure Loss (Minimums for Rated Thrust)

Modulating Valves	$\Delta P/P_{upstream}$
Fuel Valve (cavitating venturi)	0.001
Main Oxidizer Valve	0.0485
Preburner Oxidizer Valve	0.0485
Injectors	$\Delta P/P_{downstream}$
Preburner Fuel Injector	0.040
Preburner Oxidizer Injector	0.045
Main Burner Oxidizer Injector	0.045
Main Burner Hot Gas Injector	0.043

D. Thrust Chamber Heat Transfer

1. h_g - Mayer Boundary Layer Solution
2. h_c - Dittus-Boelter 1.63 μm (64 μin.) surface roughness
3. Enhancement factor to be used at throat location

The purpose of the initial cycle studies was to establish component design requirements for the selected engine configuration and operating modes. (Refer to figure 2.) Preliminary subassembly/component designs were generated for these requirements and the performance and off-design characteristics of these subassemblies were defined. This subassembly/component information was then used in the cycle computer programs to define the engine characteristics.

The initial baseline engine cycle generated, cycle No. 104 was the basis for subassembly/component designs. A flow schematic for this cycle, presented in figure 21, shows the engine operating characteristics at 100% thrust and MR = 6.

After completion of the preliminary design, the subassembly/component performance characteristics and "best-estimate" I_{vac} values were used in the cycle computer program to generate the engine characteristics for all operational modes and operating points of interest (cycle No. 106). Engine characteristics for the nominal operating point, 100% thrust and MR = 6, are presented in the schematic, figure 22. Summaries of operating characteristics at rated thrust for MR = 5.5, 6, and 6.5 are given in tables VI, VII, and VIII, respectively.

The pumped idle schematic (4% thrust, MR = 3.5) shown in figure 23 is for prepressurized vehicle tanks. Operating characteristics are presented in table IX.

Tank head idle operating conditions, after engine thermal conditioning are depicted in figure 24. Saturated liquid propellant conditions are assumed to exist at the engine fuel and oxidizer inlets. These inlet conditions produce a maximum thrust of 244.7 N (55 lb) at MR = 1.5 for tank head idle operation. At this operating point, the engine is ready to change to the pumped idle mode upon command.

The high pressure fuel turbopump speed of 9,740 rad/s (93,000 rpm) at the engine nominal operating point (rated thrust, MR = 6.0) was determined on the basis of bearing DN limits established for the ASE study. The potentially greatest bearing load in a turbopump design that employs an axial thrust balance system is the radial component. P&WA experience with high speed, high pressure turbopumps indicates that unknown or unpredicted loads in a new turbopump can cause premature bearing failures. The diameter of minimum-size bearings used by P&WA in high pressure turbopump designs is therefore 20 mm to provide adequate rotor stiffness and to prevent early bearing failure. The design point speed selection makes an allowance for off-design operating conditions at rated thrust (MR = 5.5) where fuel turbopump speed generally is about 5% higher than at the design point for single preburner, load control engine systems. This margin assures that the allowable bearing DN is not exceeded at any point within the engine operating regime.

The high pressure oxidizer turbopump design point speed of 5,760 rad/s (55,000 rpm) was set to assure satisfactory service life for the gears consistent with the present state-of-the-art for gears operating in a similar environment. The gears in the boost pump drive system are designed for a maximum pitch line velocity of 102 m/s (20,000 ft/min) and a maximum Hertz stress of 41,400 N/cm^2 (60,000 psi).

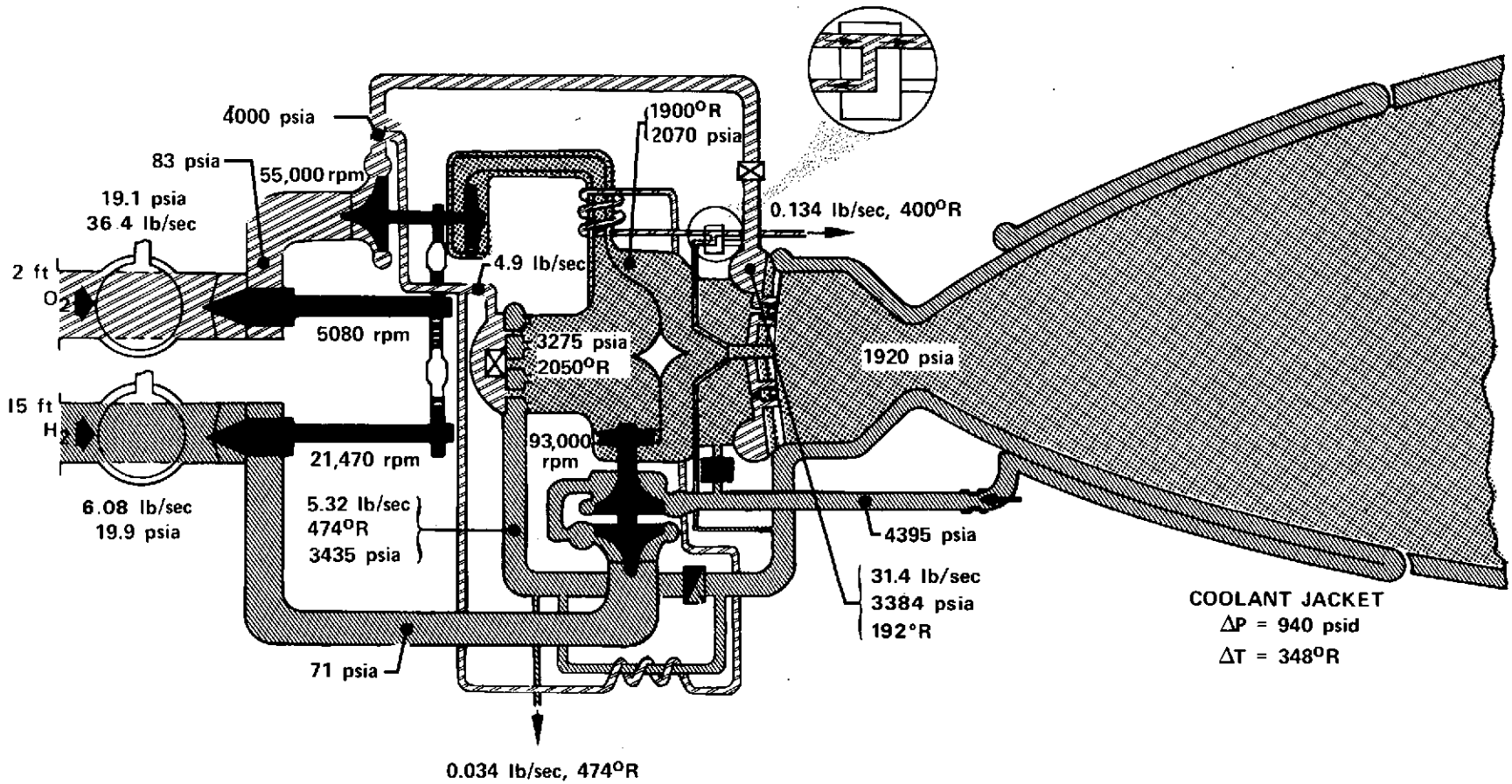

Figure 21. Baseline Cycle Balance Flow Schematic, Rated Thrust, Mixture Ratio = 6:1 (Cycle No. 104)

FD 66669

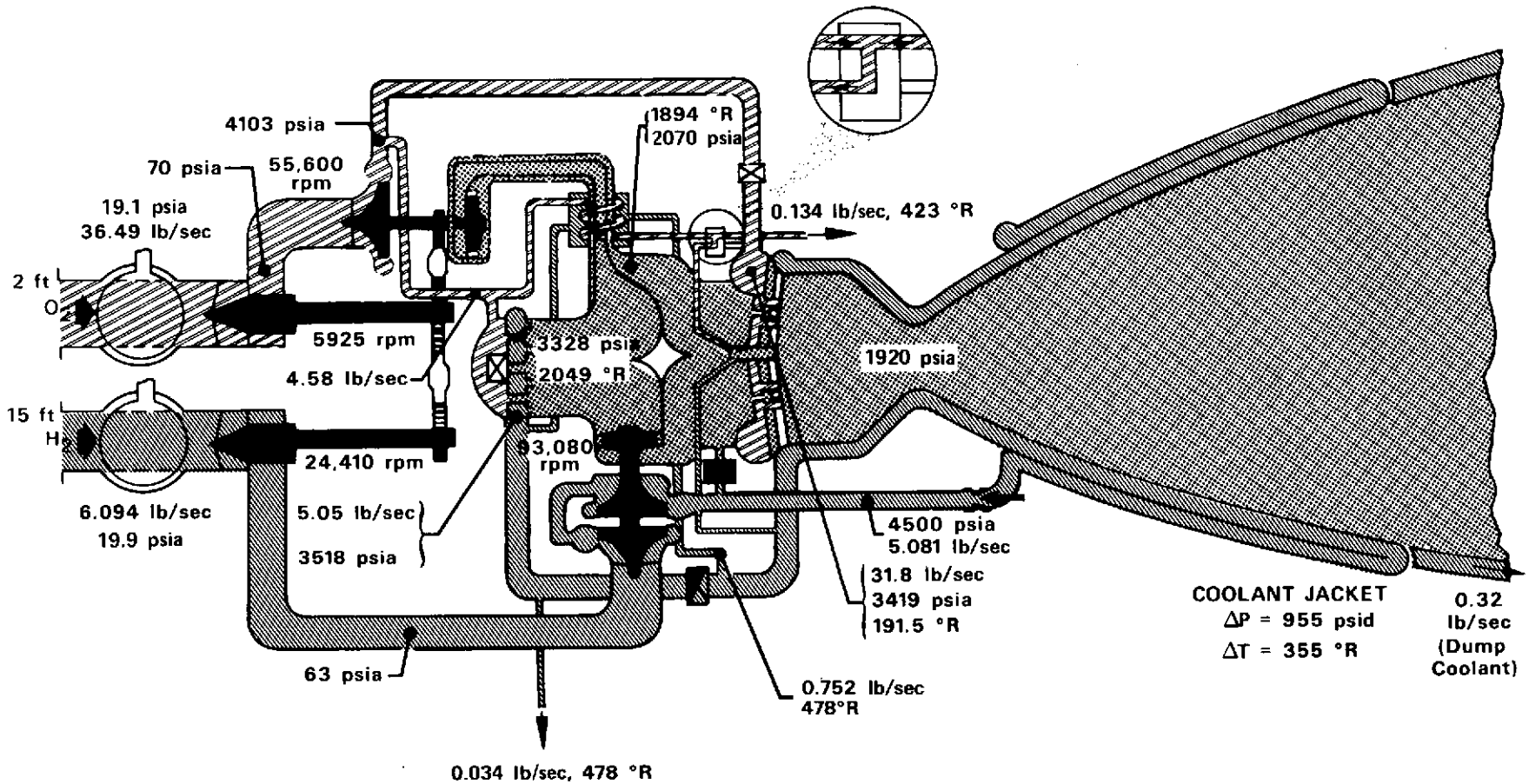

Figure 22. Final Cycle Balance Flow Schematic, Rated Thrust, Mixture Ratio = 6:1 (Cycle No. 106)

FD 66669F

Table VI. ASE Operating Characteristics,
Rated Thrust (100% Thrust, MR = 5.5)

Parameter		
Thrust, N (lb)	89,000	(20,000)
Specific Impulse, N-s/kg (sec)	4647.4	(473.9)
Inlet Fuel Flow, kg/s (lb/sec)	2.961	(6.527)
Inlet Oxidizer Flow, kg/s (lb/sec)	16.259	(35.844)
Total Propellant Flow, kg/s (lb/sec)	19.219	(42.371)
Fuel Tank Pressurization Flow, kg/s (lb/sec)	0.015	(0.034)
Oxidizer Tank Pressurization Flow, kg/s (lb/sec)	0.061	(0.134)
Chamber Pressure, N/cm^2 (psia)	1,342	(1,946)
Mixture Ratio, Vehicle	5.492	
Oxidizer Low Pressure Pump		
Inlet Total Pressure, N/cm^2 (psia)	13.2	(19.1)
Inlet NPSH, N-m/kg (ft)	5.98	(2.0)
Inlet Temperature, °K (°R)	92.2	(166.0)
Flowrate, m^3/s (gpm)	0.01438	(228)
Discharge Pressure, N/cm^2 (psia)	55.1	(79.9)
Head Rise, N-m/kg (ft)	371	(124)
Speed, rad/s (rpm)	661	(6,310)
Efficiency*, %	74.7	
Specific Speed	2,560	
Power, kwatts (horsepower)	8.13	(10.9)
Fuel Low Pressure Pump		
Inlet Total Pressure, N/cm^2 (psia)	13.7	(19.9)
Inlet NPSH, N-m/kg (ft)	47.8	(16.0)
Inlet Temperature, °K (°R)	21.3	(38.3)
Flowrate, m^3/s (gpm)	0.04252	(674)
Discharge Pressure, N/cm^2 (psia)	47.4	(68.7)
Head Rise, N-m/kg (ft)	4,824	(1,614)
Speed, rad/s (rpm)	2,723	(26,000)
Efficiency*, %	75	
Specific Speed	2,652	
Power, kwatts (horsepower)	19.02	(25.5)
Main Oxidizer Pump		
Inlet Total Pressure, N/cm^2 (psia)	51.4	(74.5)
Inlet Temperature, °K (°R)	92.4	(166.3)
Flowrate, m^3/s (gpm)	0.01438	(228)
Discharge Pressure, N/cm^2 (psia)	3,303	(4,790)
Head Rise, N-m/kg (ft)	28,916	(9,674)
Speed, rad/s (rpm)	6,203	(59,235)
Efficiency*, %	63.7	
Specific Speed	917	
Power, kwatts (horsepower)	738	(990)

*Pump efficiencies include effects of recirculated flows (thrust balance systems, bearing cooling, internal leakages, etc.).

Table VI. ASE Operating Characteristics, Rated Thrust (100% Thrust, MR = 5.5) (Continued)

Main Fuel Pump		
Inlet Total Pressure, N/cm^2 (psia)	42.9	(62.2)
Inlet Temperature, °K (°R)	21.6	(38.9)
Flowrate, m^3/s (gpm)	0.04246	(673)
Discharge Pressure, N/cm^2 (psia)	3,292	(4,774)
Head Rise, N-m/kg (ft)	490,307	(164,034)
Speed, rad/s (rpm)	10127	(96,710)
Efficiency*, %	58.2	
Specific Speed	524	
Power, kwatts (horsepower)	2,494	(3,344)
Fuel Turbine		
Inlet Total Pressure, N/cm^2 (psia)	2,398	(3,478)
Inlet Total Temperature, °K (°R)	1,122	(2,019)
Discharge Static Pressure, N/cm^2 (psia)	1,471	(2,134)
Speed, rad/s (rpm)	10,127	(96,710)
Efficiency, %	68.4	
Power, kwatts (horsepower)	2,494	(3,344)
Turbine Flow, kg/s (lb/sec)	3.285	(7.243)
Percent Admission	56	
Pressure Ratio (Total-Static)	1.630	
Oxidizer Turbine		
Inlet Total Pressure, N/cm^2 (psia)	2,386	(3,461)
Inlet Total Temperature, °K (°R)	1,122	(2,019)
Discharge Static Pressure, N/cm^2 (psia)	1,515	(2,197)
Speed, rad/s (rpm)	4,626	(59,235)
Efficiency, %	52.8	
Power, kwatts (horsepower)	764	(1,025)
Turbine Flow, kg/s (lb/sec)	1.397	(3.079)
Percent Admission	26	
Pressure Ratio (Total-Static)	1.575	
Preburner		
Chamber Pressure, N/cm^2 (psia)	2,422	(3,513)
Fuel Injector ΔP, N/cm^2 (psid)	140	(203)
Oxidizer Injector ΔP, N/cm^2 (psid)	194	(282)
Fuel Flowrate, kg/s (lb/sec)	3.744	(5.430)
Oxidizer Flowrate, kg/s (lb/sec)	2.219	(4.892)
Chamber Mixture Ratio	0.901	
Combustion Temperature, °K (°R)	1,122	(2,019)

*Pump efficiencies include effects of recirculated flows (thrust balance systems, bearing cooling, internal leakages, etc.).

Table VI. ASE Operating Characteristics, Rated Thrust (100% Thrust, MR = 5.5) (Concluded)

Thrust Chamber		
Chamber Pressure, N/cm^2 (psia)	1,342	(1,946)
Mixture Ratio	5.80	
Hot Gas Injector ΔP, N/cm^2 (psid)	115	(167)
Oxidizer Injector ΔP, N/cm^2 (psid)	973	(1,411)
Chamber Throat Diameter, cm (in.)	6.53	(2.57)
Nozzle Exit Diameter (ID), cm (in.)	132.6	(52.2)
Nozzle Expansion Ratio (Aero)	400	
Nozzle Dump Cooling Flowrate, kg/s (lb/sec)	0.152	(0.336)
Coolant Jacket		
Pressure Drop, N/cm^2 (psid)	710	(1,030)
Temperature Rise, °K (°R)	183	(330)
Tank Pressurants		
Oxidizer Flowrate, kg/s (lb/sec)	0.061	(0.134)
Oxidizer Temperature, °K (°R)	237	(426)
Fuel Flowrate, kg/s (lb/sec)	0.015	(0.034)
Fuel Temperature, °K (°R)	254	(457)

Table VII. ASE Operating Characteristics, Rated Thrust (100% Thrust, MR = 6.0)

Parameter		
Thrust, N (lb)	89,000	(20,000)
Specific Impulse, N-s/kg (sec)	4,623.8	(471.5)
Inlet Fuel Flow, kg/s (lb/sec)	2.764	(6.094)
Inlet Oxidizer Flow, kg/s (lb/sec)	16.552	(36.492)
Total Propellant Flow, kg/s (lb/sec)	19.317	(42.586)
Fuel Tank Pressurization Flow, kg/s (lb/sec)	0.015	(0.034)
Oxidizer Tank Pressurization Flow, kg/s (lb/sec)	0.061	(0.134)
Chamber Pressure, N/cm^2 (psia)	1,324	(1,920)
Mixture Ratio, Vehicle	5.99	
Oxidizer Low Pressure Pump		
Inlet Total Pressure, N/cm^2 (psia)	13.2	(19.1)
Inlet NPSH, N-m/kg (ft)	5.98	(2.0)
Inlet Temperature, °K (°R)	92.2	(166.0)
Flowrate, m^3/s (gpm)	0.01464	(232)
Discharge Pressure, N/cm^2 (psia)	48.5	(70.3)
Head Rise, N-m/kg (ft)	314	(105)

*Pump efficiencies include effects of recirculated flows (thrust balance systems, bearing cooling, internal leakages, etc.).

Table VII. ASE Operating Characteristics, Rated Thrust (100% Thrust, MR = 6.0) (Continued)

Oxidizer Low Pressure Pump (Continued)		
Speed, rad/s (rpm)	620	(5,923)
Efficiency*, %	75	
Specific Speed	2,760	
Power, kwatts (horsepower)	6.898	(9.25)
Fuel Low Pressure Pump		
Inlet Total Pressure, N/cm^2 (psia)	13.7	(19.9)
Inlet NPSH, N-m/kg (ft)	47.8	(16.0)
Inlet Temperature, °K (°R)	21.3	(38.3)
Flowrate, m^3/s (gpm)	0.03968	(629)
Discharge Pressure, N/cm^2 (psia)	43.4	(63.0)
Head Rise, N-m/kg (ft)	4,262	(1,426)
Speed, rad/s (rpm)	2,556	(24,409)
Efficiency*, %	75	
Specific Speed	2,640	
Power, kwatts (horsepower)	15.7	(21.1)
Main Oxidizer Pump		
Inlet Total Pressure, N/cm^2 (psia)	44.7	(64.9)
Inlet Temperature, °K (°R)	92.3	(166.2)
Flowrate, m^3/s (gpm)	0.01464	(232)
Discharge Pressure, N/cm^2 (psia)	2,829	(4,103)
Head Rise, N-m/kg (ft)	24,728	(8,273)
Speed, rad/s (rpm)	5,823	(55,603)
Efficiency*, %	64.4	
Specific Speed	977	
Power, kwatts (horsepower)	635	(852)
Main Fuel Pump		
Inlet Total Pressure, N/cm^2 (psia)	39.6	(57.4)
Inlet Temperature, °K (°R)	21.6	(38.8)
Flowrate, m^3/s (gpm)	0.03968	(629)
Discharge Pressure, N/cm^2 (psia)	3,103	(4,499)
Head Rise, N-m/kg (ft)	460,979	(154,222)
Speed, rad/s (rpm)	9,747	(93,078)
Efficiency*, %	58.3	
Specific Speed	510	
Power, kwatts (horsepower)	2,187	(2,933)

*Pump efficiencies include effects of recirculated flows (thrust balance systems, bearing cooling, internal leakages, etc.).

Table VII. ASE Operating Characteristics, Rated Thrust (100% Thrust, MR = 6.0) (Continued)

Fuel Turbine		
Inlet Total Pressure, N/cm^2 (psia)	2,272	(3,295)
Inlet Total Temperature, °K (°R)	1,138	(2,049)
Discharge Static Pressure, N/cm^2 (psia)	1,442	(2,092)
Speed, rad/s (rpm)	9,747	(93,078)
Efficiency, %	68.1	
Power, kwatts (horsepower)	2,187	(2,933)
Turbine Flow, kg/s (lb/sec)	3.062	(6.75)
Percent Admission	56	
Pressure Ratio (Total-Static)	1.575	
Oxidizer Turbine		
Inlet Total Pressure, N/cm^2 (psia)	2,260	(3,278)
Inlet Total Temperature, °K (°R)	1,138	(2,049)
Discharge Static Pressure, N/cm^2 (psia)	1,485	(2,154)
Speed, rad/s (rpm)	5,823	(55,603)
Efficiency, %	51.9	
Power, kwatts (horsepower)	658	(882)
Turbine Flow, kg/s (lb/sec)	1.302	(2.87)
Percent Admission	26	
Pressure Ratio (Total-Static)	1.522	
Preburner		
Chamber Pressure, N/cm^2 (psia)	2,295	(3,328)
Fuel Injector ΔP, N/cm^2 (psid)	131.7	(191)
Oxidizer Injector ΔP, N/cm^2 (psid)	170.3	(247)
Fuel Flowrate, kg/s (lb/sec)	2.289	(5.047)
Oxidizer Flowrate, kg/s (lb/sec)	2.077	(4.578)
Chamber Mixture Ratio	0.907	
Combustion Temperature, °K (°R)	1,138	(2,049)
Thrust Chamber		
Chamber Pressure, N/cm^2 (psia)	1,324	(1,920)
Mixture Ratio	6.338	
Hot Gas Injector ΔP, N/cm^2 (psid)	103.4	(150)
Oxidizer Injector ΔP, N/cm^2 (psid)	1,032	(1,497)
Chamber Throat Diameter, cm (in.)	6.53	(2.57)
Nozzle Exit Diameter (ID), cm (in.)	132.6	(52.2)
Nozzle Expansion Ratio (aero)	400	
Nozzle Dump Cooling Flowrate, kg/s (lb/sec)	0.147	(0.323)

Table VII. ASE Operating Characteristics, Rated Thrust (100% Thrust, MR = 6.0) (Concluded)

Coolant Jacket		
Pressure Drop, N/cm^2 (psid)	658	(955)
Temperature Rise, °K (°R)	197.2	(355)
Tank Pressurants		
Oxidizer Flowrate, kg/s (lb/sec)	0.061	(0.134)
Oxidizer Temperature, °K (°R)	235	(423)
Fuel Flowrate, kg/s (lb/sec)	0.015	(0.034)
Fuel Temperature, °K (°R)	266	(478)

Table VIII. ASE Operating Characteristics, Rated Thrust (100% Thrust, MR = 6.5)

Parameter		
Thrust, N (lb)	89,000	(20,000)
Specific Impulse, N-s/kg (sec)	4,581.7	(467.2)
Inlet Fuel Flow, kg/s (lb/sec)	2.605	(5.742)
Inlet Oxidizer Flow, kg/s (lb/sec)	16.889	(37.234)
Total Propellant Flow, kg/s (lb/sec)	19.494	(42.976)
Fuel Tank Pressurization Flow, kg/s (lb/sec)	0.015	(0.034)
Oxidizer Tank Pressurization Flow, kg/s (lb/sec)	0.061	(0.134)
Chamber Pressure N/cm^2 (psia)	1,311	(1,902)
Mixture Ratio, Vehicle	6.485	
Oxidizer Low Pressure Pump		
Inlet Total Pressure, N/cm^2 (psia)	13.2	(19.1)
Inlet NPSH, N-m/kg (ft)	5.98	(2.0)
Inlet Temperature, °K (°R)	92.2	(166.0)
Flowrate, m^3/s (gpm)	0.01495	(237)
Discharge Pressure, N/cm^2 (psia)	44.1	(64.0)
Head Rise, N-m/kg (ft)	275	(92)
Speed, rad/s (rpm)	593	(5,663)
Efficiency*, %	75	
Specific Speed	2,942	
Power, kwatts (horsepower)	6.19	(8.3)

*Pump efficiencies include effects of recirculated flows (thrust balance systems, bearing cooling, internal leakages, etc.)

Table VIII. ASE Operating Characteristics, Rated Thrust (100% Thrust, MR = 6.5) (Continued)

Fuel Low Pressure Pump		
Inlet Total Pressure, N/cm^2 (psia)	13.7	(19.9)
Inlet NPSH, N-m/kg (ft)	44.8	(15.0)
Inlet Temperature, °K (°R)	21.3	(38.3)
Flowrate, m^3/s (gpm)	0.03741	(593)
Discharge Pressure, N/cm^2 (psia)	41.1	(59.6)
Head Rise, N-m/kg (ft)	3,931	(1,315)
Speed, rad/s (rpm)	2,444	(23,338)
Efficiency*, %	74.9	
Specific Speed	2,604	
Power, kwatts (horsepower)	13.6	(18.3)
Main Oxidizer Pump		
Inlet Total Pressure, N/cm^2 (psia)	40.3	(58.4)
Inlet Temperature, °K (°R)	92.3	(166.2)
Flowrate, m^3/s (gpm)	0.01495	(237)
Discharge Pressure, N/cm^2 (psia)	2,515	(3,648)
Head Rise, N-m/kg (ft)	21,981	(7,354)
Speed, rad/s (rpm)	5,567	(53,164)
Efficiency*, %	64.3	
Specific Speed	1,031	
Power, kwatts (horsepower)	577	(774)
Main Fuel Pump		
Inlet Total Pressure, N/cm^2	37.6	(54.6)
Inlet Temperature, °K (°R)	21.6	(38.8)
Flowrate, m^3/s (gpm)	0.03735	(592)
Discharge Pressure, N/cm^2 (psia)	3,044	(4,415)
Head Rise, N-m/kg (ft)	452,290	(151,315)
Speed, rad/s (rpm)	9,572	(91,405)
Efficiency*, %	58.1	
Specific Speed	493	
Power, kwatts (horsepower)	2,025	(2,715)
Fuel Turbine		
Inlet Total Pressure, N/cm^2 (psia)	2,195	(3,183)
Inlet Total Temperature, °K (°R)	1,181	(2,125)
Discharge Static Pressure, N/cm^2 (psia)	1,422	(2,063)
Speed, rad/s (rpm)	9,572	(91,405)
Efficiency, %	67.9	
Power, kwatts (horsepower)	2,025	(2,715)
Turbine Flow, kg/s (lb/sec)	2.908	(6.410)
Percent Admission	56	
Pressure Ratio (Total-Static)	1.543	

Table VIII. ASE Operating Characteristics, Rated Thrust (100% Thrust, MR = 6.5) (Concluded)

Oxidizer Turbine		
Inlet Total Pressure, N/cm^2 (psia)	2,184	(3,167)
Inlet Total Temperature, °K (°R)	1,181	(2,125)
Discharge Static Pressure, N/cm^2 (psia)	1,465	(2,124)
Speed, rad/s (rpm)	5,567	(53,164)
Efficiency, %	51	
Power, kwatts (horsepower)	597	(801)
Turbine Flow, kg/s (lb/sec)	1.236	(2.725)
Percent Admission	26	
Pressure Ratio (Total-Static)	1.491	
Preburner		
Chamber Pressure, N/cm^2(psia)	2,217	(3,215)
Fuel Injector ΔP, N/cm^2 (psid)	123	(179)
Oxidizer Injector ΔP, N/cm^2 (psid)	159	(230)
Fuel Flowrate, kg/s (lb/sec)	2.137	(4.712)
Oxidizer Flowrate, kg/s (lb/sec)	2.006	(4.423)
Chamber Mixture Ratio	0.939	
Combustion Temperature, °K (°R)	1,181	(2,125)
Thrust Chamber		
Chamber Pressure, N/cm^2 (psia)	1,311	(1,902)
Mixture Ratio	6.884	
Hot Gas Injector ΔP, N/cm^2 (psid)	96.5	(140)
Oxidizer Injector ΔP, N/cm^2 (psid)	1,091	(1,583)
Chamber Throat Diameter, cm (in.)	6.53	(2.57)
Nozzle Exit Diameter (ID), cm (in.)	132.6	(52.2)
Nozzle Expansion Ratio (Aero)	400	
Nozzle Dump Cooling Flowrate, kg/s (lb/sec)	0.145	(0.319)
Coolant Jacket		
Pressure Drop, N/cm^2 (psid)	614	(891)
Temperature Rise, °K (°R)	212	(381)
Tank Pressurants		
Oxidizer Flowrate, kg/s (lb/sec)	0.061	(0.134)
Oxidizer Temperature, °K (°R)	234	(422)
Fuel Flowrate, kg/s (lb/sec)	0.015	(0.034)
Fuel Temperature, °K (°R)	278	(501)

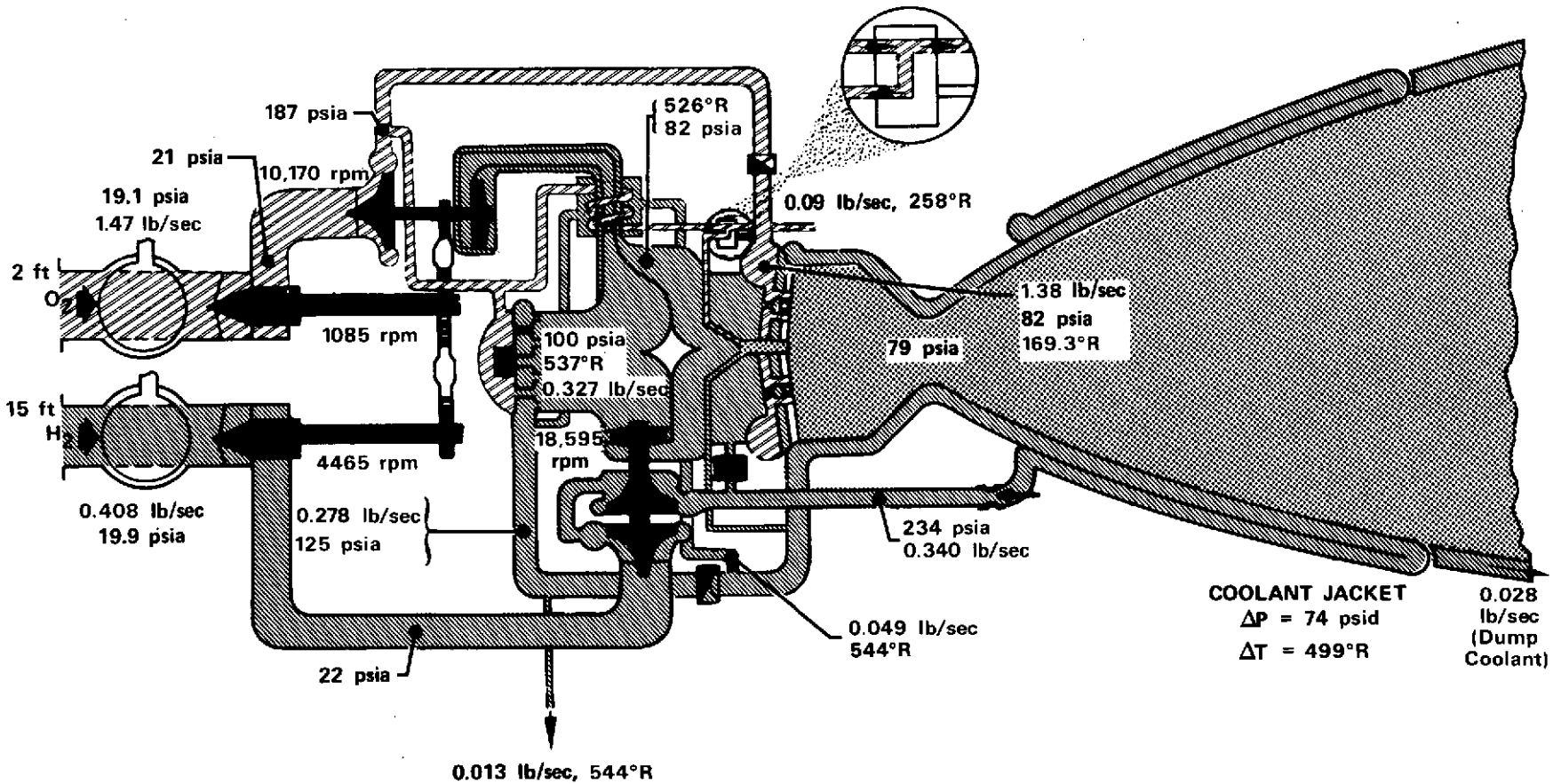

Figure 23. Pumped Idle Cycle Balance Flow Schematic, Thrust = 800 lb, Mixture Ratio = 3.5:1 (Cycle No. 106)

FD 66669D

Table IX. ASE Operating Characteristics, Pumped Idle (4% Thrust, MR = 3.5)

Parameter		
Thrust, N (lb)	3,559	(800)
Specific Impulse, N-s/kg (sec)	4,413.0	(450)
Inlet Fuel Flow, kg/s (lb/sec)	0.185	(0.408)
Inlet Oxidizer Flow, kg/s (lb/sec)	0.668	(1.473)
Total Propellant Flow, kg/s (lb/sec)	0.853	(1.881)
Fuel Tank Pressurization Flow, kg/s (lb/sec)	0.006	(0.013)
Oxidizer Tank Pressurization Flow, kg/s (lb/sec)	0.041	(0.090)
Chamber Pressure, N/cm^2 (psia)	54.5	(79.1)
Mixture Ratio, Vehicle	3.612	
Oxidizer Low Pressure Pump		
Inlet Total Pressure, N/cm^2 (psia)	13.2	(19.1)
Inlet NPSH, N-m/kg (ft)	5.98	(2.0)
Inlet Temperature, °K (°R)	92.2	(166.0)
Flowrate, m^3/s (gpm)	0.00059	(9.4)
Discharge Pressure, N/cm^2 (psia)	14.8	(21.4)
Head Rise, N-m/kg (ft)	14.9	(5)
Speed, rad/s (rpm)	113	(1,083)
Efficiency*, %	32.4	
Specific Speed	1,039	
Power, kwatts (horsepower)	0.03	(0.04)
Fuel Low Pressure Pump		
Inlet Total Pressure, N/cm^2 (psia)	13.7	(19.9)
Inlet NPSH, N-m/kg (ft)	44.8	(15.0)
Inlet Temperature, °K (°R)	21.3	(38.3)
Flowrate, m^3/s (gpm)	0.00266	(42.1)
Discharge Pressure, N/cm^2 (psia)	15.0	(21.8)
Head Rise, N-m/kg (ft)	182	(61)
Speed, rad/s (rpm)	468	(4,465)
Efficiency*, %	47.1	
Specific Speed	1,328	
Power, kwatts (horsepower)	0.075	(0.10)
Main Oxidizer Pump		
Inlet Total Pressure, N/cm^2 (psia)	14.8	(21.4)
Inlet Temperature, °K (°R)	92.2	(166.0)
Flowrate, m^3/s (gpm)	0.00059	(9.4)
Discharge Pressure, N/cm^2 (psia)	128.9	(187)
Head Rise, N-m/kg (ft)	1,019	(341)
Speed, rad/s (rpm)	1,065	(10,172)
Efficiency*, %	27.5	
Specific Speed	393	
Power, kwatts (horsepower)	2.46	(3.3)

Table IX. ASE Operating Characteristics, Pumped Idle (4% Thrust, MR = 3.5) (Continued)

Main Fuel Pump		
Inlet Total Pressure, N/cm^2 (psia)	14.6	(21.7)
Inlet Temperature, °K (°R)	21.3	(38.3)
Flowrate, m^3/s (gpm)	0.00266	(42.1)
Discharge Pressure, N/cm^2 (psia)	161	(234)
Head Rise, N-m/kg (ft)	21,426	(7,168)
Speed, rad/s (rpm)	1947	(18,595)
Efficiency*, %	40.0	
Specific Speed	262	
Power, kwatts (horsepower)	9.92	(13.3)
Fuel Turbine		
Inlet Total Pressure, N/cm^2 (psia)	68.5	(99.4)
Inlet Total Temperature, °K (°R)	298.3	(537)
Discharge Static Pressure, N/cm^2 (psia)	56.8	(82.4)
Speed, rad/s (rpm)	1947	(18,595)
Efficiency, %	41.7	
Power, kwatts (horsepower)	9.92	(13.3)
Turbine Flow, kg/s (lb/sec)	0.104	(0.23)
Percent Admission	56	
Pressure Ratio (Total-Static)	1.206	
Oxidizer Turbine		
Inlet Total Pressure, N/cm^2 (psia)	68.2	(98.9)
Inlet Total Temperature, °K (°R)	298	(537)
Discharge Static Pressure, N/cm^2 (psia)	58.5	(84.8)
Speed, rad/s (rpm)	1,065	(10,172)
Efficiency, %	31.0	
Power, kwatts (horsepower)	2.54	(3.4)
Turbine Flow, kg/s (lb/sec)	0.044	(0.098)
Percent Admission	26	
Pressure Ratio (Total-Static)	1.166	
Preburner		
Chamber Pressure, N/cm^2 (psia)	68.9	(100)
Fuel Injector ΔP, N/cm^2 (psid)	17.4	(25.3)
Oxidizer Injector ΔP, N/cm^2 (psid)	NA	
Fuel Flowrate, kg/s (lb/sec)	0.148	(0.327)
Oxidizer Flowrate, kg/s (lb/sec)	0.0	
Chamber Mixture Ratio	NA	
Temperature, °K (°R)	298.3	(537)

*Pump efficiencies include effects of recirculated flows (thrust balance systems, bearing cooling, internal leakages, etc.).

Table IX. ASE Operating Characteristics, Pumped Idle (4% Thrust, MR = 3.5) (Concluded)

Thrust Chamber		
Chamber Pressure, N/cm^2 (psia)	54.5	(79.1)
Mixture Ratio	3.766	
Hot Gas Injector ΔP, N/cm^2 (psid)	1.675	(2.43)
Oxidizer Injector ΔP, N/cm^2 (psia)	1.958	(2.84)
Chamber Throat Diameter, cm (in.)	6.53	(2.57)
Nozzle Exit Diameter (ID), cm (in.)	132.6	(52.2)
Nozzle Expansion Ratio (Aero)	400	
Nozzle Dump Cooling Flowrate, kg/s (lb/sec)	0.0125	(0.0275)
Coolant Jacket		
Pressure Drop, N/cm^2 (psid)	51.7	(75)
Temperature Rise, °K (°R)	277	(499)
Tank Pressurants		
Oxidizer Flowrate, kg/s (lb/sec)	0.041	(0.090)
Oxidizer Temperature, °K (°R)	143	(258)
Fuel Flowrate, kg/s (lb/sec)	0.006	(0.013)
Fuel Temperature, °K (°R)	302	(544)

The preburner temperature of 1140°K (2050°R) at 100% thrust and MR = 6.0 is the maximum allowable to assure that the 10 hr, 1% creep life requirements is satisfied at the severest operating point (maximum temperature) for the fuel turbine, which occurs at rated thrust, MR = 6.5. Because the oxidizer turbine is slightly smaller than the fuel turbine and operates at substantially lower speeds for the same temperatures, the oxidizer turbine blade stresses are lower and it has more temperature margin at all engine operating points.

Parasitic flows represent engine propellant flows that contribute to increased cycle power requirements, reduce power availability and/or reduce performance. Propellant flow that bypasses the turbine(s) results in an energy loss. Overboard propellant flow can be a cycle power loss or a performance loss, depending upon its source and usage. Tank pressurant flows increase pump power requirements but are not chargeable to the engine as a performance (specific impulse) loss since the propellants are returned to the vehicle tanks. High performance turbopumps and the staged combustion cycle, which uses a high energy release combustor to provide hot gases for the pump-driven turbine(s), require various cooling flows. The mainstream engine propellant flows are the sources of these cooling flows. While nozzle dump cooling flow for the ASE degrades slightly engine performance it does not, per se, reduce cycle power since the coolant source is the gearbox, which is supplied with other hydrogen parasitic flows.

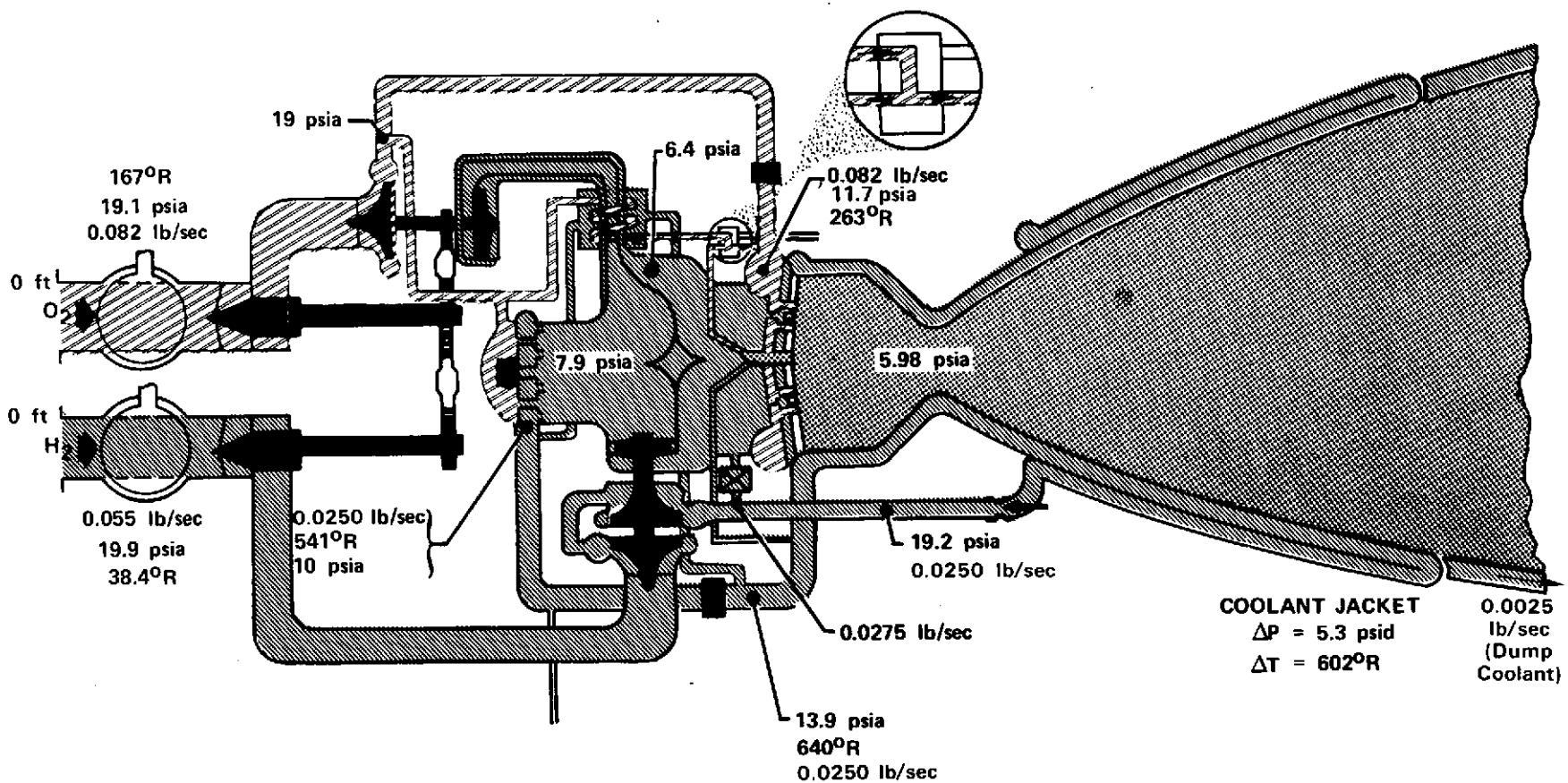

Figure 24. Tank Head Idle Cycle Balance Flow Schematic, Thrust = 55 lb, Mixture Ratio = 1.5:1 (Saturated Liquid Propellants at Pump Inlets) (Cycle No. 106)

FD 66669F

In the ASE, fuel-side parasitic losses result from the need to provide cooling flow for the turbopump bearings, turbine disks and housings, main chamber igniter, and the main case as well as tank pressurant flow, etc. The hydrogen parasitic flows that bypass the preburner and/or turbines are equivalent to approximately 17% of the engine inlet fuel flow. The sources and flow paths for fuel parasitics are shown in figure 25 for the maximum turbopump speed condition (100% thrust, MR = 5.5). Parasitic flows are taken into account in the ASE cycle analyses, and to minimize cycle power effects, therefore, the parasitic flows are routed so as to satisfy more than one requirement wherever possible.

On the oxidizer side, parasitics consist of tank pressurant flow and oxidizer pump front bearing cooling flow, which is provided by the recirculation of flow from the pump discharge to the pump inlet. These parasitics result only in increased turbine (or cycle) power requirements.

The dump coolant flowrate in figure 25 is shown to be 0.139 kg/s (0.306 lb/sec), which is the minimum flowrate required to adequately cool the lightweight nozzle extension at the full thrust, MR = 5.5 operating point. At higher mixture ratios at full thrust, a greater nozzle coolant flowrate is required. However, to provide adequate nozzle cooling over the entire mixture ratio range without the need for a coolant flow control valve, it is necessary to slightly overcool the nozzle at MR = 5.5 by approximately 10% as indicated in the engine operating characteristics tables and in the cycle balance sheets of Appendix A.

Initial cycle balances for the selected 89-kN (20,000-lb) thrust engine configuration were generated using information from the earlier P&WA Orbit-to-Orbit Engine Design Study conducted under Contract F04611-71-C-0039 for the USAF/RPL. Parametric heat transfer characteristics from the OOS study, were used to establish the thrust chamber coolant pressure loss and temperature rise. Initial high pressure turbopump speeds were also obtained from the OOS parametric study results. Engine propellant flowrates were estimated from I_{vac} obtained from the OOS parametric performance data. Component performance levels, adjusted for ASE design and operating point differences (pump specific speed, turbine velocity ratio, etc.), were also obtained from the OOS study to be used as a starting point for the initial ASE cycle work.

The initial ASE preliminary design concept included a two-stage main oxidizer pump, a low pressure loss main oxidizer injector, a hot gas (preburner combustion products) O_2 heat exchanger for oxidizer tank pressurization at rated thrust, and a GH_2/O_2 heat exchanger system to provide gaseous oxidizer to the main chamber for pumped idle (expander mode) and tank head idle operation.

However, when operating in the expander cycle mode, the oxidizer tank pressurization capability of the hot gas oxidizer heat exchanger was very limited, 0.0091 kg/s (0.020 lb/sec), with a delivered GO_2 temperature of 111.7°K (201°R). In addition, a GH_2/O_2 heat exchanger of sufficient capacity to supply superheated O_2 to the main oxidizer injector proved to be impractical. The problem could have been resolved by operating with the preburner lit (staged combustion) in the pumped idle mode, but the advantages of being able to start and operate in the expander mode at low thrust would have been lost. The engine system was therefore reconfigured to that shown schematically in figure 21, cycle No. 104.

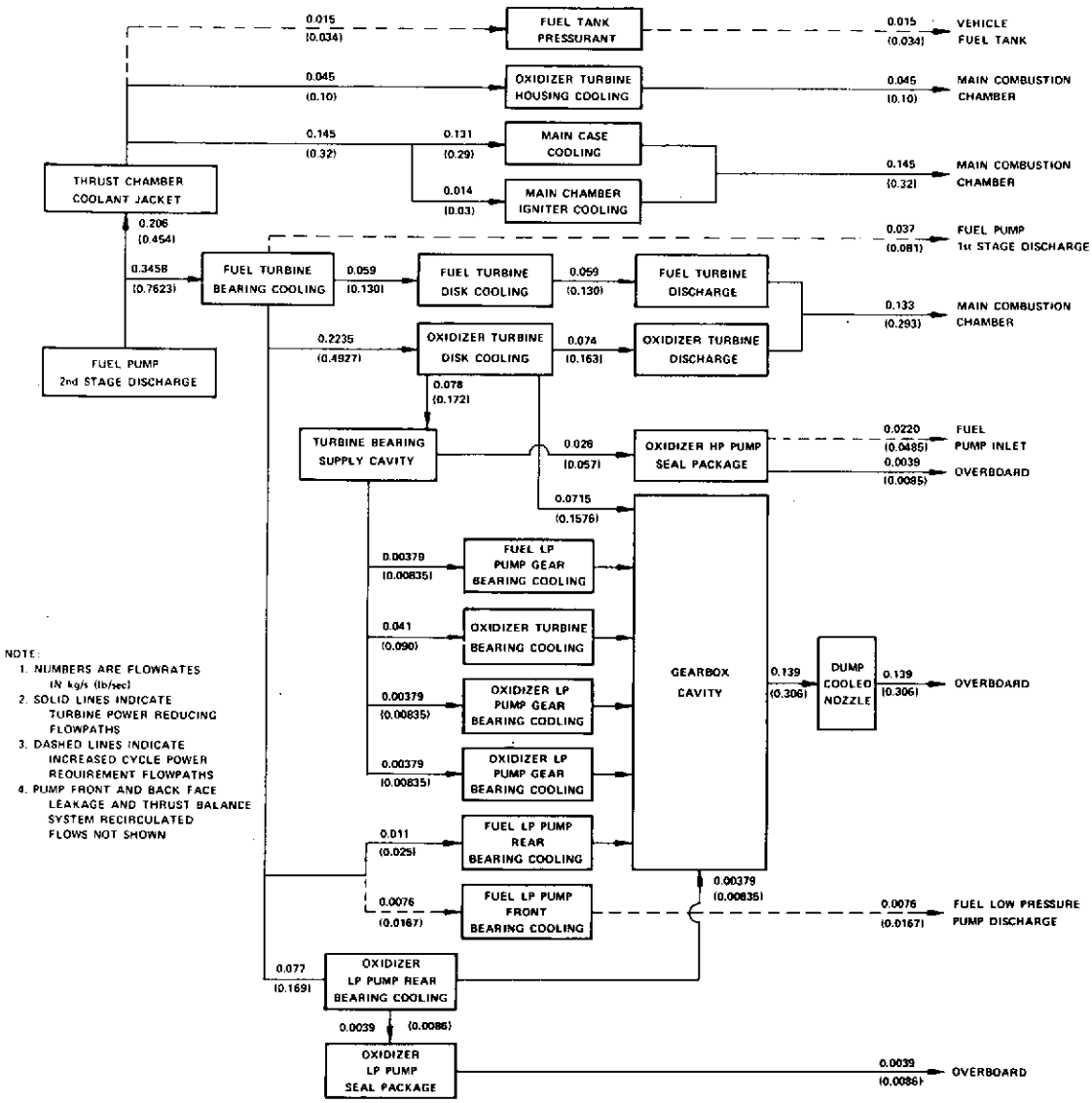

Figure 25. ASE Fuel Parasitic Flowpath Schematic; 100% Thrust, MR = 5.5

FD 75487

The engine system was modified by (1) replacing the single hot gas GO_2 heat exchanger for oxidizer tank pressurization with a dual GH_2/GO_2 and hot gas/GO_2 heat exchanger system, (2) replacing the low pressure loss main oxidizer injector with a high pressure loss injector, and (3) using a single-stage high pressure oxidizer pump instead of the two-stage (or 1 1/2 stage) pump.

To obtain adequate oxidizer tank pressurant when in the pumped idle mode, the GH_2/O_2 and hot gas/O_2 heat exchangers were combined, with all the GO_2 flow supplied to the vehicle oxidizer tank. LO_2 was supplied to the main chamber. A fuel bypass around the GH_2/O_2 heat exchanger provided adequate fuel side pressure drop during low fuel flowrate operation without incurring excessive pressure loss during full thrust operation. With liquid O_2 supplied to the main injector in the pumped idle mode, the oxidizer injection pressure drop was increased to minimize the possibility of combustion instability. The resultant increased oxidizer pressure loss at full thrust operation required the oxidizer to be supplied to the thrust chamber injector at a pressure approaching that of the preburner oxidizer injector supply pressure. The second stage of the oxidizer pump was therefore eliminated, which simplified the high pressure oxidizer turbopump design, but reduced thrust chamber pressure by some 21 N/cm^2 (30 psi) to 1324 N/cm^2 (1920 psia) because of the increased cycle power requirements resulting from higher system pressures.

Operation in pumped idle was not fully optimized to result in maximum attainable idle thrust. The cycle work was concerned primarily in establishing the feasibility of pumped idle mode operation and in determining the engine's fuel and oxidizer tank pressurization flowrate capabilities. Operating as an expander engine in pumped idle, the engine is power-limited. A pumped idle mixture ratio of 3.5 was selected as the best compromise to provide reasonable thrust and oxidizer tank pressurant flow while maintaining acceptable fuel valve (cavitating venturi) and main oxidizer injector pressure losses. An increase in mixture ratio decreases thrust capability while decreasing mixture ratio reduces the main oxidizer injector pressure loss, which tends to induce combustion instability. Preliminary optimization work indicates the nominal thrust for pumped idle operation could be increased to 5% of rated thrust.

In generating the final ASE cycles, it was determined that the fuel and oxidizer boost pump required NPSP's equaled or slightly exceeded the available NPSP's during off-design operation. The operating speeds of the boost pumps were reduced to produce sufficient NPSH margin. The small boost pump speed changes that were made in the cycle result in only minor changes to the gear ratios for the drive system. The boost pump speed changes are incorporated in cycle No. 106. Cycle balance print-outs for the baseline and final cycles are presented in Appendix A.

4. Engine Performance

Engine performance at rated thrust conditions was evaluated using JANNAF Methodology. The methodology used in the ASE study was essentially as specified in Addendum No. 1 to CPIA Publication No. 178 and Amendment No. 1. The JANNAF Methodology and evaluation procedure used in the study are described in detail in Appendix B. A summary of JANNAF performance, at rated thrust is presented in table X.

Table X. JANNAF Performance at 100% Thrust

Mixture Ratio	I_{vac}, N-s/kg (sec)
5.5	4686.6 (477.9)
6.0	4663.1 (475.5)
6.5	4620.9 (471.2)

Note: For pure propellants

The engine seal overboard leakages were considered to have a negligible effect on engine performance. The JANNAF procedure and computer programs used for evaluating performance at full thrust were also used to determine delivered vacuum specific impulse at the tank head and pumped idle operating points. Estimates of energy release for tank head and pumped idle were obtained using a P&WA correlation parameter determined from test results, which takes into account injector and chamber geometry and propellant injection conditions. Idle mode performance is shown in table XI.

Table XI. Idle Mode Performance

Operating Point	Mixture Ratio	I_{vac}, N-s/kg (sec)
Tank Head Idle (0.3% Thrust)	1.5:1	3939.3 (401.7)
Pumped Idle (4% Thrust)	3.5:1	4415.0 (450.2)

The significantly reduced delivered vacuum specific impulses for idle mode operation, particularly for tank head idle, are primarily the result of lower I_{vac} values caused by the low mixture ratio and chamber pressure. For a detailed breakdown of JANNAF performance, see Appendix B.

Experience has indicated that JANNAF-predicted performance levels have been 29.4 to 39.2 N-s/kg (3 to 4 sec) higher than the specific impulses obtained from hardware testing. Therefore, the P&WA best estimate of the ASE performance at rated thrust is the JANNAF-predicted value reduced by 39.2 N-s/kg (4 sec). There is presently no JANNAF procedure available for determining energy release when propellants are at subcritical pressures. Therefore, the idle mode performance presented in table XI obtained using JANNAF computer programs to determine kinetics, divergence and boundary layer losses, and P&WA estimates for energy release represent best-estimate values. A summary of best-estimate performance is presented in table XII.

Figure 26 shows best estimate vacuum specific impulse characteristics for the various ASE operating points.

Table XII. ASE Best-Estimate Performance

Operating Point	Mixture Ratio	Delivered I_{vac}, N-s/kg (sec)
Rated	5.5:1	4647.4 (473.9)
	6.0:1	4623.8 (471.5)
	6.5:1	4581.7 (467.2)
Pumped Idle (4% of Rated Thrust)	3.5:1	4415.0 (450.2)
Tank Head Idle (0.3% of Rated Thrust)	1.5:1	3939.3 (401.7)

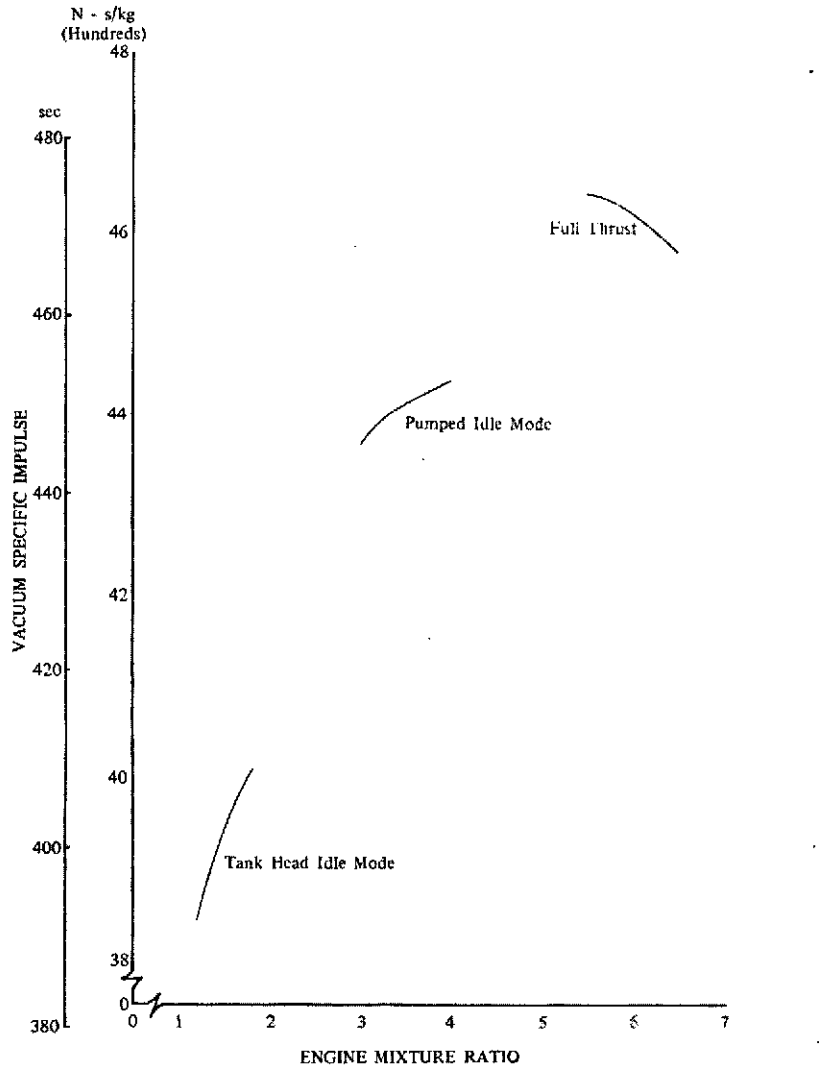

Figure 26. Advanced Space Engine "Best Estimate" Vacuum Specific Impulse DF 96273

C. ENGINE OPERATION

1. General

The following paragraphs describe how the Advanced Space Engine is controlled during the various operating modes (idle and rated thrust). Valve locations and their functions are also described.

A transient computer deck was developed to predict the engine operation of the ASE. The simulation models the components of cycle No. 104. The deck was programed with the capability to predict turbopump cooldown, tank head idle, pumped idle, full thrust, and transients between the operating modes. Full details of the simulation are described in the User's Manual for Customer Computer Deck CCD 1066.0.0, FR-5657. This dynamic simulation was used to predict the operating characteristics of the ASE and to establish control requirements.

2. Control Functions

Control of the P&WA ASE is accomplished with eight valves. Locations of the valves used on the engine are shown schematically in figure 27. Shutoff of engine propellants is accomplished by fuel and oxidizer suction (inlet) valves. A fuel (cavitating venturi) valve, a main oxidizer valve, and a preburner oxidizer valve provide propellant control during full thrust operation. A GO_2 control valve, a fuel bypass valve, and a fuel shunt valve complete the control system necessary for idle mode operation and tank pressurization requirements.

The function of the suction valves, which are located at the inlets to the low pressure pumps, is to provide positive shutoff of the propellants when the engine is not operating.

The fuel valve is located downstream of the second stage of the high pressure fuel pump and controls the hydrogen flow into the thrust chamber cooling jacket. Selection of a cavitating venturi as the valve type is based upon pumped idle mode requirements. During pumped idle operation, the venturi throat area is set to cavitate to provide hydraulic isolation of the fuel pump from boiling instability, which occurs in the thrust chamber cooling jacket when the hydrogen coolant pressure is subcritical. At full thrust the valve is scheduled to control fuel flow to the engine and, with other valves, provides the desired mixture ratio.

The main oxidizer valve is located in the line to the main oxidizer injector downstream of the high pressure oxidizer pump. The preburner oxidizer control valve is located on the preburner at the end of the line to the preburner oxidizer injector to minimize the volume between the valve and injector. The main oxidizer valve and preburner oxidizer valves control the oxidizer flowrates to the main chamber and preburner, respectively.

The fuel bypass valve is located downstream of the high pressure fuel pump and allows fuel to bypass thrust chamber coolant jacket, preburner, and turbines during tank head idle. This valve is opened at tank head idle to schedule more fuel flow through the turbopumps for cooldown. In the tank head idle mode, the fuel bypass valve also helps prevent turbopump rotation by bypassing fuel around the turbines. The transition to pumped idle is accomplished by closing the fuel bypass valve thereby increasing the fuel flow to the turbines, which initiates turbopump rotation.

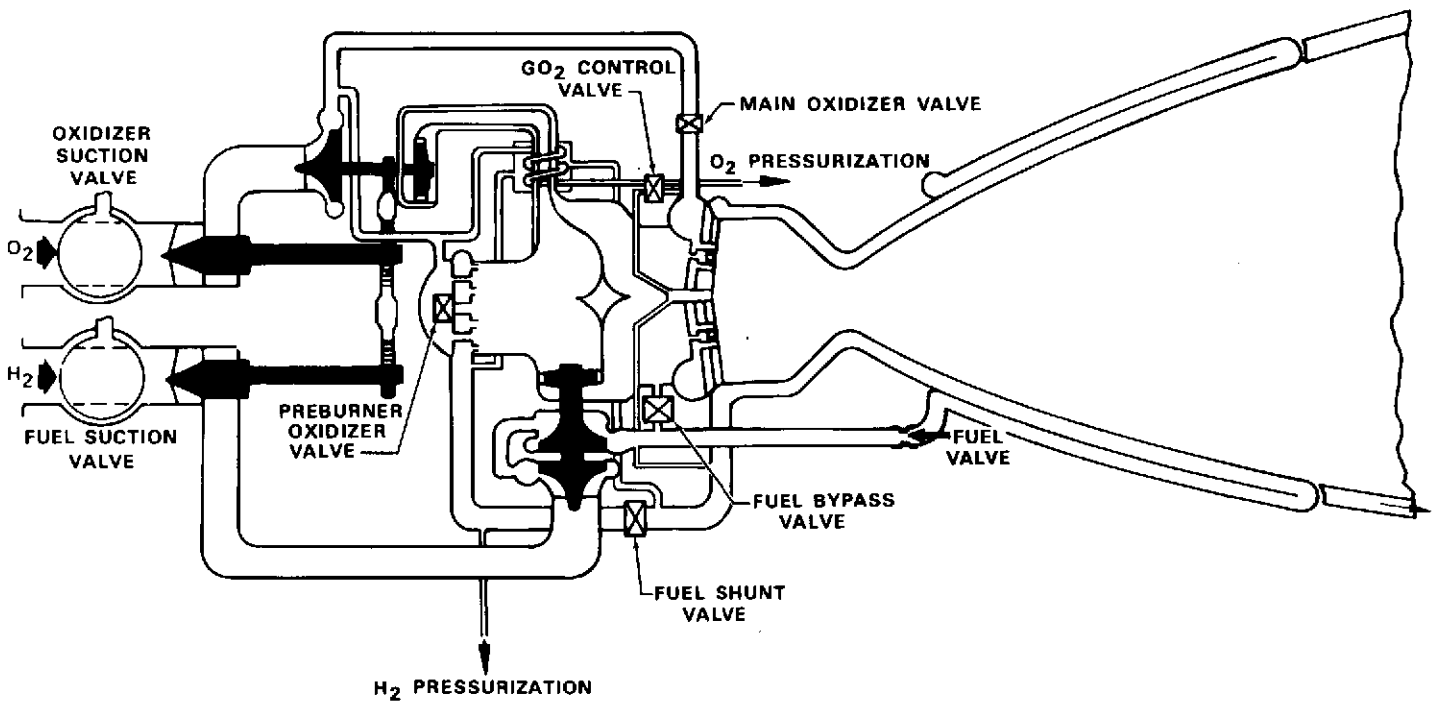

Figure 27. Advanced Space Engine Control Locations

FD 71369

The GO_2 control valve is located downstream of the GO_2 heat exchanger and supplies GO_2 to the main injector during tank head idle mode while cutting off flow to the vehicle oxidizer tank pressurization system. For pumped idle operation, the GO_2 valve is positioned to shut off the GO_2 supply to the main injector and to supply instead GO_2 to the vehicle tank pressurization system.

The fuel shunt valve is located in the fuel line at the discharge of the chamber cooling jacket and upstream of the preburner fuel injector. The shunt valve diverts fuel to the GO_2 heat exchanger. The bypass allows adequate fuel-side pressure drop to be maintained with low fuel flow at tank head idle without incurring excessive pressure loss during full thrust operation.

The ASE is controlled by three commands from the vehicle - start/stop, propellant utilization, and mode selection (tank head idle, pumped idle, and mainstage). The ASE control system provides precise mainstage thrust control over the specified range of mixture ratio. The control can compensate for expected engine component variability and also includes protective overrides to provide additional engine life margin.

Thrust at mainstage is set by using two levels of control (figure 28). The first level, which also sets mixture ratio, consists of basic schedules that set predetermined valve positions in accordance with nominal schedules of valve areas. These basic valve schedules set thrust and mixture ratio without dependence upon engine sensors. The second level is a supervisory trim of valve areas to more precisely obtain thrust based on sensed chamber pressure. Mixture ratio trim is obtained by adjustment of the mixture ratio input by the vehicle propellant utilization (PU) signal. In addition, there is a protective trim of valve areas to prevent engine operation from exceeding component physical limits. The protective trim provides additional engine safety by limiting maximum valve areas when unexpected component deterioration results in operation near design limits. Whenever a design limit is approached, protective trim reduces or limits supervisory trim as required to preclude exceeding engine limits. Six engine parameters have been identified to provide protection for the engine - vibration sensors for each of the four pumps to detect turbopump damage, turbine inlet temperature and chamber pressure.

Recovery of the vehicle (stage) from a synchronous orbit is not considered practical, while recovery from a wide range of elliptical orbits appears to be feasible. It is thus desirable to operate the engine in a degraded mode, even tank head idle, until the propellants have been exhausted to place the stage in an elliptical orbit. While the mission may be lost, and even if the engine is damaged, the stage may still be recoverable thereby representing a small cost savings. The threshold levels of these malfunction detection parameters are therefore set high to protect against a complete vehicle/engine failure only.

During start and shutdown transients the control's basic schedules are time-based and the schedules are extended to cover the envelope of transient operation. Before the engine can be started the control must be in a ready condition. This ready condition is given after the control self check has been completed. The engine can then be started by the issuance of the three vehicle commands - mode selection, propellant utilization, and start signal. Figure 29 shows the engine start sequencing of valves.

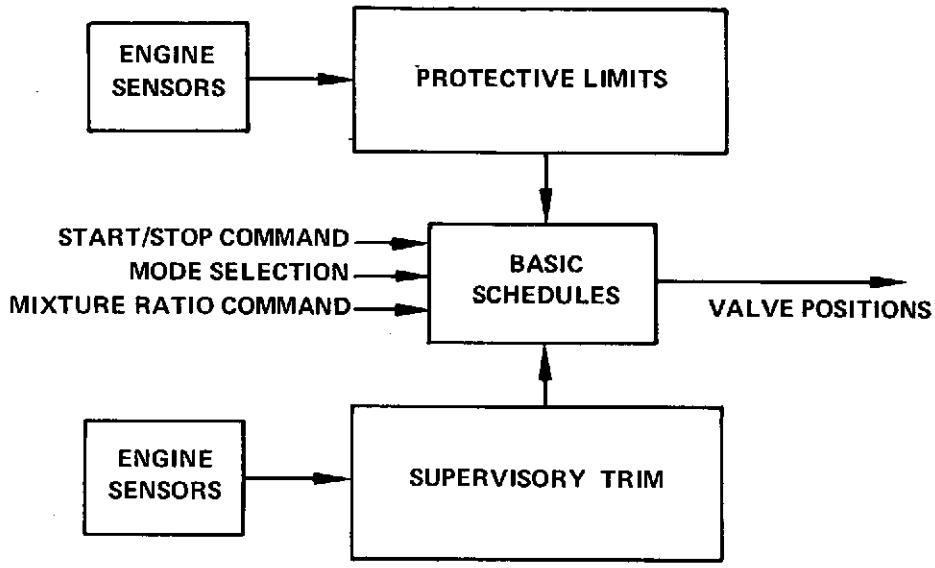

Figure 28. Advanced Space Engine Control Block Diagram FD 72145

3. Tank Head Idle - Thermal Conditioning

Prior to engine start the ASE will be in a zero-gravity environment and will be subjected to a thermal environment ranging from 111°K to 311°K (200°R to 560°R). The propellants in the tanks will be saturated and unsettled and the engine will be hot, depending upon the environmental conditions. Before the pumps can operate properly, they must be sufficiently prechilled and the propellants must be settled. This conditioning is accomplished during tank head idle operation.

Tank head idle is a pressure fed mode of operation with the preburner unlit and the fuel bypass valve open to prevent turbopump rotation and to increase the fuel pump flow, thereby decreasing cooldown time. The main chamber is lit and, with saturated liquid propellants at the engine inlets, operates at a pressure of approximately 4.1 N/cm^2 (6.0 psia) and a mixture ratio of 1.5, thus producing about 245 N (55 lb) of thrust (figure 24).

The ASE dynamic deck was used to study the transient characteristics of tank head idle and cooldown. The inputs were an engine temperature of 222°K (400°R) and saturated liquid propellants at the engine inlets.

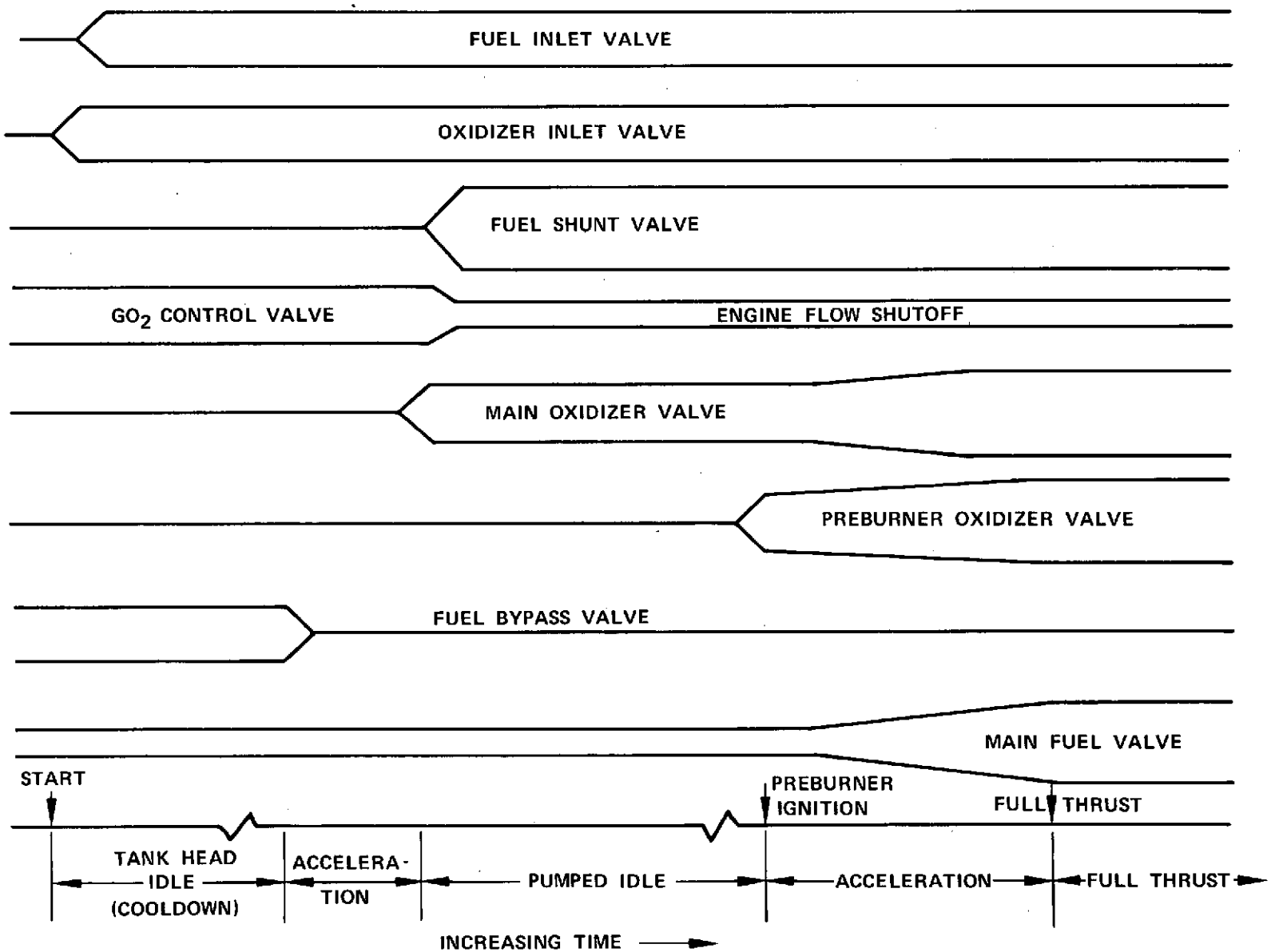

Figure 29. Advanced Space Engine Start Sequence

FD 71619

The engine start sequence is shown in figure 29. Prior to start, the igniter, the fuel venturi and the fuel bypass valves are open, and the GO_2 control valve is positioned to provide gaseous oxidizer to the main chamber. The main oxidizer, the fuel shunt, and preburner oxidizer valves are closed. At start signal, the main burner torch igniter is energized, the oxidizer suction valve opens, and oxidizer flows to the engine. After a short oxidizer lead, the fuel suction valve opens. Main chamber ignition occurs and the engine operates in tank head idle (nonrotating) while the pumps are being thermally conditioned. During tank head idle, part of the hydrogen discharging from the high pressure fuel pump bypasses the thrust chamber cooling jacket to increase the pump thermal conditioning flowrate. All of the fuel discharging from the chamber cooling jacket is directed first through the GO_2 heat exchanger system by the closed fuel shunt valve, and then into the preburner. The preburner oxidizer valve remains closed to keep oxidizer out of the preburner. The main oxidizer valve remains closed and the oxidizer pumps are cooled by the flow that passes to the GO_2 heat exchanger system. The gaseous oxygen generated is injected into the main chamber and burned with the hydrogen-side cooldown flow. With gas/gas injection, stable and controllable main chamber operation in the tank head idle mode is assured.

Figures 30 through 33 present the transient characteristics through 175 sec of tank head idle operation with fixed control valve areas. As the fuel and oxidizer pumps cool down, the densities of the propellants increase thereby increasing flowrates. The GO_2 heat exchanger minimizes oxidizer flow change while fuel flowrate through the fuel bypass valve increases slowly as the fuel density increases. As a result, the mixture ratio changes from 9.0 eventually to 2.0 during the transient. When saturated vapor conditions exist at the hydrogen inlet, the mixture ratio change is larger. The high chamber temperature associated with the high mixture ratio is detrimental to thrust chamber integrity when the engine is operated under these conditions for a prolonged time period, therefore some type of closed loop control is required. The RL10 was run successfully in the tank head idle mode by measuring the fuel temperature at the discharge of the thrust chamber cooling jacket, and then reducing oxidizer flowrate if excessive temperature was indicated. A similar control logic is used on the ASE, the GO_2 control valve position being determined by the fuel coolant jacket discharge temperature.

Chamber pressure will increase as the engine continues to cool and mixture ratio will decrease until the engine approaches the tank head idle cycle point as defined by cycle No. 104 (figure 24).

4. Pumped Idle - Propellant Tank Prepressurization

After propellant settling and thermal conditioning of the engine fuel and oxidizer systems have been completed, the engine operation can be changed to the pumped idle mode on command. This is accomplished by closing the fuel bypass valve, which initiates turbopump rotation. The main oxidizer valve is opened partially to its first step position, allowing liquid oxygen to be supplied to the thrust chamber injector. The GO_2 control valve is repositioned to shut off GO_2 flow to the main injector and to supply GO_2 for oxidizer tank pressurization from the hot gas duct heat exchanger. The fuel shunt valve will be partially opened and the cavitating venturi set to its pumped idle mode position. The engine operates in pumped idle in the expander mode (unlit preburner) while GH_2 and GO_2 are tapped from the cycle to prepressurize the vehicle tanks.

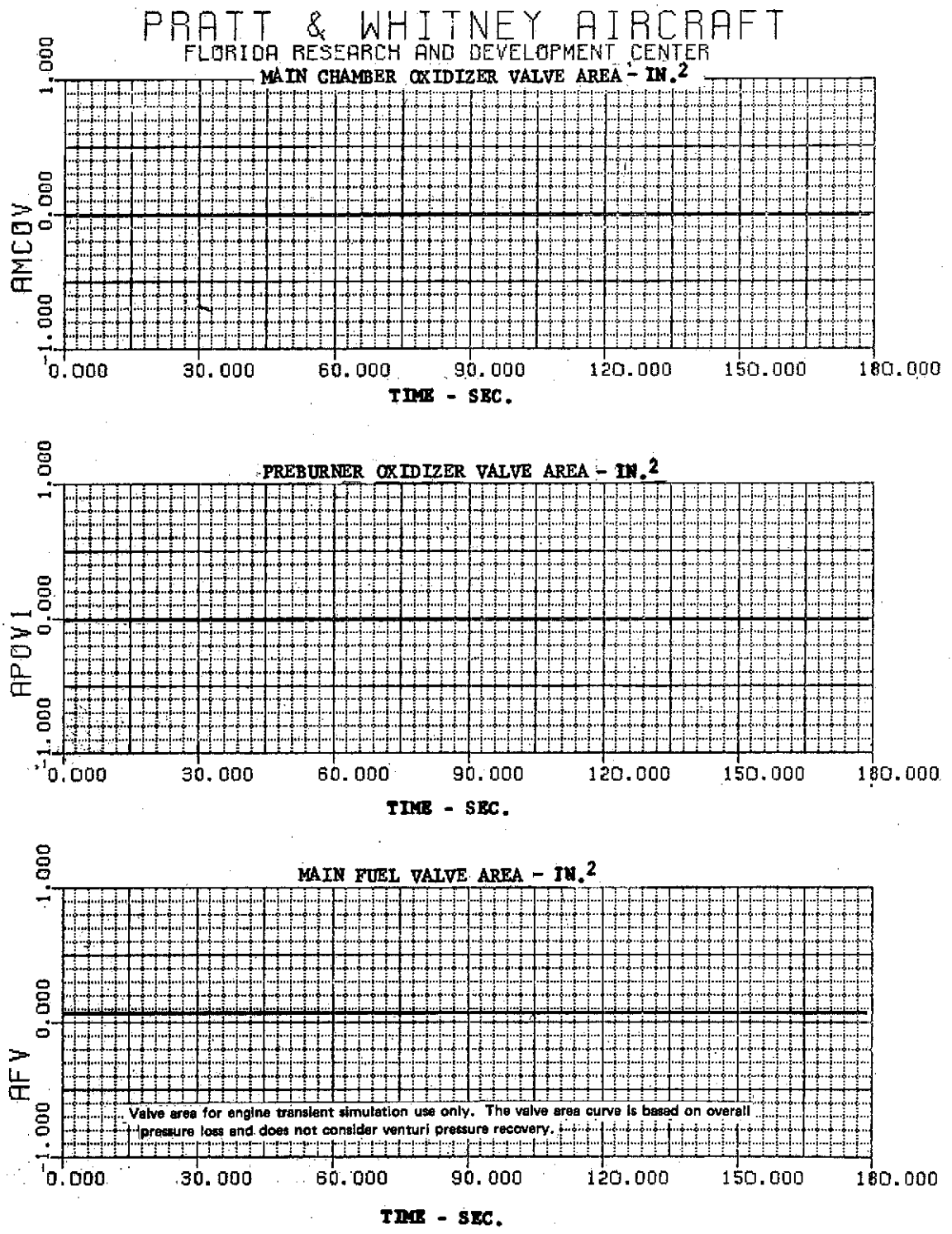

Figure 30. Tank Head Idle Cooldown: Main Chamber Oxidizer Valve Area, Preburner Oxidizer Valve Area, Main Fuel Valve Area DF 96321

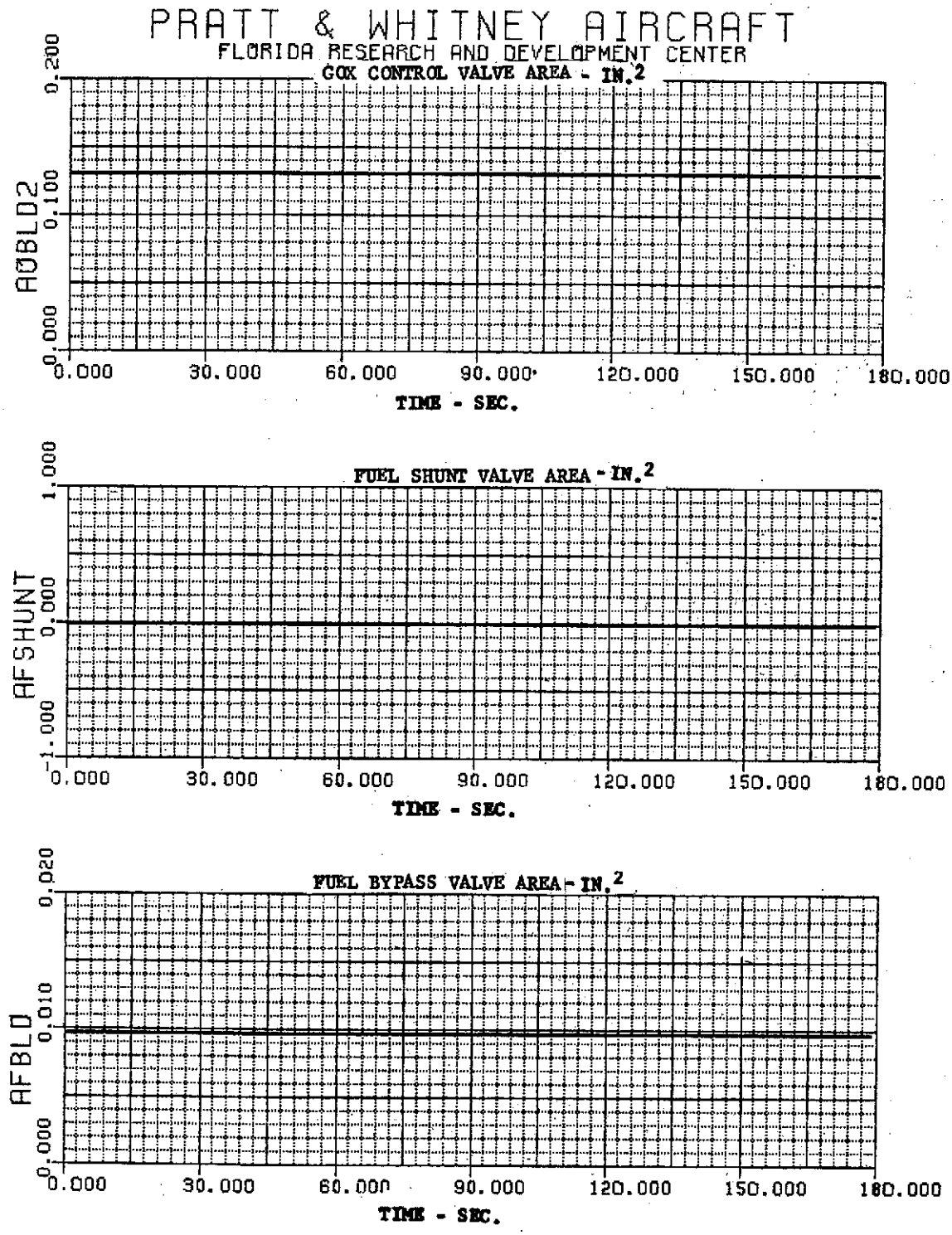

Figure 31. Tank Head Idle Cooldown: GO_2 Control Valve Area, Fuel Shunt Valve Area, Fuel Bypass Valve Area DF 96322

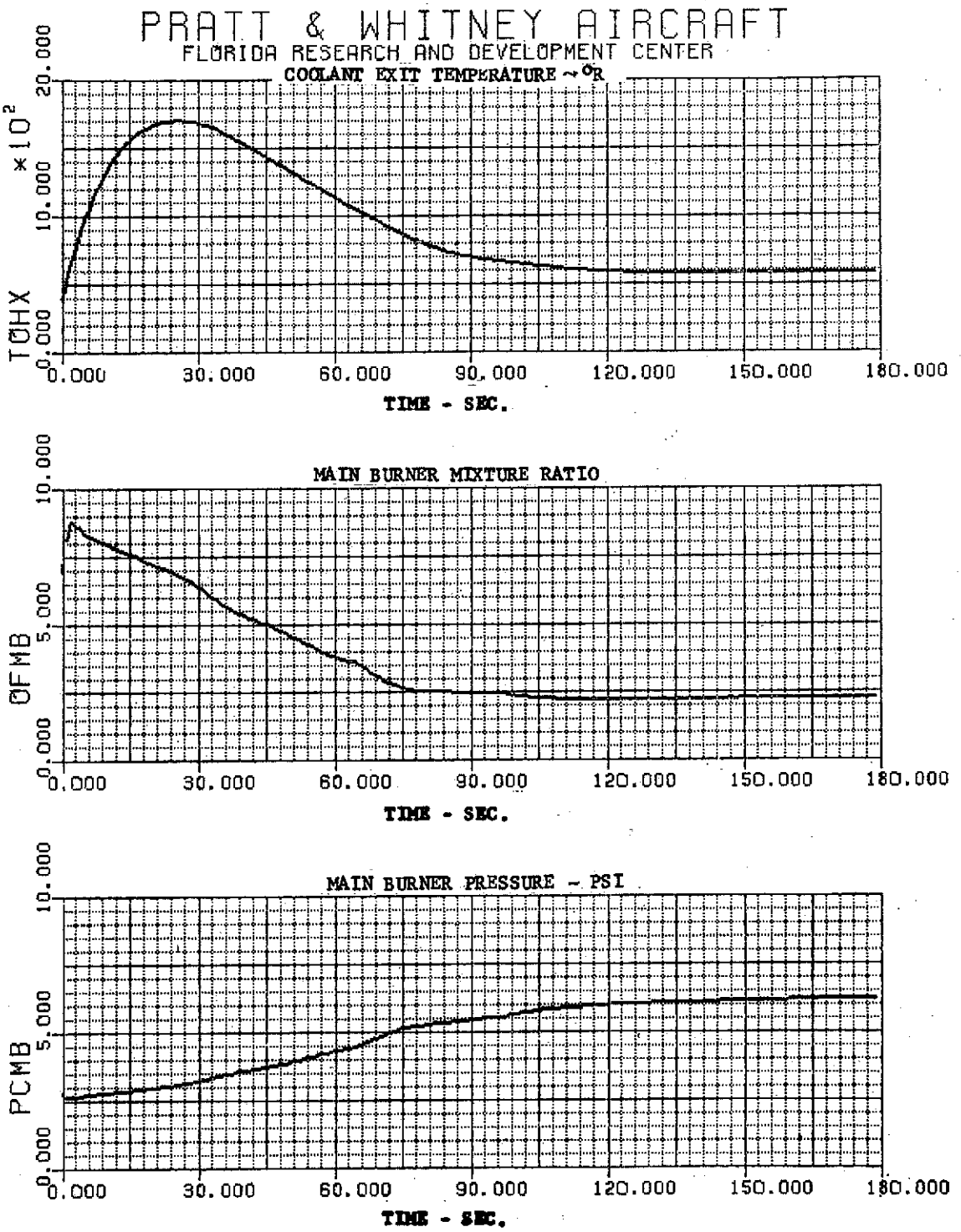

Figure 32. Tank Head Idle Cooldown: Coolant Exit Temperature, Main Burner Mixture Ratio, Main Burner Pressure

DF 96323

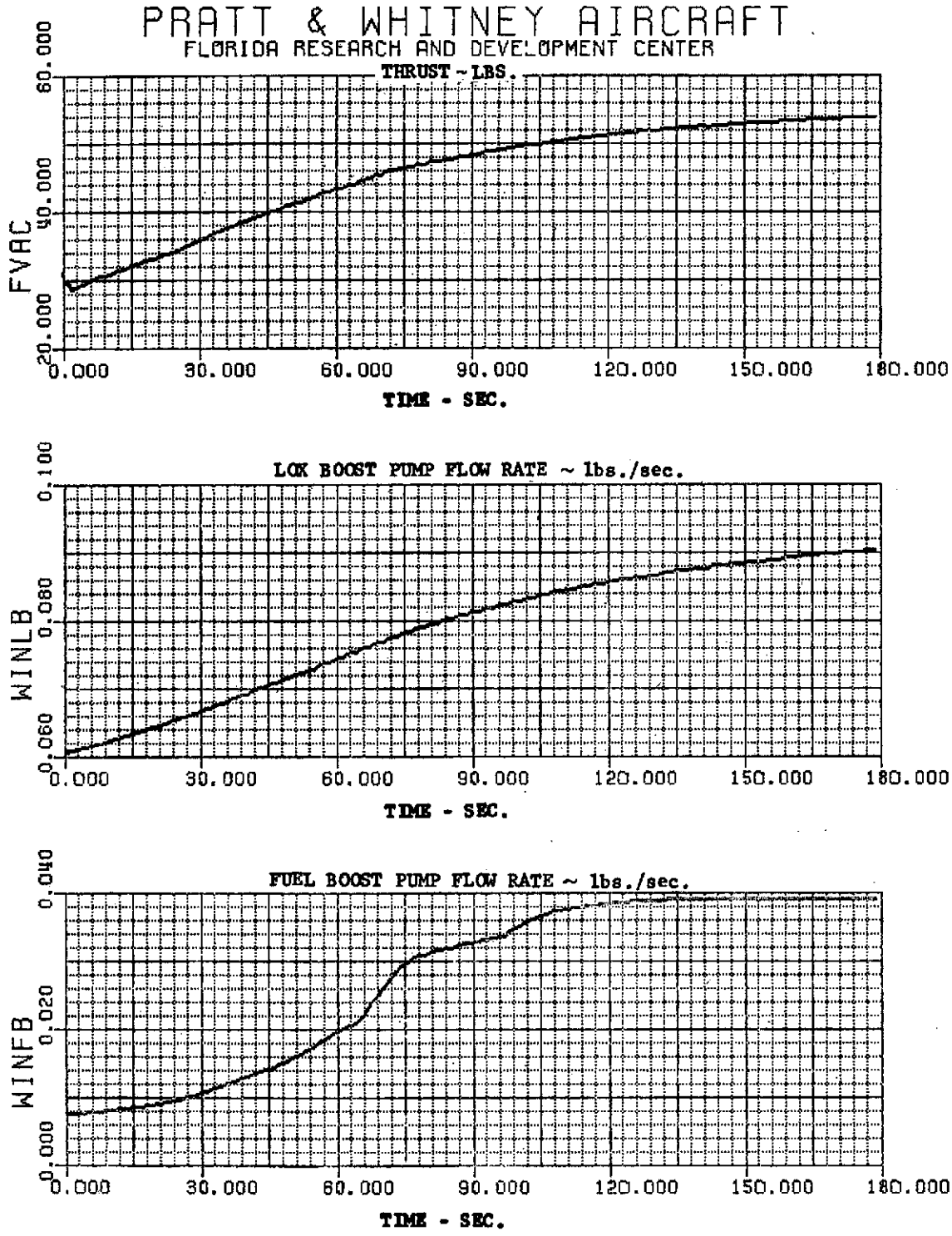

Figure 33. Tank Head Idle Cooldown: Thrust, LO_2 Boost Pump Flowrate, Fuel Boost Pump Flowrate

DF 96324

Nominal pumped idle engine operation is shown in figure 23. Figures 34 through 37 show results from the transient simulation, which predict the engine transient from breakaway at tank head idle to pumped idle. The engine will operate in pumped idle until a command is given for full thrust operation.

While operating in pumped idle, the engine system can supply tank pressurization flow. These flowrates will vary depending on the vehicle demand. Figures 38 and 39 show the effect of varying tank pressurization flowrate while the engine is operating with fixed control valve areas. The small variations in engine mixture ratio and chamber pressure show that the engine can be run satisfactorily in the pumped idle mode with open loop controls.

5. Rated Thrust

After the propellant tanks have been pressurized to the required levels, the engine is ready for operation at rated thrust. The preburner spark igniters are energized, and after the preburner oxidizer injector has been purged with helium for 1 sec, the preburner oxidizer valve is opened. The fuel shunt valve is fully opened and preburner combustion supplies fuel-rich gases to the turbines and the engine is accelerated to rated thrust. Acceleration control is maintained by scheduling the preburner oxidizer valve, the main oxidizer valve, and the fuel cavitating venturi valve.

The control valves are scheduled open loop as a function of time between pumped idle and full thrust. The valve area change rates are matched to the acceleration of the turbopumps. Figures 40 through 43 are simulation results from the dynamic deck that show the engine accelerating from pumped idle to full thrust in 2.5 to 3.0 sec. This particular simulation was run with open loop controls; however, the control protective loops would be operative during the transient and as the engine nears full thrust the chamber pressure trim would set the engine at the precise desired chamber pressure.

6. Shutdown

The ASE will be shut down upon receipt of a shutdown signal. The shutdown procedure is essentially the reverse of the start sequence. The valve sequence during shutdown is shown in figure 44. The control valves are scheduled as a function of time from full thrust to pumped idle as shown in figures 45 and 46. As the engine thrust nears pumped idle level the preburner oxidizer valve is closed, the preburner oxidizer injector purged and the engine is allowed to stabilize at pumped idle, again operating in the expander cycle mode. To complete shutdown, the main oxidizer and oxidizer suction valves are closed and the GO_2 control valve opened, thus shutting off all oxidizer to the engine. The fuel bypass valve opens, the fuel suction valve closes and fuel to the engine is shut off. The turbopumps coast to a stop and the engine is ready for another cycle. If desired, the engine can be commanded to operate in tank head idle instead of completely shutting down from pumped idle. Figures 47 and 48 show the characteristics of the shutdown.

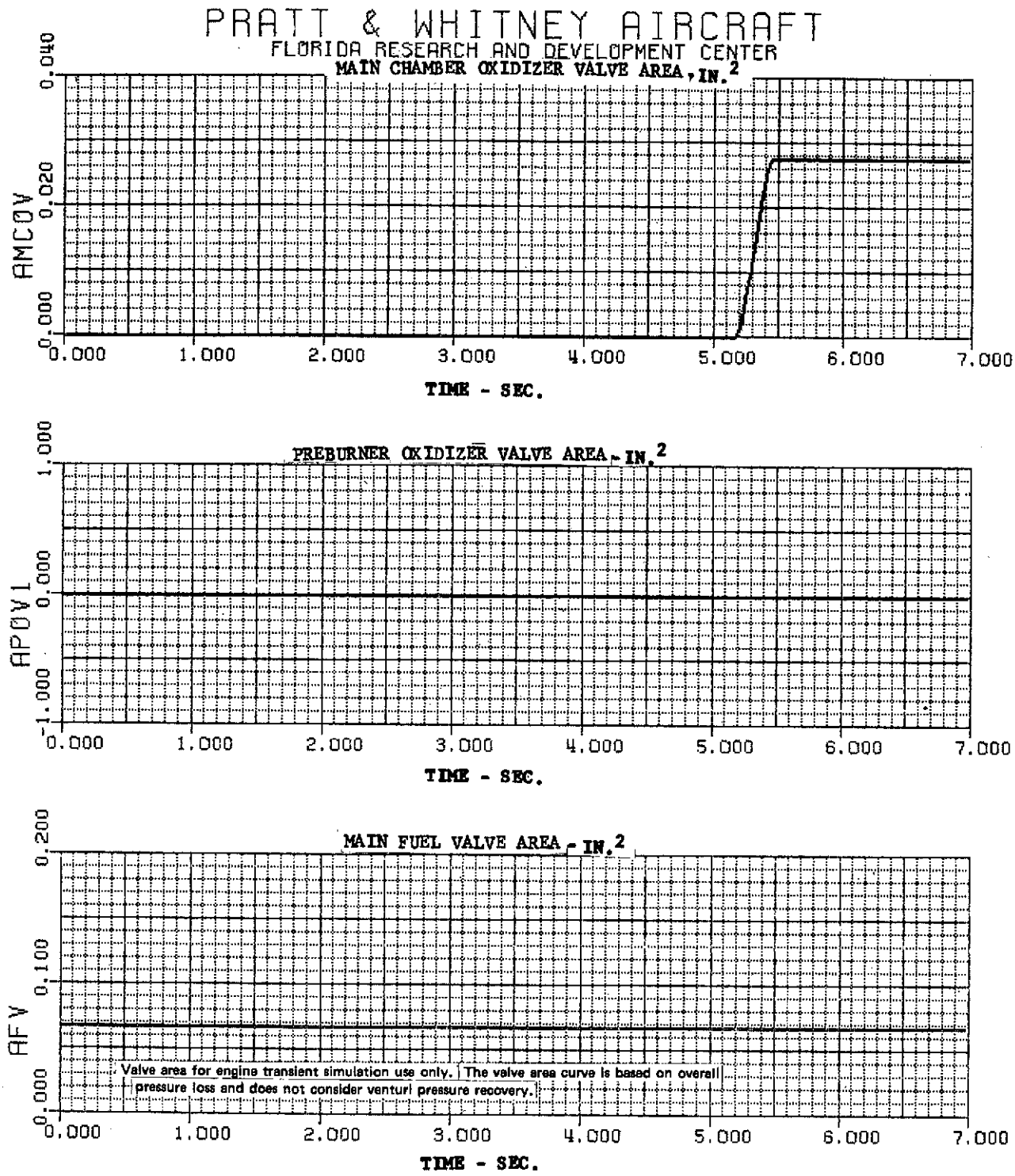

Figure 34. Start Transient, Tank Head Idle - Pumped Idle: Main Chamber Oxidizer Valve Area, Preburner Oxidizer Valve Area, Main Fuel Valve Area

DF 96325

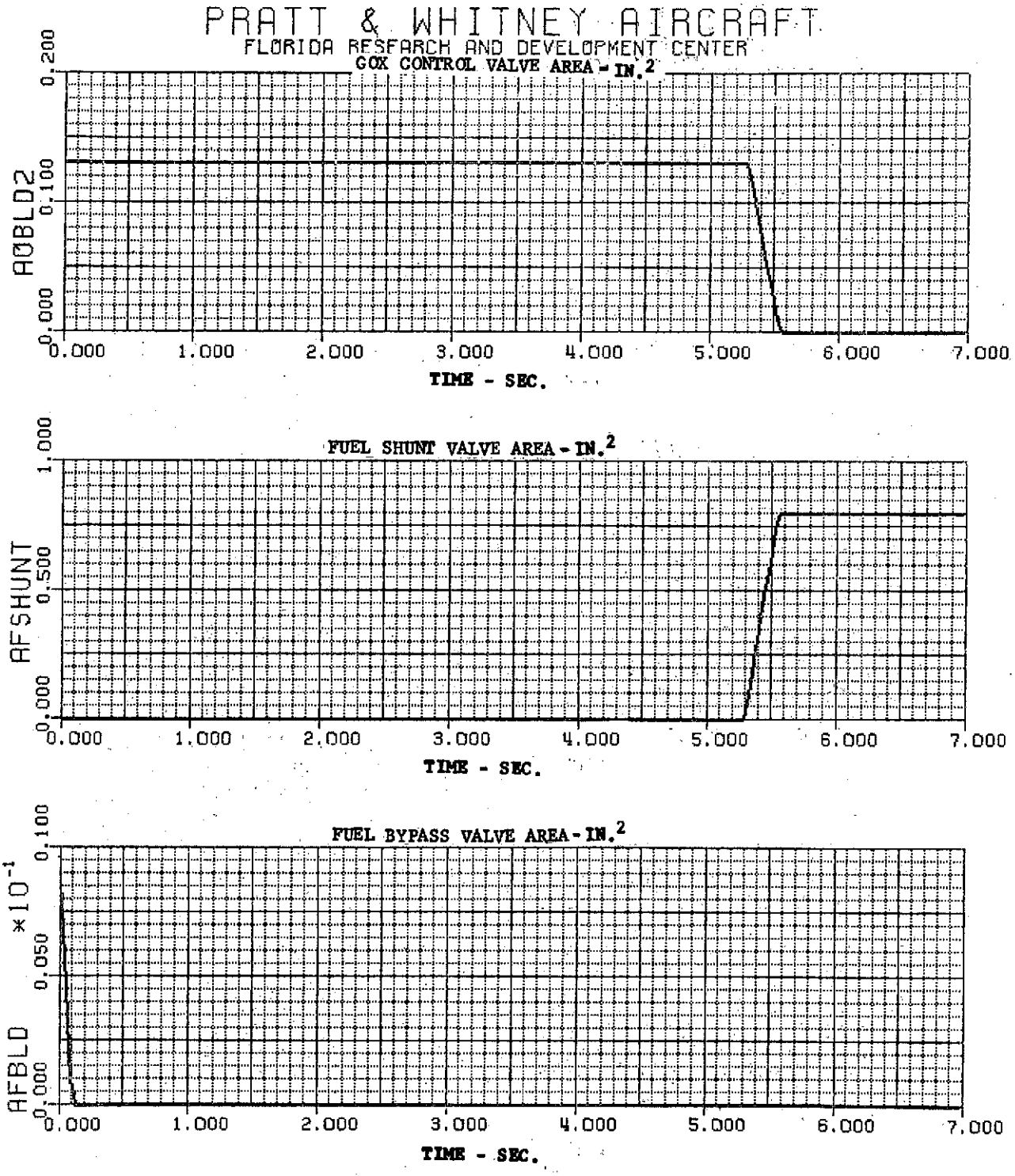

Figure 35. Start Transient, Tank Head Idle - Pumped Idle: GO_2 Control Valve Area, Fuel Shunt Valve Area, Fuel Bypass Valve Area

DF 96326

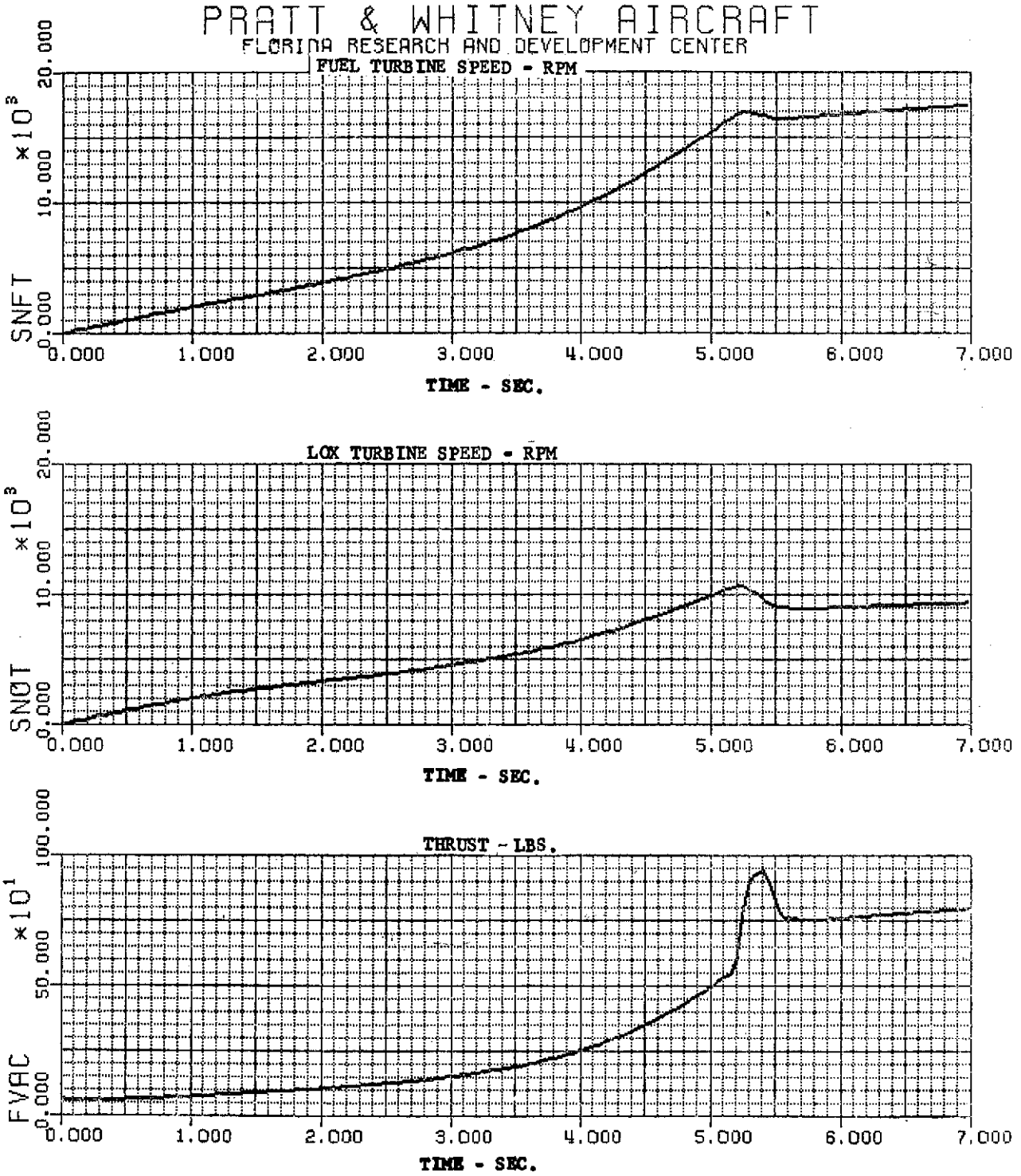

Figure 36. Start Transient, Tank Head Idle - Pumped Idle: Fuel Turbine Speed, LO_2 Turbine Speed, Thrust

DF 96327

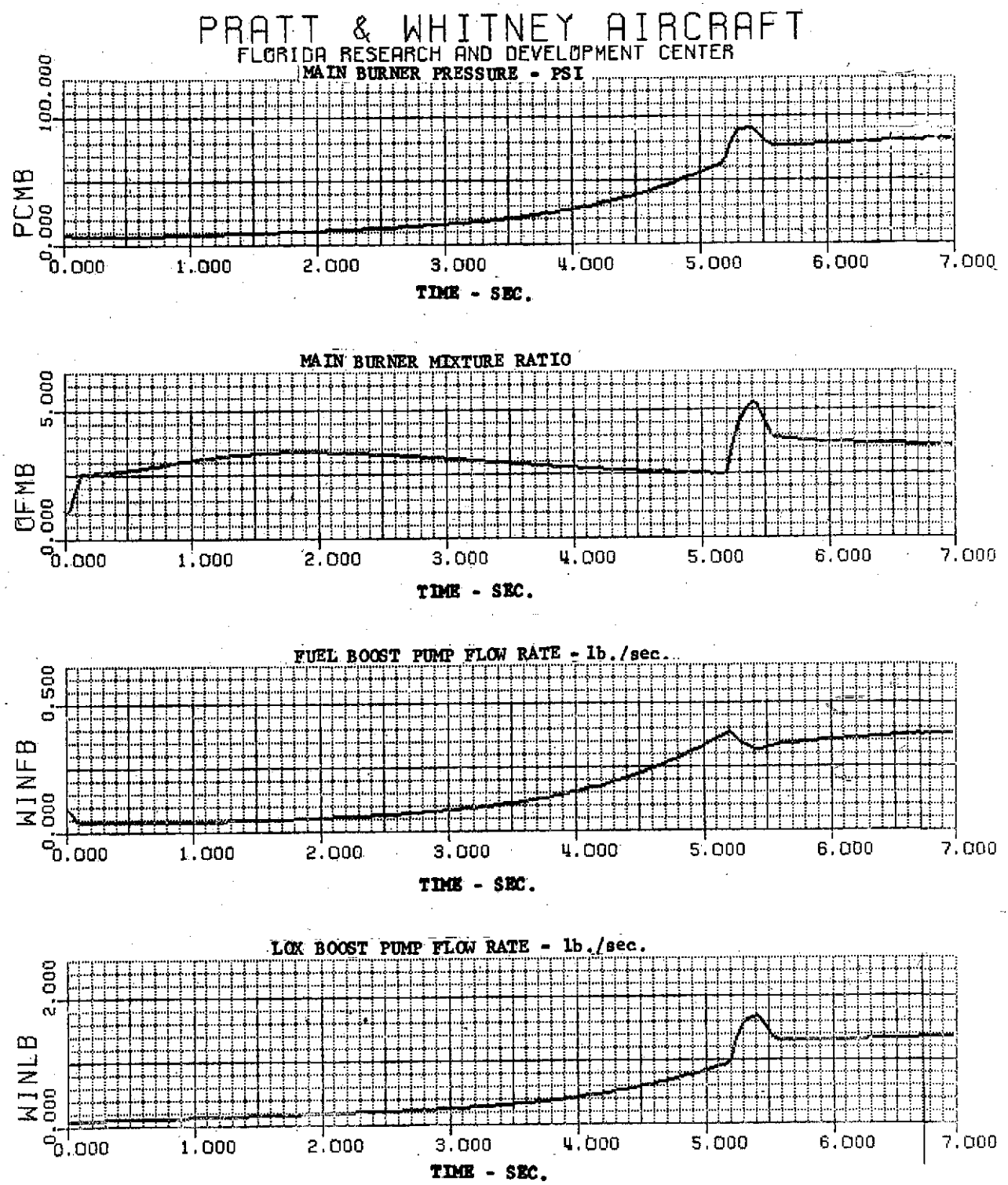

Figure 37. Start Transient, Tank Head Idle - Pumped Idle: Main Burner Pressure, Main Burner Mixture Ratio, Fuel Boost Pump Flowrate, LO_2 Boost Pump Flowrate

DF 96328

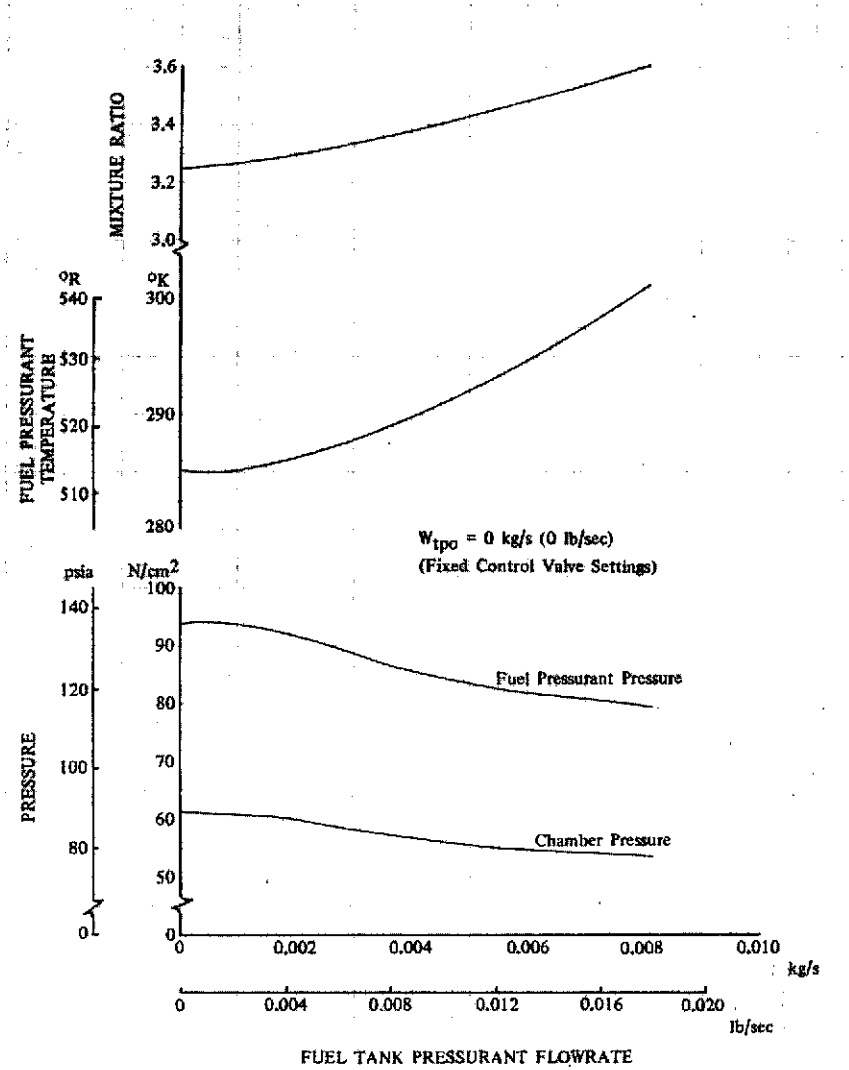

Figure 38. Effect of Varying Fuel Tank Pressurization Flow at Pumped Idle

DF 96259

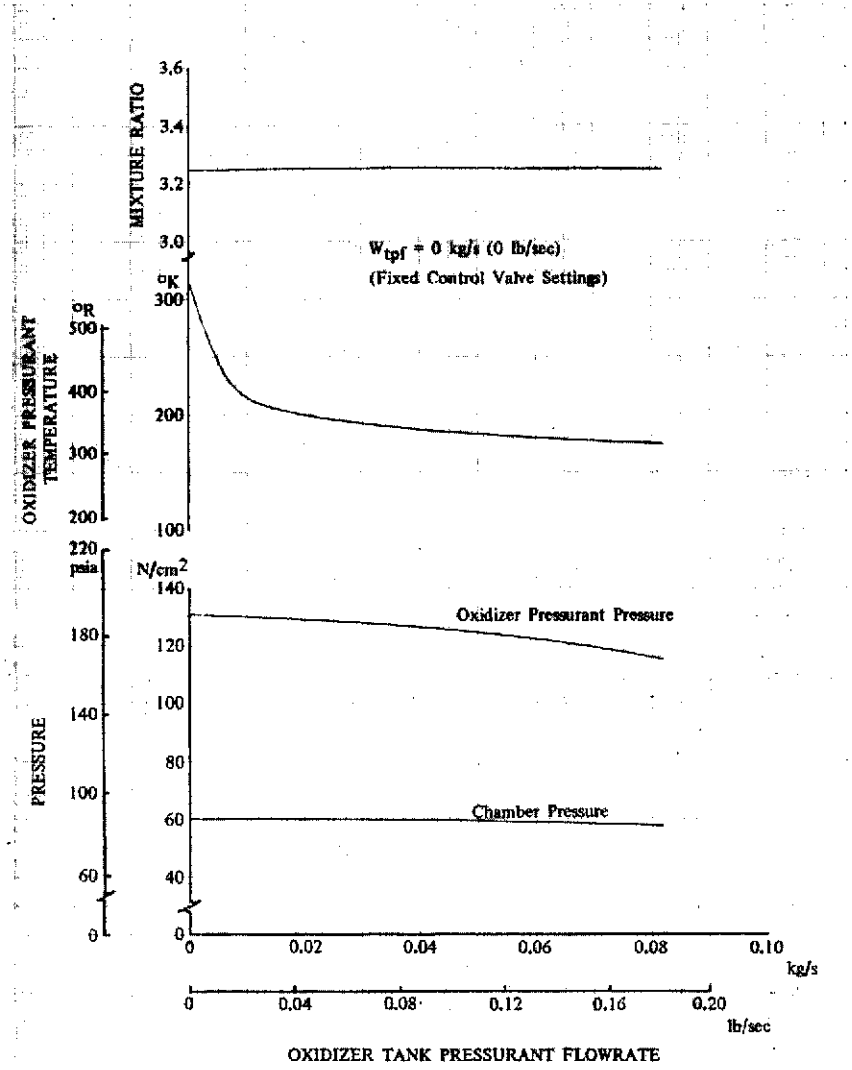

Figure 39. Effect of Varying Oxidizer Tank Pressurization Flow at Pumped Idle

DF 96258

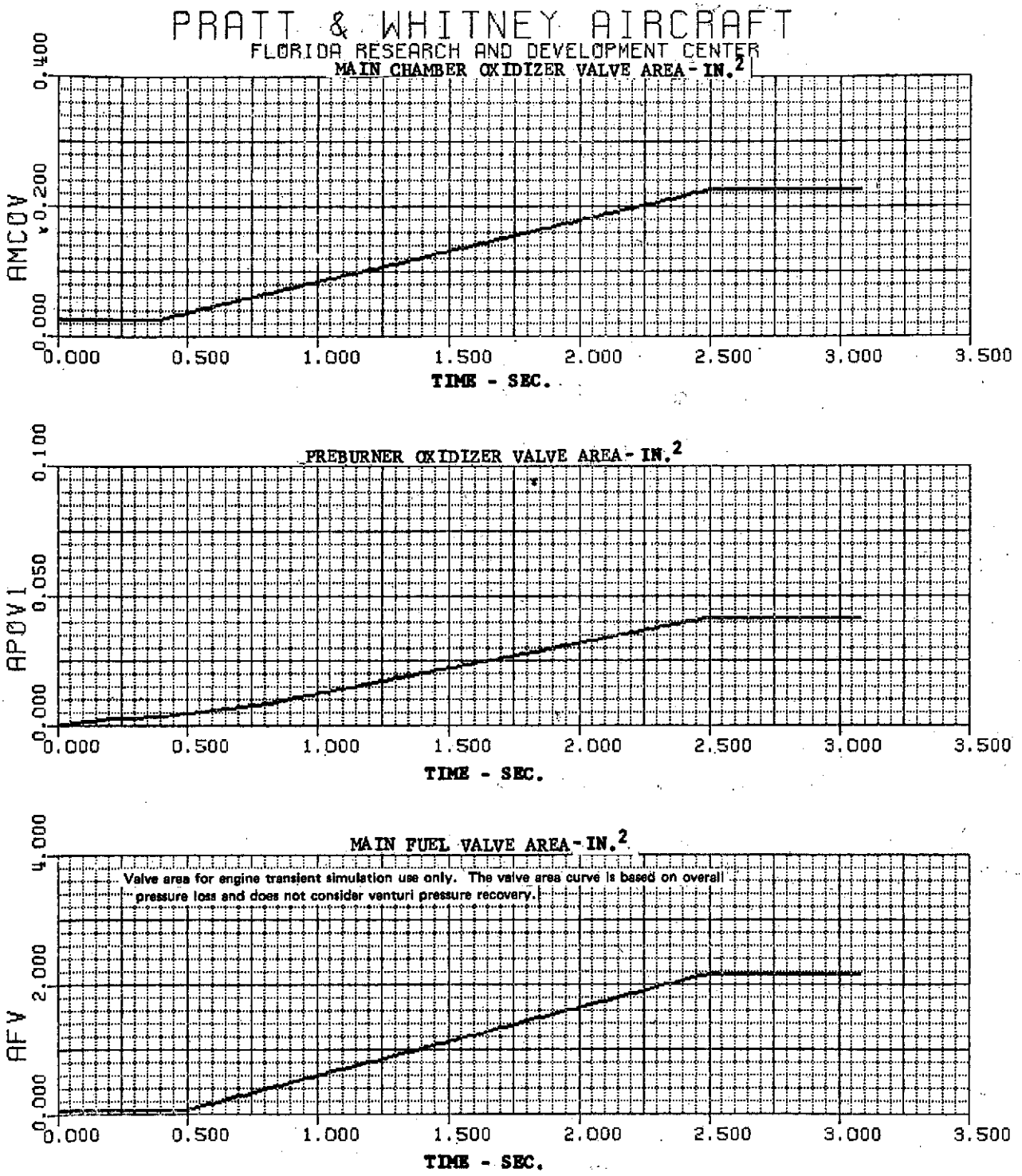

Figure 40. Pumped Idle - Full Thrust Transient, Main Chamber Oxidizer Valve Area, Preburner Oxidizer Valve Area, Main Fuel Valve Area

DF 96329

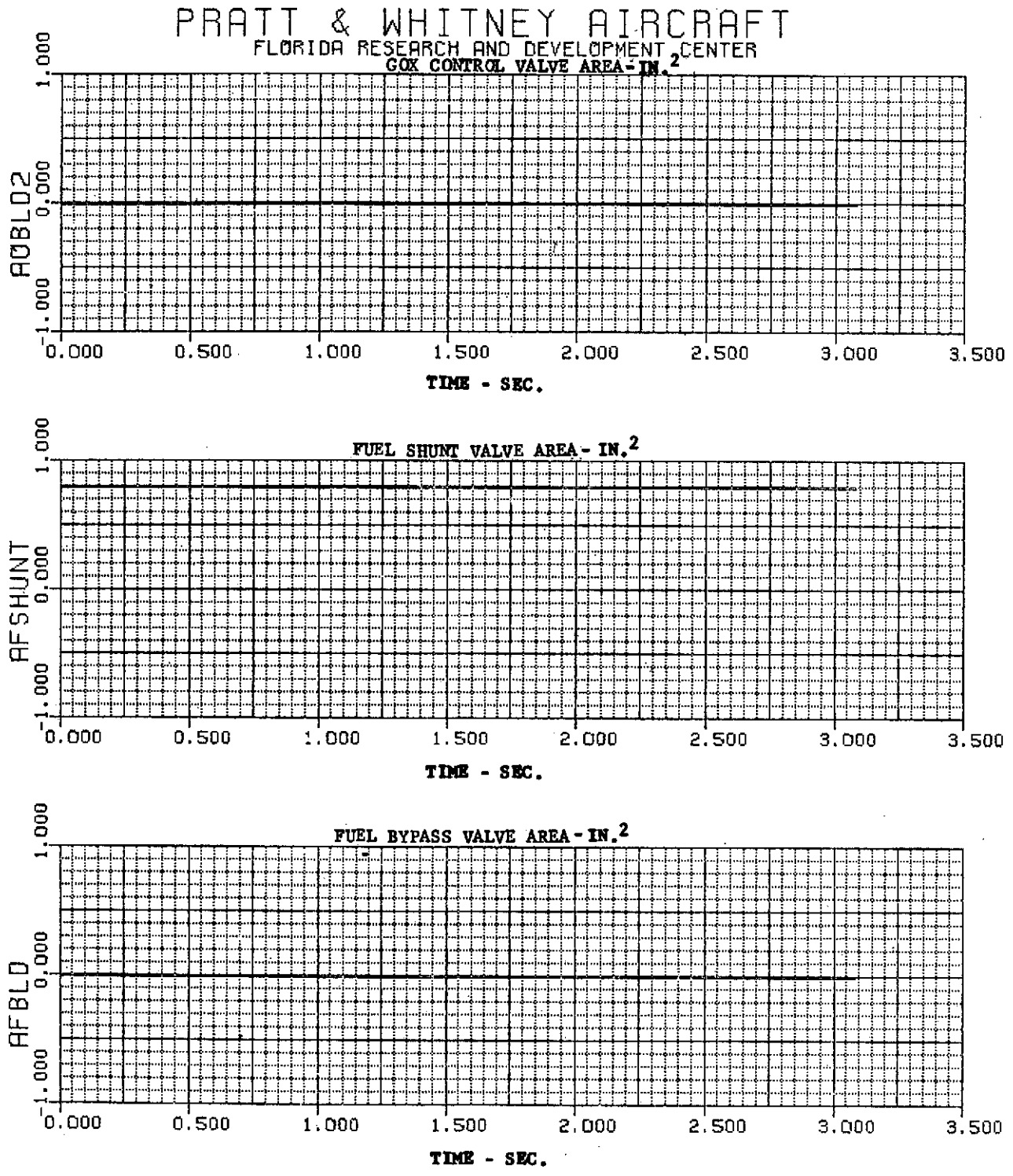

Figure 41. Pumped Idle - Full Thrust Transient, GO_2 Control Valve Area, Fuel Shunt Valve Area, Fuel Bypass Valve Area DF 96330

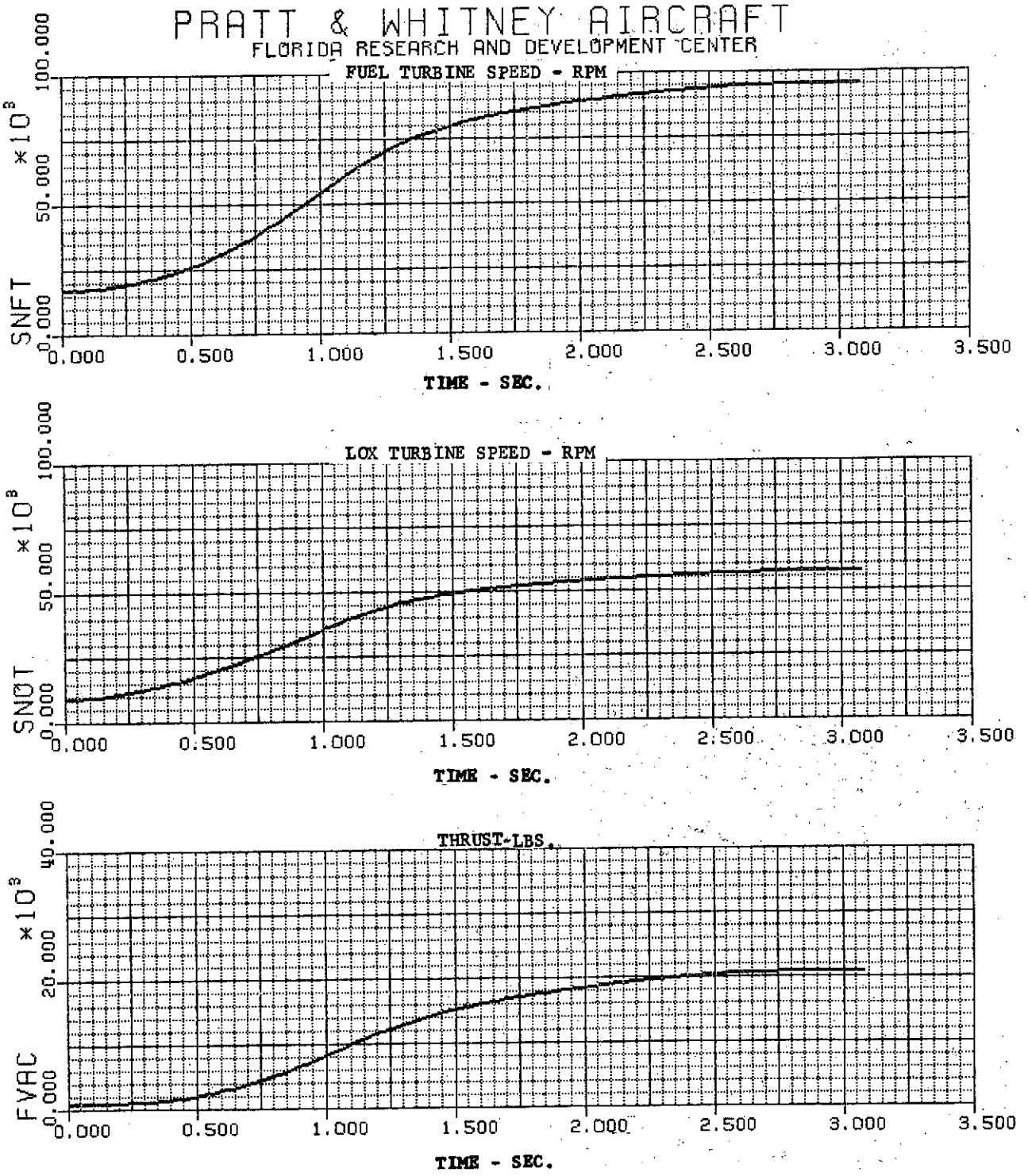

Figure 42. Pumped Idle - Full Thrust Transient, Fuel Turbine Speed, LO_2 Turbine Speed, Thrust

DF 96331

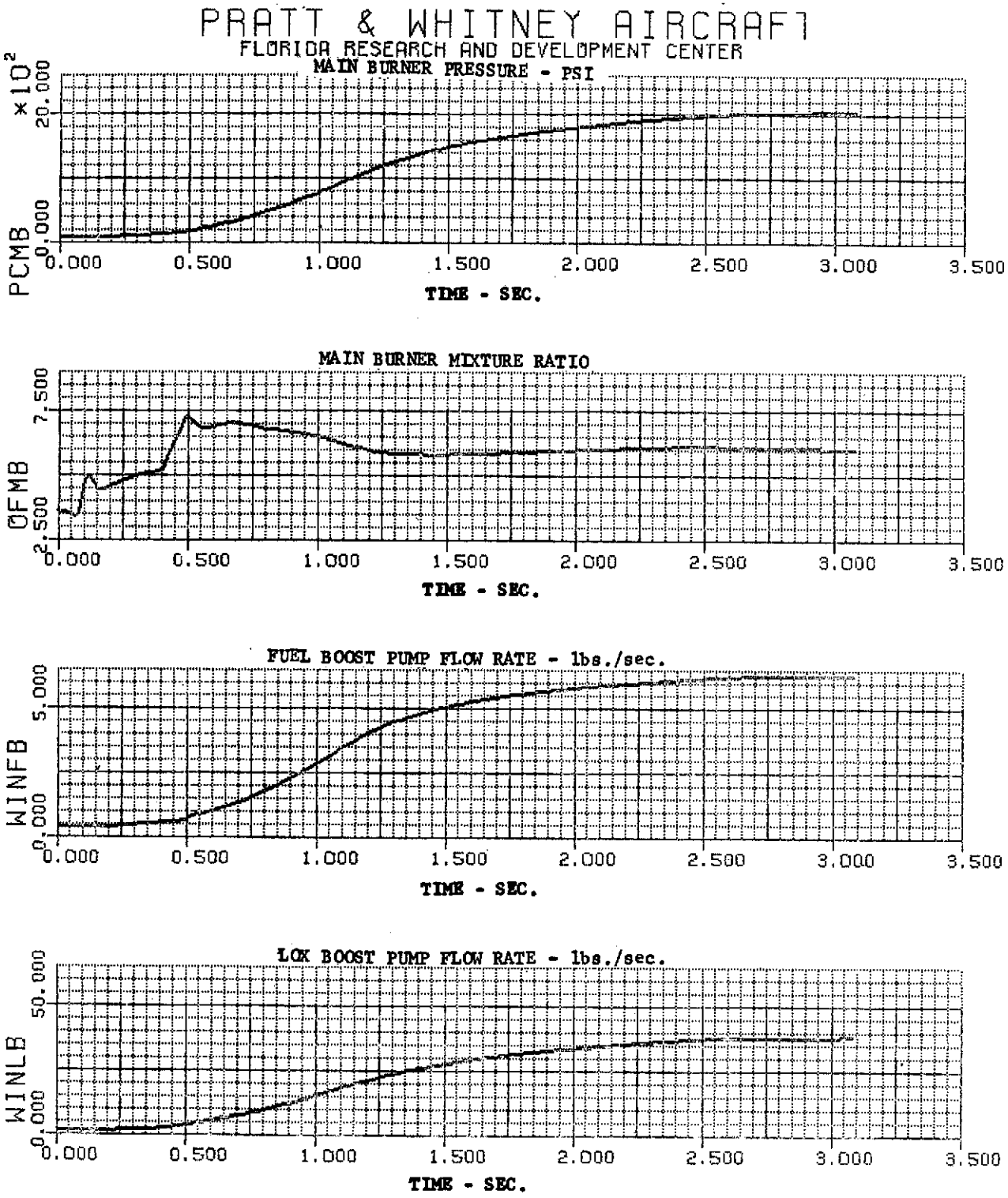

Figure 43. Pumped Idle - Full Thrust Transient, Main Burner Pressure, Main Burner Mixture Ratio, Fuel Boost Pump Flowrate, LO_2 Boost Pump Flowrate

DF 96332

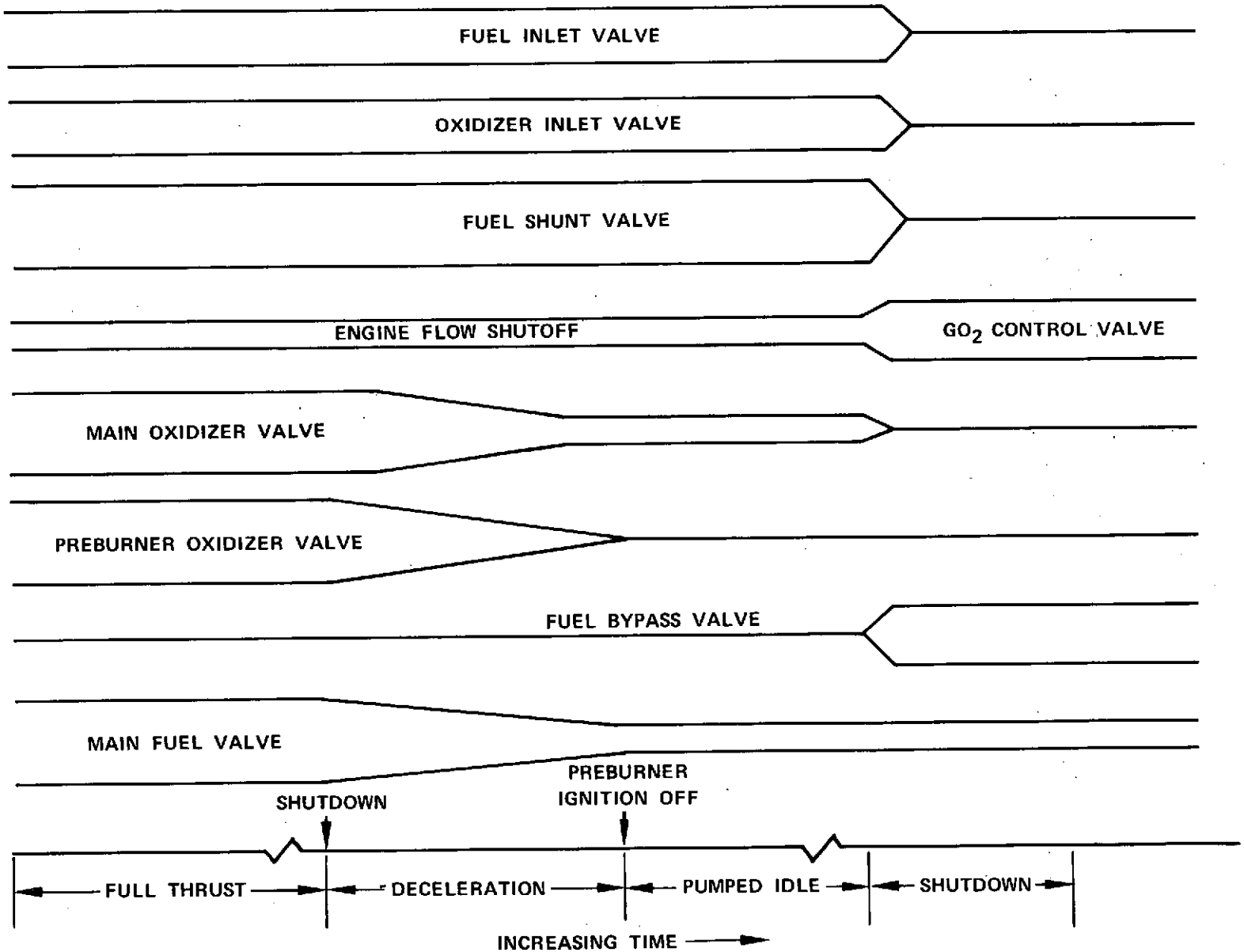

Figure 44. Advanced Space Engine Shutdown Sequence

FD 71620

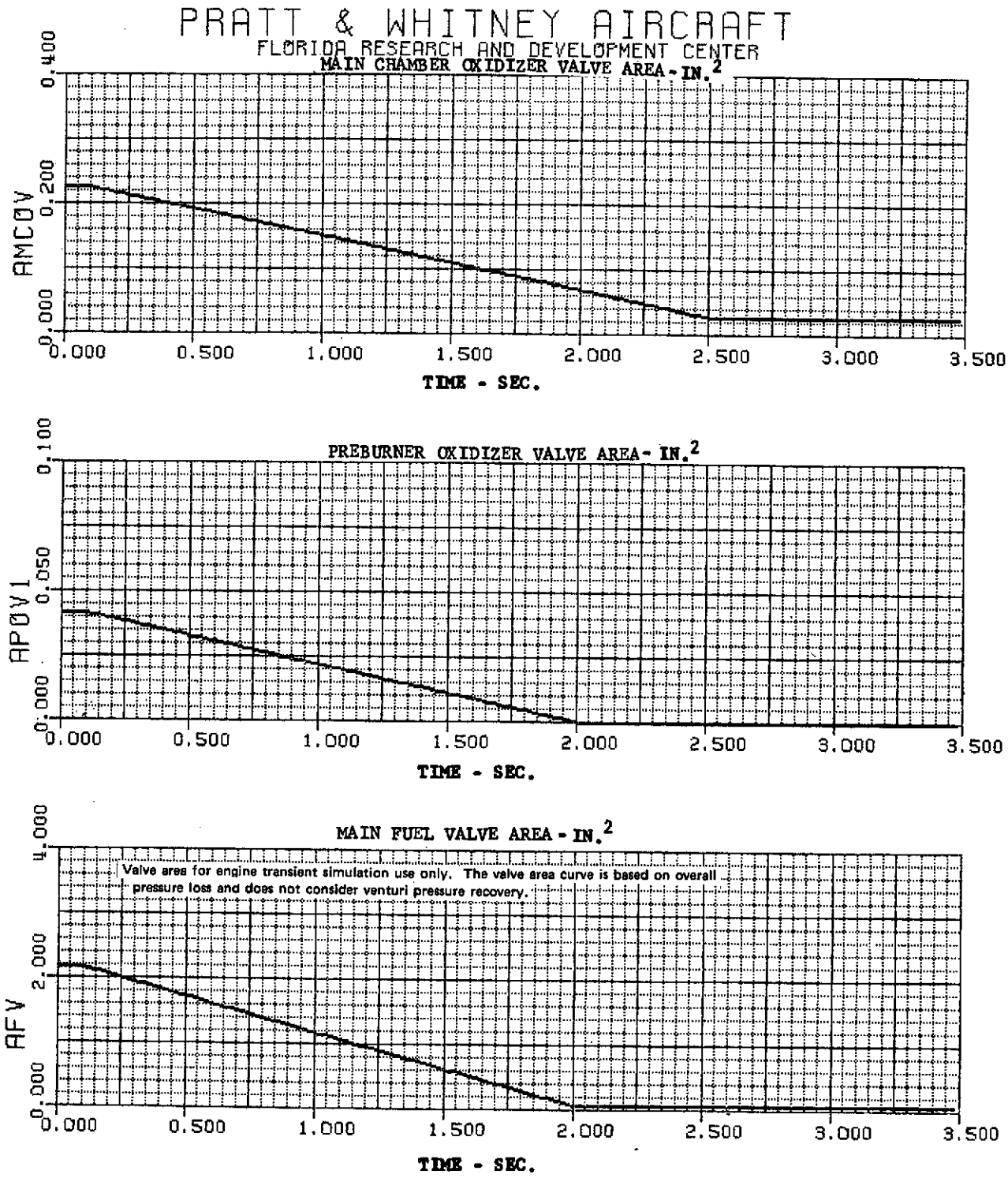

Figure 45. Shutdown Transient, Full Thrust - Pumped Idle: Main Chamber Oxidizer Valve Area, Preburner Oxidizer Valve Area, Main Fuel Valve Area

DF 96333

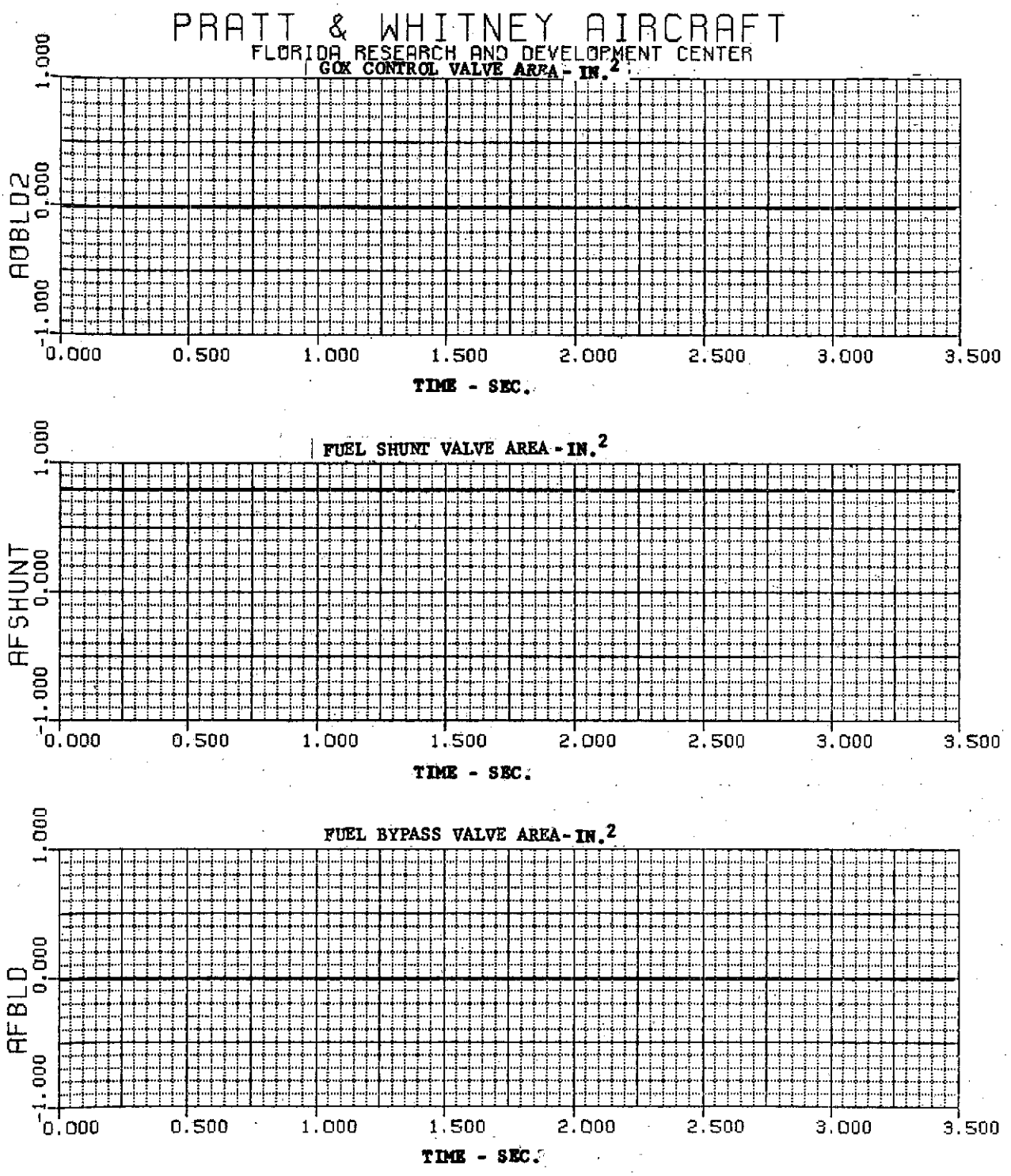

Figure 46. Shutdown Transient, Full Thrust - Pumped Idle: GO_2 Control Valve Area, Fuel Shunt Valve Area, Fuel Bypass Valve Area DF 96334

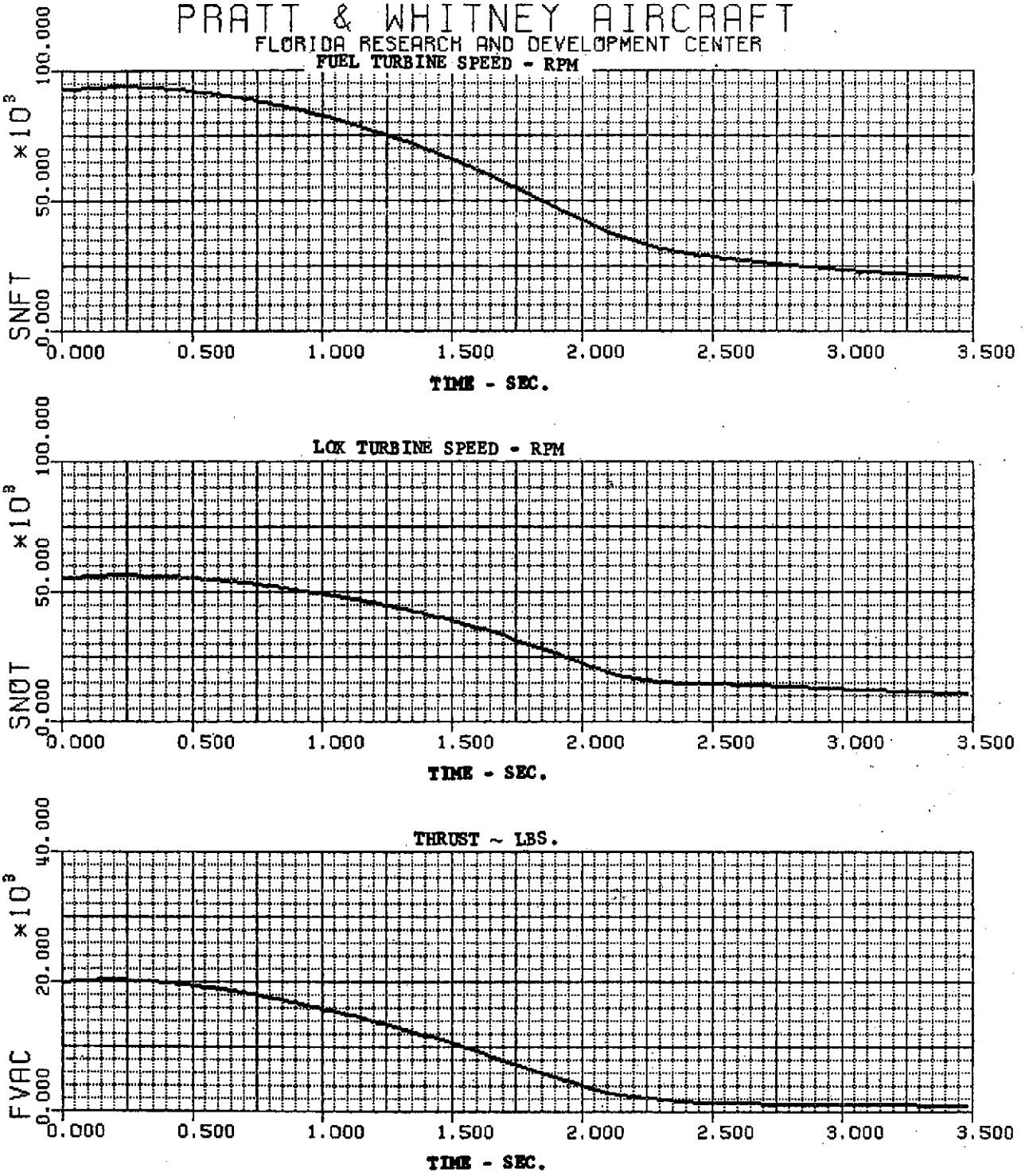

Figure 47. Shutdown Transient, Full Thrust - Pumped Idle: Fuel Turbine Speed, LO_2 Turbine Speed, Thrust

DF 96335

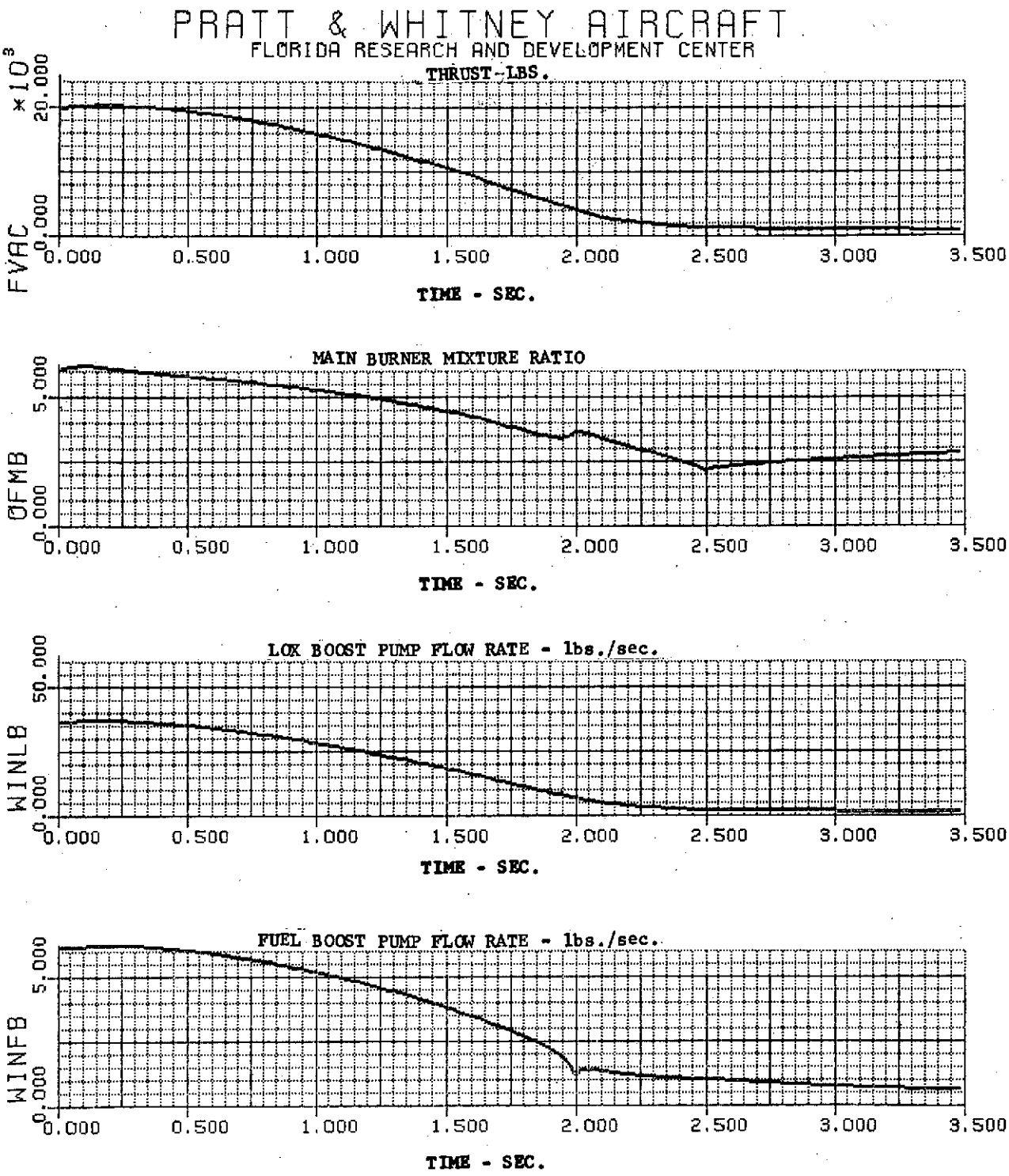

Figure 48. Shutdown Transient, Full Thrust - Pumped Idle: Thrust, Main Burner Mixture Ratio, LO_2 Boost Pump Flowrate, Fuel Boost Pump Flowrate

DF 96336

7. Propellant Dumping

Sequential dumping of propellants through the engine can be accomplished without additional valves. Fuel can be dumped with the valves in their tank head idle position - i.e., fuel suction valve open, fuel venturi full open, fuel bypass valve full open, and the fuel shunt valve full open. The oxidizer can be dumped with the oxidizer suction, GO_2 control valve, and main oxidizer valve in their full open positions.

It is assumed that some form of purge gas is available to assist in the dumping of the propellants by maintaining tank pressure near nominal level while the propellants are being dumped. Without this purge the propellants would have to boil-off to maintain tank pressure to force the propellants out and dumping would take a long time.

Fuel can be dumped by opening the suction valve to allow flow through the engine. The fuel venturi, the fuel shunt, and fuel bypass valves would be positioned full open to allow maximum flowrate. With the tank saturated at 21.3°K (38.4°R) and 14 N/cm^2 (20 psia) the flowrate would be approximately 0.025 kg/s (0.055 lb/sec). If this rate is maintained it will take approximately 45.5 min to dump 68 kg (150 lb) of fuel.

Oxidizer can be dumped by opening the oxidizer suction, GO_2 control, and main oxidizer valves to provide maximum flowrate. With the tank saturated at 92.7°K (167.0°R) and 13.2 N/cm^2 (19.1 psia) approximately 1.95 kg/s (4.3 lb/sec) of oxidizer flowrate can be maintained. With this flowrate the oxidizer tank can be emptied of 408 kg (900 lb) in 3.5 min.

If faster dumping of propellants, particularly fuel, is desired the valve sizes can be increased to provide higher flowrates. This would represent a complexity to the control system, not only in weight, but the fuel bypass valve would have to have position control to maintain flowrates during normal operation. Another alternative to providing more rapid dumping of propellants is to provide additional vent and dump valves.

8. Critical Areas of Engine Operation

A dynamic simulation has been developed to investigate the dynamics and component interactions that are unique to the tank head idle and pumped idle modes of operation. The simulation has identified several critical areas where detailed investigation is beyond the scope of the ASE program. These areas and their importance to the overall program are as follows.

The critical areas of engine operation have been grouped into three general categories. These are:

1. Pump cooldown
2. Turbopump breakaway
3. Two-phase propellant pumping.

a. Cooldown

Prior to start command the ASE will be in a zero gravity environment and the engine temperature will be between 111°K (200°R) and 311°K (560°R). After

receipt of a start command the engine will operate at tank head idle while the turbopumps cool down. The main burner will be lit to produce about 245 N (55 lb) of thrust and the preburner remains unlit.

The dynamic deck was used to predict turbopump cooldown during tank head idle operation. The assumed input was an ambient temperature of 222°K (400°R) and saturated liquid propellants. The results of a simulated cooldown run of 175 sec are shown in figures 49 through 54 (also refer to figures 30 through 33). These data indicate the relative cooldown of the pump housings and impellers.

The RL10 was successfully started to pumped idle after turbopump cooldown. The go/no-go conditions were established by a cooldown test program. After the completion of cooldown the average turbopump housing temperature will have reached some level.

The simulation of the ASE cooldown indicates that the average housing temperature of the turbopumps at the end of 175 sec of cooldown are approximately:

Pump	Temperature, °K (°R)
Fuel Boost	61 (110)
Fuel Pump (1st stage)	21 (38)
Fuel Pump (2nd stage)	21 (38)
Oxidizer Boost	106 (190)
Oxidizer Pump	94 (170)

When the simulated transient is extrapolated until housing temperatures are in the range that the RL10 achieved at "go" conditions (assumed to be 44.4 and 100°K (80 and 180°R) on the fuel and oxidizer pump, respectively) the cooldown time would be:

Pump	Time, sec
Fuel Boost	234
Oxidizer Boost	198

Cooldown criteria for the ASE turbopumps have not been established. It is not known if housing temperature is a sufficient indication for cooldown. If it is, it is also not known if the same temperature would be required for all fuel or oxidizer pumps. When the internal surface temperatures of the impeller and housing approach liquid temperatures, the pumps should be capable of producing a pressure rise. A search of available literature has indicated that the requirements for cooldown and pumping may be more complex than the use of metal temperature criteria. For example, the propellant quality (vapor volume) at the pump inlet must be below a given value to prevent head falloff caused by choking in the pump. It was concluded that cooldown and pumping with saturated inlet conditions involved complex phenomena that require more detailed study as well as some experimental work. This area of operation is identified as an area that requires additional effort beyond the scope of the ASE program.

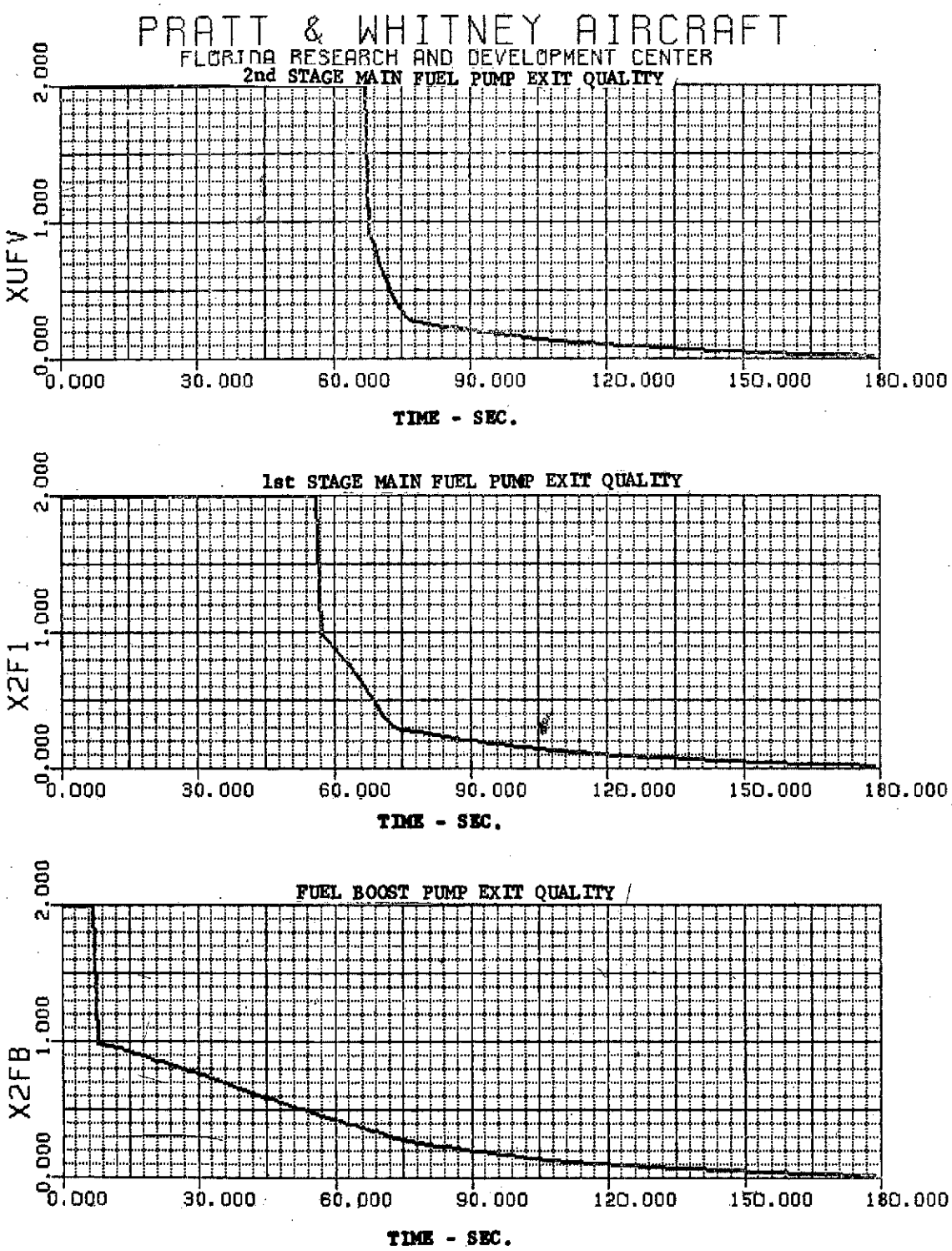

Figure 49. Tank Head Idle Cooldown - 2nd Stage Main Fuel Pump Exit Quality, 1st Stage Main Fuel Pump Exit Quality, Fuel Boost Pump Exit Quality

DF 96337

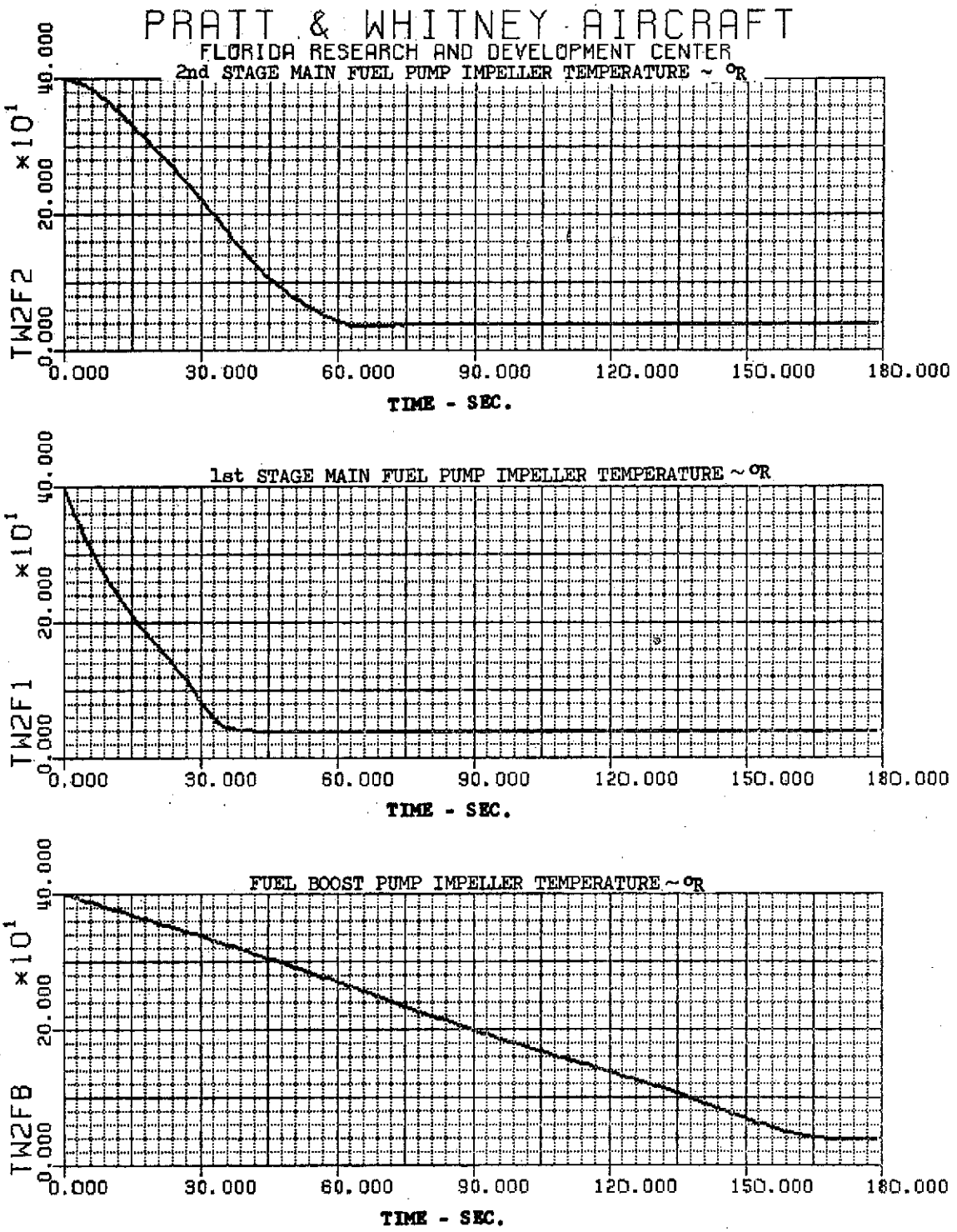

Figure 50. Tank Head Idle Cooldown - 2nd Stage Main Fuel Pump Impeller Temperature, 1st Stage Main Fuel Pump Impeller Temperature, Fuel Boost Pump Impeller Temperature DF 96338

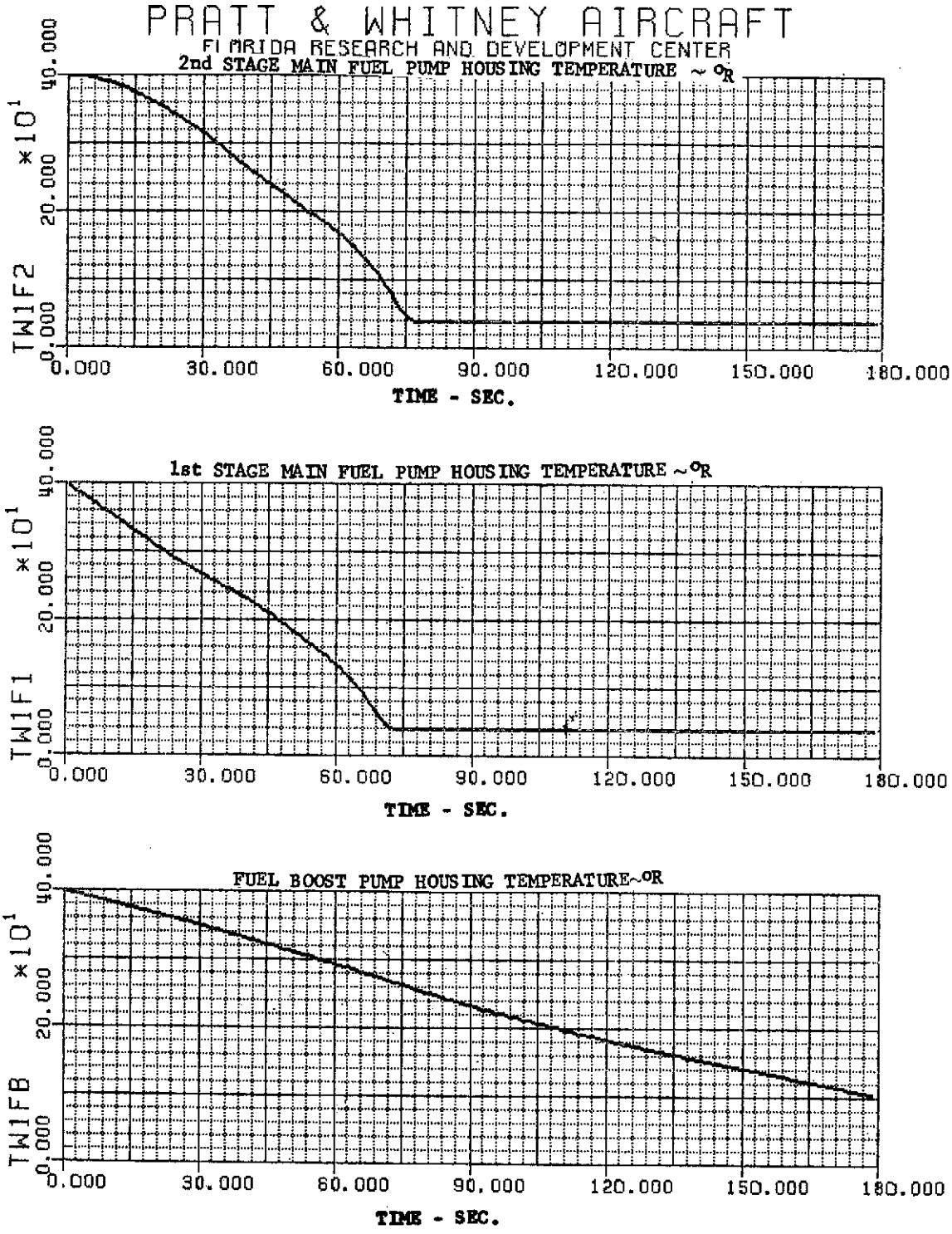

Figure 51. Tank Head Idle Cooldown - 2nd Stage Main Fuel Pump Housing Temperature, 1st Stage Main Fuel Pump Housing Temperature, Fuel Boost Pump Housing Temperature

DF 96339

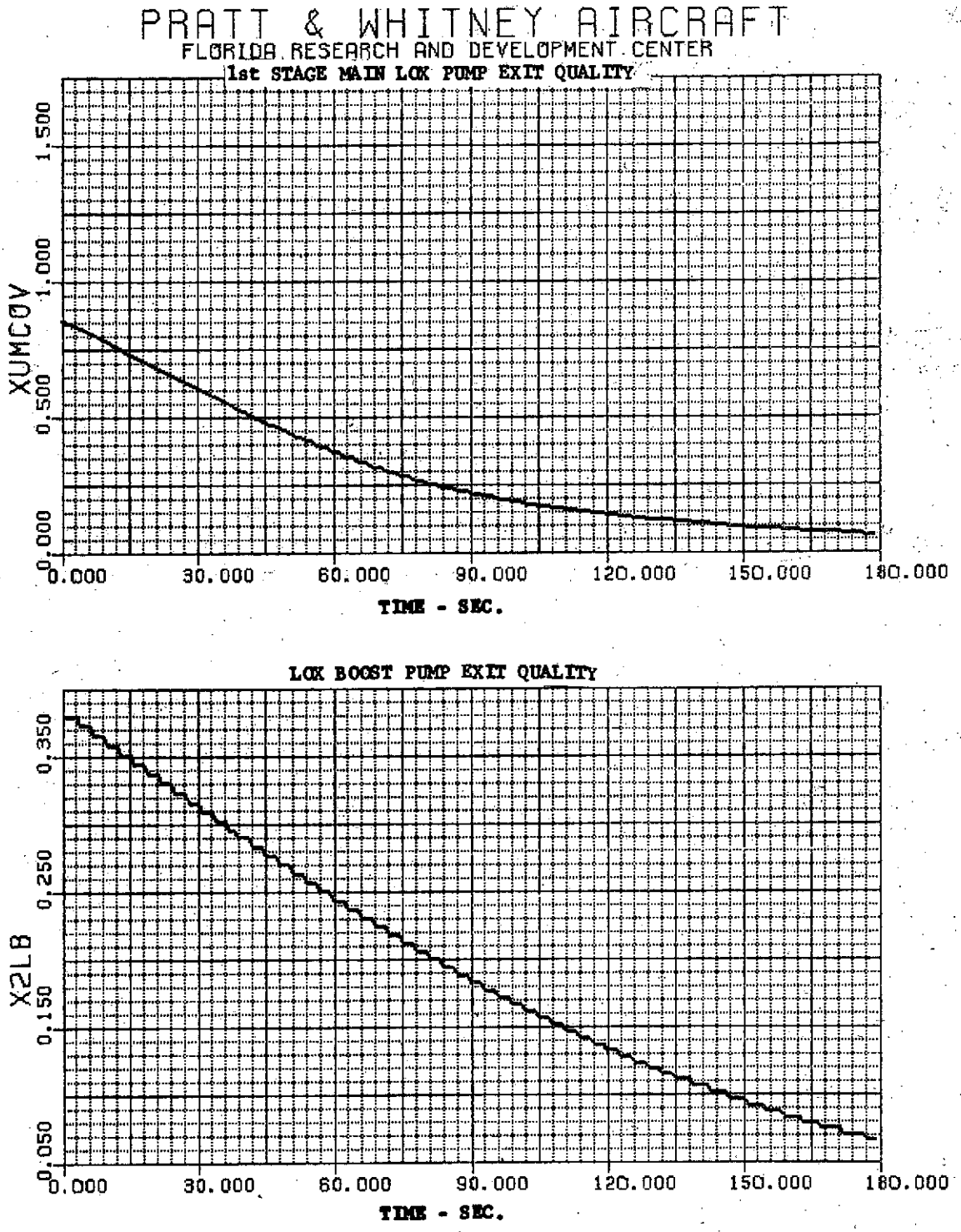

Figure 52. Tank Head Idle Cooldown - 1st Stage Main LO_2 Pump Exit Quality, LO_2 Boost Pump Exit Quality

DF 96340

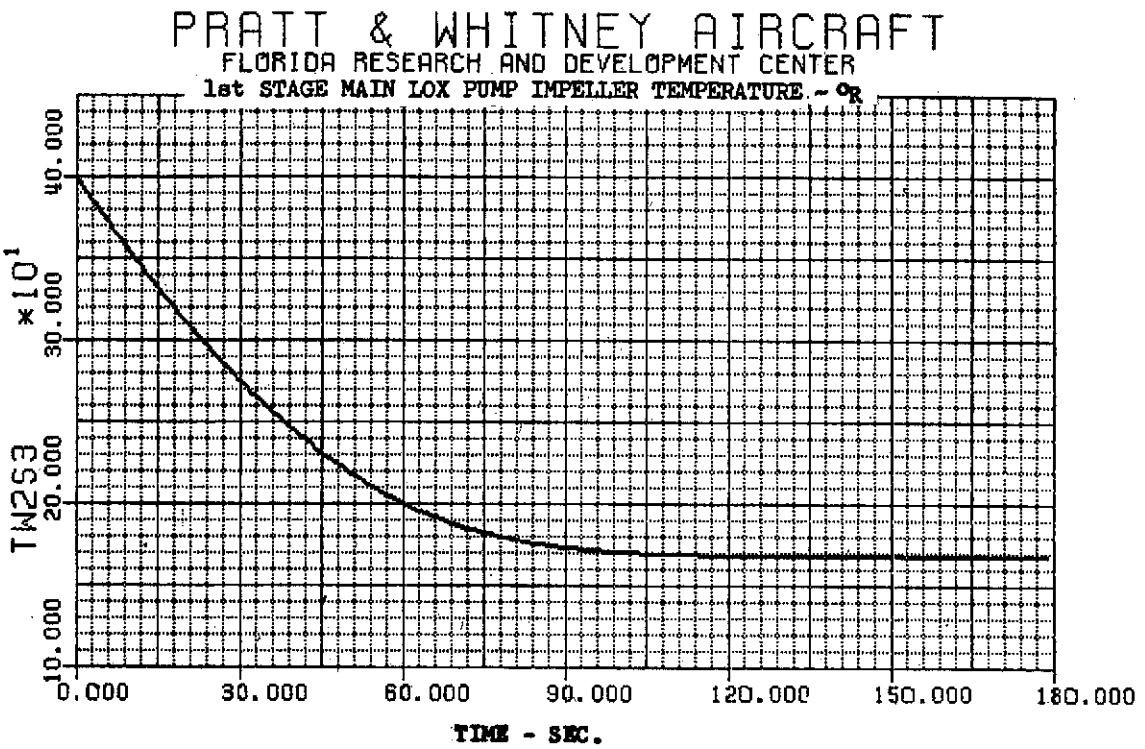

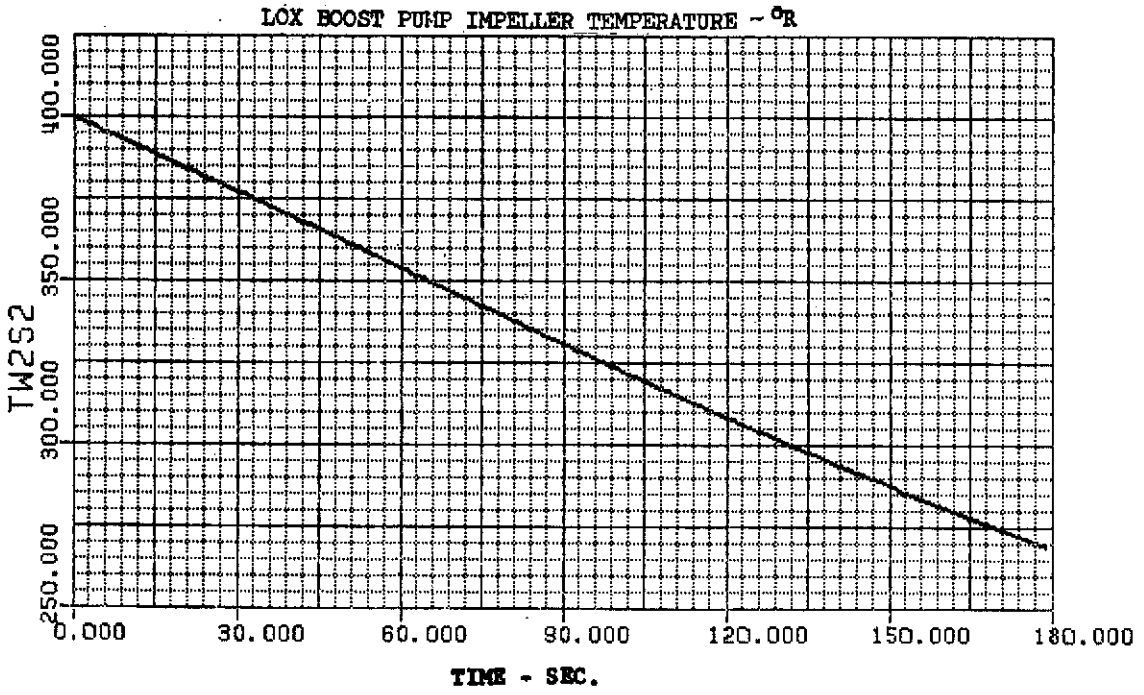

Figure 53. Tank Head Idle Cooldown - 1st Stage Main LO_2 Pump Impeller Temperature, LO_2 Boost Pump Impeller Temperature DF 96341

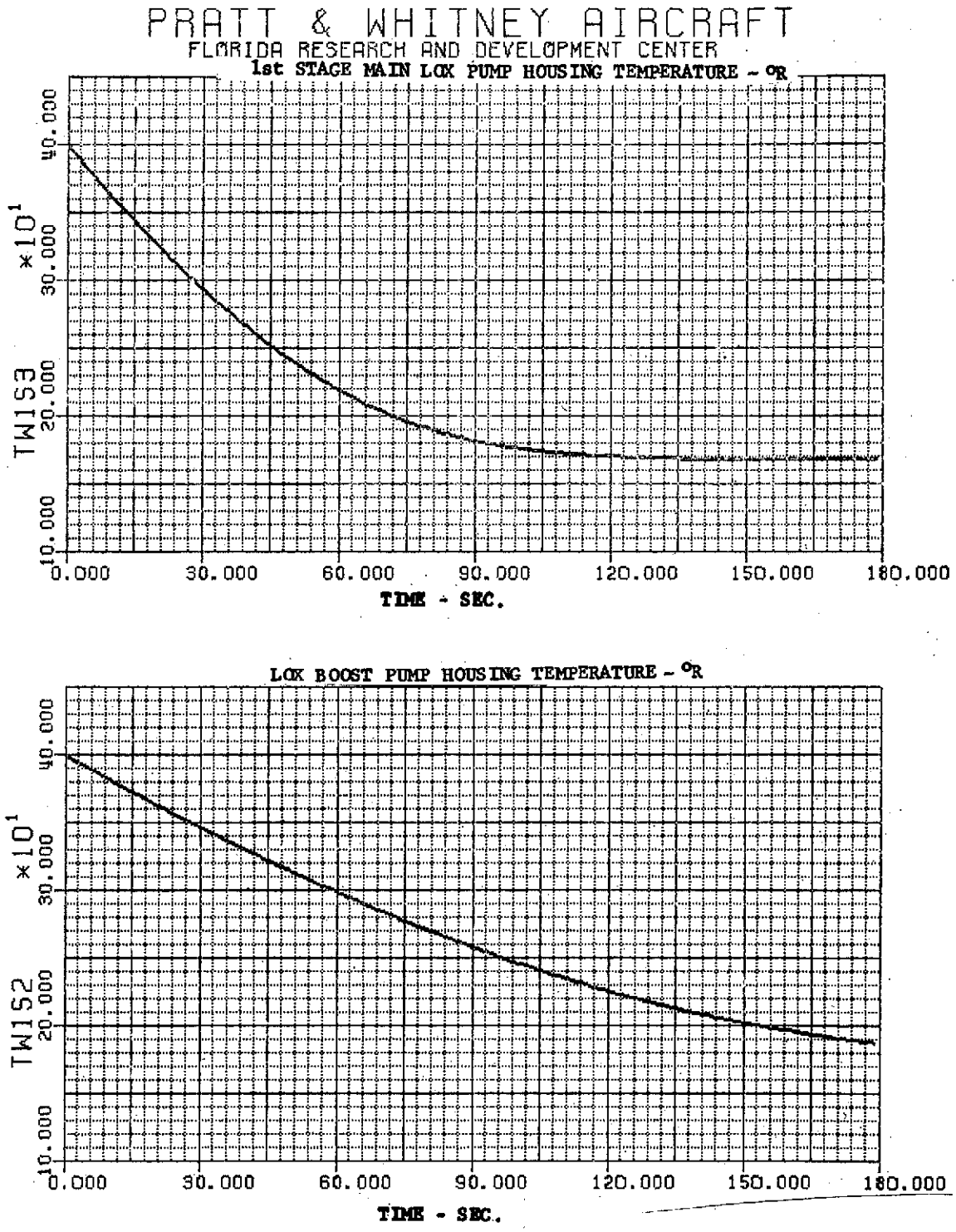

Figure 54. Tank Head Idle Cooldown - 1st Stage Main LO_2 Pump Housing Temperature, LO_2 Boost Pump Housing Temperature DF 96342

b. Turbopump Breakaway

At the conclusion of tank head idle, the control valves are sequenced to increase turbine pressure ratio and start turbopump rotation for pumped idle operation. During pumped idle the engine is operating as an expander cycle (preburner unlit). The turbine areas are designed for 1140°K (2050°R) combustion products, therefore with 305.6°K (550°R) fuel at tank head idle the turbine pressure ratios are low. The calculation of turbine zero speed torque has been substantiated with results from RL10 tests and predict that at breakaway the turbine torques will be 0.68 N-m (0.50 ft-lb) and 0.34 N-m (0.25 ft-lb) for fuel and oxidizer, respectively. The exact amount of friction that must be overcome has not been determined. The rubbing seals in the RL10 turbopump assembly require up to 7.9 N-m (70 in.-lb) of torque for breakaway. The liftoff seals of the 1.11 MN (250,000 lb) high pressure fuel pump required 1.36 N-m (12 in.-lb) of breakaway torque. The ASE oxidizer turbopump assemblies therefore use floating ring and hydrodynamic face seals in order to ensure a low breakaway torque. It is recommended that additional studies be made of turbine and pump breakaway to study methods of generating greater turbine power and to study seal designs to minimize friction.

c. Two-Phase Propellant Pumping

During tank head idle and acceleration to pumped idle, the propellant tanks will be at saturation conditions (zero NPSH). Line losses and heat leak will produce two-phase propellant at the engine inlets. The boost pumps will be required to start, accelerate, and pump with these conditions. Detailed studies and experimental tests should be conducted to determine the maximum quality at the inlet that will allow the boost pumps to produce pressure rise and to establish the pump performance while pumping two-phase propellant. It should also be established if the main pumps can pump two-phase propellants at zero NPSH or if the boost pumps must always supply positive NPSH to the main pumps. It is recommended that a detailed investigation of two-phase pumping be conducted beyond the scope of the ASE program.

D. ENGINE PHYSICAL CHARACTERISTICS

1. General

The following paragraphs present the physical characteristics of the fixed bell nozzle ASE configuration. Similar information, including a dimensional comparison of the ASE fixed nozzle and retractable nozzle configuration and the RL10A-3-3, is given in Section V, Engine Development Program Plans. Helium and electrical power requirements for the engine are also presented in Section V.

2. Engine Arrangement

The component arrangement for the ASE is shown in the installation drawings, figures 55 and 56. The engine dimension from the gimbal point (or gimbal center plane) to the nozzle exit plane is 229.1 cm (90.2 in.) and the gimbal face plane (engine reference plane) is 4.7 cm (1.85 in.) forward of the gimbal point for an overall length of 233.9 cm (92.07 in.). The maximum engine diameter occurs at the nozzle exit plane (ϵ = 400) and is 135.1 cm (53.2 in.).

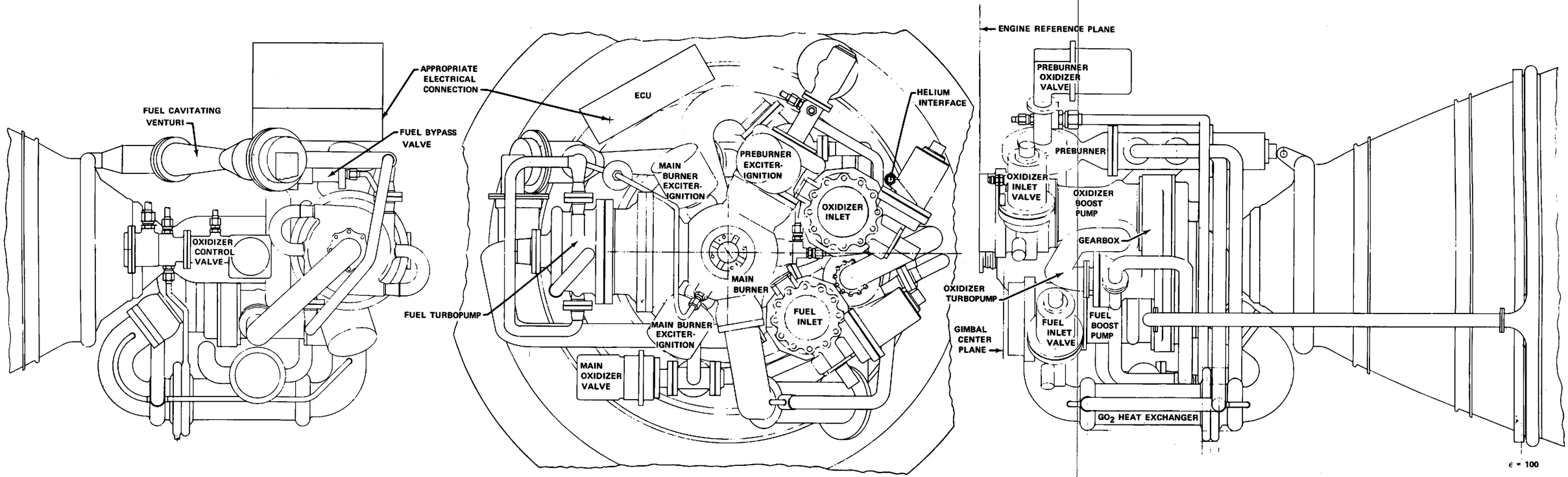

Figure 55. Advanced Space Engine Installation (Sheet 1)

FD 68857A

FOLDOUT FRAME 1

FOLDOUT FRAME 2

FOLDOUT FRAME 3

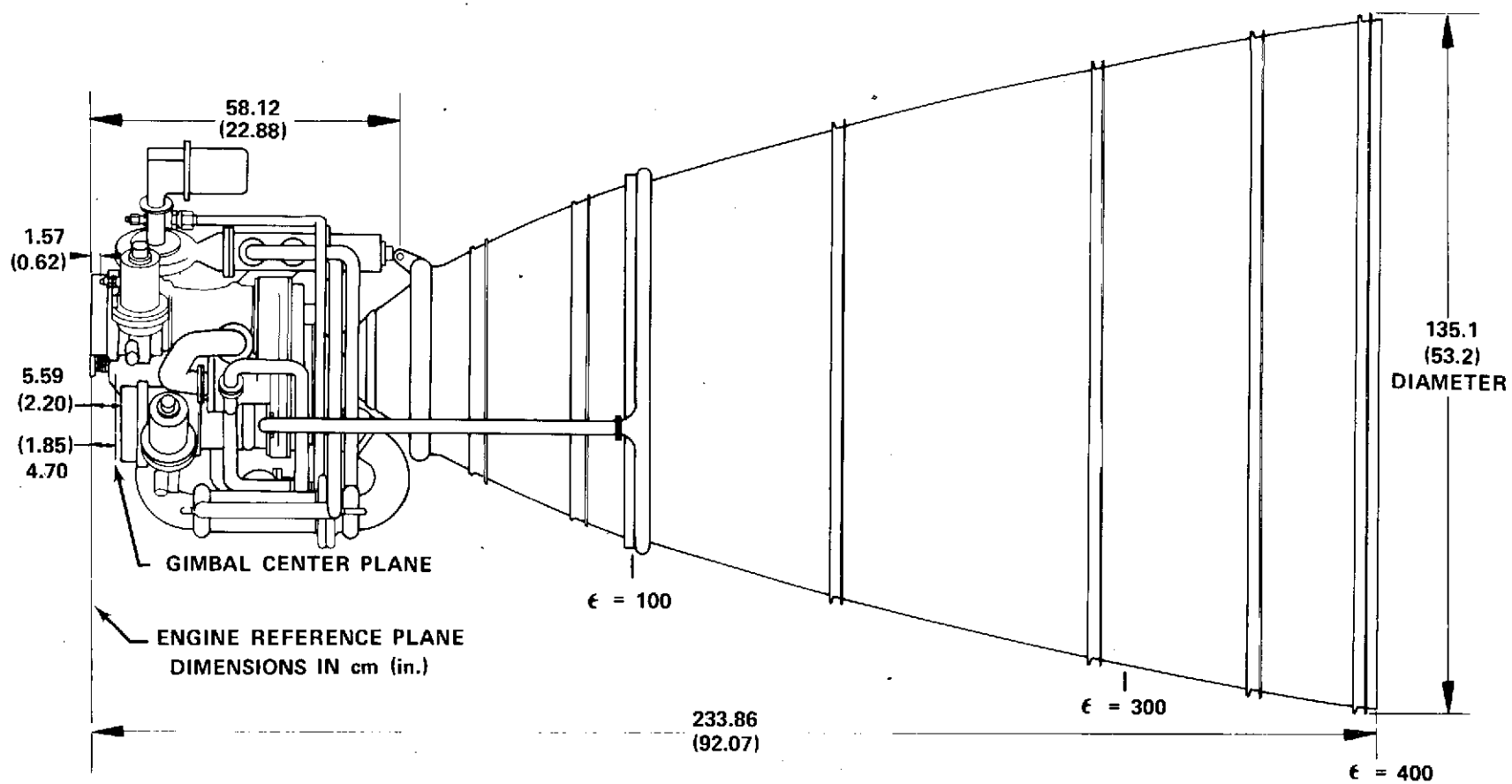

Figure 56. Advanced Space Engine Installation (Sheet 2)

FD 68858B

Gimbaling capability of ±0.122 rad (7 deg) through a square pattern is provided. Gimbaling actuator attach points are located on a stiffening ring on the main chamber downstream of the throat.

The centerline spacing between the fuel and oxidizer boost pumps is set at 21.5 cm (8.45 in.) to be the same as the RL10. However, the boost pump inlets are still located in as close to the engine centerline as possible to reduce gimbaling loads. The boost pump centerline spacing was selected by P&WA so that the ASE could be made more readily interchangeable with the RL10 by providing common vehicle/engine inlet interface locations. This is accomplished, as shown in Section V, Engine Development Program Plans, by repositioning the ASE oxidizer turbopump assembly (including the gearbox and boost pumps) on the engine.

The engine oxidizer and fuel inlets are the inlet flanges of the two inlet shutoff (suction) valves, which are mounted on the low pressure pumps. The oxidizer and fuel inlet ID's are 9.68 cm (3.81 in.) and 8.53 cm (3.36 in.), respectively.

The high pressure fuel turbopump and the preburner are mounted in a main case on top of the main chamber, which also contains the gimbal point. The fuel turbopump and preburner are plug-in units that can readily be removed and replaced to facilitate engine maintenance. The oxidizer turbopump is mounted separately with its centerline parallel to that of the thrust chamber; its turbine is supplied with preburner gases from the main case through a coaxial supply/return line.

The engine arrangement shown in figures 55 and 56 evolved as the one that minimized engine weight compared to a design with both turbopumps and the preburner mounted in the main case located at the side of the engine. Examination of estimated weights for the components showed that the main injector and main case both were relatively heavy, and that combining them would offer significant weight savings. Approximately a 6.3 kg (14 lb) reduction in weight was achieved in the final design.

The concept of a plug-in (into the main case) oxidizer high pressure turbopump proved to be impractical for a design in which the fuel and oxidizer low pressure pumps are driven by a gear system from the main oxidizer turbopump shaft. Locating the main oxidizer turbopump parallel to the thrust chamber centerline and outboard of the main case allowed the engine propellant inlets to be located close in. The coaxial preburner gas supply/return line provides a convenient location for the oxidizer heat exchanger for vehicle tank pressurization and eliminates the possible problems associated with hot plumbing lines.

3. Engine Mass Properties

a. Engine Weight and Center of Gravity

The final engine assembly dry weight was found to be 206.9 kg (456.3 lb). This is the present design weight, and the target weight for the final flight version of the ASE would be set at approximately 85% of this value to bring the weight to below 181 kg (400 lb). The weight of the turbopumps (including the low pressure pumps and gearbox) represents 23.3% of the total engine weight, and the thrust chamber 26.6%. The control system represents a major portion of the engine

weight, 36.1%, with the valves being the largest contributor, and it is in this system that the major effort to reduce engine weight would be made. The weight breakdown of the ASE, including target weights, is summarized in table XIII. Location of the engine center of gravity is shown in figure 57.

Table XIII. Advanced Space Engine Dry Weight Summary

Component	Design Weight, kg (lb)	Target ΔWeight, kg (lb)
1. High pressure fuel turbopump	19.1 (42.1)	-0.9 (-2)
2. High pressure oxidizer turbopump and gearbox	22.6 (49.9)	-0.9 (-2)
3. Low pressure fuel pump	2.6 (5.8)	-0.5 (-1)
4. Low pressure oxidizer pump	3.8 (8.3)	
5. Preburner	3.9 (8.5)	-0.9 (-2)
6. Main case	10.7 (23.5)	
7. Thrust chamber (to ϵ = 100)	22.5 (49.6)	-1.8 (-4)
8. Dump cooled nozzle	32.5 (71.6)	-6.3 (-14)
9. Controls:		
ECU	11.3 (25.0)	
Exciter-igniter (4)	7.4 (16.4)	
Fuel inlet valve	7.8 (17.1)	
Oxidizer inlet valve	8.2 (18.1)	
P/B oxidizer valve	5.5 (12.2)	
Main chamber oxidizer valve	5.4 (11.9)	
Fuel shunt valve	5.9 (12.9)	
Fuel bypass valve	1.3 (2.9)	
Fuel cavitating venturi	9.5 (21.0)	
Gox control valve	4.4 (9.8)	
Electrical harness	8.0 (17.6)	
Total Controls	74.7 (164.9)	-15.9 (-35)
10. Plumbing (includes GO_2 heat exchanger)	14.5 (32.1)	-1.4 (-3)
Total Design Dry Weight	206.9 (456.3)	-28.6 (-63)
Total Target Dry Weight		178.3 (393)

NOTE: Valve weights include weight of valve actuators.

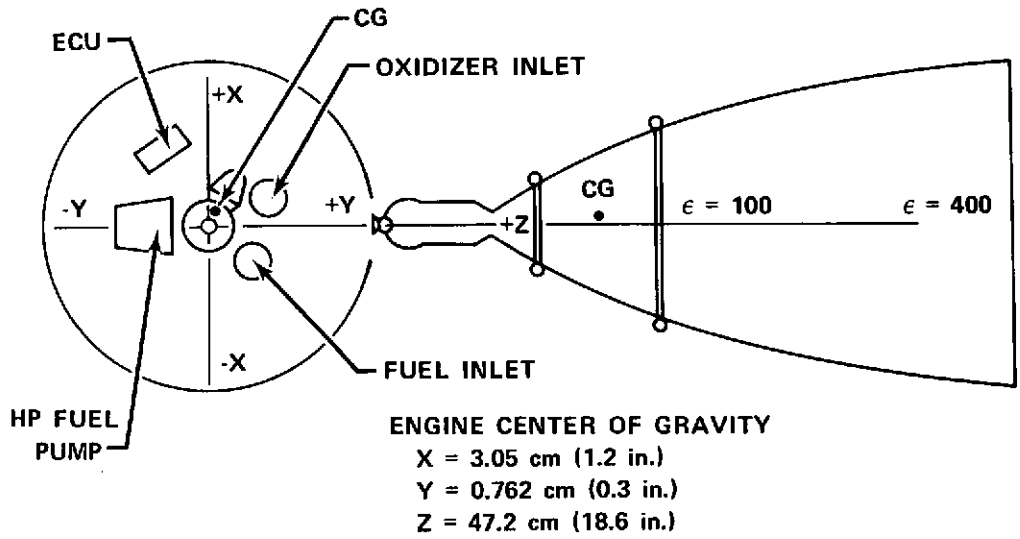

Figure 57. Advanced Space Engine Center of Gravity (Fixed Nozzle Configuration) FD 72114

b. Gimbaled Moment of Inertia

The engine can be gimbaled through a ±0.122 rad (7 deg) square pattern at rates not exceeding 20 radians/sec^2. The gimbaled moments of inertia are presented in table XIV. Figure 58 shows the ASE dynamic envelope.

Table XIV. Gimballed Moments of Inertia

I_{xx}, mm-kg-s^2 (in-lb-sec^2)	13,283 (1,155)
I_{yy}, mm-kg-s^2 (in-lb-sec^2)	13,110 (1,140)
I_{zz}, mm-kg-s^2 (in-lb-sec^2)	2,013 (175)

E. ENGINE SUBASSEMBLY/COMPONENT DESIGNS

1. General

This subsection provides operating characteristics and mechanical descriptions of the various engine subassemblies/components. The designs of the components for the ASE were based upon the requirements of cycle No. 104. The component operating characteristics presented herein reflect the results of the component design analyses which were then used to generate the engine characteristics presented in paragraph B, Engine System.

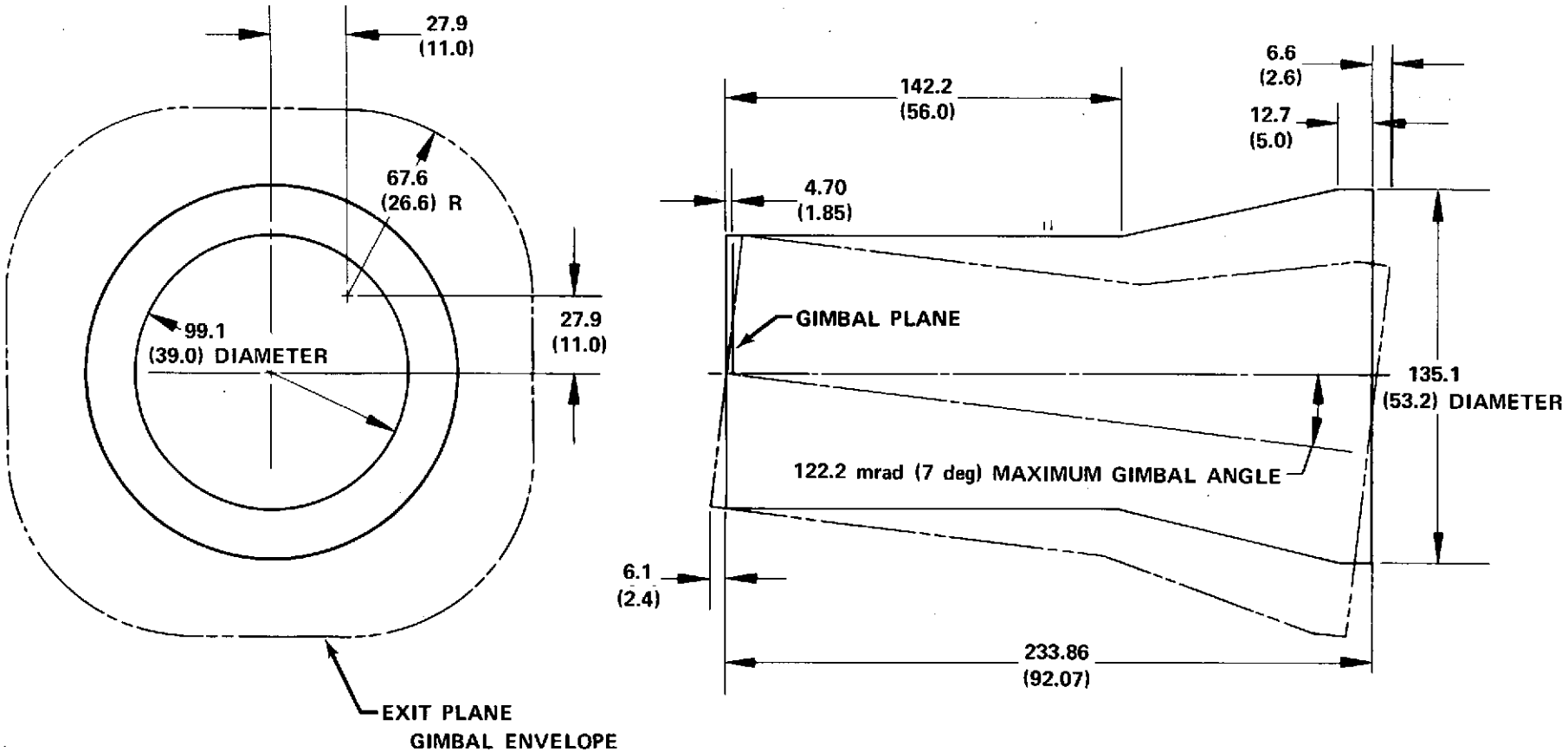

Figure 58. Advanced Space Engine (Baseline) Dynamic Envelope

FD 68854A

Figures and tables in this subsection are based upon the engine characteristics of the baseline cycle No. 104. The characteristics of final engine cycle No. 106 presented in section IV.B are only slightly different from those of cycle No. 104. These variances resulted from the differences in component performance estimates for the baseline cycle obtained from the OOS study compared to the performance obtained from the analytical evaluation of the ASE mechanical designs.

Ground rules supplied by the NASA/LeRC for the ASE preliminary design study have been reproduced and are presented herein.

NASA GROUND RULES FOR ADVANCED SPACE ENGINE

PRELIMINARY DESIGN

General

Components which are subject to a low cycle fatigue mode of failure shall be designed for a minimum of 300 cycles times a safety factor of 4.

Components which are subject to a fracture mode of failure shall be designed for a minimum of 300 cycles times a safety factor of 4.

Components which are subject to a high cycle fatigue mode of failure shall be designed within the allowable stress range diagram (based on the material endurance limit). If stress range material property data are not available, modified Goodman diagrams constructed as shown below shall be utilized.

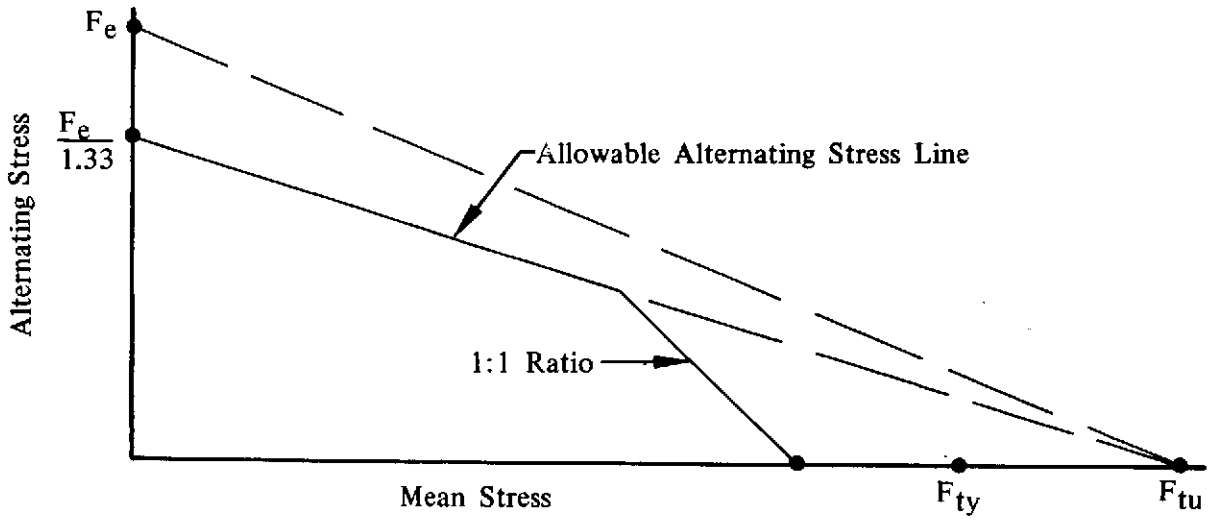

F_e = Material Endurance Limit
F_{ty} = Material Yield Strength (0.2% Offset)
F_{tu} = Material Ultimate Strength

Effective stress shall be based on the Mises-Hencky constant energy of distortion theory.

Unless otherwise noted under component ground rules specified herein, the following minimum factors of safety shall be utilized:

Factor of Safety (.2% yield) = 1.1 x Limit Load

Factor of Safety (Ultimate) = 1.4 x Limit Load

Limit Load: The maximum predicted load or pressure at the most critical operating condition

Components subject to pressure loading shall be designed to the following minimum proof and burst pressures:

Proof Pressure = 1.2 x Limit Pressure

Burst Pressure = 1.5 x Limit Pressure

Inducer

Inducer inlet NPSH shall not be less than the following:

LH_2, NPSH = 1.3 $cm^2/2g$

LO_2, NPSH = 2.3 $cm^2/2g$

Impeller

Inducers and/or impellers utilized in the high pressure pumps shall be designed for operation above incipient cavitation.

Impeller burst speed shall be at least 20% above the maximum operating speed.

Impeller effective stress at 5% above the maximum operating speed shall not exceed the allowable .2% yield stress. (Does not apply to areas in which local yielding is permitted.)

Turbine

Blade root steady-state stress shall not exceed the allowable 1% ten hour creep stress.

Stress state at the blade root as defined by the steady-state stress and an assumed vibratory stress equal to the gas bending stress shall be within the allowable stress range diagram or modified Goodman diagram.

No blade natural frequencies within ±15% of known sources of excitation at steady-state operating speeds.

Disk burst speed shall be at least 20% above the maximum operating speed.

Disk maximum effective stress at 5% above the maximum operating speed shall not exceed the allowable .2% yield stress. (Does not apply to areas in which local yielding is permitted.)

Bearings

Turbopump designs shall utilize rolling element bearings.

Maximum DN (mm x rpm):

	LO_2	LH_2	GH_2
Roller	1.5×10^6	2.0×10^6	$.5 \times 10^6$
Ball	1.5×10^6	2.0×10^6	1.2×10^6

B_{10} life ≥100 hours

Material:

Rolling Elements	440C
Races	440C

Seals

Turbopump designs shall utilize conventional type seals.

Face contact seal maximum PV, FV, and P_fV factors:*

	LO_2	LH_2	GH_2	$H_2 + H_2O$
PV Factor	25,000	50,000	20,000	10,000
FV Factor	2,000	4,000	1,500	800
P_fV Factor	60,000	200,000	50,000	20,000

*PV = unit load times rubbing velocity ($lb/in.^2$ x ft/sec)
FV = face load per unit length times rubbing velocity (lb/in. x ft/sec)
P_fV = fluid pressure differential times rubbing velocity (psig x ft/sec)

Gears (Hydrogen Gas Cooled)

Pitch line velocity (max) 20,000 fpm

Hertz stress (max) 60,000 psi

Material AMS 6260

Critical Speed

Rotor bending frequency shall be at least 25% above the rotor maximum operating speed.

A minimum margin of 20% shall be maintained between rotor rigid body critical speeds and rotor steady-state operating speeds at full thrust and the 6:1 throttled thrust condition. Rigid body critical speeds within the throttled-to-full thrust range shall be permitted only if deemed necessary by both the contractor Program Manager and the NASA Project Engineer.

Thrust Chamber

High heat flux portion of chamber shall be of nontubular construction. It shall be of milled construction with dimensional limits of:

minimum slot width = 0.030 in.

minimum slot depth/width = 4 to 1

minimum web thickness = 0.030 in.

minimum wall thickness = 0.025 in.

Use lightweight construction (tubular with high strength, high temperature alloys) starting at lowest feasible expansion ratio.

2. Low Pressure Pumps and Gearbox

a. Low Pressure Pumps

(1) General Description

Boost pumps, termed "low pressure pumps," are incorporated in both the fuel and oxidizer systems of the ASE design. The boost pumps provide the inlet NPSH conditions required by the high speed main pumps for operation without cavitation. The main pumps, in the interest of efficiency must be operated at rotational speeds too high for good suction performance. The low pressure pump designs, which have three-bladed, axial flow, helical pumping elements, provide the capability for operation at the engine inlet NPSH's of 6 N-m/kg (2 ft) for the oxidizer and 45 N-m/kg (15 ft) for the fuel. The oxidizer low pressure pump provides a pressure rise of 44.3 N/cm^2 (64.3 psi) and the low pressure fuel pump provides a pressure rise of 35.0 N/cm^2 (50.8 psi) at design point to supply the main pumps, which have maximum suction specific speeds of 34,000 and 13,000 respectively. Both low pressure pumps are gear driven from the main oxidizer turbopump shaft.

(2) Operating Characteristics

The hydrodynamic criteria and resultant geometric configurations selected for the ASE fuel and oxidizer boost pumps are based upon extensive test results and developed technology from several prior axial inducer programs. Primary emphasis for the boost pump designs was directed toward achievement of cycle suction requirements over the specified operating ranges of thrust level and mixture ratio, while providing sufficient head rise to preclude cavitation of the main fuel and oxidizer turbopumps.

Maximum suction requirements for both the fuel and oxidizer boost pumps occur at the maximum thrust, MR = 5.5 operating point. A peak suction specific speed level of 38,000 was selected for each pump at this condition, and is compatible with demonstrated values from several earlier designs.

One significant ground rule provided by the NASA/LeRC (Reference 5) to assure acceptable margin against inlet cavitation, established a maximum limit to the inlet fluid velocity as a function of the available NPSH,

$$\text{NPSH } (LO_2) = 2.3 \text{ cm}^2/2g = 2.3 \text{ x inlet velocity head}$$

$$\text{NPSH } (LH_2) = 1.3 \text{ cm}^2/2g = 1.3 \text{ x inlet velocity head}$$

The specified cycle NPSH requirements for the fuel and oxidizer boost pumps of 45 N-m/kg (15 ft) and 6 N-m/kg (2 ft), respectively, thus determined the required flow areas and resultant inlet diameters for the established cycle flowrates and maximum allowable velocities. Boost pump speeds were set in turn for each design by the selected values of suction specific speed, inlet diameter, and optimum inlet tip flow coefficient given by the suction performance correlations of figure 59.

Off-design suction capability for the fuel and oxidizer boost pumps is shown in figure 60. A linear falloff in capability with flow coefficient is used based on available inducer data as indicated in figure 59.

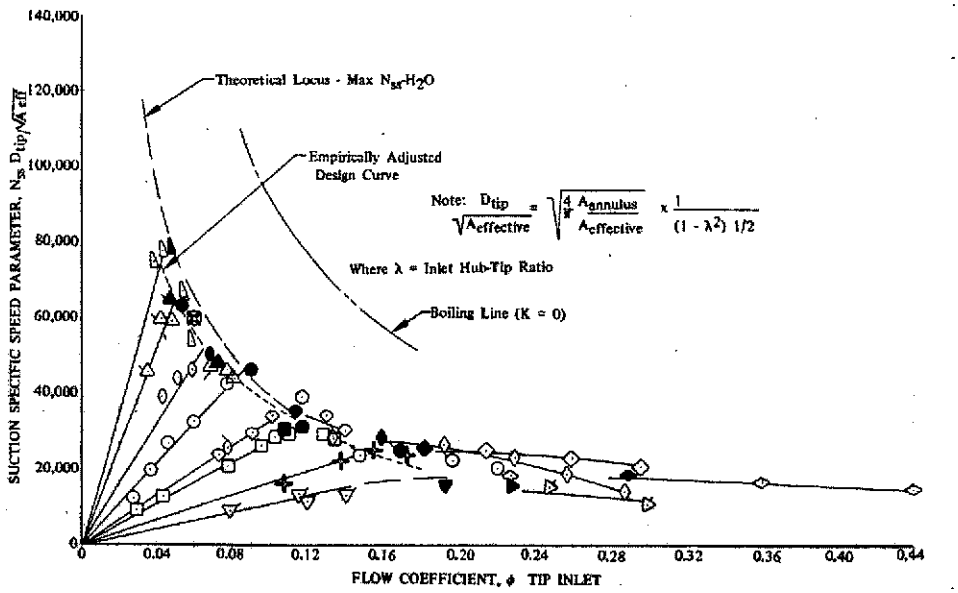

Figure 59. ASE Low Pressure Turbopump Suction Capability DF 95448

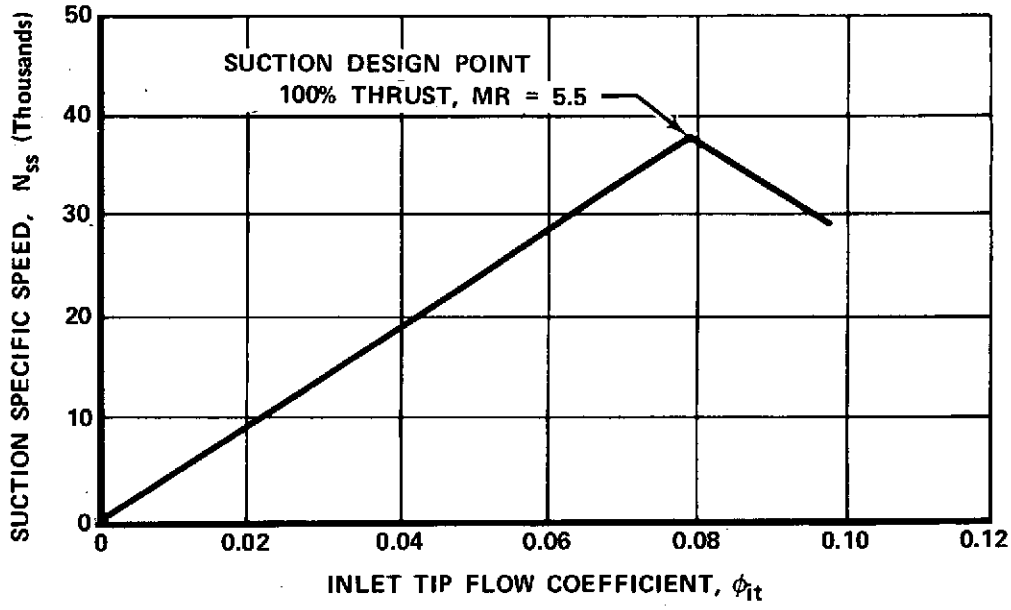

Figure 60. Advanced Space Engine Fuel and Oxidizer Boost Pump Design and Off-Design Suction Capability FD 68818

Head-flow and efficiency characteristics for both the fuel and oxidizer boost pumps were based directly upon empirical results from a series of model inducer tests conducted under a previous pump contract (Reference 6). Typical test results of one of the inducers, which formed the basis for the ASE boost pump designs, is given in figure 61. One modification to the inlet geometry of the tested configuration was required for the ASE designs because the inducer model was designed for, and tested at a lower suction capability than that selected for the ASE engine. This modification, illustrated in figure 62, uprates the suction specific speed capability from 32,000 to 38,000. The latter value is considered feasible in light of several past demonstrations on other designs.

As noted in the boost pump design tables (see table XIV), identical head and flow coefficients, efficiency, and specified speed characteristics were selected for both the fuel and oxidizer boost pumps. As a result, both designs are geometrically scaled versions of one another and of the tested inducer model, with the additionally uprated suction specified speed capability.

The collection system provided at the inducer exit is comprised of a single discharge axial volute and diffuser. The volutes are designed for a linear increase in area with circumference, resulting in a constant fluid velocity throughout the collector. Diffuser configurations were sized to provide acceptable area ratio without exceeding established empirical diffuser stall limits (Reference 7).

(3) Mechanical Description

(a) Oxidizer Low Pressure Pump

The oxidizer low pressure pump design is presented in figure 63. The oxidizer low pressure pump is driven at approximately 660 rad/s (6300 rpm) at

its 100% thrust, MR = 5.5 design point by the main oxidizer turbopump through a spur gear reduction of 9.35:1. All components of the boost pump, except for the drive gear and the aft tie bolt, are assembled in a single package to permit the pump to be unbolted as a unit from the drive gearbox. This feature allows servicing, and inspection or replacement of boost pump components without disturbing the gearbox and oxidizer turbopump components.

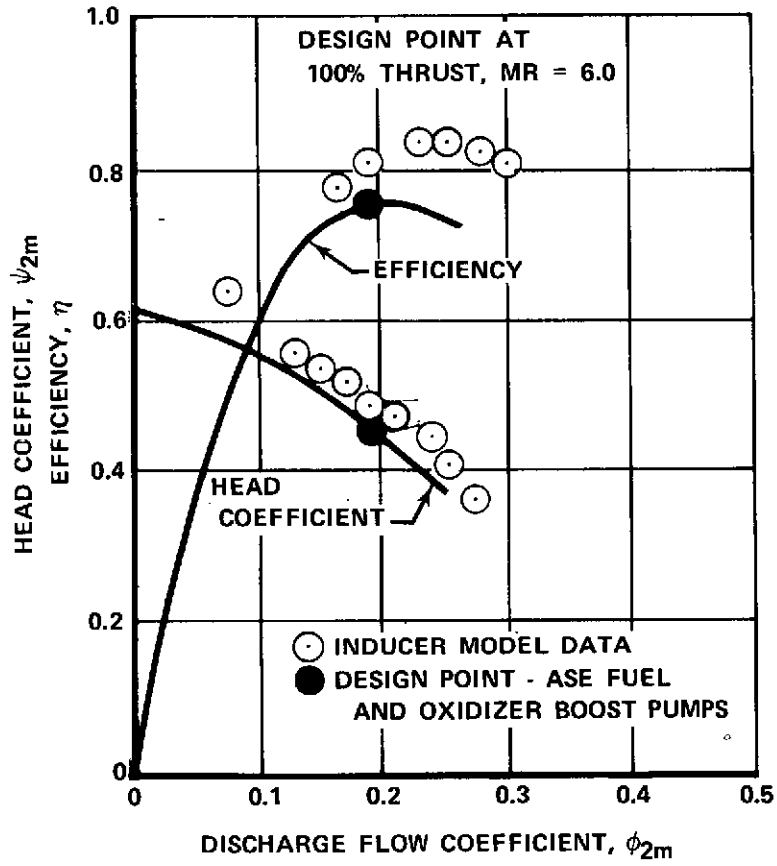

Figure 61. Advanced Space Engine Boost Pumps Head Coefficient - Efficiency Characteristics FD 68819A

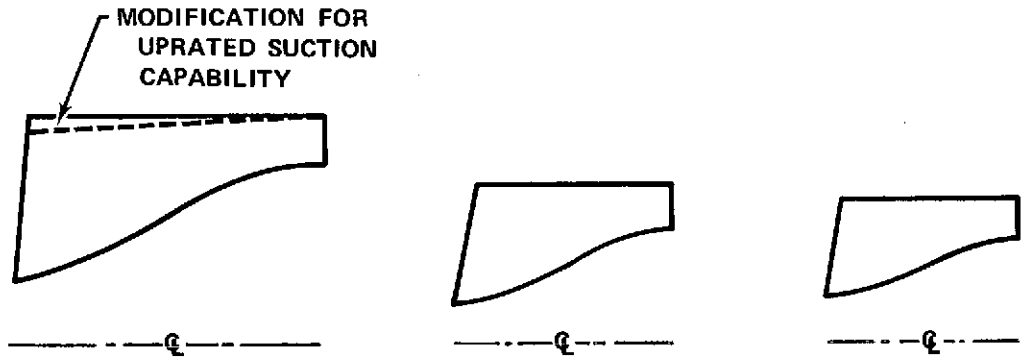

Figure 62. Inlet Geometry Modification Uprates Suction Capability FD 72389

Table XIV. ASE Low Pressure Pump Best Efficiency (BEP) Design Parameters, 100% Thrust, MR = 5.5

	Oxidizer	Fuel
Pump Speed, N, rad/s (rpm)	660 (6,300)	2,723 (26,000)
Weight Flow, $\dot{w}$, kg/s (lb/sec)	16.2 (35.8)	29.5 (6.51)
Specific Speed, N_S	2,700	2,700
Suction Specific Speed, $N_{SS_{max}}$	38,000	38,000
Mean Head Coefficient, Ψ_{2m}	0.45	0.45
Discharge Mean Flow Coefficient, ϕ_{2m}	0.195	0.195
Inlet Tip Flow Coefficient, ϕ_{it}	0.0788	0.0788
Head Rise, ΔH, N-m/kg (ft)	359 (120)	4,782 (1,600)
*Volumetric Flowrate, Q, m^3/s (gpm)	0.015 (241.5)	0.043 (684)
NPSH, N-m/kg (ft)	5.98 (2)	44.8 (15)
Efficiency, η, %	75.	75.
Power, kw (hp)	7.75 (10.4)	18.9 (25.3)
Inlet Tip Diameter, D_{it}, cm (in.)	9.68 (3.81)	8.53 (3.36)
Inlet Hub Diameter, D_{ih}, cm (in.)	2.9 (1.143)	2.56 (1.008)
Inlet Pressure, N/cm^2 (psia)	13.2 (19.1)	13.7 (19.9)
Inlet Temperature, °K (°R)	92.2 (166.0)	21.3 (38.3)
Discharge Pressure, N/cm^2 (psia)	53.7 (77.9)	47.0 (68.2)
Discharge Tip Diameter, D_{2t}, cm (in.)	9.68 (3.81)	8.53 (3.36)
Discharge Hub Diameter, D_{2h}, cm (in.)	7.32 (2.88)	6.45 (2.54)
Inlet Tip Blade Angle, β_{1t}^*, rad (deg)	0.122 (7)	0.122 (7)
Discharge Tip Blade Angle, β_{2t}^*, rad (deg)	0.524 (30)	0.524 (30)
Number of Blades	3	3

*At maximum temperature specified for ASE study, see table IV.

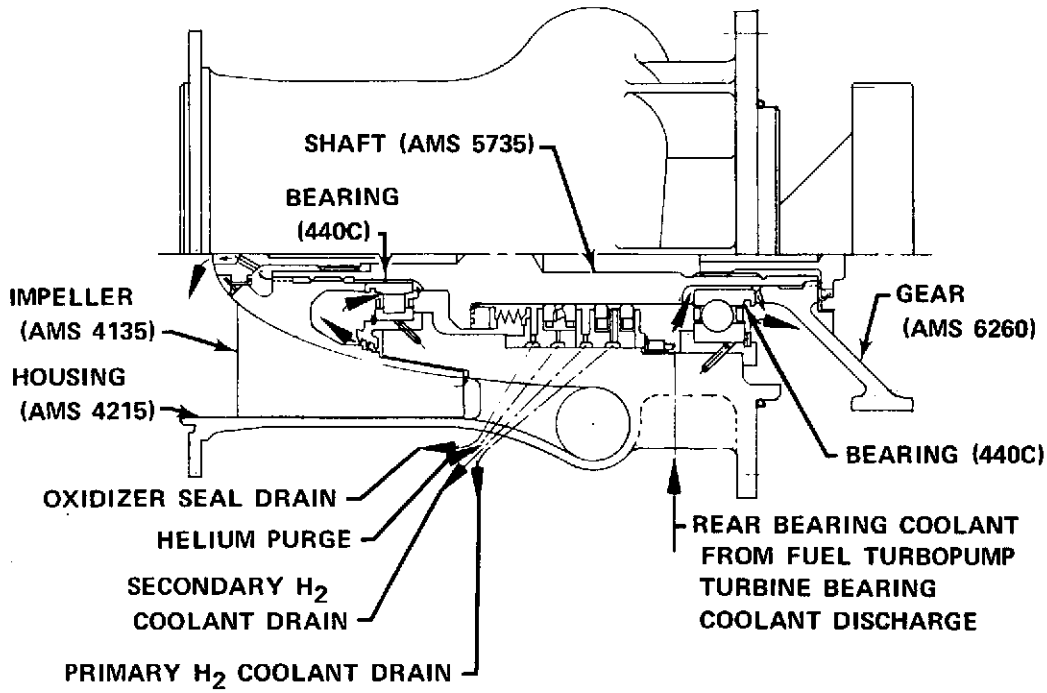

Figure 63. ASE Low Pressure Oxidizer Pump Design FD 72314

The rotor assembly of the low pressure oxidizer pump consists of the impeller, impeller drive shaft, bearings, drive gear and fore and aft tie rods.

The impeller is designed with three full wrapped blades, which are machined from an aluminum forging (AMS 4135). The selection of this material was based on its ease of fabrication, lightweight properties and compatibility with liquid oxygen. Substantiation of this material selection was based on RL10 experience, which used AMS 4135 for the fuel pump impeller, which had a diameter approximately that of ASE, 8.978 cm (3.535 in.), and operated at a speed of 3310 rad/s (31,625 rpm).

The axial flow impeller is piloted to the drive shaft at two locations. The use of twin pilots assures proper alignment of the impeller within the housing and resists the bending moment attributable to the hydraulic unbalance load of the impeller. This permits the establishment of close radial running clearances at the impeller tips needed for maximum performance. Impeller drive torque is supplied through loose fit splines located between the pilots. These splines are sized to a contact stress of 5516 N/cm^2 (8000 psi). This relatively low allowable stress is required because the separate pilots may prevent the splines from centering themselves under torque load because of eccentricity between spline pitch diameter and pilot diameters. This causes the spline tooth load to be less evenly distributed than when the parts are allowed to locate directly on the splines.

The impeller is secured axially by the forward tie rod, which is secured and piloted to the shaft. Tie rod loosening is prevented by providing slots in the impeller hub and mating slots in the tie rod to accommodate a tab type locking

device. The impeller is anodized per PWA 830-1, except for the impeller hub area which bears against the forward bearing race. To deter wear, this hub area is hardcoated per PWA 2468. The impeller hub tip fairing is formed by the contour head of the tie rod. To ensure minimal discontinuity at their junction, both the tie rod and impeller are piloted to the shaft.

The material selected for the oxidizer low pressure inducer shaft was A-286 (AMS 5735). This selection was based on the material's strength and thermal compatibility with the impeller material. The inducer shaft is also center-drilled for purposes of weight reduction.

The hydrodynamic seal rub surface on the shaft shoulder is chrome plated (AMS 2406) for wear resistance, and both this surface and the adjacent floating ring seal shaft surface are finished to a waviness height of 0.00051 mm (0.00002 in.) and a roughness height of 0.127 μm (5 μin.) The forward and aft bearing inner race seats are machined to tolerance conditions commensurate with RBEC Class 5 and ABEC Class 7 bearing tolerances, respectively. These inner race seats are also provided with slots for bearing under-race cooling.

The oxidizer boost pump drive gear is made of AMS 6260 material. This material was selected for its high strength, compatibility with hydrogen and its successful use as a gear material in a similar application in the RL10. The drive gear employs twin pilots to align it with the pump shaft and to offset the bending moment attributable to the tooth loads being out of plane with the hub centerplane. Minimizing the shaft overhang beyond the rear bearing dictated the conical shape of the gear web. The potential vibration problem attributable to the cone vs radial web is compensated for by increasing the web thickness of the former web configuration. The gear hub is secured to the shaft by the aft tie rod which is locked by means of a cup washer. Torque is transmitted by a lug engaging a shaft slot.

The oxidizer low pressure pump rotor assembly is supported by an LO_2-cooled, 17 x 40 mm roller bearing in front and an LH_2-cooled, 20 x 52 mm ball bearing in the rear, which operate at DN's of 0.107 x 10^6 and 0.126 x 10^6 mm-rpm, respectively. Both bearings operate at DN values less than the allowable 1.5 x 10^6 mm-rpm for a roller bearing in LO_2, or 2.0 x 10^6 mm-rpm for a ball bearing in LH_2, respectively. The rear bearing is sized to carry the combined thrust and radial load of the system. The combined load was calculated to be 3314N (745 lb) resulting in a bearing life of 133 hours, which is well above the 100 hour design requirement. The front bearing is loaded radially by the impeller hydraulic unbalance load of 2669N (600 lb), and has an estimated bearing life of 648 hours. The front bearings of the oxidizer fuel boost pumps may be identical in design if the results of a fit and clearance analysis indicate that the oxidizer and fuel bearing internal geometries are compatible. If the aforementioned is not possible, these bearings would be similar in design maintaining as many standard and common features as possible to minimize cost. The bearings are constructed from 440C material, as required by the study design ground rules. This material has high strength and is compatible with both oxygen and hydrogen environments and was successfully used as a bearing material in the RL10 engine.

It is important to note that rotation of the bearing race relative to its support causes wear and results in failure of the bearing to perform its function. Therefore, each bearing inner race has an interference fit with the shaft and is prevented from rotating relative to the shaft by an axial pinch load. The forward bearing axial load is applied by means of the forward tie rod loading through the impeller hub. The rear bearing pinch load is applied through the drive gear hub by means of the aft tie rod. Each bearing outer race is encased within a stainless steel liner (AMS 5646), which is pinned into the pump housing as shown in figure 63. These liners are required because the bearings would otherwise be installed in housings of a more pliant material than the bearing race. The dissimilar thermal expansion properties of the bearing and housing materials could cause undesirable changes in the bearing fits. The function of the bearing liner is to hold the bearing in a fixed position and maintain the capability of being replaced without subsequent damage to the pump housing. A design study revealed that the paramount advantage of using pinned liners over flanged (bolt-on) liners, is that upon initial installation the required tight fit between the pinned liner and housing reduces the probability of alignment disorders. Because alignment is critical to bearing life, this advantage coupled with the slight weight and cost decrease resulted in the use of the pinned liner instead of a bolted-on liner.

The bearing liner ID is carburized to resist galling and wear. Specific dimensions were selected to ensure that the liner would tighten at operating conditions to preclude the possibility of outer race spinning. The outer race is retained axially by a spiral lock ring. The forward bearing liner incorporates an integrally machined labyrinth seal thereby eliminating the need for a separate seal and its inherent positional tolerances and retention features. The location of the knife edges with respect to the shaft pilot surfaces and the location of these surfaces to the lands on the impeller hub can be closely established. These considerations allow for the establishment of close seal running clearances because position tolerance and eccentricity between the seal knife edge and the land will be minimal.

Recirculated LO_2 is supplied for cooling the forward bearing of the oxidizer boost pump. Boost pump discharge LO_2 leaks through the labyrinth seal, circulates through the rollers, reverses direction and exits under the bearing race. The LO_2 flows forward between the impeller hub and the shaft through slots and omitted splines until it reaches the impeller dome cavity. The LO_2 then exits to the impeller inlet through holes and is recirculated through the pump. The estimated coolant flow requirement for this bearing is 0.0038 kg/s (0.00835 lb/sec). The rear bearing coolant, hydrogen, originates from the main fuel pump turbine bearing coolant discharge. An external supply line introduces this coolant to the rear bearing compartment where it circulates under the rear bearing race through shaft slots. The coolant flow exits from the bearing and enters the gearbox cavity. The estimated hydrogen coolant flow requirement for this bearing is 0.0038 kg/s (0.00835 lb/sec).

Rotor dynamic analysis indicated the first critical speed to be a bounce mode at 8290 rad/s (79,184 rpm) with a span strain energy of 23.9%. This first critical speed represents a 1157% margin over the nominal operating speed. The second and third critical speeds occurred at 14,100 rad/s (134,444 rpm) and 25,000 rad/s (238,473 rpm), respectively.

The oxidizer boost pump housing is a one-piece aluminum casting (AMS 4215), which incorporates the impeller running area, the forward and aft bearing supports, the seal package support, and the volute collector and discharge diffuser horn. Minimum pump housing weight was realized by the selection of aluminum material. The aluminum has adequate strength to resist the hydraulic and external forces generated by the ASE application.

The bearing supports are machined into the fore and aft ends of the housing. The liners are installed with a slight interference fit and subsequently pinned onto these surfaces at assembly. The seal support surface within the housing is anodized to preclude galling due to axial nut load and radial, thermally-induced, loading between the seal components and the housing. A 0.279 mm (0.011 in.) fluorocarbon plastic coating is provided in the region of the impeller blades in the housing to minimize erosion and to prevent metal-to-metal contact in the event of high speed rubbing between impeller tips and housing material. Attainment of satisfactory performance requires close running radial clearances of 0.0127 mm (0.005 in.) at the impeller tips, and this coating will provide protection in case of transient rubbing. The volute collector is one of the increasing cross sectional areas which provides for a constant peripheral fluid velocity. A number of support vanes interconnect the inner and outer housing structures. Vanes are required for strength and contain drilled access holes for the seal package fluid drain and supply. To minimize weight while providing adequate strength, fins are cast into the pump housing between the volute collector and the attachment flange. These fins provide an increased moment of inertia to withstand bending moments at the otherwise reduced housing section.

Fuel and oxidizer at either end of the oxidizer boost pump are prevented from mixing by a seal package. This seal package is identical to the LO_2 turbopump seal package, whose components are entirely interchangeable with the boost pump components, requiring only the addition of a spacer. This spacer, located at the aft end of the package, compensates for the fact that the spanner nut and direction of loading is reversed between the main and boost pump stackups. Although this seal package is overdesigned for the boost pump application, it is felt that the cost savings inherent in developing a common seal package justifies its use in the boost pump. A detailed description of this seal package is presented in paragraph E4, Oxidizer High Pressure Turbopump.

(b) Fuel Low Pressure Pump

The fuel low pressure pump design is shown in figure 64. The fuel low pressure pump is driven at 2723 rad/s (26,000 rpm) at its 100% thrust, MR = 5.5 design point by the main oxidizer turbopump through a gear reduction of 2.26:1. All components of the fuel boost pump are assembled in one package to facilitate removal of the pump from the gearbox.

The rotor assembly of the fuel boost pump consists of the same elements as in the oxidizer boost pump, except for the addition of a rear labyrinth seal. This seal has an interference fit with the shaft and provides bearing coolant flow control. Both the seal and shaft are constructed of the same material, AMS 5663, to achieve thermal compatibility. The impeller is designed with three full-wrapped blades that are machined from a titanium forging (AMS 4924). Titanium was selected because of its low weight, high strength, and shaft thermal and hydrogen

compatibility. All other components of the rotor assembly are similar to corresponding oxidizer pump rotor assembly components in design considerations, materials and configuration.

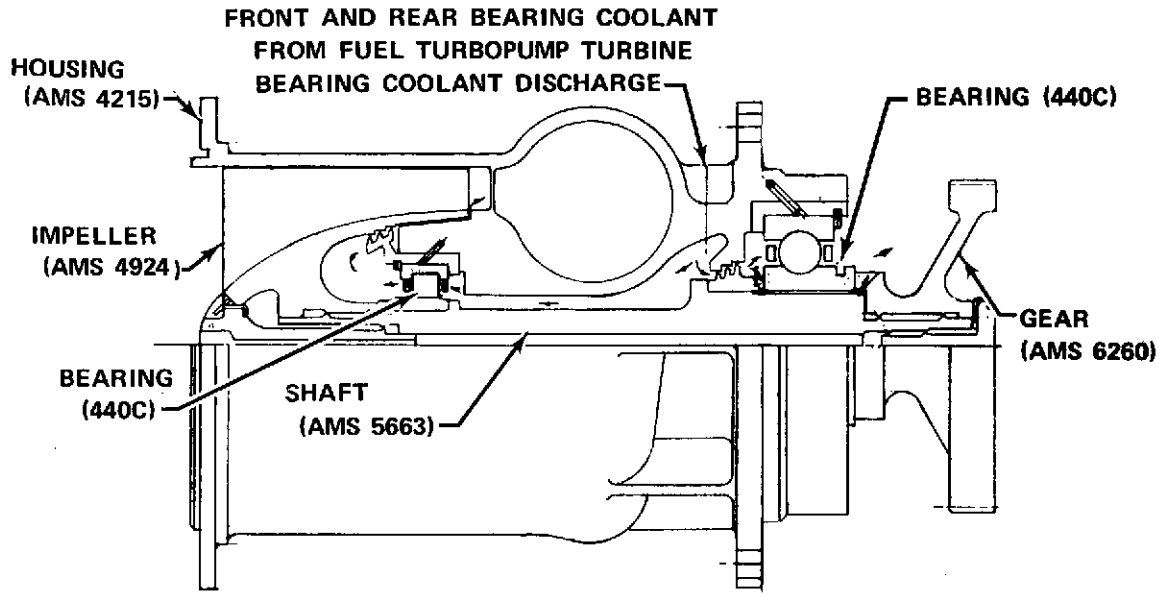

Figure 64. ASE Low Pressure Fuel Pump Design FD 72315

The fuel low pressure pump rotor is supported by a 17 x 40 mm front roller bearing and a rear 25 x 62 mm, ball bearing. These bearings operate at DN values of 0.442×10^6 mm-rpm and 0.650×10^6 mm-rpm, respectively. Both bearings are operating at DN values well below the allowable DN of 2×10^6 mm-rpm for ball and roller bearings operating in LH_2. The rear bearing is sized to carry the combined thrust and radial load of the system. The combined load is calculated to be 2860N (643 lb) resulting in a bearing life of 119 hours. The front bearing is loaded radially by an impeller hydraulic unbalance load of 2148N (483 lb) and results in a bearing life estimated at 333 hours.

The provisions used on the oxidizer boost pump for bearing race retention and antitorque are similarly taken for the fuel pump bearings. Material selections for bearings and liners are identical for the two pumps. Hydrogen cooling flows for the forward and rear bearings are supplied from the same source as for the oxidizer boost pump rear bearing. The coolant flow is introduced into a cavity in the pump housing. Front and rear bearing coolant flow is controlled by leakage from this cavity through labyrinth seals. Under-race cooling is provided at the rear bearing by means of slots in the shaft. The coolant flow to the forward bearing is recirculated to the fuel boost pump discharge volute. The coolant to the rear bearing enters the gearbox and continues its cooling function. The estimated coolant flow to each of these bearings is 0.0113 kg/s (0.025 lb/sec) to the rear and 0.0076 kg/s (0.0167 lb/sec) to the forward bearing.

Rotor dynamic analysis indicated the first critical speed to be a bending mode at 6650 rad/s (63,764 rpm) with a span strain energy of 60%. This first critical speed represents a 145% margin over the design point speed of 2710 rad/s (26,000 rpm). The second and third critical speeds occurred at 9370 rad/s (94,912 rpm) and 24,400 rad/s (234,206 rpm), respectively.

The housing of the fuel boost pump is made of AMS 4215 aluminum. The housing design features and considerations are similar to those for the oxidizer boost pump, except for the omission of seal package installation provisions in the housing which are not required for the fuel boost pump.

b. Turbopump Gearbox

The ASE turbopump gearbox design is shown in figure 65. The main oxidizer turbopump drives the gearbox, which in turn drives the oxidizer and fuel boost pumps. The gearbox has a two-piece housing that is piloted to maintain critical dimensions at assembly. The two-piece configuration of the gearbox is required for ease of assembly. To provide a compact package, the front gearbox housing is common with the oxidizer turbopump housing, whereas the rear gearbox housing mates with the oxidizer turbopump turbine housing.

The gearbox housing is fabricated from forged rings and sheet metal of A-286 (AMS 5735) material. This material selection was dictated by thermal compatibility considerations at the high pressure turbine flange. Strength requirements in the turbine area of the turbopump necessitate the use of A-286 material. To ensure a positive seal at the high pressure flange formed by the gearbox and the turbine dome, A-286 material is used for the gearbox, which will eliminate thermal incompatibility at this critical junction. Thermal incompatibility considerations at the gearbox split line indicated that the front housing should also be of A-286 material. A critical item of concern with respect to achieving the 10-hr life requirement for gears is alignment. Close alignment of all gears is more easily attained by cantilever mounting all gear and pump shafts from a common housing, i.e. the front housing, than by straddle mounting of the gear and pump shafts between the front and the rear housings. Misalignment of the gears due to housing deflections is also minimized in this fashion.

The hydrogen from the gearbox is supplied to the dump cooled nozzle through a boss located on the gearbox front housing. This location was selected to provide ease of egress of the required plumbing to the nozzle and because it was centrally located with respect to flow removal. Removing the hydrogen at a central location ensures that no stagnant areas affecting cooling exist within the gearbox.

The remaining major feature of the gearbox housing is the access boss, which allows unplugging of the oxidizer boost pump from the gearbox. As shown on figure 66, the pump drive gear will not clear the intermediate shaft front bearing. Several attempts were made to permit this by sizing various gear meshes. All these arrangements led to unacceptable package sizes and violated various ground rules. Therefore, a boss is provided on the gearbox housing, which permits access to the pump shaft tie rod without disassembly of the aft end of the LO_2 main pump and gearbox. Removal of this tie rod allows the boost pump to be removed from the gearbox pad while leaving the drive gear enclosed. The gear is provided with three equally spaced lands on the web, which engage the boss and center the gear after the pump shaft is removed. Three equally spaced lugs on the gearbox housing engage the gear rim to allow the pump shaft to be pulled from the gear bore. Upon reassembly, the gear engages the boss, which provides resistance and allows the shaft to be centered and pulled into the bore by the tie rod. The boss also precludes the possibility of dropping the tie rod into the gearbox assembly. This provision serves a secondary purpose by providing access for a preflight torque check.

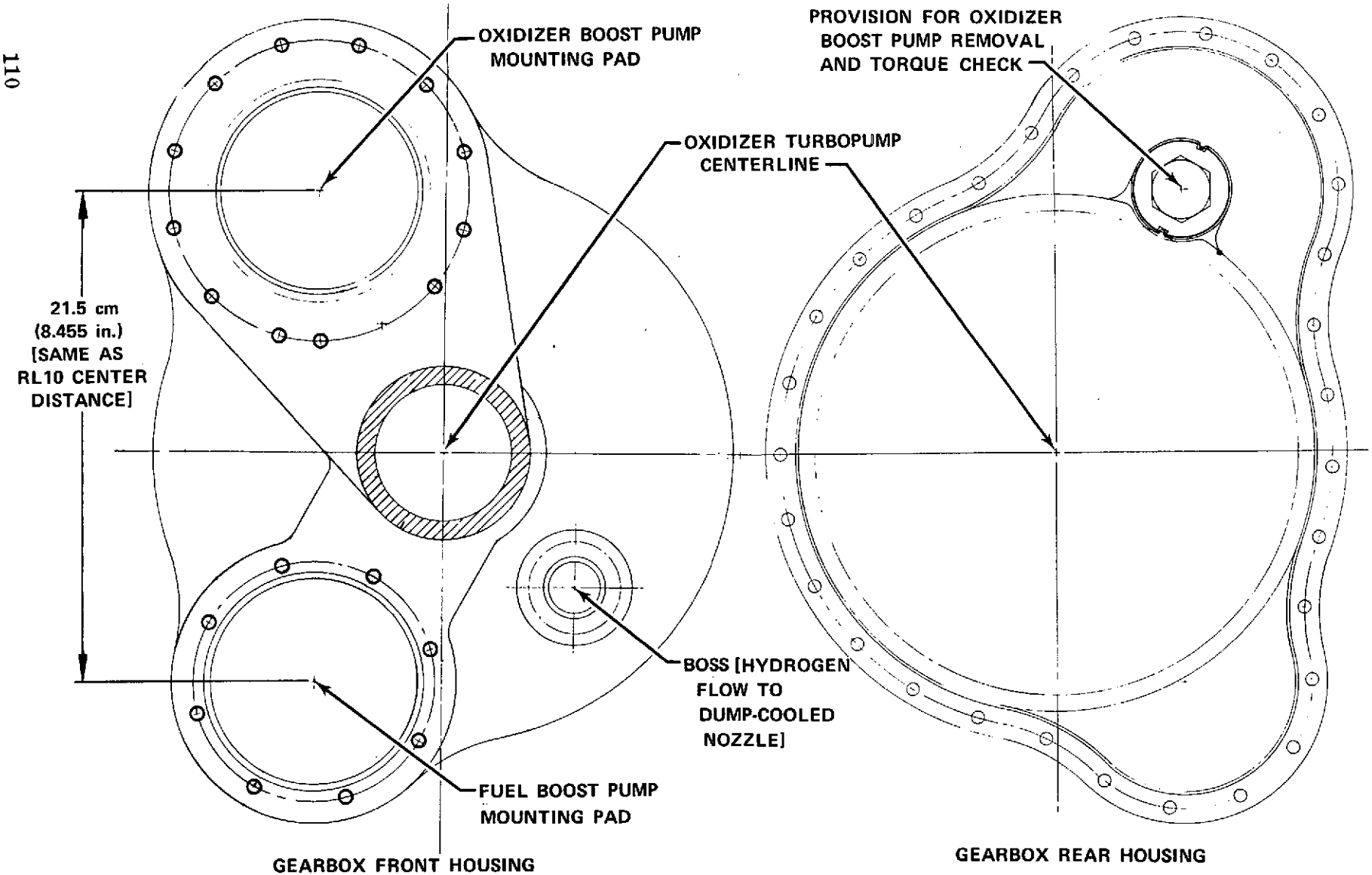

Figure 65. ASE Gearbox Housing Exterior Configuration

FD 72388

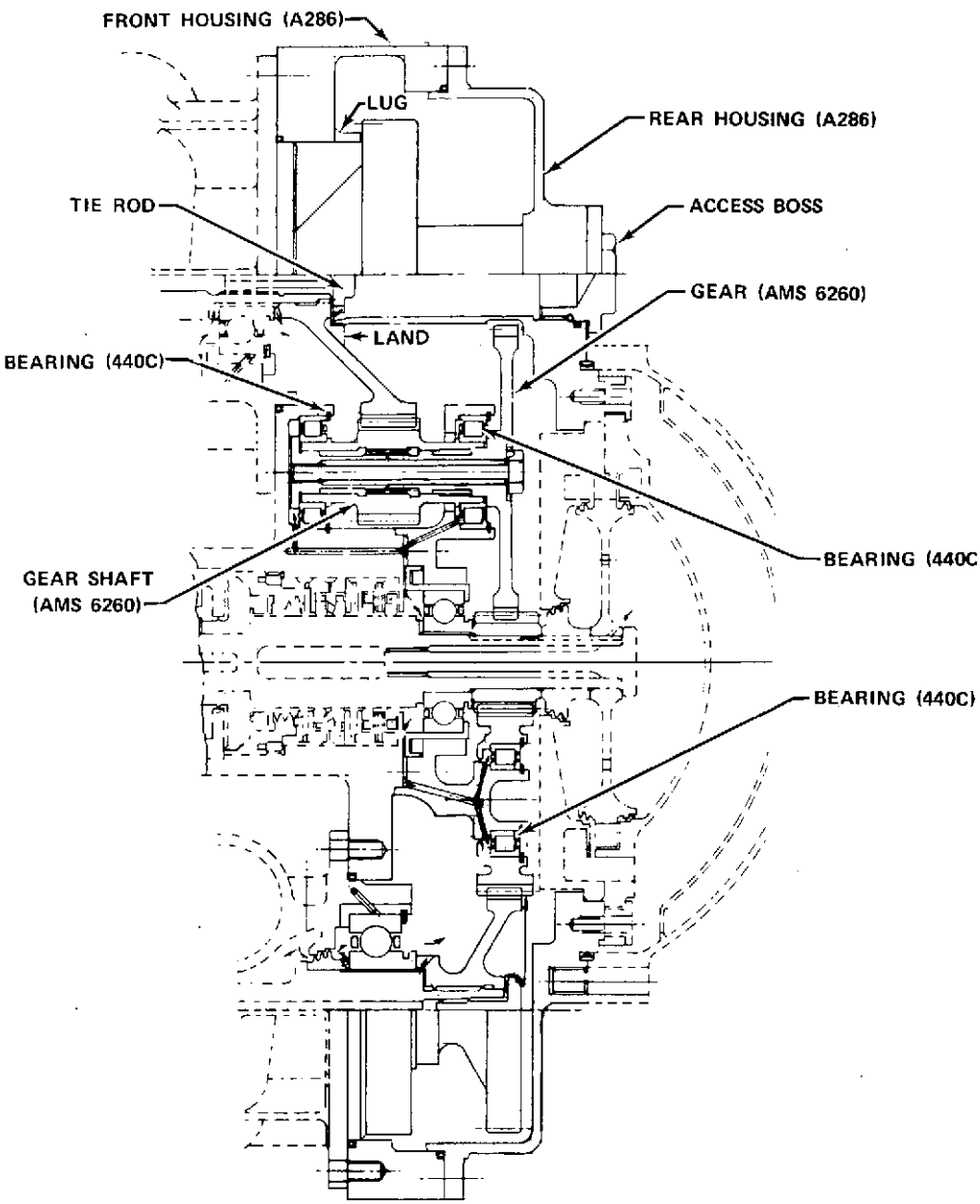

Figure 66. ASE Turbopump Gearbox FD 72316

The final gearbox housing configuration was established by considering several factors. These were:

1. Providing gear reductions that give the proper speeds at the boost pump pads

2. Ensuring that the gear reductions comply with P&WA and the NASA gear design criteria

3. Providing a minimum gearbox package

4. Maintaining the RL10 center distance of 21.5 cm (8.455 in.) between the oxidizer and fuel boost pump inlets

5. Providing an unplugging feature for the oxidizer and fuel boost pumps.

The oxidizer low pressure pump (boost pump) is driven at 660 rad/s (6300 rpm) by the oxidizer turbopump through a spur gear reduction of 9.35:1. This reduction gearing consists of an LO_2 turbopump mounted pinion gear, an intermediate shaft driven-gear and secondary pinion, and a boost pump mounted drive gear. These gears transfer a maximum of 12.0 kw (16.11 hp) for driving the oxidizer boost pump. The oxidizer pump drive gears give a 9.35:1 speed reduction through two steps, 3.1:1 and 3.02:1. The intermediate shaft consists of two parts (for ease of assembly), which are piloted at two places for maximum alignment. A single tie rod is used to axially load the two bearing inner races and to tie the two shaft pieces together. Torque transmission is accomplished with a common spline. The intermediate shaft is supported by two hydrogen-cooled 20 x 37 mm roller bearings. These bearings are interchangeable and the maximum load carried by either bearing is 445N (100 lb). The bearing life is estimated to be 49,500 hours. The bearings operate at a DN value of 0.382×10^6 mm-rpm, which is well below the allowable value. The bearing outer races are retained with spiral lock rings and have tight operating fits to prevent rotation. One bearing support is machined into the main LO_2 pump housing while the other is one of two local projections from the main LO_2 pump bearing support. Alignment of the intermediate shaft from one bearing to another is maintained by a pilot diameter between the separate bearing support structures. The bearing material is 440C while that of the intermediate shaft is AMS 6260. The aforementioned material selection was based on the criteria used in selecting the gear and bearing material for the oxidizer and fuel boost pumps. Final gear sizes and pertinent design information for the oxidizer boost pump drive gear are contained in the gear data table in figure 67.

Cooling for the intermediate shaft support bearings originates from the main oxidizer turbopump rear bearing coolant discharge. This hydrogen flow is routed to each intermediate shaft bearing through a series of slots and drilled passages in the bearing support structure. Although this coolant flow has properties very much the same as the hydrogen filling the gearbox cavity, the fact that the coolant is flowing and not stagnant will provide bearing cooling by transporting the heat away from its generation source. The required coolant flow to each bearing is estimated to be 0.0038 kg/s (0.00835 lb/sec).

GEAR NUMBER	PITCH DIAMETER, mm (in.)	PITCH LINE VELOCITY, m/min (fpm)	ROTATIONAL SPEED, rad/s (rpm)	MINIMUM FACE WIDTH, mm (in.)	HERTZ STRESS, N/cm^2 (psi) / PRESS ANGLE, rad (deg)	POWER, kw (hp)	TORQUE, N-m (in. - lb)	UNIT LOAD, N/mm (lb/in.)
1	30.48 (1.200)	5,638 (18,500)	6,161 (58,846)	15.24 (0.600)	41,369 (60,000) / 0.436 (25)	12./26. 16.11/34.79)	1.95/4.20 (17.25/37.2)	356 (2,010)
2	94.08 (3.704)	5,638 (18,500)	1,996 (19,064)	6.17 (0.243)		12 (16.11)	6.03 (53.4)	401 (2,265)
3	32.21 (1.268)	1,929 (6,330)	1,996 (19,064)	17.07 (0.672)		12 (16.11)	6.03 53.4	436 (2,465)
4	97.92 (3.855)	1,929 (6,330)	657 (6,272)	17.07 (0.672)		12 (16.11)	18.36 (162.5)	436 (2,465)
5	65.02 (2.560)	5,638 (18,500)	2,890 (27,600)	15.24 (0.600)		26 (34.79)	8.98 (79.5)	356 (2,010)
6	69.20 (2,720)	5,638 (18,500)	2,722 (26,000)	9.04 (0.356)		26 (34.79)	9.51 (84.2)	587 (3,310)

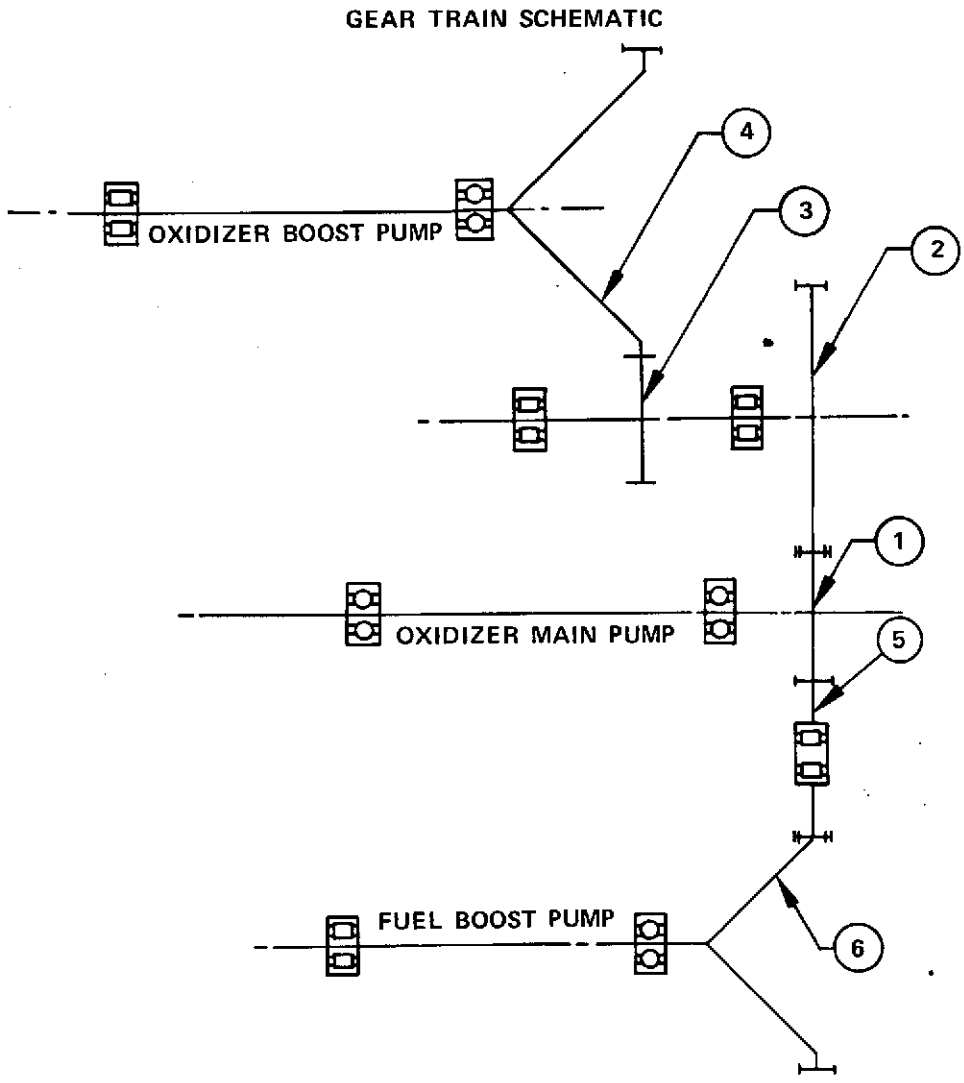

Figure 67. Advanced Space Engine Turbopump Gearbox Gear Data Table FD 71596

The fuel low pressure pump (boost pump) is driven at 2723 rad/s (26,000 rpm) at its BEP by the oxidizer turbopump through a gear reduction of 2.26:1. This reduction gearing consists of an LO_2 turbopump mounted pinion gear, a single bearing mounted idler gear and a shaft mounted boost pump drive gear. These gears transfer a maximum of 26 kw (34.79 hp) for driving the fuel boost pump. The fuel side gears have characteristics as defined by the gear data table (figure 67). The idler gear is supported by a single hydrogen-cooled roller bearing, 20 x 37 mm, operating at a DN value of 0.552×10^6 mm-rpm. The idler gear bearing support is the second of two local projections extending from the main LO_2 turbopump bearing support. The idler gear bearing load is calculated to be 445N (100 lb), which yields a life of 18,100 hours for the 20 mm bearing.

Hydrogen cooling flow to the idler gear is supplied by a series of drilled passages and slots which direct the oxidizer turbopump bearing coolant flow to the idler bearing. A cavity is provided on one side of the idler bearing to ensure that the coolant flow is directed through the bearing and does not exit directly into the gearbox cavity. The use of a well-cooled, single bearing idler gear which is closely toleranced and positioned will provide the 10-hr life required for the ASE. The required cooling flow to the idler bearing is estimated to be 0.0038 kg/s (0.00835 lb/sec).

The single bearing idler gear has been successfully demonstrated in the RL10. This system, although not a production item in the RL10, was well established in experimental operation and was qualified for production use. The single bearing system allows the idler gear freedom to adjust its plane of revolution to maximize the amount of line contact between the gear teeth in the event of shaft misalignment and hence minimizes the amount of load shift due to misalignment. The oxidizer and fuel boost pump drive train gears were designed to satisfy established design criteria for gears operating in cryogenic environments. The guidelines set forth in the NASA Monograph for turbopump gears, (Reference 8) are incorporated in the final design. The gears are, therefore, an involute form satisfying the following requirements:

1. Pitch line velocity $<$ 102 m/s (20,000 fpm) (maximum)
2. Pressure angle - 0.436 rad (25 deg)
3. Hertz stress level - 41,400 N/cm^2 (60,000 psi) (maximum)
4. Maximum reduction per mesh - 5:1 (maximum)
5. Gear configuration for 5:1 reduction - spur
6. Number of pinion teeth for 0.436 rad (25 deg) pressure angle - 20 (minimum)
7. Ratio of face width/pitch diameter $\leq$ 1:1
8. Number of gear teeth - 100 (maximum)

9. Design overload - 20% greater than design load (minimum)

10. Gear heat generation - 1.5% of HP transmitted/mesh

11. Hunting-tooth action (number of teeth in gear and pinion have no common factors)

Pertinent preliminary design and geometry information for the fuel and oxidizer boost pump gear trains are presented in figure 67.

The primary concern with gear-driven boost pumps is the ability of the gears to achieve the 10-hr ASE life requirement. A number of factors considered to be indicators of gear life were evaluated. These factors are: gear loading, cooling, lubrication and material. This evaluation indicated that the ASE gears would require only a test program to demonstrate life capability rather than an extensive development program. The rationale used for evaluation of each factor and their effects are given below.

The ASE gears were designed to face loading criteria not as great as those of the RL10 gears and to pitch line velocities and stress levels within current, NASA approved, state-of-the-art maximums. For example:

	Pitch Line Velocity, m/s (fpm)	Unit Load, N/cm (lb/in)	Hertz Stress, N/cm^2 (psi)
ASE	94 (18,500) maximum	5850 (3340) maximum	41,400 (60,000) maximum
RL10	80 (15,720) maximum	5870 (3350) maximum	38,900 (56,400) maximum

One set of gears on the RL10 engine accumulated 5.56 hours of running time at the nominal engine operating conditions with gear tooth stress levels of 51,700 N/cm^2 (75,000 psi) and a pitch line velocity of 81 m/s (16,000 fpm). The gears, when removed, were badly worn but still usable. The accumulated time on the gear set was more than three times the required engine design service life. RL10 gears have also been successfully operated at tooth stress levels and pitch line velocities of 66,190 N/cm^2 (96,000 psi) and 102 m/s (20,000 fpm), respectively. The parts involved in all these tests were of an early design, and modifications to improve life, such as the use of a single bearing idler gear to improve alignment, have since been demonstrated, but have not been subjected to maximum life duration tests.

The use of RL10 test results, the ASE's detailed attention to tolerances and a single bearing idler gear in the ASE gearbox to improve gear face alignment should result in increasing gear life to the required 10 hr.

Gear cooling needed to prolong gear life is provided by the hydrogen environment in which the gears operate. A heat transfer analysis of the oxidizer turbopump pinion gear indicates a maximum tooth temperature of 389°K (700°R). The heat transfer analysis was extremely conservative in that it assumed all the heat input occurred at the gear tip and that all the heat generation was absorbed by only one gear of the two gear mesh. However, even this temperature has little effect upon the properties of AMS 6260 material. This temperature is similar to the operating temperatures experienced by gears operating

in an oil cooled gearbox. The major difference is that hydrogen provides no lubricity, whereas oil does. From a material strength at operating temperature standpoint, the ASE gears have sufficient toughness to resist wear provided some lubrication is supplied.

Gear lubricity for the RL10 was attained by the use of a dry film lubricant, PWA 61. This lubricant consists of molybdenum disulfide and graphite powder in a varnish binder. The part to be lubricated is coated with the compound and subsequently heat treated. Satisfactory service life was attained with this lubricant for the RL10, but the longer life requirement of the ASE necessitates the use of a better gear lubricant. Some candidates representing state-of-the-art advancements are PWA 550 and PWA 474. These lubricants combine molydisulfide with antimony oxide to produce a lubricant with wear properties 100% improved over those of PWA 61. PWA 550 is an air cured lubricant. This feature permits its use as a preflight maintenance procedure, whereby the gear lubricant may be replenished, as required, by spraying the gears within the gearbox. The gears of the ASE are to be with an improved dry film lubricant having higher wear resistance than PWA 61 and should result in increased gear life.

Gear life could also be increased by changing the material from the conventional AMS 6260 to a more exotic material such as a copper-beryllium alloy. An idler gear made of this alloy ran successfully in the RL10 engine. Some advantages offered by a gear of this material operating in a cryogenic environment are as follows. Copper-beryllium has a low modulus of elasticity and is therefore more tolerant to impact load. This feature is important in rocket turbomachinery where accelerations from stop to full thrust are rapid, thereby generating high impact loads. Copper-beryllium has a high thermal conductivity. This characteristic is advantageous for cryogenic gear applications in that the heat generated at the teeth contact point is quickly conducted into the gear web. Because of its relative softness (RC35-45 vs RC60 for carburized AMS 6260), copper-beryllium is resistant to galling. The gears tend to wear in, thereby lasting longer than a gear undergoing galling. If testing indicates that wear-in life is not adequate, a type of hardcoating would have to be developed for use on the gear teeth because copper-beryllium cannot be carburized.

Another possibility for increasing gear life is the use of Borcote on corrosion resistant high strength alloys. Borcote is a boride coating provided by Stuart Metallurgical Division of Vac-Hyd, Stuart, Florida. This coating is harder than a carburized surface but is less costly to apply and produces no change in surface finish, dimensions or corrosion resistance of the parent material. This coating could be used upon a gear made of nickel alloy, thereby providing a cheap, high strength gear which is resistant to corrosion.

Attainment of the required gear life of 10 hr therefore appears feasible without the necessity for a development program because (1) gear design parameters are within the state-of-the-art, (2) gear face alignment is improved compared with that of the RL10 gearbox, and (3) a greatly improved dry film gear lubricant, will be used.

3. High Pressure Fuel Turbopump

a. General Description:

The high pressure fuel turbopump consists of a two-stage fuel pump with integrally shrouded impellers without inducers driven by a single-stage, low reaction, 56% admission turbine. The pump increases the pressure of the liquid hydrogen supplied by the fuel boost pump to the levels necessary to supply hydrogen for the regeneratively cooled portion of the thrust chamber, and for preburner injection. The high pressure fuel turbopump arrangement is shown in figure 68. The modular plug-in design was selected for ease of maintenance.

b. Operating Characteristics

(1) Main Fuel Pump

The high pressure fuel pump was designed for its best efficiency point (BEP) at 100% thrust and MR = 6.0. At the design point, the pump rotational speed is 9740 rad/s (93,000 rpm) and produces a pressure rise of 3003 N/cm^2 (4355 psi) to provide the necessary pressure to provide fuel for the regeneratively cooled portion of the thrust chamber and for injection into the preburner. The main pump is inducerless to increase critical speed and has a design maximum suction specific speed capability of 15,000 and an actual operating maximum of 11,600. Inducerless suction capability at the N_{SS} = 13,000 level has been demonstrated by P&WA in hydrogen pump tests (Reference 9). Suction capability of the main fuel pump is presented in figure 69 which shows a linear falloff with flow coefficient as described in paragraph E2, Low Pressure Pumps and Gearbox.

Head-flow coefficient and efficiency characteristics for the main fuel pump first and second stages, which have the blades swept back 0.436 rad (25 deg) (figures 70 and 71) were based upon correlated slip factors and impeller-collector loss coefficients from several centrifugal pump programs including the RL10, high pressure pump and XLR129 test programs (References 9, 10, 11, 12 and 13). The resultant hydrodynamic parameters are given in table XV as derived from the empirical data with adjustments for specific speed, suction specific speed and other geometric variations.

Each pump stage has a shrouded impeller to reduce blade tip leakage and thereby improve overall pump efficiency. Efficiency levels indicated in the design tables are consistent with values demonstrated on past designs of the same specific speed. The main fuel pump efficiency, after an adjustment for thrust piston recirculation flows, matches that of an RL10 fuel pump first stage that was shrouded and tested at the same specific speed. The number of impeller blades selected for each design was chosen to provide acceptable hydrodynamic loadings consistent with demonstrated values. Partial splitter blades were incorporated to eliminate excessive fluid blockage through the impeller inlet sections.

A double discharge volute-diffuser system is used to minimize radial thrust loads at off-design operating conditions. The volute-collectors are designed for a linear increase in flow area, resulting in a constant fluid velocity within the volute. Each diffuser is sized to provide an acceptable area ratio for reduced pressure loss downstream of the pump without exceeding established empirical diffuser stall limits given in Reference 7.

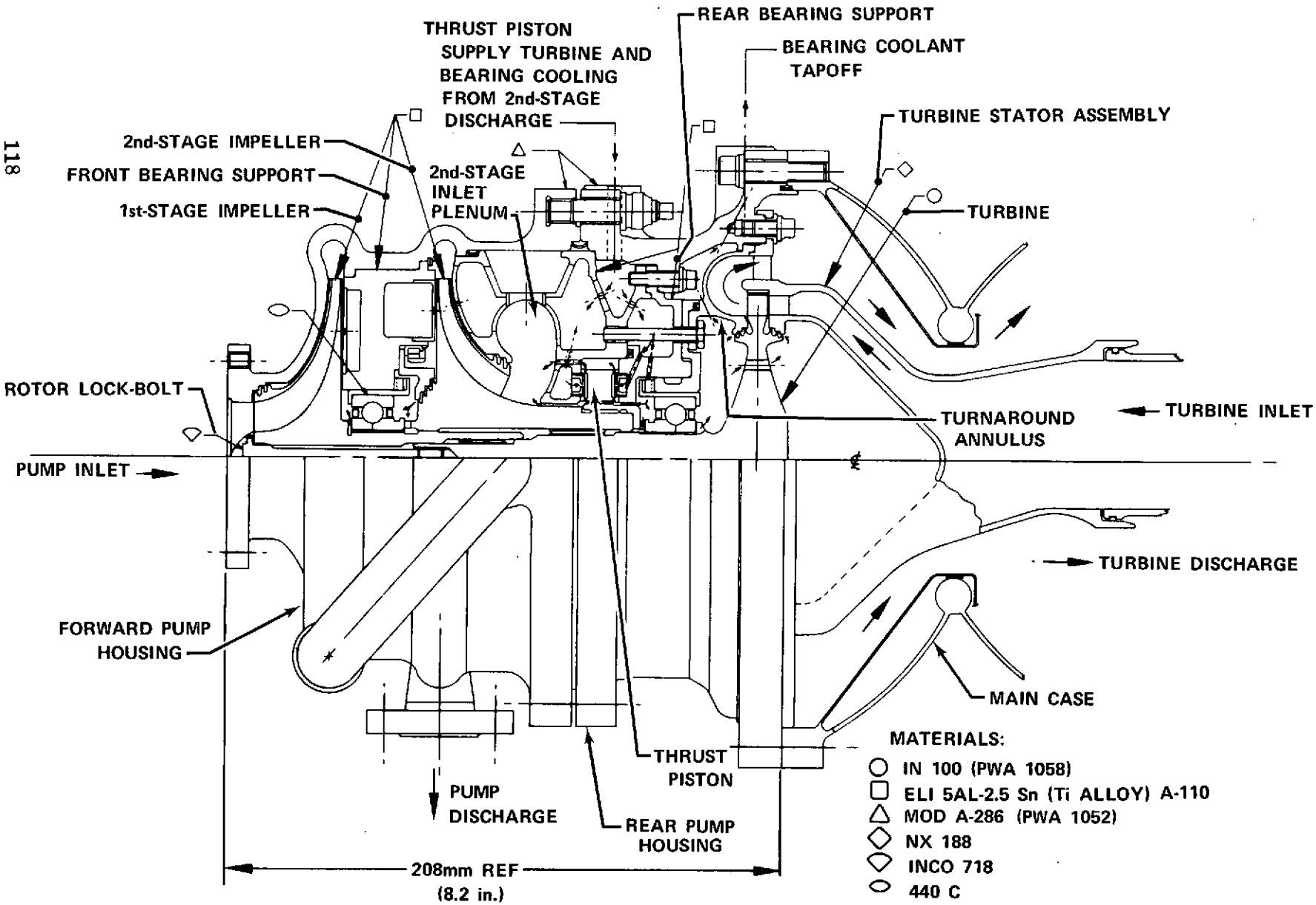

Figure 68. High Pressure Fuel Turbopump

FD 72396

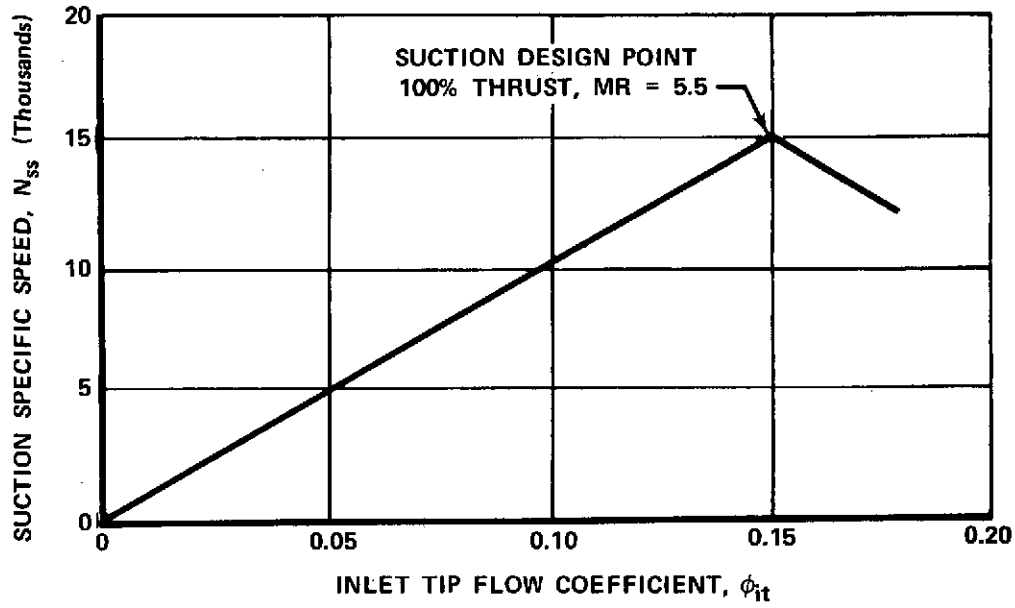

Figure 69. Advanced Space Engine High Pressure Fuel Suction Capability FD 68868

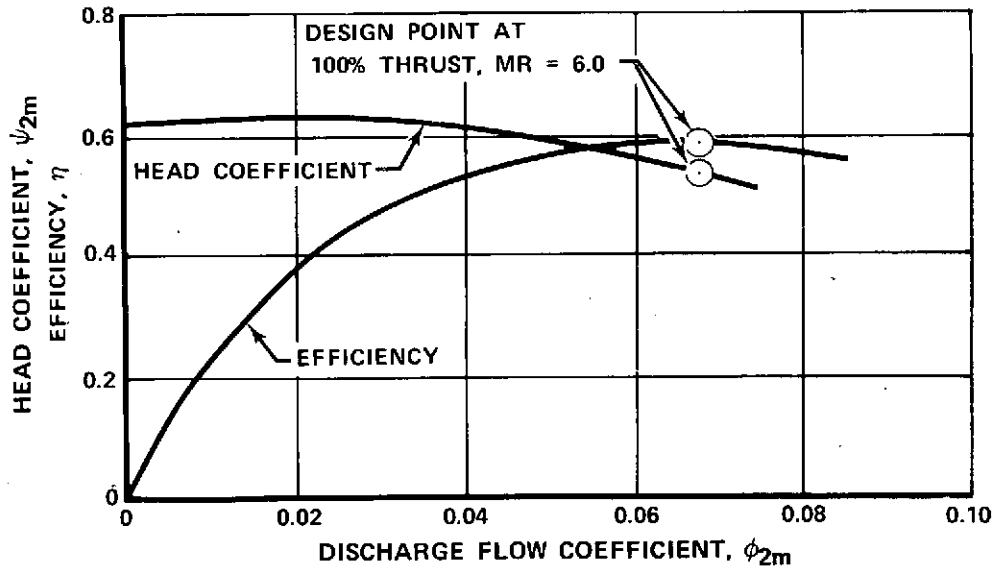

Figure 70. Advanced Space Engine High Pressure Fuel Pump: 1st Stage Head Coefficient - Efficiency Characteristics FD 68825A

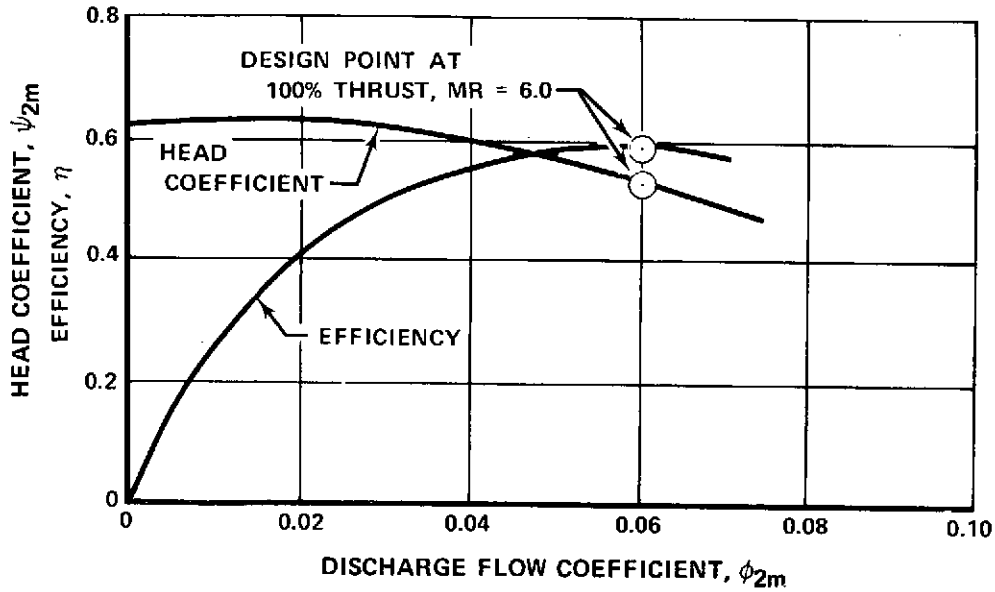

Figure 71. Advanced Space Engine High Pressure Fuel Pump: 2nd Stage Head Coefficient - Efficiency Characteristics FD 68826

Table XV. Advanced Space Engine High Pressure Fuel Pump Best Efficiency Point Design Parameters

100% Thrust, MR = 6.0		
	First Stage	Second Stage
Pump Speed, N, rad/s (rpm)	9,740 (93,000)	9,740 (93,000)
Specific Speed, N_S	514	514
*Design Suction Specific Speed, $N_{SS_{max}}$	15,000	N/A
Mean Head Coefficient, Ψ_{2m}	0.527	0.539
Discharge Mean Flow Coefficient, ϕ_{2m}	0.068	0.060
*Design Inlet Tip Flow Coefficient, ϕ_{it}	0.015	N/A
Head Rise, ΔH, N-m/kg (ft)	224,780 (75,200)	233,790 (78,215)
Volumetric Flowrate, Q, m^3/s (gpm)	0.0396 (628)	0.0422 (669)
**Efficiency, η, %	58.1	58.4
Power, kw (hp)	1,104 (1,480)	1,141 (1,530)
Inlet Tip Diameter, D_{it}, cm (in.)	4.50 (1.77)	5.97 (2.35)
Inlet Hub Diameter, D_{ih}, cm (in.)	1.52 (0.6)	4.83 (1.9)
Inlet Pressure, N/cm^2 (psia)	44.8 (65)	1,517 (2,200)
Inlet Temperature, °K (°R)	21.7 (39)	45.6 (82)
Discharge Pressure, N/cm^2 (psia)	1,538 (2,230)	3,034 (4,400)
Impeller Tip Diameter, D_{2t}, cm (in.)	13.4 (5.276)	13.6 (5.37)
Impeller Tip Speed, U_T, m/s (ft/sec)	653 (2140)	659 (2160)
Discharge Blade Height, h_b, cm (in.)	0.25 (0.1)	0.25 (0.1)
Inlet Tip Blade Angle, β_{1t}*, rad (deg)	0.192 (11)	0.192 (11)
Discharge Mean Blade Angle, β_{2t}*, rad (deg)	0.436 (25)	0.436 (25)
Number of Blades	3-6-12	
Discharge Temperature, °K (°R)	45.6 (82)	70.3 (126)

*Suction Design Point, 100% Thrust and MR = 5.5

**Pump efficiency includes effects of recirculated flows (thrust balance system, bearing cooling, internal leakages, etc.).

N/A - Not Applicable

Critical speed for high pressure, high speed pumps is an important design consideration. The NASA groundrules for the ASE study requires the rotor bending frequency to be at least 25% above the rotor maximum operating speed, and a minimum margin of 20% is to be maintained between rotor rigid body critical speeds and rotor steady-state operating speeds at full thrust. (Refer to paragraph E1 for the complete NASA-prescribed groundrules.) The use of relatively stiff rotor support spring rates in the design of the fuel turbopump assures that the critical speed groundrule requirements will be satisfied. With a ball bearing spring rate of 525 MN/m (300,000 lb/in.), the first and second critical speeds are bounce modes and occur within the transient operating range at 4922 rad/s (47,000 rpm) and 7749 rad/s (74,000 rpm), respectively. The third critical speed is a bending mode and occurs at a speed of 27,646 rad/s (264,000 rpm), nearly three times the maximum steady-state operating speed.

To reach the rated thrust operating region, the fuel turbopump must pass through the first two critical speeds. P&WA experience has shown that the rotor strain energy must be less than 25% of the strain energy of the entire system, with 75% or more absorbed by the rotor supports, to ensure quiet passing through rigid rotor (bounce modes) critical speeds. The rotor strain energies for these two critical speeds are each less than 5% of the system total strain energy. Because of the rapidity (~450 ms) with which the fuel turbopump passes through the first and second critical speeds during the transient from pumped idle to full thrust, and the low rotor strain energies, no detrimental operational effects are anticipated. The relationship of critical speeds to operating speeds is shown in figure 72.

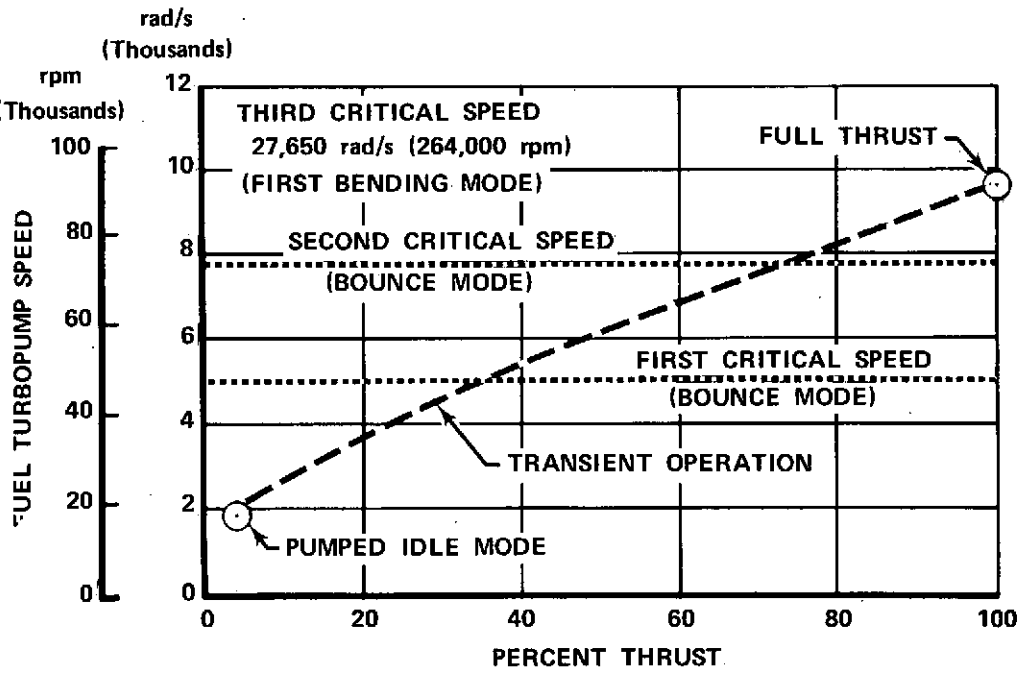

Figure 72. ASE High Pressure Fuel Turbopump Critical Speeds FD 70549

(2) Turbine

The high pressure fuel pump drive turbine is an axial flow, partial admission, single stage impulse design, deriving its power from the expansion of preburner combustion products. The turbine develops 2240 kw (3,000 hp) at the design point with a total-to-static pressure ratio of 1.55 and an efficiency of 68.9%. The turbine design point is at 100% thrust and MR = 6.0. Table XVI presents the turbine design point operating conditions; mean velocity diagrams are shown in figure 73. Turbine off-design efficiency is presented in figure 74. The turbine mean diameter of 11.7 cm (4.6 in.) was sized to satisfy the 10-hr, 1% creep life requirement with wrought IN100 (PWA 1058) material.

The fuel turbine elevation is shown in figure 75. The exit blade height was set at 0.762 cm (0.300 in.), a P&WA study groundrule minimum. A 0.254 cm (0.10 in.) overlap at the ID and OD of the blades results in a vane height of 0.71 cm (0.28 in.). The axial chord lengths for the vanes and blades were set at 0.762 cm (0.30 in.). These were selected as being the smallest allowable to minimize aerodynamic losses of each airfoil. For a given blade height, small chords yield high aspect ratios, which in turn maintain low airfoil end losses. Because of the small size of the fuel turbine, end losses represent a high percentage of total airfoil loss; maximizing the aspect ratio will minimize these end losses. Based on XLR129 experience, vane and blade Zweifel load coefficients (Reference 14) are set at 0.78 and 0.87, respectively, to avoid low efficiencies. Thirty vanes and 74 blades are required. Figure 76 shows that an arc of admission of 56% provides optimum performance without requiring an excessively low exit vane angle.

Table XVI. Advanced Space Engine High Pressure Fuel Turbopump Turbine Operating Conditions at Design Point (100% Thrust, MR = 6.0)

Rotor Speed, rad/s (rpm)	9,730 (93,000)
Mean Wheel Speed, m/s (ft/sec)	569.5 (1,870)
Mean Diameter, cm (in.)	11.697 (4.605)
Velocity Ratio, (Total/Static, Isentropic)	0.401
Flowrate, kg/s (lb/sec)	3.215 (7.095)
Inlet Temperature, °K (°R)	1,140 (2,050)
Inlet Pressure, N/cm^2 (psia)	2,234 (3,240)
Pressure Ratio, (Total/Static)	1.554
Efficiency, (Total/Static)	0.689
Power, kw (hp)	2,240 (3,006)
Number of Stages	1
Percent Admission	56

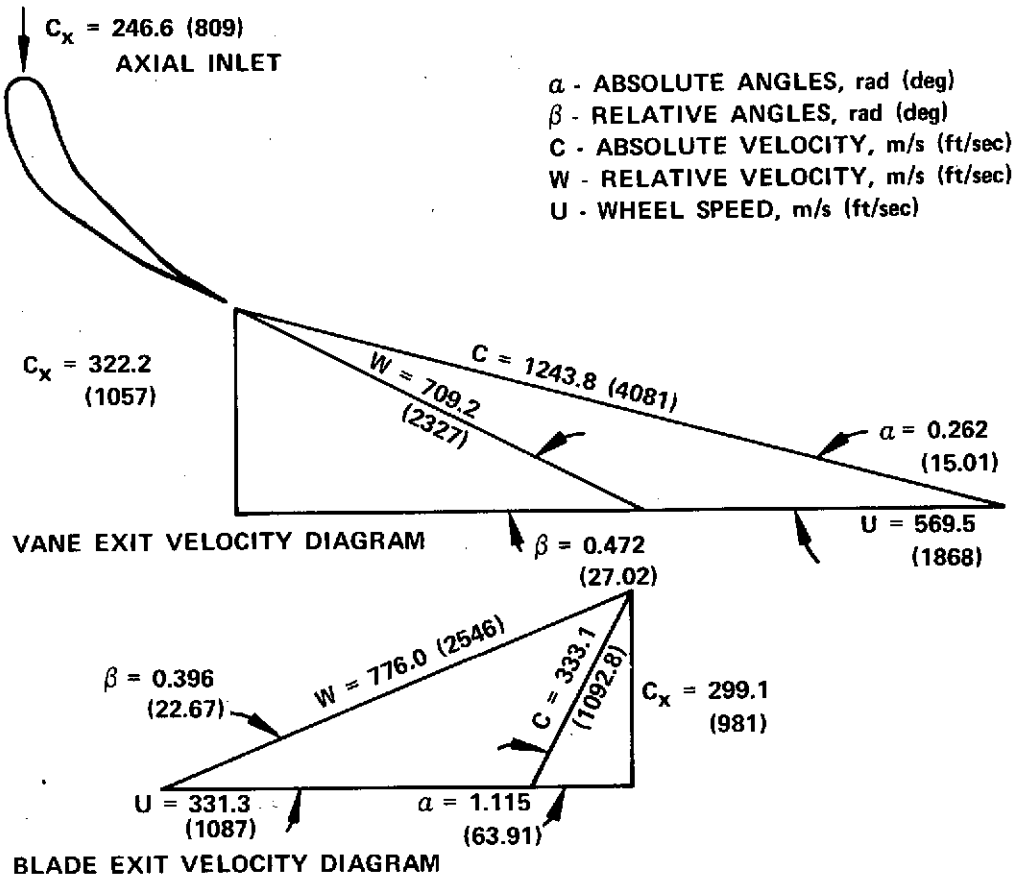

Figure 73. Advanced Space Engine Fuel Turbopump Turbine Design Point Mean Velocity Diagrams

FD 71599

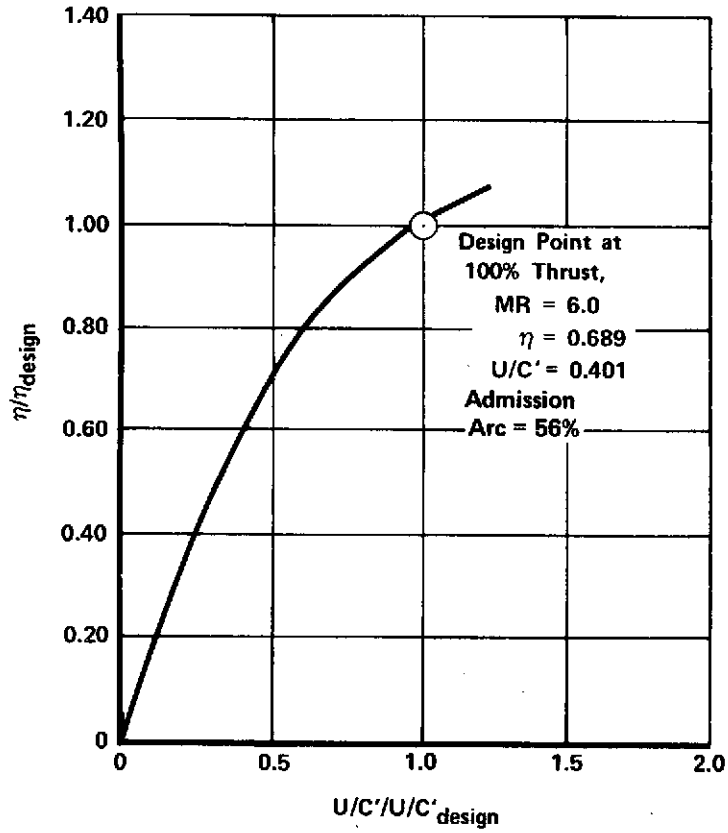

Figure 74. ASE Fuel Turbine Off-Design Efficiency Characteristic FD 70531A

PERCENT ADMISSION	56	
MEAN DIAMETER	117 mm (4.605 in.)	
RADIUS, TIP	62 mm (2.4425 in.)	62.25 mm (2.4525 in.)
BLADE LENGTH	7.11 mm (0.280 in.)	7.62 mm (0.300 in.)
	1st-STAGE VANE	1st-STAGE BLADE
RADIUS, ROOT	55 mm (2.1625 in.)	54.6 mm (2.1525 in.)
CHORD LENGTH, AXIAL	7.62 mm (0.300 in.)	7.62 mm (0.300 in.)
		0.762 mm (0.030 in.)

Figure 75. Fuel Turbopump Turbine Elevation FD 71602

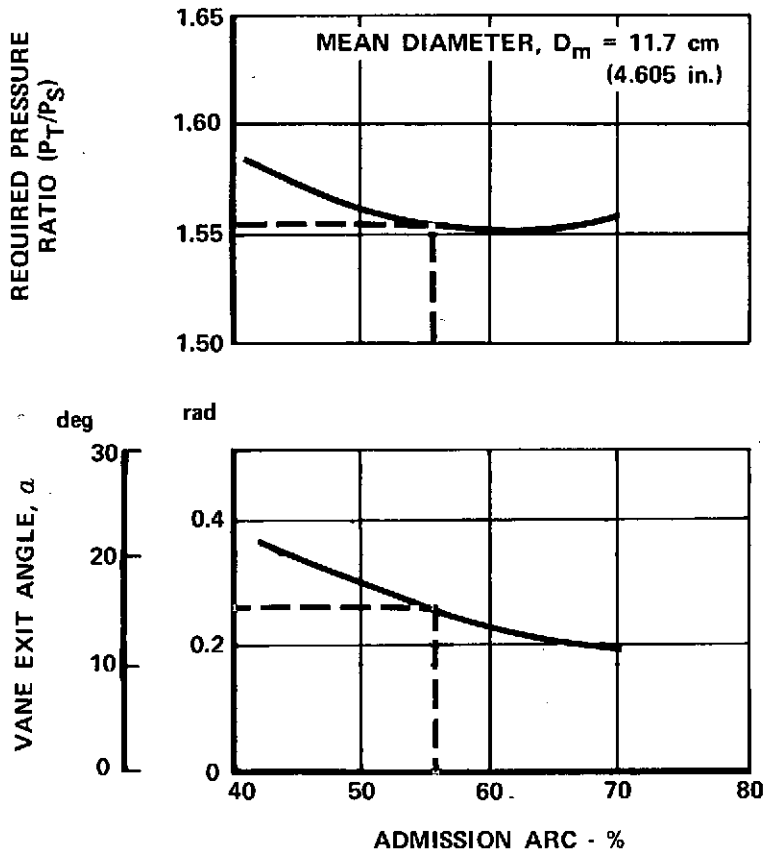

Figure 76. Effect of High Pressure Fuel Turbopump Turbine Admission Arc (Unshrouded) FD 68827

Fuel turbine leakage flows are accounted for in turbine efficiency predictions. The total turbine leakage is 6.61% of the inlet flow and consists of circumferential and tip leakages, which are 1.73% and 4.88%, respectively. To minimize leakage, a low mean static pressure reaction of 73.5% is used, which is sufficient to maintain a 5% positive root reaction. Table XVII presents predicted operating characteristics at 100% thrust for design and off-design operation. The turbine efficiency is virtually constant for the entire mixture ratio excursion.

Table XVIII presents a blade life summary at the 100% thrust operating points, and shows that a minimum turbine temperature margin of 8.9°K (16°R) for 10 hr, 1% creep life occurs at MR = 6.5 which is the maximum turbine operating temperature condition. At the engine nominal operating point, MR = 6.0, the turbine blade temperature margin is 53°K (95°R).

c. Mechanical Description

The hydrogen turbopump consists of two, back-to-back, integrally shrouded impellers, a high pressure thrust balance piston, two internally preloaded ball bearings, a single stage, partial admission, unshrouded impulse turbine, and two main exterior housings.

Table XVII. Advanced Space Engine Fuel Turbine Performance at 100% Thrust

Mixture Ratio	5.5	6.0	6.5
Pressure Ratio (T/S)	1.616	1.554	1.532
Inlet Temperature, °K (°R)	1,140 (2,053)	1,140 (2,051)	1,184 (2,132)
Inlet Pressure, N/cm^2 (psia)	2,372 (3,440)	2,236 (3,242)	2,185 (3,169)
Inlet Flow, kg/s (lb/sec)	3.384 (7.64)	3.218 (7.095)	3.071 (6.77)
Efficiency, (T/S)	0.688	0.689	0.687
Isentropic Mean U/C, (T/S)	0.402	0.401	0.398
Rotor Speed, rad/s (rpm)	10,184 (97,251)	9,738 (92,991)	9,714 (92,761)
Power, kw (hp)	2,610 (3,500.4)	2,240 (3,006.3)	2,150 (2,878.3)

Table XVIII. Advanced Space Engine Fuel Turbopump Turbine Blade Stress and Allowable Temperature at 100% Thrust Wrought IN100 (PWA™ 1058) Material

Mixture Ratio	5.5	6.0	6.5
T_{tbr}, °K (°R)	1,107 (1,993)	1,111 (2,000)	1,156 (2,081)
Root Stress, N/cm^2 (psi)	35,649 (51,705)	32,587 (47,264)	32,370 (46,948)
Allowable T_{tbr}, °K (°R)	1,148 (2,067)	1,164 (2,095)	1,165 (2,097)

where:

T_{tbr} - Average blade relative temperature, includes burner profile of 30°K (54°R) and control tolerance of 11°K (20°R)

Root Stress - Constant section, untapered blade

Allowable T_{tbr} - Based on 10 hr, 1% creep life

The two pump stages produce a pressure range from 3034 N/cm^2 (4400 psia) to 3261 N/cm^2 (4730 psia), which is required to provide fuel for thrust chamber cooling and injection into the preburner at full thrust. The 1st- and 2nd-stage impellers have respective tip diameters of 13.4 and 13.5 cm (5.276 and 5.317 in.) and tip velocities of 652 and 658 m/s (2140 and 2160 ft/sec). These velocities are below the generally accepted limit of 700 m/s (2300 ft/sec) for integrally shrouded titanium impellers. The material for both impellers is a titanium alloy (AMS 4924) which was selected to minimize rotating mass.

A preliminary stress analysis of the 1st-stage impeller was conducted to verify the feasibility of using integral shrouds. The first stage rather than the second was chosen for analysis because the former has the conditions that are more conducive to producing deflections, i.e., the more flexible disk and the larger blade area. While the stress analysis was performed on a preliminary impeller design that was not completely detailed, the maximum calculated effective stress levels and deflections indicated that shrouded impellers operating at the conditions of the baseline engine cycle are feasible.

The Contura Corp., Los Angeles, California, was contacted in regard to the machining problems involved with an integrally shrouded impeller. The impeller fabrication should be feasible as long as blade heights are maintained at a reasonable minimum of 0.254 to 0.381 cm (0.100 to 0.150 in.) with an ultimate minimum of 0.127 cm (0.050 in.) and the wrap angles are less than 3.14 rad (180 deg).

A separate thrust balance piston is used in the ASE fuel turbopump to compensate for axial load unbalance during turbopump operation. The relatively high pressures acting on the pump and turbine rotor disks create axial loads. These axial forces tend to cancel, and theoretically by varying disk diameters and seal locations, a perfectly balanced machine could be obtained for a single operating condition. However, varying operating conditions during engine mixture ratio excursions and acceleration/deceleration transients would upset the balance and cause axial loads. Since the maximum predicted load is only 2335 N (525 lb) toward the pump end, the direction of the unbalance force may reverse during off-design operation. Therefore, a double acting thrust piston was selected for the ASE fuel turbopump because it can balance the loads in either direction.

An appreciation of the variations in axial thrust loads that may occur (especially during turbopump development) can be obtained by considering the magnitudes of the thrust encountered. The axial thrust on the single backface of the fuel pump second stage, for example, was calculated to be greater than 334 kN (75,000 lb). A 1% error in pressure level and/or pressure distribution prediction on this one disk could produce a difference of 3336 N (750 lb) in the axial thrust unbalance of the turbopump shaft.

The self-compensating characteristic of the thrust balance piston system is achieved through displacement-sensitive flow metering resistances. Figure 77 illustrates the basic elements of a double-acting thrust piston. High pressure hydrogen is supplied to cavities on either side of the piston from the pump 2nd-stage discharge through supply orifices. The hydrogen flows from the cavity through clearances between the piston and lands in the housing that form flow metering resistance, and back to the inlet of the second stage. An axial shaft unbalance in either direction causes the rotor assembly to displace in the direction of the external load. The displacement alters the metering resistances, resulting in cavity pressure changes which generate an axial pressure gradient (across cavities) opposite in direction and equal in magnitude to the externally applied load. This effect is similar to that of a hydraulic spring, in which displacement increases until load equilibrium is obtained.

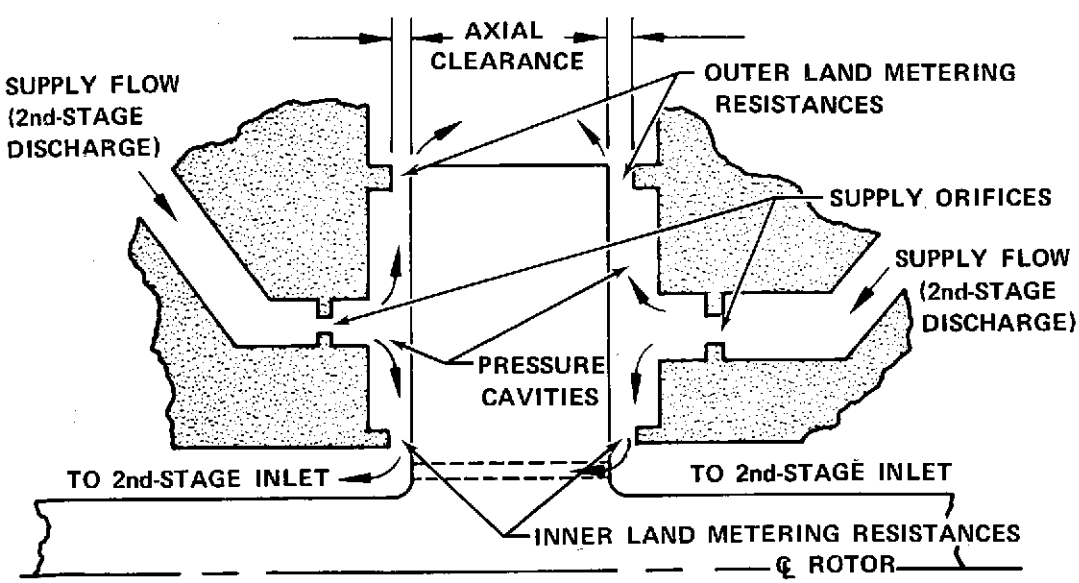

Figure 77. Representative Cross Section of Double-Acting Thrust Piston FD 68828

The thrust piston size (metering resistances at 2.29 cm (0.9 in.) and 3.3 cm (1.3 in.) radii) can provide a maximum force capability of approximately 17.35 kN (3900 lb). However, since the predicted maximum unbalance is only 2335 N (525 lb), the force capability can be reduced to decrease piston flow and thereby improve overall pump efficiency after turbopump development trims unbalance. This can be readily accomplished by replacing the supply orifices shown in figure 78.

The predicted maximum unbalance was 2335 N (525 lb) at 100% thrust and MR = 5.5, where maximum fuel pump pressures occur. At any off-design operating condition (except transient overshoot) the magnitude of axial unbalance will be less. Based on prior turbopump experience, 4448 N (1000 lb) thrust capability (90% margin above predicted maximum unbalance) was recommended for developed turbopump operation. This thrust capability requires a flowrate of 0.24 kg/s (0.52 lb/sec) equivalent to 8% recirculation flow around the second stage of the fuel pump.

The rotor assembly is supported by two angular contact ball bearings. (Refer to figure 68.) The use of ball bearings permits critical speed to be varied by allowing changes to be made in rotor support spring rate. Angular contact ball bearings are subject to less heat generation than preloaded roller bearings. In general, there is greater experience with ball bearings, making them desirable for this application where a high degree of stiffness is not required, as it would be in a variable thrust engine. Angular contact 55 mm ball bearings for a large thrust size high pressure hydrogen pump, which were fabricated from 440C material, had similar internal geometry (except for number of balls) and were successfully operated in hydrogen at a DN of 2.2×10^6 mm-rpm for over 10 hr in a P&WA test program (Reference 15).

The two identical ball bearings used to support the shaft are 20 mm x 47 mm and have a split inner race. Bearing internal geometry is:

Number of balls	8
Diameter of balls, cm (in.)	0.794 (0.3125)
Pitch diameter, cm (in.)	3.35 (1.3189)
Inner race curvature, cm (in.)	1.47 (0.58)
Outer race curvature, cm (in.)	1.32 (0.52)
Operating contact angle, rad (deg)	0.314 (18)

Internal geometry selection was based on results of extensive parametric studies performed under the Space Shuttle Main Engine Definition (Phase B) program (Reference 16). The study results, applied to ASE, indicate that the bearing internal geometry provides a sufficiently high radial spring rate to prevent shaft bending critical speed problems. The selected internal geometry also limits ball excursion to values below the cage pocket clearance, thus avoiding cage problems. Values of internal kinematic parameters were kept within the range of previous experience in order to limit wear and heat generation. The bearings operate at a DN of 1.86×10^6 mm-rpm, which is well below the limit of 2.0×10^6 mm-rpm for LH_2 operation set by study groundrules. The front bearing is cooled by controlled hydrogen leakage from the fuel pump 2nd-stage discharge to the 1st-stage discharge. Clearances of the labyrinth seals on the 2nd-stage impeller backface are sized to control the leakage flow to the 0.20 kg/s (0.45 lb/sec) required for bearing cooling.

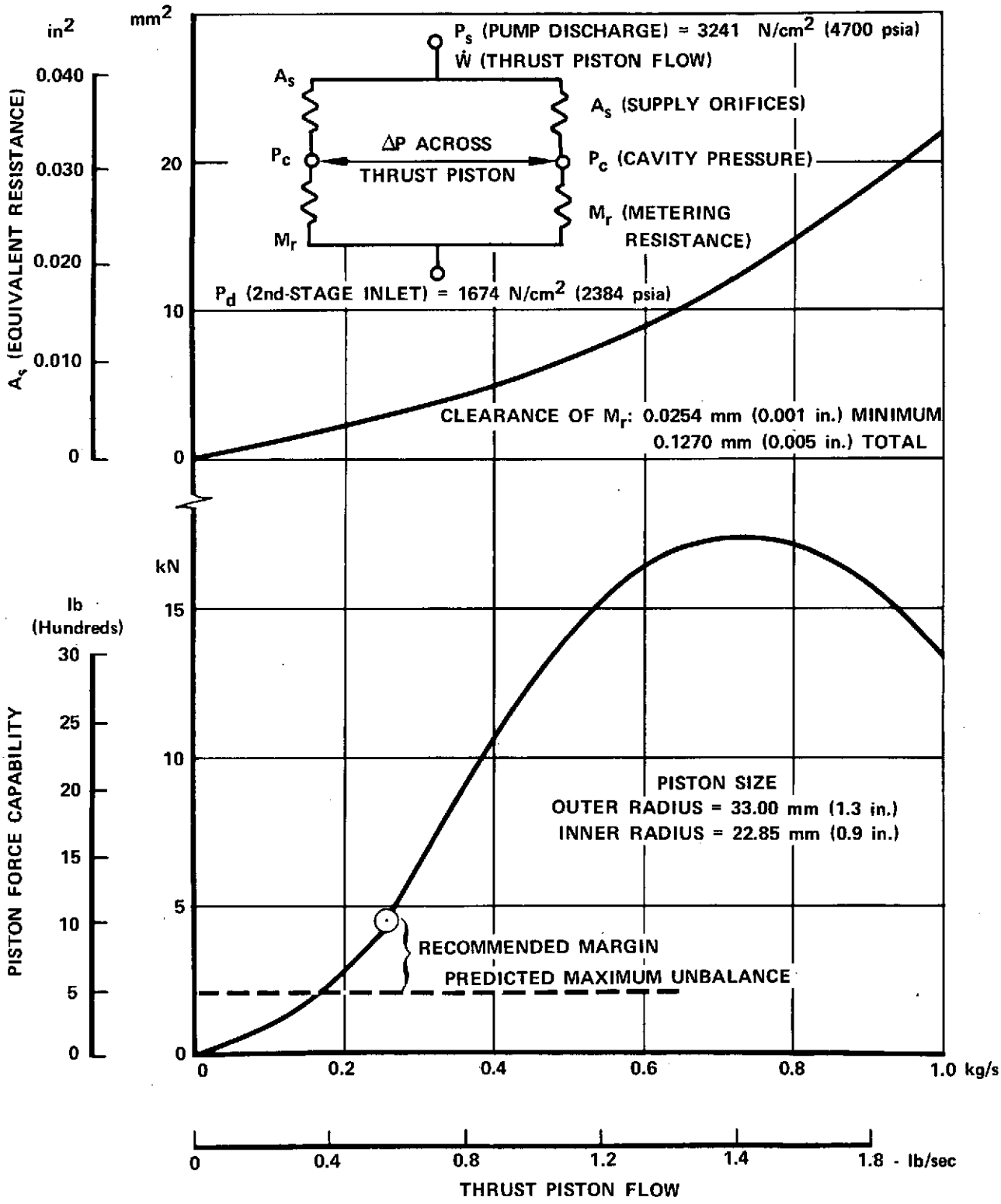

Figure 78. Advanced Space Engine Fuel Turbopump Thrust Balance System Characteristics FD 71594

The rear bearing coolant flow is supplied from the fuel turbopump thrust piston cavity. Part of this flow, 0.0036 kg/s (0.008 lb/sec), is routed to the 2nd-stage pump inlet, and 0.077 kg/s (0.169 lb/sec) cools the fuel turbine disk and then flows into the turbine flowpath to act as a dam against inflow of hot preburner gases. The remainder of the coolant flow is transferred externally to the gearbox for use in cooling the bearings of the other pumps and the gears.

The bearings are fabricated from vacuum melt 440C (AMS 5630) stainless steel as have been all other cryogenic bearings in P&WA designs. The cages are stainless steel shielded Salox-M (bronze filled fluorocarbon plastic) of one piece inner land riding design. Cages of this type have been used in 1.11 MN (250,000 lb) and 1.56 MN (350,000 lb) thrust high pressure engine turbopump bearings and have demonstrated 10 hr life. This cage type has also been qualified for use in the RL10. The bearings are mounted in spring loaded slipper rings to permit motion in compliance with the thrust piston movement. Rotor overtravel during startups, transient and shutdowns is limited to the amount of travel permitted by the thrust piston. The thrust piston is limited in axial travel by Bearium B10 rub strips, which are fastened into the housing fore and aft of the thrust piston. The thrust piston will rub lightly on the Bearium B10 during startups until the 2nd-stage discharge flow to the thrust piston cavity is such that it will regulate the thrust piston properly. The axial clearance on each side of the thrust piston is nominally 0.0063 cm (0.0025 in.).

Pump power is supplied by a single-stage turbine. The turbine rotor has unshrouded blades that are integral with the disk. The rotor is fabricated from wrought IN100 (PWA 1058) material. The turbine rotor blades could not be shrouded without reducing the operating temperature because the blade root stresses are approaching the maximum allowable stresses for the required operating conditions. (See table XVIII.) IN100 (PWA 1058) was selected because of its superior strength-to-weight ratio at elevated temperatures and its ability to withstand hydrogen embrittlement (Reference 17). The turbine disk is cooled by flow supplied from the rear bearing. The blades are uncooled, but some blade root cooling is provided by leakage from the rim labyrinth seals. The tandem set of three labyrinth seals form a hydrogen-cooled dam at the disk outer diameter to prevent the inflow of hot turbine gases. The running labyrinth seal clearance is 0.005 cm (0.002 in.) radially. The assembly clearance will be set to compensate for the thermal expansion difference between the turbine disk and the turbine inner housing. The turbine disk is integral with the main shaft. The 1st- and 2nd-stage impellers are splined to the turbine shaft.

Sizing of the turbine disk was based on P&WA design criteria with the exception of criteria specified in this contract. The average tangential stress allowable, using a material utilization factor of 0.85, was set at 77,200 N/cm^2 (112,000 psi), and the effective stress allowable (0.2% yield strength) is 99,970 N/cm^2 (145,000 psi). The resulting disk weighs 0.862 kg (1.9 lb) with a diametric growth at the live rim of 0.038 cm (0.015 in.) and 0.034 cm (0.012 in.) at the labyrinth seals. The disk is designed to the average tangential stress limit of 77,200 N/cm^2 (112,000 psi) and the largest effective stress in the disk is 95,800 N/cm^2 (139,000 psi).

Pump main housings (forward and rear) are fabricated from forged rings of PWA 1052 (MOD A-286) material welded together and finish machined. Use of multiple forgings eliminates machining steps necessary to obtain the complex inner and outer contours from a single billet. The material was selected for its strength at cryogenic temperatures and resistance to hydrogen embrittlement at elevated temperatures.

The forward pump housing contains the 1st- and 2nd-stage volutes, the 2nd-stage inlet plenum, and front bearing support. The front rotor bearing support is fabricated from AMS 4924 titanium alloy. Cavities are machined out of the front and back face of the support to reduce weight. These cavities are covered with plates to provide a close running clearance at the impeller back faces, and thereby enhance stage performance by minimizing the mass of fluid being swirled by the impeller. The cavities are vented to the impeller cavities to minimize deflection generated by differential pressures. Crossover pipes between the first and second stages are welded into the impeller housing.

Each pump stage has dual horn type discharge diffusers located 3.14 rad (180 deg) apart. The dual discharge design, because of lower flowrates and fluid velocities, increases static pressure recovery, and minimizes bearing radial loads. Diffusers are sized to provide a maximum area ratio without exceeding diffuser stall criteria.

The rear pump housing which extends over the double-acting thrust piston and rear bearing, provides the attachment for the turbine stator assembly and incorporates the flange by which the fuel turbopump assembly is mounted to the main case.

The 2nd-stage inlet plenum, rear bearing support, and thrust piston housing are a welded and mechanical assembly of AMS 4924 titanium alloy conical shapes to provide structural stiffness and reduce weight. The 2nd-stage inlet flow enters a cavity between the main housing and the plenum structure, and passes through radial transfer tubes into the impeller inlet plenum.

Thrust piston flow and bearing coolant flow are supplied through a boss in the pump rear housing. Drilled passages in the assembly of conical shapes admit flow to the desired cavities and serve to distribute the thrust piston supply flow to the front and rear of the piston.

The turbine stator assembly is made from PWA 643 (NX 188), a castable nickel base alloy. The turbine gas flowpath is from the main case centerbody duct to the turbine stators, through the rotor to an annulus where the gas flow is turned back 3.14 rad (180 deg), parallel to the entrance flow, and then into the main case plenum. The turbine stator assembly incorporates the turbine stators over an admission arc of 56%, the transition section from the stator OD that mates with the main case centerbody and separates inlet and discharge flow, and an inner shell that provides a cover for the back face of the turbine to keep hot gases away from the shaft area.

4. High Pressure Oxidizer Turbopump

a. General Description

The high pressure oxidizer turbopump consists of a single stage pump with shrouded impeller and a high speed inducer driven by a single-stage, 26% admission, low reaction impulse turbine. The high pressure pump (or main pump) increases the pressure of the liquid oxygen supplied by the low pressure pump to the level required for injection into the preburner and main chamber. The turbine also provides power for the low pressure fuel and oxidizer pumps which are driven through gearing from the oxidizer turbopump shaft.

The arrangement of the high pressure oxidizer turbopump is shown in figure 79. The turbopump rear bearing is located forward of the boost pump drive gear to permit removal or gear inspection without removing the bearing.

b. Operating Characteristics

(1) Main Oxidizer Pump

The high pressure oxidizer pump was designed for its best efficiency point (BEP) at 100% thrust and MR = 6.0. At its design point speed, 5760 rad/s (55,000 rpm), the pump produces a pressure rise of 2710 N/cm^2 (3930 psi) to provide the required pressures for oxidizer injection into the preburner and main chamber. The main oxidizer pump has a high speed inducer with a design maximum suction specific speed capability of 34,000. Suction capability of the pump is shown in figure 80. The linear reduction in suction specific speed for off-design operation shown in figure 80 is based upon inducer characteristics cited in the low pressure pump section, figure 59.

Head-flow coefficient and efficiency characteristics for the main oxidizer turbopump (figure 81) were based upon correlated slip factors and impeller-collector loss coefficients from several centrifugal pump programs including the RL10, 50K and XLR129 test programs. The resultant hydrodynamic parameters are given in table XIX as derived from the empirical data with adjustments for specific speed, suction specific speed and other geometric variations.

The pump has a shrouded impeller to reduce impeller blade tip leakages and thereby improve efficiency. The efficiency indicated in the design table is consistent with values demonstrated by prior designs of the same specific speed. For example, the main oxidizer pump efficiency, after an adjustment for thrust piston recirculation flows, matches that of a shrouded RL10 oxidizer pump at the same specific speed.

The number of impeller blades (refer to table XIX) was chosen to provide acceptable hydrodynamic loadings consistent with demonstrated values. Partial splitter blades were incorporated to eliminate excessive fluid blockage through the impeller inlet sections.

A double discharge volute-diffuser system is provided for the purpose of minimizing radial thrust loads at off-design operating conditions. The volute-collectors are designed for a linear increase in flow area with circumference, resulting in a constant fluid velocity within the volute. Each diffuser is sized to provide an area ratio that reduces pressure losses downstream of the pump without exceeding established empirical diffuser stall limits given in Reference 7.

With the bearing arrangement shown in figure 79, and spring rates of 525 MN/m (300,000 lb/in.) and 350 MN/m (200,000 lb/in.) for the forward and rear bearings, respectively, the high pressure oxidizer turbopump operates between the first and second critical speeds when at full thrust. The third critical speed (the first bending mode) occurs at 20,600 rad/s (196,500 rpm). The first critical speed occurs at 4252 rad/s (40,600 rpm) and has a margin of 24% below the minimum full thrust rotational speed while the second critical speed, 8524 rad/s (81,400 rpm), is 38% above the operating range. The relationship of critical speeds to operating speeds is presented in figure 82.

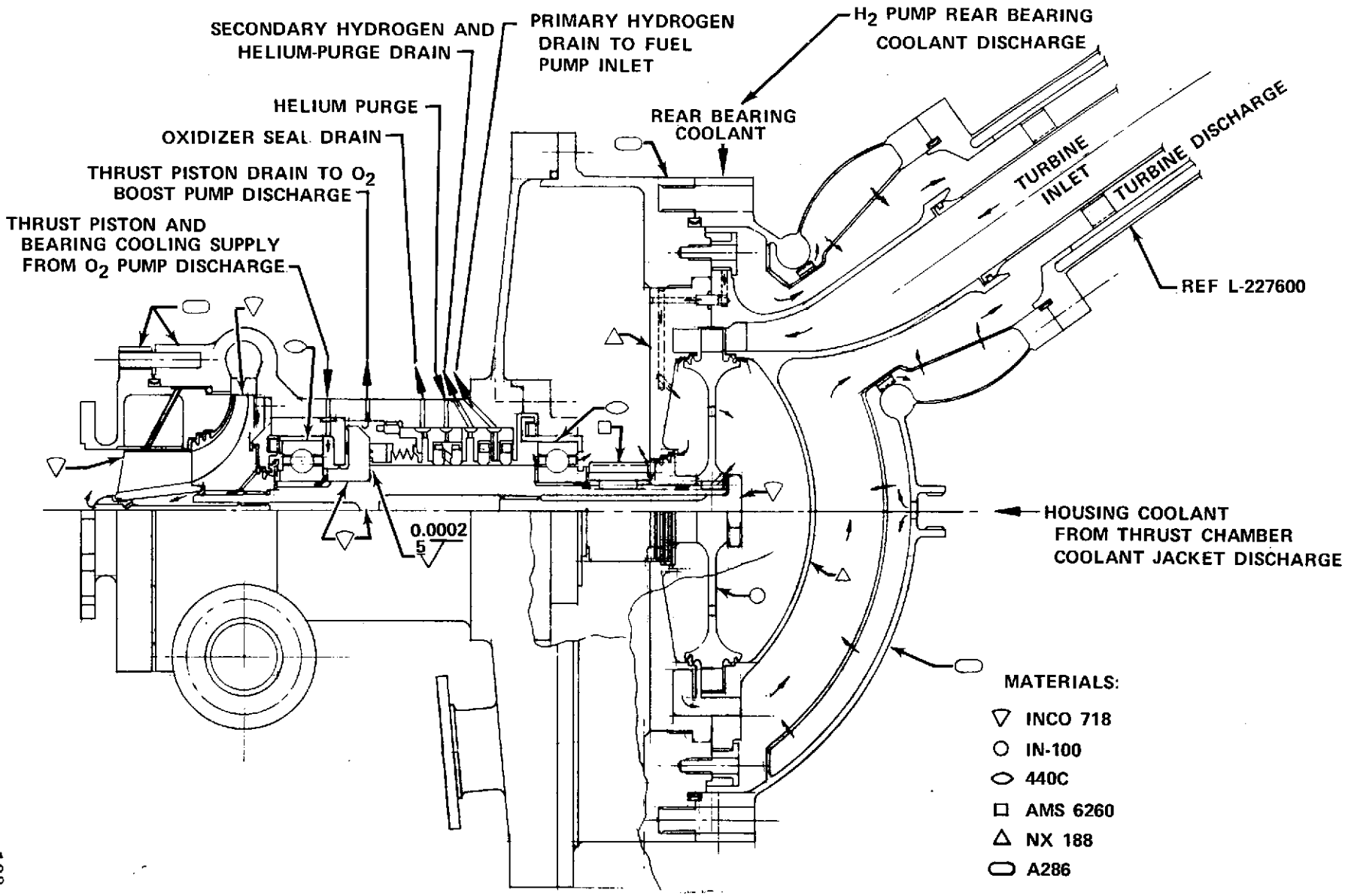

Figure 79. ASE Oxidizer Turbopump Design

FD 72480

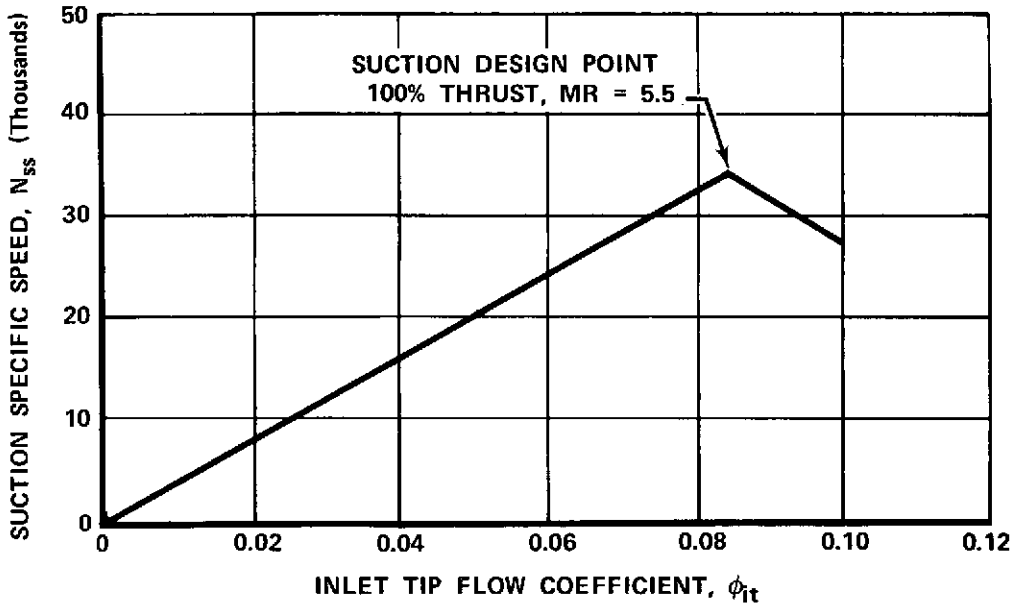

Figure 80. Advanced Space Engine High Pressure Oxidizer Pump Suction Capability

FD 68836

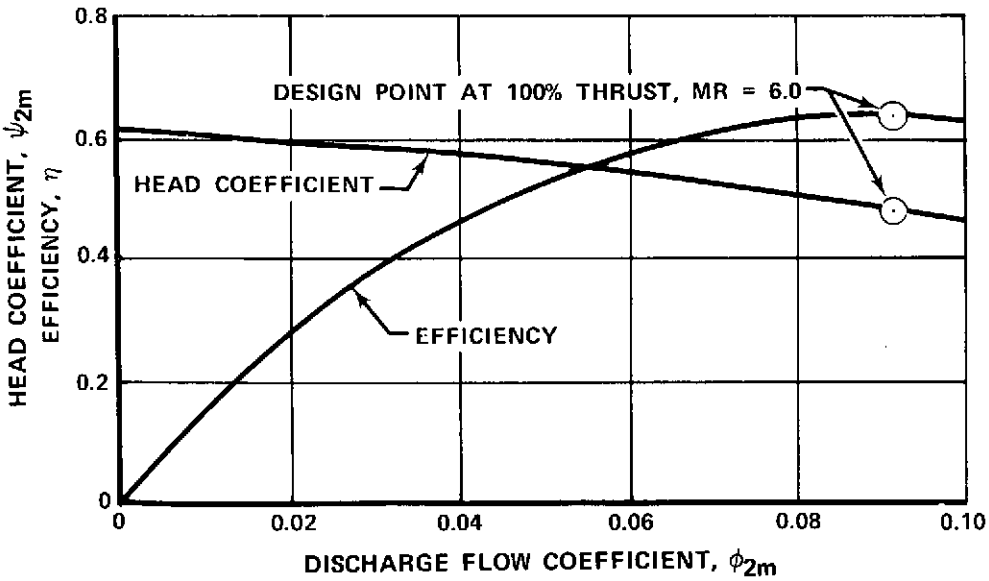

Figure 81. Advanced Space Engine High Pressure Oxidizer Pump Head Coefficient - Efficiency Characteristics

FD 68837A

Table XIX. ASE High Pressure Oxidizer Pump Best Efficiency Point Design Parameters

100% Thrust, MR = 6.0	
Pump Speed, N, rad/s (rpm)	5,760 (55,000)
Weight Flow, $\dot{w}$, kg/s (lb/sec)	165 (36.38)
Specific Speed, N_s	983
*Design Suction Specific Speed, $N_{ss_{max}}$	34,000
Mean Head Coefficient, Ψ_{2m}	0.482
Discharge Mean Flow Coefficient, ϕ_{2m}	0.091
*Design Inlet Tip Flow Coefficient, ϕ_{it}	0.084
Head Rise, ΔH, N-m/kg (ft)	24,115 (8,068)
Volumetric Flowrate, Q, m^3/s (gpm)	0.0146 (232)
**Efficiency, η, %	64.5
Power, kw (hp)	636 (853)
Inlet Tip Diameter, D_{it}, cm (in.)	4.57 (1.8)
Inlet Hub Diameter, D_{ih}, cm (in.)	1.02 (0.4)
Inlet Pressure, N/cm^2 (psia)	49.2 (71.3)
Inlet Temperature, °K (°R)	92.4 (166)
Discharge Pressure, N/cm^2 (psia)	2,760 (4,000)
Impeller Tip Diameter, D_{2t}, cm (in.)	7.76 (3.055)
Impeller Tip Speed, U_T, m/s (ft/sec)	223 (732)
Discharge Blade Height, h_b, cm (in.)	0.33 (0.13)
Inlet Tip Blade Angle, β_{1t}*, rad (deg)	0.131 (7.5)
Discharge Mean Blade Angle, β_{2t}*, rad (deg)	0.436 (25)
Number of Blades	3-6-12
Discharge Temperature, °K (°R)	107 (192)

*Suction Design Point, 100% Thrust and MR = 5.5
**Pump efficiency includes effects of recirculated flows (thrust balance system, bearing cooling, internal leakages, etc.)

During the start transient from pumped idle to rated thrust, the oxidizer turbopump passes rapidly through the first critical speed. (See figure 82.) The rotor strain energy for the first critical speed is 8.7% of the system total strain energy and, as cited in the fuel turbopump section, therefore assures quiet passing.

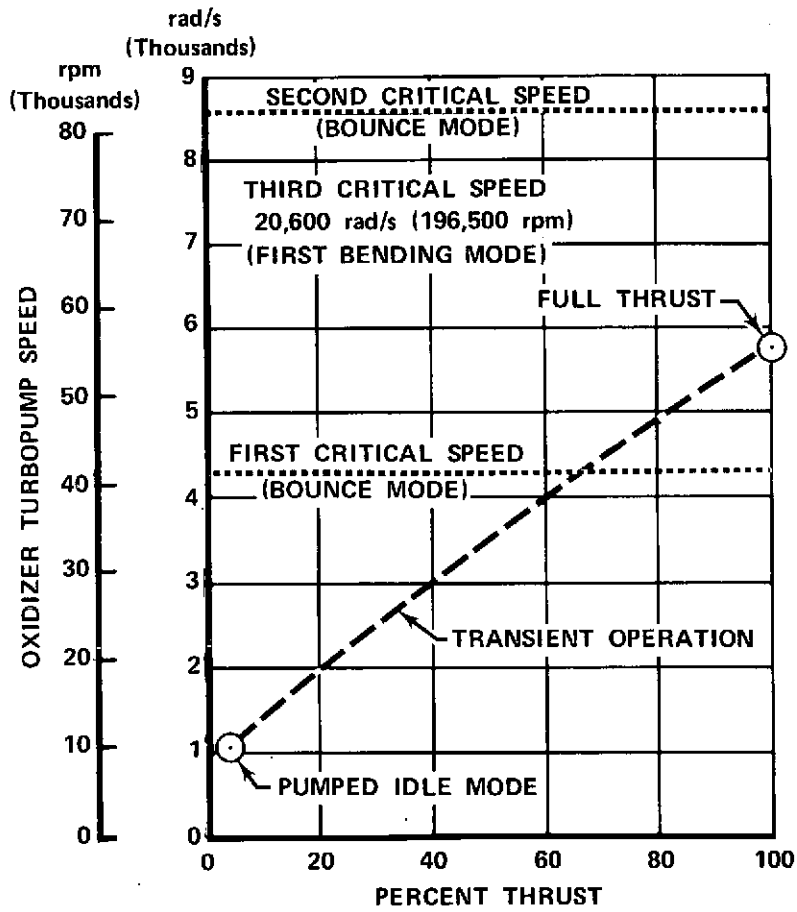

Figure 82. ASE High Pressure Oxidizer Turbopump Critical Speeds FD 71567

(2) Oxidizer Turbopump Turbine

The ASE high pressure oxidizer pump drive turbine is an axial flow, partial admission, single-stage impulse design. The aerodynamic sizing point for the oxidizer turbine is 100% thrust and mixture ratio of 6. At the design point the turbine develops 666 kw (892 hp) with a total-to-static efficiency of 53%. Table XX presents the operating conditions at the design point and figure 83 presents the mean velocity diagrams. The turbine off-design efficiency characteristic is shown in figure 84. The optimum arc of admission is 26% as shown in figure 85 for the 11.54 cm (4.545 in.) mean diameter oxidizer turbine. This results in minimum pressure ratio without requiring an excessively low vane exit angle. The oxidizer turbine elevation is shown in figure 86. As in the fuel turbine, blade height was set at 0.762 cm (0.30 in.) (a P&WA study groundrule minimum) which with a 0.0254 cm (0.010 in.) overlap at ID and OD yields a corresponding vane height of 0.711 cm (0.280 in.). To maintain a high airfoil aspect ratio to minimize airfoil end losses, chord lengths for the vane and blade were set at 0.762 cm (0.30in.). The small size of the oxidizer turbine makes airfoil end loss a large percentage of total airfoil loss. Vane and blade Zweifel load coefficients (Reference 14) were set at 0.78 and 0.87 based on P&WA XLR129 experience; 30 vanes and 68 blades are required.

Table XX. ASE High Pressure Oxidizer Turbopump Turbine

Turbine Operating Conditions at Design Point 100% Thrust, MR = 6.0	
Rotor Speed, rad/s (rpm)	5,760 (55,000)
Mean Wheel Speed, m/s (ft/sec)	332 (1091)
Mean Diameter, cm (in.)	11.54 (4.545)
Velocity Ratio, (total/static, isentropic)	0.249
Flowrate, kg/s (lb/sec)	1.410 (3.118)
Inlet Temperature, °K (°R)	1140 (2050)
Inlet Pressure, N/cm^2 (psia)	2230 (3226)
Pressure Ratio, (total/static)	1.468
Efficiency, (total/static)	0.530
Power, kw (hp)	666 (892)
Number of Stages	1
Percent Admission	26

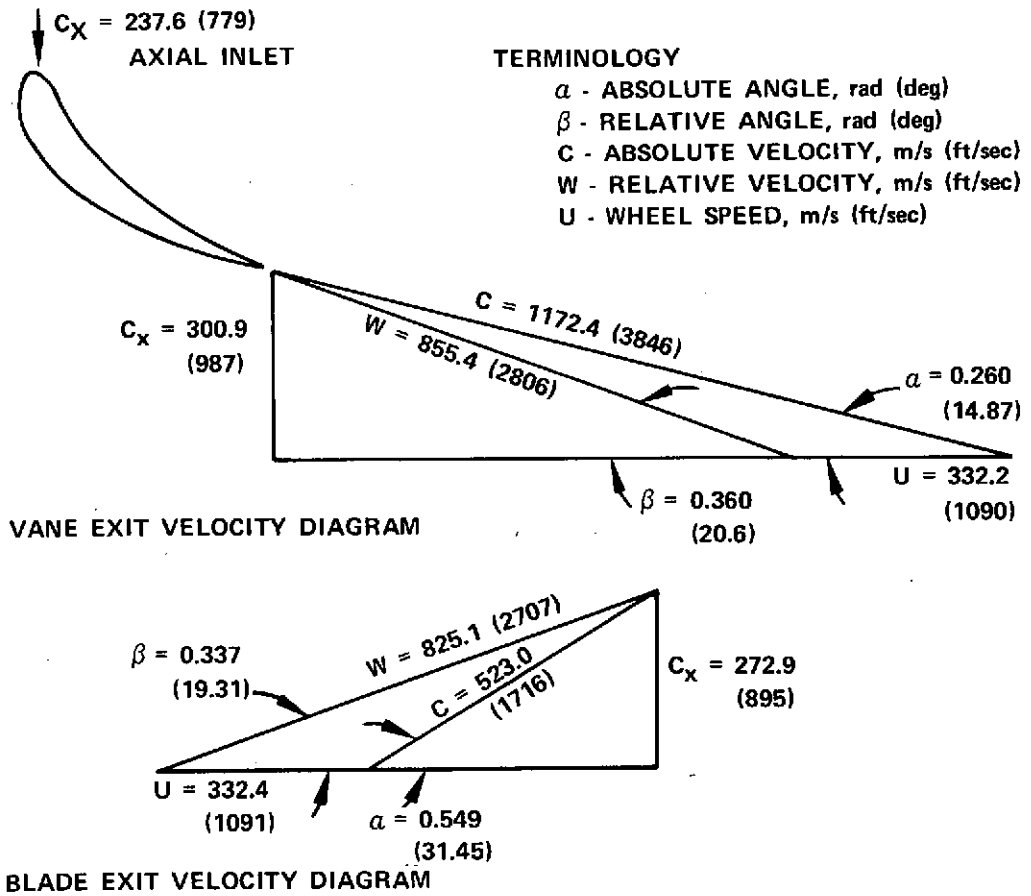

Figure 83. Advanced Space Engine Oxidizer Turbopump Turbine Design Point Mean Velocity Diagrams

FD 71598

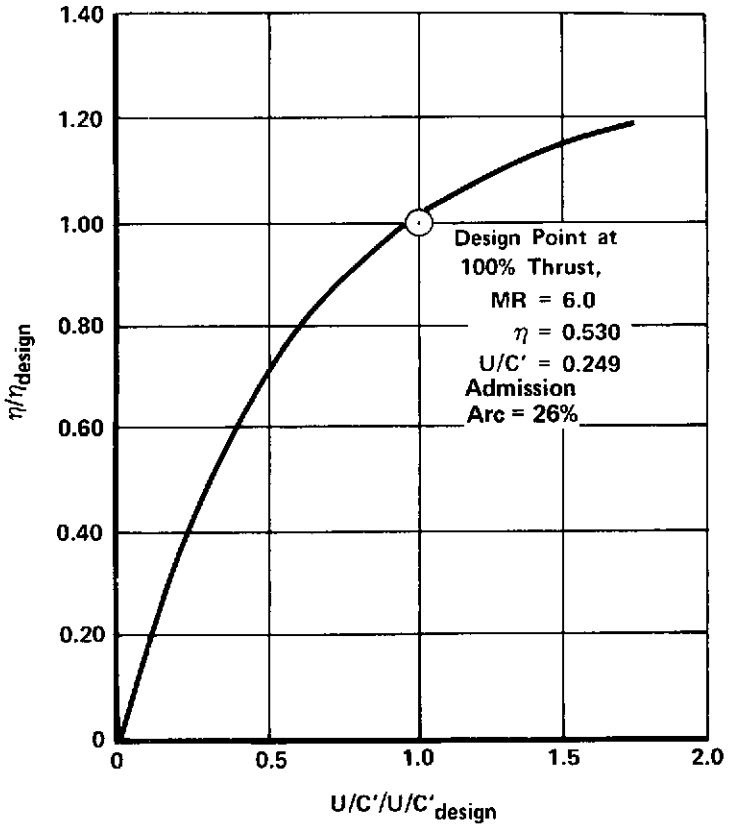

Figure 84. ASE Oxidizer Turbine Off-Design Efficiency Characteristic

FD 70529A

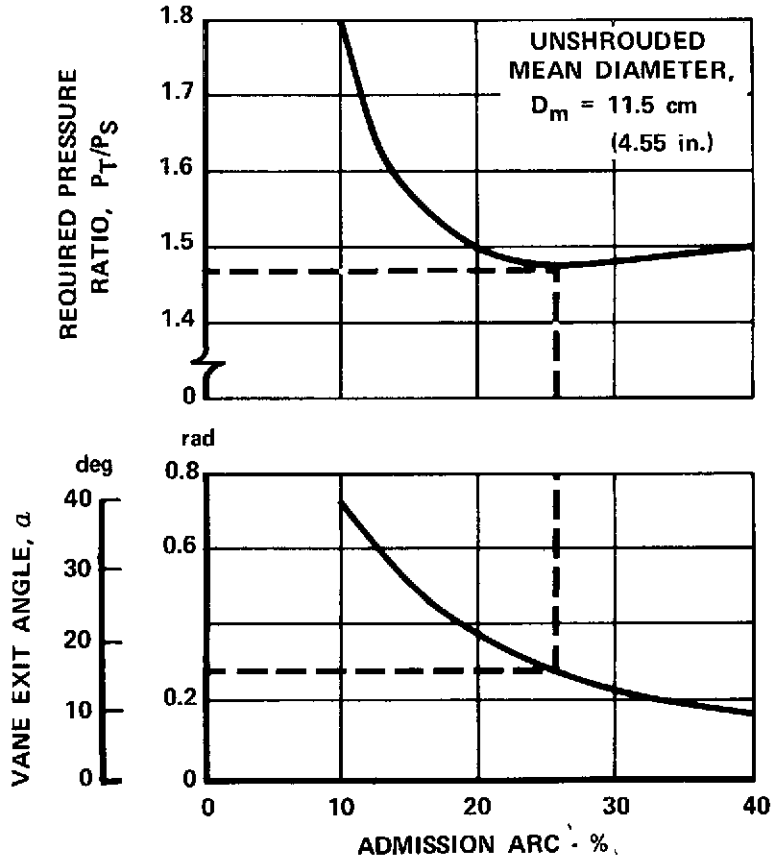

Figure 85. Effect of High Pressure Oxidizer Turbopump Turbine Admission Arc

FD 71597

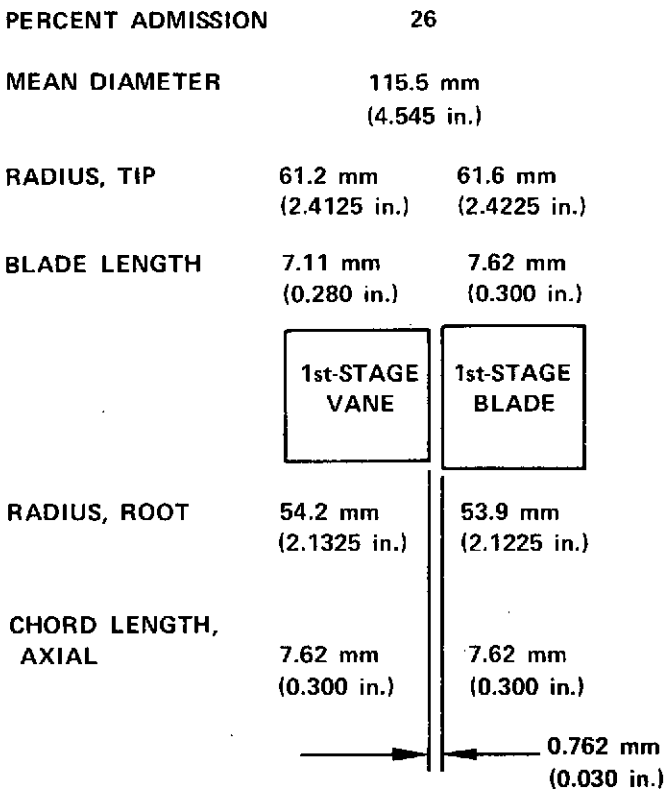

Figure 86. Oxidizer Turbopump Turbine Elevation FD 71601

The oxidizer turbine total leakage loss is 8.38% of the inlet flow and the effects are accounted for in turbine efficiency predictions. Blade tip leakage represents 4.65% of turbine inlet flow while 3.73% of the flow is circumferential leakage between the vanes and blades.

Table XXI presents predicted oxidizer turbine off-design performance based on ASE preliminary cycle 104A at 100% thrust, mixture ratios of 5.5, 6, and 6.5. This shows only a small variation in turbine isentropic mean velocity ratio (U/C) and corresponding small (≈1 point) variation in efficiency.

Table XXII presents at 100% thrust a blade stress and allowable temperature summary. The operating stress and temperature levels of the oxidizer turbine present no problem in the attainment of 10 hr, 1% creep life for IN100 (PWA™ 658/ AMS 5397) material.

c. Mechanical Description

The high pressure oxidizer turbopump consists of a high speed inducer, a single-stage impeller, a single acting thrust piston, a single-stage low reaction, unshrouded turbine, two ball bearings, two exterior housing sections, a pinion gear and a seal housing. (See figure 79.)

A single-stage shrouded impeller, in conjunction with the high speed inducer, provides a pressure range from 2551 N/cm^2 (3700 psia) to 3241 N/cm^2 (4700 psia) which is required for flow injection into the preburner and the main burner. The impeller has a 7.75 cm (3.055 in.) tip diameter with a maximum

tip velocity of 239 m/s (783 ft/sec) which is well below the limit of 640 m/s (2100 ft/sec) for an integrally shrouded Inco 718 impeller based on results of P&WA testing of a shrouded impeller rig which used a titanium alloy. Bore stress is ~124,000 N/cm^2 (180,000 psi).

Table XXI. ASE Oxidizer Turbopump Turbine Off-Design Performance at 100% Thrust

Mixture Ratio	5.5	6.0	6.5
Pressure Ratio (T/S)	1.52	1.468	1.447
Inlet Temperature, °K (°R)	1140 (2053)	1140 (2051)	1184 (2132)
Inlet Pressure, N/m^2 (psia)	2359.4 (3422.1)	2224.2 (3226)	2174.1 (3153.3)
Inlet Flow, kg/s (lb/sec)	1.52 (3.36)	1.41 (3.118)	1.29 (2.97)
Efficiency (T/S)	0.535	0.53	0.522
Isentropic Mean U/C, (T/S)	0.256	0.249	0.242
Rotor Speed, rad/s (rpm)	6162 (58,846)	5759 (55,000)	5594 (53,425)
Power, kw (hp)	785.4 (1053.3)	665.3 (892.2)	626.6 (840.4)

Table XXII. ASE Oxidizer Turbopump Turbine Blade Stress and Allowable Temperature at 100% Thrust IN100 (PWA™ 658/AMS 5397) Material

Mixture Ratio	5.5	6.0	6.5
T_{tbr}, °K (°R)	1,136 (2,044)	1,138 (2,048)	1,184 (2,131)
Blade Root Stress, N/cm^2 (psi)	12,882 (18,685)	11,253 (16,322)	10,617 (15,400)
Allowable T_{tbr}, °K (°R)	1,298 (2,336)	1,321 (2,377)	1,328 (2,390)

where:

T_{tbr} - Average Blade Relative Temperature, includes burner profile of 30°K (54°R) and Control Tolerance of 11°K (20°R)

Blade Root Stress - Constant section, untapered blade

Allowable T_{tbr} - Based on 10 hr, 1% creep life.

Both the impeller and inducer are fabricated from Inco 718 (AMS 5662) forgings. Inco 718 was selected because of its high strength to weight ratio. If an integral shroud is not economically feasible, a gold-nickel brazed-on shroud could be used since tip velocity is still below the design braze criteria limit of 488 m/s (1600 ft/sec). The impeller is splined to the shaft with snap diameters provided at each end of the hub. The impeller retaining bolt threads to the shaft and traps the inducer and impeller. The forward part of the retaining bolt projects into the LO_2 flow providing a smooth contour to the inducer inlet. A hexagonally shaped slot is provided in the forward part of the bolt for torquing.

A separate thrust balance piston is used in the ASE oxidizer turbopump to compensate for axial load unbalance during turbopump operation. As in the fuel turbopump, the axial loads are created by the relatively high pressures acting on the pump and turbine rotor disks. The oxidizer turbopump axial load is in only one direction since the single-stage pump load is in the same direction

as the turbine load, toward the pump inlet end of the turbopump. To compensate for the force unbalance, a single-acting thrust piston is used.

The single-acting thrust piston (figure 87) has high pressure fluid supplied to only one side of the piston while the other is vented to pump inlet pressure. The high pressure fluid flows from the single cavity through a clearance between the piston and lands on the housing. With shaft axial thrust in only one direction, but of varying magnitude, the single cavity is still self-compensating since displacement of the piston alters the exit metering resistance to produce cavity pressure changes which generate axial forces equal in magnitude to the applied load.

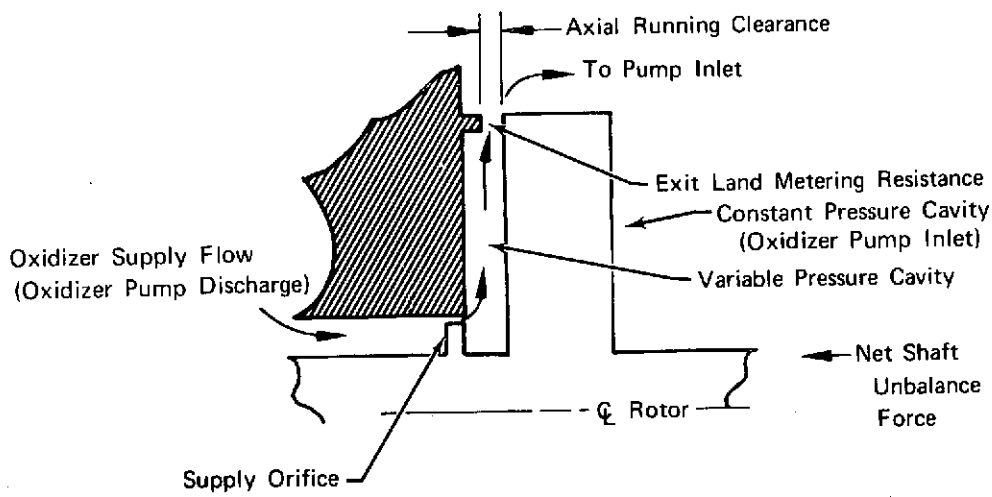

Figure 87. Representative Cross Section of Single-Acting Thrust Piston FD 51502A

The maximum predicted rotor unbalance (axial) occurs at maximum pressures (100% thrust and MR = 5.5) and is 40.8 kN (9170 lb). This consists of a 22.7 kN (5109 lb) pump load and a 8.1 kN (4061 lb) turbine load. The seal on the back-face of the pump, and a $\Delta P = 31$ N/cm^2 (45 psi) placed across the turbine disk sets the load at this level. The thrust piston (metering resistances of 5.72 cm (2.25 in.) diameter) provides an axial load compensation capability of 49.8 kN (11,200 lb) which is a margin of 22% above the predicted maximum unbalance. This condition requires a 1.1 kg/s (2.5 lb/sec) flowrate or 7.2% recirculation flow around the oxidizer pump.

The rotor assembly is supported by two angular contact ball bearings. Angular contact ball bearings are subject to less heat generation than preloaded roller bearings. Greater experience has been accumulated with angular contact ball bearings, which makes them desirable for this application where high stiffness is not required as it would be in a variable thrust engine. Angular contact 50 mm ball bearings for a large thrust size high pressure oxidizer pump, which were fabricated from 440C (AMS 5630) material, had similar internal geometry (except for number of balls) and were successfully operated in oxygen at a DN of 1.3×10^6 mm-rpm for over 10 hours in a P&WA program (Reference 18).

The single 20 mm x 47 mm bearings used to support the turbopump shaft are identical split inner race types. Internal bearing geometry is:

Number of balls	8
Diameter of balls	0.7938 cm (0.3125 in.)
Pitch diameter	3.35 cm (1.3189 in.)
Inner race curvature	1.47 cm (0.58 in.)
Outer race curvature	1.32 cm (0.52 in.)
Operating contact angle	0.31 rad (18.0 deg)

Internal geometry selection was based on results of extensive parametric studies performed under Contract NAS8-26186, SSME Definition (Phase B) Program. These studies indicated that bearing internal geometry will yield sufficiently high radial spring rates to prevent bending critical speed problems. This geometry also limits ball excursion to values below the cage pocket clearance, thus avoiding cage problems. Values of internal kinematic parameters were kept within the range of previous experience in order to limit wear and heat generation. The bearings operate at a DN of 1.1×10^6 mm-rpm at the engine nominal operating point. The front bearing is cooled by 0.17 kg/s (0.37 lb/sec) of LO_2 from the thrust piston supply. The coolant is circulated through grooves provided on the bearing inner race, then through a two-step labyrinth seal and through drilled passages and grooves in the impeller hub. Flow is then directed through drilled holes in the retaining bolt and into the oxidizer pump inlet.

Rear (turbine) bearing hydrogen coolant is supplied from the fuel turbopump rear bearing discharge flow. The coolant first passes into the oxidizer turbine housing compartment where it serves three purposes: one, to provide a coolant for the turbine disk, two, to provide a dam to prevent leakage of hot combustion products into the gearbox, and three, to provide thrust balance pressure on the turbine disk. Part of the coolant passes through a three step labyrinth seal into the gearbox. The remainder of the flow passes through holes in the turbine disk hub and into grooves in the turbine drive shaft which runs under the rear bearing inner race. These grooves vent the flow to the gearbox cavity in front of the bearing. The rear bearing hydrogen coolant flowrate is 0.08 kg/s (0.17 lb/sec).

The bearings are constructed from vacuum melt 440C (AMS 5630) stainless steel as required by the NASA/LeRC study ground rules. This material has high strength and is compatible with oxygen/hydrogen environments. Substantiation of this material's integrity was based on its successful use as a bearing material in the RL10 engine. The cages are stainless steel shielded Salox-M (bronze filled fluorocarbon plastic) of one piece inner land riding design. Cages of this type have demonstrated 10 hr life in 1.11 MN (250,000 lb) and 1.56 MN (350,000 lb) thrust high pressure engine bearings and have been qualified for use in the RL10. The bearings are mounted in spring loaded slipper rings to permit motion in compliance with thrust piston movement. Rotor overtravel during transients is limited by stops on the outer bearing races.

Power is delivered to the oxidizer pump and hydrogen/oxygen boost pumps by a single-stage turbine. The turbine features blades that are integral with the disk, because of the small blade size, and fabricated from PWA 658 (IN100) material which was selected because of its superior strength-to-weight ratio at elevated temperatures and its compatibility with hydrogen. The oxidizer turbine disk is cooled by 0.22 kg/s (0.49 lb/sec) of hydrogen supplied from the fuel turbopump rear bearing. The turbine blades are uncooled, although disk cooling is provided between

labyrinth seals. A tandem set of dual labyrinth seals are provided to form a hydrogen cooled dam at the disk outer diameter. The running labyrinth seal clearance is 0.015 mm (0.002 in.) radially whereas the assembly clearance is larger due to the disk having a higher thermal expansion coefficient than the turbine inner housing. Power is transferred from the disk to the shaft by a 3.05 mm (0.120 in.) diameter pin inserted halfway in the shaft and disk bore.

Sizing of the disk was based on Space Shuttle Main Engine design criteria with exception of the burst margin, which is 20%. The average tangential stress allowable, using a material utilization factor of 0.85, was set at 77221 N/cm^2 (112,000 psi). The effective stress allowable was set at 99974 N/cm^2 (145,000 psi). The resulting disk weighed 0.29 kg (0.63 lb) which was light enough to be beneficial in meeting critical speed margins. The diametrical growth at the live rim was 0.030 cm (0.012 in.) The average tangential stress was 60,674 N/cm^2 (88,000 psi) and the effective stress 99,285 N/cm^2 (144,000 psi).

The effect of gear loads from the fuel and oxidizer boost pumps displace the turbine disk seal clearances. Maximum deflection is less than 0.013 mm (0.0005 in.) with bearing spring rates in the 0.350 MN/cm (200,000 lb/in.) range. With 0.051 mm (0.002 in.) radial running clearance, seal rub will not be encountered.

The impeller and turbine shaft is machined from Inco 718 (AMS 5662) forgings to provide a midspan shaft stiffness necessary for critical speed dampening and thermal compatibility with the impellers and inducer. Maximum torsional stress is 30,337 N/cm^2 (44,000 psi) with an allowable stress of 57,227 N/cm^2 (83,000 psi).

The pinion gear which transmits power to the LO_2 and LH_2 boost pumps is located between the turbine and rear bearing. The gear is piloted on the shaft and coupled to it by a 0.318 cm (0.125 in.) diameter pin installed lengthwise between the gear and shaft. This method of attachment provides concentricity control which ensures close tolerances on the gear mesh for extended gear life. The gear was sized for the LH_2 boost pump power of 25.950 kw (34.8 hp), a pitch line velocity of 94 m/s (18,500 fpm), and a Hertz stress of 41,369 N/cm^2 (60,000 psi). For additional gear information see Paragraph E2, Low Pressure Pumps and Gearbox.

The inducer and impeller-seal housings are fabricated from A-286 (AMS 5735) material to provide high strength in high pressure areas and thermal compatibility with gearbox. The impeller-seal housing is integral with the gearbox housing. (See paragraph E2.) The A-286 housings, having a greater thermal expansion than the Inco 718 impeller and inducer, allow a larger seal clearance at assembly than at operating conditions. This condition provides a closely controlled seal clearance at rated thrust.

The impeller-seal housings contains a removable structural piece which supports the outer bearing race and also forms the stationary face for the thrust balance piston. This piece is trapped by the impeller seal land which also supports the bearing axial spring. A polyimide coating of 0.254 mm (0.010 in.) is applied to the housings in the impeller labyrinth seal running areas to prevent potential metal-to-metal contact between housing and rotor.

The inducer housing contains a seal drain which allows impeller discharge seal leakage to flow back to the inducer via a tube. This drain reduces pressure load on the flange toroidal seal. The tube allows the inducer flowpath wall to be very thin, thus reducing cooldown boil-off during startup. If flow were allowed to enter the cavity instead of the tube at startup, heat would be drawn from the outer housings causing the oxidizer to boil-off producing a high percentage of gas to liquid fluid at the pump inlet.

Twin discharge volutes are provided to minimize bearing radial loads caused by uneven pressure distribution around the impeller. The volutes are welded into the impeller seal housing to simplify the forging configuration.

The turbine discharge housing provides a plenum for preburner combustion gases to collect for return to the main case through the outer annulus of a coaxial supply/return line. The housing is a welded assembly of A-286 (AMS 5731) and was designed for a burst safety factor of 1.5. A porous inner liner of sintered woven AISI 347 is transpiration cooled by hydrogen so the outer housing can be maintained at a relatively low temperature for maximum strength. Coolant is supplied from the thrust chamber coolant jacket discharge flow at a rate of 0.045 kg/s (0.10 lb/sec). After passing through the liner, the coolant mixes with the preburner gases discharging from the turbine and returns to the main case.

Within the turbine discharge housing an inner section fabricated from NX-188 (PWA 643-castable nickel alloy) connects a circular cross section inlet connection with the inner conduit of the coaxial supply/return line from the main case. The circular cross section transitions into the integral vanes forming a 26% arc of admission. A dome covering the face of the turbine wheel protects the shaft area from the hot gases and forms a passage for the exhaust gases.

An inner housing just forward of the turbine disk separates the high pressure turbine coolant from the low pressure gearbox. This housing contains the turbine flow turnaround cavity and drilled passages for transmitting coolant flow into the turbine compartment. The housing is fabricated from NX-188 (PWA 643) material and is sized for a pressure differential of 1379 N/cm^2 (2000 psi). A dual pilot is provided on the outer diameter to minimize deflection at the inner diameter seal land.

The shaft seal compartment, located between the pump and gearbox, consists of an oxidizer (hydrodynamic face) seal, a helium purge (double floating ring) seal, and a gearbox (double floating ring) seal. The seal holders which contain the floating ring seals are held in place by a locknut on the inner surface diameter of the impeller-seal housing.

The same seal package is used on the oxidizer boost pump. This seal package was selected to ensure low breakaway torque for pumped idle mode and to provide minimal seal leakage. Furthermore, this seal package provides a failsafe separation of liquid oxidizer and hydrogen-rich turbine hot gases, and to allow safe engine operation in the event of a single seal failure. The RL10 seal package, which includes rubbing face and split ring seals, could not be used in the ASE because of its high loads and the low starting torque capability of the ASE.

The hydrodynamic face seal was selected over the conventional rubbing contact seal for use as the primary oxidizer seal to meet operating life. The floating ring shaft seal was rejected because of higher leakage loss. The single and double floating ring seal was selected over the labyrinth seals for the secondary oxidizer and primary and secondary fuel seals because of higher helium consumption and additional weight penalty.

The floating ring seals are fabricated from a P5N carbon insert with an Inco 750 retainer band. To increase carbon wear resistance, the mating ring surfaces are chrome plated. To establish a static seal within the ring compartment the seals are axially loaded against the ring housing by wave springs and pressure load.

Shaft to seal ring radial operating clearance of 0.013 mm (0.0005 in.) minimizes seal leakages. Oxidizer seal overboard leakage is 0.014 kg/s (0.03 lb/sec). Primary fuel seal leakage (recirculated to the fuel pump inlet) is 0.0334 kg/s (0.0485 lb/sec) and the secondary (overboard) fuel seal leakage is 0.0059 kg/s (0.0085 lb/sec).

5. Preburner Assembly

a. General Description:

The preburner is an oxygen-hydrogen combustor that generates fuel-rich hot gases to power the oxidizer and fuel pump drive turbines during mainstage operation only (acceleration from pumped idle to and for rated thrust operation). During tank head and pumped idle only gaseous hydrogen is supplied to the preburner. The engine operates in pumped idle in the expander mode (unlit preburner) which eliminates many of the problems of preburner design and operation associated with staged combustion at low thrust levels. The preburner is designed to provide a stable turbine working fluid, possessing uniform temperature and total pressure profiles.

Liquid oxygen and gaseous hydrogen are supplied to the preburner injector at rated thrust. The hot gases, resulting from the combustion of these propellants, are divided and ducted into the oxidizer and fuel pump drive turbines before being injected into the main chamber through the hot gas (fuel) injector. The arrangement of the preburner is shown in figure 88.

In establishing the design for the ASE preburner, experience gained in the XLR129 Air Force Reusable Rocket Engine Program was used extensively. A multiple concentric jet-type injector with single orifice oxidizer elements was selected. The concentric jet injector configuration produces low temperature profile variations. Because the ASE is a fixed-thrust engine, and operates as an expander cycle engine with no combustion in the preburner when in idle mode, dual-orifice oxidizer elements are not required to provide adequate injector pressure losses for the high flow turndown ratios associated with deep throttling. Use of single orifice oxidizer elements results in simpler mechanical designs for the injector and preburner oxidizer control valve.

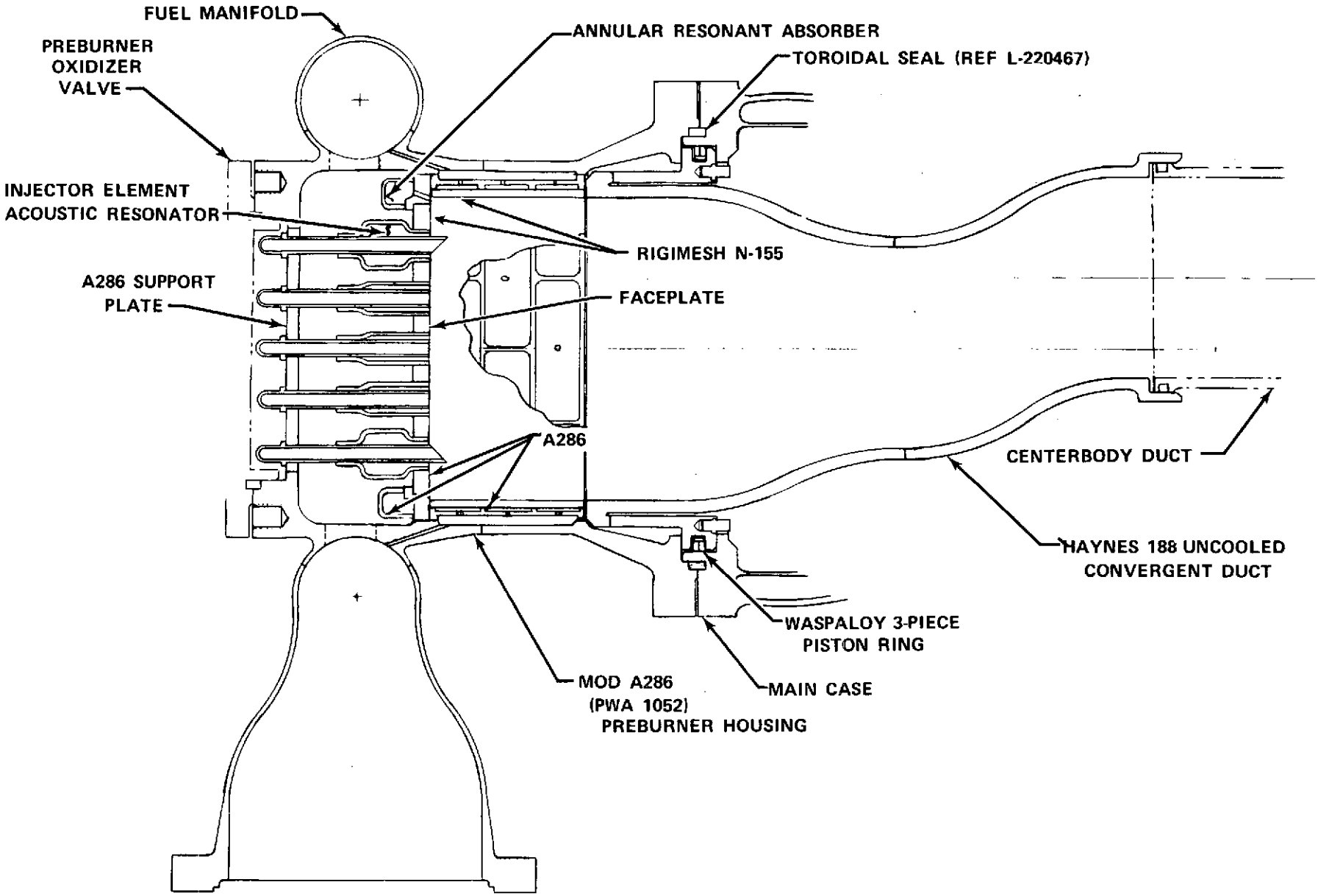

Figure 88. ASE Preburner

FD 72392

The preburner duct has a transpiration-cooled liner immediately downstream of the injector face and is sized to ensure a low throughput Mach number and long residence time for thorough mixing of the combustion products. Acoustic resonators are included in the injector design to suppress acoustic combustion instability. Ignition is accomplished with dual spark igniters located in the side of the preburner, 1.91 cm (0.75 in.) downstream of the injector faceplate.

The preburner is mounted on the main case with its centerline perpendicular to the engine thrust axis.

b. Operating Characteristics

(1) Ignition

Preburner ignition is accomplished with two spark igniters mounted in the side of the preburner approximately 2.1 rad (120 deg) apart and in different mixture ratio regions, with one igniter in line with an outer row oxidizer injector element and the other igniter located between elements. The deliberate positioning of igniters in regions of different mixture ratios increases the range of the mixture ratio at the igniters when the preburner oxidizer valve is first opened. Since ignition in the preburner initially takes place when the engine operating mode changes from pumped idle (with only fuel in the preburner) to mainstage operation, the pressure in the preburner is at a relatively high level, 68.9 N/cm^2 (100 psia). The combination of self-atomizing oxidizer injector elements, high preburner pressure and warm fuel at 294°K (530°R) in the preburner will ensure reliable ignition with minimal delay time. With the fuel lead in the preburner, there is less chance of an ignition temperature spike caused by an oxidizer flow overshoot. Good control of the oxidizer flow through the injector during the ignition phase is obtained by having the valve very close-coupled to the injector, by taking the flow to the GO_2 heat exchanger from immediately upstream of the preburner oxidizer valve pintle, and by minimizing the volume of the injector manifold downstream of the valve pintle.

Use of spark igniters avoided the complexity of a torch ignition system. Furthermore, locating a torch igniter in the center of the preburner injector would have prevented the close-coupling of the preburner oxidizer valve. Mounting a torch igniter in the side of the preburner in the same location as for the spark igniter(s) could have resulted in burnout of the preburner wall opposite the igniter since the preburner diameter is small, 7.62 cm (3 in.), and results in proximity of the wall to the tip of the torch igniter.

(2) Combustion Performance

Preburner combustion performance is determined from the engine cycle power balance and design requirements, while operating within the turbomachinery maximum allowable temperature. For the ASE, the combination of expander cycle operation in the low idle modes and staged combustion operation only at the 100% thrust level means that the preburner design requirements can be relaxed in comparison with staged combustion engines which are required to operate over a large throttling range. The combustion performance has only to satisfy the comparatively minor accommodations required for operation at off-design engine mixture ratios.

Figures 89 and 90 show the preburner combustion temperature and chamber pressure, respectively, which were required to satisfy the engine cycle power balance for the baseline cycle No. 104. The preburner injector propellant flowrates and the resulting mixture ratios are shown in figures 91 and 92. The fuel/oxidizer momentum ratios are shown in figure 92.

To make maximum power available to the turbines while ensuring turbine and preburner integrity, the performance of the preburner has to combine high efficiency with thorough mixing for uniform temperature profile while maintaining stable combustion. The preburner injector configuration, which has been selected to accomplish these objectives, is a fixed-area fuel, single-orifice oxidizer coaxial element concept, which incorporates tangential-entry slot-swirler oxidizer injection elements.

Performance prediction techniques for rocket combustors are typically concerned only with overall performance in terms of c* (characteristic velocity) efficiency. In comparison with main burner chambers, preburners are characterized by longer residence times, lower throughput velocities, greater combustor lengths, and lower mixture ratios; all of which are favorable for higher combustion efficiencies. Since combustion efficiencies in excess of 99% are readily attainable in main burner chambers either with hot, 1000°K (1800°R), or cold, 222°K (400°R) fuel, in theory combustion efficiencies of essentially 100% can be expected. In actual tests, the XLR129 preburner consistently demonstrated this level of performance.

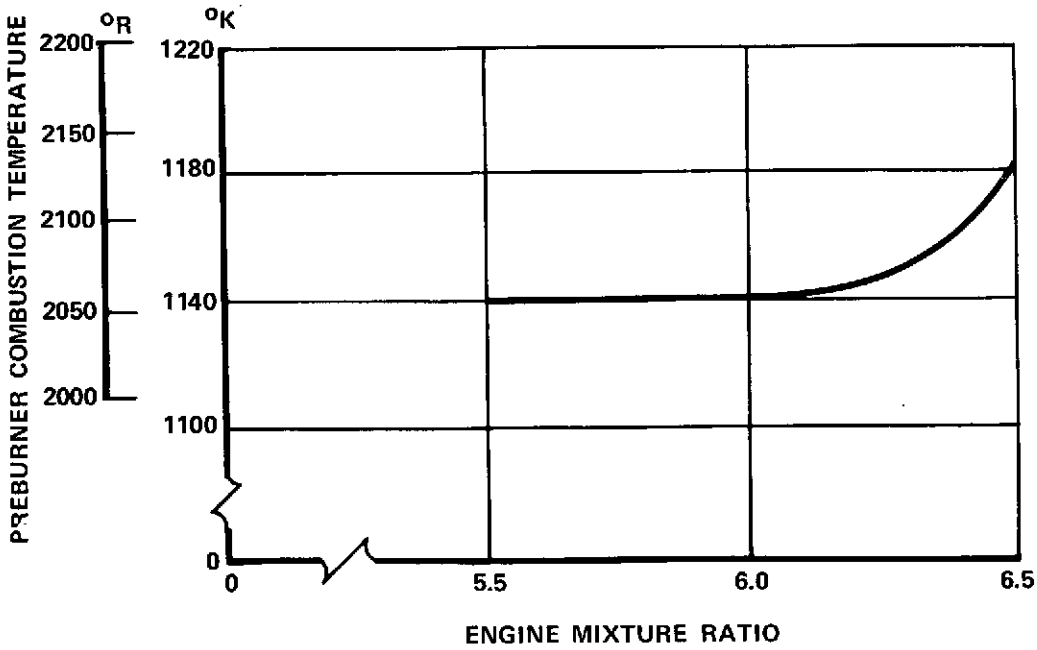

Figure 89. Advanced Space Engine Preburner Combustion Temperature at Rated Thrust FD 68810

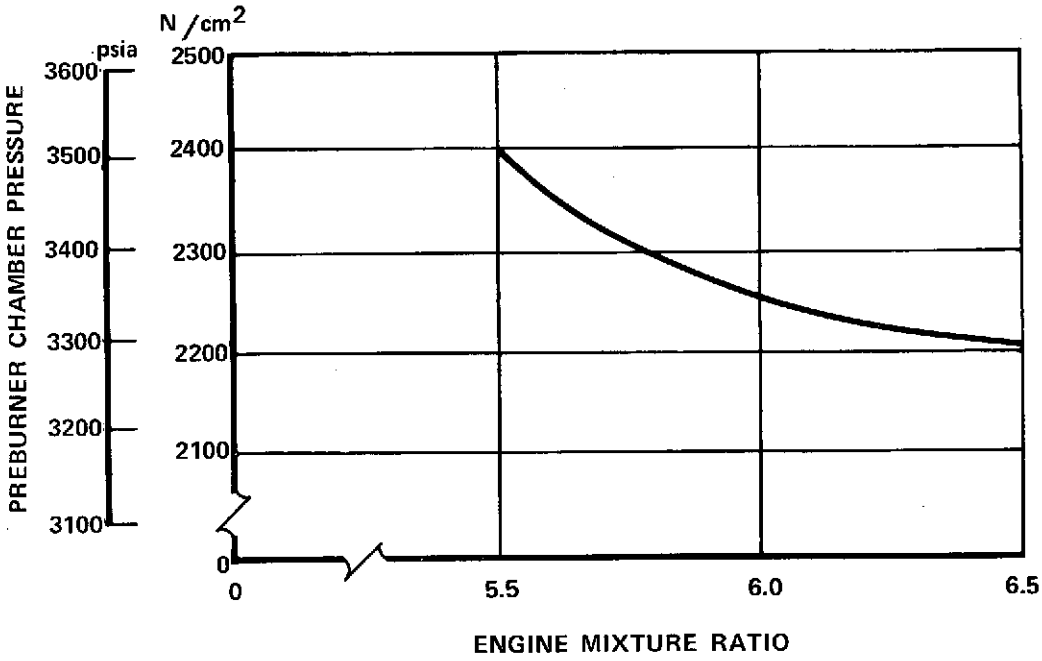

Figure 90. Advanced Space Engine Preburner Chamber Pressure at Rated Thrust

FD 68811

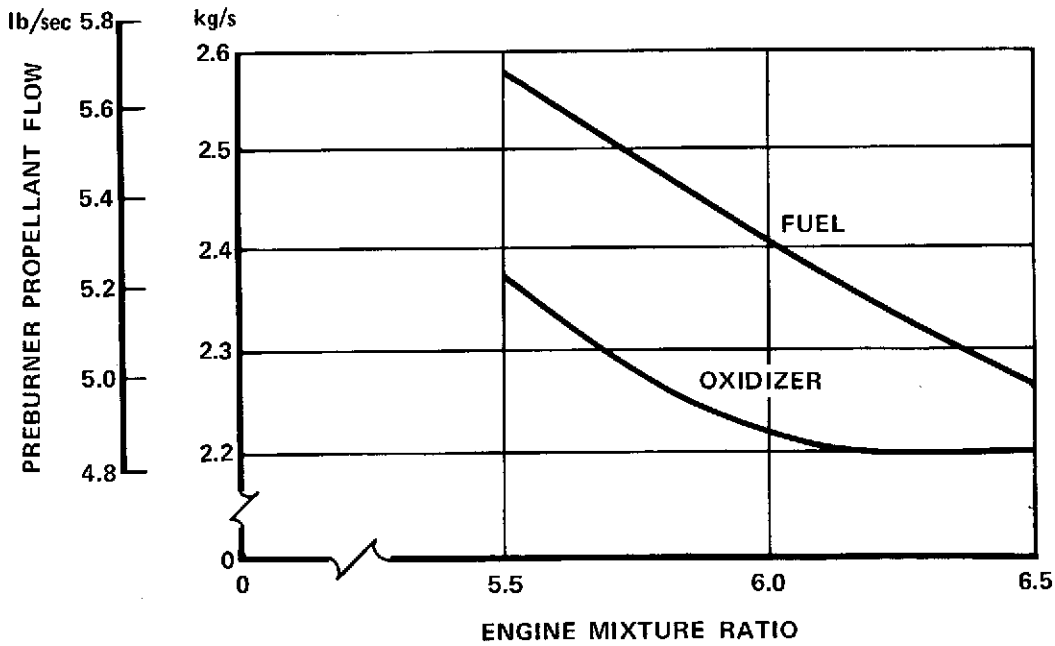

Figure 91. Advanced Space Engine Preburner Propellant Flows at Rated Thrust

FD 68812

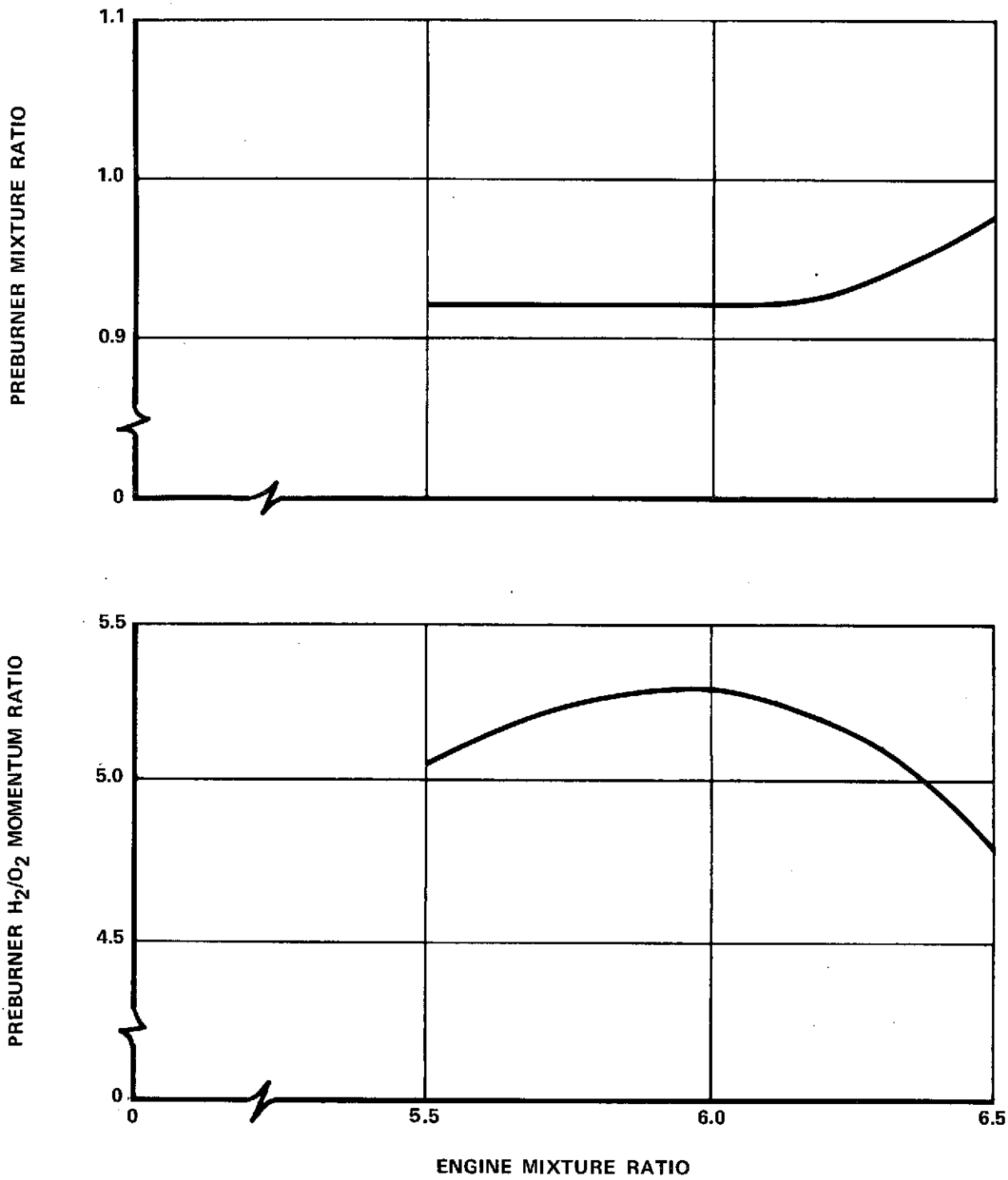

Figure 92. ASE Preburner Mixture Ratio and Fuel/Oxidizer Momentum Ratio at Rated Thrust

FD 68813

Of the two performance goals, combustion efficiency and temperature profile, the attainment of a uniform temperature profile is the more difficult to attain. To evaluate the effect of engine cycle and geometric variables upon performance, P&WA has developed an analytical design correlation to relate the above to exit temperature profile. This correlation is

$$\text{Peak minus average exit temperature} = 50.6e^{0.75B}$$

The value of B is obtained from an empirical correlation which includes engine cycle and geometric variables to predict exit temperature profiles.

$$B = \frac{V_c}{(MR)\left(\frac{L}{D_c}\right)\left(\frac{AN \times N}{A_c}\right)^{0.3} e^{0.008\,T_f}}$$

where:

V_c = Combustion chamber propellant throughput velocity
MR = Fuel/oxidizer momentum ratio or fuel velocity/oxidizer velocity x mixture ratio
L = Effective combustor length or total duct and chamber volume/injector face area
D_c = Injector face diameter
AN = Atomization number
N = Number of injection elements
A_c = Injector face area
T_f = Fuel temperature

Substitution of representative values from the current engine design and engine cycle show $\Delta T = 30°K$ (54°R).

Results of the above-mentioned correlation indicate that the design and engine cycle provide a very favorable environment for attainment of a low temperature profile. The design may therefore be scaled directly from previous high pressure rocket engine preburner designs without technical risk. In particular, XLR129 test experience and previous design studies indicate that a favorable scaling parameter is the engine thrust divided by the number of preburner injection elements; this number should be very close to 1,000. This criterion is satisfied with 20 elements. A minimum injection element spacing of 1.22 cm (0.48 in.) is also standard. This value was increased slightly to 1.27 cm (0.5 in.) in order to provide room for the faceplate resonator cavities. The injection element spacing and pattern selected for the ASE preburner injector provides the desired number of elements and element minimum spacing.

(3) Injector Flow

The injector manifolds and cavities were sized for minimum total pressure loss so that maximum pressure would be available for injection, while at the same time providing sufficient pressure loss, where required, to ensure proper distribution of propellants. Dynamic loss coefficients based upon XLR129 flow tests were used in these analyses, supplemented where necessary with loss coefficients from the SAE Aerospace Applied Thermodynamic Manual.

Fuel enters the injector from a single inlet horn and passes into a wrap-around manifold. The manifold diameter was sized to the same criterion as the 44 kN (10,000 lb) and 111 kN (25,000 lb) thrust P&WA OOS engine designs: an inlet region velocity of 91 m/s (300 ft/sec). This resulted in a manifold diameter of 2.95 cm (1.16 in.). The inlet horn diameter was set by the fuel shunt valve size at 6.35 cm (2.5 in.). The resulting total pressure loss for the 100% thrust, MR = 6 design point, and using SAE loss coefficients, from the inlet horn to the manifold, is 6 N/cm^2 (9 psi). The manifold velocity head is 14 N/cm^2 (21 psi), resulting in a manifold-to-chamber static pressure differential of 116 N/cm^2 (168 psid). This must be apportioned among the fuel crossover passages, the injection element spacer (or acoustic resonator) inlet slots, and the injection element fuel annuli at the faceplate itself. All these differential pressures are static-to-static.

Approximately 8.5% of the total pressure loss, or 10 N/cm^2 (15 psi), is taken across the fuel crossover passages. This is sufficient to ensure a uniform circumferential flow distribution as the fuel enters the injector cavity. The height of the cavity, 2.92 cm (1.15 in.), results in a maximum transverse velocity of 18 m/s (60 ft/sec) equivalent, to a dynamic head of less than 0.3 N/cm^2 (0.5 psi). This ensures that there will be no static pressure gradients across the fuel injector cavity. The remaining static pressure differential is 105 N/cm^2 (153 psi), 25% of this, or 26 N/cm^2 (38 psi), is taken across the element spacer (or resonator cavity) inlet slots; the remainder, or 79 N/cm^2 (115 psi), is taken across the injection element fuel annuli.

Oxidizer flow to the preburner injector is controlled by a pintle valve mounted directly to the injector body. This valve also incorporates a shutoff function for idle operation. Oxidizer tank pressurization flow is tapped off just upstream of the control and shutoff point. This combination ensures that the preburner oxidizer supply system will be continually preconditioned, during idle mode operation when the preburner is not lit, to a point as close as possible to the injector. Gaseous and two-phase oxidizer flow during the preburner start transient is held to a minimum, as the cryogenic oxidizer cools the oxidizer side of the injector. This, in turn, reduces the risk of rough combustion or severe temperature spikes.

The flow area downstream of the valve control point is 1.897 cm^2 (0.294 sq in.) which results in an oxidizer flow dynamic head of 6 N/cm^2 (9 psi) at the maximum oxidizer flowrate. Although this is only 3.6% of the total oxidizer injection differential pressure and can result in at most a 1.6% mixture ratio variation, a diverter plate has been incorporated in the valve to prevent flow impingement upon oxidizer injection elements. The height of the oxidizer cavity, 0.89 cm (0.35 in.) results in a transverse oxidizer dynamic head of less than 0.4 N/cm^2 (0.6 psi). Transverse static pressure gradients across the oxidizer injector cavity are thus eliminated.

(4) Duct Cooling Requirements

Prior to the XLR129 Demonstrator Engine Program, extensive testing of a dual orifice oxidizer, fixed area fuel preburner injector, under the supporting data and analysis program, was conducted. These tests clearly indicated that an uncooled preburner duct should not be located within 1.27 cm (0.5 in.) of the outer injection elements. During the test program, the uncooled

scrub liner repeatedly suffered localized damage. Many of the damaged areas could be directly related to outward-directed flow patterns created from the counter-rotating injection element pattern. The rest of the damaged areas could not be attributed to the aforementioned flow pattern produced by the concentric injector elements. As a result of these tests, the XLR129 preburner was designed with an uncooled scrub liner 1.8 cm (0.7 in.) from the outermost elements. Testing showed that even with this separation a cooled liner was necessary. A Rigimesh liner was therefore built and incorporated in all subsequent preburner, powerhead, and staged combustion tests.

Because the ASE preburner duct is located slightly less than 1.3 cm (0.5 in.) from the outermost row of elements, a transpiration-cooled Rigimesh liner is incorporated for protection. In addition, the outer row of elements is scarfed 0.785 rad (45 deg); this scarfing has the effect of shifting the spray cone axis by half this angle, thereby reducing the mixture ratio adjacent to the wall. Testing of the No. 2 preburner injector for the XLR129, which incorporated scarfed elements, indicated that the effects of the localized mixture ratio variations upon the temperature profile are negligible.

(5) Combustion Stability

Combustion instability that might be encountered in the Advanced Space Engine preburner is of two general types: feed-system-coupled nonacoustic instability (chugging) and acoustic instability (screech). The ASE preburner design and engine cycle incorporate measures to prevent both types of instability.

Chugging has previously been encountered in high-pressure rocket engine programs; most notably during the supporting data and analysis efforts. During preburner injector tests, chugging was encountered at all equivalent thrust levels below 25% of full thrust. Tests were scheduled to evaluate the effects of primary-to-secondary oxidizer flow split, fuel temperature, and test stand volumes. Some minor effects of the first variable were noted, but raising the fuel temperature above 167°K (300°R) eliminated the instability. To further investigate the problem analytically, an analog computer simulation of the preburner using the Double Dead Time model was formulated and tested. These studies signified that chugging could be eliminated by reducing the volume of the secondary oxidizer cavity by 20%. This change, incorporated into the nearly identical XLR129 demonstrator engine preburner injector, did in fact result in stable combustion at the 20% thrust operating point.

The importance of the preceding discussion, as applied to the single-orifice oxidizer ASE preburner, is that chugging is most likely to be suppressed by using very small injector cavity volumes; commensurate, of course, with minimum pressure loss for proper propellant distribution and high fuel temperatures characteristic of the ASE. Additionally, injector pressure losses at the injection plane should be held to minimum values of 4.5% for liquid propellants and 3.0% for gaseous. The only occasion in which chugging is likely to occur is during transient conditions from pumped idle to full thrust. A rapid start transient would raise the injection pressure losses to above their respective lower stability bounds before an instability can develop.

Acoustic resonator devices located in the preburner faceplate provide damping for acoustic instability, or screech. These absorbing devices are

reliable and effective and can be provided in a variety of configurations. The ASE preburner features two different configurations: one is similar to the annular cavity of the main chamber, the second is unique, consisting of a tuned resonator cavity around each of the peripheral oxidizer injection elements. The fuel flows through these resonator cavities before its injection into the combustion chamber, providing a constant known gas temperature and composition inside the resonator. The regulated properties of the working gas provide a far more reliable prediction of absorption characteristics of the device at the design frequency of 13,500 Hz. The flow through the aperture has the effect of reducing the total absorption and increasing the bandwidth of the device. The outer row of elements was selected because the first tangential mode was to be damped, i.e., located where the maximum and minimum of the pressure oscillation occurs. This type of acoustic resonator (absorber) device is believed to be new and has not yet been tested at FRDC; however, its innovative characteristics lean to an attractive configuration.

The annular cavity located at the periphery of the faceplace is also tuned to provide damping at the frequency of the first tangential mode. As in the main chamber resonator, the acoustic cavity is purged with fuel and divided into eight separate resonators by baffles.

Figures 93 and 94 show the design absorption coefficient and frequency bandwith of the preburner resonators. The length of the oxidizer injection elements was sized so that their first longitudinal acoustic mode frequency is sufficiently different from that of the first tangential mode of the preburner combustion chamber, thereby assuring that instability due to coupling between these two modes will not occur.

c. Mechanical Description

The preburner for the Advanced Space Engine is mounted on the engine main case, with its centerline perpendicular to the engine thrust axis. Two spark igniters and the preburner oxidizer control valve are mounted directly to the preburner housing. A 6.4 cm (2.5 in.) diameter line brings warm hydrogen from the main chamber coolant exit manifold to the preburner fuel distribution manifold. Figure 88 shows the preburner cross section.

The preburner is a welded assembly with pressed-in cooled chamber liner and separate uncooled chamber and duct. This assembly forms a plug-in component for the main case to facilitate removal and replacement. The uncooled chamber-duct is a mechanically separate assembly and is mounted by trapping its mounting flange between the main case and the preburner mounting flange. The gap between the uncooled and cooled chambers is purged with cool hydrogen. The Rigimesh liner of the cooled chamber is welded to a coolant distribution sleeve and pressed into place just downstream of the faceplate. The preburner housing is a body of revolution with the igniter bosses and the fuel manifold added as welded attachments. The injector is manufactured by welding its components into the housing to form one assembly. The major components of the ASE preburner are described in the following pages.

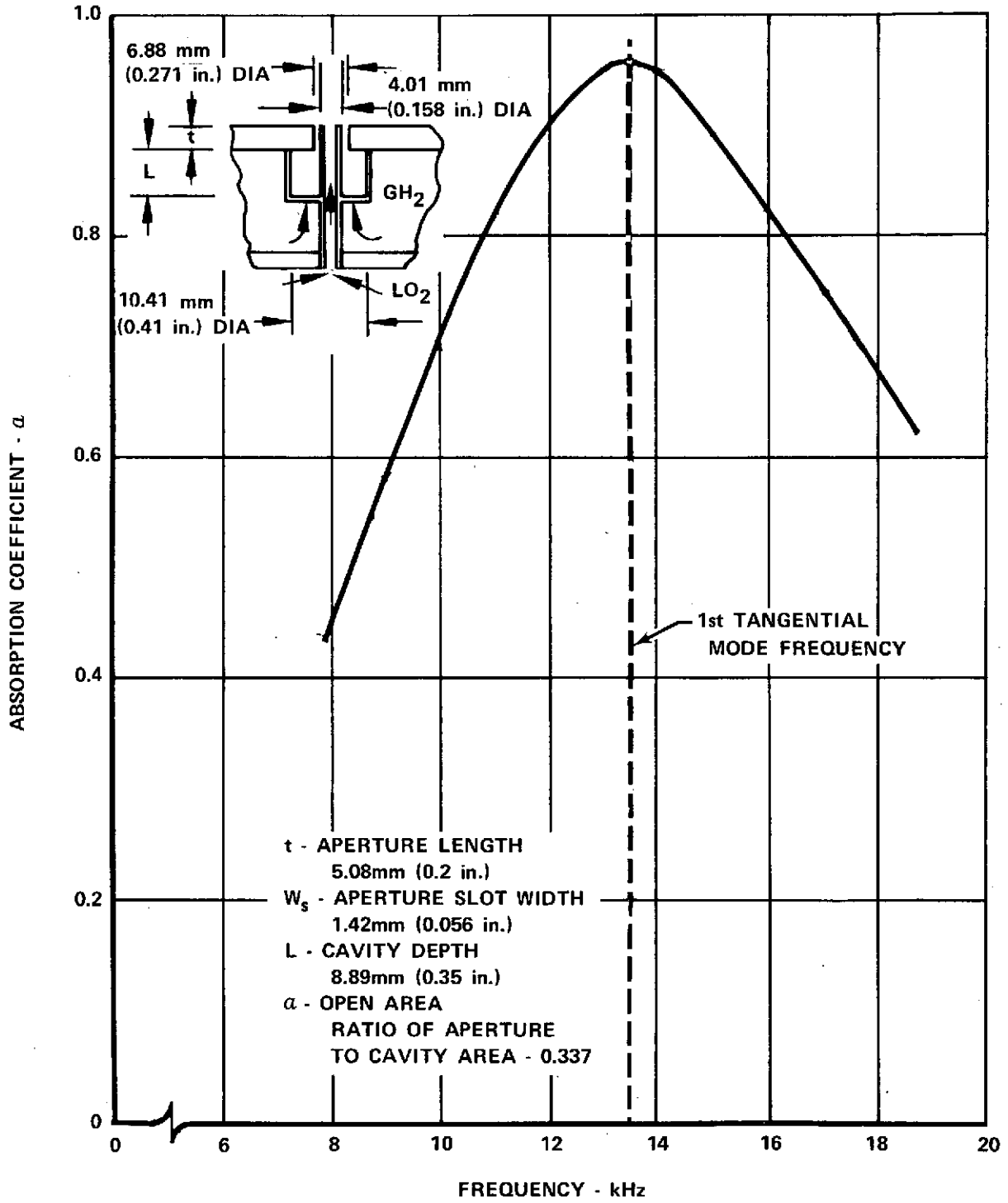

Figure 93. Advanced Space Engine Preburner First Tangential Mode Resonant Absorber

FD 68817

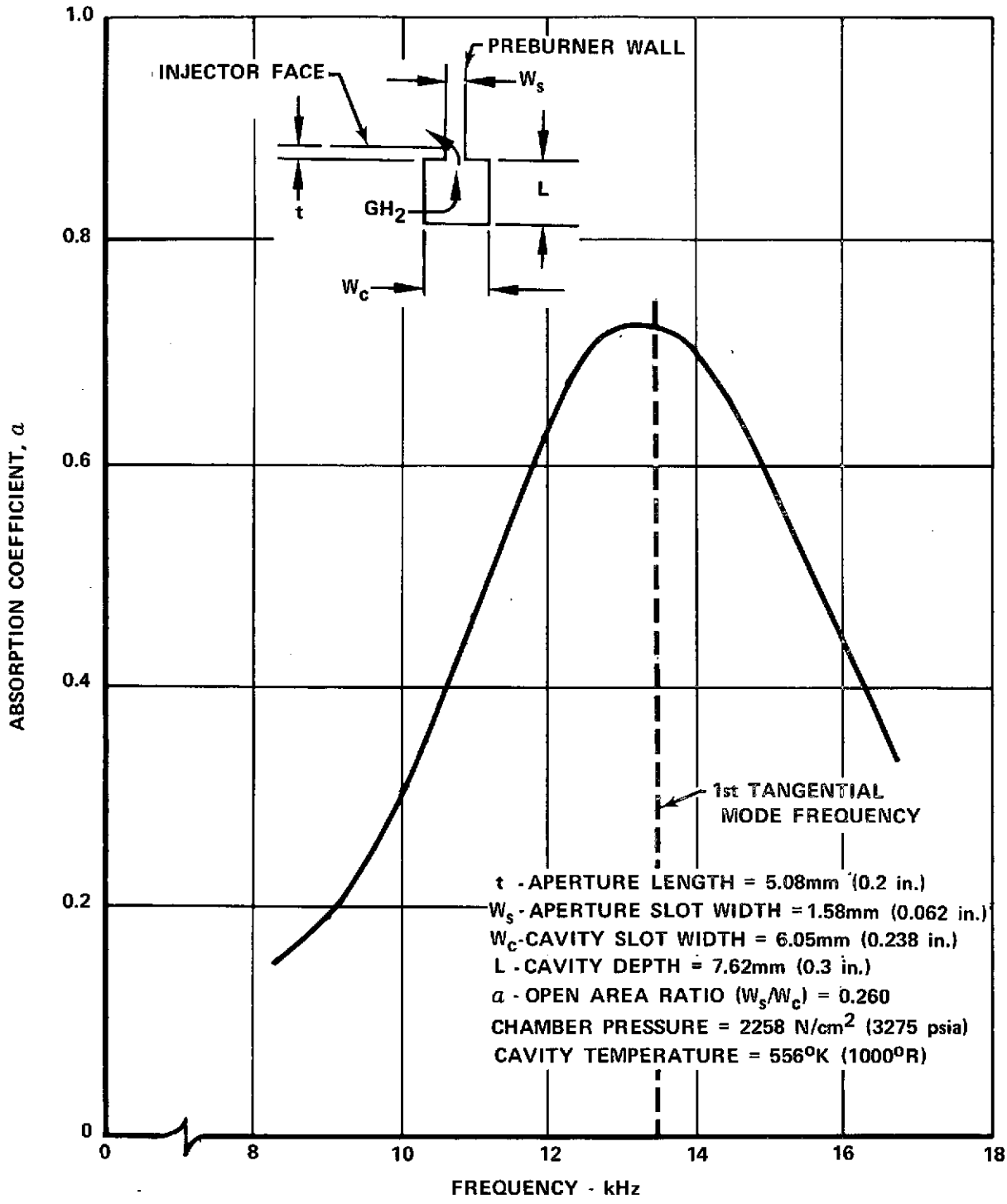

Figure 94. Advanced Space Engine Preburner First Tangential Mode Slot Resonator FD 68816

(1) Housing

The main housing of the preburner is fabricated from modified A-286 (PWA 1052). Selection of this material ensures a positive seal with the main case by eliminating thermal incompatibility. Further desirable properties of this material are its strength and compatibility with warm hydrogen. The housing can be manufactured in two parts and joined with a butt electron beam (EB) weld. The fuel manifold, inlet horn, and igniter bosses are all EB-welded into the housing to form the main structural assembly. The housing assembly has been sized by a preliminary stress analysis for maximum operating loads.

The fuel manifold is constant in diameter, 2.95 cm (1.16 in.), with 12 equally spaced slots, which yield a total flow area of 15.35 cm^2 (2.38 in^2) into the fuel cavity. These slots are arranged so that each oxidizer control valve attaching stud is located in a corresponding web between the slots.

Housing weight is minimized by cooling all highly stressed structural members. Low cycle fatigue problems are not anticipated because of the absence of high temperatures and thermal strains.

(2) Injector

The preburner injector configuration is based on a fixed-area fuel, single-orifice oxidizer, coaxial-element concept. It incorporates tangential-entry slot swirler oxidizer injection elements. This lightweight configuration allows mechanical simplicity, and simplification of valving and control. Tangential-entry slot-swirler injection elements provide finely atomized oxidizer for rapid combustion and attainment of uniform temperature profiles. The relatively large flow area, 0.245 cm^2 (0.038 in^2) per element, required by the warm gaseous fuel results in less sensitivity of the injector to nonconcentricity of the oxidizer and fuel orifices. Therefore, the concentricity requirement has been relaxed to 0.051 mm (0.002 in.) R.

The injection elements are mechanically simple and fabricated from drawn AISI 347 stainless steel tubing. The closed end is created by rolling a tube end to a spherical configuration and brazing it closed. The tangential entry slots are electro-discharge machined into the tubes, as shown in figure 95. The elements are mounted in an injector housing support plate that extends across the injector and serves as the main structural diaphragm separating the fuel and oxidizer in the injector. This plate is AISI A-286 and is EB-welded into the housing. The elements and their faceplate support sleeves are brazed into place with a gold-nickel braze (PWA 19). The faceplate support structure, which also creates the circumferential annular acoustic cavity, is welded to the housing. The final part of the injector, the faceplate, is then installed with a circumferential weld and is silver brazed to each injector element support sleeve.

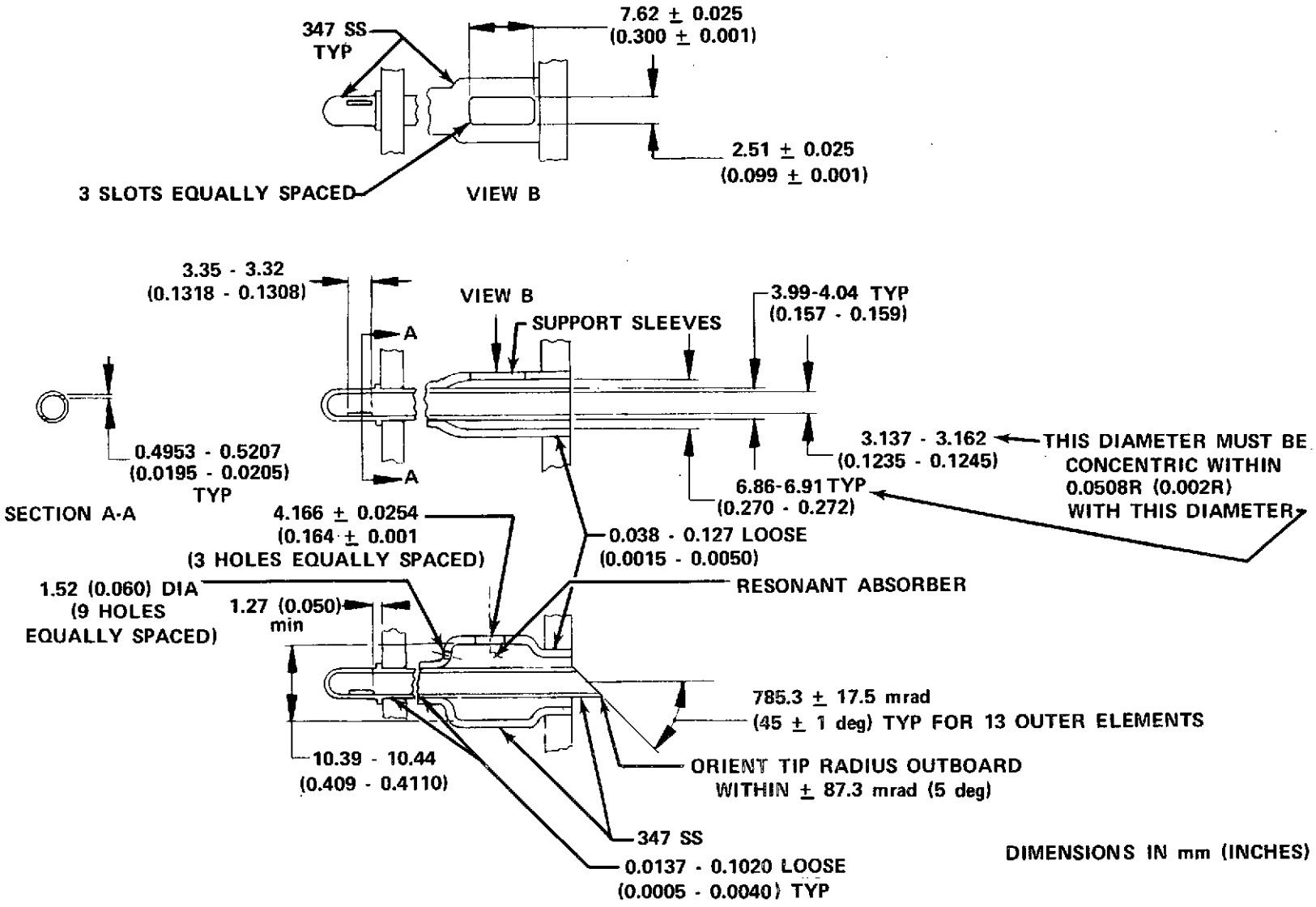

Figure 95. Preburner Injector Elements and Support Sleeves

FD 72391

The faceplate is fabricated from a woven and sintered wire mesh of N-155 (AMS 5794). The design porosity is 65 scfm/ft^2 (air) at a pressure differential of 1 N/cm^2 (2 psi) at ambient pressure and temperature. The faceplate support rings are fabricated from AISI A-286 and EB-welded to the housing to form an acoustic cavity. The member separating the acoustic resonator from the fuel cavity provides this cavity with a purge flow, which results in a known gas temperature and composition for more accurate tuning to the desired resonant frequency. The ring that supplies the main load-carrying capability of the faceplate, has 20 equally spaced circumferential slots, 0.1575 cm (0.062 in.) wide, which occupy 75% of the faceplate circumference. These slots, shown in figure 96, are sized in conjunction with the depth and volume of the acoustic cavity into which they open.

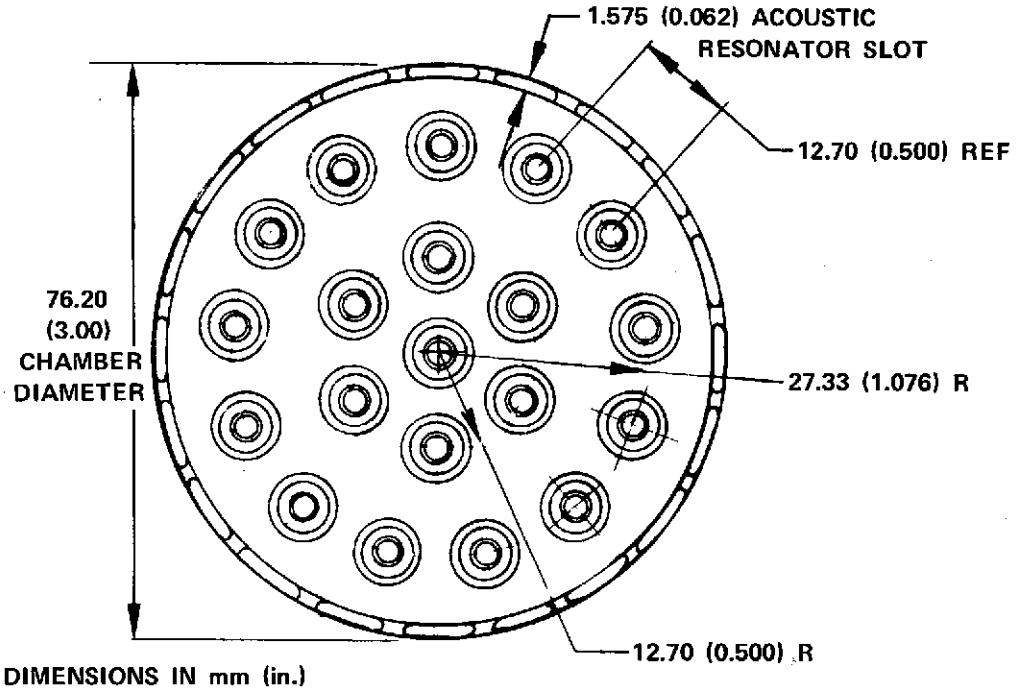

Figure 96. Preburner Faceplate FD 72390

There are two types of faceplate support sleeves with the location determining the type. Of the 20 injector elements, 13 are on the outer radius. These peripheral support sleeves incorporate an independent acoustic resonator. They are manufactured from AISI 347 stainless steel tubing by hydraulically expanding a heavy walled tube into an external die. The peripheral support sleeves serve as acoustic resonators, faceplate supports, and element positioners. The seven inner elements provide faceplate support and injector element positioning. They are manufactured from AISI 347 stainless steel tubing by a swaging operation onto a mandrel to hold the inner diameter to a close tolerance.

(3) Chamber and Duct

There are two sections to the combustion chamber: a short transpiration cooled section near the faceplate and a downstream uncooled section that funnels the combustion products into the centerbody duct. The cooled section consists of a

3.81 cm (1.500 in.) long cylinder constructed of 0.178 cm (0.070 in.) thick N155 woven and sintered wire mesh (Rigimesh). This cylinder is welded inside an AISI A-286 sleeve, which distributes coolant flow into 18 different compartments under the Rigimesh to assure an even coolant flow distribution. This sleeve is then pressed into the preburner housing with tight fits forming the desired seals. Flowrate through this cooled liner will be 92 scfm, according to XLR129 experience.

The uncooled portion of the chamber is manufactured in three parts. The flange and the converging section are symmetrical about the centerline and are a welded assembly for manufacturing ease. Downstream of the convergent portion of the chamber, a constant diameter offset duct is welded onto the assembly. This duct transfers the combustion gases from the chamber into the centerbody duct, where they are distributed to the two turbines. The uncooled chamber assembly is installed by insertion into the main case and trapping its flange between the main case flange and the preburner attaching flange. Because of the absence of tight fits, the chamber flange is free to grow thermally. In respect to this loose fit, the large flange diameter coupled with the total chamber length, prevent centerbody movement of more than a few thousandth inches. There are four positioning pins located between the uncooled chamber and the main case flange. These positioning pins prevent rotation, and align the cooled and uncooled chambers.

(4) Igniters

The two spark igniters, as shown in figure 97, are located 1.91 cm (0.750 in.) downstream of the preburner faceplate. At this axial location, the GH_2 and LO_2 are sufficiently mixed for ignition and the igniters are upstream of the flamefront thereby preventing flame erosion of the igniter tips. To assure ignition with minimum delay time, the igniters are located at angular positions of extreme mixture ratio variations. Therefore one igniter is aligned with the centerline of a perimeter injector element. The second igniter is approximately 2.1 rad (120 deg) from the first and located midway between two injector elements.

The igniters are completely independent of each other to provide system redundancy. Each igniter, which has its own exciter (figure 97), is mounted on a preburner housing boss employing a Dynatube® fitting. The igniters are mounted through the cooled liner and hydrogen is available to purge the gap between the igniter and liner. The hydrogen purge prevents back-leakage of hot combustion products. The mounting arrangement of the igniters provides accessibility for service and inspection. Another attractive feature is that internal inspection by a borescope of the preburner injector and chamber may be accomplished by removing an igniter assembly.

6. Thrust Chamber Assembly

a. General

The thrust chamber assembly consists of the main case subassembly and the thrust chamber. The main chamber injector and main case form a welded subassembly that attaches to the thrust chamber. The design of the thrust chamber is presented in this section first and is followed by the design of the main case subassembly.

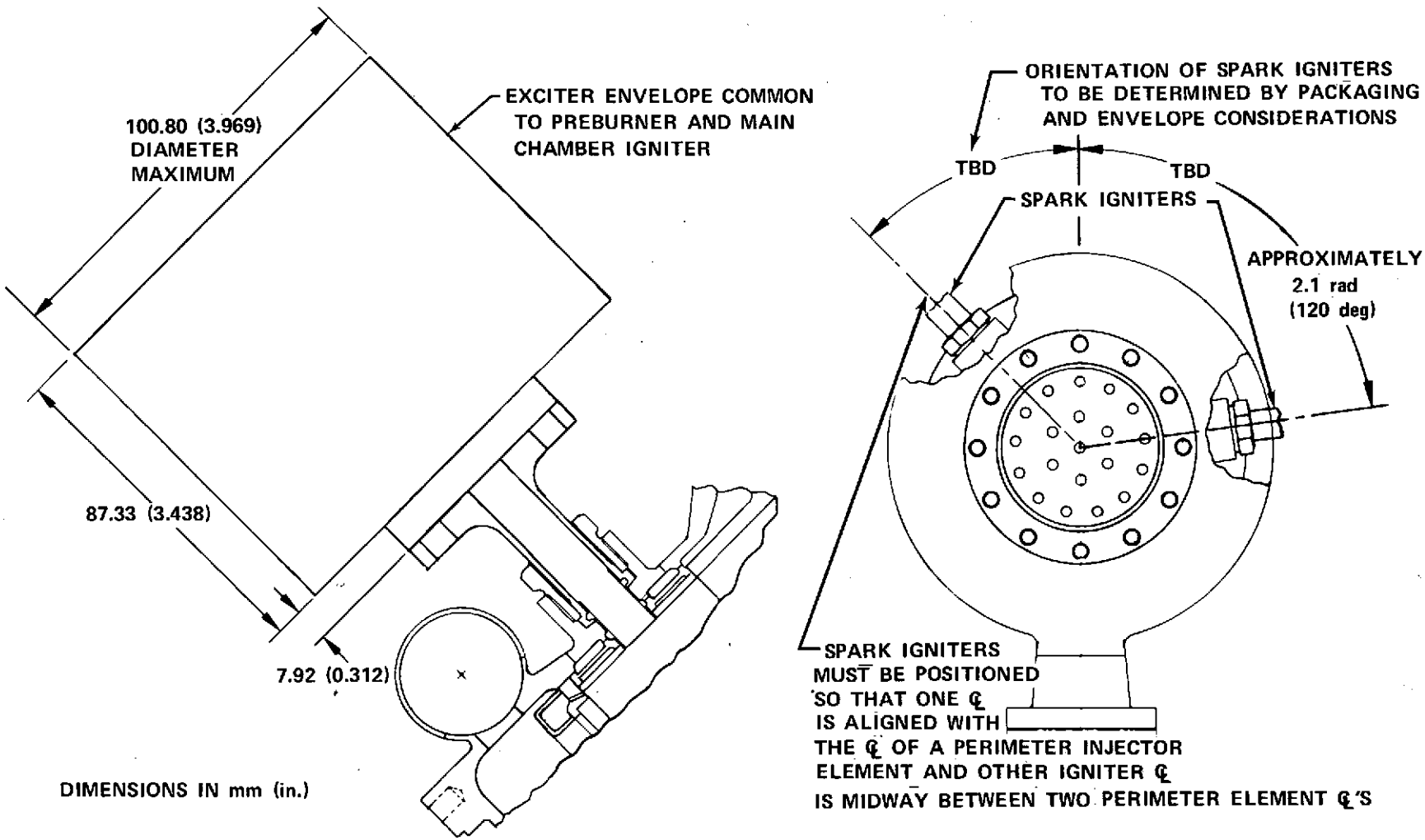

Figure 97. Preburner Igniter Orientation and Exciter Envelope

FD 75495

b. Thrust Chamber

(1) General Description

The thrust chamber contains the high temperature and high pressure combustion gases and expands them in the 400:1 expansion ratio nozzle to produce thrust. The thrust chamber consists of three sections; a nontubular regeneratively cooled section to $\epsilon = 6$, in series with a tubular regeneratively cooled nozzle to $\epsilon = 100$, and a corrugated, lightweight dump-cooled nozzle skirt to $\epsilon = 400$.

Cold, high-pressure hydrogen from the main fuel pump serves as the coolant for the regeneratively cooled portions of the thrust chamber using a pass-and-a-half cooling scheme. The coolant jacket acts as a heat exchanger to supply superheated hydrogen to the preburner.

(2) Operating Characteristics

The high heat fluxes encountered in the combustion chamber and throat sections at the nominal chamber pressure of 1324 N/cm^2 (1920 psia) require the use of high conductivity material for the hot-side wall, coupled with small flow area cooling passages. The heat flux at the throat section is 11.8 kw/cm^2 (72 Btu/in^2-sec). A machined copper alloy AMZIRC liner with an electroformed nickel closure was used to satisfy this requirement, but such construction is comparatively heavy. Therefore, lighter weight construction was used where possible in the lower heat flux regions, as discussed in the following paragraphs. This approach produced the three-section chamber of the ASE, which consists of (1) the nontubular regeneratively cooled combustion chamber and nozzle to an expansion ratio of 6:1, (2) a tubular regeneratively cooled nozzle section between expansion ratios of 6:1 and 100:1, and (3) a corrugated-construction, dump-cooled nozzle from the expansion ratio of 100:1 to the exit expansion ratio of 400:1. (See figures 98 and 99.)

The throat diameter of the chamber is 6.53 cm (2.57 in.). The 2.93 contraction ratio permits satisfactory injector element density. The bell nozzle has a minimum surface area (MSA) contour, which was selected as the best compromise for length, weight, and performance. A 22.9 cm (9 in.) combustion chamber length was selected to provide minimum length without compromising combustion performance.

The thrust chamber and nozzle cooling concept illustrated in figure 100 which was selected for the ASE is extremely important because it interacts strongly with the overall system performance and may determine the engine thermal cycle life (LCF). The regenerative cooling limit of the thrust chamber is a major factor in determining the design chamber pressure. Furthermore, the pressure drop in the coolant jacket directly affects fuel pump discharge pressure and therefore the required level of turbine power and fuel pump technology. The basic objectives of the regenerative cooling system are to permit operation at the highest possible heat flux with minimum coolant pressure drop consistent with meeting chamber cycle life requirements while having the lightest weight. However, the actual system design is a compromise of the basic objectives to best suit the engine system.

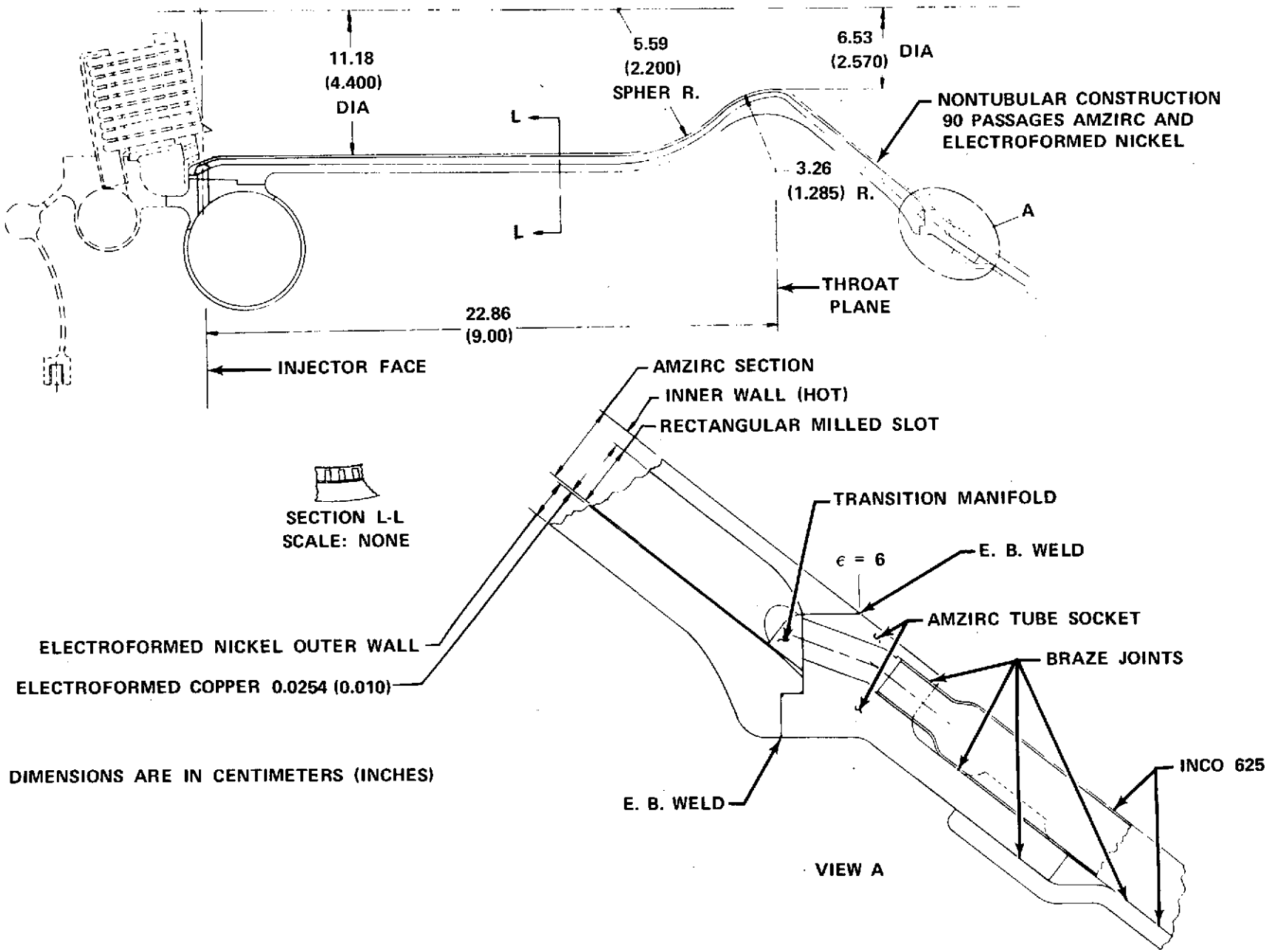

Figure 98. ASE Thrust Chamber

FD 68747B

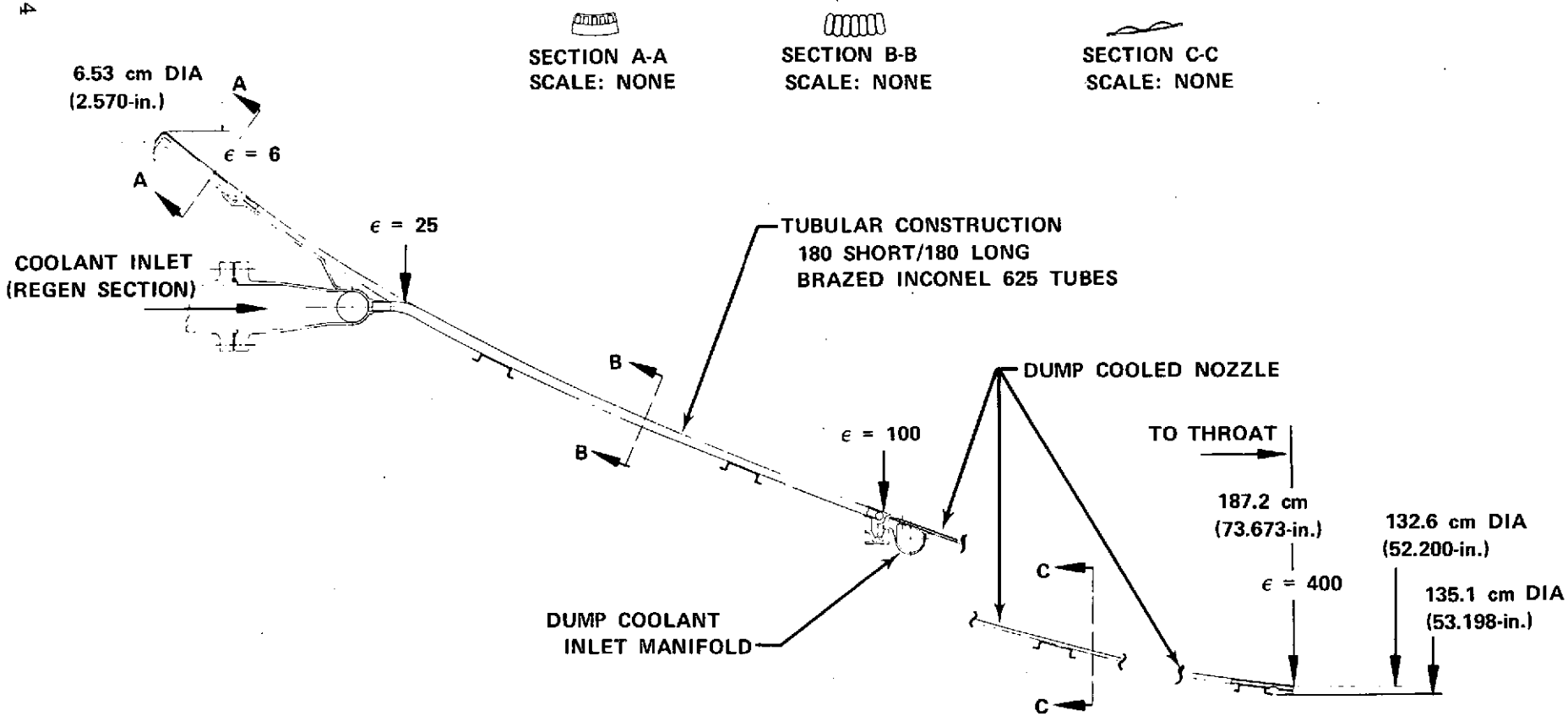

Figure 99. ASE Thrust Chamber Nozzle

FD 66676B

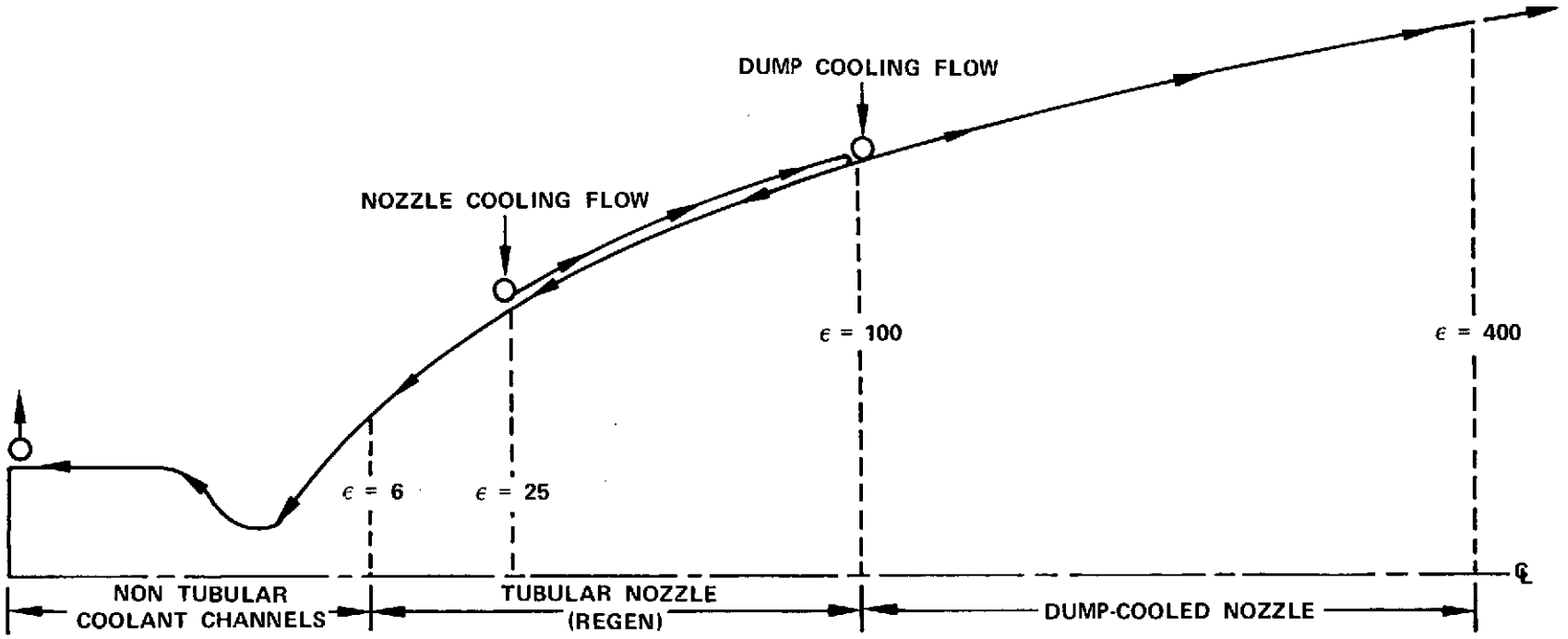

Figure 100. Advanced Space Engine Thrust Chamber Cooling Concept FD 68838

The rectangular (nontubular) coolant passage design illustrated in figure 101 is mandatory for the ASE combustion chamber and nozzle throat region. High chamber pressures result in high heat fluxes at the chamber throat as shown in figure 102 for an 89 kN (20,000 lb) thrust engine. These heat flux levels require high coolant velocities and, therefore, small coolant passages. A high thermal conductivity material such as copper must be used to maintain combustion-side wall temperatures at low levels to provide adequate cycle life. Furthermore, two-dimensional heat transfer into the material between coolant passages provides increased heat transfer area. This fin effect provides more efficient heat transfer thereby increasing the allowable heat flux and/or reducing the required coolant pressure drop.

For the remaining (lightweight) sections of the chamber, the breakpoint between the nontubular section and the tubular section ($\epsilon = 6$), was established based on the minimum tube wall thickness that can be reasonably fabricated and cooled, and the flow passage cross-sectional area requirements. The $\epsilon = 100$ point at which the dump-cooled section is started was set by the contract statement of work.

A dump-cooled extension was selected for the thrust chamber nozzle from an area ratio of 100:1 to 400:1. The dump-cooled nozzle extension is light in weight and relatively simple to fabricate. The coolant source for the dump cooled nozzle is cold hydrogen from the gearbox, which would ordinarily be dumped overboard without providing useful thrust. With the dump-cooled nozzle concept, the coolant is expanded through small nozzles in each of the coolant passages at the chamber nozzle exit plane, with a vacuum specific impulse of approximately 4266 N-s/kg (435 sec). The nozzle extension is attached to the tubular portion of the nozzle by a Marmon-type clamp that seals the joint and assures proper alignment of the extension.

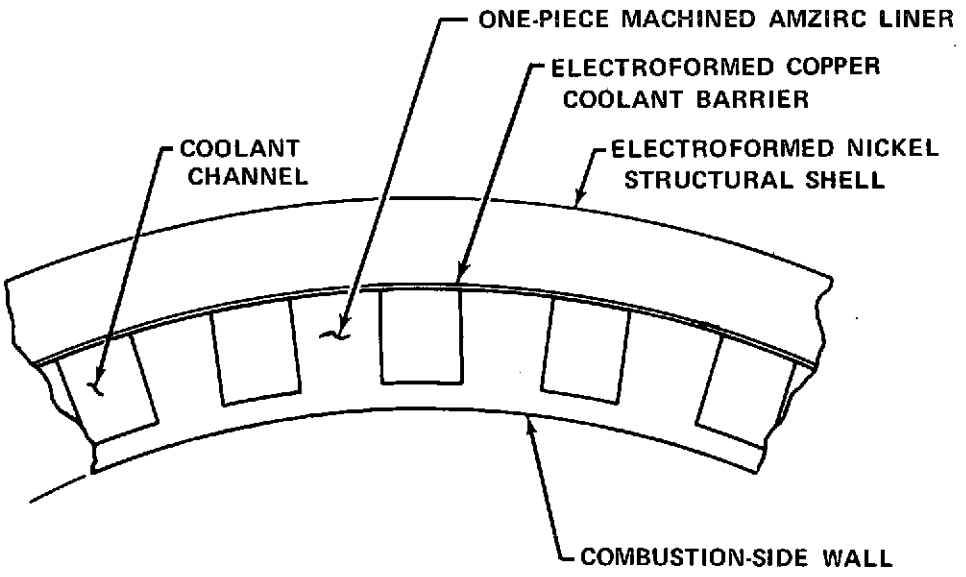

Figure 101. Typical Nontubular Wall Structure FD 68839

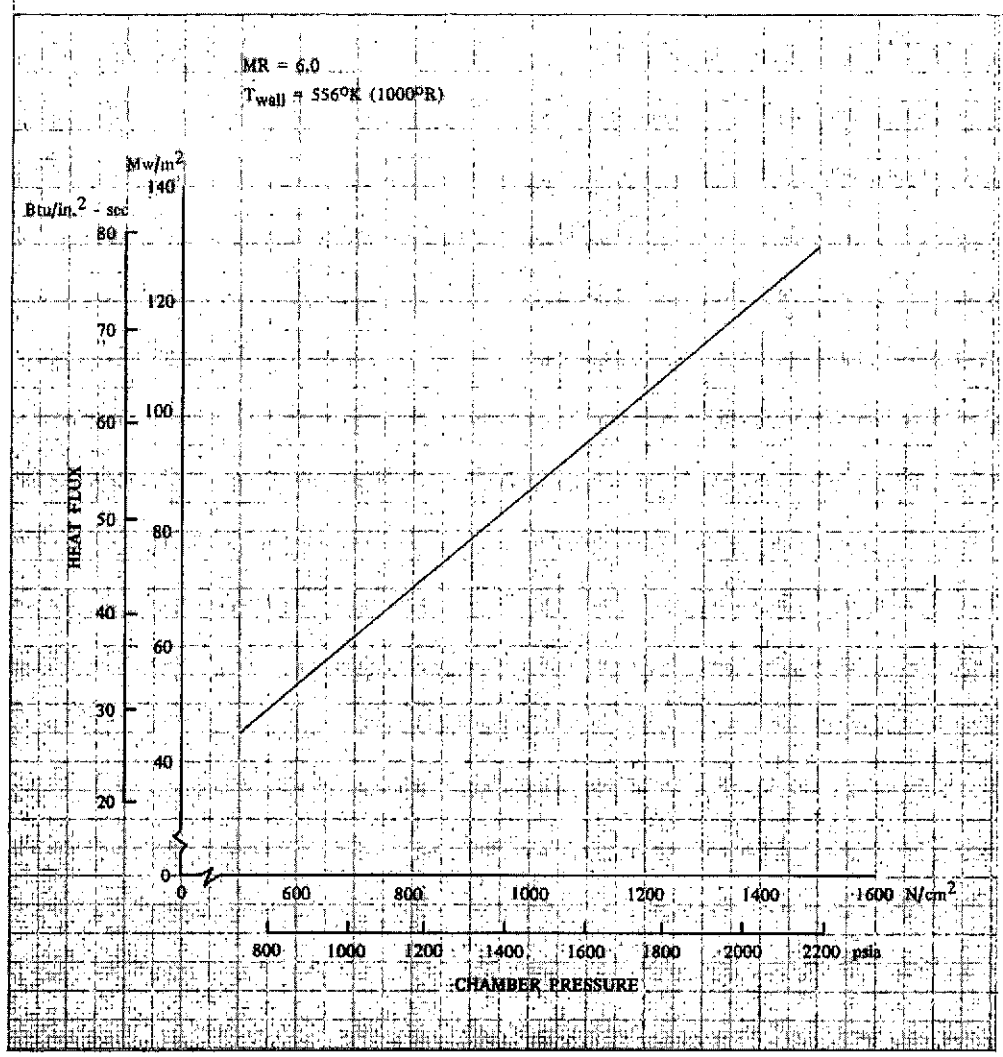

Figure 102. Effect of Chamber Pressure on Throat Heat Flux for 89 kN (20,000 lb) Thrust Engine DF 95449

The corrugated dump-cooled design was selected for the large surface area section of the nozzle because it has the following advantages over the tubular type construction: (1) lighter weight, (2) resistance-welded flat-sheet construction is less costly than brazed tubular construction, (3) coolant passage cross section is readily varied to achieve desired coolant velocity profiles; and (4) hoop stresses are carried by the cooled outer wall, whereas external bands must be used in tubular sections. The feasibility of corrugated sheet construction was demonstrated in hot firing tests of a modified RL10A-3-3 thrust chamber conducted in August 1967.

A radiation-cooled skirt was also considered and rejected as an alternative to dump cooling because the most suitable material from a temperature capability standpoint, columbium, is subject to embrittlement when exposed to hydrogen. Materials not susceptible to hydrogen embrittlement can only be used in the region between expansion ratios of 300:1 and 400:1. In addition, the prospective weight savings through the use of a radiation-cooled nozzle compared to a

corrugated dump-cooled nozzle would be slight, if any. The equivalent wall thickness of the corrugated construction on the ASE nozzle is only 0.495 mm (0.0195 in.) from expansion ratios of 100:1 to past the ϵ = 300 nozzle station. The gearbox hydrogen ventage flow is used as the coolant for the corrugated nozzle section. The dump coolant flow is expanded through small nozzles with an area ratio of 3.5:1 at the end of each passage to produce useful thrust. There is sufficient gearbox vent flow to provide adequate nozzle cooling for all engine operating points.

An additional advantage of a dump-cooled nozzle is its lower outside wall temperature, which would require less or no heat shielding compared to a radiation-cooled nozzle.

(3) Mechanical Description

(a) Nontubular Chamber

The nontubular regeneratively cooled portion of the thrust chamber has a one-piece copper alloy liner. The high chamber heat fluxes require the use of a high thermal conductivity material such as copper. The thermal fatigue properties of pure copper can be improved with only a small reduction in conductivity by alloying with small amounts of other metals. The alloy selected for the ASE design is AMZIRC, an oxygen-free copper alloy containing 0.15% Zirconium, produced by AMAX, Inc. The AMZIRC is obtained as a forging and cold-worked by spinning to rough shape on a mandrel to increase strength. After spinning, the ID surface is final-machined and coolant channels are milled in the OD. A thin copper layer, about 0.254 mm (0.010 in.) in thickness, is provided as the primary passage protective barrier closure material between the hydrogen coolant and a nickel outer shell to alleviate possible property-reducing hydrogen embrittlement of the nickel. The structural nickel outer closure is electroformed over the milled liner outer surfaces to complete the cooling passages. The above-described materials and fabrication techniques were used in the construction of a 1.11 MN (250,000-lb) engine thrust chamber that was subjected to three 100% thrust, 2068 N/cm^2 (3000 psia) chamber pressure test firings conducted by P&WA during 1971. A photograph of the milled-slot liner used in the 1.11 MN (250,000 lb) thrust engine testing is presented in figure 103.

Thrust chamber LCF life may be a major consideration in the selection of engine chamber pressure. Low cycle fatigue of the regeneratively cooled thrust chamber results from the large thermal strains that are introduced between the heated inner wall of the chamber and the cooler outer structural wall.

The problem of evaluating thrust chamber LCF life capability has been approached by (1) identifying the critical locations in the thrust chamber for analysis, (2) determining the LCF life capability at those locations, and (3) making modifications to the chamber geometry and/or engine operation to ensure that the life requirements have been met.

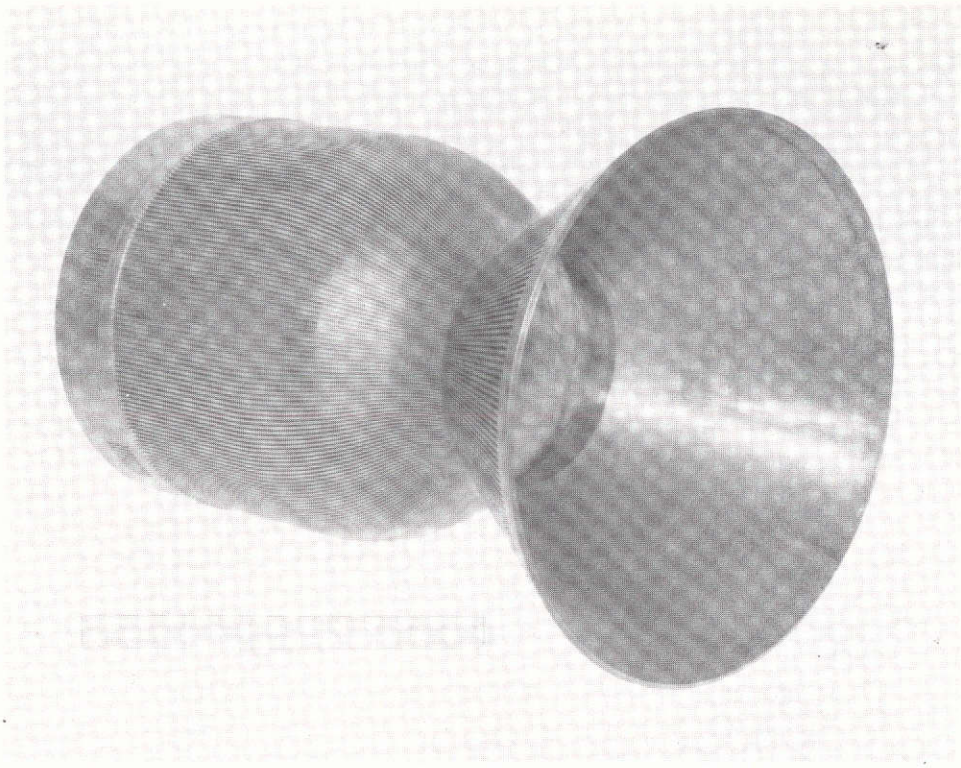

Figure 103. Milled-Slot Chamber Liner for a 1.11 MN (250,000 lb) Thrust Engine FE 105647

Large thermal gradients are generated in high performance rocket engine regeneratively cooled thrust chambers during operation. These gradients affect the expected cyclic life of the chamber walls. Further aggravating this condition is the presence of high-pressure coolant within the wall passages. Pratt & Whitney Aircraft has developed a method for the analysis of nontubular thrust chambers that provides a complete evaluation of thermal life in that thermal gradients and the pressure differential across the hot wall are treated simultaneously. See Appendix C for a discussion of the method of analysis.

Low cycle fatigue analysis of the ASE milled slot chamber shows a minimum life of 760 cycles at the coolant inlet with 920 cycles at the chamber throat and 1000 cycles at the injector. The ASE thrust chamber LCF life capability can be improved to the required 1200 cycles during a detailed design in two ways: the thermal and mechanical strains can be reduced by passage redesign, or if necessary, the thrust chamber heat flux can be lowered by chamber pressure reduction.

Reducing the chamber thermal and mechanical strains through passage redesign is the preferred approach to LCF life improvement since engine performance is not affected as long as the coolant pressure losses remain within the engine cycle power capability. The passage redesign is made difficult by the fact that the chamber cycle life predictions are based on the combined effects of thermal and mechanical strains and the separation of their effects is not straightforward.

A two-dimensional finite element conduction heat transfer analysis was used to determine the passage temperature fields shown in figure 104. At each selected location, the passage cross section has been divided into a fixed number of unit depth masses or nodes. The interior and exterior boundary nodes that have been subjected to the coolant-side and combustion-side environments are also illustrated in figure 104. Heat transfer by radiation is considered to be negligible. A steady-state heat balance has been made for each node simultaneously to determine its operating temperature.

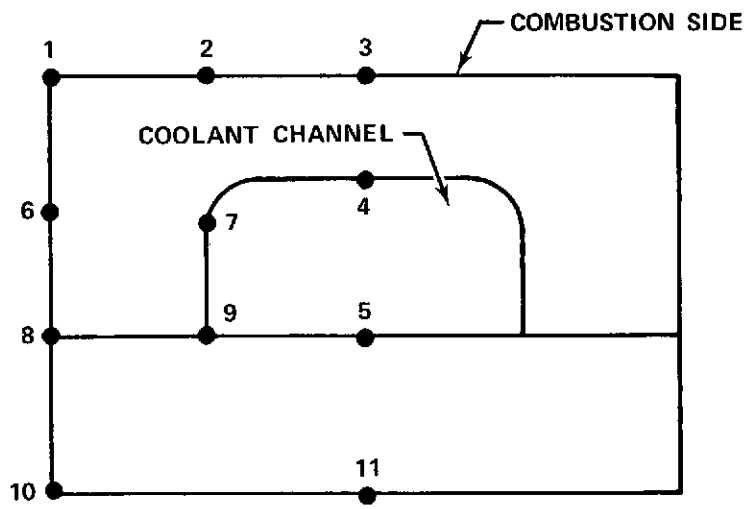

LOCATION	TEMPERATURES, °K (°R) INJECTOR	THROAT	ϵ = 6
1	650 (1171)	589 (1060)	516 (929)
2	646 (1162)	581 (1045)	521 (937)
3	644 (1159)	574 (1033)	525 (945)
4	511 (919)	300 (540)	449 (809)
5	280 (503)	152 (273)	190 (342)
6	516 (928)	341 (614)	420 (756)
7	488 (879)	288 (518)	424 (763)
8	338 (609)	175 (314)	225 (404)
9	318 (573)	165 (297)	216 (389)
10	321 (578)	166 (299)	217 (391)
11	313 (564)	166 (298)	208 (375)

Figure 104. Advanced Space Engine Nontubular Thrust Chamber Section Two-Dimension Temperature Distribution at Nominal Operating Conditions FD 68840

The coolant-side and combustion-side convective environments have been determined from a steady-state heat transfer analysis of the entire thrust chamber. (See Appendix D.) Computer formulations are currently available that allow the determination of the combustion-side and coolant-side convective environments (temperatures and convective film coefficients) from the input thrust chamber geometries and engine operating conditions (chamber pressure and mixture ratio).

Coolant pressure losses and wall temperatures along the chamber walls (based on one-dimensional analyses) were also predicted. The combustion gas convective environment was determined using the Mayer integral boundary layer analysis (Reference 19) and enthalpy driving potential. The coolant side environment was predicted using empirically determined correlations for hydrogen heat transfer coefficients (Reference 20) modified to account for the effects of passage surface roughness using the method of Dipprey and Sabersky (Reference 21), and passage curvature as reported in Reference 22.

A surface roughness of 1.63 μm (64 microinches) has been used for the heat transfer analysis as this is a standard value for machined surfaces and should be readily attainable.

The analytical method used to predict thrust chamber and nozzle heat transfer has been verified in tests of both the RL10 and the ADP tandem combustion test rig as shown in table XXIII.

Table XXIII. Comparison of Experimental Engine Data With Predicted Combustion-Side Heat Transfer

Engine	Approx. Thrust, kN	(lb)	Propellant Combination	Mixture Ratio	Chamber Pressure, N/cm^2	(psia)	Deviation From Test Data, %
RL10A-3-1	66.7	(15,000)	H_2/O_2	4.46	199	(289)	2.5
				5.08	201	(292)	2.8
				5.70	202	(293)	1.0
RL10A-3-3	66.7	(15,000)	H_2/O_2	4.45	245	(356)	3.6
				5.06	267	(387)	2.2
				5.68	267	(388)	2.8
ADP Combustion Test Rig	1,112.	(250,000)	H_2/O_2	5.87	2,123	(3,080)	0.0
				6.84	2,063	(2,992)	-0.7
				7.12	2,061	(2,990)	0.7

Coolant passage dimensions for the nontubular chamber are shown in figure 105 as functions of axial distance from the nozzle throat plane. Both slot width and height have been varied along the coolant path. This approach is the same as that used for the 1.11 MN (250,000 lb) thrust engine thrust chamber shown in figure 103, and provides maximum latitude in passage design to tailor coolant film coefficients to local heat fluxes. The hot-wall thickness has been similarly varied along the chamber length to maintain nearly constant passage bending stresses. The passage bending stresses are functions of the slot width to hot-wall thickness ratios and can become significant factors in the chamber cycle life capability if not carefully controlled.

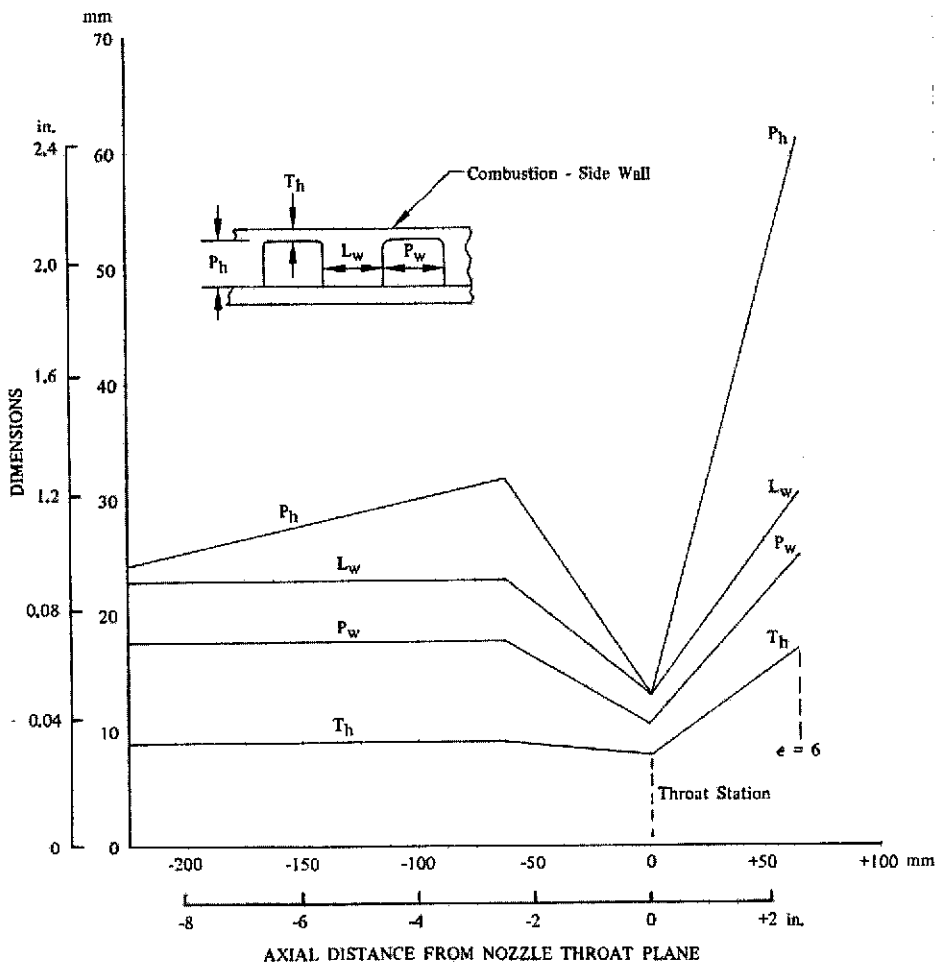

Figure 105. Advanced Space Engine Regeneratively Cooled Nontubular Chamber Section Geometry DF 95839

A passage thermal map showing the three critical locations identified in the nontubular chamber (ϵ = 6, throat, and injector) are presented in figure 104. Coolant and hot wall temperature profiles are presented in figures 106 and 107 respectively; the tubular section of the nozzle (ϵ = 6 to 100) is also included. A coolant pressure profile, again for both the tubular and nontubular sections, is shown in figure 108.

(b) Tubular Nozzle

The tubular regenerative nozzle is identical in concept to the tubular nozzle used on the RL10 production engine. It consists of a pass-and-a-half heat exchanger made up of 180 long and 180 short tubes extending from the end of the nontubular section at ϵ = 6 to the start of the dump-cooled nozzle at ϵ = 100. The tube split, required to accommodate the change in circumference while providing tube cross sections consistent with cooling requirements and fabrication limitations, is at an area ratio of 25:1. Flow is from the inlet manifold at ϵ = 25, parallel to the combustion gases through the short tubes, to a turnaround manifold

at $\epsilon = 100$, and then through the long tubes, counterflow, to the nontubular section.

Tube dimensions for the pass-and-a-half counterflow regenerative nozzle are summarized in figure 109. Coolant- and hot-wall temperature profiles for the tubular nozzle are included in figures 106 and 107, respectively, while the coolant pressure profile is similarly included in figure 108.

Inconel 625 (AMS 5599) was selected as the tube material based on results of studies for a similar application in the XLR129 engine (Reference 13). Inconel 625 has good low cycle fatigue properties at elevated temperatures, high ductility at cryogenic temperatures (50% elongation at 77.8°K (140°R)) and good yield strength at high temperature (19.3 kN/cm^2 (28,000 psia) at 1056°K (1900°R)). Based on strength-temperature characteristics, a maximum wall temperature of 1061°K (1910°R) was assumed for design; at this temperature level, thermal cycle life is not a limiting factor.

Bands are used on the outside of the skirt to take hoop stress. To establish band locations, tubes are treated analytically as beams subjected to thermal stress by the hot-cold wall temperature differential and bending stress from nozzle static wall temperature differential and bending stress from nozzle static wall pressure; longitudinal loads due to thrust, maneuver loads, and gimballing acceleration are also considered. Bands are placed to establish beam lengths, which limit tube stress to a level below the material yield strength at a factor of safety of 1.1.

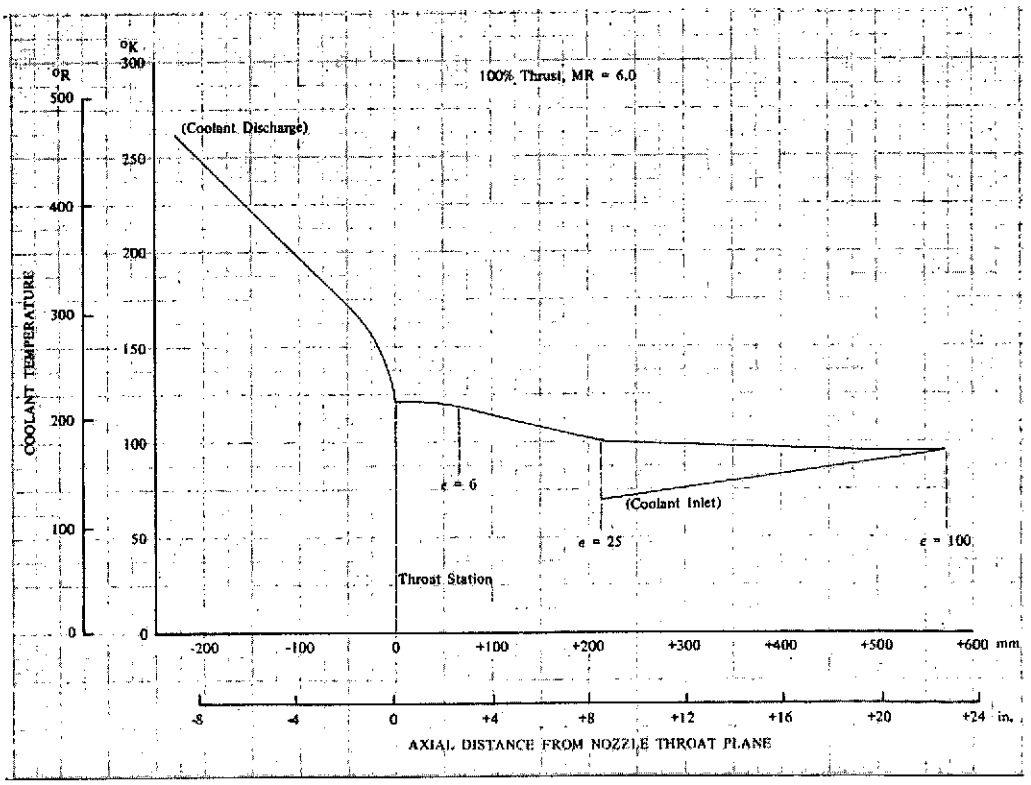

Figure 106. Advanced Space Engine Regeneratively Cooled Thrust Chamber Coolant Temperature DF 95450

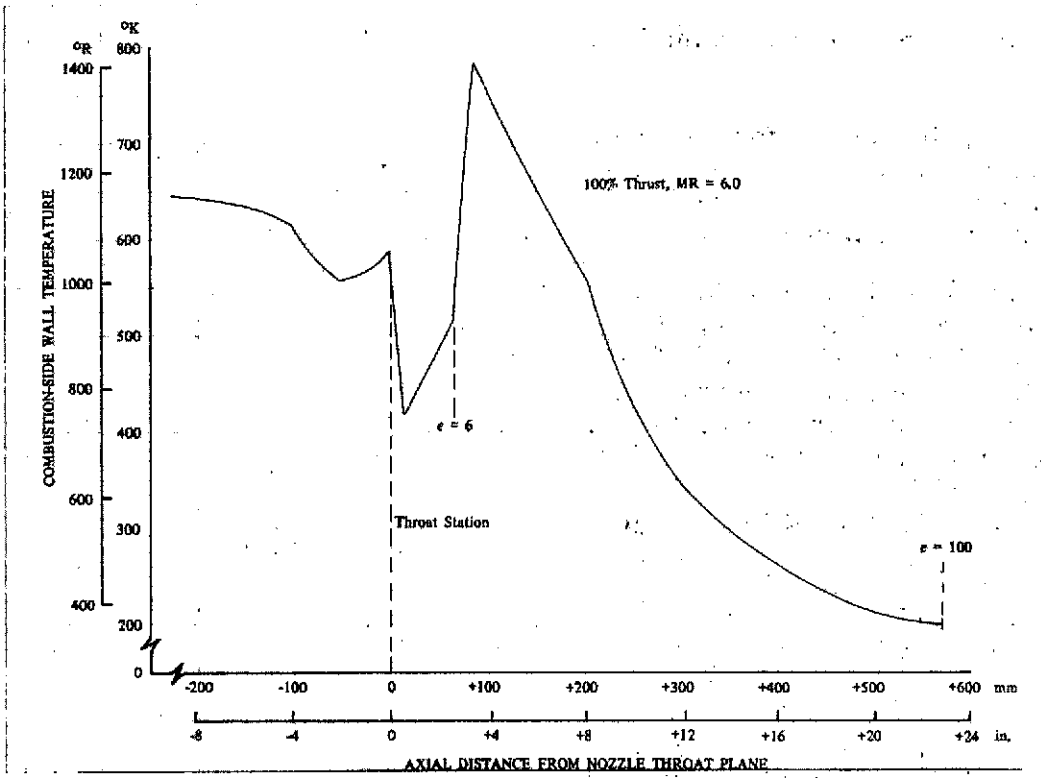

Figure 107. Advanced Space Engine Regeneratively Cooled Thrust Chamber Wall Temperature DF 95840

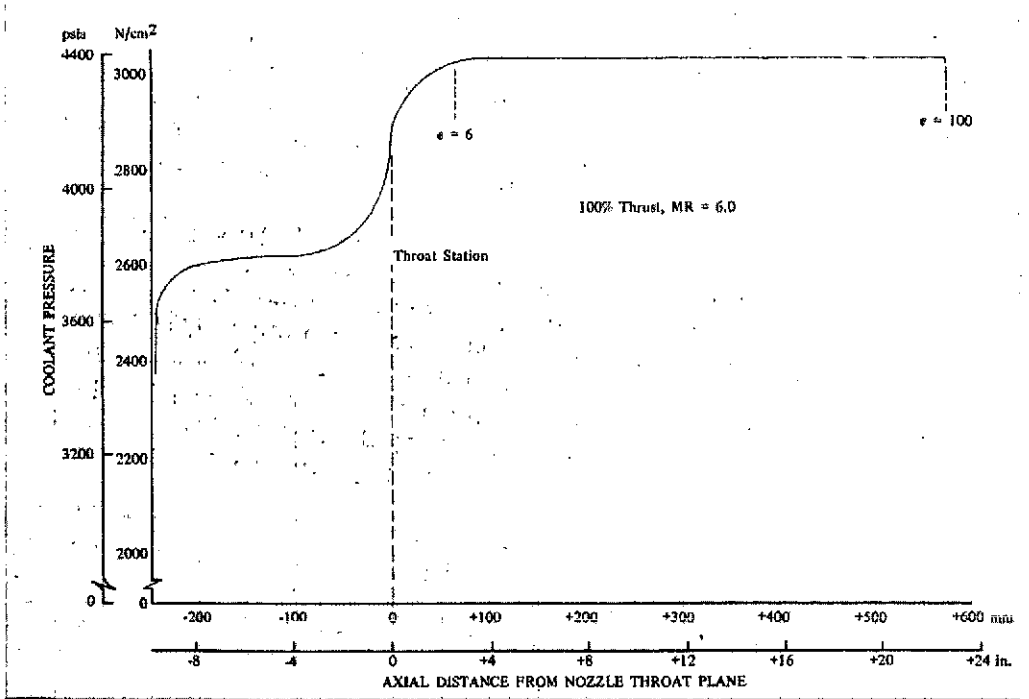

Figure 108. Advanced Space Engine Regeneratively Cooled Thrust Chamber Coolant Pressure DF 95841

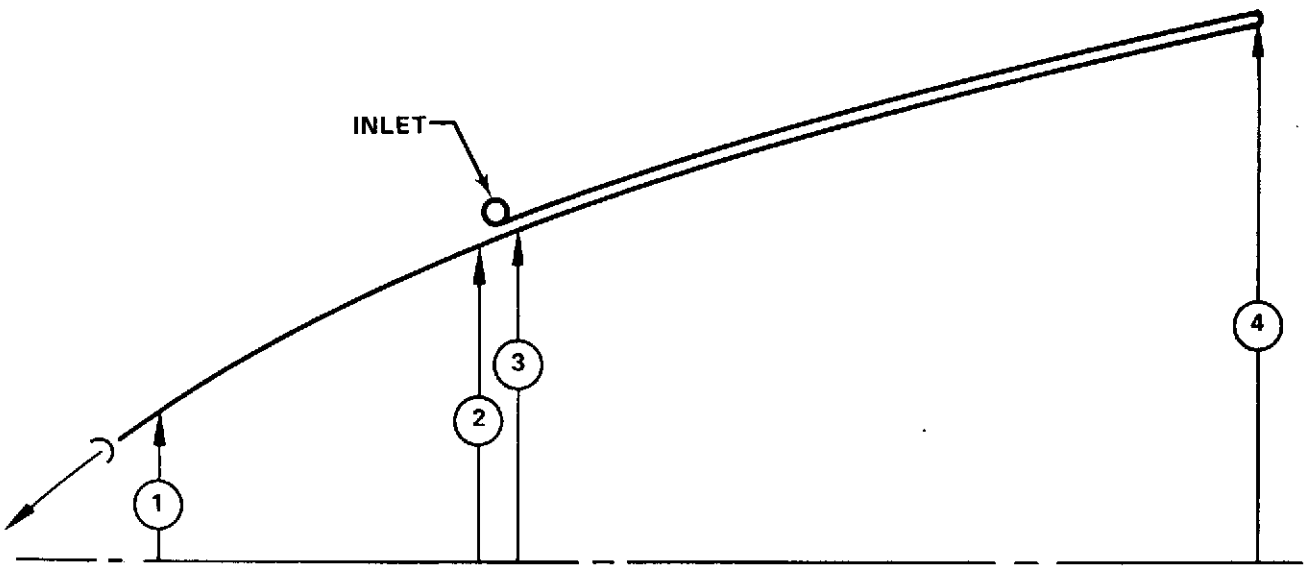

PARAMETER	LOCATION			
	1	2	3	4
AREA RATIO	6.0	25.0	25.0	100.0
NO. TUBES	180	180	360	360
TUBE OUTER WIDTH, W, mm (in.)	2.82 (0.111)	5.61 (0.221)	2.95 (0.116)	5.74 (0.226)
TUBE OUTER HEIGHT, h, mm, (in.)	3.28 (0.129)	5.82 (0.229)	7.37 (0.290)	5.74 (0.226)
TUBE WALL THICKNESS, t, mm, (in.)	0.241 (0.0095)	0.343 (0.0135)	0.343 (0.0135)	0.343 (0.0135)

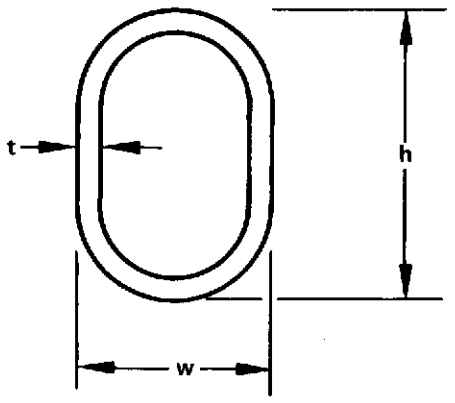

Figure 109. Advanced Space Engine Thrust Chamber Tubular Nozzle Section Geometry FD 71588

Stiffening bands at the inlet and turnaround manifolds of the tubular skirt section are Inconel 625 to maintain thermal compatibility with the tubes for brazing. The sides of the tubes are "spanked" to give a minimum of 0.762 mm (0.030 in.) flat braze contact area. Processing is patterned after that of the RL10 engine thrust chamber, of which more than 300 have been made, and that used for a 1.11 MN (250,000 lb) thrust size nozzle skirt of the XLR129 program made under Contract F04611-68-C-0002. (See Reference 13, table II.) While the RL10 and XLR129 parts were not fabricated from Inconel 625 material, extensive laboratory testing of the material has been conducted to confirm the fabrication processes.

(c) Dump-Cooled Skirt

The dump-cooled skirt is formed by a smooth outer skin and a corrugated inner skin that are resistance seam welded longitudinally together. (See figures 110 and 111.) The corrugations form coolant passages for hydrogen from the gearbox vent from a nozzle area ratio of 100:1 to an exit area ratio of 400:1. Indentations near each passage exit form restrictions to choke the flow in each passage for uniform flow distribution. The nozzles formed by these indentations have an expansion ratio of 3.5 and provide useful thrust from the heated dump coolant.

The hydrogen used as the coolant in the dump-cooled nozzle is taken from the gearbox discharge, where it is at a temperature of 61.7°K (111°R) and a pressure of 138 N/cm^2 (200 psia) at the nominal operating point. An orifice in the supply line reduces the pressure to 41.4 N/cm^2 (60 psia) to provide a flowrate of 0.143 kg/s (0.315 lb/sec) through the coolant passages. The coolant temperature is increased to 1011°K (1820°R) before it is expanded by the 3.5:1 area ratio nozzles to produce 623 N (140 lb) of thrust at 4266 N-s/kg (435 sec) vacuum specific impulse. Variation of wall temperature along the nozzle at selected locations in the corrugations is shown in figure 112.

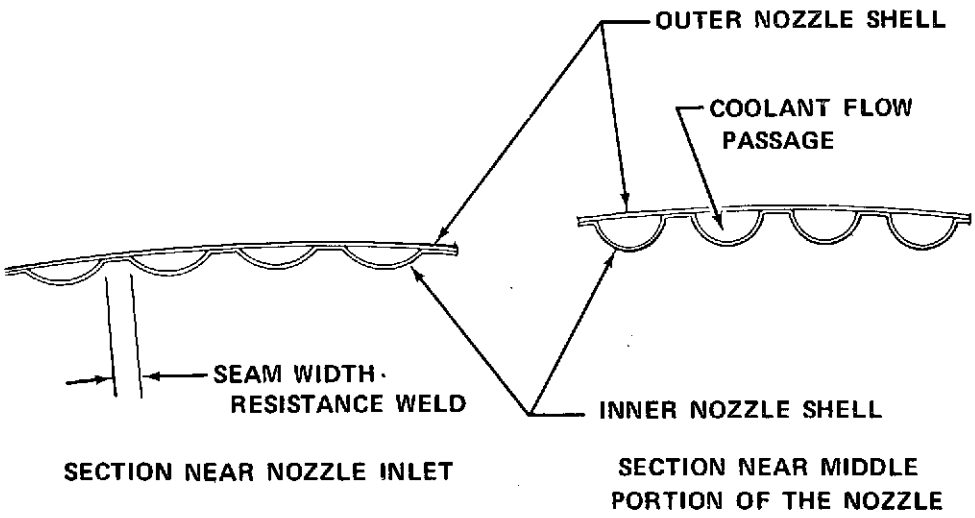

Figure 110. Representative Corrugation Sections for Dump-Cooled Nozzle FD 68841

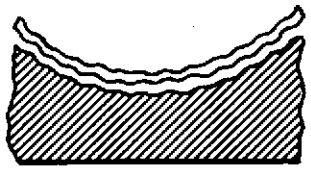

DRAW-FORM-CLAMP SEQUENCE PRODUCES COOLANT PASSAGES ON INNER PANEL

INLET CORRUGATED PANELS AND OUTER SHEET PANELS ARE SIZED AND RESISTANCE WELDED TO FORM SUBASSEMBLIES

SUBASSEMBLIES ARE BUTT-WELDED FORMING SETS OF PANELS

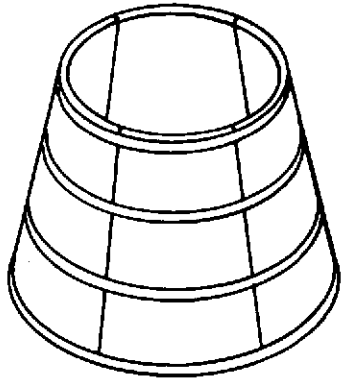

PANELS ARE BUTT-WELDED TO FORM THE BASIC NOZZLE. REINFORCING BANDS ARE INDUCTION BRAZED IN PLACE

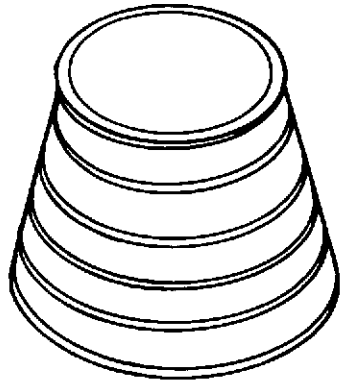

COOLANT MANIFOLD IS INDUCTION BRAZED COMPLETING THE DUMP COOLED NOZZLE

Figure 111. Dump Cooled Nozzle Fabrication Sequence

FD 68842

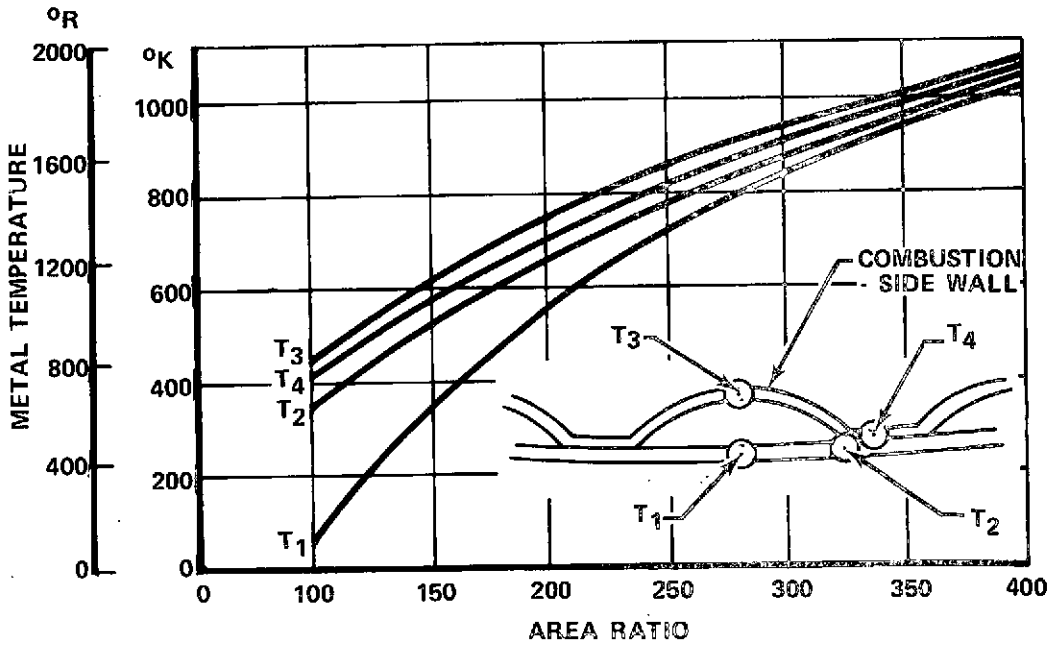

Figure 112. Advanced Space Engine Dump Cooled Nozzle Metal Temperature Profiles FD 68869

Coolant velocities were established in the dump-cooled skirt to limit the maximum wall temperature to 1061°K (1910°R). The loss of material properties for Inco 625 above this temperature is excessive. The maximum wall temperature occurs at the crown of the corrugation at the coolant exit. Since the corrugation is subject only to the differential pressure between the coolant and the high temperature gas flow, use of 0.203 mm (0.008 in.) thick sheet for the corrugation layer assures that the stress can be maintained below both the 0.2% yield stress and below the 10-hr, 0.5% creep life range in the temperature environment present. Sheet material no thinner than 0.203 mm (0.008 in.) was considered advantageous to avoid material handling and fabrication difficulties. Corrugation cross-sectional dimensions vs nozzle stations are presented graphically in figures 113 and 114.

The outer layer of the dump-cooled skirt was sized for both the hot gas static pressure distribution and for the coolant pressure. This layer was treated as a fixed beam at operating temperature with length equal to the corrugation width and a uniformly applied load equal to the coolant pressure. The tensile hoop stresses resulting from the static wall pressure is combined with bending stresses using an iteration equation (Reference 13). The resulting outer skin is a constant 0.203 mm (0.008 in.) thickness, from a nozzle area ratio of 100:1 to an area ratio of 300:1. From area ratio of 300:1 to the nozzle exit (area ratio of 400:1) the outer skin is tapered by chemical milling from 0.203 mm (0.008 in.) thickness to 0.457 mm (0.018 in.) thickness at the exit plane. (See figure 114.) The additional thickness at the nozzle exit plane is needed because the wall temperatures in this region are in the creep range of the Inco 625 material (AMS 5599).

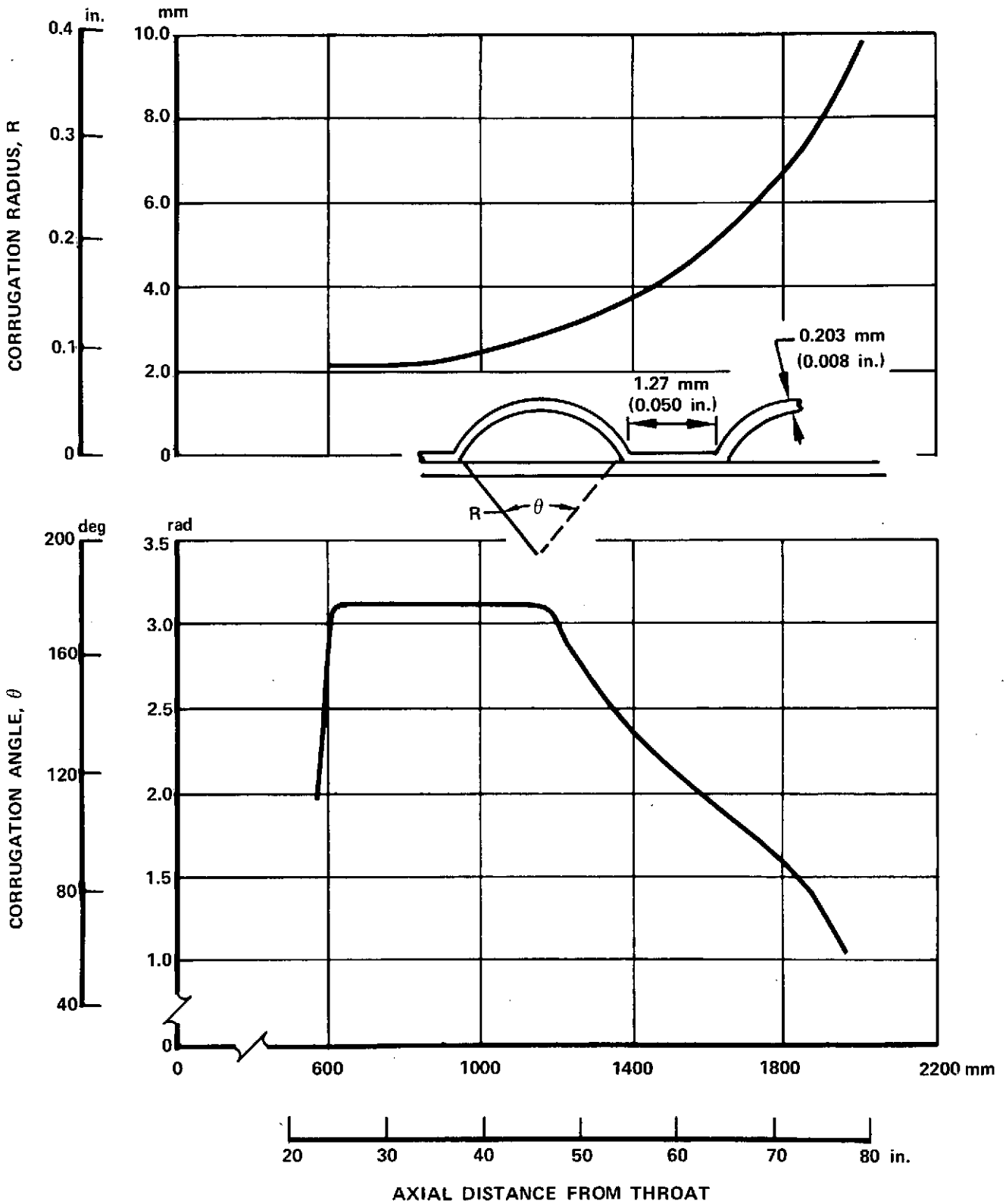

Figure 113. Advanced Space Engine Dump Cooled Nozzle Passage Geometry (360 Corrugations) FD 68871

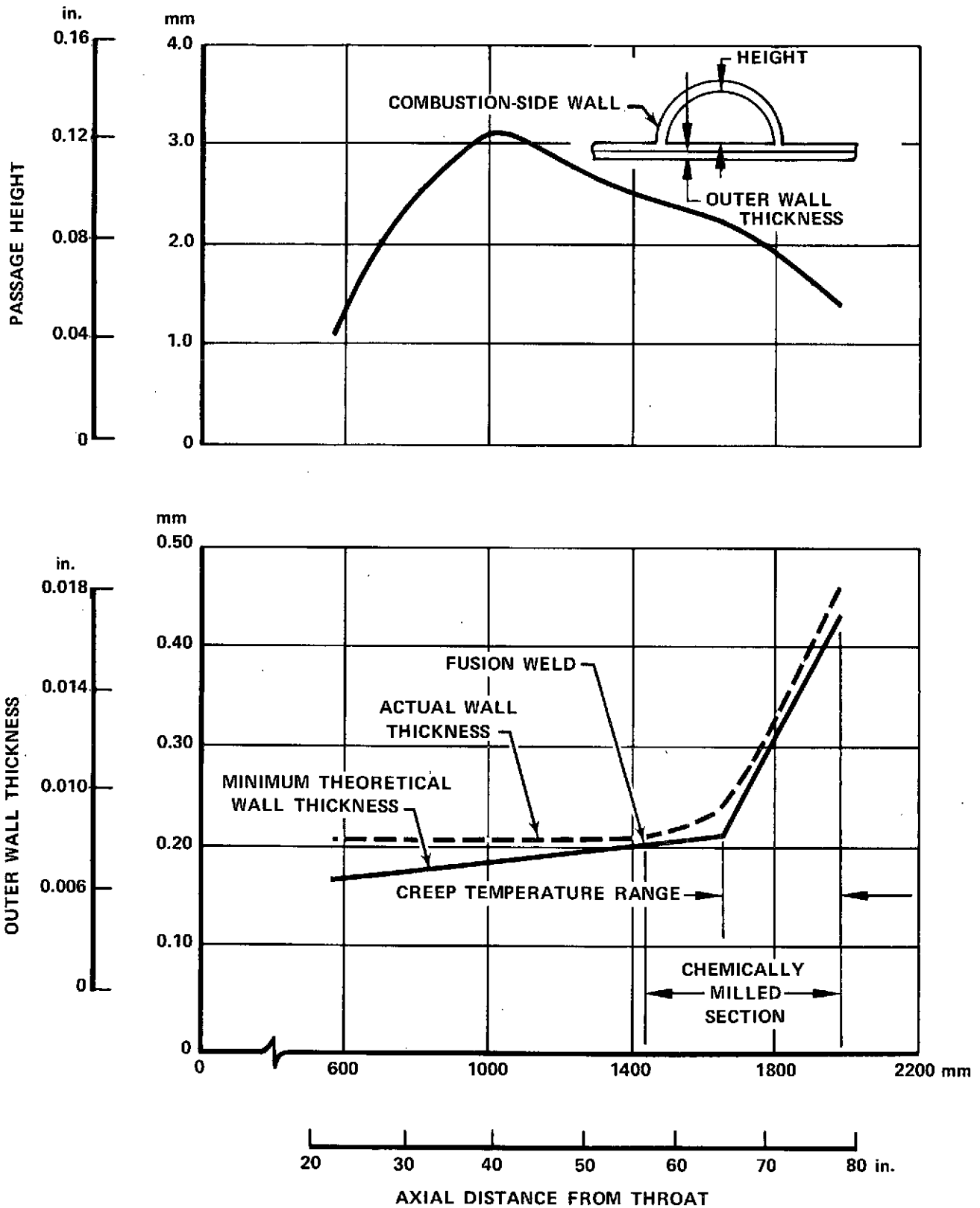

Figure 114. ASE Dump Cooled Nozzle Passage Geometry (360 Corrugations) FD 72570

(d) Nozzle Joints and Stiffeners

- Tubular to Nontubular Transition Joint

Coolant enters the nontubular nozzle section at its maximum expansion ratio of 6:1 from the tubular section in a counterflow direction. To avoid the weight and pressure loss penalties of two separate manifolds, flanges, and fasteners, direct attachment between the two sections is provided. (See figure 98.) The tubes at the end of the tubular section are brazed into sockets in an AMZIRC ring, which is electron-beam welded both to the nontubular AMZIRC inner wall and to the structural nickel outer wall. This joint, in addition to being lightweight relative to flange type joints, makes use of the high thermal conductivity of the AMZIRC combined with higher coolant velocities in the transitional flow region (compared to coolant velocities in the tubular section) to prevent excessive hot-wall temperatures.

- Inlet Manifold and Gimbal Attachment Brackets

The liquid hydrogen coolant is introduced into the regeneratively cooled chamber at an area ratio of 25:1 through an annular inlet manifold with a 3.81 cm (1.50 in.) ID. The coolant flows into the short tubes of the parallel flow section of the skirt heat exchanger through braze joints between the manifold and the 180 short nozzle tubes.

The coolant inlet manifold is also used as the attach point for the two gimbal actuator brackets. (See figure 115.) This eliminates the weight penalty of a separate stiffening ring. The vertical (radial) gimbal actuator force required to achieve the 20 rad/sec^2 (1146 deg/sec^2) specified angular acceleration rates is 3.65 kN (820 lb). The total force required of the actuator at the 0.523 rad (30 deg) nominal operating angle is 7.3 kN (1640 lb).

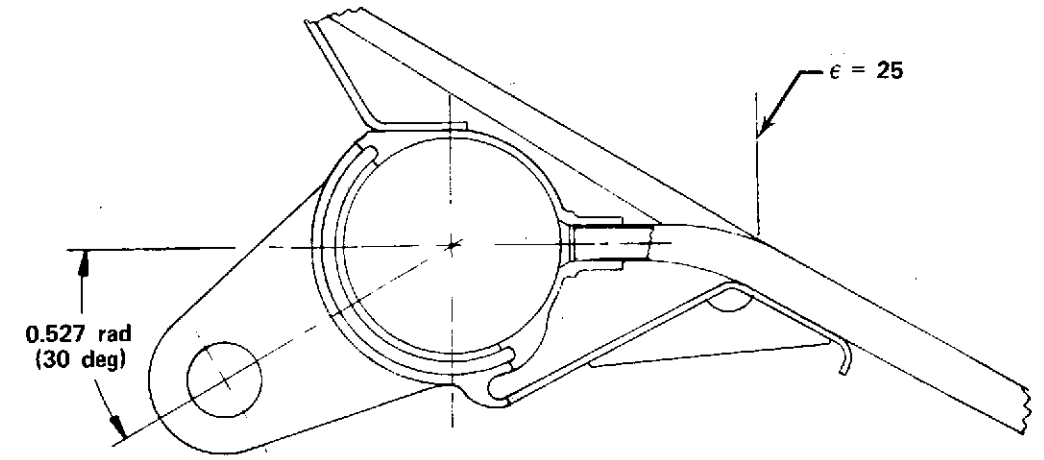

Figure 115. Advanced Space Engine Gimbal Actuator Bracket FD 72482

Stress resulting from the combined actuator and internal pressure loads on the inlet manifold are calculated to result in a factor of safety in excess of 1.1 with respect to yield strength at room temperature. A still greater factor of safety exists at lower operating temperatures.

- Dump-Cooled Nozzle Attachment and Turnaround Manifold

The dump-cooled nozzle is attached to the regeneratively cooled nozzle at an area ratio of 100:1 by a Marmon-type clamp, which fastens mating flanges on each side of the joint in place. (See figure 116.) On the dump-cooled nozzle side of the joint, the flange is integral with the coolant inlet manifold. Radial positioning of the flange is maintained by a snap joint, and angular (circumferential) position of the flange are maintained by dowel pins joining the flanges. Hot exhaust gases are prevented from escaping at the junction of these two flanges by a metallic O-ring seal.

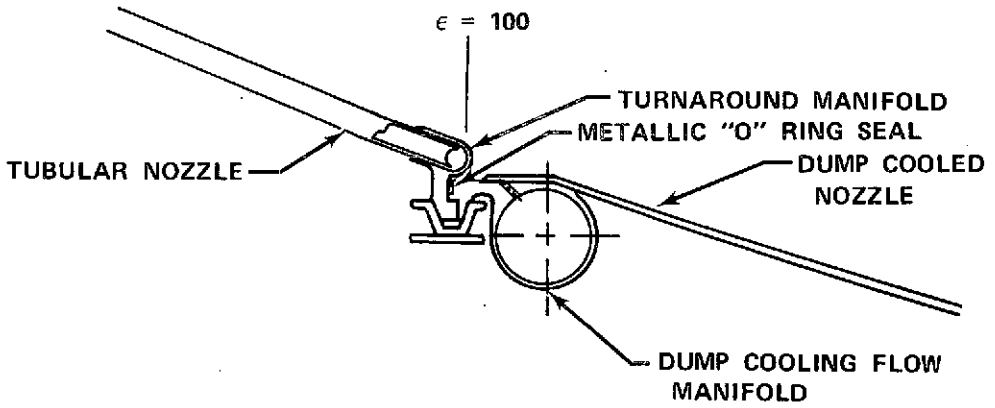

Figure 116. Dump Cooled Nozzle/Tubular Nozzle Turnaround Manifold Junction FD 68844

The coolant inlet manifold has a 2.54 cm (1.0 in.) inside diameter and a 0.762 mm (0.030 in.) thick outer wall. It is brazed to the sheet metal outer skin at the forward end of the dump-cooled skirt. The manifold restrains the nozzle shell in the radial, axial and rotational directions.

On the regeneratively cooled nozzle side of the joint, the flange makes up the outer portion of the tubular nozzle turnaround manifold. It is necessary to break the turnaround manifold into inner and outer portions because of tube assembly problems resulting from the slope of the nozzle at this station. After the 180 long tubes are inserted individually into their sockets in the transition joint at $\epsilon = 6$, the 180 short tubes are placed between them and the two stiffening rings are brought into position. The inlet manifold at $\epsilon = 25$ is then brought into place on the short tubes. The turnaround manifold parts are finally brought together. The outer section comes down from the direction of the nozzle throat while the inner section is brought up from the direction of the nozzle exit. The ends of the tubes are then wedged together between the manifold segments and the manifold segments were joined together with a 2π rad (360 deg) fusion weld. The entire tubular portion of the nozzle (from $\epsilon = 6$ to $\epsilon = 100$) is then furnace brazed.

- Dump-Cooled Nozzle Stiffening Rings

As shown in figure 99, four inverted hat-section stiffening rings are incorporated on the dump-cooled section of the nozzle. These rings have been sized and positioned to provide support for loads from gimballing, maneuvering and vibration.

Studies were conducted to determine optimum stiffening ring cross sections to give the greatest moment of inertia for the least weight (I/A). Considered were "I" and "Z" sections, channels, equilateral triangles, squares, circles and semicircles. The "I" and "Z" sections were ruled out because of the lack of torsional rigidity. After the other sections were sized for crippling and buckling stability, the study showed the three sections having the highest I/A to be the circle, followed by the semicircle and the square. As the circle and semicircle both entailed excessive manufacturing difficulty and expense to use as stiffening rings, and as the hat section is closely related to the square stiffening ring section in I/A and is more easily manufactured than any of the other three sections, the hat section was chosen for the dump-cooled nozzle stiffening rings.

Stresses and deflections resulting from gimballing depend upon unknown excitation and damping. The design approach has been to assure that the natural frequency exceeds the maximum gimballing frequency. The hat section generated for the ASE dump-cooled nozzle was initially sized to provide a moment of inertia sufficient to keep the exit end of the nozzle from vibrating in an ovalizing mode at less than 13 Hz, thereby providing a 30% margin over the 10 Hz specified for the gimbal frequency. The other three stiffening rings were located to prevent cylindrical buckling caused by dynamic loading.

c. Main Case Subassembly

(1) General Description

The main chamber injector and main case of the ASE forms a welded assembly that attaches to the thrust chamber. The main case is, in effect, the fuel (hot preburner combustion gases) manifold for the main chamber injector. The injector must introduce the propellants into the main chamber in a manner that will assure efficient, stable combustion at all engine operating points.

A multiple concentric jet injector with single orifice oxidizer elements was selected for the preburner. The concentric jet injector configuration produces low temperature profile variations. Because the ASE is a fixed-thrust engine, and operates as an expander cycle engine with no combustion in the preburner when in idle mode, dual-orifice oxidizer elements were not required to provide adequate injector pressure losses for the high-flow turndown ratios that were required on the OOS engine. Use of single orifice oxidizer elements permits a simpler mechanical design of the injector and control valve and allows a small decrease in engine weight.

The main case supports the preburner and the high-pressure fuel pump, contains the ducting that routes preburner gases to the turbines, and accepts the return flow from the turbines to serve its function as the main injector hot gas manifold. The main case also contains the spherical gimbal joint, and transmits thrust through it to the vehicle mount interface.

The main burner ignition system is composed of a low-energy, spark-ignited oxygen/hydrogen torch. Dual spark plug igniters are provided with separate exciter boxes for system redundancy.

The main case assembly is shown in figure 117.

(2) Operating Characteristics

(a) Main Chamber Injector

- Combustion Performance

The η_c* performance levels used in the ASE studies for evaluation of the main injector were based on an empirical curve generated from results of high-pressure thrust chamber testing. Chamber and injector designs were established to assure the predicted levels would be achieved. As noted in the preceding discussion of the injector design, selection of design parameters was based on experience with the XLR129 engine designs, which provided a portion of the data used to generate the empirical curve.

The capability of the ASE injector design was evaluated using equations developed through regression analysis of RL10, 222 kN (50,000-lb) thrust high pressure and 1.11 MN (250,000-lb) thrust high pressure engine and rig test data. Use of this analysis determined that η_c* in excess of 99.7% at 100% thrust and η_c* greater than 99% over the entire operating range can be conservatively predicted, as shown in figure 118. The analysis was based on a 22.9 cm (9 in.) long thrust chamber which, according to the analysis, is reasonably close to the maximum desirable length.

- Injector Flow Characteristics

The main chamber injector operating characteristics are determined by the engine cycle power balance. The variation in chamber pressure with mixture ratio at rated thrust is shown in figure 119. Injector characteristics described in the following paragraphs are from the baseline cycle operating conditions.

The fuel flowing to the main burner injector at full thrust is actually hot, fuel-rich preburner combustion gas that has been expanded through the turbines that drive the high pressure fuel and oxidizer pumps. The temperature of the hot gas is shown in figure 120. Figure 121 shows the hot gas injector pressure drop as a percentage of chamber pressure.

Because of pumped idle operational requirements (see paragraph B, Engine System), an oxidizer injector pressure drop larger than necessary to provide combustion stability resulted at full thrust. Figure 122 shows the oxidizer injector pressure drop as a percentage of main chamber pressure over the engine mixture ratio operating range at full thrust. The main chamber injector propellant momentum ratios are shown in figure 123.

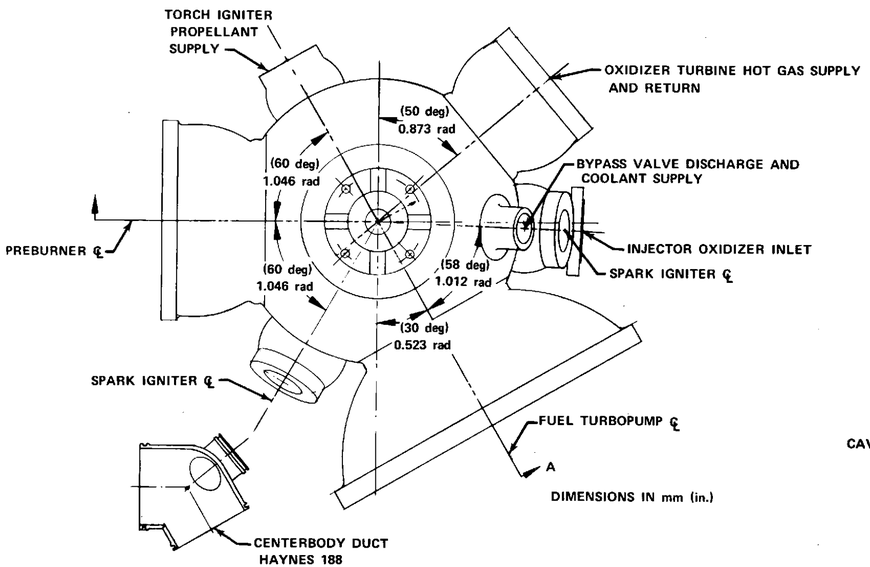

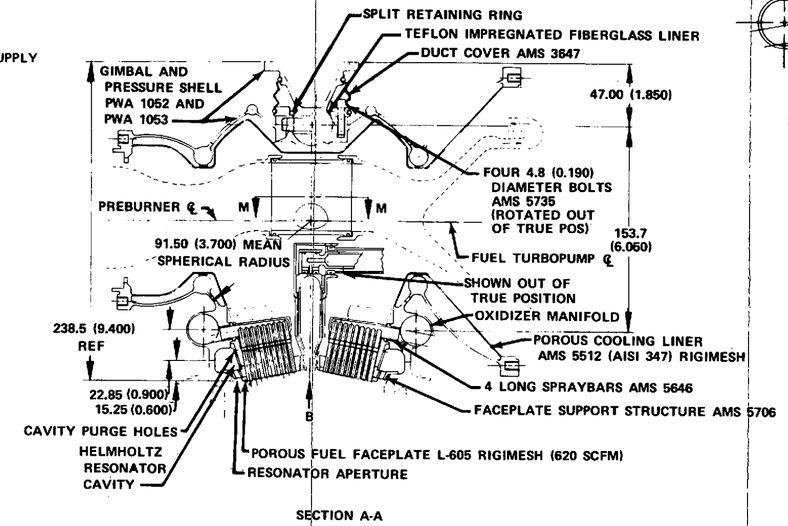

SECTION A-A

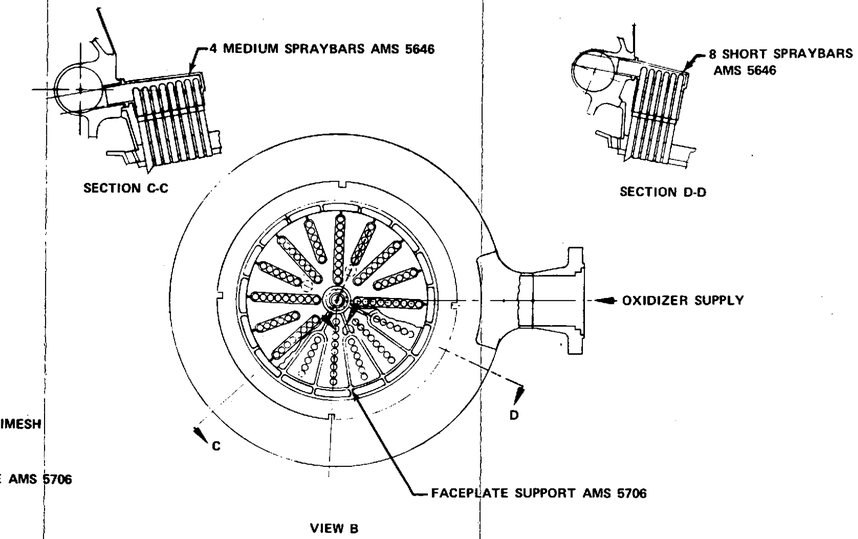

VIEW B

Figure 117. ASE Main Case and Injector Cross Section

FD 72483

FOLDOUT FRAME 1

FOLDOUT FRAME 2

FOLDOUT FRAME 3

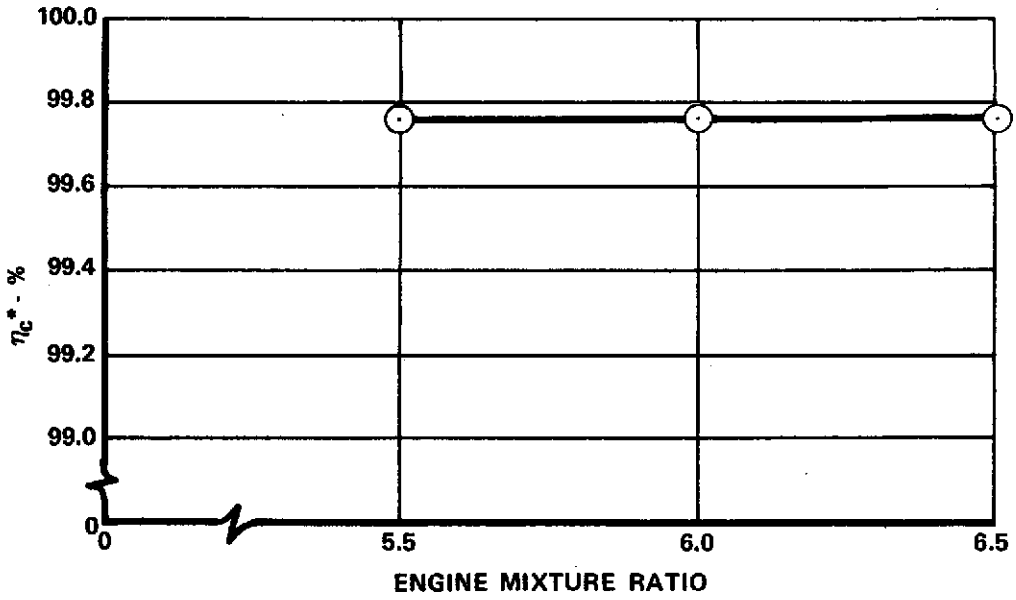

Figure 118. Advanced Space Engine Main Chamber Predicted η_c* (Based on Regression Analysis) FD 71593

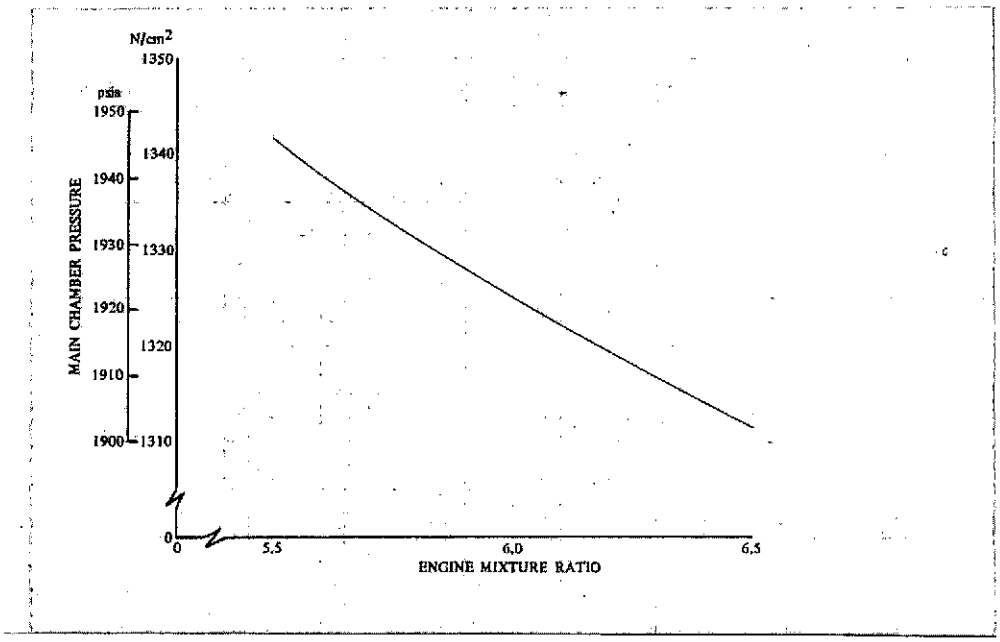

Figure 119. Advanced Space Engine Main Chamber Pressure at Rated Thrust DF 96018

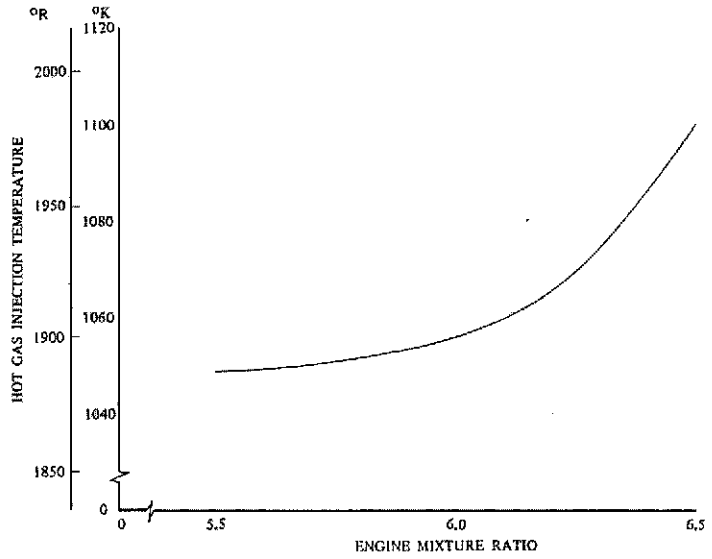

Figure 120. Advanced Space Engine Main Injector Hot Gas Injection Temperature at Rated Thrust

DF 96017

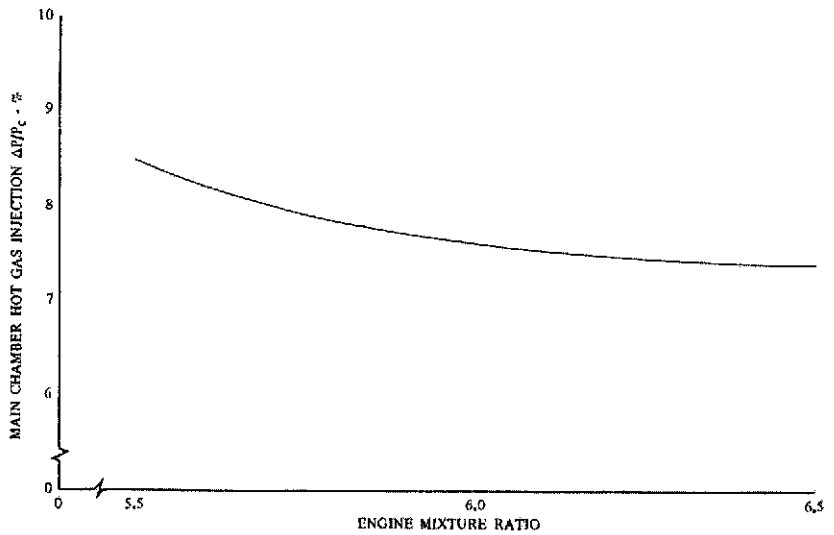

Figure 121. Advanced Space Engine Main Chamber Hot Gas Injection $\Delta P/P_c$ at Rated Thrust

DF 96016

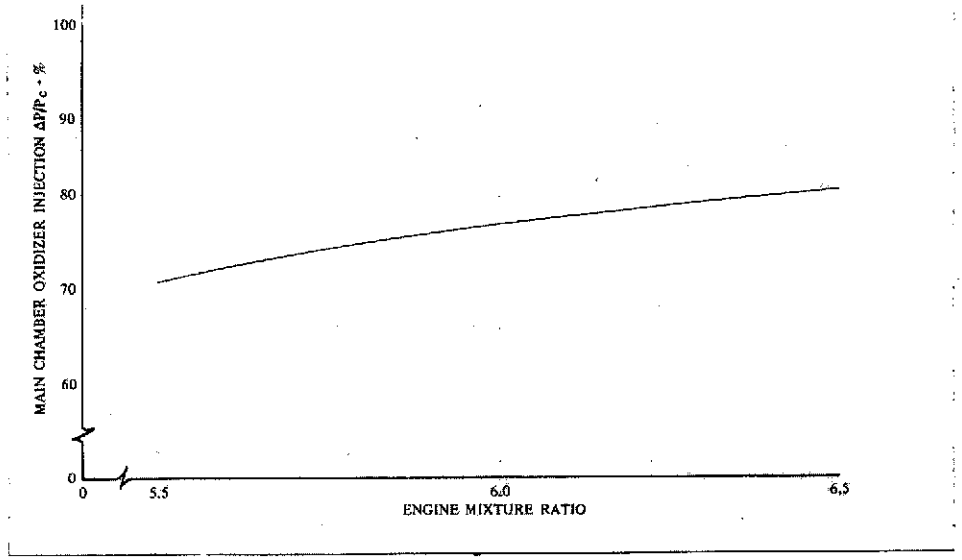

Figure 122. Advanced Space Engine Main Chamber Oxidizer Injection $\Delta P/P_c$ at Rated Thrust DF 96015

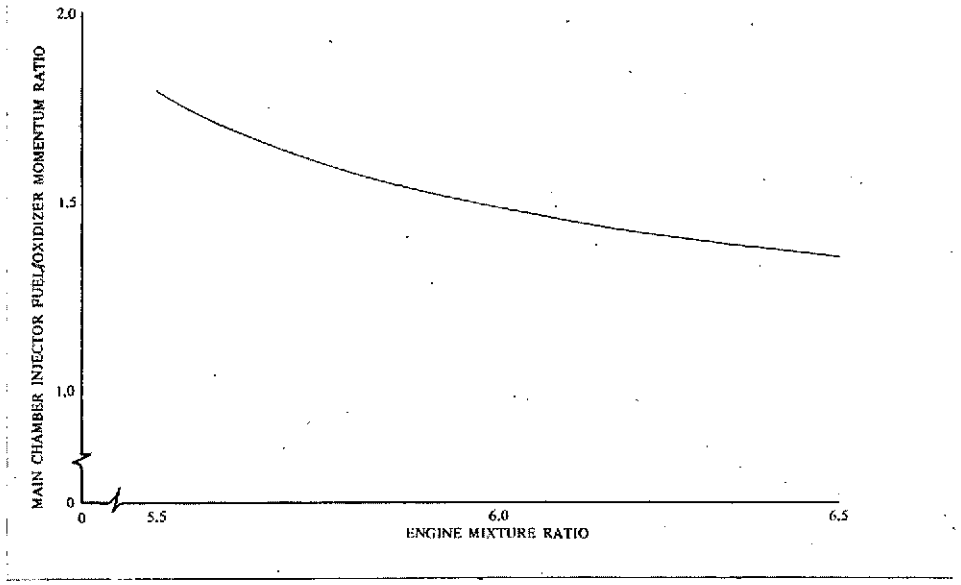

Figure 123. Advanced Space Engine Main Chamber Injector Fuel/Oxidizer Momentum Ratio at Rated Thrust DF 96019

The oxidizer element design provides excellent atomization. The injection elements are self-atomizing in that they do not depend upon the interaction of separate fluid streams to form droplets, but rather use the energy available in the element injection pressure drop for atomization. The tangential orientation of the entrance slots induces a flow that forms a thin fluid film upon the wall of the tube. A portion of the total injection pressure drop is consumed in the velocity of the film. The vortex flow field creates a gas core within the element, and the fluid film is maintained by the centripetal force exerted upon the fluid by the wall. When the fluid film leaves the element, the higher-velocity fluid toward the center of the element tends to penetrate outward through the slower-moving fluid at the outer boundary of the fluid sheets. As the fluid sheet of each oxidizer injection element expands, the sheet thins out, and the combination of thinning and violent internal mixing atomizes the fluid into extremely small droplets.

The atomization characteristics of tangential entry injector elements were investigated in water flow tests conducted by the Delavan Corporation, a Pratt & Whitney Aircraft supplier. The Sauter mean diameter and droplet size distribution obtained with typical elements are shown in figure 124. The water test data were corrected for liquid oxygen flow using the empirical equation derived by Delavan Corporation, which is:

$$\frac{SMD_{LO_2}}{SMD_{H_2O}} = \left(\frac{\mu LO_2}{\mu H_2O}\right)^{1/4} \left(\frac{\sigma LO_2}{\sigma H_2O}\right)^{1/3} \left(\frac{\rho H_2O}{\rho LO_2}\right)^{1/2}$$

where:

SMD = Sauter Mean Diameter
μ = viscosity
σ = surface tension
ρ = density

A JANNAF droplet size group vaporization efficiency correlation developed for Space Shuttle Main Engine Phase B Contractors was provided to Pratt & Whitney Aircraft during our participation in the Contract NAS8-26186 program. The droplet size vaporization efficiency vs initial droplet size group diameter curves from this correlation for the contraction ratio of 3.0 for the ASE are presented in figure 125 for 1034 N/cm^2 (1500 psia) chamber pressure and in figure 126 for 2068 N/cm^2 (3000 psia) chamber pressure, levels that bracketed the 1324 N/cm^2 (1920 psia) design point of the ASE engine. The atomization characteristics (maximum droplet size) of the tangential swirler elements are well under the maximum allowed for 100% vaporization efficiency at either chamber pressure level for chamber lengths less than the design value, so vaporization is not a limiting combustion performance factor.

- Provisions for Combustion Stability

Combustion instability that might be encountered in the Advanced Space Engine main injector is of two general types: feed-system-coupled nonacoustic instability (chugging) and acoustic instability (screech). The ASE main burner injector design and engine cycle incorporate measures to prevent either type of instability.

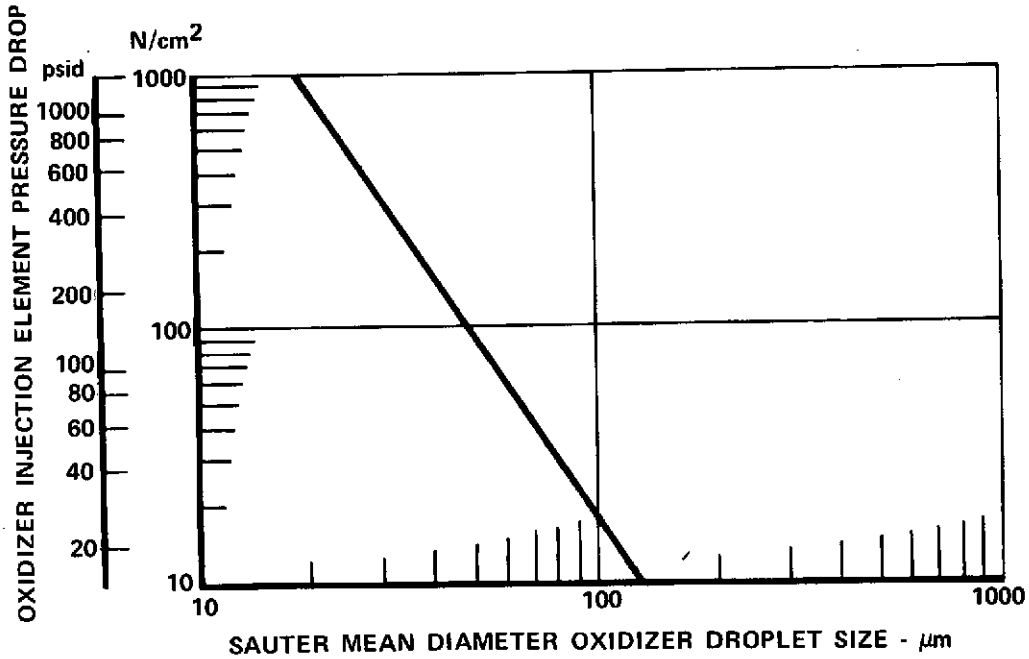

Figure 124. Advanced Space Engine Injector Element Performance FD 72541

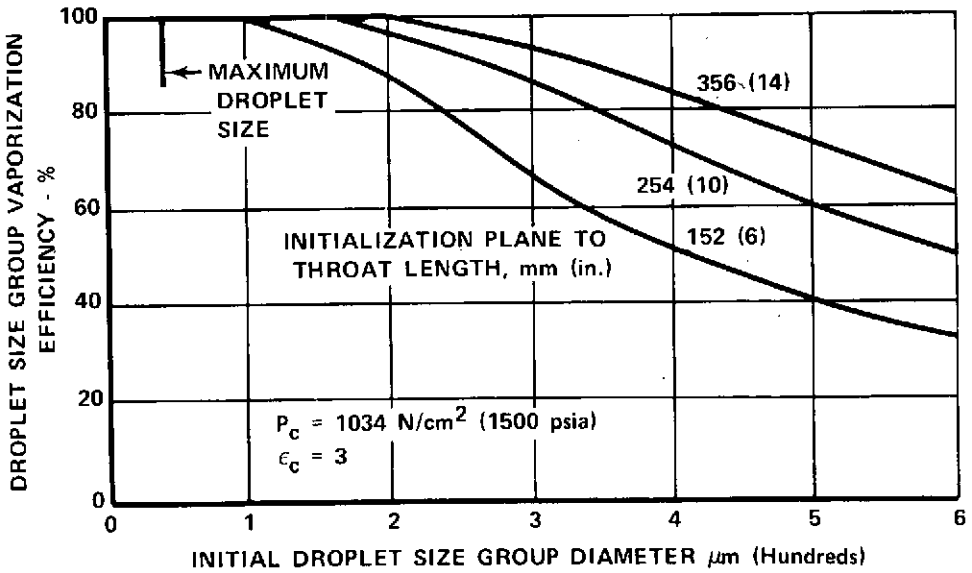

Figure 125. Main Injector Vaporization Efficiency, 1034 N/cm2 (1500 psia) Chamber Pressure FD 71576

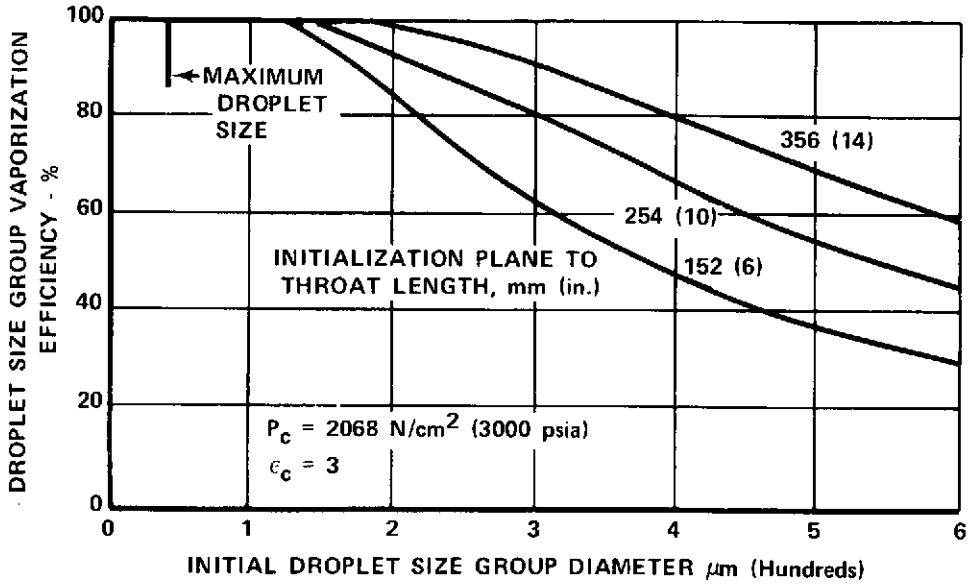

Figure 126. Main Injector Vaporization Efficiency, 2068 N/cm2 (3000 psia) Chamber Pressure FD 71577

Two areas are of primary concern for idle-mode nonacoustic instability (chugging). Operation in the pumped idle mode involves very low propellant $\Delta P/P_C$. The analog computer studies performed during the XLR129 program for the preburner injector showed that fuel temperatures above 167°K (300°R) had a powerful stabilizing influence because of its effect upon reducing the ignition delay time. It is anticipated, therefore, that the main chamber can be operated at these low pressure drops for pumped idle without chugging.

The second area of concern involves the transition from tank head idle, when the main injector is supplied with gaseous oxygen, to pumped idle, when the main injector is supplied with liquid oxygen. The liquid oxygen must chill the injector body; during this cooldown, the injector is flowing two-phase fluid. This cooldown period should be as short as possible. Although much of this potential problem area requires a transient system analysis for proper definition, the main chamber injector design contributes to providing a rapid cooldown by minimizing the weight of hot-gas-contacting material that must be cooled down. In particular, the spraybars and oxidizer injection elements are comparatively thin-walled items and are light in weight.

Acoustic instability (screech) will be damped by an acoustic resonator cavity. This type resonator is approximately twice as effective as other damping devices of the same aperture area and cavity volume and has a wider effective absorbing bandwidth.

The annular acoustic cavity, as shown in figure 117, is located at the periphery of the injector faceplate and is tuned to provide damping at the frequency of the first tangential mode. The acoustic cavity is purged with a low fuel flow and divided into eight circumferential compartments to eliminate circumferential flow. The design absorption coefficient and frequency bandwidth of the main burner resonator are shown in figure 127.

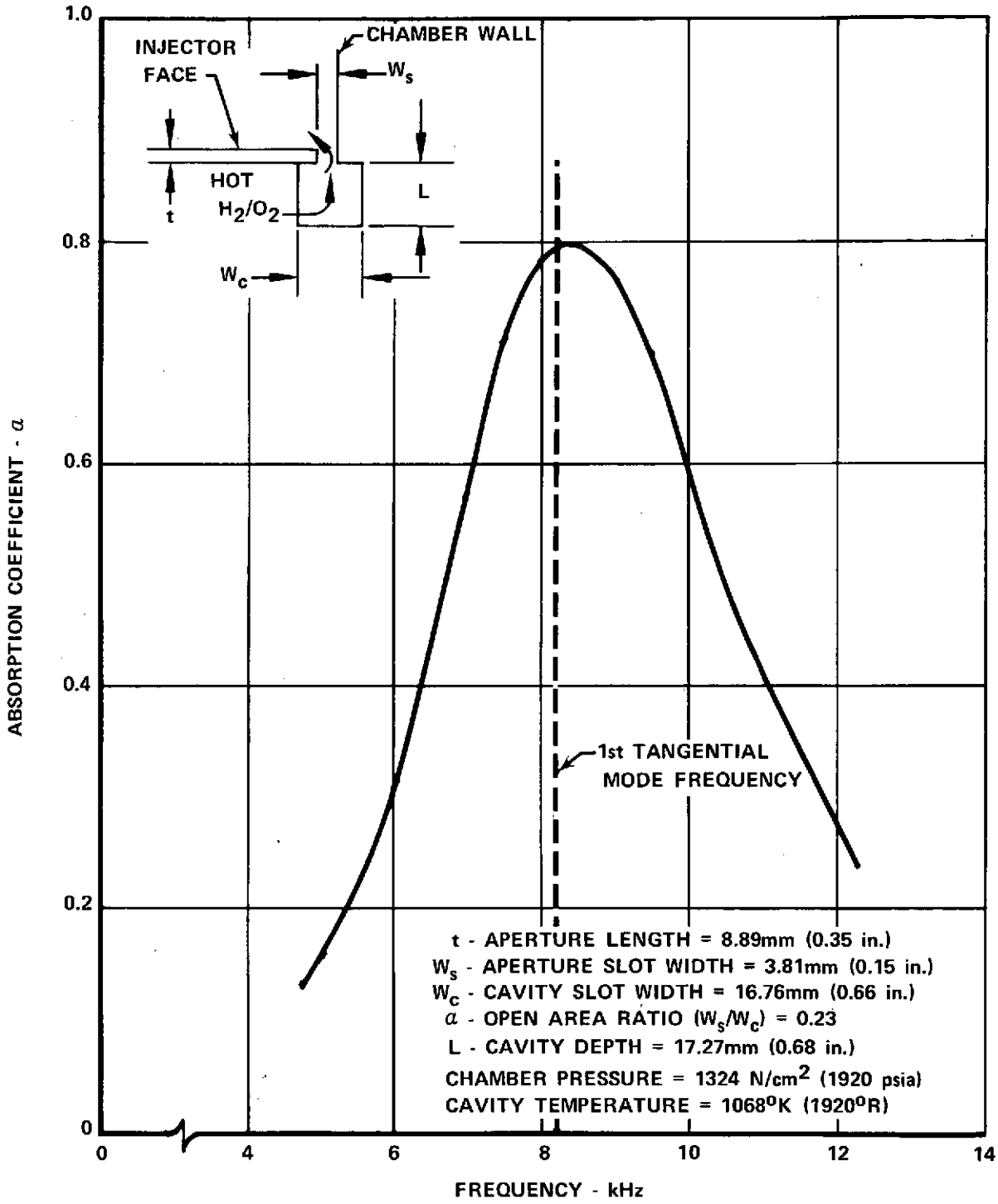

Figure 127. Advanced Space Engine Main Chamber First Tangential Mode Slot Resonator FD 68872

(b) Igniters

Torch igniter operating characteristics depend on supply orifice sizes, igniter discharge port diameter, igniter cooling configuration, and propellant supply tapoff locations. These are established to satisfy the following design objectives:

1. Igniter pressurization by the startup igniter propellant flowrates in order to attain a pressure above the lower limit for ignition

2. Sufficient spark energy and discharge rate to ensure ignition of the igniter flow

3. Sufficient energy release rate to ensure ignition of the main combustor startup flows

4. Sufficient torch momentum to penetrate into the mainstream of the engine propellants

5. Igniter cooling and low mixture ratio combustion to permit safe, continuous operation at all throttle points.

Analyses performed for the XLR129 and Space Shuttle Main Engines showed that an energy release rate of 1.69 kw (1.6 Btu/sec) will provide a reliable lightoff. This requires an igniter flowrate of 0.00068 kg/s (0.0015 lb/sec) at a mixture ratio of 2.0. Figure 128 depicts the igniter supply conditions, required flowrates, and resulting orifice effective areas for the main chamber torch igniter to satisfy this condition at startup. The discharge port diameter is sized to provide an unlit chamber pressure of 2.76 N/cm^2 (4.0 psia). As noted above, approximately 15% of the total fuel flow is diverted to the transpiration liner, which raises the igniter injector mixture ratio to 2.35. Figure 129 shows that this combination of mixture ratio and chamber pressure is within the ignition envelope.

The engine is designed to start with an oxidizer lead. Hence, as figure 129 shows, the ignition envelope will be traversed by the mixture ratio/P_c trace before the steady-state point is attained, providing the most favorable conditions for reliable ignition. Because the main chamber igniter flows bypass the turbines and therefore reduces available power, valves are included in the supply lines. The oxidizer valve closes completely, but the fuel valve permits approximately 15% of normal igniter flow to pass while in the closed position to provide igniter cooling during steady-state operation.

(3) Mechanical Description

(a) Main Case

The ASE main case configuration, as shown in figure 117, was adpated from the transition case design used in the XLR129 engine. Additional studies of the OOS 111 kN (25,000 lb) thrust engine, provided many benefits in engine packaging.

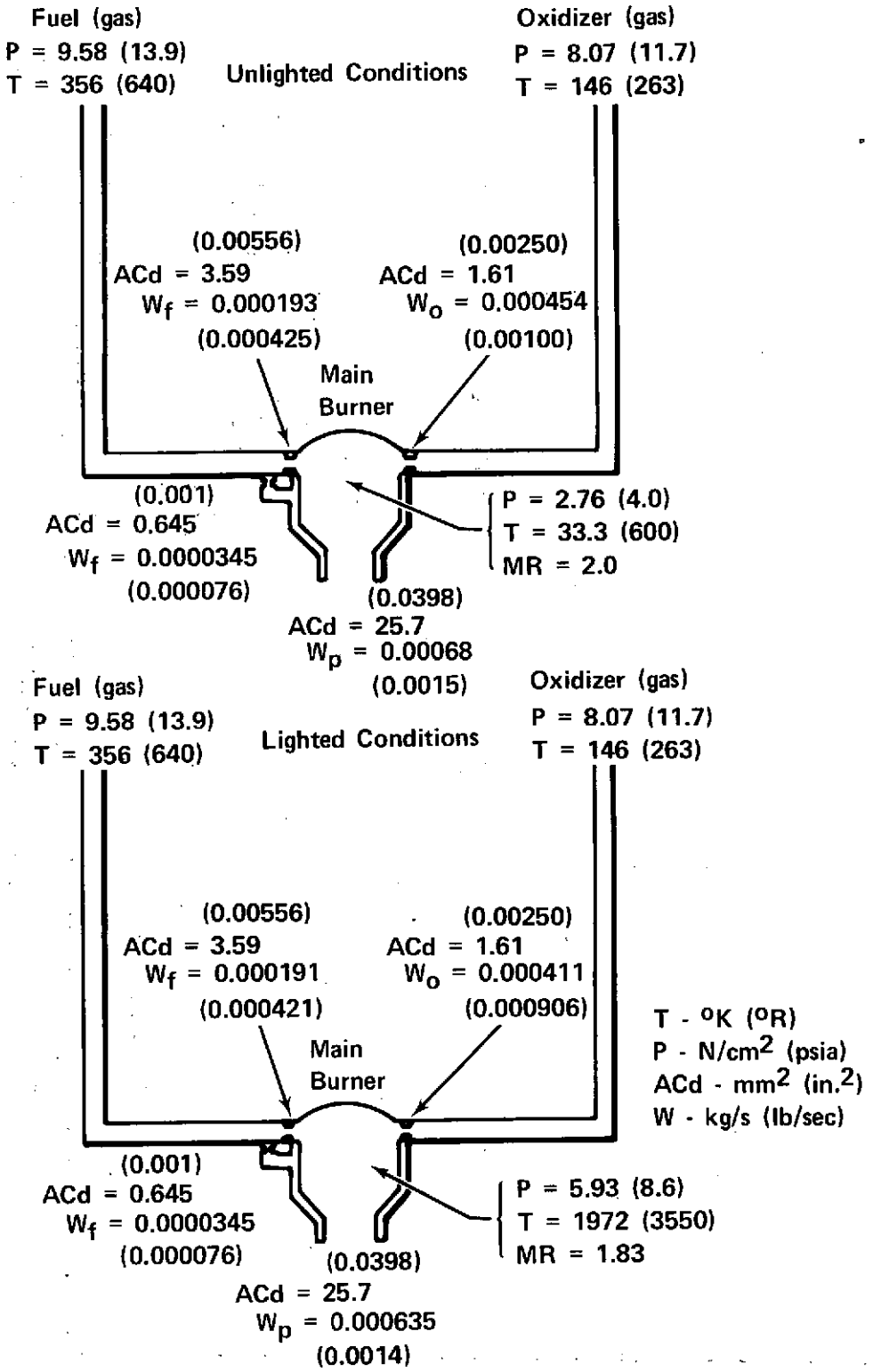

Figure 128. Advanced Space Engine Main Burner Torch Igniter Lighted and Unlighted Conditions

FD 71591

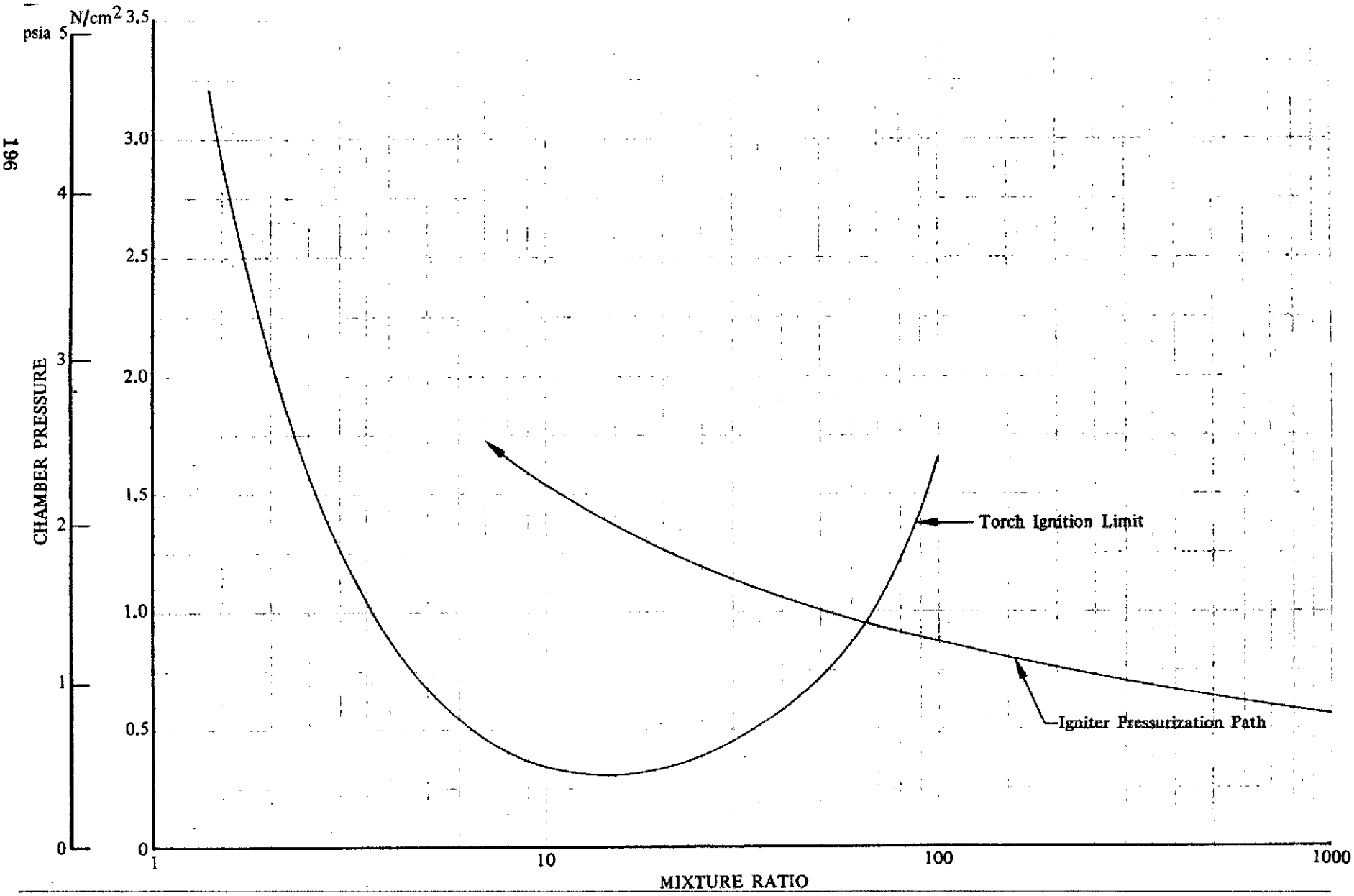

Figure 129. Advanced Space Engine Main Chamber Torch Igniter Ignition Envelope DF 96020

The spherical main case design is based on a modular plug-in approach for the preburner and fuel turbopump assembly. The main burner injector forms a weldment with it to eliminate an additional large diameter flange, which would be necessary in a bolt-on injector configuration. The two spark igniters, igniter propellant supply assembly, and torch igniter are all removable. The case diameter of 18.8 cm (7.4 in.) was established by the size of the main injector and acoustic cavity and the space required to install the torch igniter under the centerbody. Adapting sections from the case body to component attaching flanges are also spherical; the spherical shape inherently lends itself to the use of action line flanges. In action line flanges, the centerline of the shell wall intersects the centroid of the flange. This eliminates the bending movement normally encountered with L-flanges, since the shell load produces no unbalanced moment in the flange.

The main case is fabricated from two hydroformed hemispheres and ring-rolled forgings. The forgings form the component flanges and stiffening rings. Mod A-286 (PWA 1053, sheet) material is used because of its hydrogen compatibility and high strength. A porous sintered woven wire cooling liner shields the case structural shell from the high temperature turbine exhaust gases. The liner is hydrogen transpiration cooled by 0.131 kg/s (0.29 lb/sec) of hydrogen to maintain the case at or slightly above room temperature. This also protects surrounding engine components from adverse radiation effects, minimizing component interface thermal growth problems, and allowing efficient use of the case material. The liner, made in segments and welded in place in the sphere, is 0.099 m^3/s (21 scfm) porosity AISI 347 Rigimesh with an operating pressure differential of 6.9 N/cm^2 (10 psid) at 100% thrust.

A 0.254 cm (0.1 in.) gap between the ASE case and the liner is adequate for coolant distribution. A small gap is desirable to reduce the volume trapped between the case and liner, providing rapid transient pressure response. Coolant is supplied from the main chamber heat exchanger through the bypass valve with the pressure reduced sufficiently to maintain only a slight external pressure.

The centerbody duct in the main case routes the turbine drive gases from the preburner to the turbopumps. The centerbody also forms an enclosed duct system, which provides mixing length for preburner gases to promote uniform temperature profiles for the turbines. The duct of the ASE, 5.08 cm (2.00 in.) ID, is sized for a lower Mach number than comparable parts in the XLR129 engine. This provided greater residence time ensuring complete combustion. The centerbody is formed by three intersecting cylinders fabricated from Haynes 188 high temperature material. It is supported by the plug-in components in the main case. Sealing is accomplished by using a piston ring at each intersection, thereby allowing quick plug-in assembly.

The orientation of the component attachments is shown in figure 117. The case contains the gimbal mount assembly by means of a support cone which intersects the central sphere at a diameter that provides a pressure area term to balance engine thrust. Thrust is therefore taken in the main case as an additional hoop load only; the case is never in compression.

(b) Injector

The injector configuration selected for the ASE is a radial-slot spraybar design. The advantages of this arrangement over concentric element and circumferential slots were established in both design studies and testing conducted on XLR129 engine main chamber injectors. A large number of injection elements can be incorporated in the interest of good combustion efficiency, and the structural features permit free thermal expansion of parts for durability and long life.

The main burner injector introduces, atomizes, and mixes liquid oxidizer with the hot, fuel-rich turbine discharge gases (preburner combustion products) in such a way that efficient and stable combustion is achieved over the full operating range of thrust and mixture ratio.

The turbine discharge gases flow around injector spraybars and elements to the injector faceplate, which is constructed of Rigimesh. Part of these gases flows through the Rigimesh faceplate; however, the major portion of the gases flows through openings that are machined in the faceplate around the oxidizer elements.

The liquid oxygen enters the main burner injector through a single inlet horn. It then flows into the oxidizer inlet manifold that is wrapped around the circumference of the injector, maintaining essentially equal distribution to all the spraybars. The liquid oxygen flows from the wraparound manifold through crossover passages to the radial spraybars that serve as internal manifolds for the oxidizer injection elements. A single, tapered hole along the length of each spraybar allows sufficient area to maintain the overall injector pressure loss within the cycle limits.

The oxidizer manifold is integral with the major structural circumferential element of the injector, which forms the attachment to the main case. This inner section is a machined Mod A-286 (PWA 1052) forging, and the manifold closure is fabricated from Mod A-286 (PWA 1053) sheet material.

As shown in figure 117, there are four long, four medium length, and eight short spraybars. The long spraybars contain nine elements, the medium eight, and the short spraybars six elements. The spraybars are welded into bosses on the inner structural piece. The spraybars were brazed on the XLR129 engine but testing revealed small cracks in the braze joint. In the ASE, eight short spraybars are welded on bosses that are located above and between bosses for the long and medium spraybars. This configuration allows the spraybars to be located closer together for a higher-element density in a smaller diameter.

The spraybars are subjected to hot preburner combustion gases at 1056°K (1900°R) on outside surfaces and cold liquid oxygen at 111°K (200°R) on inside surfaces. The resulting thermal gradient across the wall produces thermal strains that make thermal fatigue life a consideration, even though it is not a limiting one. AISI 347 provides better cycle life than the Inconel 625 that was used in XLR129 spraybars. As AISI 347 has adequate strength, it was selected for the application, in which thickness is established by web stresses resulting from loads on the material between adjacent oxidizer elements. The selection reduces cost and machining effort. Stress analyses show that LCF life is 2000 cycles, well above the 1200 cycle criteria.

Injection elements are brazed into the spraybars to form radial rows as illustrated in figure 130. Each element is formed from a small diameter tube with one end rolled closed. The oxidizer enters through slots cut through the tube wall tangent to the inside diameter near the closed end.

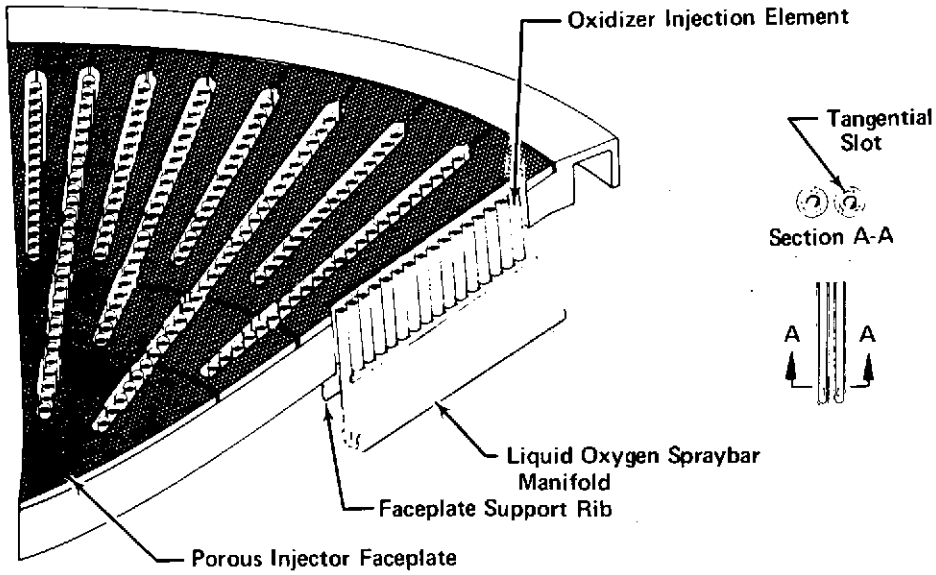

Figure 130. Main Chamber Injector Spraybar Configuration FD 46271A

The elements are mechanically simple, durable, and can be easily manufactured from drawn tubing (AMS 5571) of 0.338 cm (0.133 in.) OD and 0.209 cm (0.0824 in.) ID. The tangential entry causes the flow to leave the elements and enter the main combustion chamber in a hollow swirl cone made up of very small droplets. The discharge coefficient of the elements can be changed by varying the entrance slot area/discharge area ratio as illustrated in figure 131. The tangential entry slots can be accurately electric-discharge machined into the tubes, so individual element flowrates can be varied to produce the uniform injected mass flux necessary to achieve high performance. The individual elements can also be flow-calibrated before they are used in an injector assembly.

The element density for the ASE design is greater than that of XLR129 injectors that were tested: 116 elements with an 11.2 cm (4.4 in.) diameter compared to 996 elements with a 46.5 cm (18.3 in.) diameter. This increased element density should enhance the propellant injection profile and performance levels.

Figure 132 shows that by using distinct classes of elements configured for three different flows, the oxidizer radial mass flux variations can be held within ±10% of nominal. Mixture ratio is uniformly maintained by varying the fuel slot widths. Table XXIV summarizes the injector flow characteristics at 100% thrust, MR = 6.0. Use of a greater number of element classes would permit even closer tolerances for radial mass flux. Alternative injection elements are counterswirled for uniformity of injection pattern. To prevent the spray cone from impinging on the chamber wall, the outer element discharge tips are cut at an angle. As for the individual elements, spraybars can be flow-calibrated before being used in an assembly.

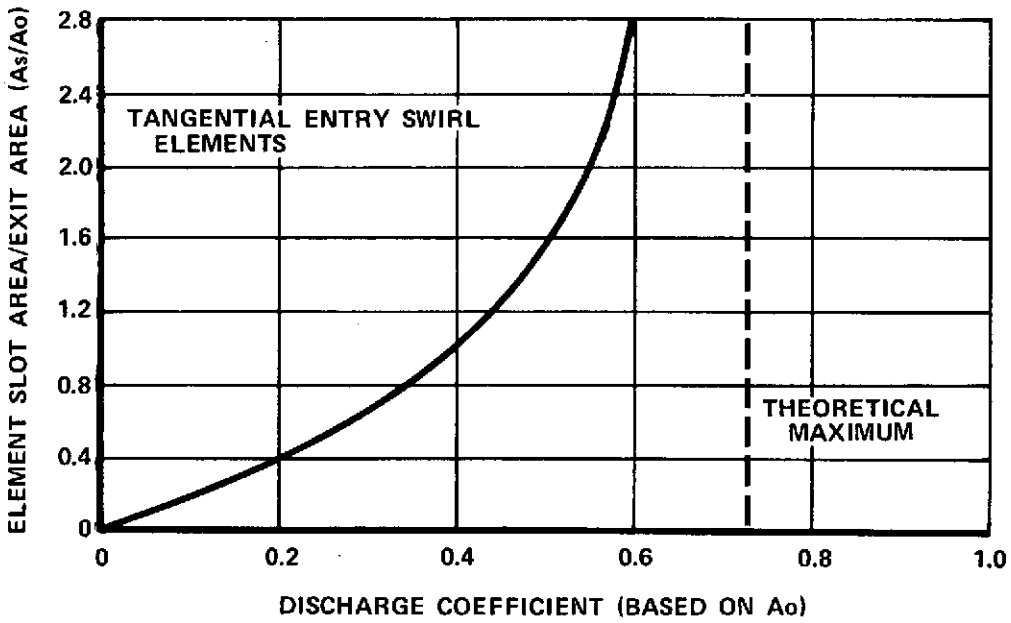

Figure 131. Tangential Entry Oxidizer Injector Element Discharge Coefficient Characteristic FD 72682

The fuel faceplate is a two-piece assembly consisting of an L-605 (AMS 5796) sintered wire matrix porous faceplate and a Waspaloy (AMS 5706) radial beam support structure. The faceplate and support structure are electron-beam welded together to form the two-piece faceplate assembly. Approximately 95% of the fuel-rich hot preburner combustion gas is distributed through slots surrounding the oxygen injection elements. The slot width is shaped to supply an amount of fuel at a given location that matches the classed oxidizer flow to create a uniform mixture ratio. The remainder of the flow passes through the surface of the plate to create a protective barrier against burning caused by recirculation.

The radial slots in the faceplate are sufficiently long to permit differential radial thermal growth between the hot faceplate and cooler spraybars. The radial layout of both the spraybar and fuel slot is in line with radial thermal growth, thereby minimizing the effects of thermal growth on injection pattern. The fuel faceplate assembly is pressure-loaded against the main chamber. Provisions are incorporated in the injector housing to provide for centering of the faceplate, and radial and axial stops are provided.

The 0.292 m^3/s (620 scfm) Rigimesh faceplate has a 101 N/cm^2 (146 psid) pressure drop at 100% thrust and the Rigimesh bulk temperature will be 1056°K (1900°R which is 133.3°K (240°R) hotter than that of the SSME cycle. The higher Rigimesh temperature increases the transient temperature difference between the slowly responding support web and the rapidly responding Rigimesh. Thermal analysis shows the support web temperature to be 611°K (1100°R) and the Rigimesh 111.1°K (200°R). Thus, LCF life was evaluated and determined to be greater than 1200 cycles.

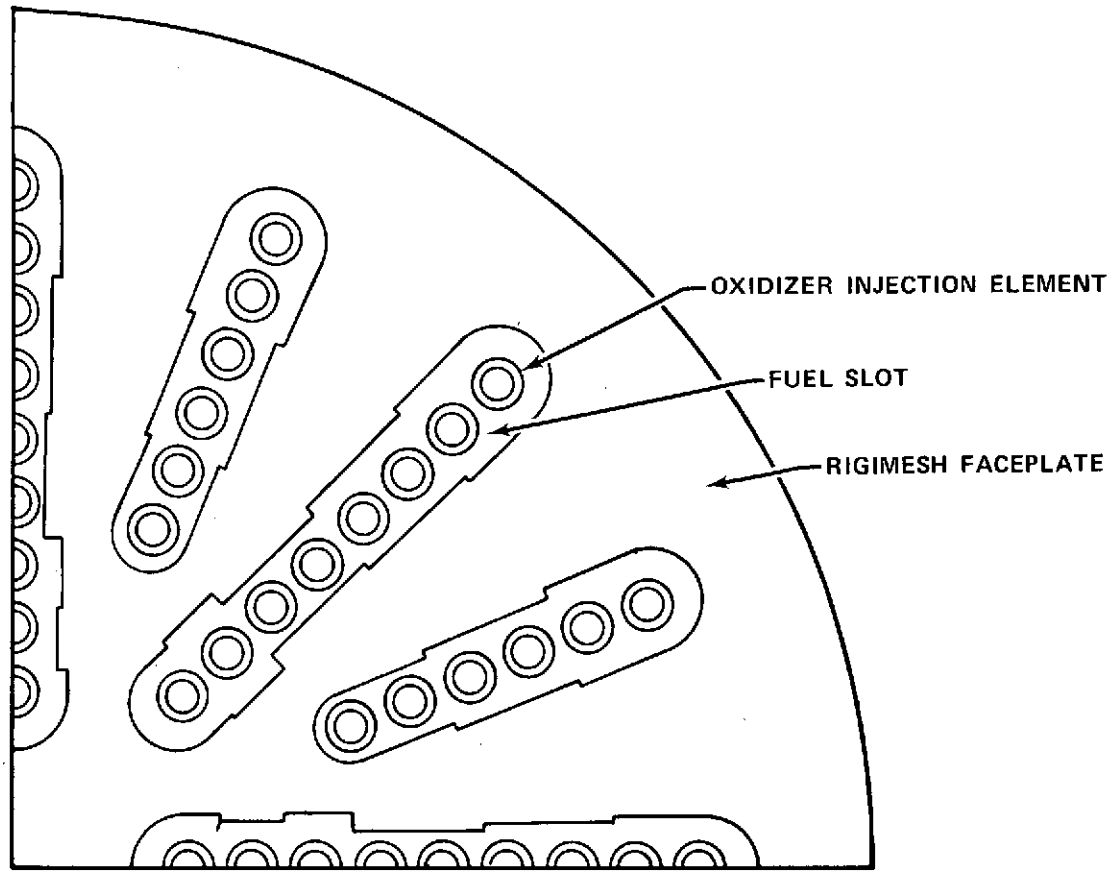

(SEE TABLE XXIV FOR INJECTOR DIMENSIONS)

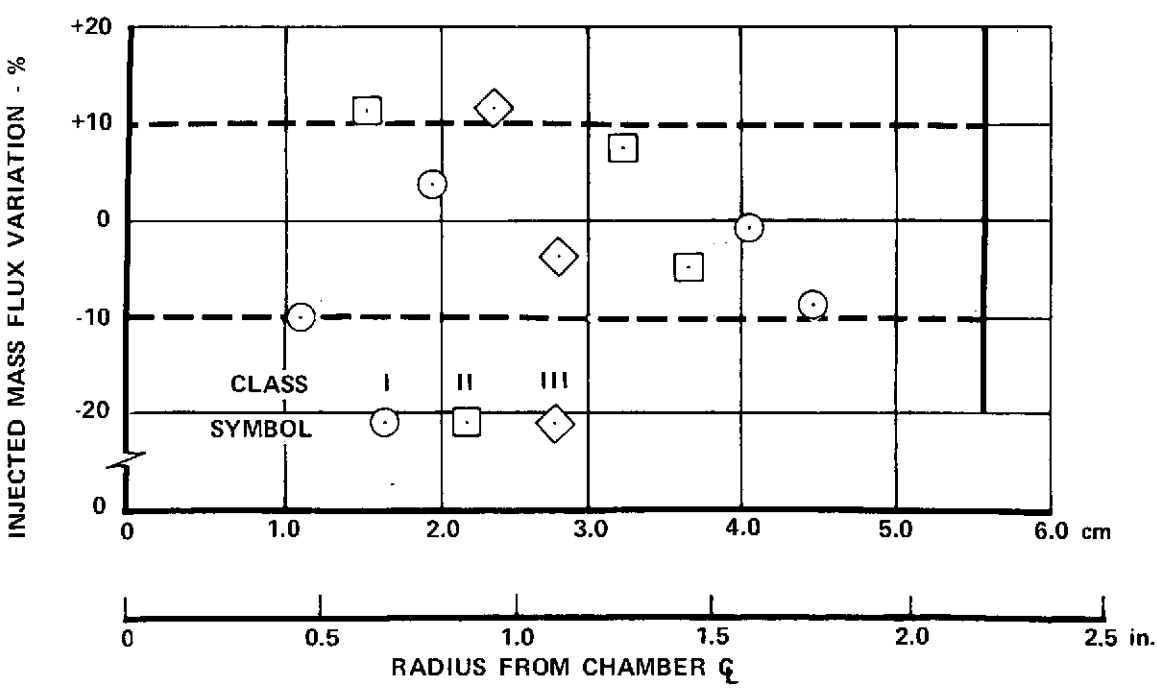

Figure 132. Advanced Space Engine Main Injector Element Classing FD 71592

Table XXIV. ASE Main Chamber Injector Dimensions and Flow Characteristics

OXIDIZER SIDE				
Element ID	2.095 mm (0.0824 in.)			
Element OD	3.380 mm (0.1330 in.)			
CLASS		I	II	III
Slot Width, mm (in.)	3 per element	0.437 (0.0172)	0.437 (0.0172)	0.437 (0.0172)
Slot Length, mm (in.)	3 per element	1.615 (0.0636)	1.283 (0.0505)	0.945 (0.0372)
Slot Area/Exit Area		0.615	0.490	0.360
Discharge Coefficient		0.284	0.240	0.186
Flowrate, kg/s (lb/sec)		0.1149 (0.2529)	0.0891 (0.1965)	0.0762 (0.1680)
Oxidizer Manifold Pressure Losses:				
Inlet Horn Loss, N/cm^2 (psi)		14 (21)		
Manifold Loss, N/cm^2 (psi		6 (9)		
Element Loss, N/cm^2 (psi)		430 (624)		
Total Loss, N/cm^2 (psi)		450 (654)		
FUEL SIDE				
CLASS		I	II	III
Radial Slot Width, mm (in.)		6.86 (0.270)	5.80 (0.228)	4.47 (0.176)
Rigimesh Faceplate				
Porosity Rating, m^3/s (scfm)		0.1415 (300)		
Faceplate Flow, % of Total:		9.1		
Fuel Pressure Losses:				
Entrance Loss, N/cm^2 (psi)			14 (21)	
Spraybar Blockage Loss, N/cm^2 (psi)			6 (9)	
Faceplate Loss, N/cm^2 (psi)			137 (199)	
Total Loss, N/cm^2 (psi)			157 (229)	

An acoustic resonator cavity as shown in figure 117 is incorporated in the main injector design to suppress high frequency instability in the injector. This resonator is approximately twice as effective as other damping devices of the same aperture area and cavity volume and has a wider effective absorbing bandwidth.

The acoustic cavity selected for the ASE has a volume of 131 cm^3 (8 cu in.) and an aperture width of 0.381 cm (0.150 in.). The aperture slots are part of the faceplate structure and thus remain constant in size throughout the thermal cycles. The cavity is directly behind the apertures and is formed when the main case assembly is welded to the thrust chamber and a ring was welded to the faceplate web support structure. The ring has a 0.0127 cm (0.005 in.) loose radial fit with the main case at assembly and fits tight at pump idle, tank head idle and 100% power conditions. To obtain the necessary 131 cm^3 (8 cu in.) for the cavity, the spraybar elements were increased in length about 1.27 cm (0.50 in.). This

was done not only to keep the acoustic cavity directly behind the apertures, but also to keep the main case diameter at a minimum, save weight, and not increase the blowoff load at the weld joint of the main case to thrust chamber.

The injector elements are short enough to have adequate combustion stability and are well supported by the copper braze joint into the spraybar. The acoustic cavity is purged with 0.025% of the total faceplate fuel supply through sixteen 0.074 cm (0.029 in.) diameter holes in the ring welded to the web support structure. This is done to maintain the cavity at a known temperature and absorption frequency. Eight baffles are welded to the cavity ring and support structure to break up transverse flow in the cavity.

(c) Main Burner Torch Igniter

Reliable ignition is provided by a low-energy, spark-ignited torch igniter for the ASE main chamber. The torch igniter features self-pressurization (choked flow conditions) for altitude ignition combined with propellant supply locations within the engine flowpaths, which permits safe, continuous operation when required.

The torch igniter is provided with two independent exciter-plug spark igniter assemblies for redundancy. Fuel is provided to the igniter from a tap immediately upstream of the fuel shunt valve; oxidizer is provided from a tap downstream of the oxidizer heat exchanger. These locations were selected based on the tank head idle operating characteristics of the ASE, in that preconditioning propellants are available. The main chamber igniter propellants bypass the turbines but are mixed with the main chamber flow for efficient expansion through the thrust chamber nozzle. Since igniter flows represent turbine power losses, a spring-loaded valve actuated by GO_2 pressure from the oxidizer control valve shuts off oxidizer flow to the igniter during full thrust, steady-state operation. The igniter fuel flow is reduced to an amount sufficient for igniter cooling by a valve similar to that used in the igniter oxidizer supply system.

The main burner torch igniter configuration, as shown in figure 133, consists of a housing, chamber, orifice and supply assembly, and two spark igniter assemblies (only one of which is shown; the other is out-of-plane with the view shown).

The igniter housing, support ring, orifice and supply assembly are fabricated from AMS 5735. AMS 5735 was selected for strength and compatibility with main case materials. The chamber is fabricated from 40 scfm nickel (AMS 5553) Rigimesh to provide transpiration cooling. The chamber is welded to a support ring and to the igniter housing at the main burner injector face. The housing is bolted to the main injector faceplate structure. The support ring incorporates four predrilled orifices, 0.051 cm (0.020 in.) diameter, which meter approximately 15% of the igniter total fuel flow to the transpiration cooled igniter liner. Three fuel slot orifices in the igniter injector meter the remaining 85% of the fuel into the igniter combustion chamber. The igniter chamber is part of the orifice and supply assembly which consists of a presized oxidizer orifice nozzle and a fuel supply duct. A set of seal rings forms a support and seal between the oxidizer orifice nozzle and the support ring. A seal ring is provided between the igniter housing and the fuel supply duct. The purpose of the seal ring is to seal off turbine exhaust fuel in the main case, while simplifying assembly

and disassembly of the orifice and supply assembly. The igniter spark plug assemblies are provided with heat shields. Seal rings are used to form a seal between the spark plug and the igniter housing. The heat shield and seal rings cool and seal the spark plug from the hot turbine exhaust fuel.

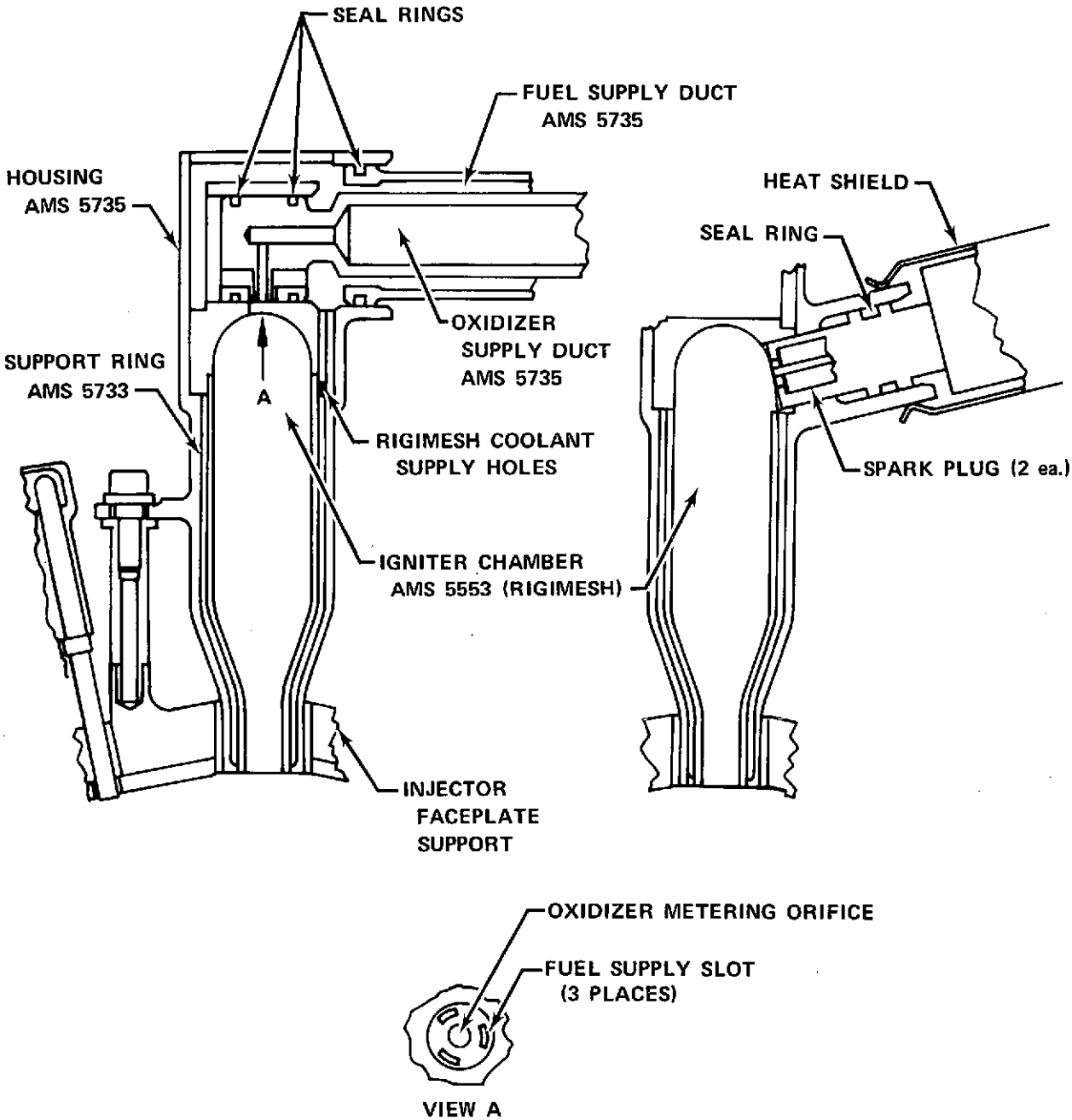

Figure 133. ASE Engine Main Burner Igniter Design FD 72395

The ASE main burner torch igniter design is based on a proven concept, which has been designed and tested for the RL10 and 1.11 MN (250,000 lb) thrust engines. The 1.11 MN (250,000 lb) thrust engine torch igniter was bench-tested (firing of torch igniter only) 116 times for a total duration of 2670.5 sec. This testing occurred over a range of mixture ratios from 0.5 to 3.0 and a temperature

range of 722 to 2556°K (1300 to 4600°R). Chamber tests (igniter firing chamber propellants at sea level) of the 1.11 MN (250,000 lb) thrust engine igniter was initiated 209 times for a total duration of 2879 sec. Altitude chamber tests of the RL10 torch igniter were conducted 714 times for a total duration of 73,259 sec.

Sea level ignition of the torch igniter was proven to be 100% reliable in the 1.11 MN (250,000 lb) thrust engine test program. Altitude torch ignition is verified by successful altitude chamber testing as well as in flight operation of the RL10 engine. Engine ignition has been successfully demonstrated by the RL10 in both altitude chamber testing and flight operation and in 1.11 MN (250,000 lb) thrust engine sea level chamber testing.

(d) Gimbal Assembly

The gimbal assembly configuration, as shown in figure 134, provides the ASE with the capability of being gimballed through a ± 122 mrad (7 deg) square pattern at acceleration or deceleration rates up to 20 rad/sec^2 (1146 deg/sec^2).

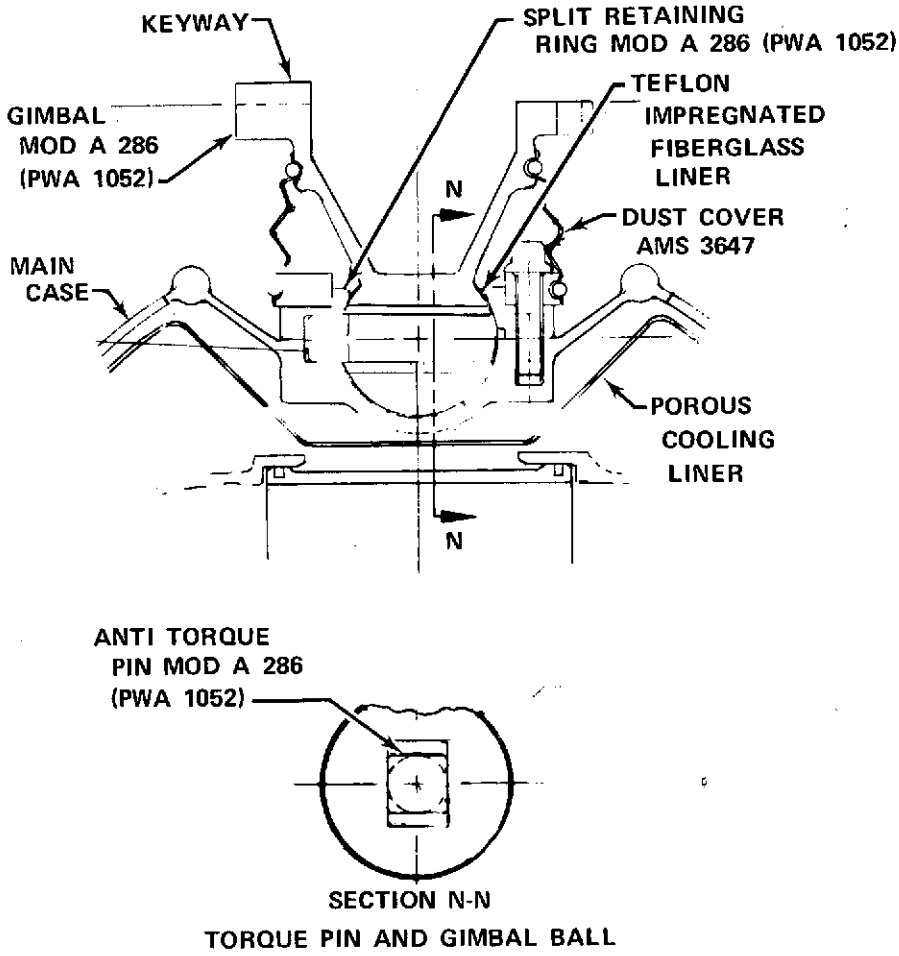

Figure 134. ASE Gimbal Assembly FD 72484

Engine thrust is transferred through a spherical ball intersected by a flanged cone which attaches to the vehicle interface. The flanged cone contains four keyways which accept engine torque and also facilitate bolt hole alignment at assembly. This eliminates the need for a standard cross pin universal joint, thereby producing a simpler, lighter and more stable joint.

The gimbal assembly is fabricated from forged Mod A-286 (PWA 1052) material because of its high strength and thermal compatibility with the main case structure. The design of the ball joint incorporates an antitorque pin which accepts the torque produced by the engine and transmits it to the vehicle. The ball features a bonded fluorocarbon plastic impregnated fiberglass liner to provide low friction and to distribute the bearing loads. The ball was sized to 3.05 cm (1.2 in.) diameter such that the bearing load on the plastic liner would not exceed 13,790 N/cm^2 (20,000 psi). This type liner has been used successfully at these bearing loads in the XLR129 program. Engine hanging loads are carried by a retaining ring which is split for assembly. A dust cover is provided to protect the low friction liner from deposit of abrasive particles. The gimbal loads were determined for the ASE system by reviewing 1.11 MN (250,000 lb) and 1.56 MN (350,000 lb) thrust engine calculations where 45% of the total moment was due to acceleration, 35% for side G-loads, and 20% for friction, hose restraints, and thrust-offset.

The thrust gimbal ball fits into a socket in the upper end of the outer case upon a support cone. This cone intersects the outer case sphere at a circle diameter which provides a pressure area term that balances against engine thrust. As a result, thrust is transmitted efficiently through the main case with only an increase in hoop load.

An alternative flanged cone gimbal pedestal design is provided to incorporate the exact mounting bolt holes and interface as the RL10 engine mount. It would increase the gimbal assembly weight by 0.419 kg (0.924 lb).

The total gimbal load represents approximately 8% of the total engine loads. When the total gimbal system is designed, including actuators, the minimum operational life criteria of 10,000 cycles will be met. The total gimbal system has not yet been defined, so the natural frequency of that system cannot yet be determined. The criterion that the natural frequency of the gimbal system shall not be less than 10 Hz should easily be met. All the engine components, including the dump-cooled nozzle, have natural frequencies above 10 Hz.

7. Vehicle Tank Pressurization Heat Exchangers

a. General Description

The ASE is required to provide a system for the autogenous pressurization of the vehicle propellant tanks. This is accomplished by heat exchangers, which provide gaseous fuel and oxidizer. The gaseous fuel and oxidizer are supplied to the vehicle fuel and oxidizer propellant tanks, respectively, as needed to maintain the desired tank pressures at full thrust and pumped idle. A GO_2 heat exchanger is also required to provide gaseous oxidizer for injection into the main combustion chamber at tank head idle.

The gaseous fuel for tank pressurization is supplied from the coolant discharge line of the regeneratively cooled thrust chamber. Fuel discharging from

the chamber cooling jacket will be at temperatures greater than 22°K (400°R) at all engine operating conditions and thus is well suited for fuel tank pressurization.

The gaseous oxidizer for tank pressurization is supplied from a heat exchanger incorporated in the oxidizer turbine supply/return line.

b. Operating Characteristics

A heat exchanger is required to supply the gaseous oxidizer pressurant since there are no readily available sources of heated oxidizer in the engine system. A schematic showing candidate areas for location of the oxidizer heat exchanger is shown in figure 135.

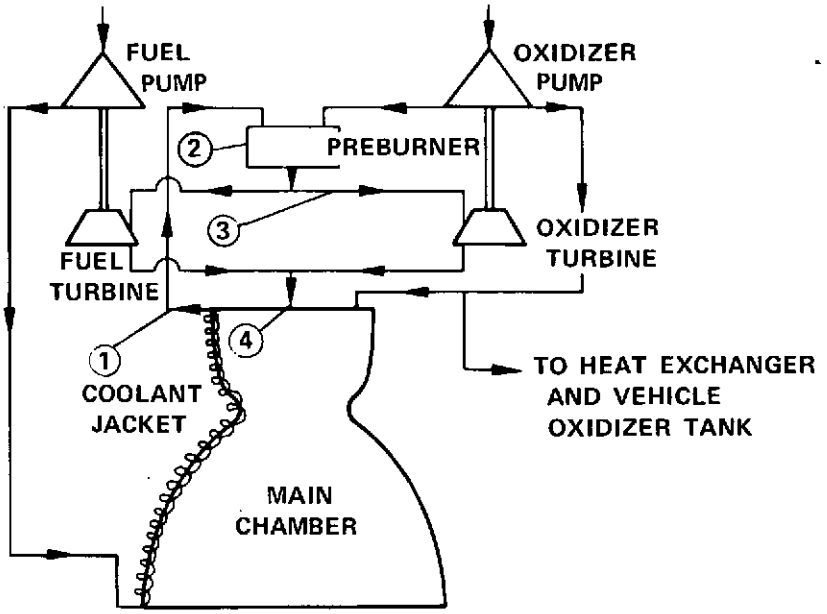

Figure 135. Potential Locations for Oxidizer Heat Exchanger FD 68823

The four locations shown are (1) the fuel line connecting the regeneratively cooled thrust chamber and the preburner fuel injector, (2) the preburner combustion chamber walls, (3) the line connecting the preburner and the oxidizer turbine, and (4) the oxidizer turbine discharge line returning to the main chamber injector.

An investigation of possible heat exchanger configurations has shown that the heat exchanger requirements, summarized in table XXVa, can best be met by locating a single heat exchanger in the oxidizer turbine supply/return line, shown schematically in figure 136 as the turbine discharge line. Table XXVb provides a summary of the GO_2 heat exchanger characteristics.

Table XXVa. Oxidizer Heat Exchanger Requirements

Requirement	Full Thrust (Oxidizer Tank Pressurization)	Pumped Idle (Oxidizer Tank Pressurization)	Tank Head Idle (Gaseous Injection Into Main Chamber)
Oxidizer Flowrate, kg/s (lb/sec)	0.061 (0.134)	0.041 (0.090)	0.037 (0.082)
Minimum Oxidizer Temperature Rise, °K (°R)	116 (208)	47 (84)	(vaporize oxidizer)
Minimum Oxidizer Inlet Temperature, °K (°R)	107 (192)	94 (169)	93 (168)
Minimum Oxidizer Inlet Pressure, N/cm^2 (psia)	2758 (4000)	108 (157)	13 (19)
Maximum Oxidizer Pressure Loss, N/cm^2 (psi)	14 (20)	7 (10)	6 (8)
Minimum Oxidizer Heat Pickup, joule/s (Btu/sec)	12,010 (11.40)	8720 (8.28)	7525 (7.15)
Maximum Fuel Flowrate, kg/s (lb/sec)	2.427 (5.351)	0.156 (0.345)	0.0124 (0.0274)
Maximum Fuel Pressure Loss, N/cm^2 (psi)	13.8 (20.0)	4.1 (6.0)	2.1 (3.0)

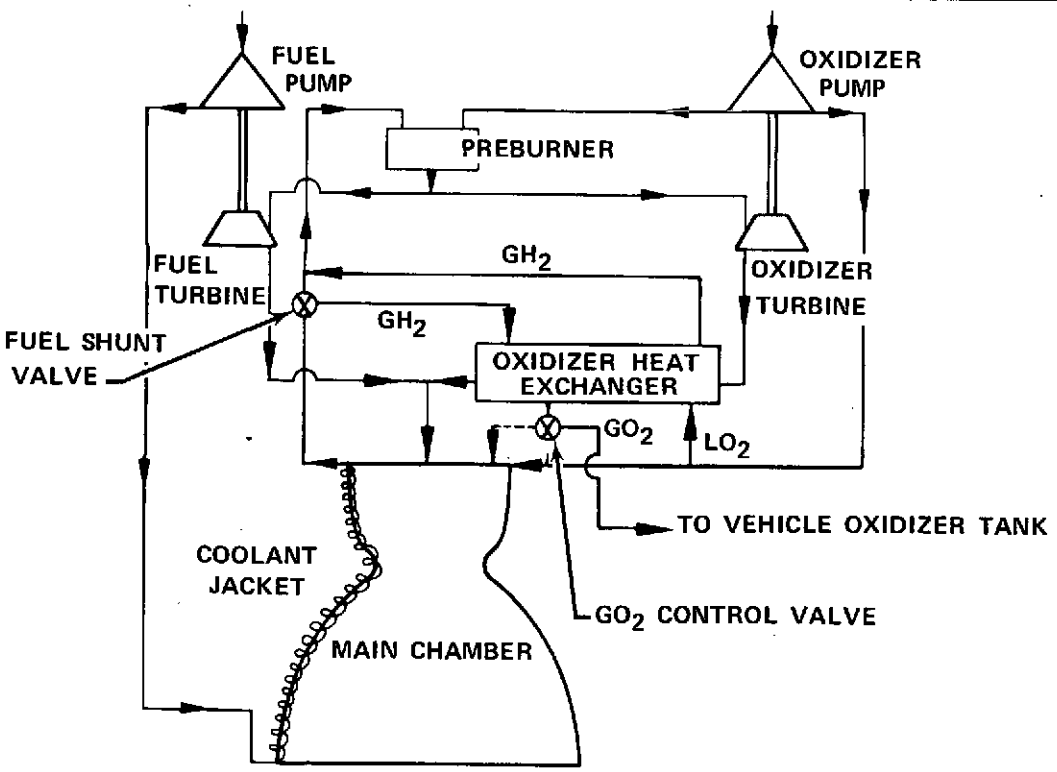

Figure 136. Single Oxidizer Heat Exchanger in Oxidizer Turbine Return Line

FD 68824

Table XXVb. Oxidizer Heat Exchanger Characteristics

Parameter	Full Thrust	Pumped Idle	Tank Head Idle
Thrust Chamber (Fuel) Coolant Flowrate, kg/s (lb/sec)	2.427 (5.351)	0.156 (0.345)	0.0124 (0.0274)
Thrust Chamber Coolant to Heat Exchanger and Elbows, %	20	20	100
Elbow Cooling Flowrate, kg/s (lb/sec)	0.147 (0.325)	0.0094 (0.0207)	0.0037 (0.0082)
Heat Exchanger Fuel Flowrate, kg/s (lb/sec)	0.342 (0.755)	0.022 (0.0483)	0.0087 (0.0192)
Heat Exchanger Oxidizer Flowrate, kg/s (lb/sec)	0.061 (0.134)	0.041 (0.090)	0.037 (0.082)
Oxidizer Inlet Temperature, °K (°R)	107 (192)	94 (169)	93 (168)
Oxidizer Temperature Rise, °K (°R)	128 (231)	49 (88)	36 (64)
Oxidizer Pressure Loss, N/cm^2 (psid)	<0.69 (<1)	<0.69 (<1)	0.76 (1.1)
Oxidizer Heat Pickup, joule/s (Btu/sec)	13,300 (12.60)	9,390 (8.88)	9,200 (8.70)
Fuel Inlet Temperature, °K (°R)	263 (474)	299 (538)	356 (640)
Fuel Exit Temperature, °K (°R)	330 (594)	273 (491)	283 (510)
Fuel Pressure Loss, N/cm^2 (psid)	9.66 (14.0)	0.97 (1.4)	1.52 (2.2)

The heat exchanger assembly procedure is as follows. (Refer to figure 137.)

Step

1. Resistance seam weld the fuel inlet and exit manifolds to the outer sleeve per spec PWA 15 (plus braze per spec PWA-S-2671 over 60% of the remaining area).

2. Insert each oxidizer tube (radial installation), then braze the tubes to the oxidizer inlet and exit manifolds and also to the fuel exit manifold per spec PWA-S-2671.

3. Insert the Berylco 10 core into the outer sleeve and braze to sleeve and the fuel inlet and exit manifolds per spec PWA 85 except use PWA 707 or AMS 4785 filler at 1200°K maximum - then cool as fast as possible.

4. Age assembly at 756° ± 8°K (1360° ± 15°R) for 3 hours.

5. Weld the fuel inlet and exit manifolds to the transition duct per spec PWA 16-2.

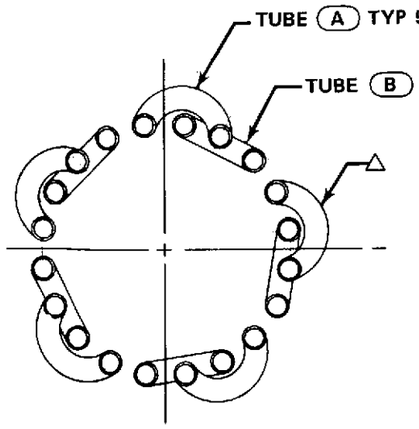

SECTION B-B
(SHOWING OXIDIZER
TUBES ONLY)

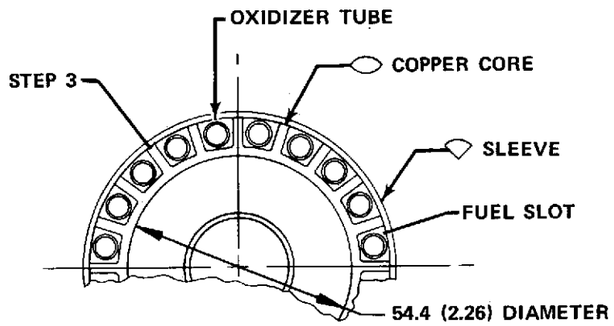

SECTION A-A

ASSEMBLY PROCEDURE (WELDING AND BRAZING SCHEDULE)

STEP NO.	DESCRIPTION
1	RESISTANCE SEAM WELD THE H_2 INLET EXIT MANIFOLDS TO THE OUTER SLEEVE PER PWA 15 PLUS BRAZE PER PWA-S-2671 OVER 60% OF REMAINING AREA
2	INSERT THE OXIDIZER TUBES AND BRAZE THEM TO THE H_2 EXIT MANIFOLD AND THE OXIDIZER INLET AND EXIT MANIFOLDS PER PWA-S-2671
3.	INSERT COPPER CORE INTO SLEEVE AND BRAZE TO SLEEVE AND H_2 INLET AND EXIT MANIFOLD PER PWA 85, EXCEPT USE PWA 707 OR AMS 4785 FILLER AT 1200°K (1700°F) MAXIMUM - COOL AS FAST AS POSSIBLE
4	AGE AT 755° ± 8°K (900 ± 15°F) FOR 3 hr
5	WELD H_2 INLET AND EXIT MANIFOLDS TO TRANSITION DUCT PER PWA 16-2
6	X-RAY SYSTEM

MATERIALS:
- ⬭ BERYLCO 10 (COPPER-BERYLLIUM)
- △ PWA 770 (347 SST)
- □ AMS 5646 (347 SST)
- ◇ AMS 5512 (347 SST)

DIMENSIONS IN mm (in.)

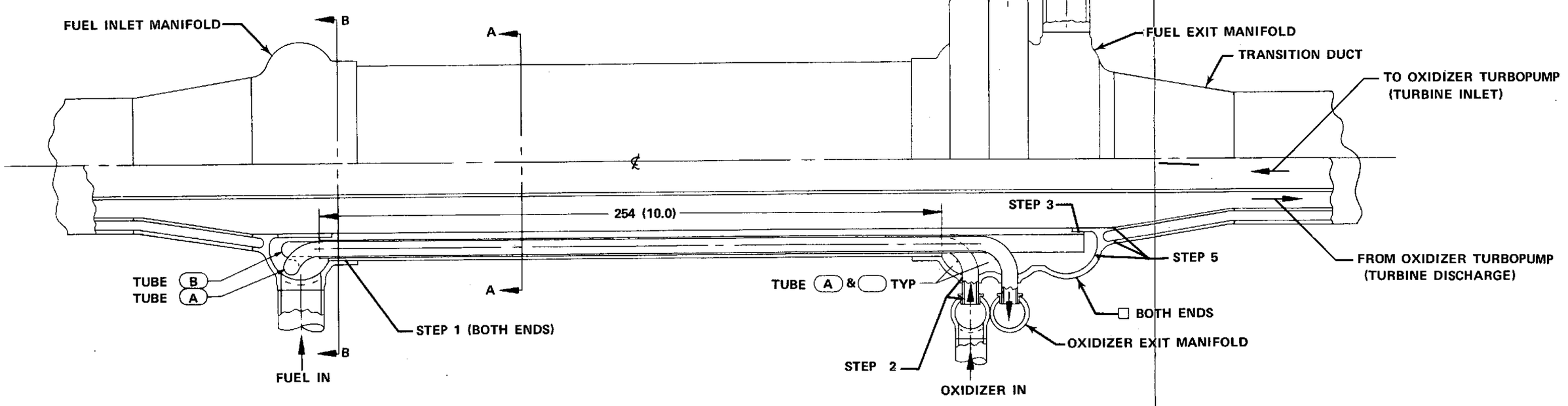

Figure 137. Oxidizer Heat Exchanger

FD 72481

The oxidizer turbine external line is easily accessible for interface connections to the vehicle. The primary advantage of this selection is the fact that one heat exchanger can satisfy the GO_2 requirements for both idle modes and full thrust operation. Investigation of location 1 in the regeneratively cooled thrust chamber discharge line, indicated the heat transfer surface area requirements at full thrust conditions were at least twice as large as those at pumped idle and tank head idle conditions (for fixed fuel and oxidizer flow areas). It was further found that if an auxiliary heat source were used to augment the heat transfer process at full thrust, a single heat exchanger could meet the requirements at all operating conditions. The high temperature oxidizer turbine discharge gases returning to the main case provide an auxiliary heat source at full thrust conditions.

The heat exchanger configuration selected (a combination tubular and sandwich design), figure 137 has a fuel-cooled hot gas return line with oxidizer tubes suspended in the fuel passages. During pumped idle and tank head idle operation, heat is transferred between the fuel in the passages and the oxidizer in the tubes; at full thrust, heat is transferred from the hot turbine gases to the fuel (by cooling the duct walls) and then to the oxidizer. The double-pass oxidizer flowpath minimizes the heat exchanger length, and the single-pass fuel flowpath minimizes the fuel pressure losses. Fuel obtained from the thrust chamber coolant discharge line and that flows in parallel with the fuel in the oxidizer heat exchanger, is used to cool the remainder of the hot gas return line, which includes the elbows upstream and downstream of the heat exchanger.

A fuel shunt valve is used to divert warm fuel through the GO_2 heat exchanger and elbows in the oxidizer turbine supply/return line. For tank head idle operation, the fuel shunt valve is actuated to divert all the chamber coolant jacket discharge flow to the GO_2 heat exchanger and elbows. The fuel shunt valve is repositioned for rated thrust and pumped idle to direct approximately 20% of the fuel to the GO_2 heat exchanger and elbows. A constant flow split of approximately 70%/30% for the diverted fuel flow is maintained between the GO_2 heat exchanger and elbows for all engine operating points.

c. Mechanical Description

The heat exchanger configuration (figure 137) consists of (1) a THERMAL SKIN® or inner core with 20 milled passages, (2) ten double-pass oxidizer tubes, and (3) an outer structure plus manifolds.

The materials selected for the heat exchanger are Copper-Beryllium (Berylco 10) for the THERMAL SKIN or core and 347 SST for the oxidizer tubes and outer structure. Berylco 10 was chosen because of its high conductivity and good strength capabilities; 347 SST was chosen because of its relatively close coefficient of expansion to Berylco 10, thus lessening thermal differences.

A thermal analysis was conducted on the heat exchanger to ensure the integrity of all the braze joints caused by shrinkage of the 347 SST oxidizer tubes and the differential growths between the Berylco 10 core and the 347 SST outer structure. All braze joints stresses were designed to be less than 10,340 N/cm^2 (15,000 psi) as prescribed by P&WA design practice.

The design of the heat exchanger manifolds prevents any oxidizer to fuel leakage. Mixing of the oxidizer and fuel can occur only if an oxidizer tube has a structural failure. All oxidizer tube braze joints are located so that if a leak occurs because of a braze failure, the oxidizer will flow into the engine compartment.

To prevent the tubes from vibrating inside the Berylco 10 core, the tubes are shaped in such a manner as to make contact at one place along each core passage. A shaped tube will remain snug against the core to prevent tube chatter. Weld spots on the tubes were also considered as an antivibration scheme but weld spots, if they become worn, lose their effectiveness and could cause damage to the Berylco 10 core.

8. Controls and Valves

a. General

The control study objective for the Advanced Space Engine design was to define a system that achieved a satisfactory balance between engine capability and control system complexity. Because control system weight becomes an increasingly larger percentage of total engine weight as engine thrust size decreases, emphasis was placed on minimizing control system complexity.

The engine preliminary design incorporates a failsafe control system that will shut the engine down in a safe manner in the event of a component malfunction, or if an engine limiting parameter (such as preburner temperature), cannot be contained within an acceptable limit.

An engine control concept was established and the preliminary logic for start, shutdown, steady-state operation, mode change, and mixture ratio variation was generated. Component designs were defined for the required valves, the control unit, ignition systems, and sensors. The concept and components are described in the following paragraphs.

b. Control System Concept and Operation

(1) Approach

(a) Control Unit

In view of the requirements for engine mode change and mixture ratio variation by electrical signal within specified ranges, and for avoidance of user-monitored red line parameters for safe operation, use of an electronic command unit to monitor and control parameters is dictated for the ASE.

As a control unit, an analog computer provides output control signals that are essentially real time functions of appropriate input signals and offer the highest overall control response to process changes. However, this approach requires separate electrical circuits to accomplish each required function and results in a relatively high part count in an application of medium control complexity. More significant is the fact that each electrical component in a given functional implementation from input to output contributes an error to the output signal. This limits the potential precision of an analog control, particularly if the environmental temperature range is broad.

The accuracy limitations of an analog can be avoided with only slight sacrifice in response by using a discrete controller. This approach relies upon discrete or digital parts such as counters, comparators, and adders to accomplish the required functions and perform desired computations with discrete signals, pulse trains, and pulse widths, but without using permanent storage devices. This approach still produces a relatively high part count since there is no time-sharing of hardware.

With a further sacrifice in response, a stored program digital computer can be used thus enhancing accuracy since computations are performed with discrete on-off signals. It also minimizes the part count because algorithms are computed sequentially with common hardware. Flexibility is greatly improved because major changes in input/output relationships can be made by altering the memory contents of identical parts rather than revising and reconfiguring circuits. Conventional digital computing speeds (1-5 μsec per computation) are sufficiently high that sequential computations can be made and each output updated on the order of every 10 to 20 milliseconds, which is a response limitation that can be accepted. Therefore, the stored program digital computer approach was selected to satisfy the ASE control requirement. It offers the highest precision and greatest flexibility with minimum hardware and acceptable response.

(b) Control Points

The basic engine operating variables of thrust and mixture ratio can be controlled in the staged combustion cycle in turbine power and/or pump load control modes. Turbine power is a function of preburner flow, preburner mixture ratio (turbine inlet temperature), turbine inlet and exit pressures, and turbine areas. Any control point that influences these parameters has a direct affect on power. Pump load control can be effected by either pump recirculation or pump throttling.

Turbine throttling or bypass to vary pressure ratio or flowrate would provide control, but would necessitate the use of valves in hot gas streams, which would compromise valve durability. Variable turbine areas are another approach, but the required complexity is not consistent with current technology. The most suitable method is to control turbine inlet temperature through preburner oxidizer flow, which can be accomplished by using a cryogenic valve, and therefore is well within the current state-of-the-art.

With a parallel turbine, single preburner arrangement, turbine power control through the preburner establishes only total propellant pumping capability. Pump load control is required to achieve mixture ratio control. The alternatives here are recirculation or throttling. Recirculation of any significant flowrate is not practical, so throttling is the obvious choice.

The scope of the ASE design effort did not permit in-depth study of control point locations. However, studies of staged combustion engine control requirements had been conducted in considerable depth by P&WA in the AEB and XLR129 programs, References 13 and 23.

Results of these studies were directly applicable in view of the fact that the engine systems differed basically only in the main thrust chamber cooling method. The earlier engines were transpiration-cooled whereas the ASE is regeneratively cooled. As this difference does not have a significant influence on controls, the control point locations established for throttling valves were the same as in the

AEB study: an oxidizer valve in the line downstream of the high pressure pump discharge and a fuel valve in the line between the 2nd-stage fuel pump discharge and the inlet manifold of the thrust chamber regenerative cooling jacket.

(2) Control Logic

Closed cycle rocket engine systems such as the RL10, XLR129, OOS and ASE produce a stable thrust level with fixed valve areas. Open-loop time scheduling of valves is thus acceptable for safe engine start and shutdown, stable steady-state operation, and transients from one operating condition to another. However, because of possible variations in engine inlet conditions or minor changes in hardware as the thermal environment changes, it is necessary to supplement the open loop/time sequence scheduled with closed loop trim control using engine parameter sensors to achieve high precision. A protective trim capability is also necessary for engine safety. For these reasons, two levels of control logic are employed, i.e., open loop/time sequence scheduling and closed loop supervisory and protective trimming.

The extent of closed loop trim precision and engine protection provided significantly affects the complexity and weight of the digital electronic control unit and the number of sensors required. Initially, systems of two different levels of complexity were studied. In the first, supervisory precision trim was provided for both thrust and mixture ratio, and a relatively large number of engine parameters were sensed for protective trim, resulting in 33 sensed inputs, 26 of which were duplicated for redundancy. The computer for this system required a 6000-word memory. Based on the reasoning that mixture ratio control was required for propellant utilization, (Space Tug PU system 3σ precision specified as $\pm 0.25\%$), and therefore the loop should be closed through the vehicle PU system, it was felt that a system with only thrust trim might be satisfactory. With only one precision trim and judicious reduction in the number of protective trims, input senses were reduced to 12, with 5 redundant, which meant that the memory requirement could be reduced to approximately 2000 words, reducing the control unit weight. The single precision trim approach was recommended for ASE design.

(3) System Configuration

(a) Control Requirements

A preliminary control schematic for the ASE is presented in figure 138. The engine electronic control acts in response to commands from the vehicle system for start, mixture ratio variation, and shutdown.

Control of the P&WA ASE is accomplished with eight valves. A schematic showing the locations of the valves used on the engine is provided in figure 139. Shutoff of engine propellants is accomplished by fuel and oxidizer inlet (suction) valves. A fuel valve (cavitating venturi), a main oxidizer valve, and a preburner oxidizer valve provide propellant control during full thrust operation. A GO_2 control valve, a fuel bypass valve, and a fuel shunt valve complete the control system necessary for idle mode operation and tank pressurization requirements. Transient analysis of the tank head idle mode of operation has shown a need for closed loop control of the GO_2 valve during this mode, to maintain mixture ratio within acceptable limits. The valve position will be varied to change oxidizer flowrate, if excessive fuel temperature at the discharge of the thrust chamber coolant jacket is indicated.

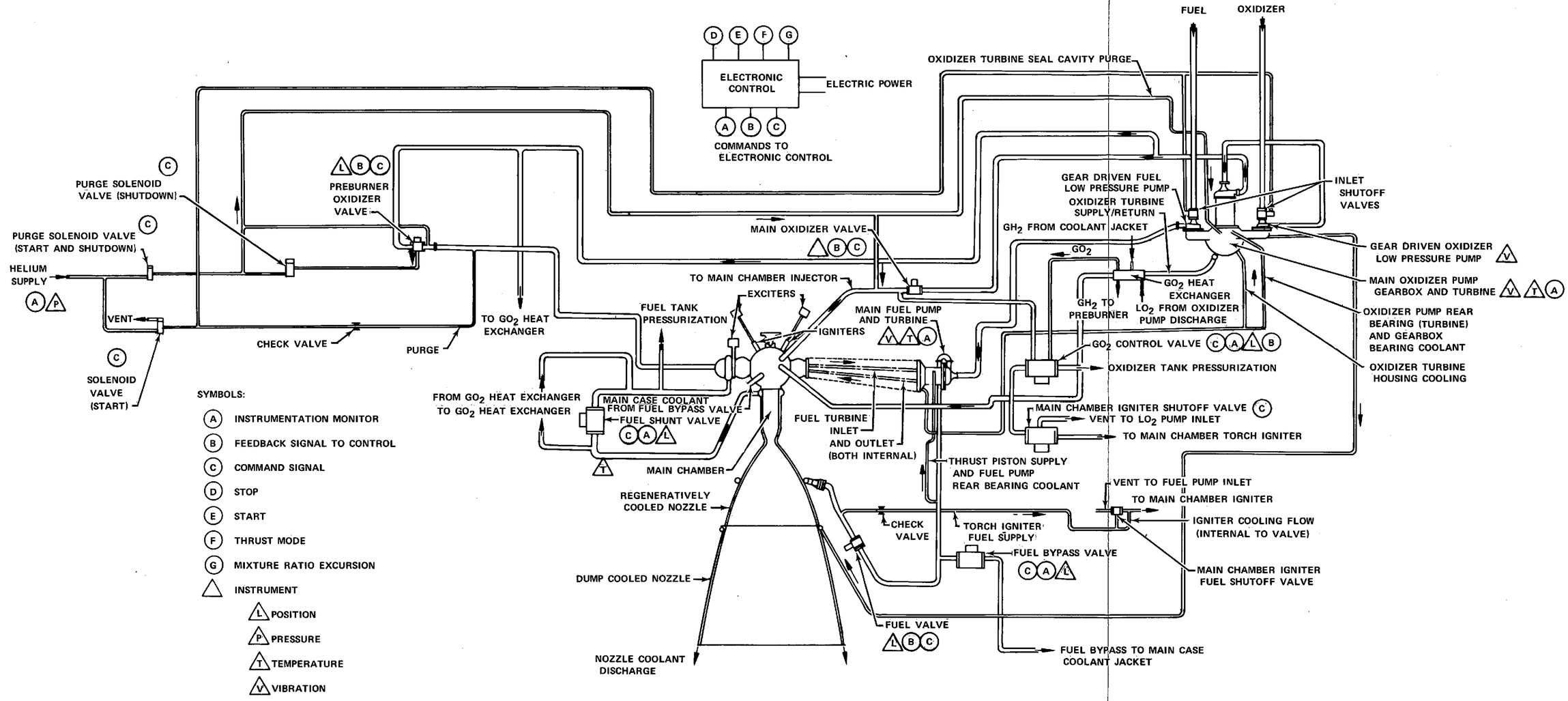

Figure 138. ASE Preliminary Control Schematic

FOLDOUT FRAME 1

FOLDOUT FRAME 2

FOLDOUT FRAME 3

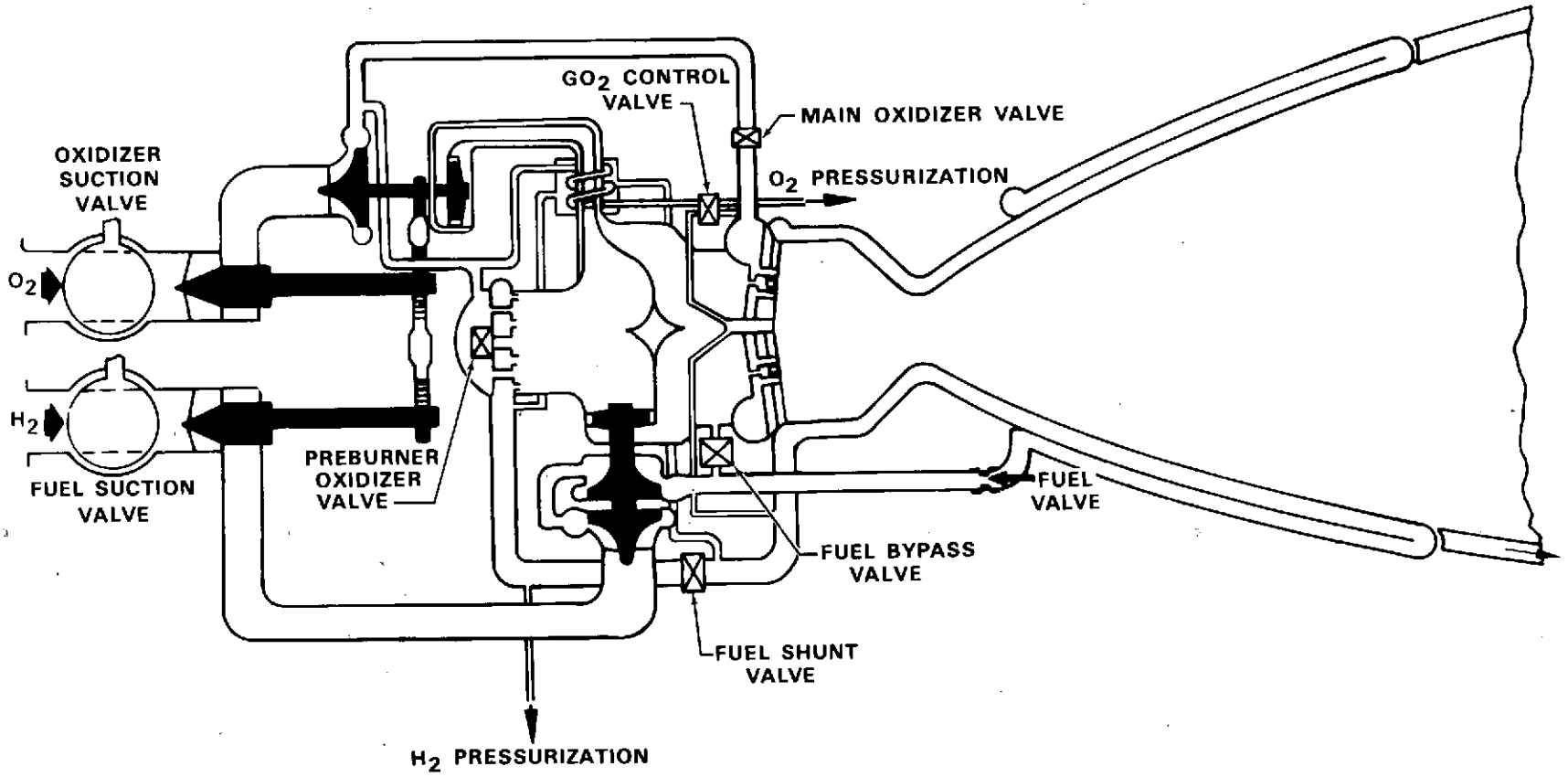

Figure 139. Advanced Space Engine Control Locations

FD 71369

The ASE valves are controlled by three commands from the vehicle - start/stop, PU, and operating mode selection (tank head idle, pumped idle, and mainstage). The ASE control provides precise thrust control over the specified range of mixture ratio and inlet conditions. The control can compensate for anticipated engine component variability and also includes protective overrides to provide additional engine life margin.

Thrust and mixture ratio are set by using two levels of control (figure 140). The first level consists of basic schedules that set predetermined valve positions in accordance with nominal schedules of valve areas. These basic schedules safely provide thrust and mixture ratio without dependence upon engine sensors. The second level is a supervisory trim of valve areas to obtain more precisely thrust based on sensed chamber pressure. Mixture ratio trim is obtained by adjustment of the mixture ratio input by the vehicle PU signal. In addition, there is a protective limit of valve areas to protect the engine by preventing it from exceeding mechanical limits. The protective limit provides additional engine safety by limiting maximum valve areas when unexpected component deterioration causes engine operation near design limits. Whenever a design limit is approached, protective trim limits supervisory trim as required to preclude exceeding engine limits. Six engine parameters are monitored for malfunctions to provide vehicle protection - vibration sensors for the four pumps, turbine inlet temperature and chamber pressure. The threshold levels of these malfunction detection parameters are set high to protect against a complete vehicle/engine failure only. In the event a malfunction is detected, action is taken to step engine operation down to the next safe level of operation. Therefore, only catastrophic engine malfunctions will abort the mission to save the vehicle. During start and shutdown transients, the control's basic schedules (figure 141) are time-based and the schedules are extended to cover the envelope of transient operation. Before the engine can be started the control must be in a ready condition. This ready condition is given after the control self check has been completed (figure 142). The engine can then be started by the issuance of the three vehicle commands - mode selection, PU, and start signal.

The supervisory trim system for thrust at steady state is a main chamber pressure control loop as shown in figure 143. The electronic control receives chamber pressure requests and measured chamber pressure signals. An error is calculated and integrated to produce the parameter trim. Each of the three valves trim to eliminate chamber pressure error and to maintain mixture ratio when trimming thrust. Stability with no overshoot is maintained by using conservatively sized trim gains. Unlike the supervisory trim, the protective trim or limit monitors are in effect from start to 100% during both steady-state and transient operation (figure 144).

Sensor redundancy is provided for the supervisory trim parameter to preclude engine shutdown or overtrim because of a sensor failure. For a second sensor failure, the control removes closed loop supervisory trim, schedules valve areas based on the predetermined open loop time sequence schedules, and requests a safe, middle mixture ratio of 6.0.

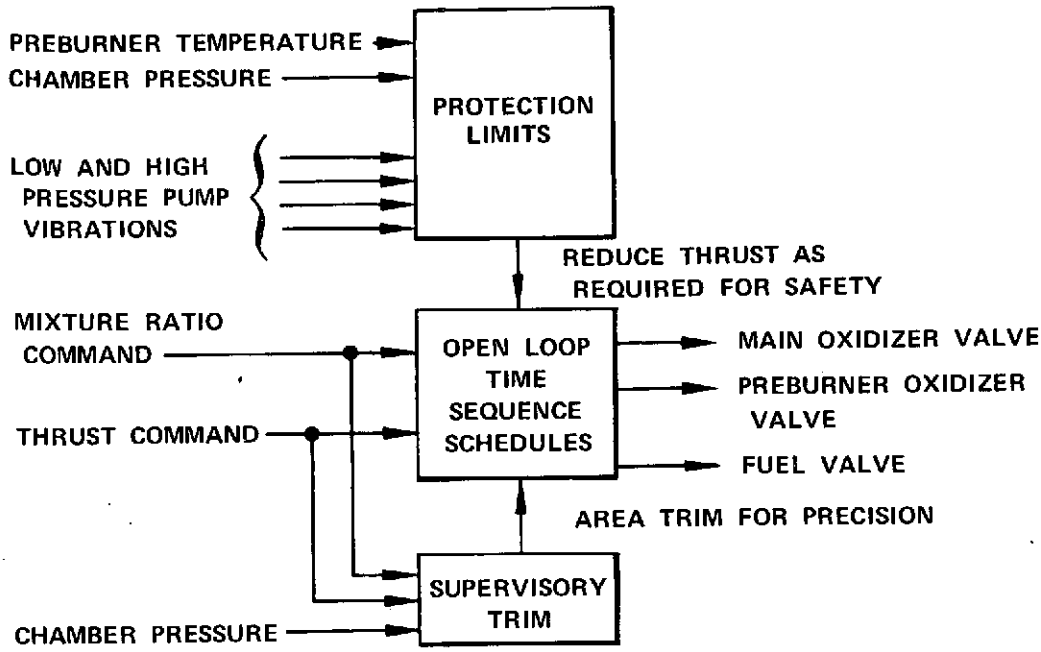

Figure 140. Advanced Space Engine Electronic Control Basic Block Diagram FD 68834

As noted previously, open loop scheduling of mixture ratio was selected in the interest of weight saving. Mixture ratio changes are thus effected by the changes in valve position based on schedules in the control computer. Open-loop precision estimates indicate that a mixture ratio precision of ±3.1% within the range of 5.5 to 6.5 at full thrust might be attainable in the ASE by sensing valve areas (position) and chamber pressure only.

(b) Failsafe Provisions

If a protective loop limit cannot be satisfied by engine power reduction (throttling), the electronic control unit will remove power from the control point actuators. With the exception of the fuel cavitating venturi, the control point valves are designed to failsafe under hydraulic or spring load. The main chamber butterfly valve normal mode of failure under hydraulic load is closed. The cavitating venturi is designed to fail open so that a cool, fuel rich shutdown will be achieved.

To complete the failsafe shutdown, the preburner oxidizer valve is spring-loaded closed. The inlet valves are also spring-loaded and will close when power is removed from the prestart solenoid valve. By orificing the helium supply line to the fuel inlet valve actuator, the fuel inlet valve closing will lag the oxidizer inlet valve, assuring that fuel will flow into the system until the oxidizer is depleted.

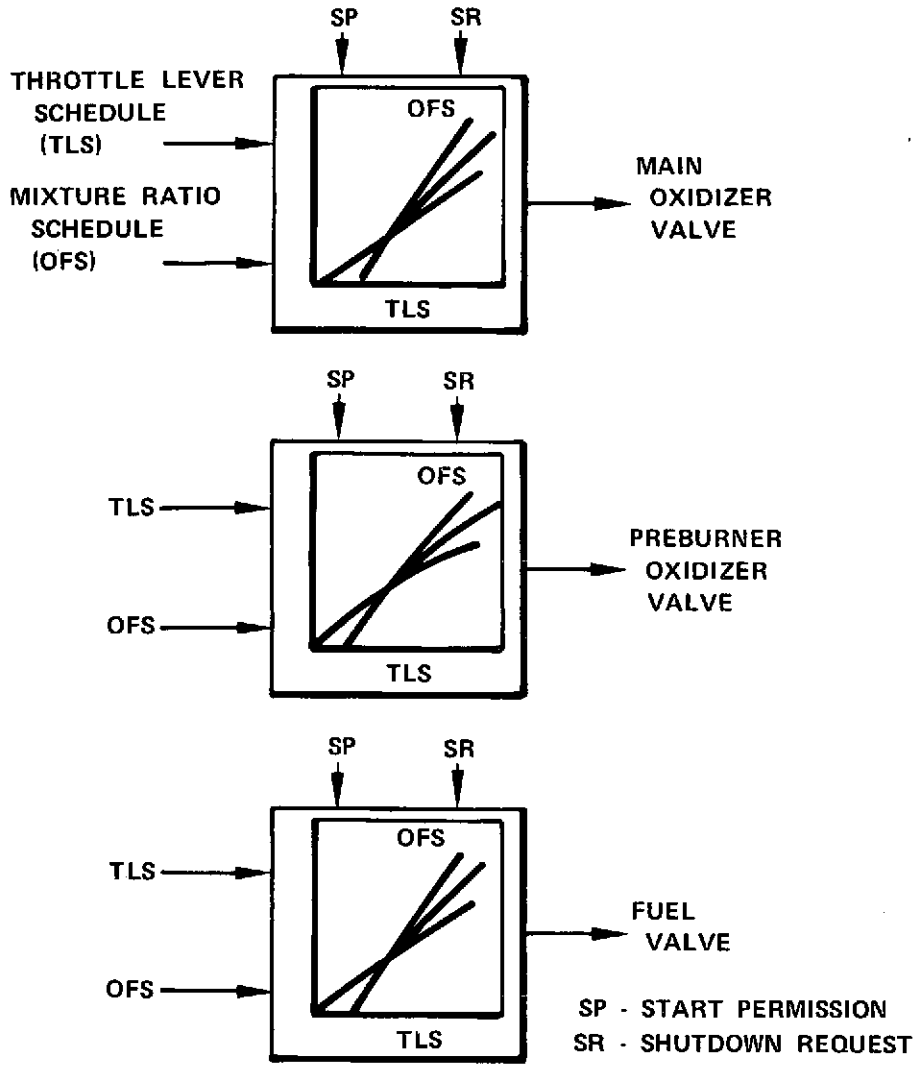

Figure 141. Electronic Control Unit Time Sequence Open Loop Valve Schedules

FD 68833

c. Components

(1) Electronic Control Unit

The electronic control unit (ECU) is an engine-mounted digital electronic control computer that controls the ASE system. Analog engine sensors provide signals representing the key engine parameters, and these signals are carried to the ECU over an engine harness in analog form. The ECU input analog circuits condition these signals, and analog-to-digital converters digitize them for use in the computer program. Multiplex circuits are used to allow signal conditioners and digitizers to process signals from a number of sensors in sequential order to reduce hardware requirements in the interface signal processing section.

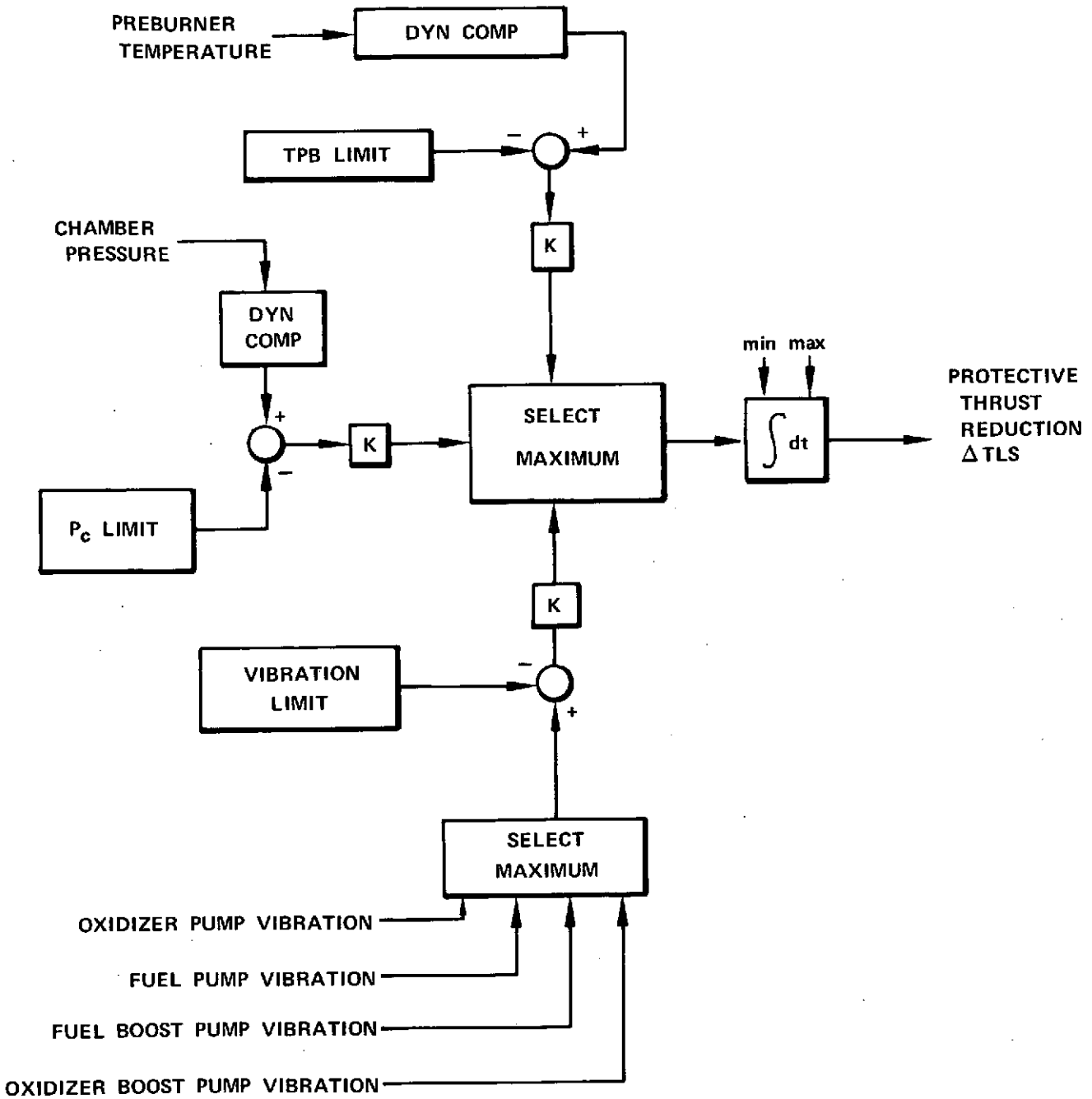

Figure 142. Electronic Control Unit Self-Check and Vehicle Command Logic

FD 68835

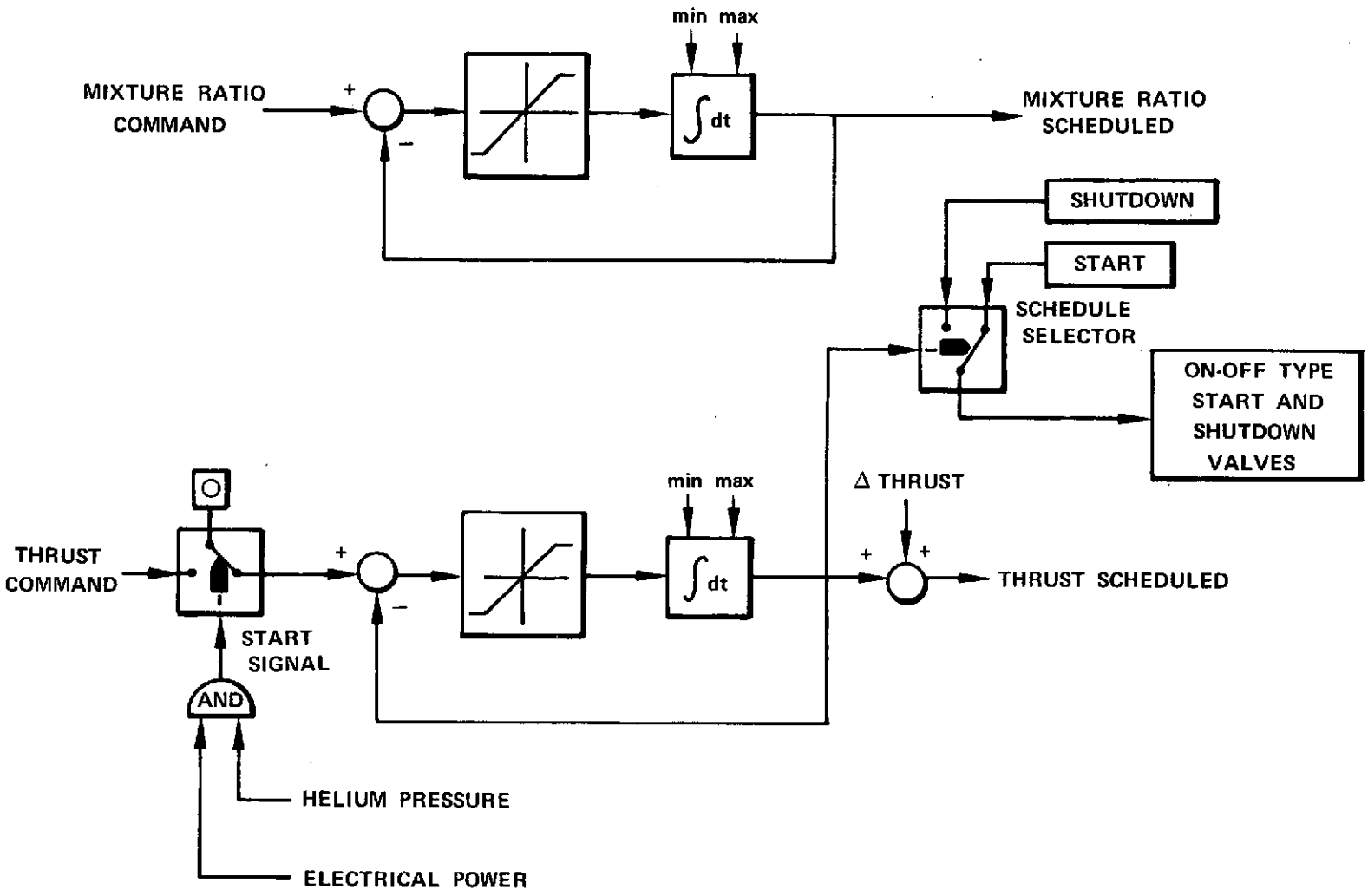

Figure 143. Closed Loop Thrust Control Block Diagram

FD 68832

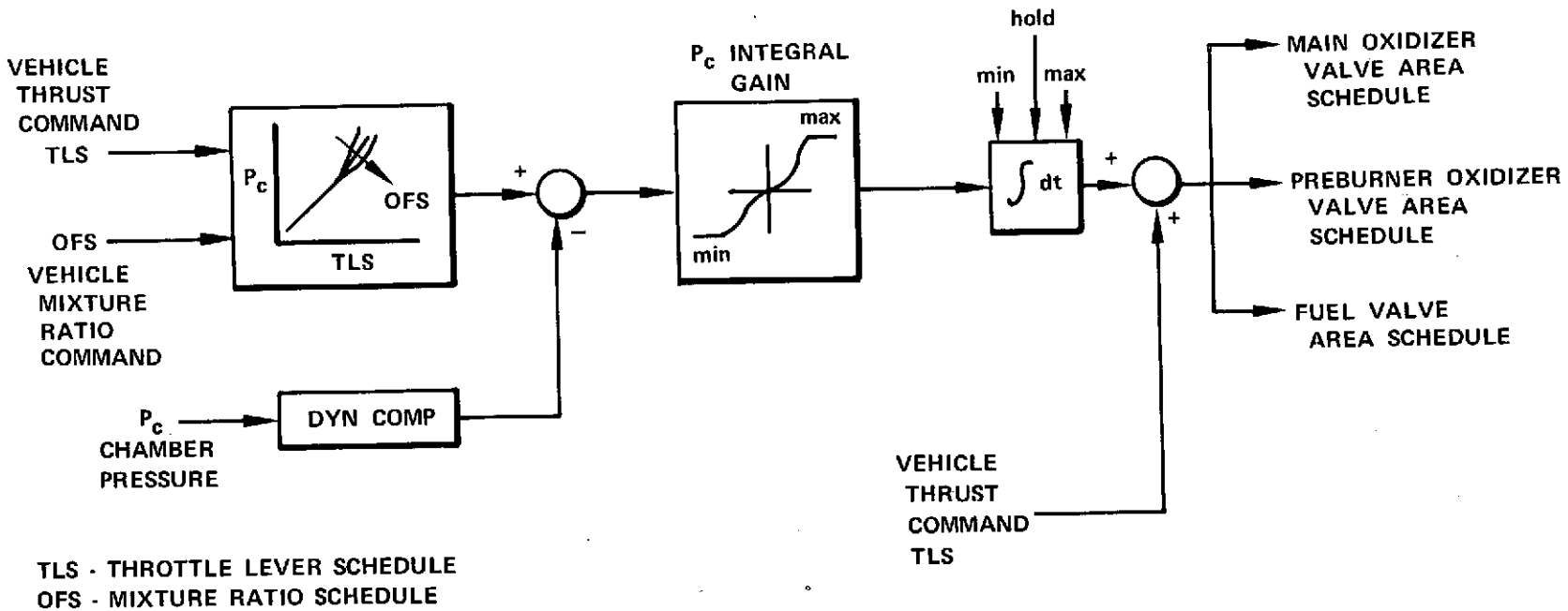

FD 68831

Figure 144. Closed Loop Protective Trim Monitor Block Diagram

The control and arithmetic operations that make up the engine commands logic are carried out in a general purpose, stored-program central processing unit (CPU). This CPU is the heart of the ECU and provides control over the memory, the input multiplexers, and the output circuits. The CPU is constructed of medium scale integrated circuit transistor logic (TTL) elements.

The stored program is implemented in a programable read-only memory. This memory provides maximum flexibility to accommodate engine ground trim and control modifications.

The programable memory contains the control and checkout programs and all the tables and constants needed by the control program. A random access read/write memory is provided to store the intermediary values of arithmetic calculations. This scratch pad memory allows the ECU to keep track of timing and short-term storage of data. The solid-state memory devices used in the scratch pad memory are compatible with the TTL logic of the CPU.

A diagram showing the inputs required by the ECU and its outputs is given in figure 145. Table XXVI lists required control senses. The vehicle sends the start, mode, mixture ratio, and shutdown commands required to govern operation of the system to the engine via a data bus. The engine reports to the vehicle, on a separate bus, the key engine parameters required for performance analysis, as well as failure information on the control system components. This information is available for recording on the vehicle data recording system to provide maintenance information at the completion of the mission.

The ECU controls the engine by positioning the engine propellant and pressurant valves in accordance with the stored valve schedules and the closed loop trims, which are derived from the sensed engine parameters. The position outputs from the ECU digital program are processed by the output drivers. These output circuits contain power switching elements that energize magnetic coils, which move the valve stepper motor, actuators, and solenoids. The modulating valves located at the engine control points provide continuous potentiometer feedback of valve position, closed loop.

The ECU provides for switching power to the preburner and main chamber ignition systems. Ignition is automatically energized at the proper time during the engine start sequence, and no vehicle monitoring or control of ignition is required.

Power is supplied to the ECU from the vehicle power system on two power buses. Electrical power of 28 vdc is required to operate the computer and its associated sensors and outputs, as well as an electrical heater. The ECU has a diode-isolated power selector logic that allows the control to operate if either power bus is energized. Isolation is maintained between the two buses to protect the vehicle power management system. Fusing resistors are used in each leg of the power input lines to isolate the vehicle from failures in the ECU which might otherwise affect other systems sharing that bus. To provide protection from very low orbital temperatures, an internal electrical heater is provided. The heater is not actively switched by the ECU and requires vehicle power to be supplied when its operation is required.

For the preliminary design, a lightweight approach with the circuit components of the ECU mounted on multilayer printed circuit boards was assumed.

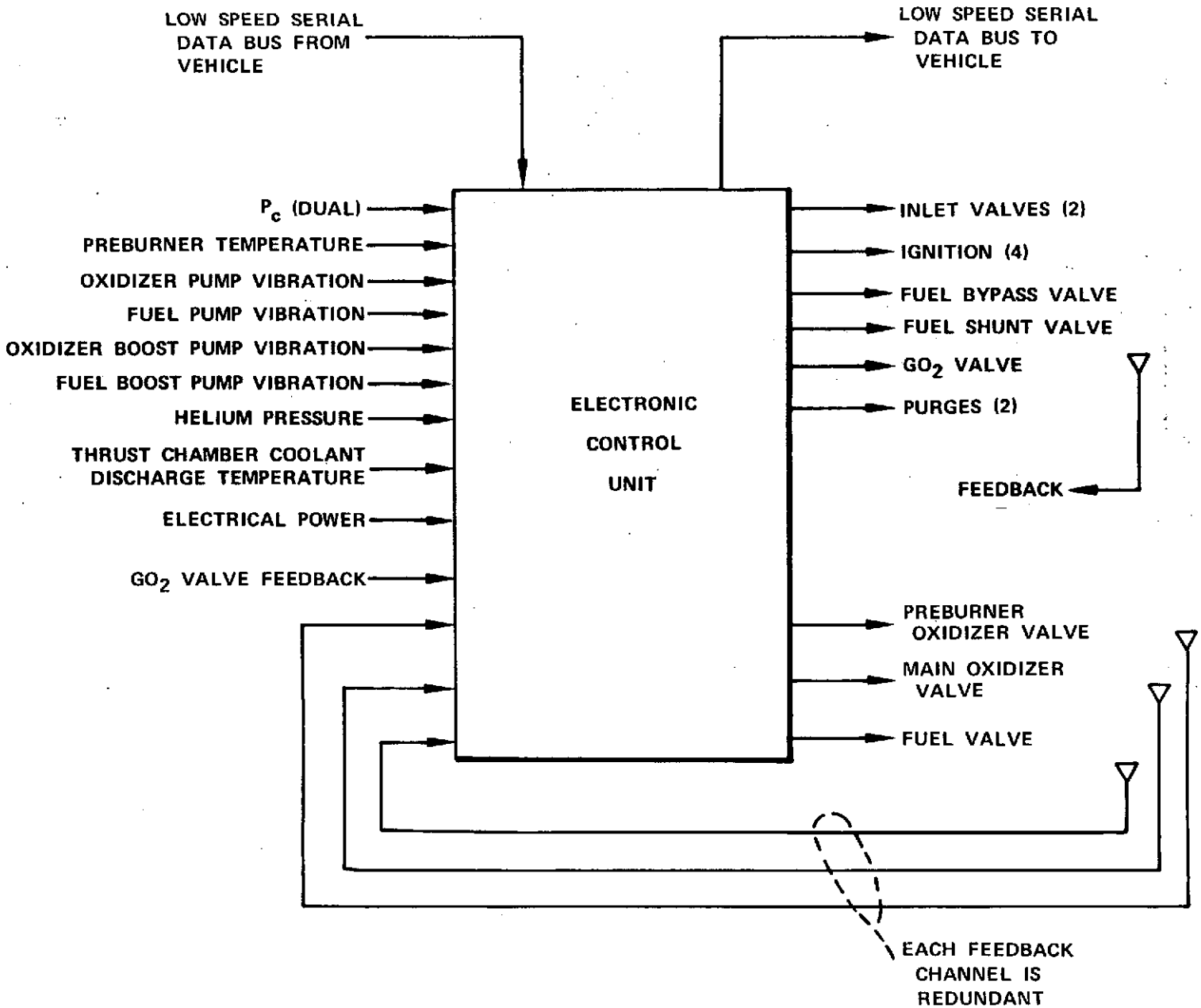

Figure 145. Engine Control Unit Input - Output Data

FD 68830

Table XXVI. Control Senses Required

Required Sense	No. Sensors
Main Chamber Pressure	2 (Averaged)
Preburner Temperature	1*
Helium Supply Pressure	1
High Pressure Oxidizer Pump Vibration	1
High Pressure Fuel Pump Vibration	1
Main Oxidizer Valve Position	2 (Averaged)
Fuel Venturi Valve Position	2 (Averaged)
Preburner Oxidizer Valve Position	2 (Averaged)
Fuel Boost Pump Vibration	1
Oxidizer Boost Pump Vibration	1
Thrust Chamber Coolant Jacket Discharge Temperature	1
GO_2 Valve Position	2 (Averaged)

*4 Thermocouple junctions in the sensor.

The circuit boards would be assembled in large frames, with an aluminum gridwork over each card to pick up the heat dissipated by each circuit element and carry it out to surrounding framerails. The frames would be stacked vertically, and be hinged along one edge so that the stack could be opened like the pages of a book to allow access without disassembling the unit. Flexible etched-circuit wiring, strain-relieved at each end, would be used from frame-to-frame and to the input/output connectors. The outer case would be formed of channel corrugated cold wall aluminum panels, rigidly mounted to the engine case. An aspirator valve would maintain a $\pm$ 1.4 N/cm^2 (2 psid) maximum pressure differential between the interior and exterior of the ECU. A sketch of the type of unit envisioned is shown in figure 146. Ten electrical harnesses connect the ECU to the:

- Vehicle Data Buses
- Vehicle Power Buses
- Engine Sensors
- Engine Solenoid Valves
- Ignition System
- Control Valve Actuators.

(2) Control Valve Actuators

(a) Modulating Valve

Four modulating valves are required to control the thrust and mixture ratio of the ASE. The actuators position the valves according to a schedule demanded by the electronic control unit (ECU) and hold them in response to the pulse train signal. Since accurate control of actuator position is necessary, the use of pneumatic or hydraulic actuation is not practical. Electrical actuators are suitable and compatible with the ECU output. The actuators chosen for use in modulating valves are four-phase, permanent magnet, inductor stepping motors that directly convert digital pulse inputs to analogous shaft motion.

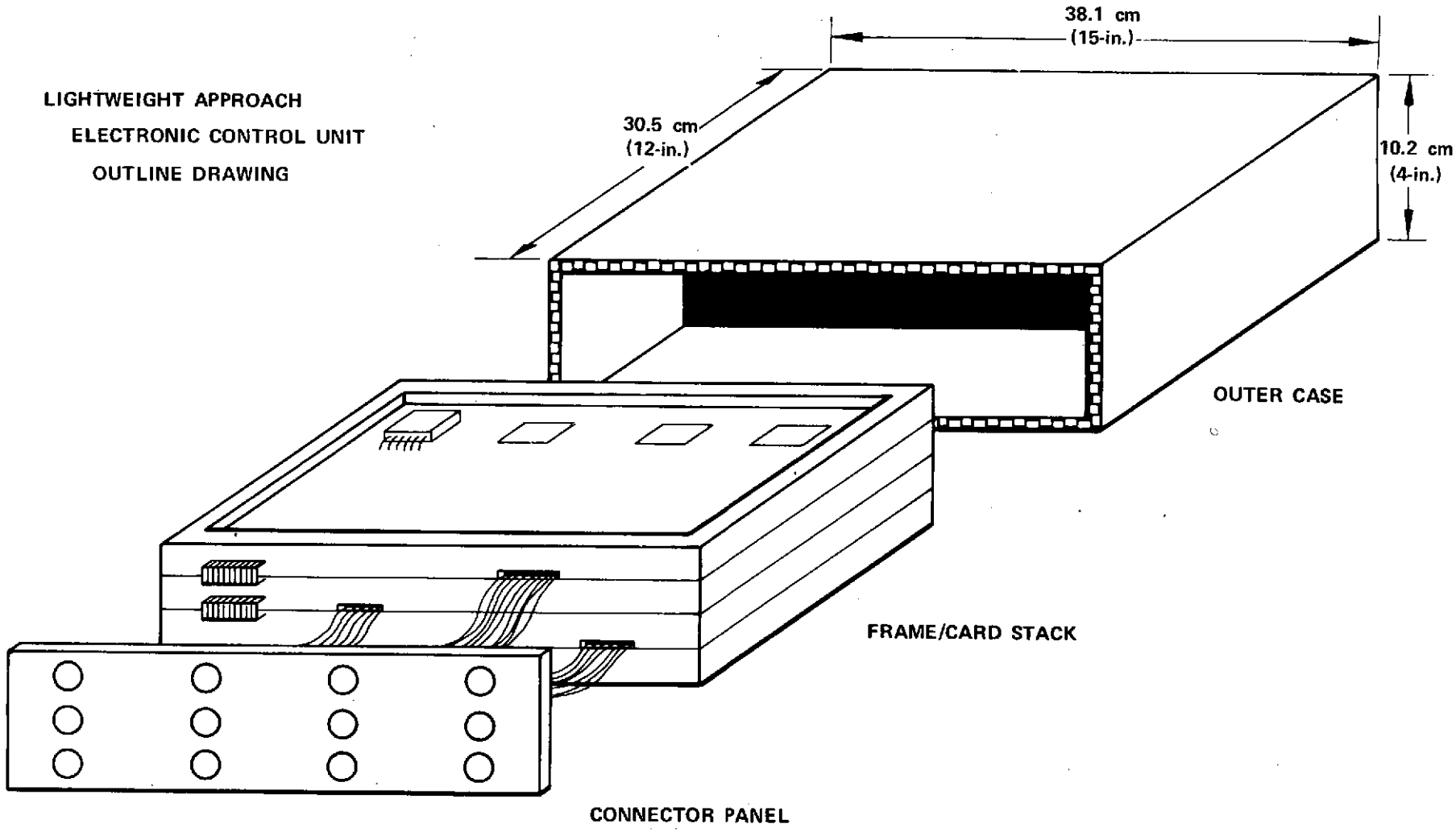

Figure 146. Conceptual Design of ECU for the Advanced Space Engine

FD 68829

By using planetary gear trains of various ratios for each valve, commercially available stepper motors can be used to satisfy the response and actuation force of each valve. Four stepper motors will satisfy all modulation requirements by using speeds of 31.4 mrad (1.8 deg) per step at a rate of 400 steps/sec.

The gear ratios selected for the valves and resulting times for the valves to slew (traverse their full range) with this actuation are summarized in table XXVII. The table shows valve response, or the reciprocal of the time required for one cycle of valve travel over ±3% of its range, which was assumed to be the area variation necessary to control a system perturbation. The response values are considered acceptable based on typical requirements determined in other staged combustion engine studies.

Table XXVII. 89 kN (20,000 lb) Thrust Engine Control Valves With Stepper Motor Actuators

	Main Oxidizer Valve	Preburner Oxidizer Valve	Fuel (Cavitating Venturi) Valve
Gear Reduction	9.95:1	8.0:1	13.3:1
Valve Movement Rate	1.26 rad/s (72.4 deg/sec)	1.98 cm/s (0.786 in./sec)	2.38 cm/s (0.942 in./sec)
Valve Operating Range	0.698 rad (40 deg)	0.88 cm (0.350 in.)	3.17 cm (1.250 in.)*
Time to Slew, sec	0.553	0.440	1.330
Time to Cycle, to 3% of Range, sec	0.105	0.083	0.250
Response, Hz	9.5	12.0	4.0

*Modulation required for only 0.38 cm (0.150 in.) of stroke. Remainder of stroke is used for extracting pintle.

Planetary gear trains present a few problems. One is lubrication, which is necessary even though the gear speed is low. Based on RL10 experience, the dry lubricant molybdenum disulfide with antimony oxide in a silicone bonder (PWA 550) will provide over 10-hr life. Another problem is gear train backlash, which will be present regardless of how close gear tolerances are maintained. Compensating for backlash on the modulating valves is accomplished by incorporating closed loop position indicators on the moving element to maintain accurate control of valve position. Additionally, gear trains for valves without a force reversal mode will be preloaded in one direction.

(b) Two-Position Valves

Four engine valves are of the two-position type. The function of these valves is to shut off flow or act as flow directors to one of two outlets. With the

exception of the two inlet suction valves, all these valves are deenergized during full thrust operation. However, should actuation power fail, the inlet valves fail closed.

The source of actuation power for the two-position valves are pneumatic pistons powered by helium. The rate of valve opening is controlled by using an orifice to set helium flow. Piston sealing is accomplished by use of a lip seal as shown in figure 147. The actuator is equipped with a return spring to ensure closing when the helium pressure is removed. Nominal helium pressure is 517 N/cm^2 (750 psi), but the actuators are sized to open the valves when the pressure is greater than 207 N/cm^2 (300 psi), which yields a safety factor of 310 N/cm^2 (450 psi).

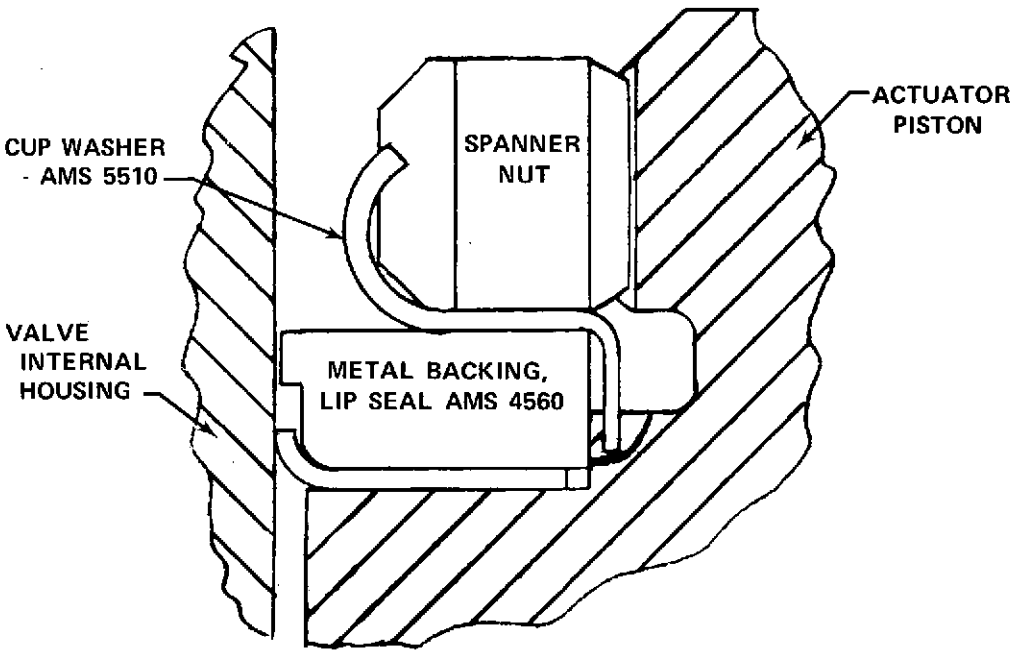

Figure 147. Valve Actuator Seal FD 72496

(3) Valve Mechanical Description

(a) General

The particular type of valve selected for each application depends upon the control requirements and cycle allowances. Table XXVIII is a comparative valve evaluation for different valve types. Poppet and ball valves are two-position only. The poppet valve requires elaborate contouring for precision flow control during modulation and the ball valve requires sealing of the valve housing with no vent during shutoff.

Static sealing in all valves is accomplished by the use of toroidal segment or inverted "C" seals. This type seal, along with nine other seals, was extensively tested under the XLR129 program. The Inconel X-750 toroidal segment was found to be the only seal to meet a maximum leakage limit of 0.01 sccs (Reference 24).

Table XXVIII. Control Valve Evaluation

Valve Type	Advantages	Disadvantages
Ball	Minimum pressure loss, simple seals, provide positive shutoff, low actuation force, low response time	High seal wear if drag type, not used on valves less than 2.54 cm (1.0 in.)
Pintle	Provides positive shutoff, good modulation, low percent leakage if no shutoff provision	Restricted to small changes in area, may require force balance, physically large
Butterfly	Good midrange control of area for 20:1 turndown ratio, compact, small actuation forces	Shutoff not positive unless liftoff seals used, high pressure loss
Poppet	Simple, two-position use, minimum seal wear, short stroke, positive shutoff, can use two poppets on one shaft for flow direction, small	Requires contouring for modulation, high pressure losses

The shaft seals are lip seals made of Kapton-F Polyimide/FEB Teflon laminations and Fep Teflon laminations (Reference 24, page VII 14-35). Substantiation of this type seal was concluded from the XLR129 test program. These test results indicated that seal leakages did not exceed 0.37 sccs after 10,000 shaft cycles with pressures up to 4137 N/cm^2 (6000 psig). A typical shaft seal configuration is shown in figure 148. Small high pressure fittings used on the valves are of the dynatube type as described in paragraph E.9, Plumbing.

Material selection for the valves is an important consideration. Inconel 718 is the material selected for valves operating in a cryogenic environment. Substantiation of this valve material is based on XLR129 experience. Titanium (AMS 4972) was selected for construction of one valve (cavitating venturi) for purposes of weight reduction.

Because of hydrogen embrittlement, titanium or Inconel 718 cannot be used in hydrogen above cryogenic temperatures. The material selected to operate in the aforementioned conditions is A-286 stainless steel.

(b) Inlet Valves

The inlet suction valves are ball, two-position, helium-actuated valves. The valves mount directly on the boost pumps and interface with the vehicle propellant lines. The difference between the fuel and oxidizer valves is the bore diameter of the ball. A common ball, seals, and surrounding housing design is a possibility if the inlet size of the pumps is standardized. The valves are actuated to start propellant flow to the engine and remain open during the entire engine operation. The valves are equipped with seals on both the inlet and outlet sides to ensure complete shutoff. In addition, the valve housing is vented overboard through the vehicle vent system to prevent propellant buildup. A leak detector to

indicate inlet seal failure will provide evidence for review and action at post flight inspection. A position indicator is attached to the splined shaft to provide a method of monitoring valve opening.

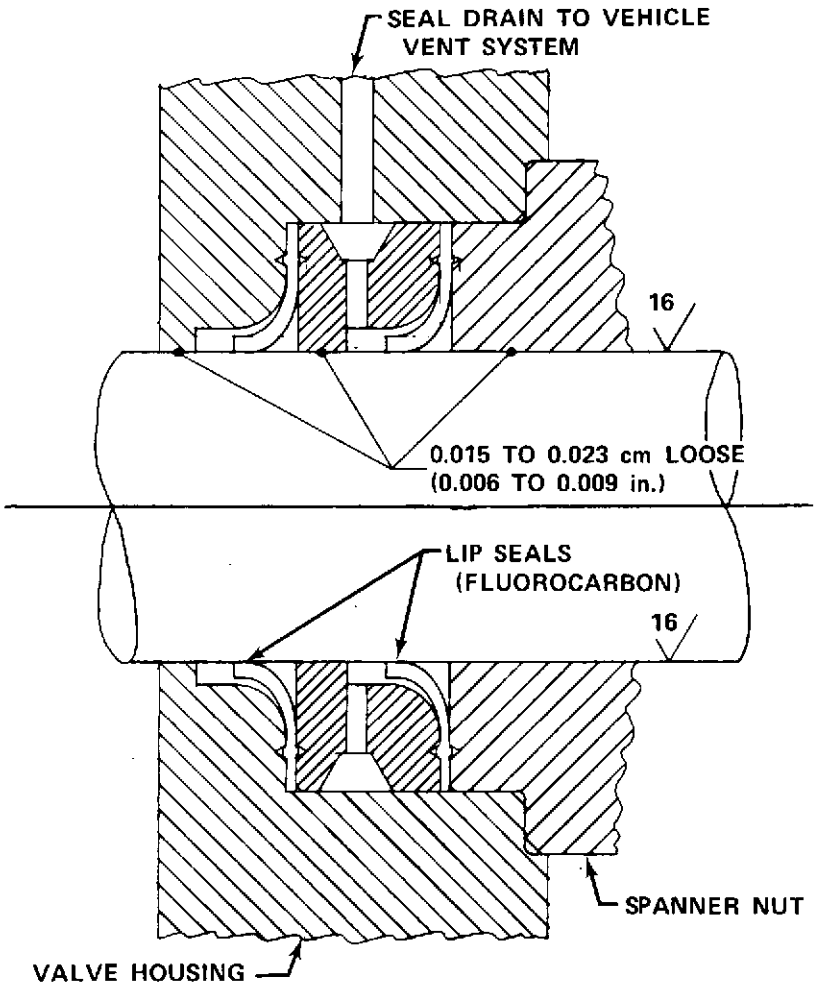

Figure 148. Typical Sliding and Rotating Shaft Seals FD 72495

A typical valve cross section is illustrated in figure 149. The valve housing and ball are made of aluminum Al 6061 (AMS 4127). The ball is anodized to increase surface hardness, which reduces seal wear. The ball is splined to a shaft that has an integral pinion gear. The pinion is driven by a rack attached to the actuator piston. The rack and pinion are A-286 stainless steel (AMS 5735). The actuator housing and piston are 347 stainless steel (AMS 5646). The return spring, which is 17-7 PH stainless steel (AMS 5673), was sized to close the valve during full flow should the actuator pressure fail. The inlet and outlet seals are fluorocarbon plastic seals held in place by an A-286 stainless steel spanner nut. These seals are preshaped so that a pressure load is induced to force the seal against the ball. The lip seal in the actuator is composite Kapton-F polyimide/Fep Teflon laminations and Fep Teflon laminations. The rack and pinion are dry-lubricated with MoS_2 to minimize wear.

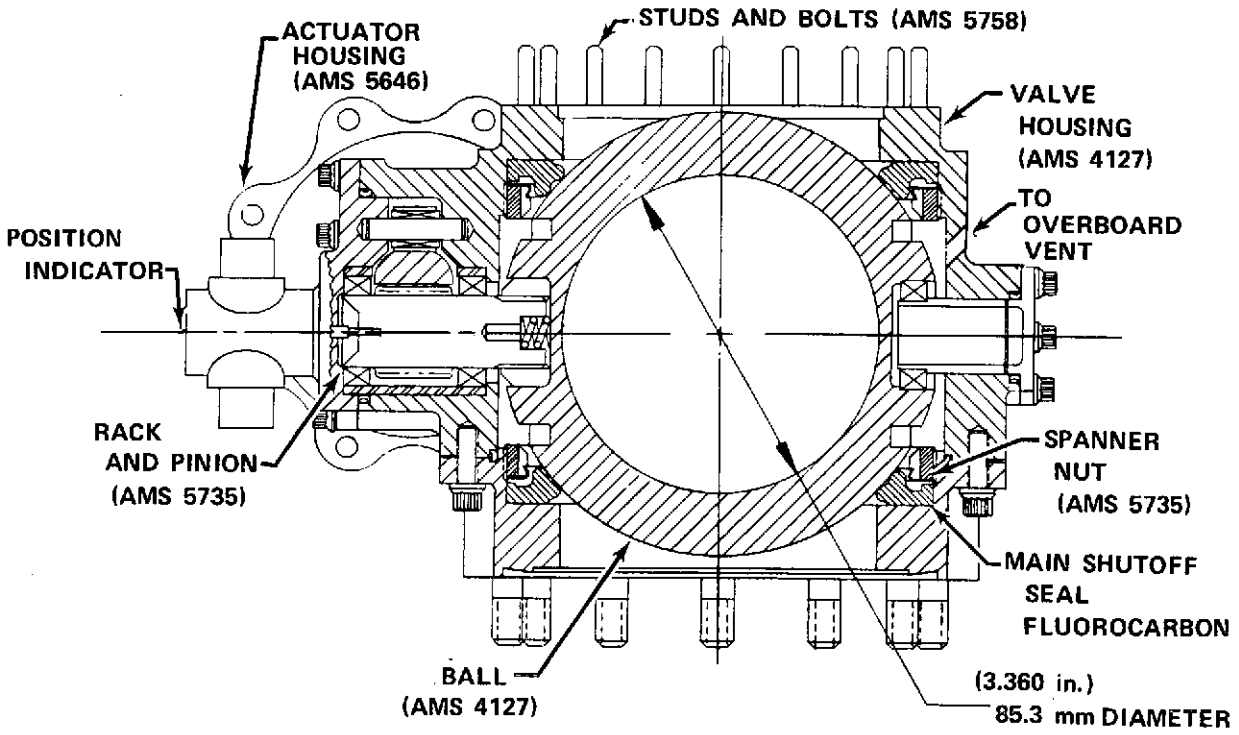

Figure 149. Representative Inlet Valve Cross Section FD 72494

(c) Main Oxidizer Valve

The control system concept requires a modulating control valve in the main chamber oxidizer line. Valve positioning is determined by demands from the ECU. A dual purpose (modulation and shutoff) butterfly type valve, driven by a stepper motor through a planetary gearbox, is used in this application.

The main oxidizer valve, as presented in figure 150, provides shutoff during prestart and shutdown. A shutoff sealing configuration for the butterfly plate was developed in XLR129 studies, which included the evaluation of 21 seal concepts and the fabrication and testing of four designs. These tests included cyclic endurance (over 10,000 cycles) at cryogenic and ambient temperatures and durability testing at high flow and high pressure.

Valve sealing for shutoff is accomplished by using a pressurized, hoop seal. An enlarged view of the seal area appears in figure 151. The sealing element is a hydroformed Inconel X-750 (AMS 5598) hoop-welded to an Inconel X (AMS 5671) support member. After heat treatment, the seal element is silver-plated to enhance sealing and durability. A toroidal static seal is installed in the housing to prevent leakage around the hoop. A loading ring is used to provide circumferential loading of the static seal. The ring also forms a flow passage liner downstream of the shutoff valve.

The valve housing, disk, shaft, and seal loading ring are Inconel 718 (AMS 5663), which exhibits a high strength-to-weight ratio and good ductility at cryogenic temperatures. The bolts, studs, and nuts are MP35N (AMS 5758) to minimize bolt size. The shaft bearings are roller bearings made of AMS 5630.

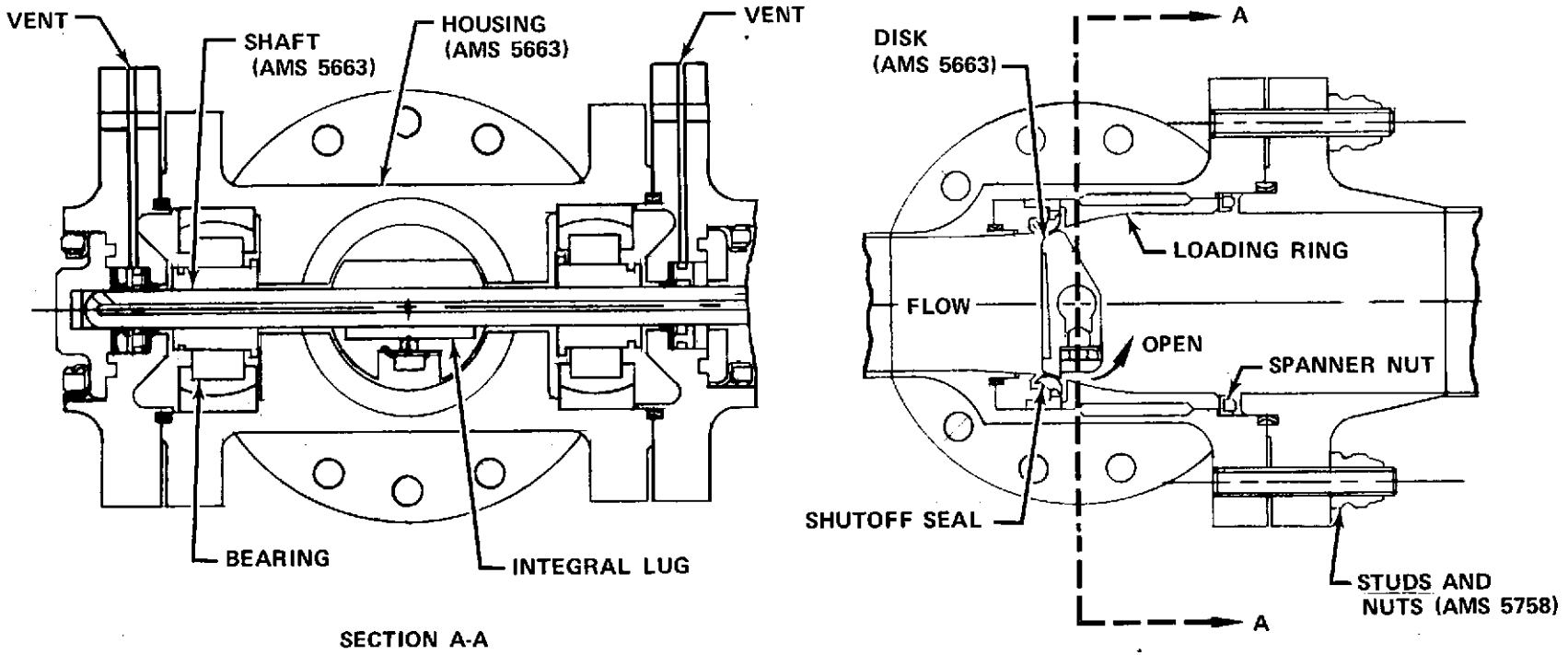

Figure 150. Butterfly-Type Main Oxidizer Valve Cross Section

FD 72493

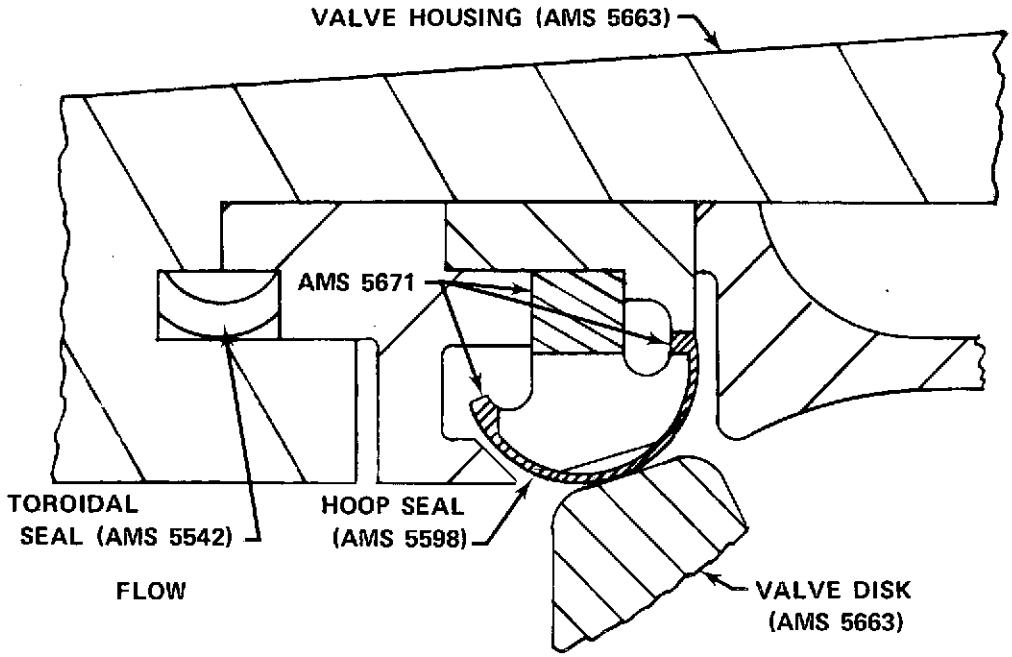

Figure 151. Butterfly Valve Seal FD 72492

Force-balancing the butterfly disk partially reduces actuation requirements. Balance is achieved by cutting a spoiler notch in the front face of the disk, which enhances uniform pressure distribution across the disk and thereby reduces the dynamic flow torque. The flow metering and torque characteristics of the valve were substantiated in XLR129 program testing.

The main chamber oxidizer valve flow characteristics are illustrated in terms of effective area in figure 152. The valve is sized so that the maximum cycle effective area occurs at 1.05 rad (60 deg) and the minimum effective area occurs at 0.35 rad (20 deg) of valve opening. This assures a relatively uniform valve metering characteristic regardless of engine operating point. The valve area margin against undetermined engine component variations is 28%. Figure 153 shows the valve percent area change per degree of valve opening as a function of valve angular position.

(d) Preburner Oxidizer Valve

The preburner oxidizer valve, as shown in figure 154, is mounted directly to the preburner housing and forms the top of the preburner pressure vessel. This design feature reduces oxidizer volume downstream of the valve, which facilitates shutdown and minimizes the amount of helium required for purging.

The preburner oxidizer valve is closed during tank head and pumped idle. Because the preburner is nonoperational during idle conditions, some heat will be conducted to the valve. To cool the valve while in the closed position, the oxidizer flow for the GO_2 heat exchanger is tapped off the valve body upstream of the control point, thereby creating continuous flow through the valve.

The preburner oxidizer valve uses a traversing contoured pintle to modulate oxidizer flow. The pintle position is controlled by a rack and pinion arrangement, driven by a stepper motor through a planetary gear train.

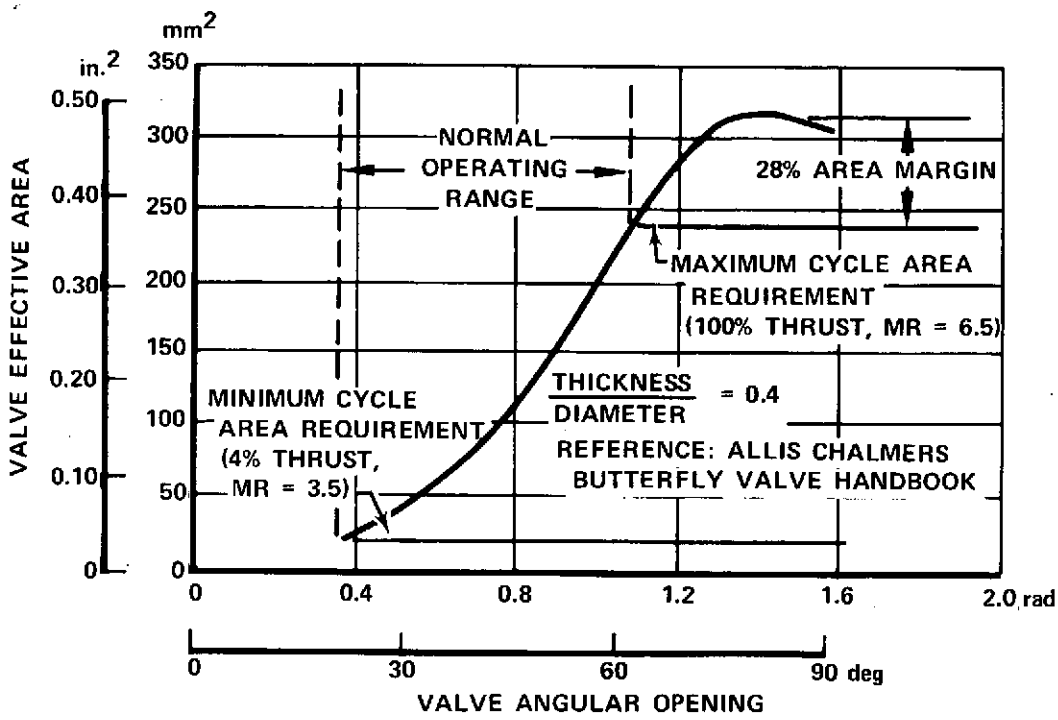

Figure 152. Advanced Space Engine Main Oxidizer Valve Flow Area Characteristics FD 71584

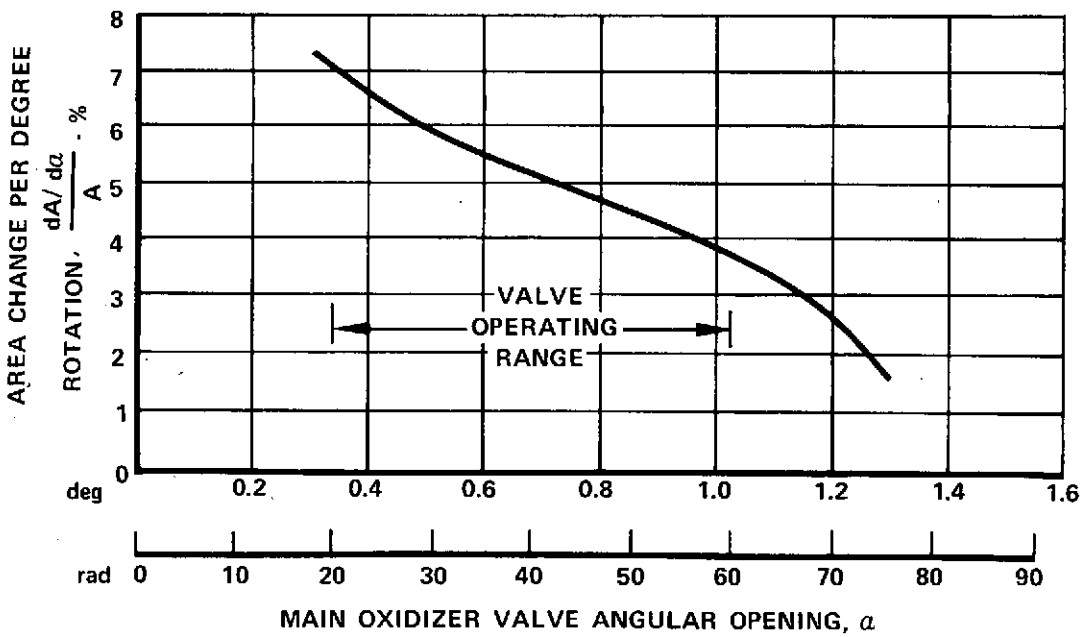

Figure 153. Advanced Space Engine Main Oxidizer Control Valve Sensitivity FD 71585

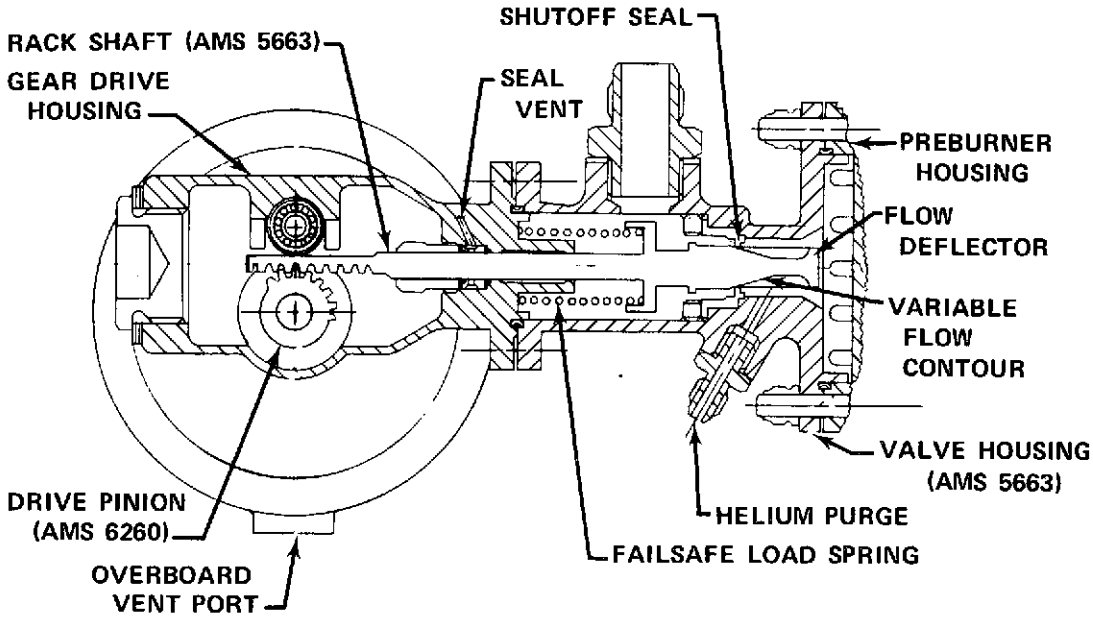

Figure 154. Preburner Oxidizer Valve Cross Section FD 72491

The pintle position is fed back to the ECU by a position indicator on the rack. Actual pintle position is set by the ECU in accordance with engine process feedback.

Figure 155 illustrates valve flow characteristics in terms of effective area. The valve area margin against undetermined engine component variations is 21%. The pintle has an integral flow deflector downstream of the control point. Combustion analysis has shown that the deflector is necessary to prevent the direct impingement of oxidizer on preburner elements.

The pintle, rack, housing and pressure fittings are high-strength Inconel 718 (AMS 5663). This material has a high strength-to-weight ratio and good ductility at cryogenic temperatures. The pinion is AMS 6260 and the lightly loaded rack bearing is 440C (AMS 5630). The bolts, nuts, and studs are high-strength, multiphase MP35N (AMS 5758).

During idle operation, when the valve is closed, leakage past the shutoff seal must be minimal. The incorporation of a smooth conical seal surface on the valve pintle ensures positive sealing. The pintle seats against the edge of the orifice plate, which conforms to the shape of the conical surface on the pintle. The shaft seals are laminated Kapton-F and Fep Teflon. The static seals are toroidal segments made of Inconel X-750 (AMS 5542).

(e) Fuel Valve (Cavitating Venturi)

The fuel valve (cavitating venturi), shown in figure 156, serves a dual function in engine operation. Located just downstream of the main fuel pump discharge, the venturi provides modulation of fuel flow as well as isolation of the fuel pump from pressure oscillations caused by boiling instability in the regeneratively cooled thrust chamber during pumped idle.

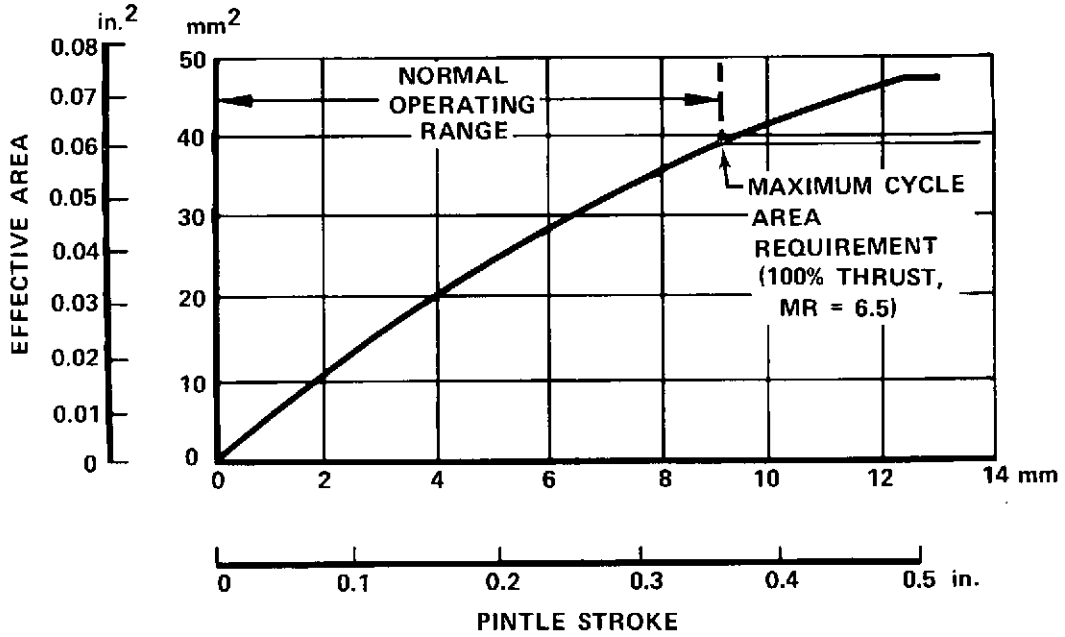

Figure 155. Advanced Space Engine Preburner Oxidizer Valve Flow Area Characteristics FD 71586

The valve housing has a diffuser section included in it downstream of the venturi throat. The diffuser is necessary to recover most of the inlet pressure and match the valve size to the regeneratively cooled thrust chamber inlet manifold. The translating pintle is contoured to aid pressure recovery while maintaining a minimum stroke.

A translating pintle, driven by a rack and pinion to vary throat area, is closed down to its cavitating position, A_{eff} = 0.495 cm^2 (0.0768 in^2) during pumped idle mode. At full thrust with a mixture ratio of 6.5, the pintle is moved to a position with an effective area of 1.69 cm^2 (0.2618 in^2). For full thrust with mixture ratios of 5.5 and 6.0, the effective area of 4.03 cm^2 (0.6245 in^2) is produced by fully withdrawing the pintle from the venturi throat. Figure 157 displays valve flow characteristics in terms of effective area. The valve uses a pressure balance piston to reduce the load on the pintle shaft, which allows use of a smaller actuator.

The pintle and rack are fabricated from Inconel 718 (AMS 5663). The housing, made of 8-1-1 titanium (AMS 4972), is sized for minimum deflection to minimize throat area deviations. In addition, ribs are included on the outside of the housing in the vicinity of the throat. These ribs provide necessary stiffening without a large increase in weight. The pintle shaft is similarly sized for stiffness.

The pinion that drives the rack is AMS 6260 and the lightly loaded rack bearing is fabricated from 440C (AMS 5630). The pinion is connected to a 13.3:1 reduction planetary gearbox, with gears of AMS 6260. The gears and the rack are lubricated with MoS_2 (PWA 550). Bolts and nuts are high-strength multiphase MP35N (AMS 5758).

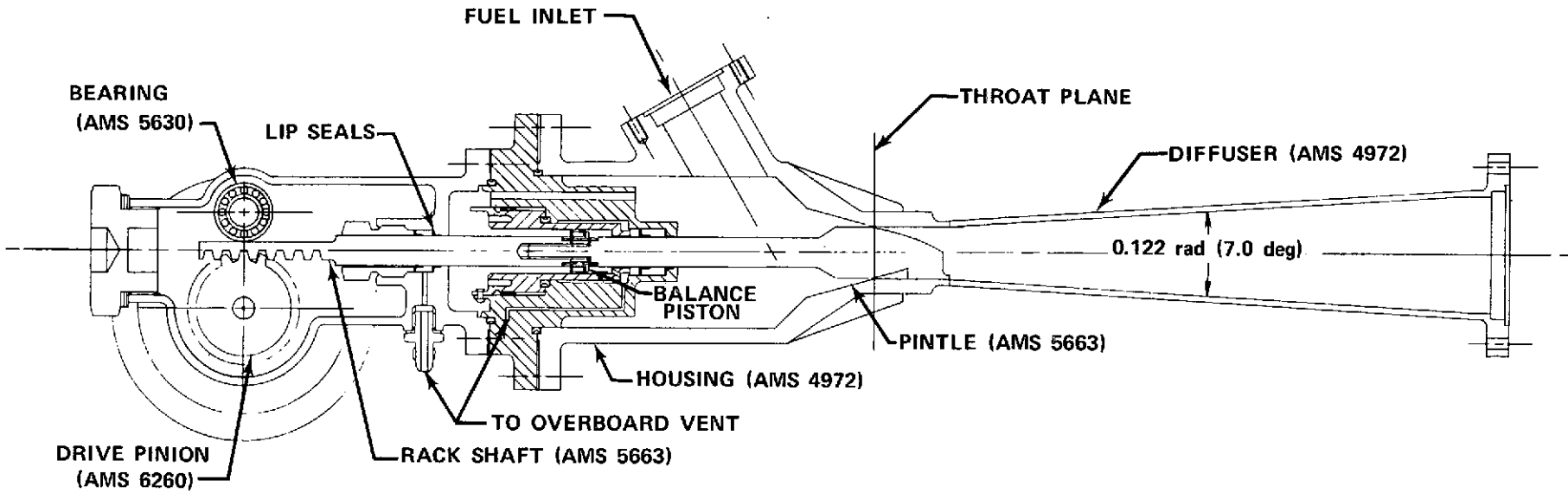

Figure 156. Fuel Cavitating Venturi Cross Section

FD 72486

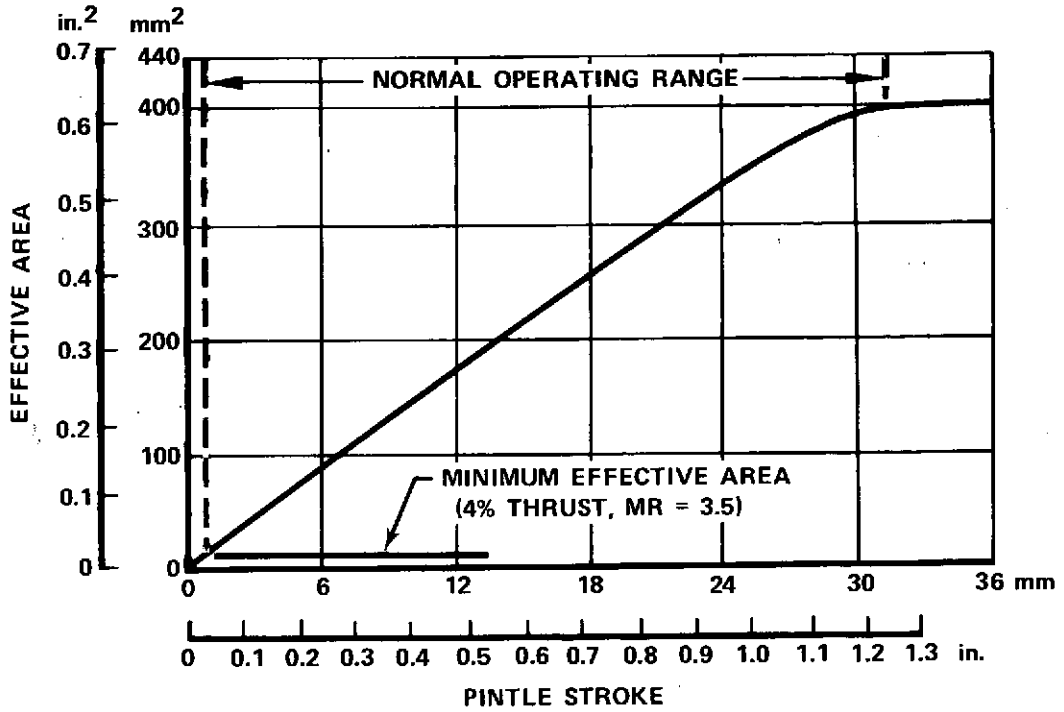

Figure 157. Advanced Space Engine Fuel Cavitating Venturi Flow Area Characteristics FD 71583

Shaft seals are used to isolate one side of the pressure balance piston from fuel pressure and prevent fuel pressure from being felt by the actuator housing. The seals are laminated Kapton-F and Fep Teflon. Static seals are toroidal segments made of Inconel X-750 (AMS 5542).

(f) Fuel Bypass Valve

The fuel bypass valve shown in figure 158 is a two-position helium-actuated valve that provides continuous cooling flow to the main case. With the valve actuated at tank head idle, approximately half the fuel flow bypasses the regeneratively cooled nozzle and dumps directly into the main case. Closing the valve, by removing helium pressure, increases fuel flow to the turbines and initiates the rotating idle mode. With the valve closed at full thrust, a flow of 0.131 kg/s (0.290 lb/sec) is supplied through a fixed orifice for main case cooling.

A poppet, the controlling element in the valve, is used to shut off bypass flow. To prevent excessive case coolant flow past the poppet, and direct the flow through the fixed orifice, the poppet face and mating valve seat exhibit a fine surface finish.

The valve housing and poppet shaft are fabricated from Inconel 718 (AMS 5663) because of the high-pressure load. This material provides high strength, high elastic modulus, and good ductility. The return spring is 17-7 PH stainless steel (AMS 5673), and the bolts are multiphase MP35N. Shaft seals are laminated Kapton-F and Fep Teflon. Static seals are Inconel X-750 (AMS 5542).

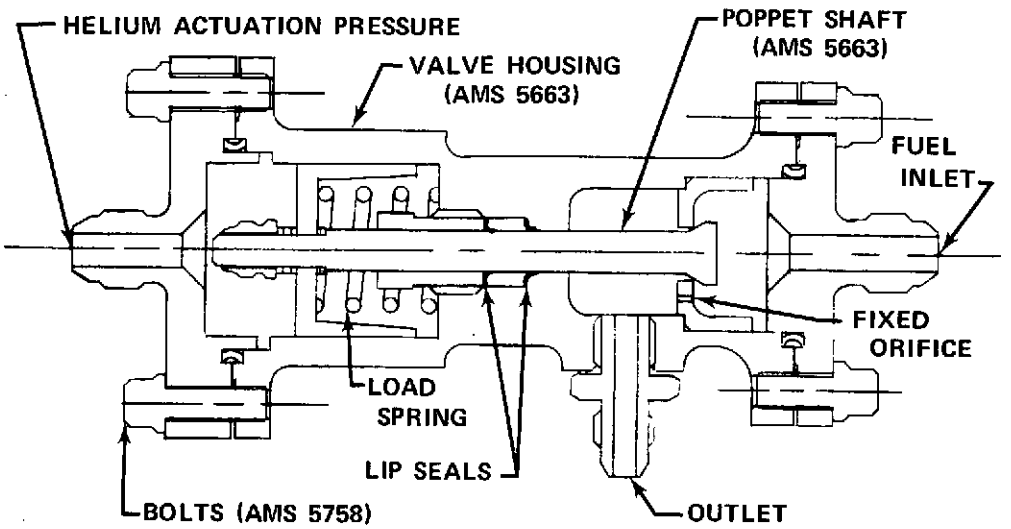

Figure 158. Fuel Bypass and Main Case Coolant Valve FD 72490

(g) Fuel Shunt Valve

ASE cycle studies indicate the need for a two-position fuel valve to control the percentage of fuel flow to the GO_2 heat exchanger. This valve, which is located downstream of the regeneratively cooled thrust chamber, is actuated during tank head idle to flow 100% of the fuel through the heat exchanger. The valve is deenergized for rotating idle and full thrust, directing 79% of the flow directly to the preburner and 15% through the heat exchanger and into the preburner. The remaining 6% of the fuel flow is used to cool the elbows in the line exterior to the heat exchanger.

Figure 159 shows the valve cross section. A plug, powered by a helium actuator, is used to shut off direct flow to the preburner. The outlet to the heat exchanger is an always-open port sized to match pressure drops in each line to the preburner.

The valve housing and plug are A-286 stainless steel (AMS 5735), a material that provides good corrosion resistance with no susceptibility to hydrogen embrittlement. The actuator housing is 347 stainless steel (AMS 5646) and the return spring 17-7 PH stainless steel (AMS 5673). Shaft seals are laminated Kapton-F and Fep Teflon and static seals are Inconel X-750 (AMS 5542).

(h) GO_2 Control Valve

The GO_2 control valve, as shown in figure 160, directs the flow of the oxidizer discharged from the GO_2 heat exchanger. During tank head idle, the shuttle valve is not actuated. Gaseous oxidizer then flows to the torch igniter and main injector. The valve contains a pintle driven by a rack and pinion to modulate flow to the injector. Flow characteristics in terms of effective area are shown in figure 161. During the transition from tank head to pumped idle, the shuttle valve is pressure-actuated and shifts position. Flow to the injector is shut off and the tank pressurization side is opened. Also, a small valve in the igniter line, illustrated in figure 162, is closed during the shift to pumped idle. This valve maintains a degree of leakage to negate contaminant back flow into the igniter line. Leakage flow is set by the diametral shaft clearance.

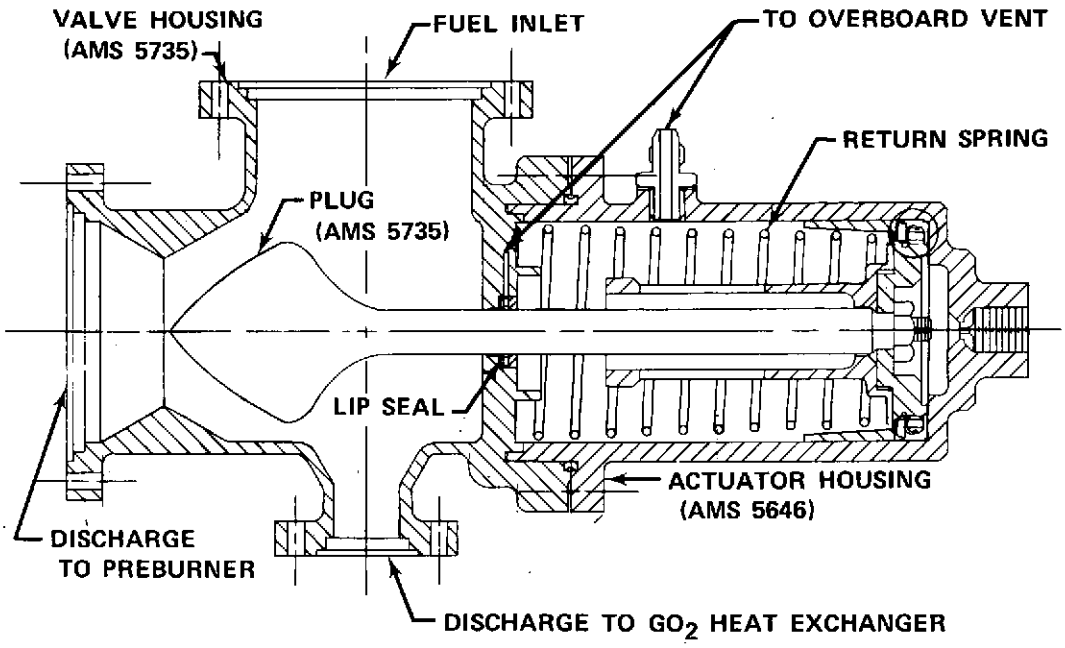

Figure 159. Fuel Shunt Valve Cross Section FD 72489

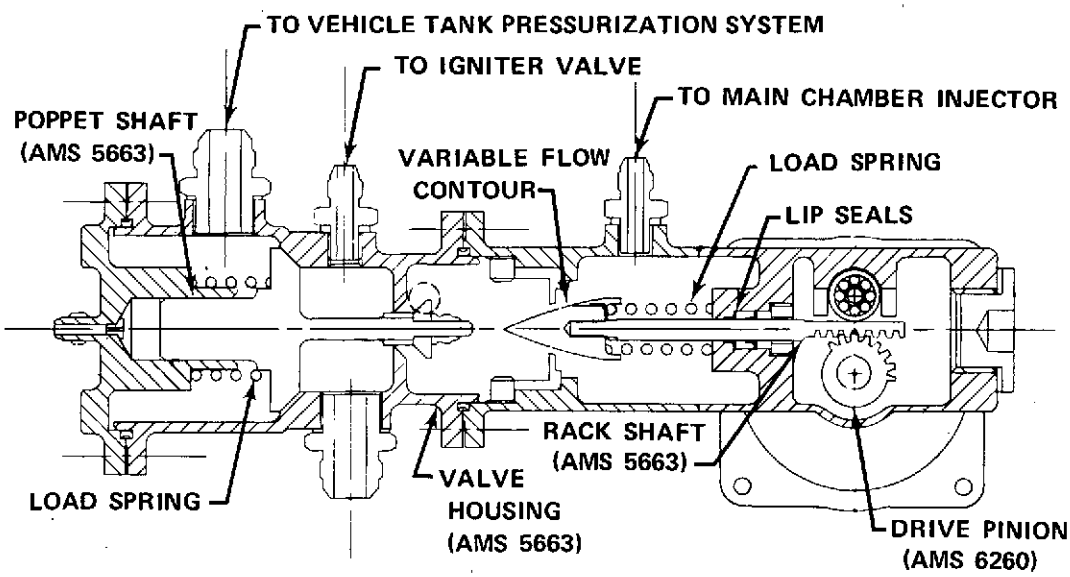

Figure 160. Gaseous Oxidizer Control Valve FD 72488

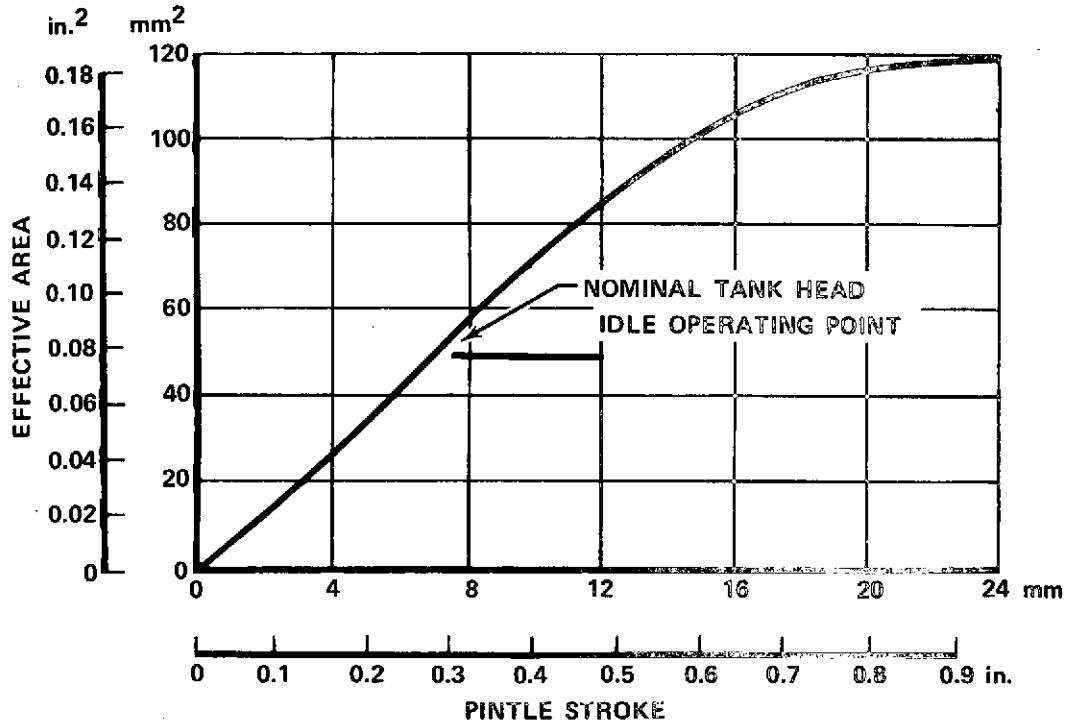

Figure 161. Advanced Space Engine Gaseous Oxidizer Control Valve Flow Area Characteristics (To Main Chamber Injector) FD 71587

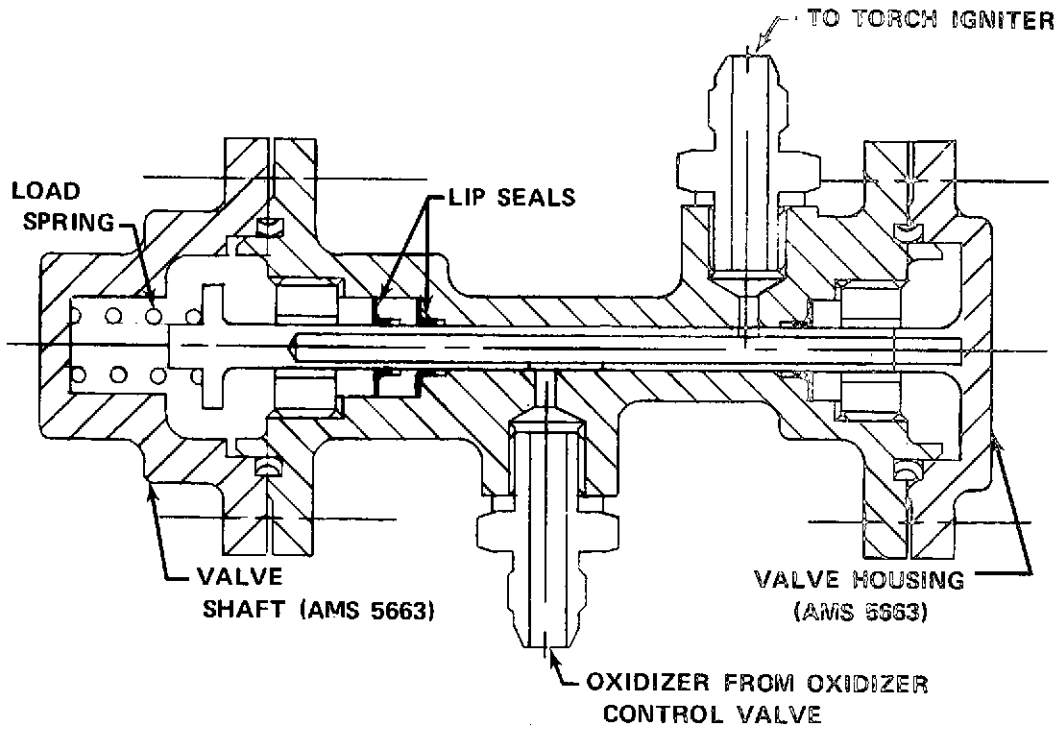

Figure 162. Igniter Flow Control Valve FD 72487

The GO_2 control valve housings, poppets, pintle and fittings are Inconel 718 (AMS 5663). The rack bearing is 440C (AMS 5630) and the pinion is AMS 6260. The return springs are 17-7 PH stainless steel (AMS 5673) and the bolts are multiphase MP35N (AMS 5758). Shaft seals are laminated Kapton-F and Fep Teflon. Static seals are Inconel X-750 (AMS 5542). The rack is lubricated with MoS_2 per PWA 550.

9. Plumbing

a. General

Lines must be provided to connect all major engine components and controls as defined in the control schematic presented in figure 138. The detail design of high pressure plumbing requires the use of sophisticated design procedures, which were not consistent with the scope of the ASE study, and therefore effort in this area was limited to preliminary sizing and routing of major lines for the engine arrangement drawing.

Under Phase II of the XLR129 program, (Reference 13) required analytical techniques were generated, a comprehensive set of ground rules was developed, and seal configurations with leakage rates acceptable for high pressure rocket engine usage were standardized to assure design consistency. The connector envelopes shown on the engine arrangement drawing reflect application of these standards. Descriptions of the connections and seal designs are given below.

b. Discussion

(1) Flanges

All conventional straight line connections employ the raised-face (cantilever) type flange shown in figure 163. Basic design of the raised-face flange requires that the distance between the static seal and the bearing face of the flange be held to a minimum. Bolt loads and blowoff loads are located as close as possible to reduce the overturning moment in the flange ring, which produces bending of the flange as shown in figure 164. This ensures that the deflection of the flange in the area of the seal surface will be small as the flange load is applied and the flange is deflected. The flange itself is designed to be relatively stiff in resistance to an overturning moment. In designing the flange, the radial thickness is held to a minimum by employing a large number of the smallest possible diameter bolts to reduce the overturning moment in the flange and to provide sufficient preload to prevent separation of the flange under applied operational loads. The flange thickness is then established, using a finite element computer analysis, to limit the rotational deflection at the seal contact point to a specific value as required for the particular application. The analytical routine generates a practical low-weight cantilever, or raised-face, flange whose deflection at the seal contact point does not exceed a specified value under maximum bolt preloading at 120% of maximum operating pressure.

By minimizing the radial thickness of the seal, bearing surface, and bolt diameter stackup, the overturning moment in the flange is minimized and the flange material is utilized to its fullest advantage. The result is to minimize both the weight and size of the flange required to meet the requirements.

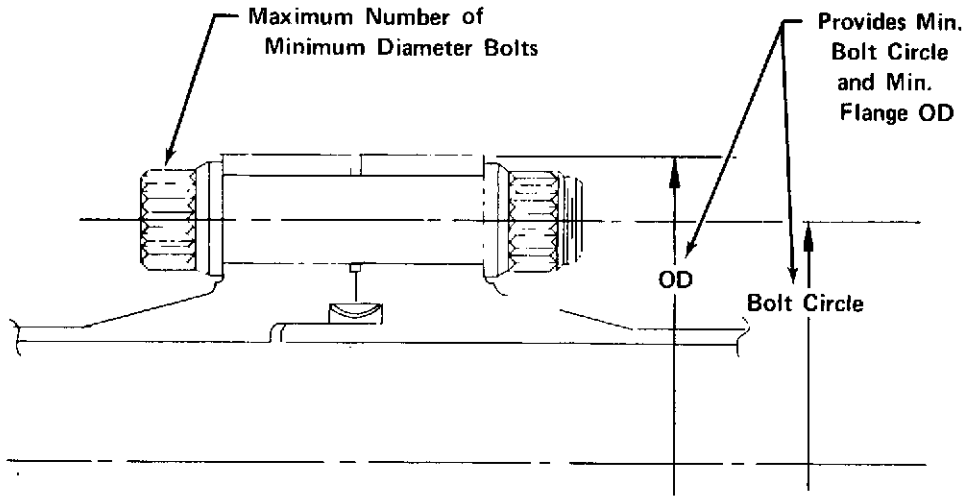

Figure 163. Raised Face Flange FD 52443

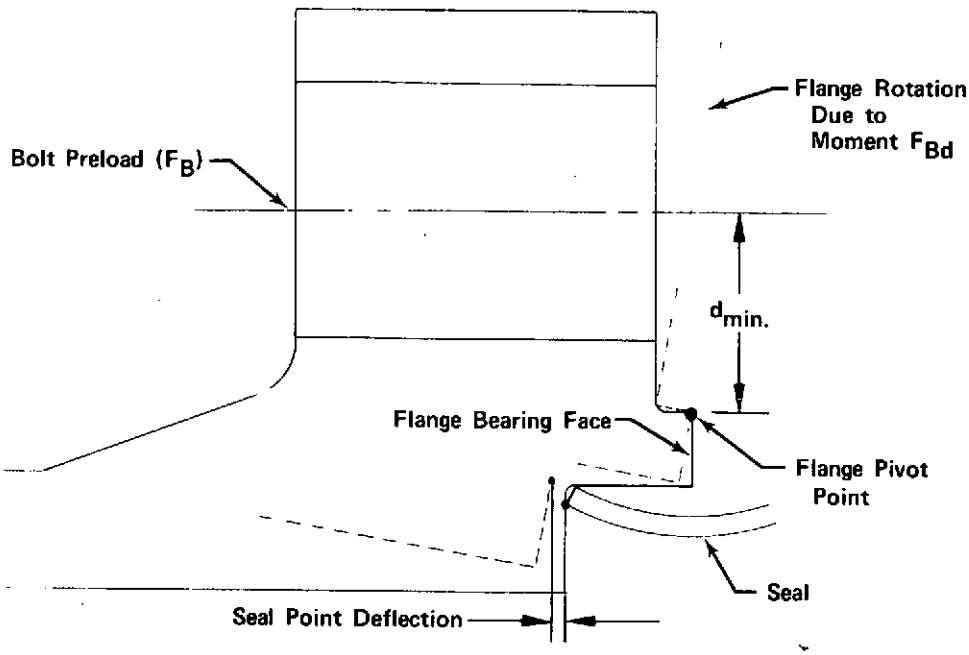

Figure 164. Rotational Effect of Flange Loading FD 46300

(2) Static Seals

A toroidal segment seal developed specifically for use in the XLR129 engine is specified for use in all high pressure connectors in excess of 25.4 mm (1 in.) diameter. The design has proved capable of meeting leakage requirements of 10^{-6} scc/sec or less. For static seals of 25.4 mm (1 in.) diameter and less, Resistoflex Corporation's Dynatube fitting is used. This fitting has been tested extensively at pressures up to 3447 N/cm^2 (5000 psia) over a wide range of temperatures with leakage rates of 10^{-7} scc/sec being maintained through 500 assembly cycles.

(a) Toroidal Segment Seal

The toroidal segment seal configuration, figure 165, provides reasonably consistent performance throughout the entire 0 to 4826 N/cm^2 (7000 psig) pressure range. This seal utilizes axial compression to produce radial deflection and high unit loads necessary for effective sealing at low operating pressures. The seal groove depth, cross section size, and thickness are varied as required to meet the load requirements over a large range of coupling diameters. Seal size information is presented as shown in figure 166.

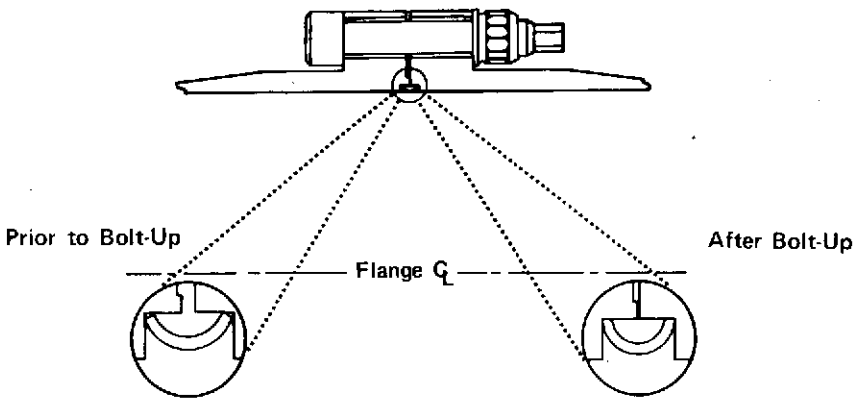

Figure 165. Toroidal Segment of Detail Part, Fit and Installed Shape FD 46260

Primary sealing is accomplished by a radial sealing force developed at installation. By keeping the radial contact width of the sealing legs equal to 0.254 mm (0.010 in.) or less, a minimum value of radial sealing stress can be set at 1379 N/cm^2 (2000 psi). This value of radial stress is sufficient to yield the lead plating on the seal. The addition of pressure increases this force. Therefore, seal pressure increases with increasing internal pressure and the integrity of the seal is maintained.

(b) Dynatube Fitting

The Dynatube fitting selected for use for static seal applications of 25.4 mm (1 in.) or less is shown in figure 167. It is available in various configurations and provides an integral, reusable seal for small lines. As shown in the illustration, initial sealing force is provided by the controlled deflection of the seal lip engaging the seal face on the mating component. The initial sealing force, developed by deflecting the lip, and the intimate contact resulting between the deflected lip and the conical seal seat provides the sealing capability necessary to maintain the low leakage requirement at the lower pressure values.

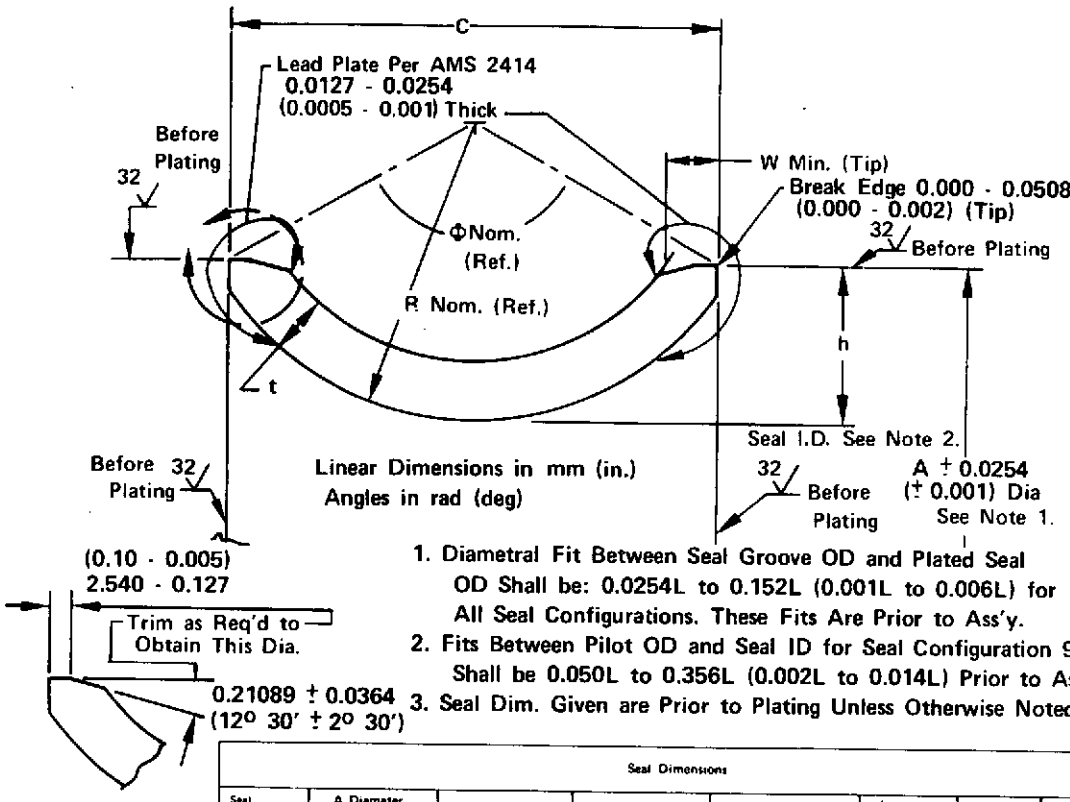

Seal Dimensions										
Seal Configuration No	A Diameter Minimum and Maximum mm (in.)	C mm	C (in.)	h mm	h (in.)	r mm	r (in.)	Φ Nominal rad (Reference)	R Nominal (Reference) mm	R Nominal (Reference) (in.)	W Minimum mm	W Minimum (in.)
1	25.400 to 50.800 (1.000 to 2.000)	2.718 4.447	(0.107) (0.109)	0.914 0.863	(0.036) (0.034)	0.279 0.330	(0.011) (0.013)	2.16 (124°)	(0.064) 1.626		(0.010) 0.254	
2	50.800 to 76.200 (2.000 to 3.000)	2.718 4.447	(0.107) (0.109)	0.914 0.863	(0.036) (0.034)	0.457 0.533	(0.018) (0.021)	2.095 (120° 12')	(0.067) 1.702		(0.019) 0.475	
3	76.200 to 107.950 (3.000 to 4.250)	4.064 4.166	(0.160 (0.164)	1.422 1.321	(0.056) (0.052)	0.584 0.660	(0.023) (0.026)	2.20 (126° 30')	(0.096) 2.438		(0.083) 2.108	
4	107.950 to 215.900 (4.250 to 8.500)	5.359 5.512	(0.211) (0.217)	1.879 1.778	(0.074) (0.070)	0.584 0.660	(0.023) (0.020)	2.27 (130° 36')	(0.122) 3.099		(0.023) 0.584	
5	215.900 to 368.300 (8.500 to 14.500	6.731	(0.265) (0.265)	2.286	(0.090) (0.090)	0.838 0.991	(0.033) (0.039)	2.182 (125° 12')	(0.158 4.013		(0.033) 0.838	
6	368.300 to 419.100 (14.500 to 16.500)	6.731 6.883	(0.265) (0.271)	2.286 2.134	(0.090) (0.084)	0.991 1.118	(0.039) (0.044)	2.147 (123°)	(0.162) 4.060		(0.039) 0.991	
7	419.100 to 457.200 (16.500 to 18.000)	6.731 6.883	(0.265) (0.271)	1.016 2.134	(0.040) (0.084)	1.168 1.295	(0.046) (0.051)	2.096 (120° 36')	(0.166) 4.216		(0.046) 1.168	
8	457.200 to 482.600 (18.000 to 19.000)	6.781 6.883	(0.267) (0.271)	2.286 2.134	(0.090) (0.084)	1.168 1.295	(0.046) (0.051)	2.095 (120° 12')	(0.166) 4.216		(0.046) 1.168	
9	Over 482.600 (19.000)	5.359 5.512	(0.211) (0.217)	1.879 1.778	(0.074) (0.070)	0.406 0.483	(0.016) (0.019)	2.269 (131° 48')	(0.120) 3.048		(0.016) 0.406	

Figure 166. Toroidal Segment Static Seal FD 71589

Increasing internal line pressure produces an additional pressure/area force behind the seal, because of the undercut section, and thereby provides additional seal load between the seal lip and the mating face. The result is a seal that is capable of maintaining its low leakage rate throughout the operating pressure spectrum.

The fact that the seal is an integral part of the coupling ensures that the seal is neither omitted or misassembled. Also, the reusability of the seal reduces maintenance time and cost by decreasing the number of replacement seals required.

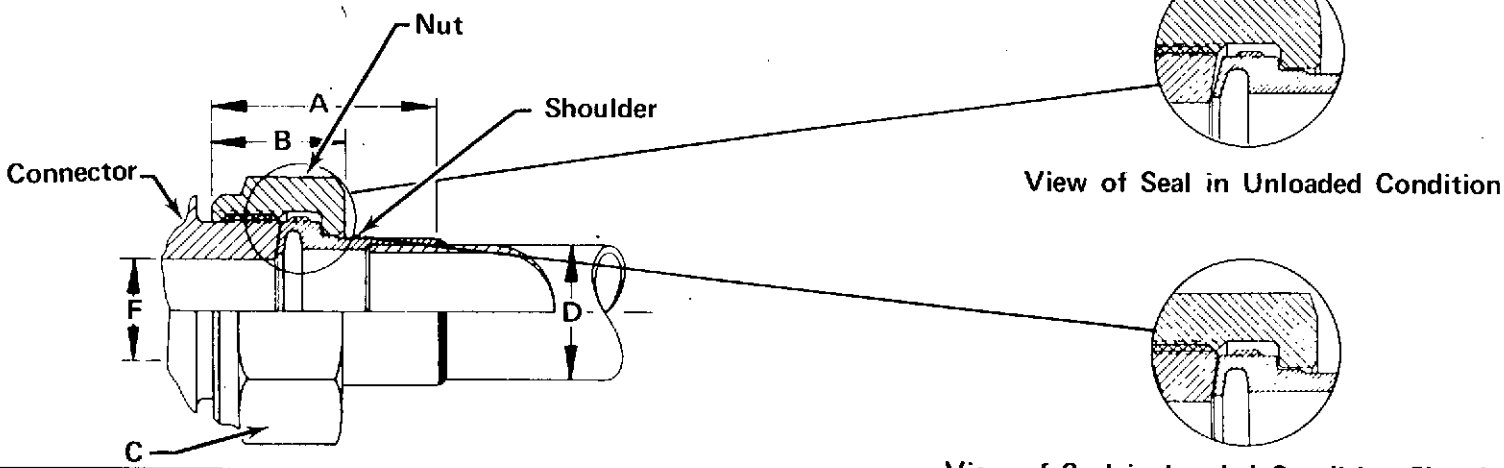

SIZE	A mm (in.)	B mm (in.)	C mm (in.)	D mm (in.)	F mm (in.)
-3	17.27 (0.680)	10.67 (0.420)	11.10 (7/16)	4.75 (3/16)	4.04 (0.159)
-4	18.01 (0.709)	11.53 (0.454)	14.27 (9/16)	6.35 (1/4)	4.80 (0.189)
-5	18.14 (0.714)	11.66 (0.459)	15.88 (5/8)	7.92 (5/16)	6.02 (0.237)
-6	18.62 (0.733)	12.95 (0.510)	17.45 (11/16)	9.53 (3/8)	7.67 (0.302)
-8	18.92 (0.745)	13.16 (0.518)	22.23 (7/8)	12.70 (1/2)	10.24 (0.403)
-10	23.01 (0.906)	14.50 (0.571)	25.40 (1.0)	15.88 (5/8)	13.16 (0.518)
-12	23.93 (0.942)	16.18 (0.637)	28.58 (1 1/8)	19.05 (3/4)	16.61 (0.654)
-16	36.25 (1.427)	17.91 (0.705)	34.93 (1 3/8)	25.40 (1.0)	22.05 (0.868)

NOMINAL INSTALLATION TORQUE VALUES								
SIZE	-3	-4	-5	-6	-8	-10	-12	-16
N - m (ft-lb)	9.49 (7)	16.27 (12)	17.63 (13)	27.12 (20)	47.46 (35)	65.09 (48)	81.36 (60)	111.19 (82)

Figure 167. Dynatube® Fitting

FD 71590

SECTION V
ENGINE PROGRAM PLANS

A. ENGINE DEVELOPMENT PROGRAM APPROACH

1. Introduction

Advanced Space Engine Program Plan I provides for the design and development of an 89 kN (20,000 lb) thrust Advanced Space Engine following a minimum cost development program approach. Program Plan II provides for design and development of an 89 kN (20,000 lb) thrust Advanced Space Engine following a minimum time development program approach.

2. Program Plan I (Minimum Cost)

Program Plan I, the minimum cost engine development program for an 89 kN (20,000 lb) thrust advanced space engine is preliminary in nature and encompasses flight certification, achievement of engine readiness for production, and field operations starting from current engine technology levels without prior demonstration. The program is directed toward minimizing the cost and the risk involved in any major development effort by (1) verifying that the engine design meets the requirements at the lowest hardware level, (2) identifying marginal conditions by conducting selective overstress tests at subcomponent, component, and engine levels, (3) monitoring critical parameters continuously to provide visibility for assessment of progress, and (4) identifying problem areas early in the program. RL10, XLR129, and the available Rocketdyne Space Shuttle experience will be used.

Emphasis in this development effort is placed on the early verification of potential failure modes and preparation of detailed contingency plans to ensure early problem solutions, thus minimizing impact on the program. Changes in the baseline design concept are made only to resolve problems, and verification that the new design features meet the specified requirements at the lowest practical hardware assembly level is made as early in the program as possible. Marginal improvements are excluded. Each requirement is terminated as soon as the stated objectives have been achieved, and the development effort is continuously shifted to those requirements not yet met.

Although high hardware and facility costs are risked because of the possibility of catastrophic failures, selective overstress testing can significantly reduce development cost and time by accelerating the learning rate. Subcomponent overstress testing (material specimen, rotating part spin, housing pressure, etc) is used extensively by P&WA to find and correct problems at the lowest possible hardware level. Risk of damage to more expensive hardware is thereby lessened. In addition to subcomponent tests, selective component and engine overstress tests will be integrated into the overall engine development programs as part of the design verification requirement.

Satisfactory verification that all requirements have been met will be followed by a formal flight certification demonstration conducted under the cognizance of the procuring agency. Certification of the service life capability of the design will also be accomplished, based on the cumulative life history of all the development hardware and a final life demonstration to be conducted using a simulated typical mission duty cycle.

3. Program Plan II (Minimum Time)

Program Plan II, the minimum time engine development program for an 89 kN (20,000 lb) thrust engine is also preliminary in nature and encompasses flight certification, achievement of engine readiness for production, and field operations starting from current technology levels without prior demonstration. The program is directed toward minimizing time by providing a program whereby a conservative design approach is used, followed by a comprehensive development program. Testing is planned so that the complete engine system and all components are subjected to all possible combinations of operational and environmental conditions to expose as quickly as possible all reliability-degrading failure modes. Alternative designs are started concurrent with the baseline design configuration. To attain an early high level of reliability, emphasis is placed on engine systems testing. Of even greater significance in development of reliability are engine systems overload tests. These include thrust, mixture ratio, cycles, and life or service duration.

Component tests are also important. These tests permit evaluation of component durability and performance characteristics over extremes of operating and environmental conditions that are not practical to test in an operating engine system, which has an interdependency of subsystems and components. Although component testing is conducted over the full range of operation, the early tests are made to the extent necessary to establish suitability for the first engine tests. Component, subsystem and engine system testing are thereafter conducted concurrently. Component overload tests such as cycle life, overpressure and vibration will be conducted on all advanced space engine components.

Alternative component and engine system configurations will be designed and tested concurrently. Additional component and engine system testing is required, which is not necessary in a minimum cost development program because development moves at a slower pace and thus allows a step-by-step process of design verification where each requirement is identified and verified. More hardware is therefore needed to accomplish the minimum time program objectives.

Certification of the engine developed in the minimum time program is verified by formal preliminary flight certification (PFC) and final flight certification (FFC) tests, which are similar to the RL10 engine preliminary flight rating tests (PFRT) and qualification tests (QT).

B. CONFIGURATION

In Task I of the program conducted under Contract NAS3-16750 an overall engine configuration for an advanced space engine at the 89,000 N (20,000 lb) thrust level was established. The configuration selected was based on the basic requirements and operating conditions given in table XXIX. The approved configuration and operating mode are as follows:

1. Boost pumps gear driven off the main oxygen pump

2. No throttling

3. NPSH magnitudes of 6 N-m/kg (2 ft) (LO_2) and 45 N-m/kg (15 ft) (LH_2)

4. Tank-head-idle start as defined in figure 168

5. Pass-and-a-half cooling configuration for the regeneratively cooled portion of the thrust chamber

6. Single preburner.

Two alternative program plans for the development of the engine assembly conforming to these requirements and conditions and the approved configuration and operating mode follow.

Table XXIX. Advanced Space Engine Configuration and Operating Conditions

Propellants	Liquid Hydrogen Liquid Oxygen
Vacuum Thrust, N (lb)	89,000 (20,000)
Vacuum Thrust Throttling Capability	No Requirement
Vacuum Specific Impulse, N-s/kg (seconds)	4624 (471.5)
Engine Mixture Ratio	6.0 (nominal at full thrust) 5.5-6.5 (operating range at full thrust)
Chamber Pressure, N/cm^2 (psia)	1324 (1920)
Drive Cycle	Staged Combustion
Envelope Restrictions	
Length (max), cm (in.)	234 (92.07)
Diameter (max), cm (in.)	135 (53.2)
Engine System Weight, kg (lb)*	178.3 (393)
Nozzle Type	Fixed Bell
Nozzle Expansion Ratio	400:1
Propellant Inlet Temperature, °K (°R):	
Hydrogen	Range: 20.3 (36.5)to 22.2 (40)
Oxygen	Range: 90 (162)to 95.6 (172)
NPSH at Pump Inlet at Full Thrust, N-m/kg (ft)	
Hydrogen	45 (15)
Oxygen	6 (2)
Engine Temperature at Normal Prestart, °K (°R)	Range: 111.1 to 311.1 (200 to 560)
Service Life Between Overhauls	300 thermal cycles or 10 hours accumulated run time.
Service Free Life	60 thermal cycles or 2 hours accumulated run time.
Maximum Single Run Duration, seconds	2000
Maximum Time Between Firings During Mission, days	14
Minimum Time Between Firings During Mission, minutes	1
Maximum Storage Time in Orbit (Dry), weeks	52

*Target Dry Weight

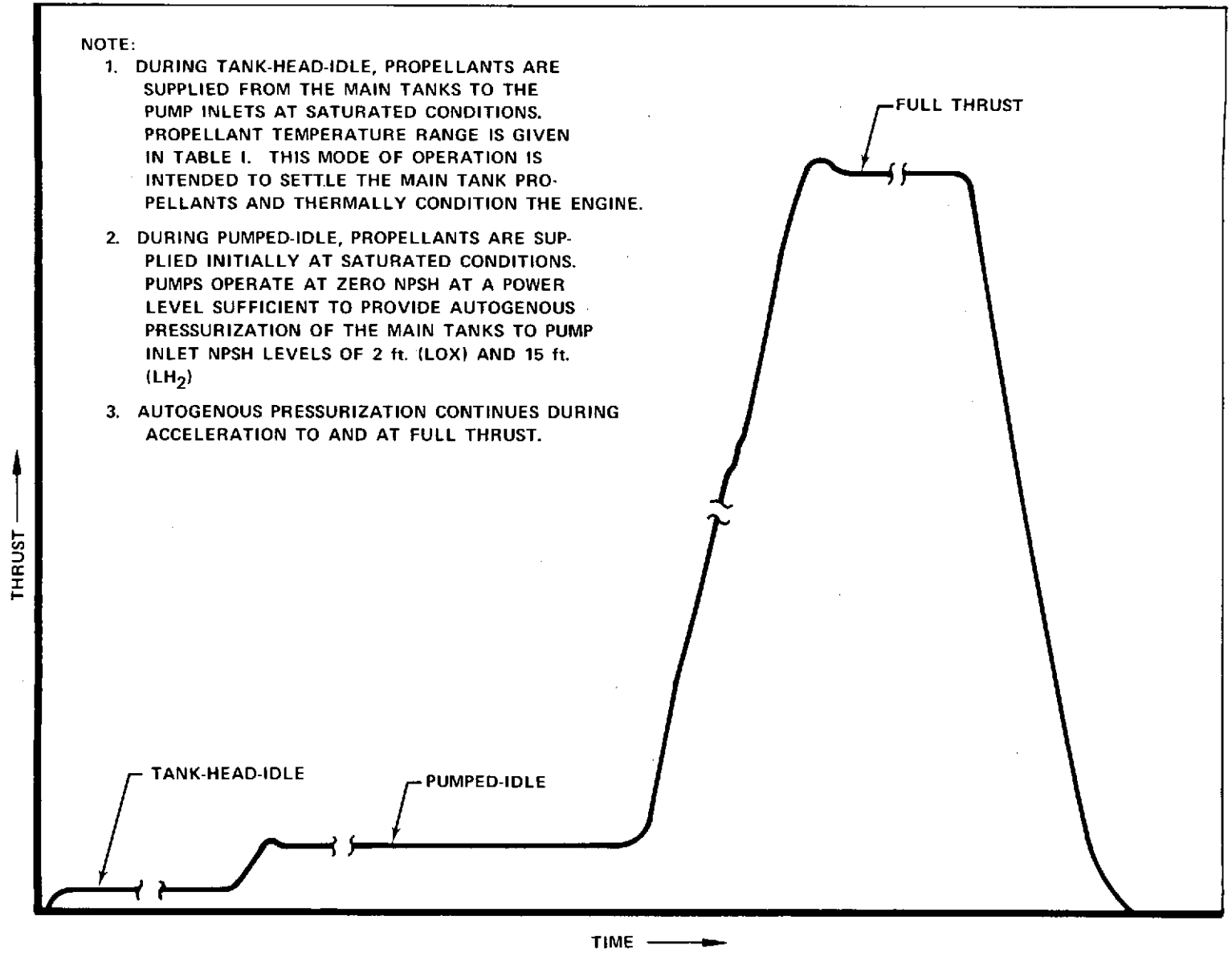

Figure 168. Tank Head Idle, Pumped Idle, and Full Thrust Definitions FD 68845

C. DESCRIPTION OF PROGRAM PLANS

1. Program Plan I (Minimum Cost)

The minimum cost development program for the advanced space engine design consists of 72 months of design, fabrication and test effort. This effort will encompass three design, build, test cycles to FFC (initial, PFC and FFC configurations). Figure 169 shows the development schedule presenting the major program milestones and key decision points as well as the overall development program. The design and fabrication schedules for this program are shown in figure 170 and the program test plan is shown in figure 171.

The design and fabrication schedules are arranged for early release of long-lead-time material procurement as well as sequential releases of drawings to support the fabrication process and permit meeting the early hardware delivery schedules. The preliminary design effort was conducted under Tasks I through V as part of this study. The extent of this design effort was conceptual, however, and not suitable for detailing and subsequent design release. It is therefore necessary to design and release the complete engine. The schedule of this effort is shown in figure 170. Emphasis is placed on fabrication and testing of the specific baseline hardware configurations as opposed to workhorse configurations, except that initially breadboard electrical control hardware will be used to define more specifically the logic and requirements of a control system to establish the approach to be used in the design of a flight system.

Major component testing will be initiated with rig tests of a preburner injector, main case, igniters, and preburner oxidizer valve, progressing to preburner subsystem testing. Other major components, such as low- and high-pressure fuel and oxygen pumps, will be rig-tested prior to subsystem testing to better define operating limits and satisfy the component design verification requirements. After these tests, the emphasis will be shifted to subsystems testing.

Subsystems testing is planned to enable component performance and interactions to be evaluated without involving an entire engine. These subsystems provide an environment that is representative of the actual engine, thereby reducing the total number of engine tests required. The design and inevitable development of special test hardware is eliminated by using actual engine hardware rather than boiler-plate rig hardware. The subsystems to be tested are:

- Preburner
- Staged Combustion (Preburner/Main Case/Main Chamber)
- High Pressure Fuel Turbopump
- High Pressure Oxidizer Turbopump
- Integrated Control
- Powerhead (Engine System Configured for Sea Level Testing)
- Altitude Ignition

These subsystems will be comprised of functioning subassemblies of the engine. The subassemblies that compose each subsystem are shown in schematic form as a portion of the engine schematic, figure 172.

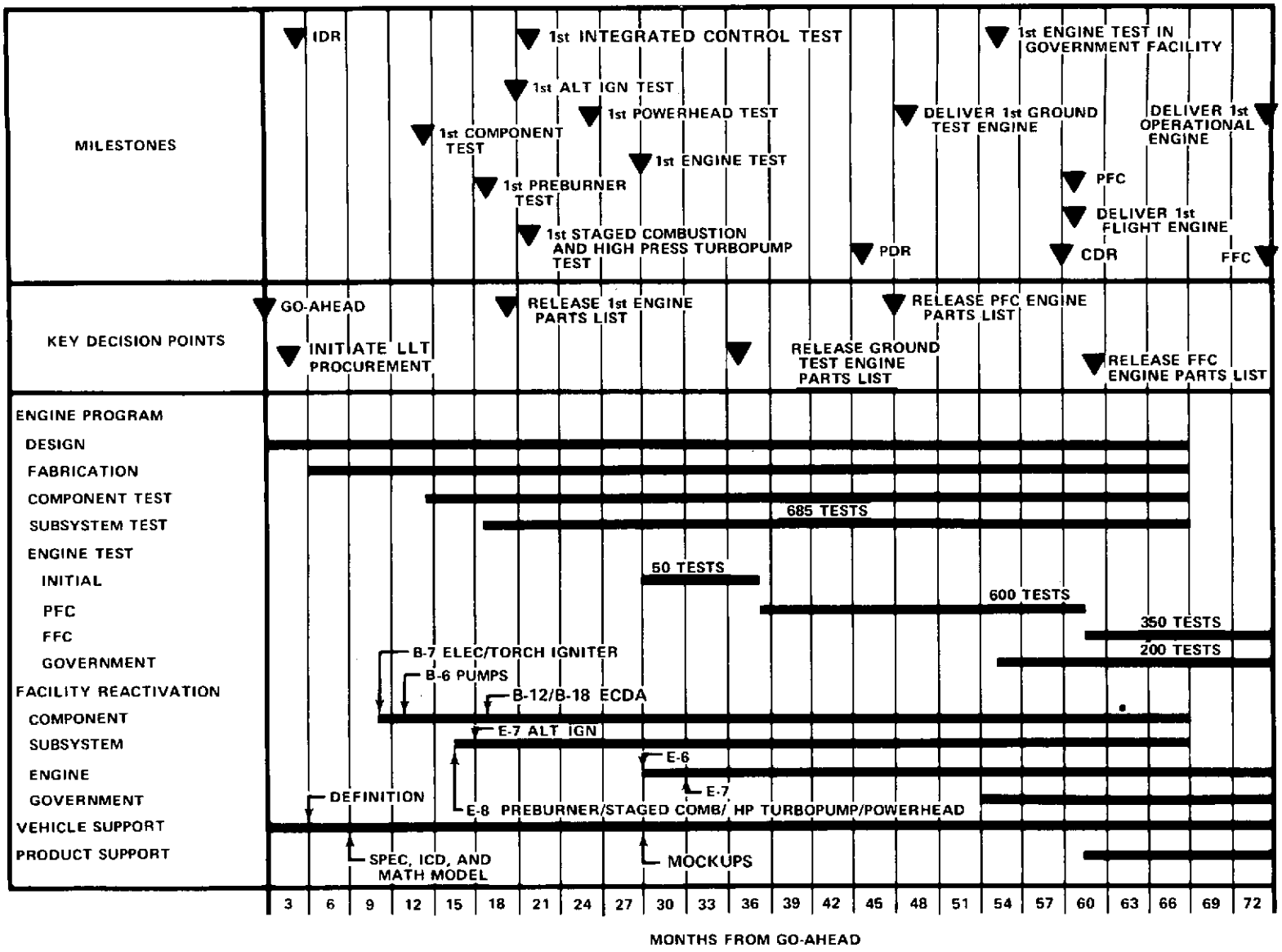

Figure 169. Minimum Cost Engine Development Program

FD 68846B

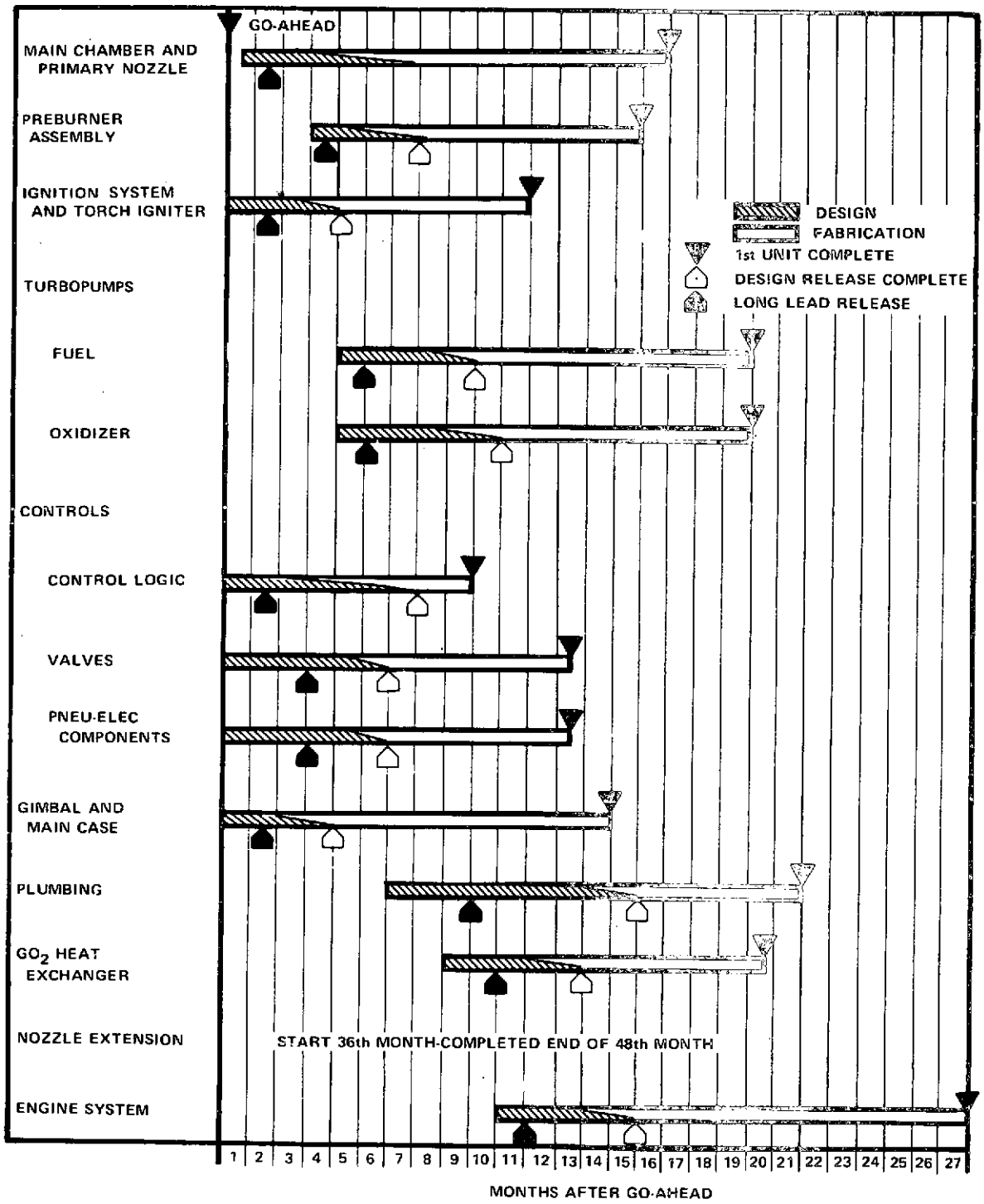

Figure 170. Design and Fabrication Schedule - First Unit Delivery, Program Plan I (Minimum Cost) FD 68847

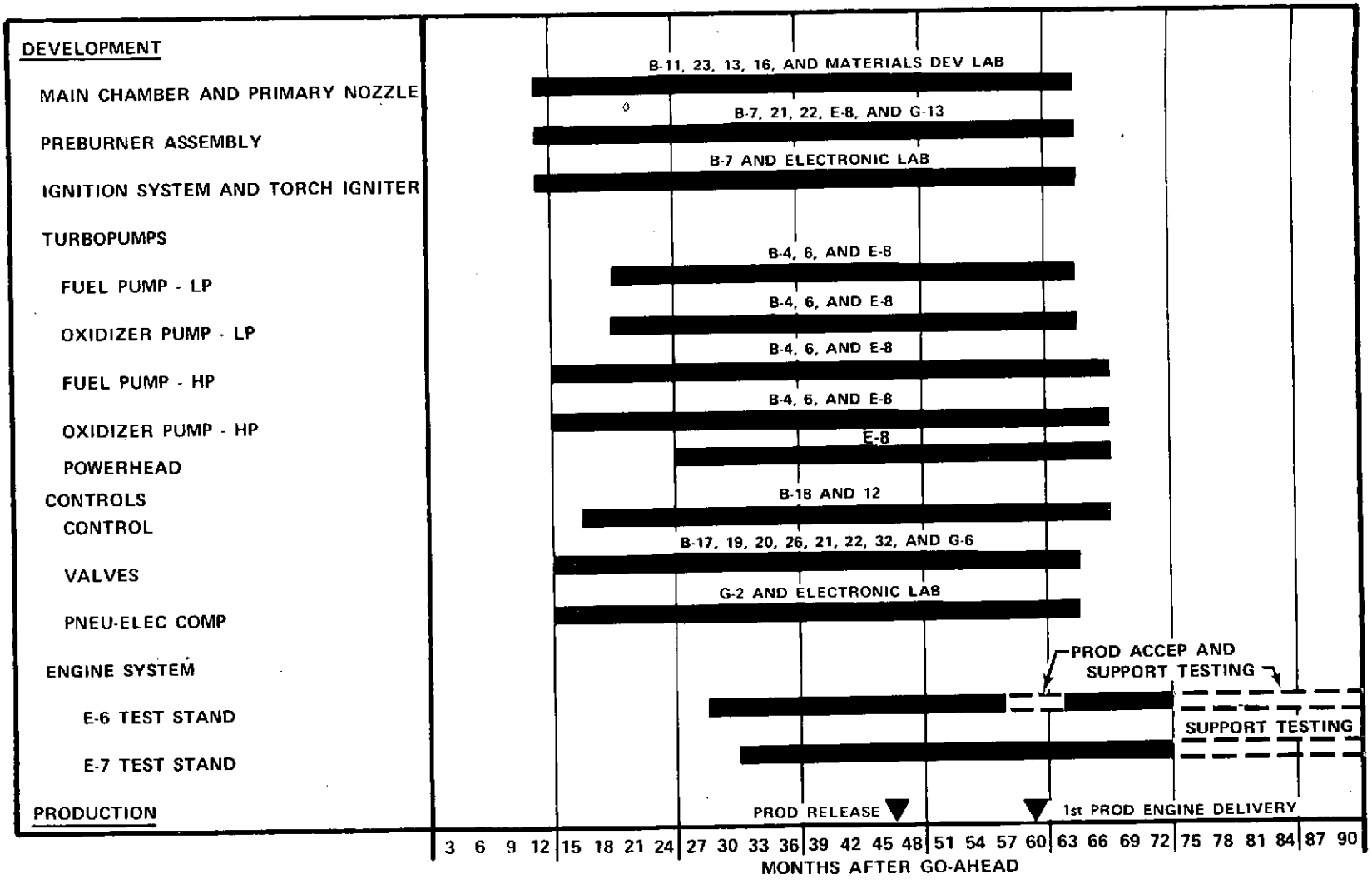

Figure 171. Test Plan, Minimum Cost Engine Development Program

FD 68848A

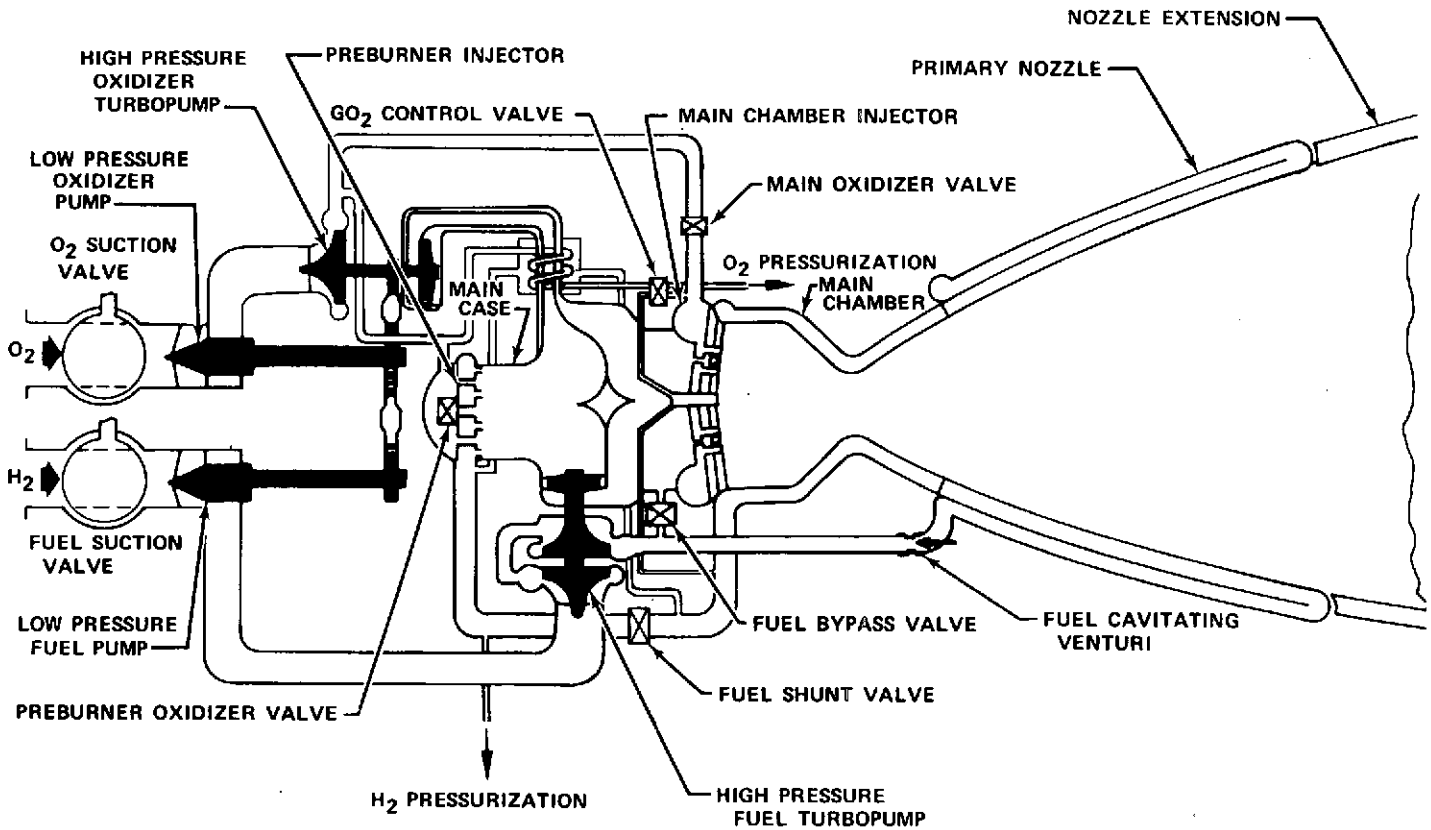

Figure 172. Advanced Space Engine System

FD 68849

The control system component testing time phasing, particularly with respect to the propellant and control valves, is planned to be concurrent with major subsystem and engine testing. This approach minimizes the possibility of duplicate valve testing resulting from subsequent engine baseline design modifications.

Simultaneous engine, subsystem and component testing will be used to eliminate those failure modes that can be resolved at lower hardware assembly levels, thereby reducing total engine system testing and cost. Emphasis will be placed on the following:

- Identification of each requirement and its verification
- Verification of requirements at the lowest hardware level practicable and as early in the program as possible
- Use of overstress testing to accelerate failure mode detection at the subcomponent, component, and engine levels.

The P&WA design and development have been formalized for this program as shown in figure 173. Design verification specification (DVS) documents, which identify each new design requirement and assumption and its verification will be used in the Advanced Space Engine minimum cost development program. Each DVS document also includes a description of the component or engine, the number of hardware components required, the number and types of tests required, the verification level, and the sequential order of verification.

The DVS documents that are planned for an eventual ASE development program are listed below:

- High Pressure Fuel Turbopump
- Low Pressure Fuel Turbopump
- High Pressure Oxidizer Turbopump
- Low Pressure Oxidizer Turbopump
- Preburner Injector
- Main Chamber Injector
- Torch Igniter
- Main Case and Gimbal
- Nozzle Extension
- Main Chamber and Primary Nozzle
- Helium System
- Preburner Oxidizer Valve
- GO_2 Control Valve
- Oxidizer Tank Pressurizing Valve
- Fuel Tank Pressurizing Valve
- Main Oxidizer Valve
- GO_2 Heat Exchanger
- Oxidizer Inlet Suction Valve
- Fuel Inlet Suction Valve
- Igniter
- Electrical Ignition System
- Fuel Shunt Valve
- Engine Command Unit

- Electrical Harnesses
- Control Instrumentation
- Igniter Flow Control Valve
- Main Fuel Valve (Cavitating Venturi)
- Fuel Bypass Valve
- Engine Plumbing, Miscellaneous Hardware
- Engine System

Six new engines were selected for the development program based on the above considerations and particular characteristics of the staged combustion turbine power cycle. A total of 160 engines, including rebuilds, will be used for the minimum cost complete development program. Approximately 57 equivalent engine sets of hardware are planned to support the assembly and test programs.

Historical RL10 and XLR129 design, fabrication, and test experience was used as a guideline for establishing the duration of the overall minimum cost development effort and the number of engine system tests. It was estimated that about 1200 engine system tests over a period of 45 months, combined with a 16-month design, fabrication, and initial component test period and an 11-month initial subsystem test period would be necessary to accomplish the minimum cost development program objectives. Duration of the overall development effort is estimated at 72 months. Development of the RL10 engine model to first qualification required about 1200 engine tests and a 71-month overall development program duration. The Rocketdyne J2 engine also required a 71-month overall development program duration to Qualification II.

Because of the limited funding under Contract NAS3-16750 for program planning and cost estimating, it was impractical to attempt a detailed analysis of the component hardware and test requirements for the ASE development program. Estimates of component requirements are therefore based on the ratio of engine-to-component activity experienced in previous RL10 engine development programs. Subsystem testing, which is a significant cost item, is planned. It is estimated that the following subsystem tests are required to accomplish the development program objectives.

Subsystem	No. of Tests
Preburner	70
Staged Combustion	70
High Pressure Fuel Turbopump	75
High Pressure Oxidizer Turbopump	90
Integrated Control	30
Powerhead	250
Altitude Ignition	100

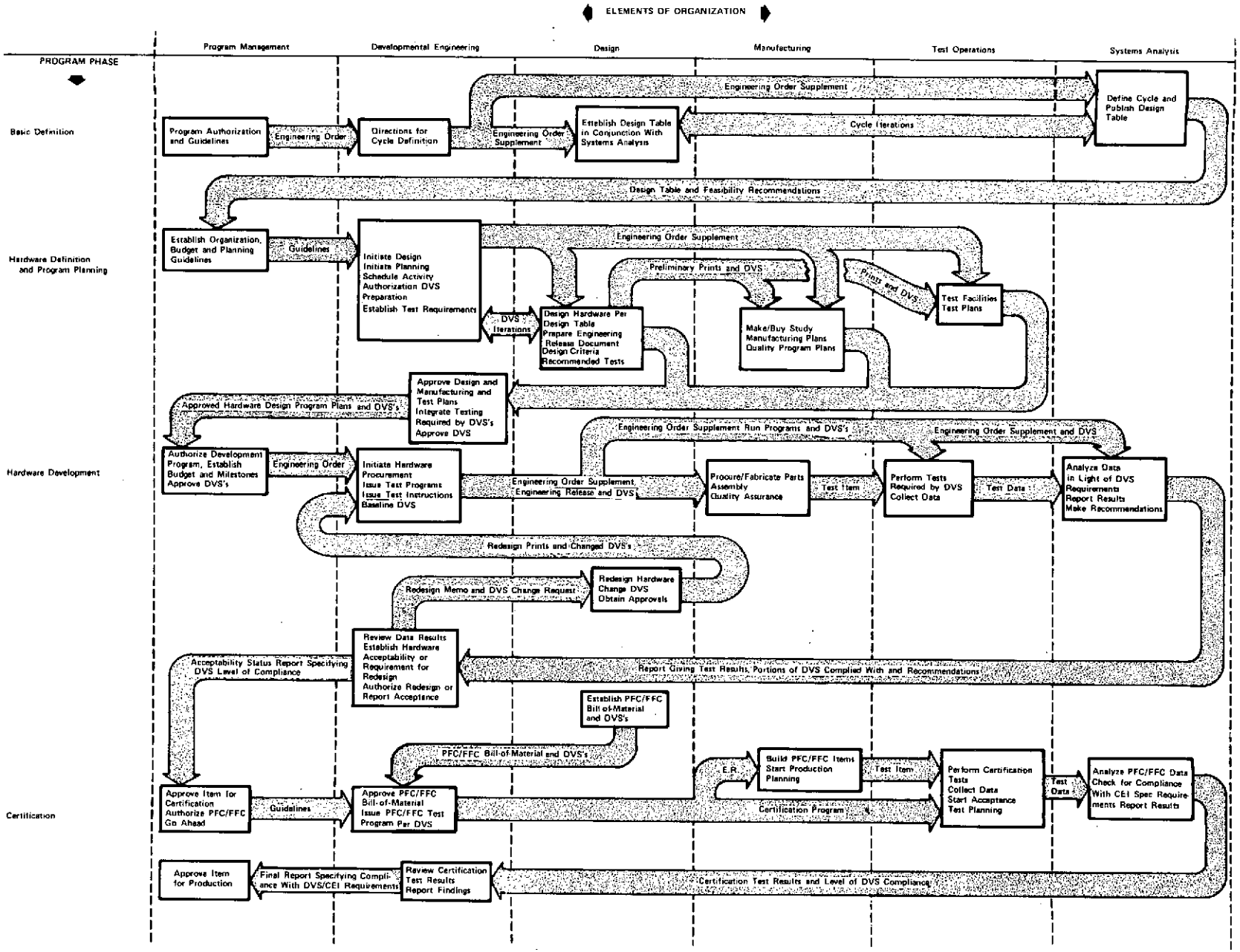

Figure 173. Incorporation of DVS Into Development Process Flow

FD 42760A

The engine test program is geared to exposing a selected sample of engines to a significant number of recycles in keeping with the long-life requirements of the program. A recycle consists of detailed teardown, inspection, and reassembly (with the original components if sufficient life remains) upon completion of a test series of up to 300 thermal cycles. This approach, in conjunction with the maintenance of detailed component and subsystem data resulting from the periodic inspections, will provide a systematic assessment of the engine life capability. Because thermal cycles rather than accumulated duration have the greatest impact on service life, the major emphasis is placed on exposing the engines to thermal cycles.

Review of testing requirements defined in the program plans indicate that basic facilities for necessary testing, excluding tests of engines with full expansion ratio (400:1) nozzles under altitude conditions, are available at FRDC but that modifications and additions would be required to satisfy all requirements. Testing of engines with full expansion ratio nozzle under altitude conditions require a facility like J-3 or J-4 test stand in the Arnold Engineering Development Center (AEDC) because the P&WA test stand (E-7) would need a new diffuser system with added capability to accomplish the planned tests. Therefore, J-3 or J-4 test stand is assumed for the full expansion ratio nozzle engine system tests. The functions and capabilities of the 24 existing test stands selected for use in the ASE development and production are given in table XXX. In addition to these stands, the FRDC Engine Control Development Area (ECDA), Instrumentation Laboratory and various test support services will be used. Estimated costs on a new item purchase basis for the additions and modifications to these facilities are included as facility/STE costs in Attachment A.

One of the more significant modifications to the test stands described in table XXX includes expansion of the existing single-bay E-8 test stand used for preburner, staged combustion, and powerhead tests to add positions for fuel and oxidizer turbopump subsystems and necessary additions to the common propellant supply capacity. Other additions and modifications include those required for testing of bearings and seals, as well as component fracture mechanics (B-4 stand), and fuel (B-17, B-19, B-20, B-22 and B-32 stands). These would largely involve addition of test positions, and expansion of propellant storage and pressurization capability and data acquisition systems. Allowance has also been made for reactivation of test stands that are not now in use.

Table XXX. Functions and Capabilities of Florida Research and Development Center Test Stands

Stand No.	Description/Use
B-4	(1) Fuel and oxidizer turbopump bearing and seal tests at engine operating temperature and speeds
	(2) Engine hardware proof-pressure and burst tests with gaseous hydrogen

Table XXX. Functions and Capabilities of Florida Research and Development Center Test Stands (Continued)

Stand No.	Description/Use
B-6	Low- and high-pressure fuel and oxidizer turbopump tests. Turbopumps would be driven by ambient temperature gaseous hydrogen; low pressure fuel and oxidizer pumps would be gear-driven by electrical motors
B-7	Preburner and main chamber torch igniter hot firings at engine operating conditions
B-11, B-23	High and low cycle fatigue material tests in hydrogen and gaseous helium environments at cryogenic and elevated temperatures
B-13	Acoustic vibration tests on nozzle panel specimens
B-16	Material tensile tests in hydrogen and gaseous helium environments at cryogenic and elevated temperatures
B-18, B-12	Engine command unit (ECU) steady-state and transient tests
B-17, B-19, B-20, B-26	Valve cyclic and seal leakage tests at engine operating pressures and temperatures, using LN_2 and LO_2
B-21, B-22	Valve, injector and flowmeter calibrations with water at pressures to 1448 N/cm^2 (2100 psi)
B-24	Temperature probe calibration at cryogenic temperatures
B-32	Valve and seal leakage tests in liquid hydrogen and gaseous hydrogen environments at pressure to 3447 N/cm^2 (5000 psi)
E-6, E-7	Simulated altitude test stand for ignition subsystem and engine system tests; exhaust pressures of 0.069 N/cm^2 (0.1 psia) can be attained at start

Table XXX. Functions and Capabilities of Florida Research and Development Center Test Stands (Continued)

Stand No.	Description/Use
E-8	Preburner, staged combustion, high pressure fuel and oxidizer turbopump tests and powerhead tests. Preburner, staged combustion and powerhead tests would be conducted in the existing center test position. Test positions for fuel and oxidizer turbopumps would be added. Run time for the pressure-fed tests (pre-combustor, staged combustion, fuel and oxidizer turbopump, and powerhead) would be approximately 200 sec at 100% thrust for the 89 kN (20,000-lb) thrust engine
E-23	Materials compatibility test with liquid oxygen
G-2	(1) Helium system flow and leakage tests at operating conditions (2) Nozzle collapse test
G-6	Engine hardware flow calibrations with low pressure gaseous nitrogen
G-13	Engine hardware flow calibration with low pressure water

Ground support equipment (GSE) will be developed concurrently with engine development to ensure compatibility between engine and GSE functions. Milestones for GSE development will be integrated with engine development milestones so that GSE will be provided for training and support of the first prototype engines to be delivered as well as for production engines. GSE development must be an integral part of engine manufacturing and development testing.

Ground support equipment items are classified into four major groups:

- Mechanical Equipment - Wrenches, covers, kits, etc.
- Electrical Equipment - Electrical checkout consoles
- Inspection Equipment - Borescopes, leak detectors, eddy current inspection equipment, radioisotope inspection equipment, etc.
- Handling Equipment - Maintenance stands, slings, adapters, and engine transporters.

A preliminary listing of the individual GSE items identified are shown in table XXXI.

Table XXXI. Preliminary Advanced Space Engine Ground Support Equipment List

Maintenance Stand

- Engine, Vertical
- Engine, Horizontal
- High Pressure Fuel/Oxidizer Turbopump
- Low Pressure Fuel/Oxidizer Turbopump
- Nozzle Extension
- Main Chamber and Primary Nozzle

Sling, Handling

- Engine
- High Pressure Fuel/Oxidizer Turbopump
- Low Pressure Fuel/Oxidizer Turbopump
- Main Chamber/Preburner Injector
- Nozzle Extension
- Main Chamber and Primary Nozzle

Adapter, Handling

- Engine, Kit
- High Pressure Fuel/Oxidizer Turbopump
- Low Pressure Fuel/Oxidizer Turbopump
- Nozzle Extension
- Main Chamber and Primary Nozzle

Adapter, Torque Wrench

- High Pressure Fuel/Oxidizer Turbopump
- Low Pressure Fuel/Oxidizer Turbopump
- Preburner Injector
- Main Chamber Injector
- Nozzle Extension
- Primary Nozzle

Inspection Unit

- Borescope
- Radioisotope
- Eddy Current
- Ultra Violet

Cover

- Engine
- Overboard Vent
- Nozzle Extension

Miscellaneous

- Pad - Protective, Primary Nozzle
- Engine Transporter
- Wrench-Borescope Plug
- Flow Tester - Pneumatic
- Pneumatic Console
- Leak Detector
- Hygrometer Unit
- Kit - Pressure Check
- Plug - Pressure Check - Main Chamber Throat
- Liquid Nitrogen Service Unit
- Inert Gas Arc Welding Set
- Adapter - Engine Installation
- Torque Check Kit - High and Low Pressure Fuel/Oxidizer Turbopump
- Plug - Main Chamber Throat
- Electrical Console - Engine Control System Static Checkout
- Component Test Console - Engine Static Checkout

The estimated propellant and ancillary fluid requirements for the ASE development program are not included in the program cost estimate and are considered to be furnished without cost by the Government. The estimated requirements are:

LH_2	8,000 tons (short, 2000 lb)
LO_2	38,000 tons (short, 2000 lb)
LN_2	6,000 tons (short, 2000 lb)
GN_2	602,000,000 scf
GHe	3,500,000 scf

2. Program Plan II (Minimum Time)

The minimum time development program for development without prior demonstration through FFC of the ASE design consists of 57 months of design, fabrication and test effort. This effort will encompass two design, build, and test cycles to FFC (PFC and FFC). The development schedule showing the major program milestones and key decision points and overall development program are shown in figure 174. The design and fabrication schedules for this program are shown in figure 175, and the program test plan is shown in figure 176.

The design and fabrication schedules are set up for early release of long-lead time material procurement and sequential drawing releases to support the fabrication process for meeting the early hardware schedules. The design effort in addition to the baseline PFC engine will include alternative designs in those areas of the ASE design that are considered to be problem areas. Emphasis will be placed on fabrication not only of the baseline hardware configurations, but also of the alternative ASE design configurations. (In a minimum time engine development effort, the problem areas must be anticipated and corrective design configurations available for test verification before the problems occur.) The alternative design configurations selected for verification are based on the results of thorough failure mode and effect analyses (FMEA).

The test program includes concurrent testing and evaluation of the baseline and alternative configurations. As soon as one configuration shows that the design requirements can be achieved and satisfy the engine system, the effort on other configurations, baseline or alternative, is immediately dropped.

The order in which testing is planned, the program objectives of this program do not differ from Program Plan I (minimum cost). More engines, hardware sets and testing are necessary, however, because of the alternative design configurations. These additional engines, hardware sets, and testing will require expenditure of premium time to meet the planned milestones. A premium time expenditure of about 20% of the total direct effort is estimated to be required for this program.

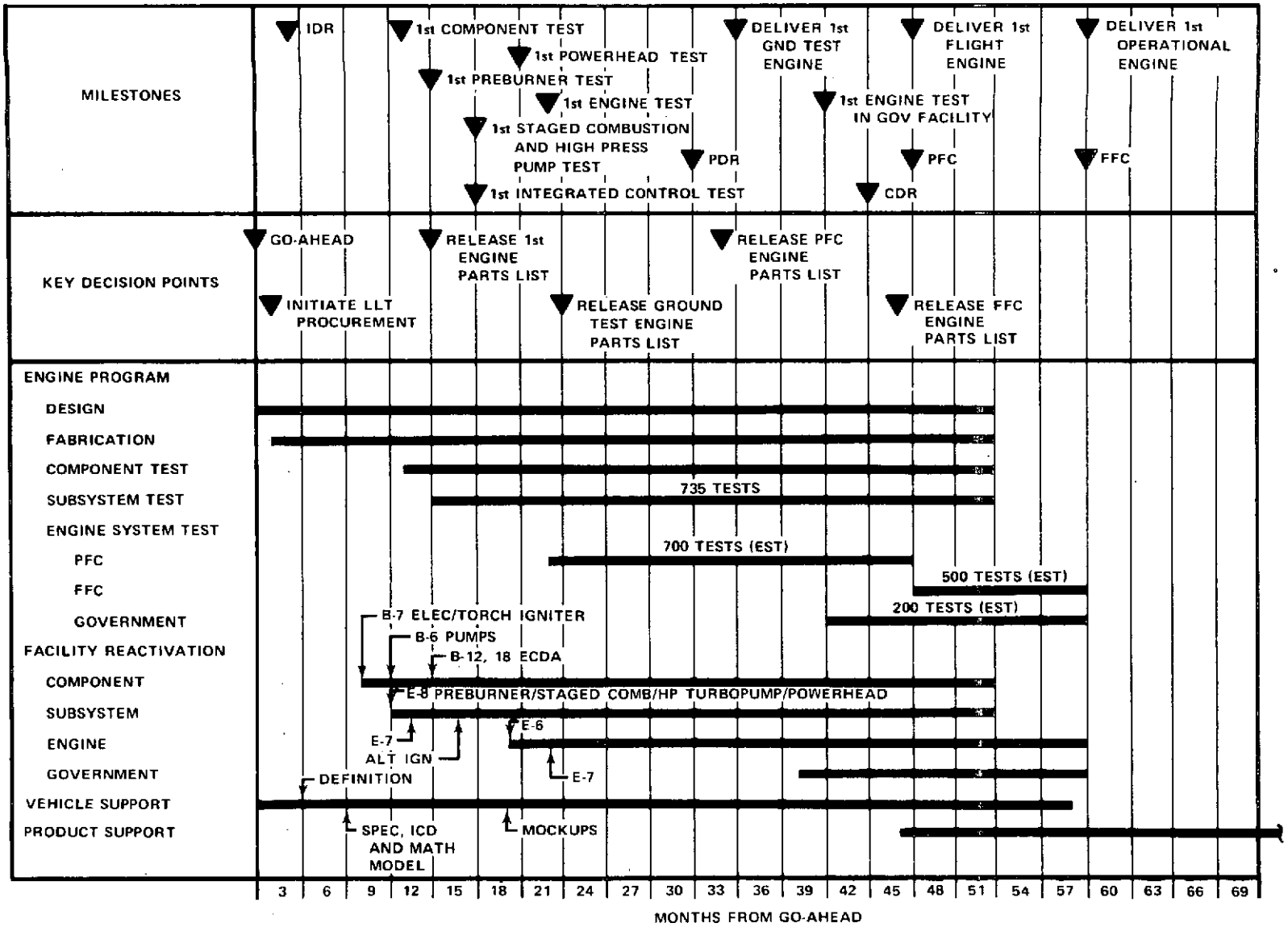

Figure 174. Schedule, Program Plan II (Minimum Time) FD 68850C

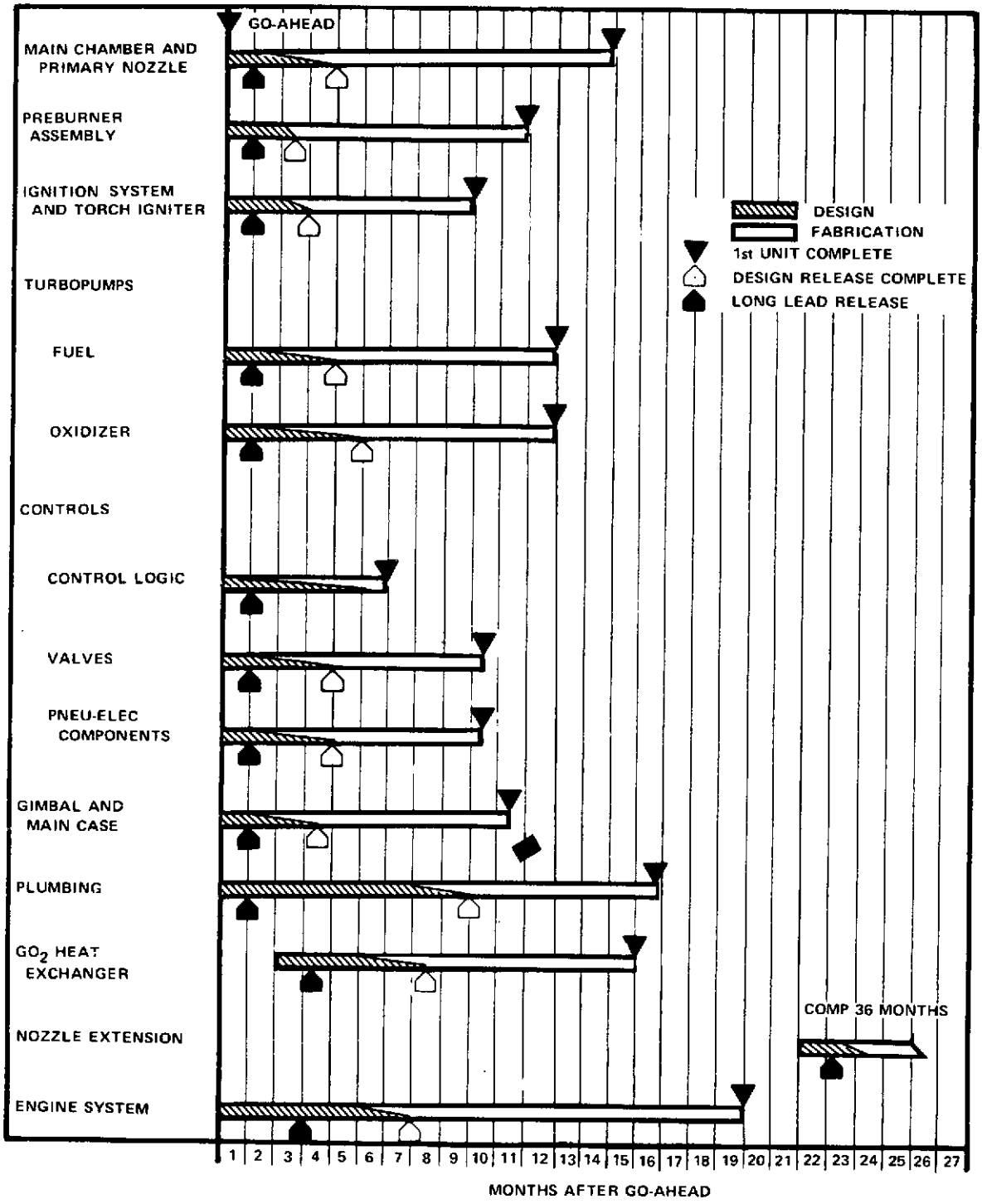

Figure 175. Design and Fabrication Schedule - First Unit Delivery, Program Plan II (Minimum Time) FD 68851A

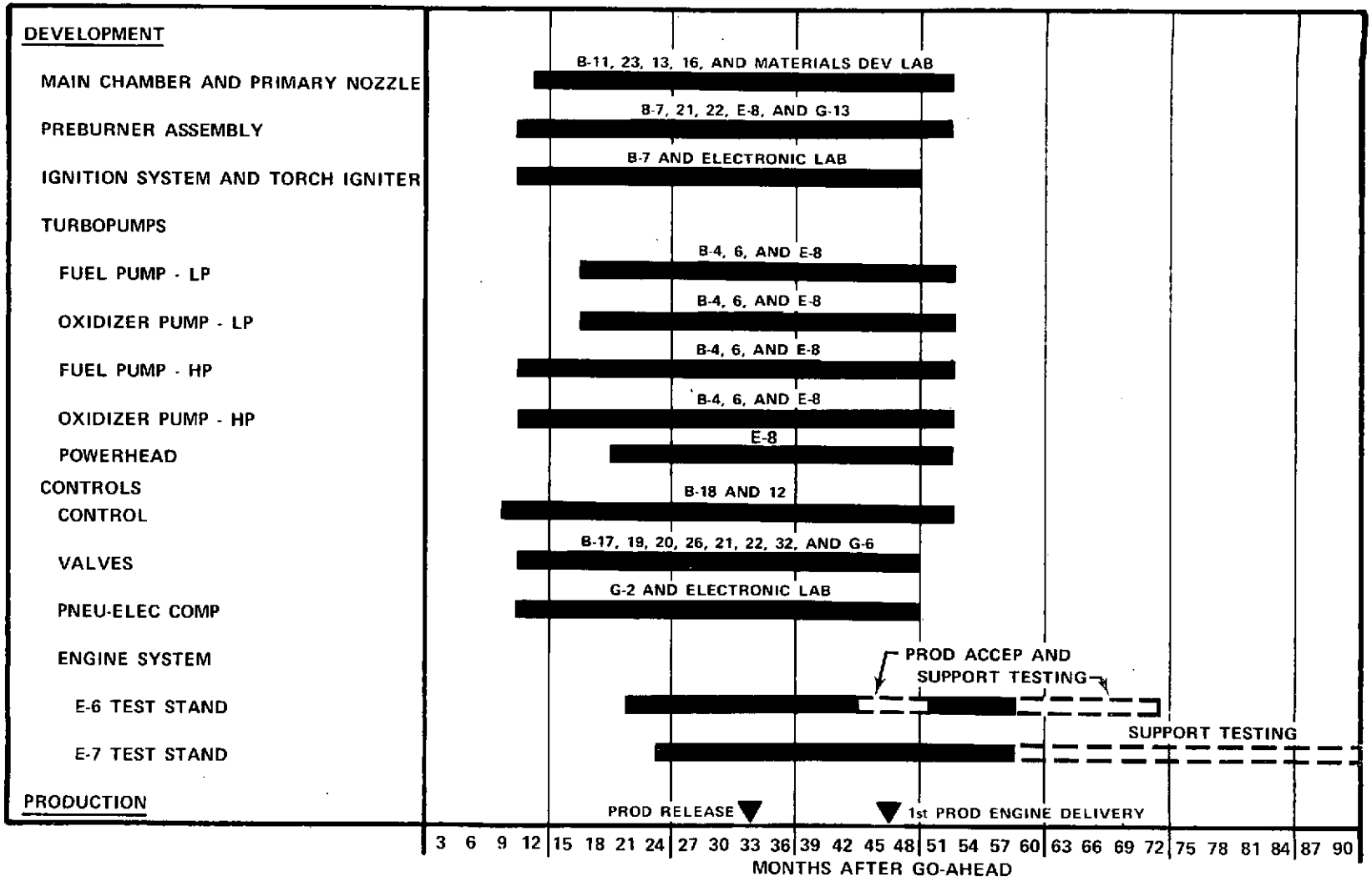

Figure 176. Test Plan, Program Plan II (Minimum Time)

FD 68852A

The initial component and subsystem testing is planned to demonstrate feasibility for engine use rather than to accomplish design verification requirements as in the minimum cost program. The emphasis is to shift as quickly as possible to engine systems testing so that the hard-to-find failures and malfunctions will be manifested within the planned schedule.

Seven new engines were selected for the development program based on the above considerations and particular characteristics of the staged combustion turbine power cycle. A total of 195 engine builds, including rebuilds, will be used for the minimum time complete development program. Approximately 67 equivalent engine sets of hardware are planned to support the assembly and test programs.

Historical RL10 and XLR129 design, fabrication and test experience was used as a guideline for establishing the duration of the overall minimum time development effort and the number of engine system tests. It was estimated that about 1400 engine system tests over a period of 37 months, combined with a 12-month design, fabrication and initial component test period and 8-month initial subsystem test period would be necessary to accomplish the minimum time development program objectives. Duration of the overall development effort is estimated to be 57 months. Duration of this program is not directly comparable to that of any RL10 program but was based on the RL10 engine system test experience on test stands E-6 and E-7 (35 engine tests/month) and by reducing by about 20% the time to the first engine system test estimated for Phase I (20 months as opposed to 27 months). The program objectives are planned to be achieved by the use of premium time during the design, fabrication, initial component testing, and subsystem testing periods.

Detailed component hardware and test requirements are not included for the same reasons as stated under Program Plan I.

Subsystem testing requirements are estimated to be the same as those specified in Program Plan I except that 50 additional powerhead tests are considered necessary for pre-engine systems testing of alternative design configurations.

Facility and STE requirements are the same as those defined in Program Plan I. Additional expense is estimated to be required, however, so that the facilities will be available to meet the planned milestones.

Ground support equipment will be handled as described in Program Plan I and includes those items listed in table XXXI.

The estimated propellant and ancillary fluid requirements for the ASE development program are not included in the program cost estimate and are considered to be furnished without cost by the Government. The estimated requirements are:

LH_2	9,500 tons (short, 2,000 lb)
LO_2	42,000 tons (short, 2,000 lb)
LN_2	7,000 tons (short, 2,000 lb)

GN_2	702,000,000 scf
GHe	4,000,000 scf

D. CONFIGURATION MODIFICATIONS

1. Retractable Nozzle Extension

An Advanced Space Engine with a retractable nozzle extension (200:1 to 400:1 area ratio) was evaluated.

The engine development program for the retractable nozzle version of the ASE is the same as described under Program Plans I and II. There will be additional design and manufacturing requirements for those items peculiar to the retractable nozzle (for example, translating mechanism and supporting structures). There is no change in the estimated development program duration or the number of engine system tests considered necessary to accomplish program objectives.

Ground support equipment requirements will change as required to handle an engine with a retractable nozzle extension. There is no change in the estimated program cost for GSE development because these requirements would be included in the initial design and, further, are considered to be relatively small and within the estimating ability of ASE ground support equipment requirements. The estimated increase in engine system dry weight for a retractable nozzle extension version of the ASE is 24.5 kg (54.0 lb), of which 8.6 kg (19 lb) is caused by the increased length of the tubular nozzle and the remaining 15.9 kg (35 lb) is the weight of the nozzle retraction system. Because of the increase in size of the regeneratively cooled portion of the nozzle, the specific impulse of this version of the ASE is increased by 11.8 N-s/kg (1.2 sec).

The estimated cost of the retractable nozzle extension version of the ASE, which is provided as a delta cost to the base engine development program cost, and the base production unit cost is presented in Attachment A.

2. Advanced Space Engine/Vehicle Interfaces Compatible With RL10A-3-3 Engine/Vehicle Interfaces

An Advanced Space Engine with engine/vehicle interfaces compatible with the RL10A-3-3 engine/vehicle interfaces was evaluated. The engine development program is the same as described under Program Plans I and II. It is estimated that there would be no change in engine development program requirements or costs for this version of the ASE as long as these features are included in the initial design of the ASE. There is no change in engine dry weight to make the ASE baseline engine/vehicle interfaces compatible with the RL10A-3-3 engine/vehicle interfaces.

Figure 177 shows the RL10 engine outline installation configuration and identifies the significant engine/vehicle dimensional interfaces. The mechanical interfaces for the retractable nozzle configured engine and the engine with vehicle/engine interfaces compatible with the RL10A-3-3 engine are shown in figures 178 and 179. Table XXXII shows the actual interface dimensional difference between RL10, ASE baseline and ASE with engine/vehicle interfaces compatible with the RL10.

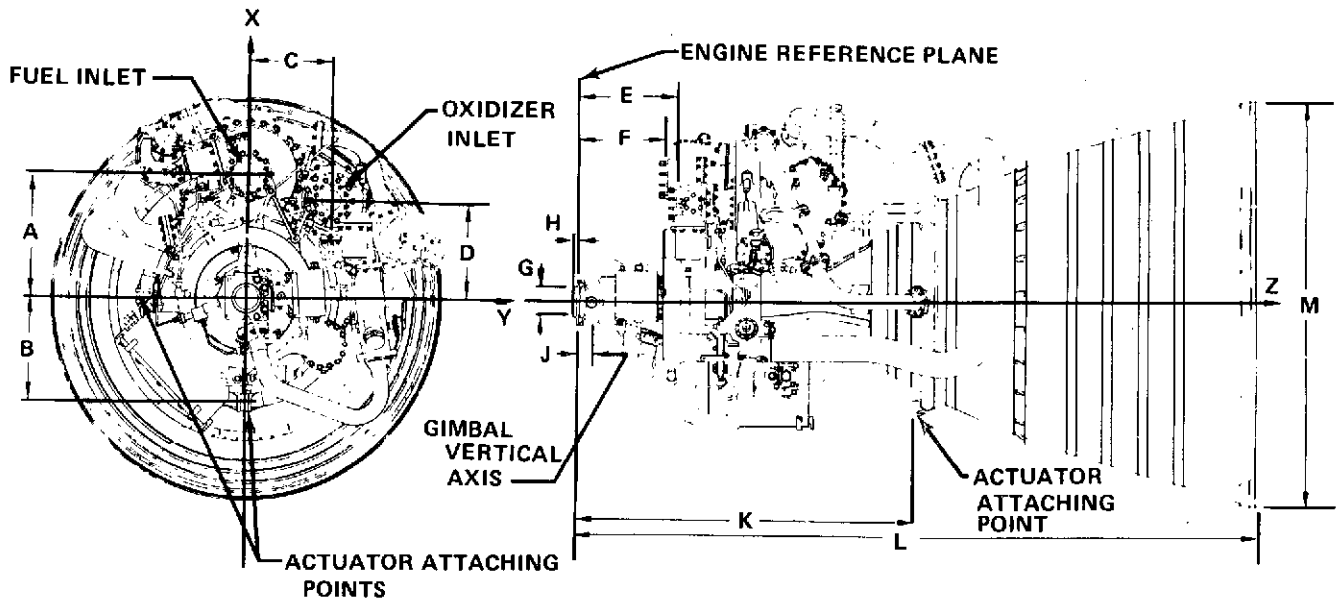

Figure 177. RL10 Outline Installation Drawing

FD 68853A

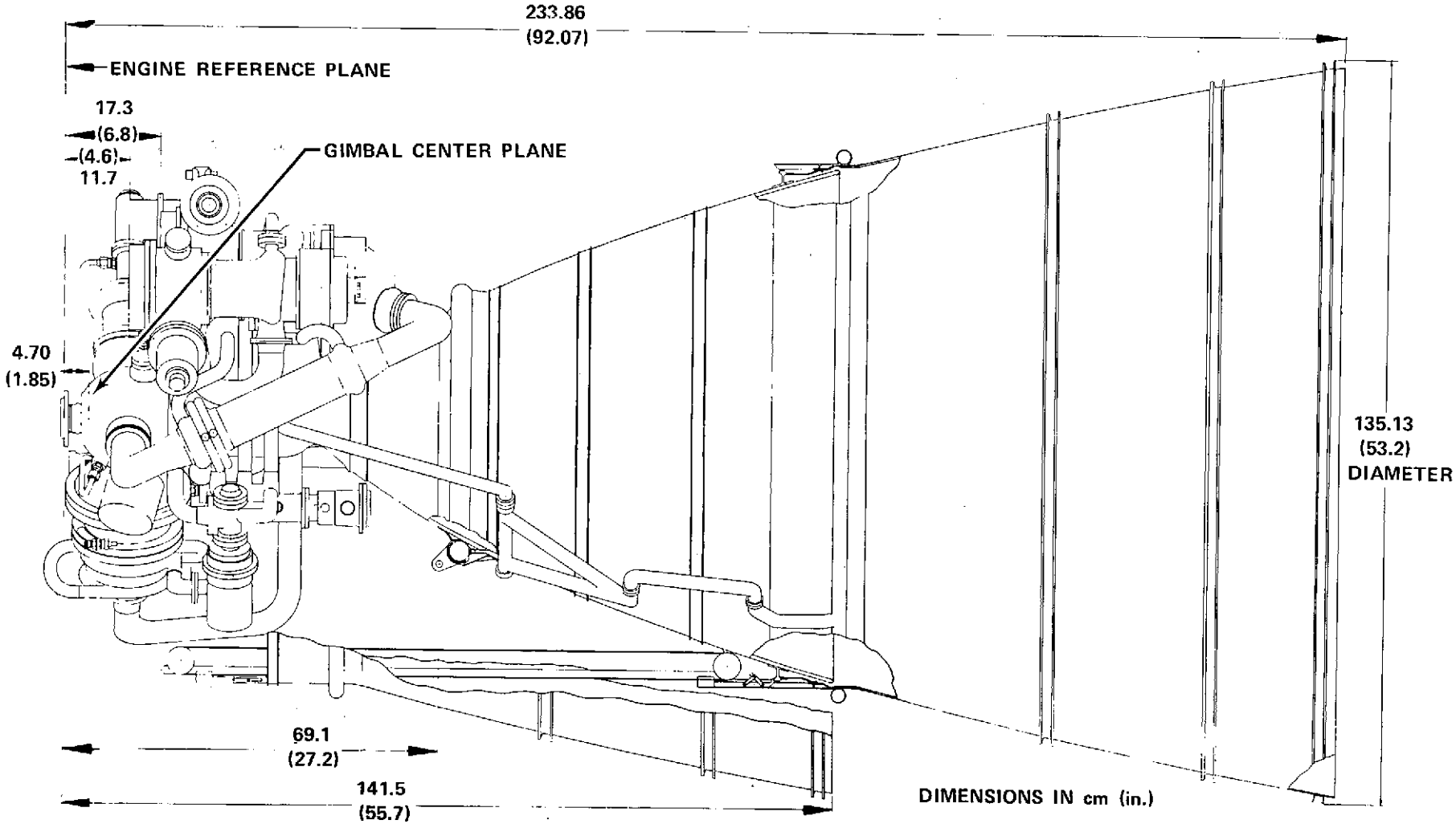

Figure 178. Mechanical Interfaces for Retractable Nozzle Engine

FD 70072A

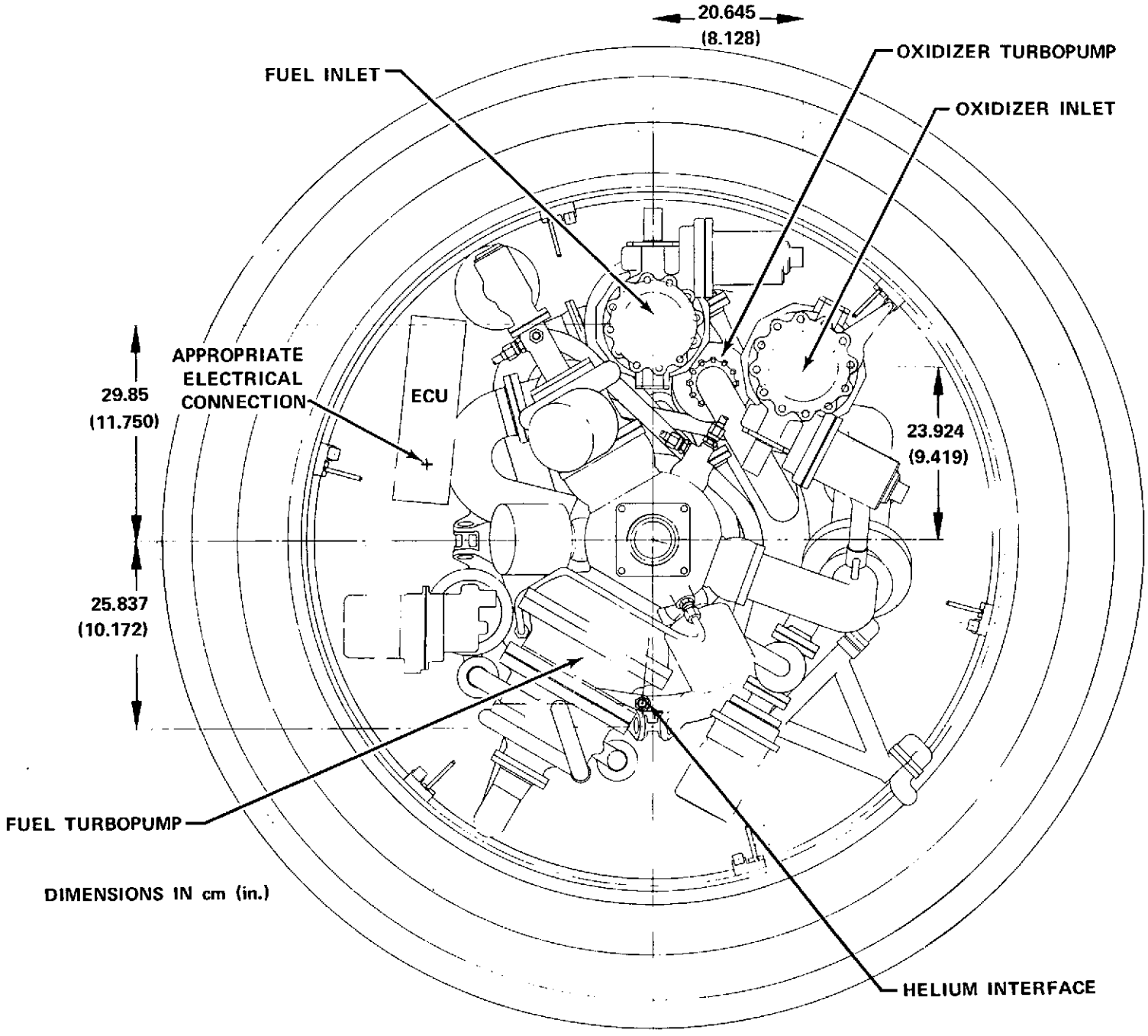

Figure 179. ASE Interfaces Compatible With RL10A-3-3 Engine

FD 70073A

Table XXXII. Dimensional Comparisons of RL10, ASE With Engine/ Vehicle Interfaces Compatible With RL10, and Baseline ASE

Dimension*, cm (inches)	Description	RL10	ASE/RL10	Baseline ASE
A	Y Axis to Fuel Inlet	29.845 (11.750)	29.845 (11.750)	6.86 (2.7)
Al	X Axis to Fuel Inlet	0.0	0.0	18.42 (7.25)
B	Radius to Actuator Attachment	25.837 (10.172)	25.837 (10.172)	19.1 (7.5)
C	X Axis to Oxidizer Inlet	20.645 (8.128)	20.645 (8.128)	4.19 (1.65)
D	Y Axis to Oxidizer Inlet	23.924 (9.419)	23.924 (9.419)	22.99 (9.05)
E	ERP to Oxidizer Inlet	24.392 (9.603)	11.6 (4.6)	0.0 0.0
F	ERP to Fuel Inlet	24.735 (8.738)	17.3 (6.8)	5.6 (2.2)
G	Interface Diameter	7.305 (2.876)	7.305 (2.876)	N/A
H	Interface Height	0.610 (0.240)	0.610 (0.240)	N/A
J	ERP to Gimbal Plane	3.810 (1.500)	4.70 (1.85)	4.70 (1.85)
K	ERP to Actuator Attachment Point	83.500 (32.874)	69.1 (27.2)	58.12 (22.88)
L	Engine Length	178.05 (70.10)	233.86 (92.07)(Ext) 141.5 (55.7) (Ret)	233.86 (92.07)
M	Exit Diameter	100.43 (39.54)	135.1 (53.2)	135.1 (53.2)
Fuel	Fuel Inlet Diameter	5.476 (2.156)	8.53 (3.36)	8.53 (3.36)
Oxidizer	Oxidizer Inlet Diameter	4.877 (1.920)	9.68 (3.81)	9.68 (3.81)

*See figure 177

N/A Not Applicable

E. VEHICLE/ENGINE REQUIREMENTS

1. Performance

The Advanced Space Engine assembly basic performance information that may be used for initial vehicle study use is shown in tables XXXIII through XXXV. Figures 180 and 181 show the predicted start and shutdown characteristics, respectively.

Table XXXIII. Full Thrust Performance Characteristics for ASE

Thrust (vac), N (lb)	89,000 (20,000)
Mixture Ratio	6 ± 0.5
Chamber Pressure, N/cm^2 (psia)	1324 ± 14 (1920 ± 20)
Expansion Ratio	400:1
Length, cm (in.)	233.86 (92.07)
Diameter (maximum), cm (in.)	135.13 (53.2)
Best Estimate Specific Impulse, N-s/kg (sec)*	4623.8 (471.5)
Nominal Fuel Inlet Conditions	
Temperature, °K (°R)	21.3 (38.3)
Pressure, N/cm^2 (psia)	13.7 (19.9)
Nominal Oxidizer Inlet Conditions	
Temperature, °K (°R)	92.2 (166.0)
Pressure, N/cm^2 (psia)	13.2 (19.1)
Required NPSH, N-m/kg (ft)	
Fuel	45 (15)
Oxidizer	6 (2)
Life	
Service Free	
Accumulated Operating Time, hr	2
Thermal Cycles	60
Minimum Operating Time, ** hr	10
Thermal Cycles**	300
Fuel Tank Pressurization Flow	
Flow, kg/s (lb/sec)	0.015 (0.034)
Temperature, °K (°R)	274 (494)
Oxidizer Tank Pressurization Flow	
Flow, kg/s (lb/sec)	0.061 (0.134)
Temperature, °K (°R)	235 (423)

*Add 11.8 N-s/kg (1.2 sec) for two-position nozzle configuration
**Between overhauls

Table XXXIV. Tank Head Idle Performance Characteristics for Saturated Liquid Propellants

Thrust (vac), N (lb)	245 (55)
Mixture Ratio	1.5:1
Chamber Pressure, N/cm^2 (psia)	4.1 (6.0)
Specific Impulse, N-s/kg (sec)	3942 (402)
Nominal Fuel Inlet Conditions	
Temperature, °K (°R)	21.3 (38.3)
Pressure, N/cm^2 (psia)	13.5 (19.6)

Table XXXIV. Tank Head Idle Performance Characteristics for Saturated Liquid Propellants (Continued)

Nominal Oxidizer Inlet Conditions	
Temperature, °K (°R)	92.8 (167.0)
Pressure, N/cm^2 (psia)	12.5 (18.1)
Minimum Fuel NPSH, N-m/kg (ft)	0 (0)
Minimum Oxidizer NPSH, N-m/kg (ft)	0 (0)

Table XXXV. Pumped Idle Performance Characteristic for ASE

Thrust (vac), N (lb)	3559 (800)
Mixture Ratio	3.5:1
Chamber Pressure, N/cm^2 (psia)	54 (79)
Specific Impulse, N-s/kg (sec)	4413 (450)
Nominal Pump Inlet Pressure, N/cm^2 (psia)	
Fuel	13.5 (19.6)
Oxidizer	12.5 (18.1)
*Minimum Fuel NPSH, N-m/kg (ft)	0 (0)
*Minimum Oxidizer NPSH, N-m/kg (ft)	0 (0)
Maximum O_2 Pressurant Flow, kg/s (lb/sec)	0.4 (0.09)
at Temperature, °K (°R)	144 (260)
Maximum H_2 Pressurant Flow, kg/s (lb/sec)	0.058 (0.013)
at Temperature, °K (°R)	299 (538)

*Without tank pressurization

2. Weight

The base ASE dry weight is 178.3 kg (393 lb). Add 24.5 kg (54.0 lb) for the retractable nozzle extension version.

3. Envelope

The base ASE envelope is shown in figure 182. The ASE envelope with RL10 interface and a retractable nozzle extension are shown in figures 183 and 184.

4. Vehicle/Engine Interfaces

The baseline engine interface design was designed to the requirements as specified in Contract NAS3-16750.

This subsection will primarily define the following interface requirements for the Baseline ASE Engine:

1. Mechanical Connections
2. Autogenous Tank Pressurization Characteristics
3. Electrical Requirements
4. Pneumatic Requirements
5. Engine Instrumentation Requirements
6. Engine Inlet Characteristics

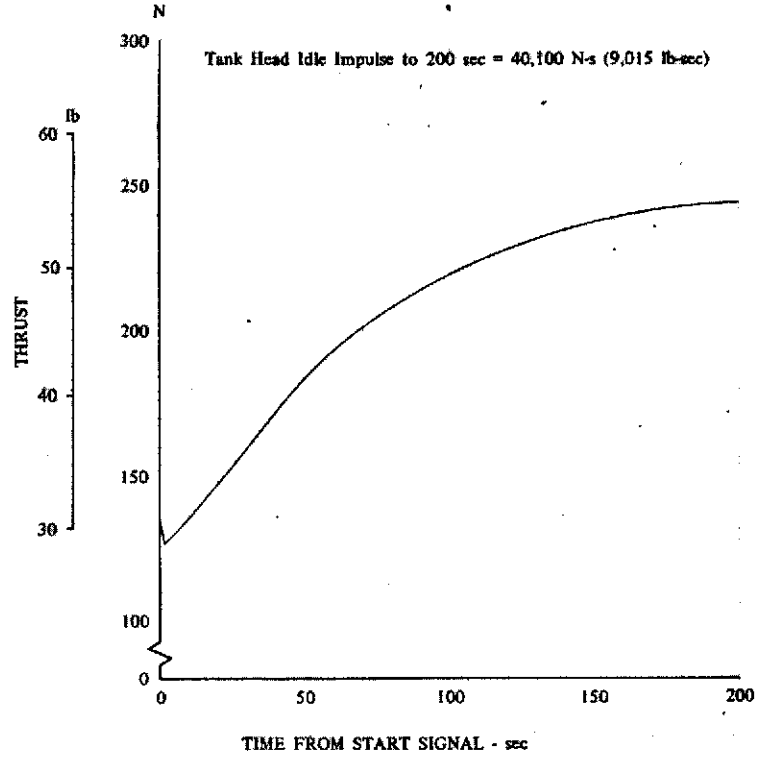

Figure 180a. Tank Head Idle Thrust Characteristic DF 97686

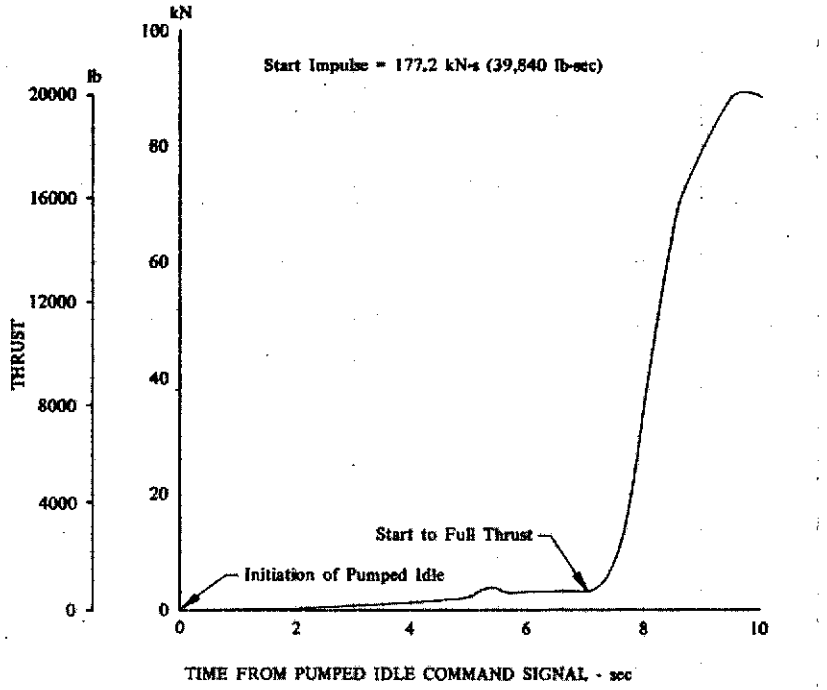

Figure 180b. Start Transient Thrust from Initiation of Pumped Idle to Full Thrust DF 97685

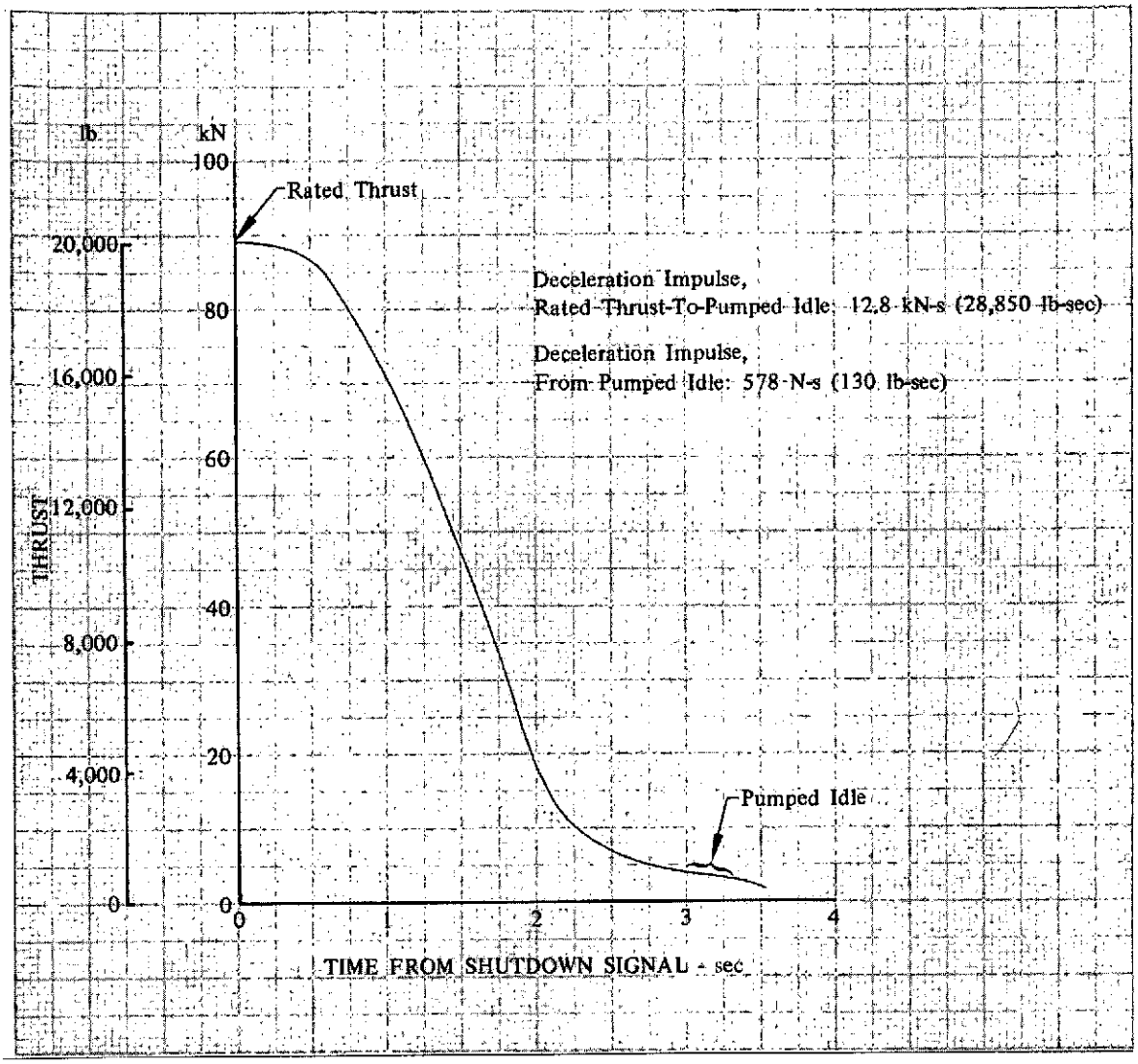

Figure 181. Advanced Space Engine Deceleration Transient DF 96262

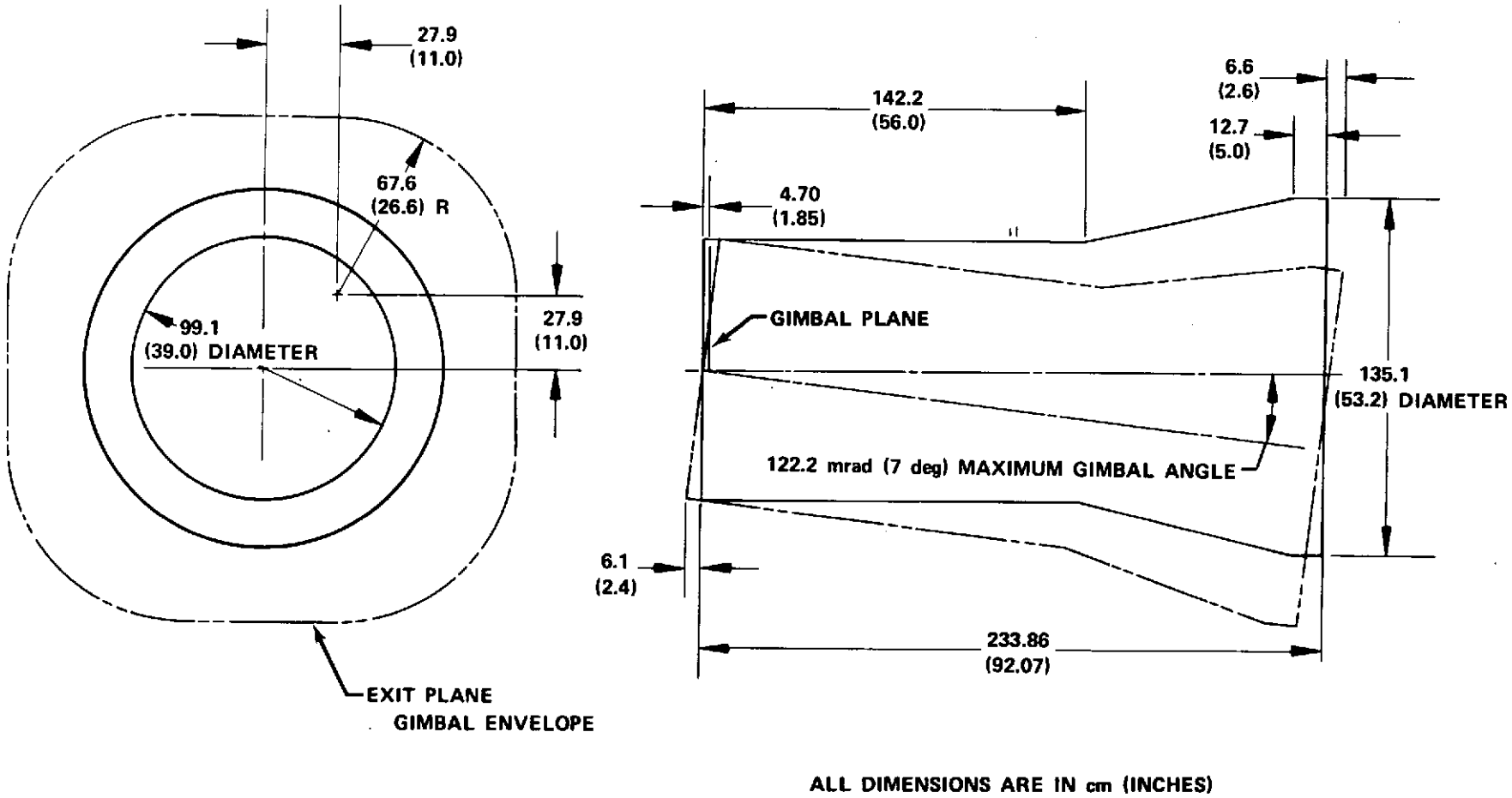

Figure 182. Advanced Space Engine (Baseline) Dynamic Envelope

FD 68854A

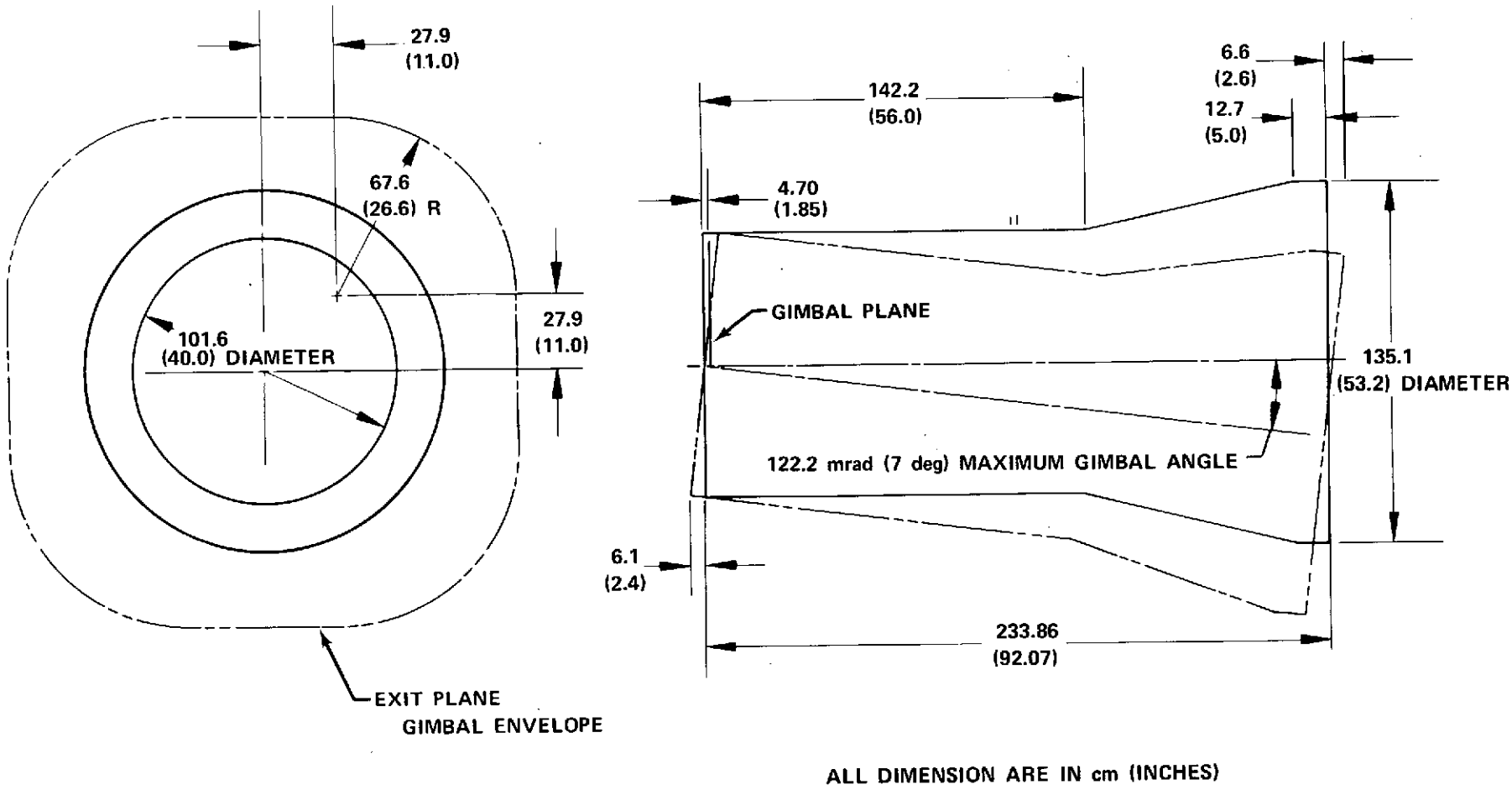

Figure 183. Extended Dynamic Envelope of Advanced Space Engine With RL10 Interfaces and Retractable Nozzle Extension

FD 68855A

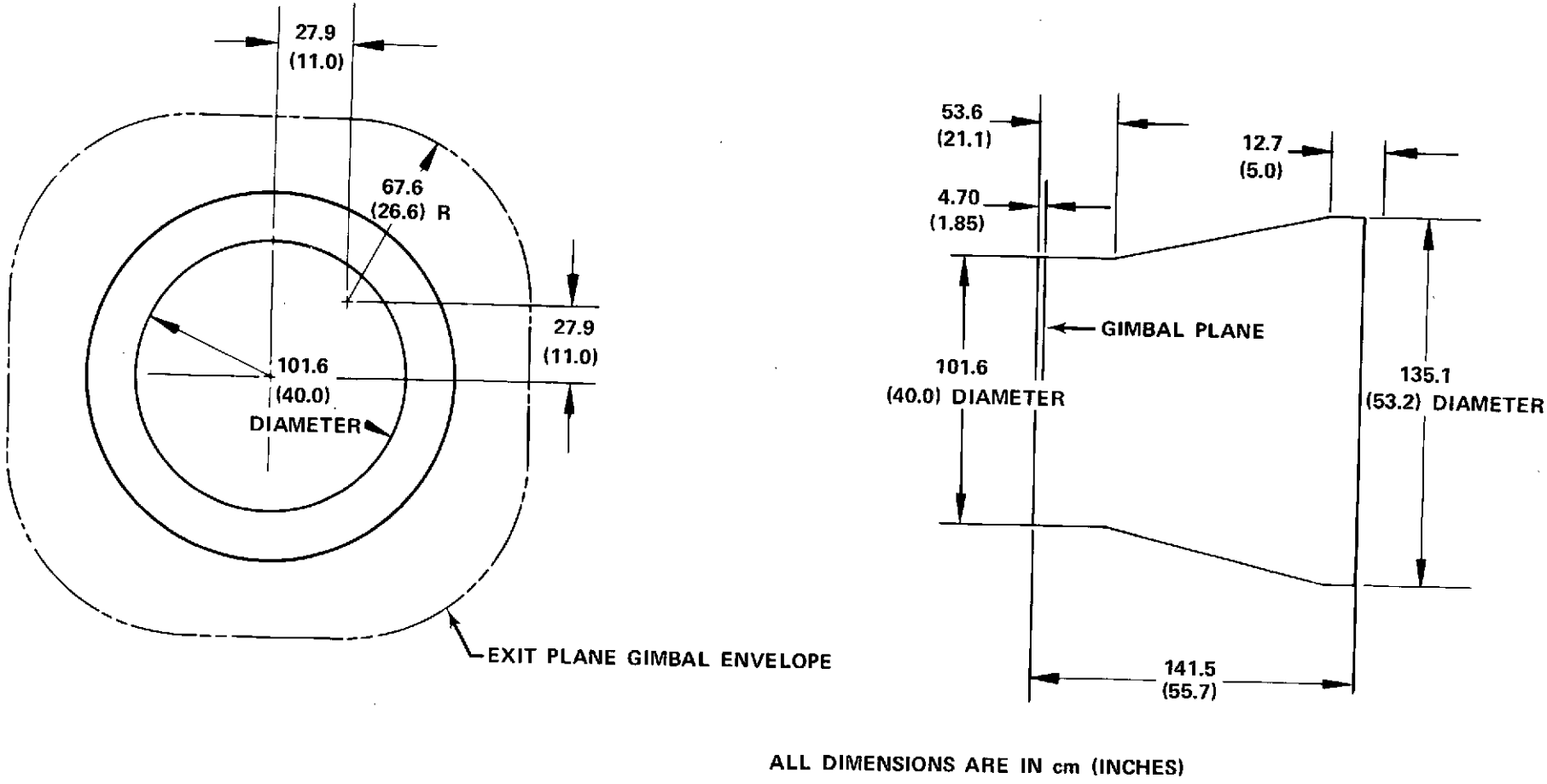

Figure 184. Advanced Space Engine With RL10 Interfaces and Retracted Nozzle Extension Envelope FD 68856A

a. Mechanical Connections

Mechanical connections between the engine and vehicle consists of the thrust mount, propellant inlets, pneumatic and electrical interface connections, and gimbal actuator attach points. The baseline engine mechanical interfaces are shown in figure 185, sheets 1 and 2.

The thrust mount is a mechanical connection at the forward end of the engine gimbal block. Propellant inlet connections are at the inlet shutoff valves with the interface slightly below the gimbal plane.

The pneumatic and electrical interfaces provide multiple-pin type connections for electrical power, control signals, and monitoring data and connections for pneumatic supply to the engine.

Two attach points for gimbal actuators are provided. The attach points and the engine are designed for gimbaling at an acceleration of 20 rad/sec^2 and a ± 122.2 mrad (7-deg) gimbal pattern. Engine design is such that no portion of the engine intrudes into the gimbal plane during any phase of operation, with the exception of the fuel pump bypass tube.

b. Autogenous Tank Pressurization

Warm hydrogen and oxygen are provided at the interface for use in vehicle pressurization. Pressurant conditions for pumped idle are shown in figures 186 and 187 for the oxidizer and fuel pressurants. The pressurant conditions for full thrust operations for the oxidizer and fuel pressurants are shown in figures 188 and 189.

c. Electrical Requirements

Electric power, shown in figure 190, is required in the following areas: engine control unit, control valves, solenoid valves, instrumentation, and ignition. The electrical controls required are: preburner ignition system, main chamber ignition system, solenoid valves, and valve control stepper motors.

The maximum power requirement based on a 28 v dc supply (all components operating simultaneously) is estimated as follows:

1.	ECU	100 w	
2.	Ignition System	210 w	
3.	Control Valve Stepper Motors	496 w	(3 at 132 w and 1 at 100 w)
4.	Solenoid Valves	196 w	
	TOTAL	1002 w maximum	

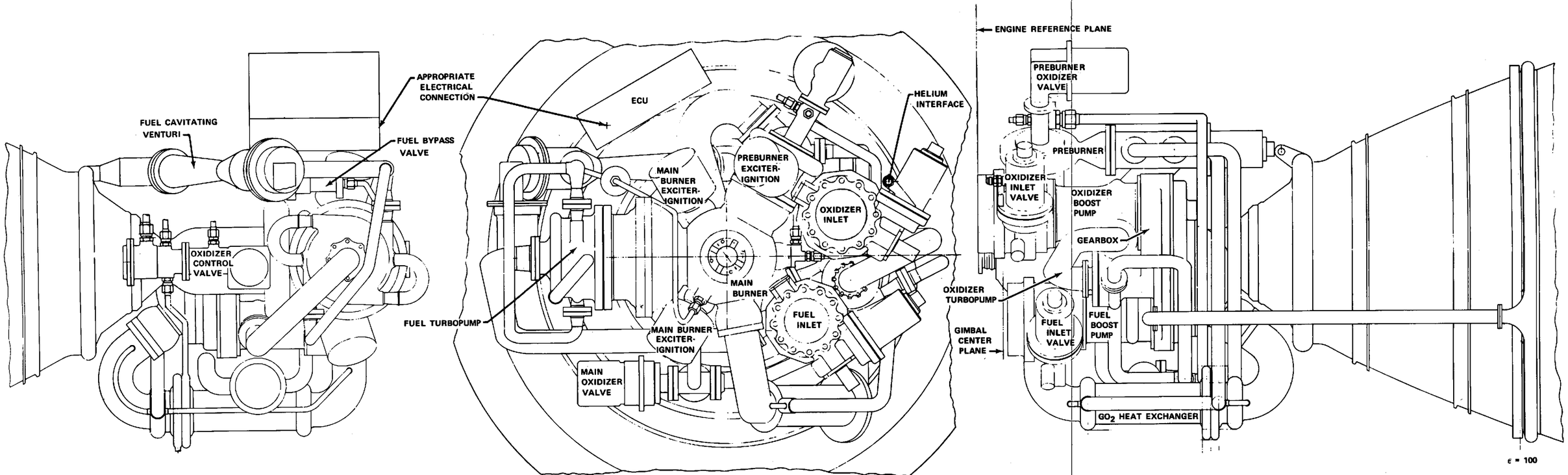

Figure 185. Advanced Space Engine Installation (Sheet 1)

FD 68857A

FOLDOUT FRAME

FOLDOUT FRAME 2

FOLDOUT FRAME 3

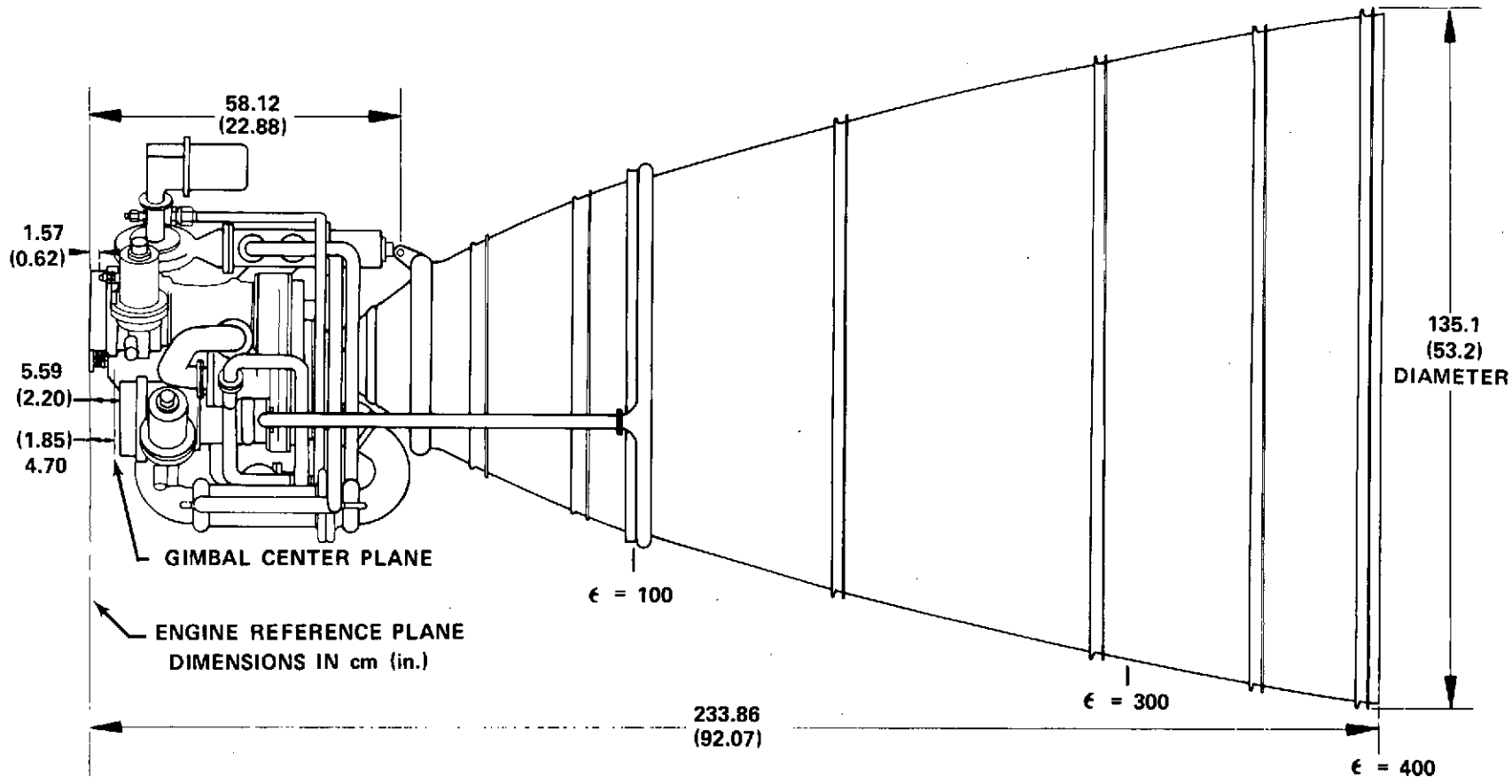

Figure 185. Advanced Space Engine Installation (Sheet 2)

FD 68858B

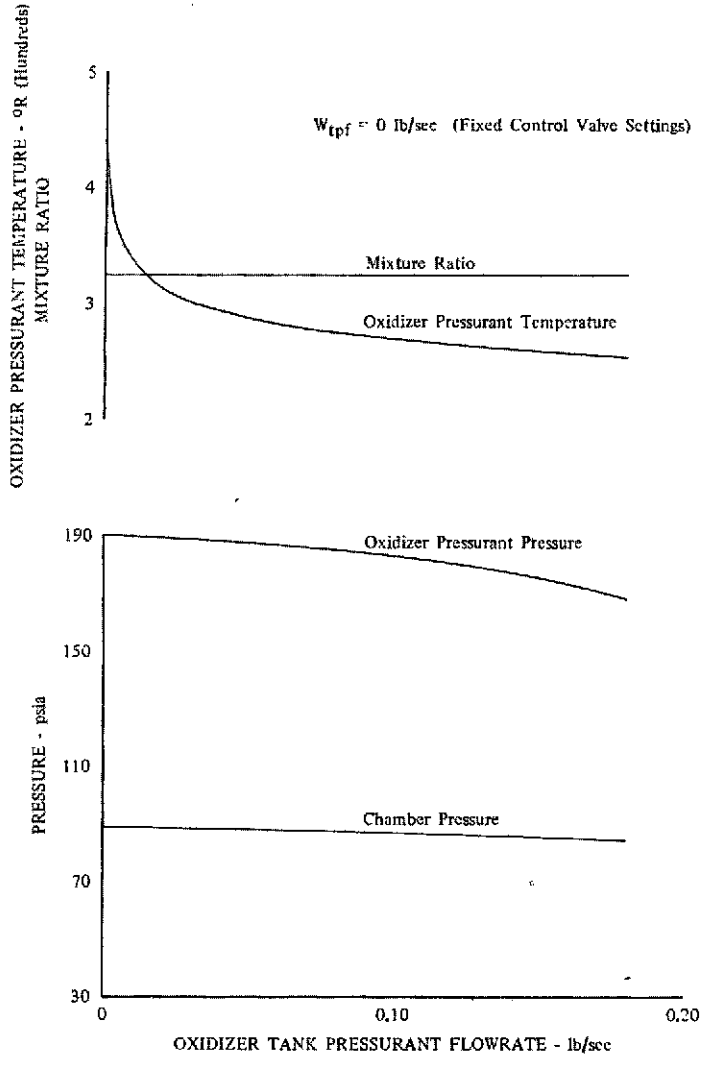

Figure 186. Effect of Oxidizer Tank Pressurant Flowrate at Pumped Idle

DF 95612

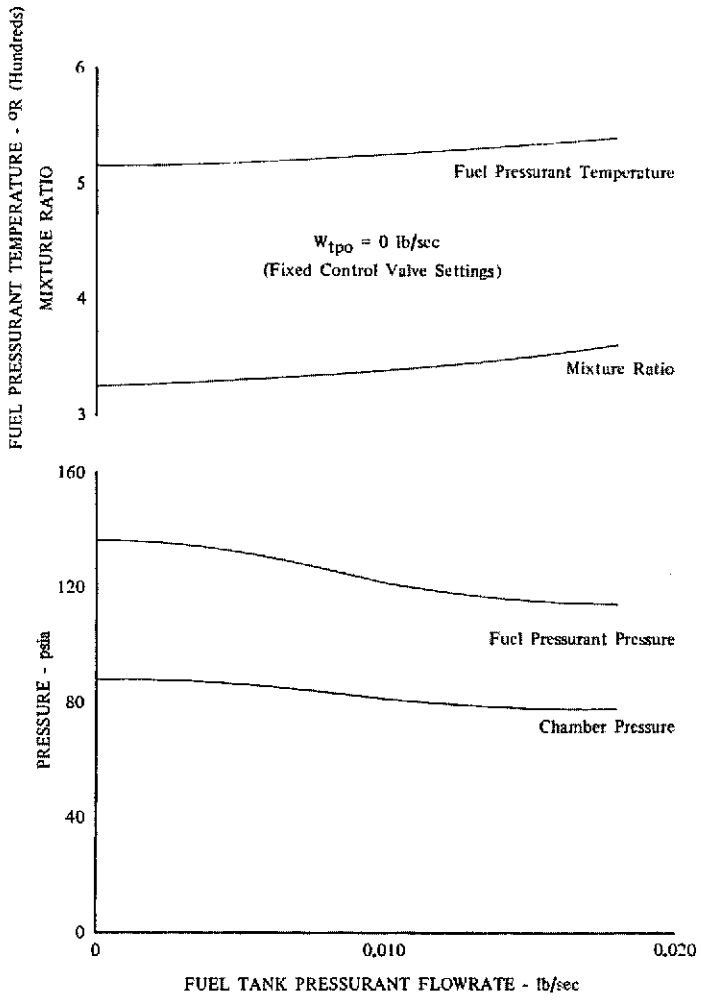

Figure 187. Effect of Fuel Tank Pressurant Flowrate at Pumped Idle

DF 95613

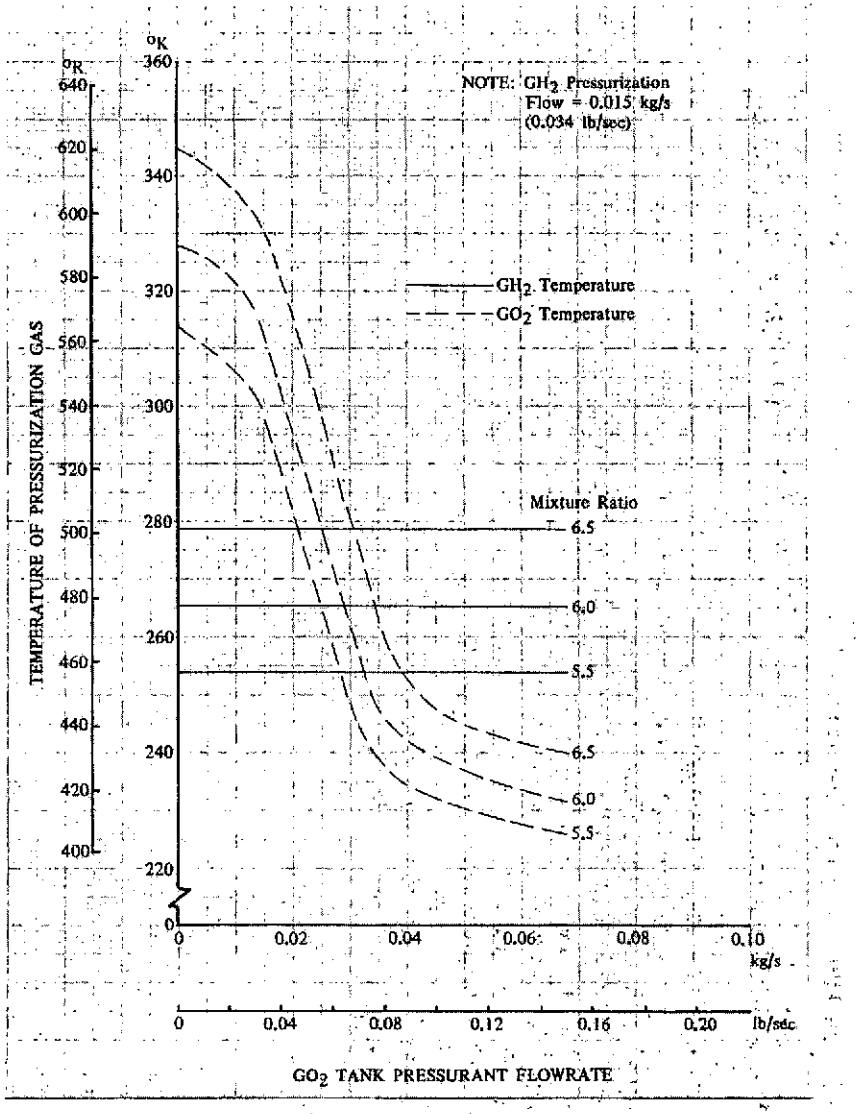

Figure 188. Advanced Space Engine Effect of Varying GO_2 Tank Pressurization Flow on Pressurization Temperature at Full Thrust

DF 96256

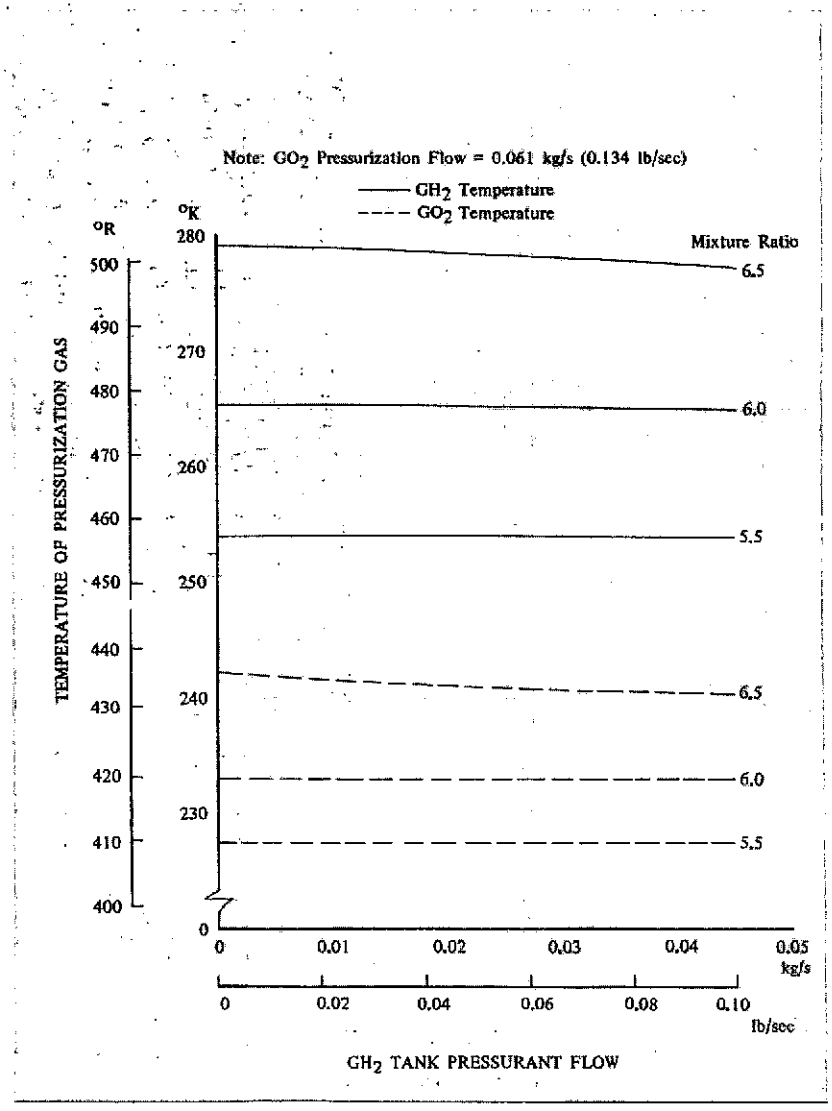

Figure 189. Advanced Space Engine Effect of Varying GH_2 Tank Pressurization Flow on Pressurization Temperature at Full Thrust

DF 96257

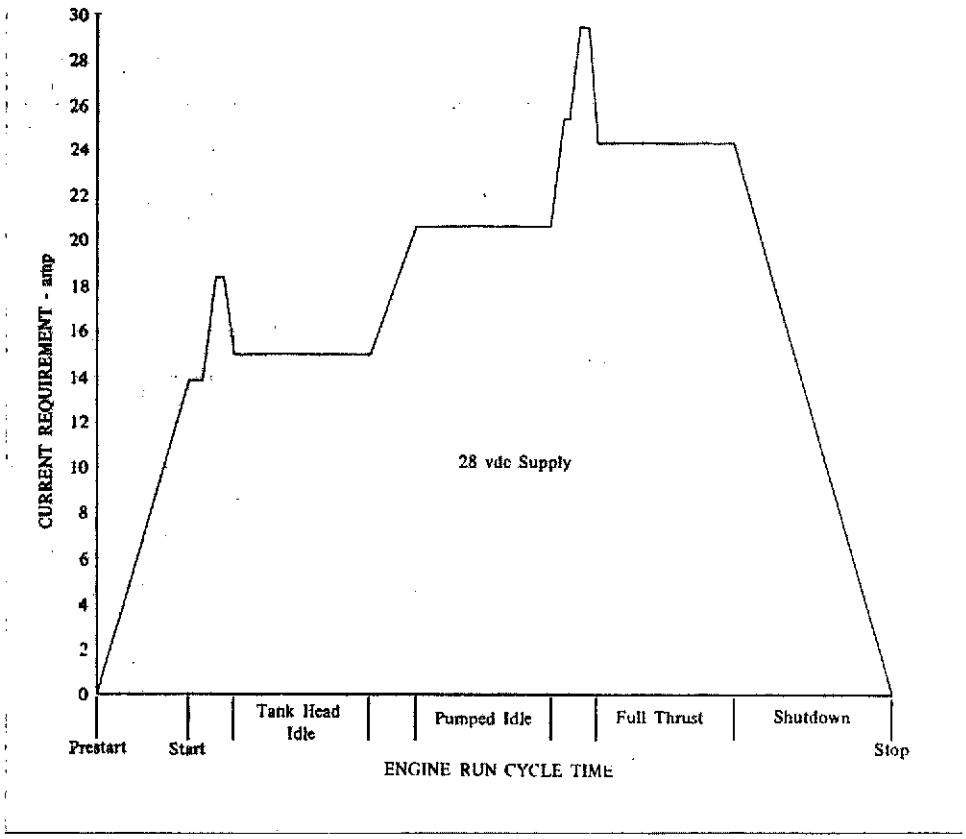

Figure 190. Engine Electrical Power Requirement DF 95616

d. Pneumatic Requirements

The engine control system will require a 345 N/cm^2 (500 psia) regulated supply of gaseous helium to the engine supply connection. Helium pressure will be used to actuate the fuel shunt valve, fuel bypass valve, oxidizer inlet suction valve and the fuel inlet suction valve. Helium flow will also be required to purge the preburner prior to ignition (rated thrust mode of operation) and to purge the propellant flow system after shutdown. Helium flow will be controlled by solenoid valves which are actuated according to the ECU controlling mode. A typical pneumatic schematic is shown in figure 191.

Maximum helium usage rate, including solenoid valve leakage, is shown in table XXXVI.

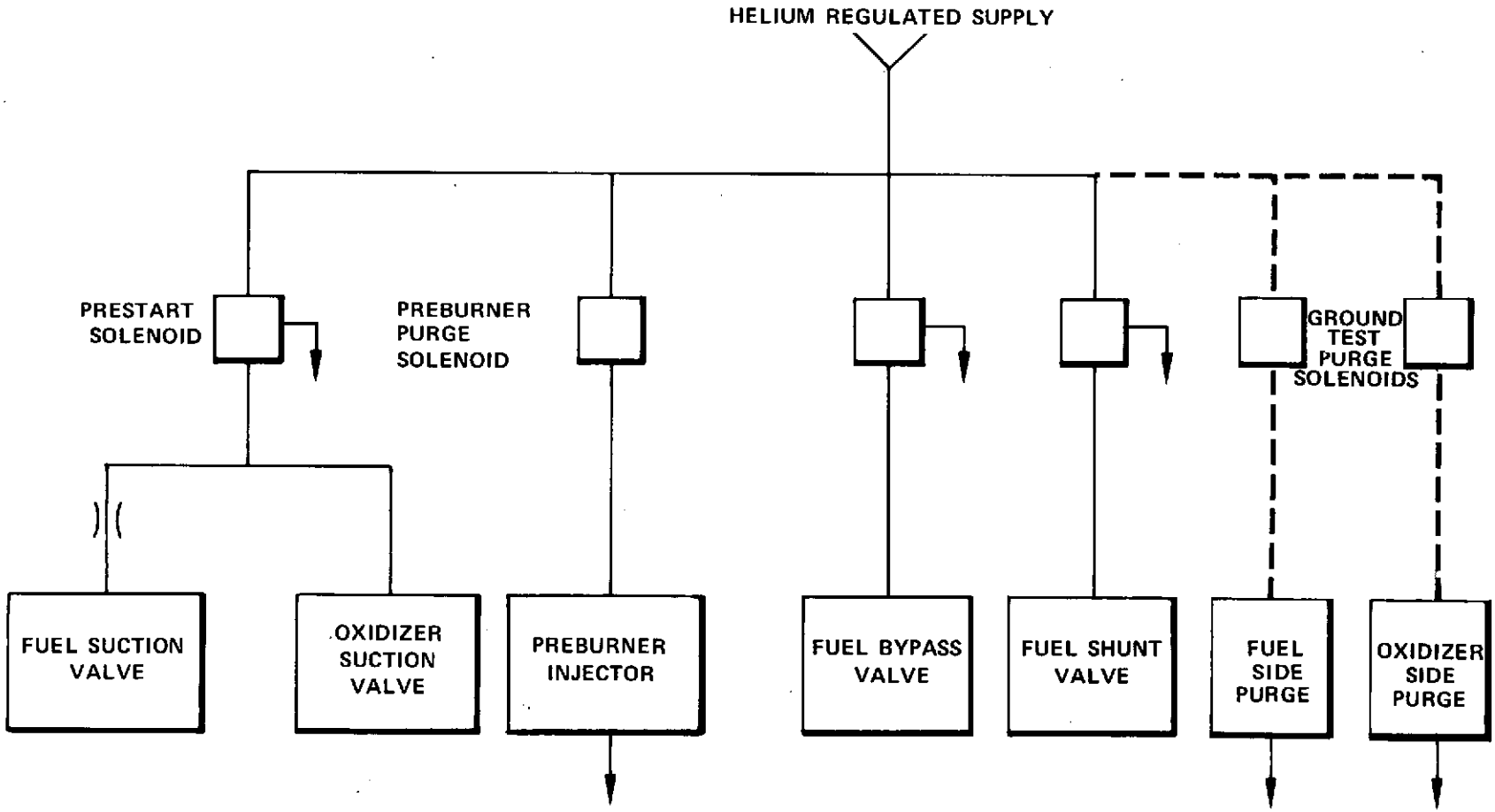

Figure 191. Estimated Helium System Requirements

FD 68859

Table XXXVI. Pneumatic Requirements

	Tank Head Idle	Pumped Idle	Rated Thrust	Shutdown
Solenoid Valves	0.08 scfm	0.08 scfm	0.08 scfm	-
Purge Flow	N/A	N/A	10.0 scfm 1 sec duration	10.0 scfm 1 sec duration

e. Engine Instrumentation

The engine instrumentation required to provide for engine readiness checkout, system performance verification, engine control, and malfunction detection is listed below:

- Vehicle Input Commands

  Engine Operation Mode

  Start/Stop
  Tank Head Idle
  Pumped Idle
  Full Thrust

  Mixture Ratio (Full Thrust Mode)

- Engine Control Instrumentation

  Thrust Chamber Pressure
  Preburner Temperature
  Vibrations - Low Pressure Fuel Pump
  Vibrations - Low Pressure Oxidizer Pump
  Vibrations - High Pressure Fuel Pump
  Vibrations - High Pressure Oxidizer Pump
  Control Valve Position - Preburner Oxidizer
  Control Valve Position - Main Chamber Oxidizer
  Control Valve Position - Main Fuel
  GO_2 Valve Position
  Jacket Coolant Discharge Temperature

- Self Check Instrumentation

  Electrical Power on-off
  Helium Supply Pressure

- Additional Engine Performance Indicators

  Inlet Pressure - High Pressure Fuel Pump
  Inlet Pressure - High Pressure Oxidizer Pump
  Discharge Pressure - High Pressure Fuel Pump
  Discharge Pressure - High Pressure Oxidizer Pump
  Rotational Speed - High Pressure Fuel Pump

Rotational Speed - High Pressure Oxidizer Pump
Gearbox Pressure
Main Injector Inlet Fuel Pressure
Main Injector Inlet Oxidizer Pressure
Main Injector Inlet Oxidizer Temperature
Inlet Pressure - Low Pressure Fuel Pump
Inlet Pressure - Low Pressure Oxidizer Pump
Inlet Temperature - Low Pressure Fuel Pump
Inlet Temperature - Low Pressure Oxidizer Pump
Housing Temperature - High Pressure Fuel Pump
Housing Temperature - High Pressure Oxidizer Pump
Preburner Igniter Spark Indicator Voltage
Main Chamber Igniter Spark Indicator Voltage
Fuel Suction Valve Position
Oxidizer Suction Valve Position
Fuel Bypass Valve Position
Fuel Shunt Valve Position

f. Engine Inlet Characteristics

The engine inlet characteristics are shown in figures 192 and 193 for the oxidizer and fuel inlet conditions required at the low pressure pump inlet.

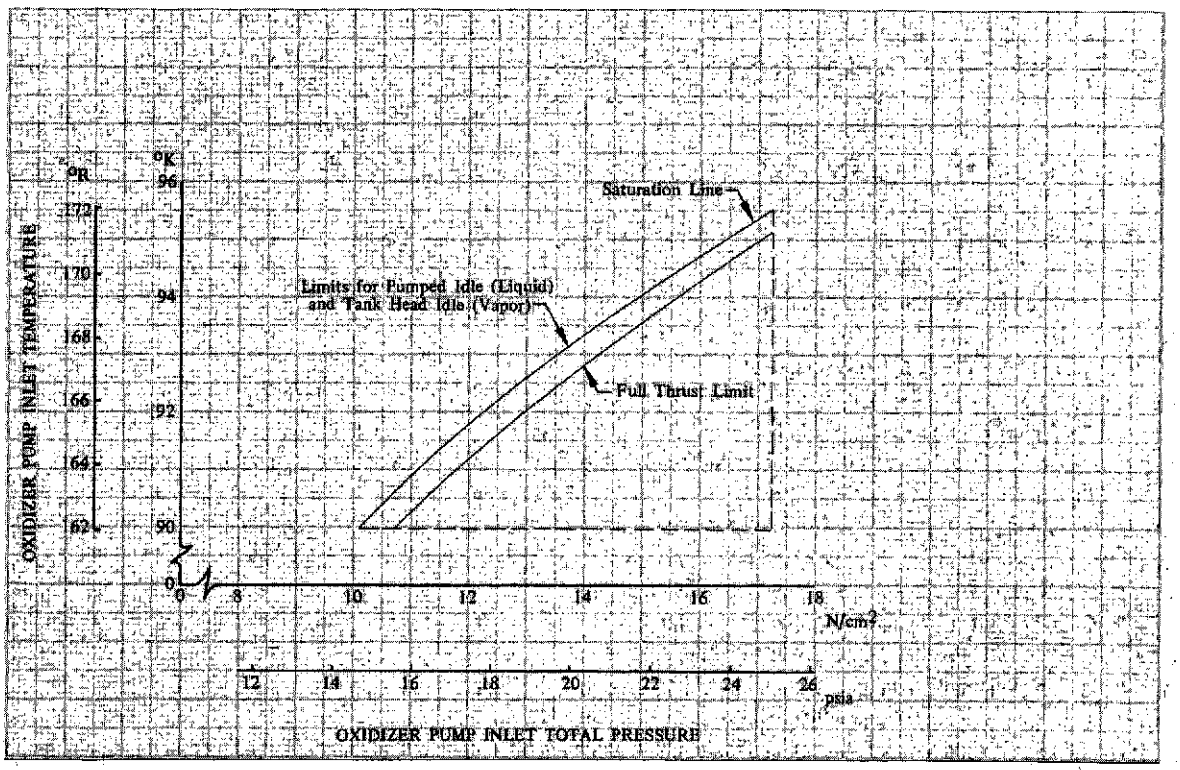

Figure 192. Advanced Space Engine Oxidizer Inlet Conditions at Low Pressure Pump DF 96260

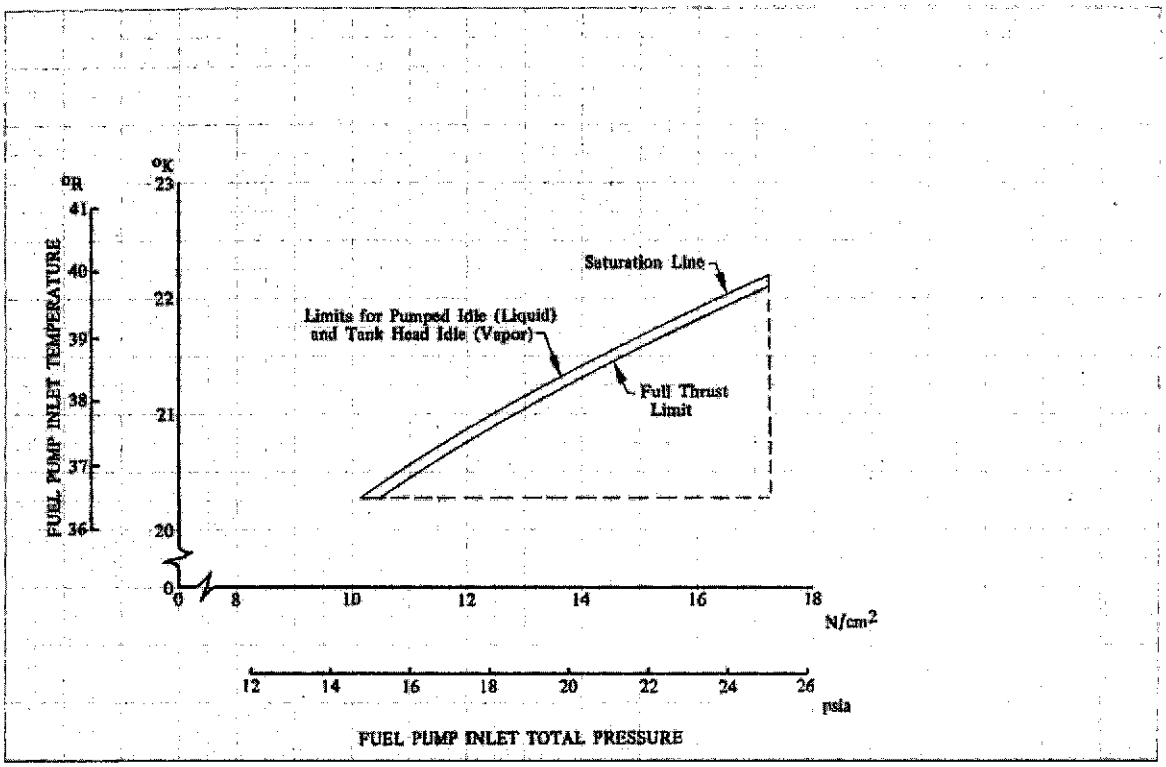

Figure 193. Advanced Space Engine Fuel Inlet Conditions at Low Pressure Pump DF 96261

F. OPERATIONAL AND FLIGHT SUPPORT PROGRAM PLAN

1. Introduction

A preliminary engine operational and flight support program plan was developed for an 89 kN (20,000 lb) thrust Advanced Space Engine considered for application for Space Tug propulsion. The plan is designed to provide all the necessary services to assure that the integrity, quality and performance of the Advanced Space Engine are maintained during any activity or associated activities involving the engine after delivery to NASA. This program will support the ground test, flight test, and operational phases of the Space Tug program. Our experience in integrating propulsion systems into reusable flight vehicles and providing operational and flight support to commercial and Government customers has led to specialized support groups within the company organization. The existing RL10 engine support program organization, which supports the Centaur launch activities, will be supplemented to consolidate the support services required to meet the objectives and needs of the Space Tug program. Tailoring our existing capabilities to the Space Tug program needs results in the following responsibilities for the four organizational elements listed below:

Operational Element	Program Responsibilities
Development Engineering Group	GSE development Flight support and anomaly resolution

Requirements Coordination Group	Government and vehicle contractor
Integrated Logistics Support Team	Logistical support and operational planning
Site Operations Team	Operational and flight support at the sites

The Space Tug engine program is divided into three major phases: design and development, delivery, and operation. Space Tug engine organizational elements of the support team will be involved in the program from the beginning except for the Site Operations teams, which are activated just before operational sites are opened. Although the Development Engineering group will be responsible for flight support and anomaly resolution throughout the Advanced Space Engine program, the size of the group will be reduced after FFC, when this work becomes a part of the support effort.

2. Design and Development

During the design and development phase, the maintainability and maintenance engineering effort started in the preliminary design study phase will be continued. Through maintainability, GSE, and human engineering reviews of new design layouts and completion of maintenance engineering analyses, various elements of the support team are able to influence new engine and GSE designs to obtain the most practical maintainable configurations. Maintenance engineering analysis is a systematic and controlled process for assessment and analysis of engine and GSE design features. Results of the maintenance engineering effort provide the basis for new maintenance planning and determination of logistical requirements by supplying data on maintenance task times, skill levels required, frequency of task occurrence, spare (support) parts required, etc. Followup observations of engine maintenance during the engine development program are used to refine the maintenance engineering data and update maintenance and logistics plans.

The Requirements Coordination group, through resident field engineers at NASA Centers and vehicle contractor plants and in-house coordinators, keeps NASA and the vehicle contractors in close technical contact with the Space Tug engine design and development program. The many technical interfaces with NASA and the vehicle contractors required to assure a reliable and maintainable integration of the engine with the overall vehicle system are achieved through the exchange of technical data, engine mockups, and technical conferences.

3. Delivery

Engineering support of the manufacturing program by the Development Engineering group will be continued after FFC as a part of the support effort. Establishment of an engine overhaul and repair capability will occur early in the manufacturing phase using the same equipment, personnel, and procedures used in the development manufacturing program. Also, early in the manufacturing phase, procurement of engine spare (support) parts, GSE and GSE spare parts will be accomplished after the P&WA recommended list of spare parts is reviewed and approved by NASA. This early procurement is required to allow placing

support parts and GSE at operational sites prior to initial engine delivery. Based on maintenance and operational planning, procurement of support parts and GSE is time-phased to take advantage of the in-production status during manufacturing. Similarly, personnel selection and training for support at the operational sites and preparation of required technical manuals is accomplished during the latter part of the engine development program and early phase of the delivery program to provide on-site support when the initial engine deliveries are made. Warehousing services and inventory control procedures for support parts at the refurbishment/repair facility is initiated with the start of support parts delivery.

4. Operations

During the operations phase, the flight support (both technical and logistical) is supplied at operational sites by a Site Operations team augmented by Space Tug engine program organizational elements shown below.

Organizational Element	Program Responsibilities
Development Engineering	Flight Support and anomaly resolution
Maintenance Engineering	Maintenance planning and routine technical support
Technical Publications	Operational and maintenance manuals and service bulletins
Refurbishment/Repair	Refurbishment and repair capabilities for engines and components
Spare Parts	Support parts, warehousing and inventory control for overhaul program parts, consumption data analysis, procurement, and field support for supply data and parts
GSE	GSE field support
Transportation	Shipment of engines and parts to and from field
Training	Preparation of training material for formal and on-the-job training for new techniques and configuration changes.

Before activation of the operational site, a Site Support team consisting of field engineers, field service representatives, GSE specialists, maintenance and inspection personnel, and performance analysts is organized and based at the site. The team is tailored in size and composition to the program needs at the site being manned and will supply all the needed engine and GSE maintenance, technical assistance to NASA and vehicle personnel on engine installation and

operation, support parts warehousing and inventory control services, and coordination on engine related planning and scheduling. A P&WA Site Manager is in charge of the support team and will provide a single focal point for NASA and vehicle contractor coordination on engine matters at the site.

On-site field engineers and field service representatives will provide technical lines of communication with the Advanced Space Engine Development Engineering group at FRDC regarding flight support and anomaly resolution matters. They also supply service engine status reports, discrepancy reports inputs, and configuration status reports on engines and GSE to the Advanced Space Engine program management. With the start of the vertical flight program the Advanced Space Engine training school will be moved from the engine assembly and test site to the launch site to provide training at a more convenient location.

PRELIMINARY COST ESTIMATES - SUPPORT DATA

Budgetary and Planning Cost Estimates have been prepared for the Development, Production and Operation and Flight Support phases for each of the NASA defined Engine Development Program Plans for an Advanced Space Engine (ASE) for Space Tug Propulsion. A matrix summarizing these Program Plan estimates by program phase is presented in Exhibit I. A detailed technical description of each of the alternative Program Plans is presented in Section III of this report. A general description of the major features of each Program Plan is presented herein. (See Exhibit II.) Exhibit III presents the Technical Characteristics of ASE.

The development program estimate has been geared to the preliminary program work breakdown structure and to the specified functional department groupings within the applicable WBS level six elements. (See Exhibit IV.) Schedules have been developed based on a December 1977 PFC date; the alternative engine development programs (through FFC) range from a minimum of 57 months (Plan II) to a maximum of 72 months (Plan I) with PFC scheduled in the 58th month on the latter program.

The production program cost estimates assume a first production lot of 40 units produced at a rate of two units per month. Cumulative average unit costs assume a 90% learning capability. A cumulative expected production program cost curve is presented and is identical for both programs. A production program schedule has also been developed from the assumed PFC date and allows 13 months lead time for long-lead procurement of hardware.

The Operations and Flight Support (O&FS) cost estimates are based on the available data provided in the preliminary mission model case 502. To satisfy the Space Tug propulsion system requirements through 1988 (10 year period), as required by the mission model, a total of 40 production ASE engines were assumed. Twenty-nine are planned for expendable missions and 13 for 197 reusable missions. O&FS estimates are presented in terms of total program cost, cost per year and cost per flight. Based on NASA mission model data, the bulk of the operations and flight support efforts will be performed from 1979 through 1988, with some efforts for tasks such as spare parts, training and publications commencing as early as 1977.

Estimated funding requirements have been developed for each engine program and program phase and presented with each detailed cost estimate on the Funding Schedule Data Form C. All cost estimates and funding data are presented in 1973 dollars. The assumptions and groundrules for these estimates are summarized in Exhibit V.

EXHIBIT I
ADVANCED SPACE ENGINE PROGRAM PLANS
Alternative Program Plans*

Program Phase	Plan I	Plan II
Development** (Through FFC)	$237.5	$273.2
Production (40 Units)	32.0	32.0
Operations and Flight Support (197 Flights)	31.6	31.6
Total Cost	$301.1	$336.8

*All Cost Figures in Millions of 1973 Dollars and Exclude Fee
**Includes $23,919,500 Facilities Estimate

EXHIBIT II
GENERAL DESCRIPTION OF PROGRAM PLANS

Engine development program plans were established for two alternate ASE programs.

The alternate program plans are based on the following requirements:

Program Plan I - Minimum cost development of Flight Certified Engine (FCE) without prior engine demonstration. For purposes of this Statement of Work, a minimum cost development program is defined as one that is not constrained to a tight (short) schedule and which makes optimum use of available facilities, hardware, and manpower to achieve the development of the engine at least cost. Overtime pay is minimized.

Program Plan II - Minimum time development of FCE without prior engine demonstration. For purposes of this plan, a minimum time development program is defined as one that is constrained to a short schedule. Duplication of facilities were considered but found to be unnecessary. Duplication of hardware for alternative designs was necessary and considerable use is made of overtime to speed up operations and accomplish the goals quickly.

The changes in development program costs, and production unit costs associated with each of the following modifications to the approved engine assembly were evaluated:

1. Change from a fixed bell nozzle (ϵ = 400:1) to a retractable nozzle (ϵ = 400:1 in extended position) such that the engine length in the nozzle retracted position is a maximum of 158.7 cm (62.5 inches).

2. Change to make engine/vehicle interfaces compatible with RL10A-3-3 engine installation.

EXHIBIT III
TECHNICAL CHARACTERISTICS OF THE BASELINE ASE

- Boost pumps gear driven off the main oxygen pump
- No throttling
- NPSH magnitudes of 6 N-m/kg (2 ft) (LO_2) and 45 N-m/kg (15 ft) (LH_2)
- Tank-head-idle start
- Pass-and-a-half regenerative cooling
- Single preburner

Engine Configuration and Operating Conditions

Propellants	Liquid Hydrogen Liquid Oxygen
Vacuum Thrust, N (lb)	89,000 (20,000)
Vacuum Thrust Throttling Capability	No Requirement
Vacuum Specific Impulse, N-s/kg (seconds)	4624 (471.5)
Engine Mixture Ratio	6.0 (Nominal at full thrust) 5.5-6.5 (Operating range at full thrust)
Chamber Pressure, N/cm^2 (psia)	1324 (1920)
Drive Cycle	Staged Combustion
Envelope Restrictions	
Length (maximum), cm (in.)	234 (92.07)
Diameter (maximum), cm (in.)	135 (53.2)
Engine System Weight, kg (lb)*	178.3 (393)
Nozzle Type	Fixed Bell
Nozzle Expansion Ratio	400:1
Propellant Inlet Temperatures, °K (°R)	
Hydrogen	Range: 20.3 (36.5) to 22.2 (40)
Oxygen	Range: 90 (162) to 95.6 (172)
NPSP at Pump Inlet at Full Thrust, N-m/kg (ft)	
Hydrogen	45 (15)
Oxygen	6 (2)
Engine Temperature at Normal, °K (°R) Prestart	Range: 111 (200) to 311 (560)
Service Life Between Overhauls	300 Thermal cycles or 10 hours accumulated run time.
Service Free Life	60 Thermal cycles or 2 hours accumulated run time.
Maximum Single Run Duration, seconds	2000
Maximum Time Between Firings During Mission, days	14
Minimum Time Between Firings During Mission, minutes	1
Maximum Storage Time in Orbit (Dry), weeks	52

*Target Dry Weight

EXHIBIT IV
PRELIMINARY WORK BREAKDOWN STRUCTURE

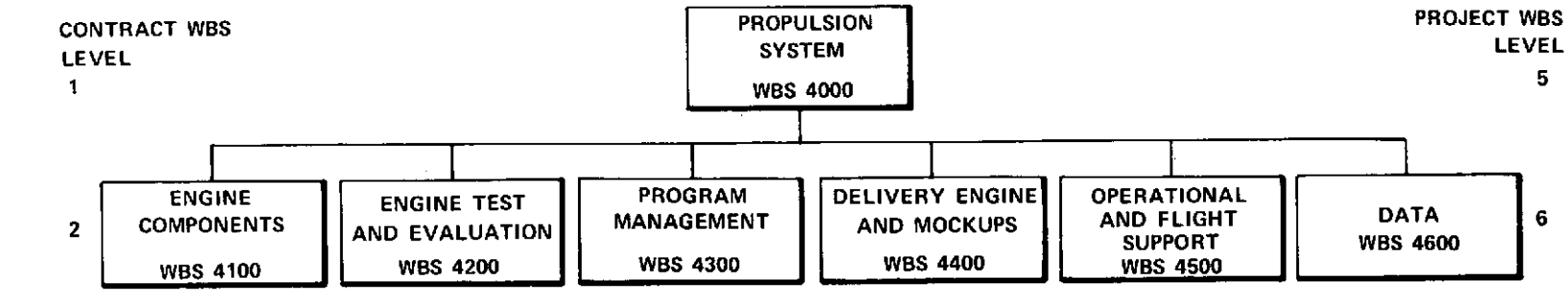

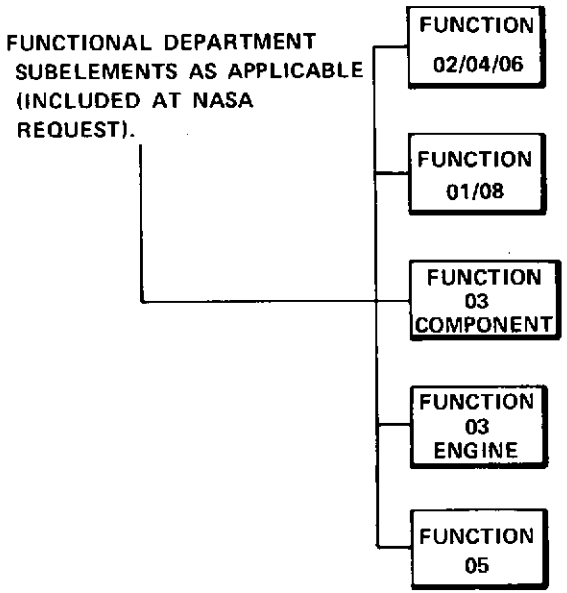

DEFINITION OF FUNCTION CODES INCLUDED IN SUBELEMENTS

FUNCTION CODE	FUNCTIONAL DEPARTMENT
01	DESIGN
02	MANUFACTURING
03	TEST
04	QUALITY
05	TOOLING
06	ASSEMBLY
08	ENGINEERING (PROGRAM MANAGEMENT)

EXHIBIT V
COST ESTIMATING ASSUMPTIONS/GROUNDRULES

A. GENERAL

1. All cost estimates exclude fee or profit. Only funding data included on the "Funding Schedule Data Form C" format include fee at 10% plus estimated open commitments.

2. All estimates are in 1973 dollars.

3. These estimates assume that the business level (and the overhead and G&A rates) during the period of performance will be the same as in 1973.

4. All propellants and ancillary fluids are to be Government-furnished and expense over and above the estimated amounts shown herein.

5. Estimates for Plan I are based on a two-shift, 5-day work week.

6. Estimates for Plan II are based on using premium time during the development program to achieve program objectives.

B. DEVELOPMENT

1. All cost estimates are "clean sheet," which exclude consideration of residual GFP material.

2. All offsite testing at Government installations will be at Government expense, over and above the estimated amounts shown herein.

3. Development estimates are for engine development through FFC.

4. Estimates are based on rent free use of all required Government owned facilities and equipment.

C. PRODUCTION

1. Production delivery requirements will approximate two engines per month.

2. Based on C.1 above, no additional production tooling or STE will be required over those specified for the development program.

3. Costs of parts and labor to incorporate engineering changes are not included in these estimates (to be negotiated separately).

D. OPERATIONS AND FLIGHT SUPPORT

1. The Operations and Flight support time period will be from 1977 through 1988.

2. Only one launch site and one vehicle manufacturer site will be used.

3. Support program will consist of a maximum of ten vehicles or tugs requiring ten engines plus three spare engines.

4. Twenty-nine additional engines will be required for expendable tug missions.

5. Spare parts will be required to support a minimum of forty engines.

6. Level 1 and 2 maintenance involving component adjustment/ replacement will be performed by NASA or vehicle contractor maintenance personnel at the launch site as well as at the vehicle manufacturer's site. Level 3 maintenance involving engine disassembly and testing will be performed by P&WA™ assembly and test personnel at the depot (FRDC) only.

7. NASA will provide spare parts warehousing at the launch site and at the vehicle manufacturer's site.

8. Training of NASA maintenance personnel will be provided by P&WA.

9. Technical supervision will be provided by P&WA at the launch site and at the vehicle manufacturer's site.

10. Engines will be installed in vehicles at vehicle manufacturer's site.

11. NASA will provide free use of Government facilities such as:

    a. Office and maintenance areas at launch site.
    b. Government vehicles for on-site transportation.
    c. Ground computers for maintenance analysis.

12. Modification kit installation costs are excluded from these estimates.

13. Estimates include flight support and anomaly resolution effort for period 1977 through 1988.

DEVELOPMENT PROGRAM COST ESTIMATES

Development program cost estimates were made for each alternative engine development program, Plan I - minimum cost and Plan II - minimum time considering previous proposal estimates, LR-129 and RL10 program cost experience. A preliminary program plan and schedule was developed for each of the ASE development programs. Analyses were made of such factors as hardware complexity, sets of hardware required, bill-of-material cost, expected weight and engine thrust requirements, mixture ratios, numbers and types of tests and program duration. These factors were compared and analyzed against similar historical requirements such as the LR-129 and RL10 development programs. Adjustments were made for differences in configuration, test programs, program duration and other factors, such as escalation, between the proposed programs and historical programs. The cost estimates for the options offered for Program Plans I and II were similarly developed from historical data. These optional program estimates are presented in Exhibits VI-E and VII-E. Exhibits VI-A through VI-E and VII-A through VII-E present the various development program cost estimates in detail.

The Program Plan estimates were structured in accordance with the preliminary program WBS and detailed at the functional discipline level (see Exhibit IV). These estimates include development efforts through final flight certification (FFC).

EXHIBIT VI-A
SCHEDULE, PROGRAM PLAN I (MINIMUM COST)

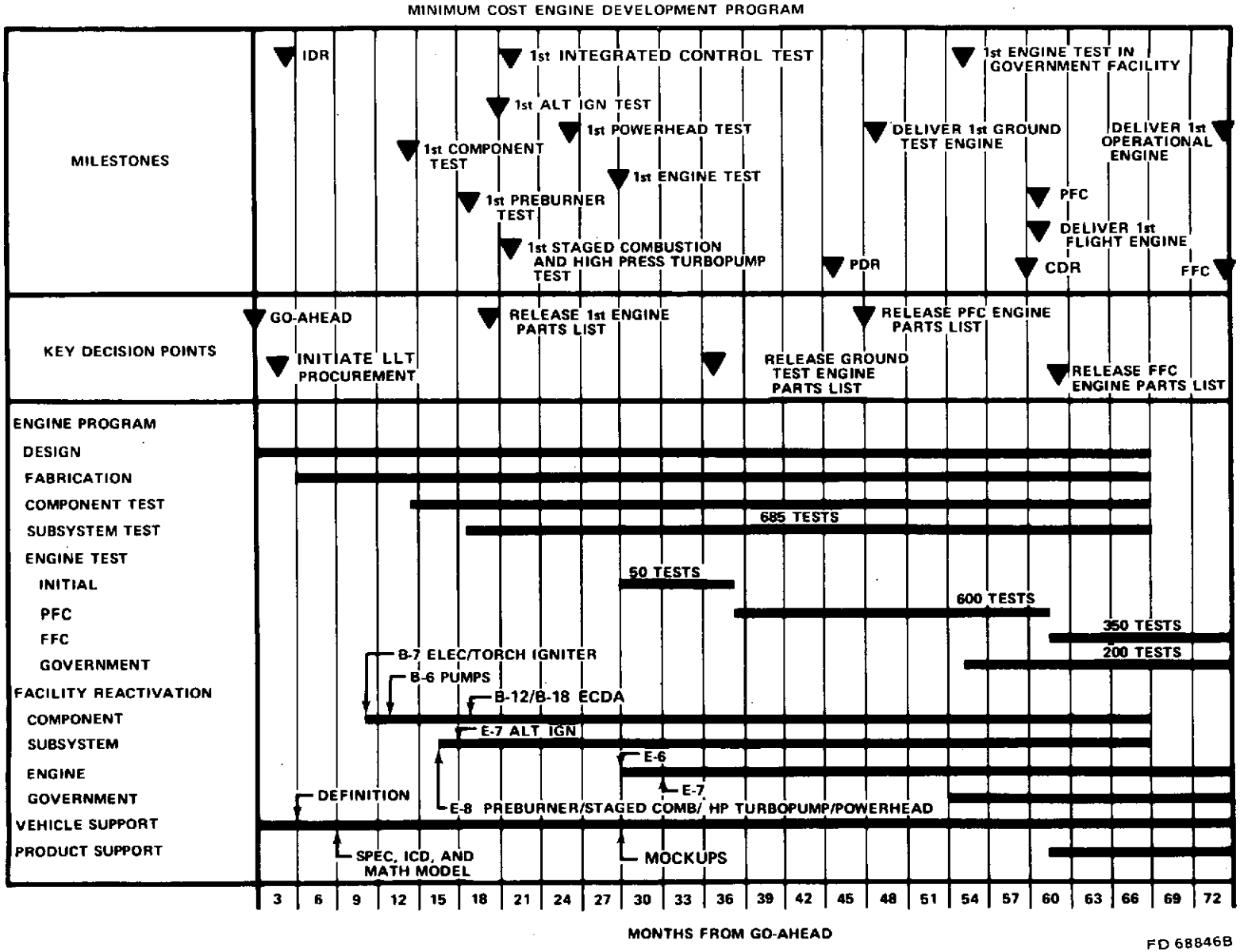

STUDY TITLE: ADVANCED SPACE ENGINE PROGRAM PLANS

CONTRACT NO. NAS3-16750

EXHIBIT VI-B
COST DATA FORM A(1)
NONRECURRING (DDT&E)*

PLAN I ENGINE

IDENTIFICATION NUMBER	WBS IDENTIFICATION	WBS LEVEL	EXPECTED COST	CONFID. RATING	T_d	T_s	SPREAD FUNCTION
4000	Propulsion System	5	$237.536				
4100	Engine-Components	6	140.922				
4200	Engine Test and Evaluation	6	87.588				
4300	Program Management	6	6.651				
4600	Data	6	2.375				
(Functional Discipline Breakouts)		Function Code					
4100	Engine-Components	02;04;06	45.734				
		01;08	43.378				
		03C	31.815				
		03E	13.490				
		05	6.505				
4200	Engine Test and Evaluation	02;04;06	28.824				
		01;08	34.177				
		03C	7.661				
		03E	12.589				
		05	4.337				
4300	Program Management	01;08	5.587				
		03C	.426				
		03E	.638				
4600	Data	01;08	2.375				

*All Costs in Millions of 1973 Dollars and Exclude Fee.

CONTRACT: NAS 3-16750

EXHIBIT VI-C
TECHNICAL CHARACTERISTICS
DATA FORM B

PROGRAM PLAN I

WBS IDEN NUMBER	WBS IDENTIFICATION	QUANTITY OR VALUE	UNITS OF MEASURE	CHARACTERISTICS	NOTES
WBS 4000	Propulsion System	471.5	Seconds	Impulse	

STUDY TITLE: ADVANCED SPACE ENGINE PROGRAM PLANS

CONTRACT NAS3-16750

EXHIBIT VI-D
FUNDING SCHEDULE DATA FORM C
PLAN I ENGINE*

[X] NON-RECURRING (DDT&E)
[ ] RECURRING (PRODUCTION
[ ] RECURRING (OPERATIONS)

PROJECT WBS ITEMS	FY 1**	FY 2	FY 3	FY 4	FY 5	FY 6
WBS 4000 Propulsion System	$19.335	$48.077	$68.458	$70.548	$39.455	$15.527
	FY____	FY____	FY____	FY____	FY____	FY____
	FY____	FY____	FY____	FY____	FY____	FY____

*All Costs in Millions of 1973 Dollars and Include Fee and Estimated Open Commitments.
**Assumes FY 1974 is FY 1

EXHIBIT VI-E
OPTIONAL COST ITEMS - PLAN I*

	Item Description	Action	Added Cost
1.	Retractable Nozzle	Add	15.586
2.	Interfaces Compatible With RL10A-3-3 Engine Installation	Add	0.000

*All cost in millions of 1973 dollars and exclude fee.

EXHIBIT VII-A
SCHEDULE, PROGRAM PLAN II (MINIMUM TIME)

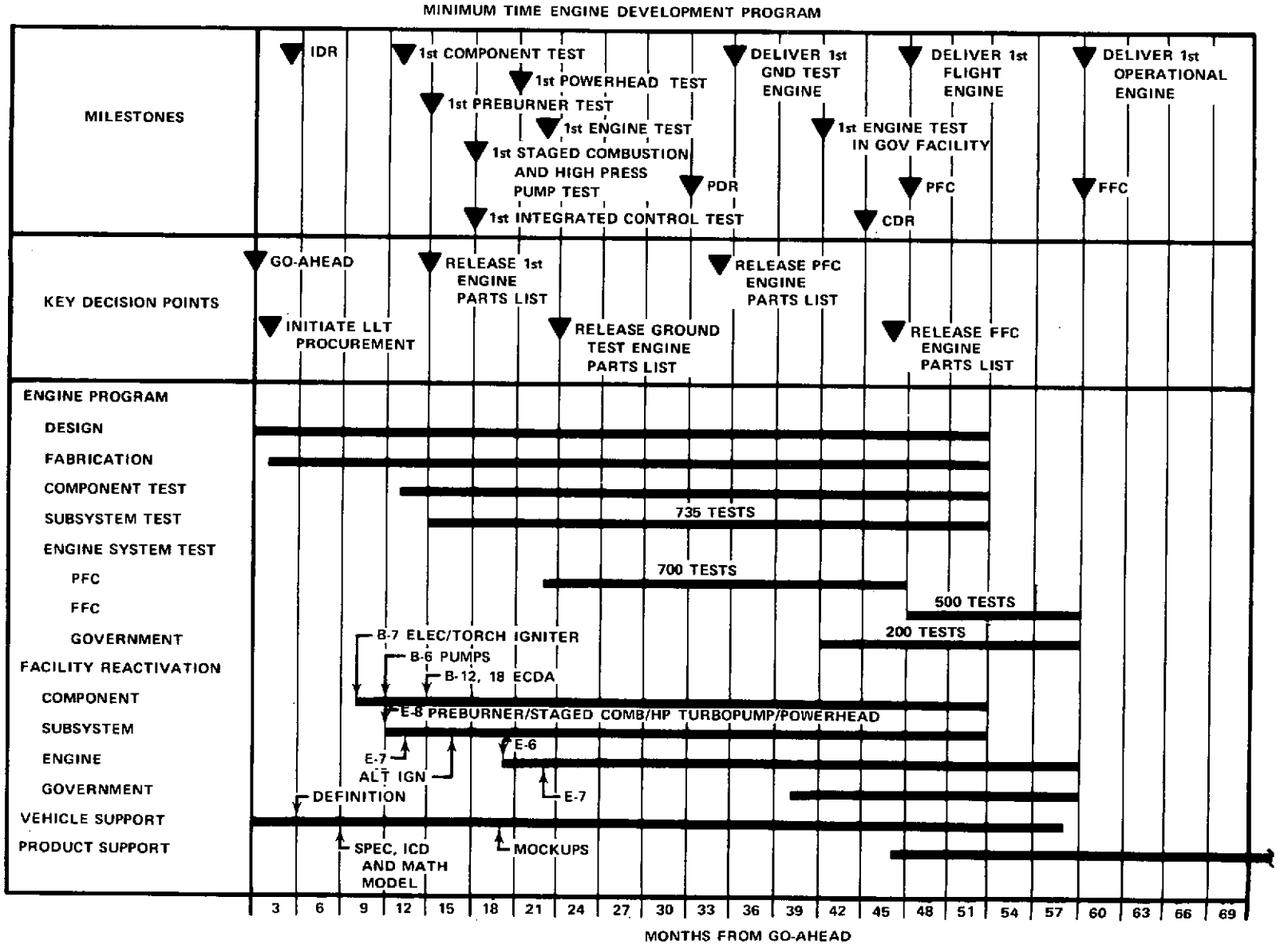

FD 68850

STUDY: ADVANCED SPACE ENGINE PROGRAM PLANS

EXHIBIT VII-B
COST DATA FORM A(1)
NONRECURRING (DDT&E)*

CONTRACT NO. NAS 3-16750

PLAN II ENGINE

IDENTIFICATION NUMBER	WBS IDENTIFICATION	WBS LEVEL	EXPECTED COST	CONFID. RATING	T_d	T_s	SPREAD FUNCTION
4000	Propulsion System	5	$273.246				
4100	Engine-Components	6	160.515				
4200	Engine Test & Evaluation	6	102.348				
4300	Program Management	6	7.651				
4600	Data	6	2.732				
(Functional Discipline Breakouts)		Function Code					
4100	Engine-Components	02;04;06	52.915				
		01;08	50.309				
		03C	33.749				
		03E	15.730				
		05	7.812				
4200	Engine Test and Evaluation	02;04;06	33.611				
		01;08	40.078				
		03C	8.933				
		03E	14.518				
		05	5.208				
4300	Program Management	01;08	6.427				
		03C	.490				
		03E	.734				
4600	Data	01;08	2.732				

*All Costs in Millions of 1973 Dollars and Exclude Fee.

STUDY TITLE: ADVANCED SPACE ENGINE PROGRAM PLANS

CONTRACT: NAS 3-16750

EXHIBIT VII-C
TECHNICAL CHARACTERISTICS
DATA FORM B

PROGRAM PLAN II

WBS IDEN. NUMBER	WBS IDENTIFICATION	QUANTITY OR VALUE	UNITS OF MEASURE	CHARACTERISTICS	NOTES
WBS 4000	Propulsion System	471.5	Seconds	Impulse	

STUDY TITLE: ADVANCED SPACE ENGINE PROGRAM PLANS

CONTRACT NAS3-16750

EXHIBIT VII-D
FUNDING SCHEDULE DATA FORM C
PROGRAM PLAN II

[X] NON-RECURRING (DDT&E)
[ ] RECURRING (PRODUCTION)
[ ] RECURRING (OPERATIONS)

PROJECT WBS ITEMS	FY 1**	FY 2	FY 3	FY 4	FY 5	FY
WBS 4000 Propulsion System	$79.050	$119.628	$67.629	$26.450	$7.815	
	FY	FY	FY	FY	FY	FY
	FY	FY	FY	FY	FY	FY

*All Costs in Millions of 1973 Dollars and Include Fee and Estimated Open Commitments.
**Assumes FY 1974 is FY 1

EXHIBIT VII-E
OPTIONAL COST ITEMS - PLAN II*

Item Description	Action	Added Cost
1. Retractable Nozzle	Add	$16.557
2. Interfaces Compatible With RL10A-3-3 engine installation		.000

*All Cost in Millions of 1973 Dollars and Exclude Fee.

PRODUCTION PHASE COST ESTIMATES

PROGRAM PLANS I AND II

PRODUCTION PROGRAM COST ESTIMATES

The production program cost estimates were developed for the base ASE using previous proposal estimates and RL10 production program experience. The first production unit cost includes the cost of fabrication and assembly, acceptance testing and preparation for shipment. For the production rate assumed (two engines per month) the development program tooling and special test equipment can be used and therefore no new production tooling will be required.

Production engine acceptance testing includes preliminary tests and final acceptance tests similar to that used to determine acceptability of current production RL10A-3-3 engines. The production engine unit cost estimates are based on previous OOS and RL10A-3-3 engine cost studies.

Initial spare parts costs are also included in the production engine cost. The types of spares and related costs are based on previous RL10 production engine program experience and the P&WA Maintenance Engineering Analysis, the prime data source for economic procurement of spares.

Estimated costs are presented for the first unit, the fortieth unit and cumulative average of forty units. These estimates assume a ninety (90) percent learning capability. The total Production Program costs are presented in Exhibit VIII and detail cost statistics are presented in Exhibits IX through XII. It was estimated that the base ASE production unit cost would increase six percent for the retractable nozzle configured engine. An ASE with interfaces compatible with RL10A-3-3 engine installation was estimated as no cost impact.

EXHIBIT VIII
PRODUCTION PHASE COST ESTIMATE

	All Plans
First Unit Cost	1.204
40th Unit Cost	0.687
CUM AVG 40 Units	0.799
40 Unit Production Program Cost	$31.960

STUDY TITLE: ADVANCED SPACE ENGINE
PROGRAM PLANS

CONTRACT NAS3-16750

EXHIBIT IX
COST DATA FORM A(2)
RECURRING (PRODUCTION)*

ALL PROGRAM PLANS

IDENTIFICATION NUMBER	WBS IDENTIFICATION	WBS LEVEL	NO. OF UNITS	EXPECTED COST	REF UNIT	REF UNIT COST	CONFID. RATING	T_d	T_s	SPREAD FUNCTION	LEARN INDEX
WBS 4400	Delivery Engines and Mockup	6	40	$31.960	N/A	$.799 **					90%

*All Cost in Millions of 1973 Dollars and Exclude Fee.
**Cumulative Average Unit Cost of 40th Unit (90% Learning)

STUDY TITLE: ADVANCED SPACE ENGINE
PROGRAM PLANS

CONTRACT NAS3-16750

EXHIBIT X
ALL PLANS PRODUCTION ENGINE CUMULATIVE
COST CURVE
(COSTS EXCLUDE FEE)

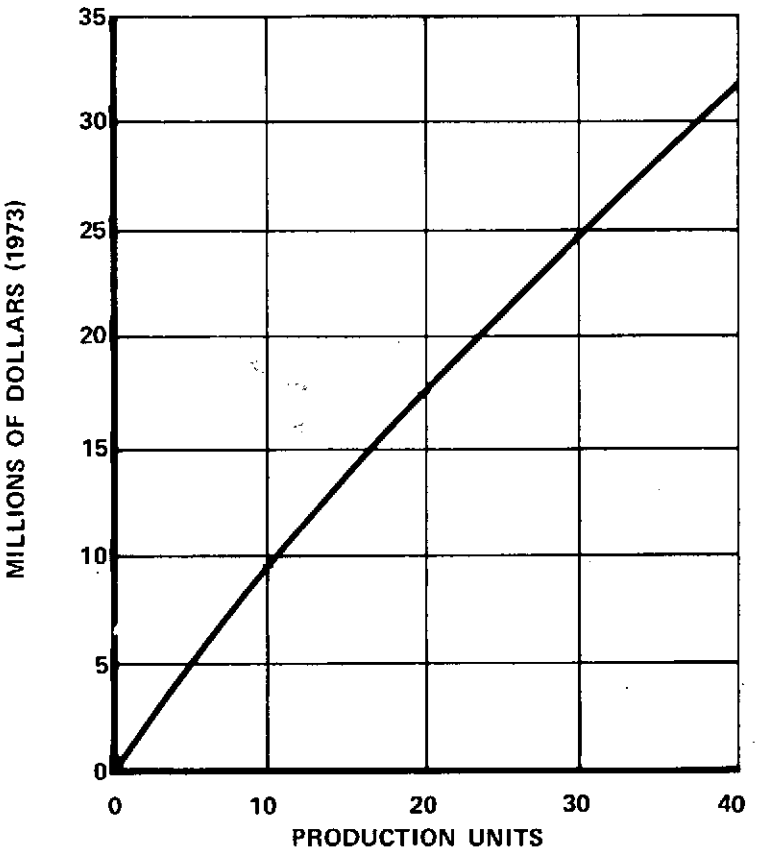

FD 70533

STUDY TITLE: ADVANCED SPACE ENGINE ALL PROGRAM PLANS

CONTRACT NAS3-16750

EXHIBIT XI
FUNDING SCHEDULE DATA FORM C

- ☐ NON-RECURRING (DDT&E)
- ☒ RECURRING (PRODUCTION)
- ☐ RECURRING (OPERATIONS)

PROJECT WBS ITEMS	FY 1**	FY 2	FY 3	FY 7	FY____	FY____
WBS 4000 Propulsion System	$17.494	$10.141	$4.057			
	FY____	FY____	FY____	FY____	FY____	FY____
	FY____	FY____	FY____	FY____	FY____	FY____

*All Costs in Millions of 1973 Dollars and Include Fee and Estimated Open Commitments.
**Assumes FY 1974 is FY 1

OPERATIONS AND FLIGHT SUPPORT PHASE COST ESTIMATES

PLANS I AND II

OPERATIONS AND FLIGHT SUPPORT COST ESTIMATES

Operations and flight support cost estimates were developed for the base ASE using data from the preliminary requirements defined in the NASA mission model*, existing support services at P&WA and our experience in supporting commercial and military aircraft and launch vehicle programs. This operations and flight support program is defined for the period 1977 through 1988 and is based on a preliminary plan to tailor the existing P&WA support organizations to Space Tug needs.

Estimates for spare parts, GSE, field service, training, publications, overhaul and maintainability have been included along with a flight support and anomaly resolution program estimate to establish the total O&FS program cost estimate.

Exhibit XII presents a summary of the operations and flight support program costs, the average cost per flight and the estimated costs per year for the period 1977 through 1988. Detail cost estimates and funding data are presented in Exhibits XIII and XIV.

*Reference NASA Mission Model case 502 provided for use on NAS8-27314

EXHIBIT XII
OPERATIONS AND FLIGHT SUPPORT ESTIMATES
PROGRAM PLANS I AND II

ITEM	ALL PROGRAM PLANS
OPERATIONS & FLIGHT SUPPORT PROGRAM COST	$31.552
AVERAGE COST PER FLIGHT (TOTAL 197 FLIGHTS)	$ .160
COST PER CALENDAR YEAR	
1977	$ 2.754
1978	4.896
1979	6.197
1980	7.698
1981	1.538
1982	1.347
1983	1.602
1984	1.133
1985	1.245
1986	.962
1987	1.068
1988	1.112
TOTAL	$31.552

*All Cost Figures in Millions of 1973 Dollars and Exclude Fee.

STUDY TITLE: ADVANCED SPACE ENGINE
PROGRAM PLANS I AND II

CONTRACT NAS3-16750

EXHIBIT XIII
COST DATA FORM A(3)
RECURRING (OPERATIONS)*

IDENTIFICATION NUMBER	WBS IDENTIFICATION	WBS LEVEL	NO. OF UNITS	EXPECTED COST	REF UNIT	REF UNIT COST	CONFID. RATING	T_d	T_s	SPREAD FUNCTION	LEARN INDEX
WBS 4500	Operational and Flight Support	6	197**	$31.552	197	$.160					
			***			****					
			Years Operation								

*All Costs in Millions of 1973 Dollars and Exclude Fee.
**197 Flights
***For Years of Operation and Expected Cost Per Year See Exhibit XII.
****Average Cost Per Flight Based on 197 Flights.

STUDY TITLE: ADVANCED SPACE ENGINE PROGRAM PLANS

CONTRACT NAS3-16750

EXHIBIT XIV
FUNDING SCHEDULE DATA
FORM C

☐ NON-RECURRING (DDT&E)
☐ RECURRING (PRODUCTION)
☒ RECURRING (OPERATIONS)

PROJECT WBS ITEMS	FY 4**	FY 5	FY 6	FY 7	FY 8	FY 9
WBS 4000 Propulsion System	$3.000	$5.400	$6.800	$8.500	$1.700	$1.500
	FY 10	FY 11	FY 12	FY 13	FY 14	FY 15
	$1.800	$1.200	$1.400	$1.100	$1.200	$1.107
	FY____	FY____	FY____	FY____	FY____	FY____

*All Costs in Millions of 1973 Dollars and Include Fee and Estimated Open Commitments.
**Assumes FY 1974 is FY 1

SECTION VI
CONCLUSIONS AND RECOMMENDATIONS

A. CONCLUSIONS

1. Advanced Space Engine Configuration Selection

- Gear-driven boost pumps to ensure satisfactory transient operation
- Single preburner with fixed-area injecter for simplicity and lightness. A close-coupled oxidizer valve is required to obtain good control response. The torch igniter is deleted and ignition is by sparkplug
- With gear-driven boost pumps, there is no advantage in the split flow cooling system, so the pass-and-a-half design was selected because of its greater inherent stability
- A two-stage, shrouded fuel turbopump with ball bearings was selected
- To obtain satisfactory operation in the pumped idle mode, a high-pressure drop thrust chamber injector has to be used, so a single-stage oxidizer turbopump was selected. A turbopump with a very low breakaway torque is essential
- A combined O_2/H_2/hot gas heat exchanger is required to supply CO_2 for THI operation and also for vehicle autogenous pressurization.

2. Advanced Space Engine Operation

- Tank head idle mode. Closed-loop control is a requirement. Thrust chamber injector stability is obtained by ensuring gas/gas propellant flow through the injector; the preburner is not in operation in this mode
- Pumped idle mode. With expander cycle operation, the engine is power limited, but this is preferred to having to operate the preburner in this mode. Autogenous pressurization capability is also limited, but closed-loop control is not required. Thrust chamber injector stability is obtained by having a high-pressure-drop oxidizer injector
- Full thrust. A thrust chamber pressure in excess of 1900 psia is obtainable. Closed-loop control is required.

B. RECOMMENDATIONS FOR TECHNOLOGY WORK REQUIRED BY THE ADVANCED SPACE ENGINES

- An oxidizer turbopump seal package with negligible breakaway torque is critical. With the turbopumps not mechanically connected and with the engine using the expander cycle when in pumped idle mode, it is essential that turbopump rotation can be initiated with a low torque

- For the small staged combustion engine to be able to meet its weight targets, reduction in the weight of the control system (valves, actuators, controller, etc.) is necessary

- Determination of the performance of high-pressure, very-high-area ratio, high-heat-flux nozzles by full-scale hot firing tests is required. No experimental data on the performance of bell nozzles of $\simeq 400{:}1$ area ratio are available

- The major problem area in this engine is not at the component level, but is in the component interactions and control of a small 3-in-1 (pressure-fed, expander-cycle pumped and staged combustion) high-pressure reusable engine. To investigate these interactions and demonstrate satisfactory operating mode changes, a breadboard engine test program is required.

APPENDIX A
ENGINE CYCLES

Cycle balance sheets (digital computer printouts) for the final cycle No. 106 are supplied in this Appendix for 100% thrust at MR = 5.5, 6.0 and 6.5, and for pumped idle (4% thrust, MR = 3.5) operation (tables A-1 through A-4). Similarly, cycle balance sheets are provided for the baseline engine cycle No. 104 (tables A-5 through A-8).

Propellant flow schematics (100% thrust, MR = 6.0) for the final engine cycle (No. 106), the baseline engine cycle (No. 104), and the ASE study initial engine cycle (No. 103) are presented in figures A-1 through A-3, respectively.

TABLE A-1

ASE OFF DESIGN DECK - CYCLE NO. 106. PAGE 1

THRUST = 20000. MRE= 5.500 PC = 1946.0

INLET CONDITIONS			**PERFORMANCE**		
FUEL TEMP	38.3	DEG R	THRUST	20000.	LB FORCE
FUEL PRESS	19.9	PSIA	IMPULSE	473.900	SEC
OX TEMP	166.0	DEG R	MIXTURE RATIO(ENG)	5.500	
OX PRESS	19.1	PSIA	CHAMBER PRESS	1946.0	PSIA
MIX RATIO(VEH)	5.492		FUEL FLOW(ENG)	6.493	LB/SEC
			OX FLOW(ENG)	35.710	LB/SEC
*** FUEL BOOST PUMP ***			**FIRST STAGE FUEL PUMP**		
DIAMETER	3.360	INCH	DIAMETER	5.276	INCH
FLOW	6.527	LB/SEC	FLOW	6.527	LB/SEC
SPEED	26003.	RPM	SPEED	96710.	RPM
EFF	0.750		EFF	0.580	
INLET PRESS	19.93	PSIA	INLET PRESS	62.21	PSIA
DISCH PRESS	68.67	PSIA	DISCH PRESS	2394.51	PSIA
DISCH TEMP	38.90	DEG R	DISCH TEMP	82.14	DEG R
EXIT DENSITY	4.351	LB/FT**3	EXIT DENSITY	4.147	LB/FT**3
VOL FLOW	674.17	GPM	VOL FLOW	673.28	GPM
HEAD	1614.	FT	HEAD	80021.	FT
POWER	25.55	HP	POWER	1636.42	HP
FLOW COEF	0.192		FLOW COEF	0.070	
HEAD COEF	0.4538		HEAD COEF	0.5187	
NPSP AVAIL	0.453	PSI	NPSP AVAIL	40.924	PSI
NPSP REQ	0.452	PSI	NPSP REQ	28.206	PSI
NPSH AVAIL	15.00	FT	NPSH AVAIL	1354.35	FT
NPSH REQ	14.97	FT	NPSH REQ	933.46	FT
SUCT SPEC SPEED	37435.		SUCT SPEC SPEED	11248.	
SECOND STAGE FUEL PUMP			*** THRUST CHAMBER ***		
DIAMETER	5.317	INCH	COOL IN PRESS	4768.9	PSIA
FLOW	6.527	LB/SEC	COOL PRESS LOSS	1029.6	PSID
SPEED	96710.	RPM	COOL TEMP RISE	330.2	DEG R
EFF	0.584		COOL DISCH TEMP	457.4	DEG R
INLET PRESS	2371.79	PSIA	COOL FLOW	5.464	LB/SEC
DISCH PRESS	4773.65	PSIA	CHAMBR PRESS	1946.0	PSIA
DISCH TEMP	127.25	DEG R	HOT GAS INJ PRESS	2112.6	PSIA
EXIT DENSITY	4.093	LB/FT**3	HOT GAS INJ TEMP	1854.2	DEG R
VOL FLOW	706.51	GPM	OX INJ PRESS	3356.8	PSIA
HEAD	84013.	FT	OX INJ TEMP	196.4	DEG R
POWER	1708.29	HP	OX FLOW	30.818	LB/SEC
FLOW COEF	0.061		HOT GAS FLOW	11.048	LB/SEC
HEAD COEF	0.5362		MC MIX RATIO	5.800	
			AREA RATIO(AERO)	400.	
			THROAT DIA(AERO)	2.570	INCH
PUMP SPECIFIC SPEED			NOZ EXIT DIA(AERO)	51.500	INCH
FUEL 1 STAGE	527.4				
FUEL 2 STAGE	520.9		**DUMP COOLED NOZZLE**		
LOX 1 STAGE	917.2		COOL FLOW	0.336	LB/SEC
FUEL BOOST	2651.7				
LOX BOOST	2560.4				

TABLE A-1 (Continued)

ASE OFF DESIGN DECK - CYCLE NO. 106. PAGE 2

THRUST = 20000. MRE= 5.500 PC = 1946.0

OXIDIZER BOOST PUMP		
DIAMETER	3.810	INCH
FLOW	35.844	LB/SEC
SPEED	6310.	RPM
EFF	0.747	
INLET PRESS	19.06	PSIA
DISCH PRESS	79.92	PSIA
DISCH TEMP	166.29	DEG R
EXIT DENSITY	70.514	LB/FT**3
VOL FLOW	228.20	GPM
HEAD	124.	FT
POWER	10.85	HP
FLOW COEF	0.184	
HEAD COEF	0.4647	
NPSP AVAIL	0.979	PSI
NPSP REQ	0.978	PSI
NPSH AVAIL	2.00	FT
NPSH REQ	2.00	FT
SUCT SPEC SPEED	36624.	

FIRST STAGE LOX PUMP		
DIAMETER	3.055	INCH
FLOW	35.844	LB/SEC
SPEED	59235.	RPM
EFF	0.637	
INLET PRESS	74.77	PSIA
DISCH PRESS	4790.18	PSIA
DISCH TEMP	196.44	DEG R
EXIT DENSITY	70.092	LB/FT**3
VOL FLOW	228.17	GPM
HEAD	9674.	FT
POWER	989.51	HP
FLOW COEF	0.083	
HEAD COEF	0.4983	
NPSP AVAIL	56.397	PSI
NPSP REQ	46.271	PSI
NPSH AVAIL	115.17	FT
NPSH REQ	94.49	FT
SUCT SPEC SPEED	25452.	

**** FUEL TURBINE ****		
FLOW	7.243	LB/SEC
NO.STAGES	1.000	
PRESS RATIO T/S	1.630	
INLET TEMP	2018.672	DEG R
POWER	3344.492	HP
INLET PRESS	3478.191	PSIA
EFF	0.684	
EXIT TEMP	1854.226	DEG R
U/C	0.398	
PERC ADMISSION	53.3	
MEAN WHEEL SPEED	1945.	FT/SEC
BLADE HEIGHT	0.30	INCH
VANE ANGLE	15.40	DEG
MEAN DIAM	4.605	INCH

*** LOX TURBINE ***		
FLOW	3.079	LB/SEC
NO.STAGES	1.000	
PRESS RATIO T/S	1.575	
INLET TEMP	2018.672	DEG R
POWER	1025.016	HP
INLET PRESS	3460.618	PSIA
EFF	0.528	
EXIT TEMP	1900.225	DEG R
U/C	0.249	
PERC ADMISSION	23.9	
MEAN WHEEL SPEED	1176.	FT/SEC
BLADE HEIGHT	0.30	INCH
VANE ANGLE	15.00	DEG
MEAN DIAM	4.545	INCH

GOX HEAT EXCHANGER		
OX INL PRESS	4790.	PSIA
OX INL TEMP	196.4	DEG R
OX PRESS LOSS	0.07	PSID
OX DISCH TEMP	426.	DEG R
GH2 FLOW	0.809	LB/SEC
GH2 INL PRES	3739.	PSIA
GH2 INL TEMP	457.	DEG R
GH2 PRESS LOSS	23.2	PSID
GH2 DISCH TEMP	565.	DEG R
GH2 TEMP TO P/B	473.	DEG R

PREBURNER		
MIXTURE RATIO	0.901	
TEMPERATURE	2019.	DEG R
PRESS	3513.	PSIA
FUEL FLOW	5.430	LB/SEC
OXIDIZER FLOW	4.892	LB/SEC
GAMMA	1.350	
CP	1.986	BTU/LB/R
GAS CONSTANT	400.8	FT-LB/LBR
PERC FUEL PARASIT	16.4	
FUEL PARASIT	1.063	LB/SEC

TABLE A-1 (Continued)

THRUST = 20000. MRE= 5.500 PC = 1946.0
ASE OFF DESIGN DECK - CYCLE NO. 106. PAGE 3

VALVES	INLET PRESS (PSIA)	DP (PSI)	DP/P1	AREA (IN**2)
FUEL VALVE	4773.7	4.77	0.0010	0.5849
PREBURNER OXIDIZER VALVE	4790.2	994.34	0.2076	0.0277
MAIN OXIDIZER VALVE	4790.2	1433.35	0.2992	0.1455
FUEL SHUNT VALVE	3739.3	23.2	0.0062	1.1672
GOX CONTROL VALVE	4790.1	0.003	0.0000	1.1100

INJECTORS	INLET PRESS (PSIA)	DP (PSI)	DP/P2	AREA (IN**2)
PREBURNER FUEL INJECTOR	3716.1	202.8	0.0577	0.5258
PREBURNER OXIDIZER INJECTOR	3795.8	282.5	0.0804	0.0520
OXIDIZER MAIN INJECTOR	3356.8	1410.82	0.7250	0.1466
HOT GAS INJECTOR	2112.6	166.60	0.0856	2.0952

TANK PRESSURANT

OX FLOW	0.134 LB/SEC
OX TEMP	426. DEG R
OX DELIV PRESS	4790.1PSIA
FUEL FLOW	0.034 LB/SEC
FUEL TEMP	457. DEG R
FUEL DELIV PRESS	3739.3PSIA

NOTES
1. VEHICLE MIXTURE RATIO - OXIDIZER/FUEL WEIGHT RATIO, INCLUDES TANK PRESSURANT FLOWS.
2. ENGINE MIXTURE RATIO - OXIDIZER/FUEL WEIGHT RATIO, EXCLUDES TANK PRESSURANT FLOWS.
3. PUMP EFFICIENCIES - INCLUDES EFFECTS OF RECIRCULATED FLOWS (THRUST BALANCE SYSTEMS, BEARING COOLING, INTERNAL LEAKAGES, ETC.)

TABLE A-2

ASE OFF DESIGN DECK - CYCLE NO. 106. PAGE 1

THRUST = 20000. MRE= 6.000 PC = 1921.6

INLET CONDITIONS		
FUEL TEMP	38.3	DEG R
FUEL PRESS	19.9	PSIA
OX TEMP	166.0	DEG R
OX PRESS	19.1	PSIA
MIX RATIO(VEH)	5.989	

PERFORMANCE		
THRUST	20000.	LB FORCE
IMPULSE	471.500	SEC
MIXTURE RATIO(ENG)	6.000	
CHAMBER PRESS	1921.6	PSIA
FUEL FLOW(ENG)	6.060	LB/SEC
OX FLOW(ENG)	36.358	LB/SEC

*** FUEL BOOST PUMP ***		
DIAMETER	3.360	INCH
FLOW	6.094	LB/SEC
SPEED	24409.	RPM
EFF	0.750	
INLET PRESS	19.93	PSIA
DISCH PRESS	63.00	PSIA
DISCH TEMP	38.83	DEG R
EXIT DENSITY	4.351	LB/FT**3
VOL FLOW	629.43	GPM
HEAD	1426.	FT
POWER	21.08	HP
FLOW COEF	0.191	
HEAD COEF	0.4551	
NPSP AVAIL	0.453	PSI
NPSP REQ	0.382	PSI
NPSH AVAIL	15.00	FT
NPSH REQ	12.65	FT
SUCT SPEC SPEED	33954.	

FIRST STAGE FUEL PUMP		
DIAMETER	5.276	INCH
FLOW	6.094	LB/SEC
SPEED	93078.	RPM
EFF	0.581	
INLET PRESS	57.37	PSIA
DISCH PRESS	2258.53	PSIA
DISCH TEMP	79.21	DEG R
EXIT DENSITY	4.163	LB/FT**3
VOL FLOW	628.67	GPM
HEAD	75305.	FT
POWER	1436.04	HP
FLOW COEF	0.068	
HEAD COEF	0.5269	
NPSP AVAIL	36.226	PSI
NPSP REQ	26.659	PSI
NPSH AVAIL	1198.98	FT
NPSH REQ	882.36	FT
SUCT SPEC SPEED	11461.	

SECOND STAGE FUEL PUMP		
DIAMETER	5.317	INCH
FLOW	6.094	LB/SEC
SPEED	93078.	RPM
EFF	0.584	
INLET PRESS	2238.80	PSIA
DISCH PRESS	4499.15	PSIA
DISCH TEMP	122.08	DEG R
EXIT DENSITY	4.094	LB/FT**3
VOL FLOW	657.03	GPM
HEAD	78917.	FT
POWER	1497.70	HP
FLOW COEF	0.058	
HEAD COEF	0.5437	

*** THRUST CHAMBER ***		
COOL IN PRESS	4494.6	PSIA
COOL PRESS LOSS	954.7	PSID
COOL TEMP RISE	355.4	DEG R
COOL DISCH TEMP	477.5	DEG R
COOL FLOW	5.081	LB/SEC
CHAMBR PRESS	1921.6	PSIA
HOT GAS INJ PRESS	2071.3	PSIA
HOT GAS INJ TEMP	1894.3	DEG R
OX INJ PRESS	3419.1	PSIA
OX INJ TEMP	191.5	DEG R
OX FLOW	31.780	LB/SEC
HOT GAS FLOW	10.315	LB/SEC
MC MIX RATIO	6.338	
AREA RATIO(AERO)	400.	
THROAT DIA(AERO)	2.570	INCH
NOZ EXIT DIA(AERO)	51.500	INCH

PUMP SPECIFIC SPEED	
FUEL 1 STAGE	513.4
FUEL 2 STAGE	506.7
LOX 1 STAGE	977.0
FUEL BOOST	2638.5
LOX BOOST	2760.0

DUMP COOLED NOZZLE		
COOL FLOW	0.323	LB/SEC

TABLE A-2 (Continued)

ASE OFF DESIGN DECK - CYCLE NO. 106. PAGE 2

THRUST = 20000. MRE= 6.000 PC = 1921.6

OXIDIZER BOOST PUMP			***FIRST STAGE LOX PUMP***		
DIAMETER	3.810	INCH	DIAMETER	3.055	INCH
FLOW	36.492	LB/SEC	FLOW	36.492	LB/SEC
SPEED	5923.	RPM	SPEED	55603.	RPM
EFF	0.750		EFF	0.644	
INLET PRESS	19.06	PSIA	INLET PRESS	64.94	PSIA
DISCH PRESS	70.28	PSIA	DISCH PRESS	4102.97	PSIA
DISCH TEMP	166.24	DEG R	DISCH TEMP	191.46	DEG R
EXIT DENSITY	70.513	LB/FT**3	EXIT DENSITY	70.222	LB/FT**3
VOL FLOW	232.33	GPM	VOL FLOW	232.30	GPM
HEAD	105.	FT	HEAD	8273.	FT
POWER	9.25	HP	POWER	851.71	HP
FLOW COEF	0.200		FLOW COEF	0.090	
HEAD COEF	0.4438		HEAD COEF	0.4836	
NPSP AVAIL	0.979	PSI	NPSP AVAIL	46.616	PSI
NPSP REQ	0.903	PSI	NPSP REQ	38.623	PSI
NPSH AVAIL	2.00	FT	NPSH AVAIL	95.20	FT
NPSH REQ	1.84	FT	NPSH REQ	78.88	FT
SUCT SPEC SPEED	34688.		SUCT SPEC SPEED	27809.	

**** FUEL TURBINE ****			*** LOX TURBINE ***		
FLOW	6.754	LB/SEC	FLOW	2.871	LB/SEC
NO.STAGES	1.000		NO.STAGES	1.000	
PRESS RATIO T/S	1.575		PRESS RATIO T/S	1.522	
INLET TEMP	2048.964	DEG R	INLET TEMP	2048.964	DEG R
POWER	2933.423	HP	POWER	881.749	HP
INLET PRESS	3294.577	PSIA	INLET PRESS	3277.932	PSIA
EFF	0.681		EFF	0.519	
EXIT TEMP	1894.283	DEG R	EXIT TEMP	1939.017	DEG R
U/C	0.394		U/C	0.241	
PERC ADMISSION	53.3		PERC ADMISSION	23.9	
MEAN WHEEL SPEED	1872.	FT/SEC	MEAN WHEEL SPEED	1104.	FT/SEC
BLADE HEIGHT	0.30	INCH	BLADE HEIGHT	0.30	INCH
VANE ANGLE	15.40	DEG	VANE ANGLE	15.00	DEG
MEAN DIAM	4.605	INCH	MEAN DIAM	4.545	INCH

GOX HEAT EXCHANGER			**PREBURNER**		
OX INL PRESS	4103.	PSIA	MIXTURE RATIO	0.907	
OX INL TEMP	191.5	DEG R	TEMPERATURE	2049.	DEG R
OX PRESS LOSS	0.07	PSID	PRESS	3328.	PSIA
OX DISCH TEMP	423.	DEG R	FUEL FLOW	5.047	LB/SEC
GH2 FLOW	0.752	LB/SEC	OXIDIZER FLOW	4.578	LB/SEC
GH2 INL PRES	3540.	PSIA	GAMMA	1.349	
GH2 INL TEMP	478.	DEG R	CP	1.986	BTU/LB/R
GH2 PRESS LOSS	21.8	PSID	GAS CONSTANT	399.7	FT-LB/LBR
GH2 DISCH TEMP	590.	DEG R	PERC FUEL PARASIT	16.7	
GH2 TEMP TO P/B	494.	DEG R	FUEL PARASIT	1.012	LB/SEC

TABLE A-2 (Continued)

THRUST = 20000. MRE= 6.000 PC = 1921.6
ASE OFF DESIGN DECK - CYCLE NO. 106. PAGE 3

VALVES	INLET PRESS (PSIA)	DP (PSI)	DP/P1	AREA (IN**2)
FUEL VALVE	4499.1	4.50	0.0010	0.5600
PREBURNER OXIDIZER VALVE	4103.0	528.16	0.1287	0.0356
MAIN OXIDIZER VALVE	4103.0	683.91	0.1667	0.2169
FUEL SHUNT VALVE	3540.0	21.8	0.0062	1.1672
GOX CONTROL VALVE	4102.9	0.003	0.0000	1.1100

INJECTORS	INLET PRESS (PSIA)	DP (PSI)	DP/P2	AREA (IN**2)
PREBURNER FUEL INJECTOR	3518.2	190.7	0.0573	0.5258
PREBURNER OXIDIZER INJECTOR	3574.8	247.0	0.0742	0.0520
OXIDIZER MAIN INJECTOR	3419.1	1497.48	0.7793	0.1466
HOT GAS INJECTOR	2071.3	149.68	0.0779	2.0952

TANK PRESSURANT

OX FLOW	0.134 LB/SEC
OX TEMP	423. DEG R
OX DELIV PRESS	4102.9PSIA
FUEL FLOW	0.034 LB/SEC
FUEL TEMP	478. DEG R
FUEL DELIV PRESS	3540.0PSIA

NOTES
1. VEHICLE MIXTURE RATIO - OXIDIZER/FUEL WEIGHT RATIO, INCLUDES TANK PRESSURANT FLOWS.
2. ENGINE MIXTURE RATIO - OXIDIZER/FUEL WEIGHT RATIO, EXCLUDES TANK PRESSURANT FLOWS.
3. PUMP EFFICIENCIES - INCLUDES EFFECTS OF RECIRCULATED FLOWS (THRUST BALANCE SYSTEMS, BEARING COOLING, INTERNAL LEAKAGES, ETC.)

TABLE A-3

ASE OFF DESIGN DECK - CYCLE NO. 106. PAGE 1

THRUST = 20000. MRE= 6.500 PC = 1902.0

INLET CONDITIONS

FUEL TEMP	38.3	DEG R
FUEL PRESS	19.9	PSIA
OX TEMP	166.0	DEG R
OX PRESS	19.1	PSIA
MIX RATIO(VEH)	6.485	

PERFORMANCE

THRUST	20000.	LB FORCE
IMPULSE	467.200	SEC
MIXTURE RATIO(ENG)	6.500	
CHAMBER PRESS	1902.0	PSIA
FUEL FLOW(ENG)	5.708	LB/SEC
OX FLOW(ENG)	37.100	LB/SEC

*** FUEL BOOST PUMP ***

DIAMETER	3.360	INCH
FLOW	5.742	LB/SEC
SPEED	23338.	RPM
EFF	0.749	
INLET PRESS	19.93	PSIA
DISCH PRESS	59.62	PSIA
DISCH TEMP	38.79	DEG R
EXIT DENSITY	4.350	LB/FT**3
VOL FLOW	593.08	GPM
HEAD	1315.	FT
POWER	18.32	HP
FLOW COEF	0.188	
HEAD COEF	0.4588	
NPSP AVAIL	0.453	PSI
NPSP REQ	0.339	PSI
NPSH AVAIL	15.00	FT
NPSH REQ	11.23	FT
SUCT SPEC SPEED	31513.	

FIRST STAGE FUEL PUMP

DIAMETER	5.276	INCH
FLOW	5.742	LB/SEC
SPEED	91405.	RPM
EFF	0.581	
INLET PRESS	54.62	PSIA
DISCH PRESS	2218.24	PSIA
DISCH TEMP	78.46	DEG R
EXIT DENSITY	4.165	LB/FT**3
VOL FLOW	592.42	GPM
HEAD	74000.	FT
POWER	1330.73	HP
FLOW COEF	0.065	
HEAD COEF	0.5369	
NPSP AVAIL	33.525	PSI
NPSP REQ	26.426	PSI
NPSH AVAIL	1109.70	FT
NPSH REQ	874.71	FT
SUCT SPEC SPEED	11578.	

SECOND STAGE FUEL PUMP

DIAMETER	5.317	INCH
FLOW	5.742	LB/SEC
SPEED	91405.	RPM
EFF	0.583	
INLET PRESS	2200.74	PSIA
DISCH PRESS	4414.89	PSIA
DISCH TEMP	120.67	DEG R
EXIT DENSITY	4.092	LB/FT**3
VOL FLOW	618.79	GPM
HEAD	77315.	FT
POWER	1384.30	HP
FLOW COEF	0.056	
HEAD COEF	0.5524	

*** THRUST CHAMBER ***

COOL IN PRESS	4305.2	PSIA
COOL PRESS LOSS	891.0	PSID
COOL TEMP RISE	380.8	DEG R
COOL DISCH TEMP	501.5	DEG R
COOL FLOW	4.746	LB/SEC
CHAMBR PRESS	1902.0	PSIA
HOT GAS INJ PRESS	2042.4	PSIA
HOT GAS INJ TEMP	1972.8	DEG R
OX INJ PRESS	3484.9	PSIA
OX INJ TEMP	188.7	DEG R
OX FLOW	32.677	LB/SEC
HOT GAS FLOW	9.813	LB/SEC
MC MIX RATIO	6.884	
AREA RATIO(AERO)	400.	
THROAT DIA(AERO)	2.570	INCH
NOZ EXIT DIA(AERO)	51.500	INCH

PUMP SPECIFIC SPEED

FUEL 1 STAGE	495.9
FUEL 2 STAGE	490.4
LOX 1 STAGE	1030.7
FUEL BOOST	2603.5

DUMP COOLED NOZZLE

COOL FLOW	0.319	LB/SEC

TABLE A-3 (Continued)

ASE OFF DESIGN DECK - CYCLE NO. 106. PAGE 2

THRUST = 20000. MRE= 6.500 PC = 1902.0

OXIDIZER BOOST PUMP			***FIRST STAGE LOX PUMP***		
DIAMETER	3.810	INCH	DIAMETER	3.055	INCH
FLOW	37.234	LB/SEC	FLOW	37.234	LB/SEC
SPEED	5663.	RPM	SPEED	53164.	RPM
EFF	0.750		EFF	0.643	
INLET PRESS	19.06	PSIA	INLET PRESS	58.40	PSIA
DISCH PRESS	63.95	PSIA	DISCH PRESS	3648.27	PSIA
DISCH TEMP	166.21	DEG R	DISCH TEMP	188.69	DEG R
EXIT DENSITY	70.511	LB/FT**3	EXIT DENSITY	70.236	LB/FT**3
VOL FLOW	237.05	GPM	VOL FLOW	237.03	GPM
HEAD	92.	FT	HEAD	7354.	FT
POWER	8.27	HP	POWER	774.41	HP
FLOW COEF	0.213		FLOW COEF	0.096	
HEAD COEF	0.4255		HEAD COEF	0.4702	
NPSP AVAIL	0.979	PSI	NPSP AVAIL	40.102	PSI
NPSP REQ	0.974	PSI	NPSP REQ	34.263	PSI
NPSH AVAIL	2.00	FT	NPSH AVAIL	81.90	FT
NPSH REQ	1.99	FT	NPSH REQ	69.97	FT
SUCT SPEC SPEED	33502.		SUCT SPEC SPEED	30066.	

**** FUEL TURBINE ****			*** LOX TURBINE ***		
FLOW	6.410	LB/SEC	FLOW	2.725	LB/SEC
NO.STAGES	1.000		NO.STAGES	1.000	
PRESS RATIO T/S	1.543		PRESS RATIO T/S	1.491	
INLET TEMP	2124.686	DEG R	INLET TEMP	2124.686	DEG R
POWER	2714.771	HP	POWER	801.031	HP
INLET PRESS	3183.181	PSIA	INLET PRESS	3167.099	PSIA
EFF	0.679		EFF	0.510	
EXIT TEMP	1972.770	DEG R	EXIT TEMP	2019.188	DEG R
U/C	0.391		U/C	0.233	
PERC ADMISSION	53.3		PERC ADMISSION	23.9	
MEAN WHEEL SPEED	1838.	FT/SEC	MEAN WHEEL SPEED	1055.	FT/SEC
BLADE HEIGHT	0.30	INCH	BLADE HEIGHT	0.30	INCH
VANE ANGLE	15.40	DEG	VANE ANGLE	15.00	DEG
MEAN DIAM	4.605	INCH	MEAN DIAM	4.545	INCH

GOX HEAT EXCHANGER			**PREBURNER**		
OX INL PRESS	3648.	PSIA	MIXTURE RATIO	0.939	
OX INL TEMP	188.7	DEG R	TEMPERATURE	2125.	DEG R
OX PRESS LOSS	0.06	PSID	PRESS	3215.	PSIA
OX DISCH TEMP	422.	DEG R	FUEL FLOW	4.712	LB/SEC
GH2 FLOW	0.702	LB/SEC	OXIDIZER FLOW	4.423	LB/SEC
GH2 INL PRES	3414.	PSIA	GAMMA	1.345	
GH2 INL TEMP	501.	DEG R	CP	1.972	BTU/LB/R
GH2 PRESS LOSS	20.5	PSID	GAS CONSTANT	393.6	FT-LB/LBR
GH2 DISCH TEMP	620.	DEG R	PERC FUEL PARASIT	17.5	
GH2 TEMP TO P/B	519.	DEG R	FUEL PARASIT	0.996	LB/SEC

TABLE A-3 (Continued)

THRUST = 20000. MRE= 6.500 PC = 1902.0
ASE OFF DESIGN DECK - CYCLE NO. 106.

VALVES **********	INLET PRESS (PSIA)	DP (PSI)	DP/P1	AREA (IN**2)
FUEL VALVE	4414.9	109.66	0.0248	0.1060
PREBURNER OXIDIZER VALVE	3648.3	202.48	0.0555	0.0555
MAIN OXIDIZER VALVE	3648.3	163.39	0.0448	0.4563
FUEL SHUNT VALVE	3414.2	20.5	0.0060	1.1672
GOX CONTROL VALVE	3648.2	0.004	0.0000	1.1100

INJECTORS **********	INLET PRESS (PSIA)	DP (PSI)	DP/P2	AREA (IN**2)
PREBURNER FUEL INJECTOR	3393.7	178.6	0.0555	0.5258
PREBURNER OXIDIZER INJECTOR	3445.9	230.5	0.0717	0.0520
OXIDIZER MAIN INJECTOR	3484.9	1582.88	0.8322	0.1466
HOT GAS INJECTOR	2042.4	140.37	0.0738	2.0952

TANK PRESSURANT

OX FLOW	0.134 LB/SEC
OX TEMP	422. DEG R
OX DELIV PRESS	3648.2PSIA
FUEL FLOW	0.034 LB/SEC
FUEL TEMP	501. DEG R
FUEL DELIV PRESS	3414.2PSIA

NOTES
1. VEHICLE MIXTURE RATIO - OXIDIZER/FUEL WEIGHT RATIO, INCLUDES TANK PRESSURANT FLOWS.
2. ENGINE MIXTURE RATIO - OXIDIZER/FUEL WEIGHT RATIO, EXCLUDES TANK PRESSURANT FLOWS.
3. PUMP EFFICIENCIES - INCLUDES EFFECTS OF RECIRCULATED FLOWS (THRUST BALANCE SYSTEMS, BEARING COOLING, INTERNAL LEAKAGES, ETC.)

TABLE A-4

ASE OFF DESIGN DECK - CYCLE NO. 106. PAGE 1

THRUST = 800. MRE= 3.500 PC = 79.1

INLET CONDITIONS

FUEL TEMP	38.3	DEG R
FUEL PRESS	19.9	PSIA
OX TEMP	166.0	DEG R
OX PRESS	19.1	PSIA
MIX RATIO(VEH)	3.612	

PERFORMANCE

THRUST	800.	LB FORCE
IMPULSE	450.000	SEC
MIXTURE RATIO(ENG)	3.500	
CHAMBER PRESS	79.1	PSIA
FUEL FLOW(ENG)	0.395	LB/SEC
OX FLOW(ENG)	1.383	LB/SEC

*** FUEL BOOST PUMP ***

DIAMETER	3.360	INCH
FLOW	0.408	LB/SEC
SPEED	4465.	RPM
EFF	0.471	
INLET PRESS	19.93	PSIA
DISCH PRESS	21.77	PSIA
DISCH TEMP	38.35	DEG R
EXIT DENSITY	4.345	LB/FT**3
VOL FLOW	42.12	GPM
HEAD	61.	FT
POWER	0.10	HP
FLOW COEF	0.070	
HEAD COEF	0.5813	
NPSP AVAIL	0.453	PSI
NPSP REQ	0.002	PSI
NPSH AVAIL	15.00	FT
NPSH REQ	0.06	FT
SUCT SPEC SPEED	1607.	

FIRST STAGE FUEL PUMP

DIAMETER	5.276	INCH
FLOW	0.408	LB/SEC
SPEED	18593.	RPM
EFF	0.404	
INLET PRESS	21.74	PSIA
DISCH PRESS	127.95	PSIA
DISCH TEMP	41.69	DEG R
EXIT DENSITY	4.267	LB/FT**3
VOL FLOW	42.13	GPM
HEAD	3561.	FT
POWER	6.53	HP
FLOW COEF	0.023	
HEAD COEF	0.6244	
NPSP AVAIL	2.151	PSI
NPSP REQ	2.203	PSI
NPSH AVAIL	71.30	FT
NPSH REQ	73.00	FT
SUCT SPEC SPEED	4918.	

SECOND STAGE FUEL PUMP

DIAMETER	5.317	INCH
FLOW	0.408	LB/SEC
SPEED	18593.	RPM
EFF	0.396	
INLET PRESS	127.86	PSIA
DISCH PRESS	233.66	PSIA
DISCH TEMP	45.04	DEG R
EXIT DENSITY	4.169	LB/FT**3
VOL FLOW	42.89	GPM
HEAD	3607.	FT
POWER	6.76	HP
FLOW COEF	0.019	
HEAD COEF	0.6228	

*** THRUST CHAMBER ***

COOL IN PRESS	202.6	PSIA
COOL PRESS LOSS	74.5	PSID
COOL TEMP RISE	499.2	DEG R
COOL DISCH TEMP	544.2	DEG R
COOL FLOW	0.340	LB/SEC
CHAMBR PRESS	79.1	PSIA
HOT GAS INJ PRESS	81.6	PSIA
HOT GAS INJ TEMP	525.6	DEG R
OX INJ PRESS	82.0	PSIA
OX INJ TEMP	169.2	DEG R
OX FLOW	1.383	LB/SEC
HOT GAS FLOW	0.367	LB/SEC
MC MIX RATIO	3.766	
AREA RATIO(AERO)	400.	
THROAT DIA(AERO)	2.570	INCH
NOZ EXIT DIA(AERO)	51.500	INCH

PUMP SPECIFIC SPEED

FUEL 1 STAGE	261.8
FUEL 2 STAGE	261.6
LOX 1 STAGE	392.8
FUEL BOOST	1328.4
LOX BOOST	1039.3

DUMP COOLED NOZZLE

COOL FLOW	0.028	LB/SEC

TABLE A-4 (Continued)

ASE OFF DESIGN DECK - CYCLE NO. 106. PAGE 2

THRUST = 800. MRE= 3.500 PC = 79.1

OXIDIZER BOOST PUMP			***FIRST STAGE LOX PUMP***		
DIAMETER	3.810	INCH	DIAMETER	3.055	INCH
FLOW	1.473	LB/SEC	FLOW	1.473	LB/SEC
SPEED	1083.	RPM	SPEED	10172.	RPM
EFF	0.324		EFF	0.275	
INLET PRESS	19.06	PSIA	INLET PRESS	21.35	PSIA
DISCH PRESS	21.36	PSIA	DISCH PRESS	187.50	PSIA
DISCH TEMP	166.04	DEG R	DISCH TEMP	169.25	DEG R
EXIT DENSITY	70.499	LB/FT**3	EXIT DENSITY	70.096	LB/FT**3
VOL FLOW	9.38	GPM	VOL FLOW	9.38	GPM
HEAD	5.	FT	HEAD	341.	FT
POWER	0.04	HP	POWER	3.31	HP
FLOW COEF	0.044		FLOW COEF	0.020	
HEAD COEF	0.5959		HEAD COEF	0.5951	
NPSP AVAIL	0.979	PSI	NPSP AVAIL	3.235	PSI
NPSP REQ	0.001	PSI	NPSP REQ	3.539	PSI
NPSH AVAIL	2.00	FT	NPSH AVAIL	6.61	FT
NPSH REQ	0.00	FT	NPSH REQ	7.23	FT
SUCT SPEC SPEED	1275.		SUCT SPEC SPEED	7557.	

**** FUEL TURBINE ****			*** LOX TURBINE ***		
FLOW	0.230	LB/SEC	FLOW	0.098	LB/SEC
NO.STAGES	1.000		NO.STAGES	1.000	
PRESS RATIO T/S	1.206		PRESS RATIO T/S	1.166	
INLET TEMP	537.276	DEG R	INLET TEMP	537.276	DEG R
POWER	13.287	HP	POWER	3.447	HP
INLET PRESS	99.370	PSIA	INLET PRESS	98.868	PSIA
EFF	0.417		EFF	0.310	
EXIT TEMP	525.587	DEG R	EXIT TEMP	530.142	DEG R
U/C	0.169		U/C	0.100	
PERC ADMISSION	53.3		PERC ADMISSION	23.9	
MEAN WHEEL SPEED	374.	FT/SEC	MEAN WHEEL SPEED	202.	FT/SEC
BLADE HEIGHT	0.30	INCH	BLADE HEIGHT	0.30	INCH
VANE ANGLE	15.40	DEG	VANE ANGLE	15.00	DEG
MEAN DIAM	4.605	INCH	MEAN DIAM	4.545	INCH

GOX HEAT EXCHANGER			**PREBURNER**		
OX INL PRESS	187.	PSIA	MIXTURE RATIO	0.0	
OX INL TEMP	169.2	DEG R	TEMPERATURE	537.	DEG R
OX PRESS LOSS	0.24	PSID	PRESS	100.	PSIA
OX DISCH TEMP	258.	DEG R	FUEL FLOW	0.327	LB/SEC
GH2 FLOW	0.049	LB/SEC	OXIDIZER FLOW	0.0	LB/SEC
GH2 INL PRES	128.	PSIA	GAMMA	1.400	
GH2 INL TEMP	544.	DEG R	CP	3.500	BTU/LB/R
GH2 PRESS LOSS	2.5	PSID	GAS CONSTANT	766.4	FT-LB/LBR
GH2 DISCH TEMP	498.	DEG R	PERC FUEL PARASIT	17.1	
GH2 TEMP TO P/B	537.	DEG R	FUEL PARASIT	0.068	LB/SEC

TABLE A-4 (Continued)

THRUST = 800. MRE = 3.500 PC = 79.1
ASE OFF DESIGN DECK - CYCLE NO. 106. PAGE 3

VALVES	INLET PRESS (PSIA)	DP (PSI)	DP/P1	AREA (IN**2)
FUEL VALVE	233.7	31.09	0.1330	0.0182
PREBURNER OXIDIZER VALVE	187.5	0.0	0.0	0.0
MAIN OXIDIZER VALVE	187.5	105.53	0.5628	0.0241
FUEL SHUNT VALVE	128.1	2.5	-0.0194	1.1672
GOX CONTROL VALVE	187.2	0.020	0.0001	1.1100

INJECTORS	INLET PRESS (PSIA)	DP (PSI)	DP/P2	AREA (IN**2)
PREBURNER FUEL INJECTOR	125.6	25.3	0.2522	0.5258
PREBURNER OXIDIZER INJECTOR	3795.8	0.0	0.0	0.0520
OXIDIZER MAIN INJECTOR	82.0	2.84	0.0359	0.1466
HOT GAS INJECTOR	81.6	2.43	0.0308	2.0952

TANK PRESSURANT

OX FLOW	0.090 LB/SEC
OX TEMP	258. DEG R
OX DELIV PRESS	187.3PSIA
FUEL FLOW	0.013 LB/SEC
FUEL TEMP	544. DEG R
FUEL DELIV PRESS	128.1PSIA

NOTES
1. VEHICLE MIXTURE RATIO - OXIDIZER/FUEL WEIGHT RATIO, INCLUDES TANK PRESSURANT FLOWS.
2. ENGINE MIXTURE RATIO - OXIDIZER/FUEL WEIGHT RATIO, EXCLUDES TANK PRESSURANT FLOWS.
3. PUMP EFFICIENCIES - INCLUDES EFFECTS OF RECIRCULATED FLOWS (THRUST BALANCE SYSTEMS, BEARING COOLING, INTERNAL LEAKAGES, ETC.)

TABLE A-5

ASE OFF DESIGN DECK - CYCLE NO. 104.8 PAGE 1

THRUST - 20000. MR = 5.500 PC = 1946.0

INLET CONDITIONS		**PERFORMANCE**	
FUEL TEMP	38.3 DEG R	THRUST	20000. LB FORCE
FUEL PRESS	19.9 PSIA	IMPULSE	474.900 SEC
OX TEMP	166.0 DEG R	MIXTURE RATIO	5.500
OX PRESS	19.1 PSIA	CHAMBER PRESS	1946.0 PSIA
		FUEL FLOW	6.479 LB/SEC
		OX FLOW	35.635 LB/SEC

*** FUEL BOOST PUMP ***		**FIRST STAGE FUEL PUMP**	
DIAMETER	3.966 INCH	DIAMETER	5.276 INCH
FLOW	6.513 LB/SEC	FLOW	6.513 LB/SEC
SPEED	22969. RPM	SPEED	97251. RPM
EFF	0.656	EFF	0.560
INLET PRESS	19.93 PSIA	INLET PRESS	72.35 PSIA
DISCH PRESS	78.04 PSIA	DISCH PRESS	2398.61 PSIA
DISCH TEMP	39.21 DEG R	DISCH TEMP	85.67 DEG R
EXIT DENSITY	4.344 LB/FT**3	EXIT DENSITY	4.055 LB/FT**3
VOL FLOW	672.75 GPM	VOL FLOW	672.94 GPM
HEAD	1926. FT	HEAD	81185. FT
POWER	34.79 HP	POWER	1715.59 HP
FLOW COEF	0.143	FLOW COEF	0.070
HEAD COEF	0.3915	HEAD COEF	0.5204
NPSP AVAIL	0.453 PSI	NPSP AVAIL	49.971 PSI
NPSP REQ	0.479 PSI	NPSP REQ	35.001 PSI
NPSH AVAIL	15.00 FT	NPSH AVAIL	1656.35 FT
NPSH REQ	15.89 FT	NPSH REQ	1160.17 FT
SUCT SPEC SPEED	35548.	SUCT SPEC SPEED	12687.

SECOND STAGE FUEL PUMP		*** THRUST CHAMBER ***	
DIAMETER	5.317 INCH	COOL IN PRESS	4725.0 PSIA
FLOW	6.513 LB/SEC	COOL PRESS LOSS	1039.0 PSID
SPEED	97251. RPM	COOL TEMP RISE	342.6 DEG R
EFF	0.563	COOL DISCH TEMP	475.6 DEG R
INLET PRESS	2375.47 PSIA	COOL FLOW	5.736 LB/SEC
DISCH PRESS	4729.77 PSIA	CHAMBR PRESS	1946.0 PSIA
DISCH TEMP	133.05 DEG R	HOT GAS INJ PRESS	2111.1 PSIA
EXIT DENSITY	3.985 LB/FT**3	HOT GAS INJ TEMP	1888.4 DEG R
VOL FLOW	720.92 GPM	OX INJ PRESS	3322.3 PSIA
HEAD	84421. FT	OX INJ TEMP	197.8 DEG R
POWER	1775.25 HP	OX FLOW	30.385 LB/SEC
FLOW COEF	0.061	HOT GAS FLOW	11.729 LB/SEC
HEAD COEF	0.5328	AREA RATIO	400.
		THROAT DIA	2.570 INCH
		NOX EXIT DIA	51.500 INCH

PUMP SPECIFIC SPEED	
FUEL 1 STAGE	524.5
FUEL 2 STAGE	527.2
LOX 1 STAGE	920.6
LOX 2 STAGE	0.0
FUEL BOOST	2049.2
LOX BOOST	1854.6

TABLE A-5 (Continued)

ASE OFF DESIGN DECK - CYCLE NO. 104.β

THRUST = 20000. MR = 5.500 PC = 1946.0

OXIDIZER BOUST PUMP		
DIAMETER	4.532	INCH
FLOW	35.769	LB/SEC
SPEED	5436.	RPM
EFF	0.632	
INLET PRESS	19.06	PSIA
DISCH PRESS	95.64	PSIA
DISCH TEMP	166.49	DEG R
EXIT DENSITY	70.495	LB/FT**3
VOL FLOW	227.72	GPM
HEAD	156.	FT
POWER	16.11	HP
FLOW COEF	0.115	
HEAD COEF	0.4348	
NPSP AVAIL	0.979	PSI
NPSP REQ	0.867	PSI
NPSH AVAIL	2.00	FT
NPSH REQ	1.77	FT
SUCT SPEC SPEED	35562.	

FIRST STAGE LOX PUMP		
DIAMETER	3.055	INCH
FLOW	35.769	LB/SEC
SPEED	58845.	RPM
EFF	0.618	
INLET PRESS	83.51	PSIA
DISCH PRESS	4716.45	PSIA
DISCH TEMP	197.76	DEG R
EXIT DENSITY	69.842	LB/FT**3
VOL FLOW	227.75	GPM
HEAD	9531.	FT
POWER	******	HP
FLOW COEF	0.084	
HEAD COEF	0.4975	
NPSP AVAIL	64.940	PSI
NPSP REQ	43.322	PSI
NPSH AVAIL	132.65	FT
NPSH REQ	88.49	FT
SUCT SPEC SPEED	30775.	

SECOND STAGE LOX PUMP		
DIAMETER	0.0	INCH
FLOW	0.0	LB/SEC
SPEED	58845.	RPM
EFF	0.0	
INLET PRESS	4716.45	PSIA
DISCH PRESS	4716.45	PSIA
DISCH TEMP	197.76	DEG R
EXIT DENSITY	69.842	LB/FT**3
VOL FLOW	0.0	GPM
HEAD	0.	FT
POWER	0.0	HP
FLOW COEF	0.0	
HEAD COEF	0.0	

*** PREBURNER ***		
MIXTURE RATIO	0.921	
TEMPERATURE	2053.	DEG R
PRESS	3474.	PSIA
FUEL FLOW	5.702	LB/SEC
OXIDIZER FLOW	5.250	LB/SEC
GAMMA	1.348	
CP	1.975	BTU/LB/R
GAS CONSTANT	397.0	FT.LB/LBR
FUEL PARASIT	0.120	

**** FUEL TURBINE ****		
FLOW	7.608	LB/SEC
NO.STAGES	1.000	
PRESS RATIO T/S	1.597	
INLET TEMP	2053.128	DEG R
POWER	3500.275	HP
INLET PRESS	3439.491	PSIA
EFF	0.705	
EXIT TEMP	1888.372	DEG R
U/C	0.406	
PERC ADMISSION	0.516	
MEAN WHEEL SPEED	1955.	FT/SEC
BLADE HEIGHT	0.30	INCH
VANE ANGLE	15.40	DEG
MEAN DIAM	4.605	INCH

*** LOX TURBINE ***		
FLOW	3.344	LB/SEC
NO.STAGES	1.000	
PRESS RATIO T/S	1.540	
INLET TEMP	2053.128	DEG R
POWER	1053.234	HP
INLET PRESS	3422.114	PSIA
EFF	0.521	
EXIT TEMP	1940.326	DEG R
U/C	0.252	
PERC ADMISSION	0.242	
MEAN WHEEL SPEED	1168.	FT/SEC
BLADE HEIGHT	0.30	INCH
VANE ANGLE	15.00	DEG
MEAN DIAM	4.545	INCH

TABLE A-5 (Continued)

ASE OFF DESIGN DECK - CYCLE NO. 104.8 PAGE 3

THRUST = 20000. MR = 5.500 PC = 1946.0

VALVES	INLET PRESS (PSIA)	DP (PSI)	DP/P1	AREA (IN**2)
FUEL VALVE	4729.8	4.73	0.0010	2.2444
PREBURNER OXIDIZER VALVE	4716.5	915.66	0.1941	0.0311
MAIN OXIDIZER VALVE	4716.5	1394.18	0.2956	0.1457
GOX CONTROL VALVE	0.0	0.0	0.0	0.0

INJECTORS	INLET PRESS (PSIA)	DP (PSI)	DP/P2	AREA (IN**2)
PREBURNER FUEL INJECTOR	3669.1	172.73	0.0494	0.6004
PREBURNER OXIDIZER INJECTOR	3800.8	326.56	0.0940	0.0520
OXIDIZER MAIN INJECTOR	3322.3	1376.28	0.7072	0.1466
HOT GAS INJECTOR	2111.1	165.15	0.0849	2.0952

TANK PRESSURANT

OX FLOW	0.134 LB/SEC
OX TEMP	409. DEG R
OX DELIV PRESS	4707.5PSIA
FUEL FLOW	0.034 LB/SEC
FUEL TEMP	476. DEG R
FUEL DELIV PRESS	3669.1PSIA

TABLE A-6

ASE OFF DESIGN DECK - CYCLE NO. 104.8 *REVISED* PAGE 1

THRUST - 20000. MR = 6.000 PC = 1921.6

INLET CONDITIONS		**PERFORMANCE**	
FUEL TEMP	38.3 DEG R	THRUST	20000. LB FORCE
FUEL PRESS	19.9 PSIA	IMPULSE	472.900 SEC
OX TEMP	166.0 DEG R	MIXTURE RATIO	6.000
OX PRESS	19.1 PSIA	CHAMBER PRESS	1921.6 PSIA
		FUEL FLOW	6.042 LB/SEC
		OX FLOW	36.250 LB/SEC

*** FUEL BOOST PUMP ***		**FIRST STAGE FUEL PUMP**	
DIAMETER	3.966 INCH	DIAMETER	5.276 INCH
FLOW	6.076 LB/SEC	FLOW	6.076 LB/SEC
SPEED	21468. RPM	SPEED	92991. RPM
EFF	0.656	EFF	0.561
INLET PRESS	19.93 PSIA	INLET PRESS	65.17 PSIA
DISCH PRESS	70.77 PSIA	DISCH PRESS	2228.66 PSIA
DISCH TEMP	39.09 DEG R	DISCH TEMP	81.79 DEG R
EXIT DENSITY	4.344 LB/FT**3	EXIT DENSITY	4.078 LB/FT**3
VOL FLOW	627.58 GPM	VOL FLOW	627.72 GPM
HEAD	1685. FT	HEAD	75184. FT
POWER	28.37 HP	POWER	1480.68 HP
FLOW COEF	0.143	FLOW COEF	0.068
HEAD COEF	0.3920	HEAD COEF	0.5271
NPSP AVAIL	0.453 PSI	NPSP AVAIL	43.232 PSI
NPSP REQ	0.317 PSI	NPSP REQ	30.513 PSI
NPSH AVAIL	15.00 FT	NPSH AVAIL	1432.96 FT
NPSH REQ	10.52 FT	NPSH REQ	1011.39 FT
SUCT SPEC SPEED	35479.	SUCT SPEC SPEED	12988.

SECOND STAGE FUEL PUMP		*** THRUST CHAMBER ***	
DIAMETER	5.317 INCH	COOL IN PRESS	4391.3 PSIA
FLOW	6.076 LB/SEC	COOL PRESS LOSS	941.6 PSID
SPEED	92991. RPM	COOL TEMP RISE	347.7 DEG R
EFF	0.564	COOL DISCH TEMP	474.0 DEG R
INLET PRESS	2208.64 PSIA	COOL FLOW	5.351 LB/SEC
DISCH PRESS	4395.73 PSIA	CHAMBR PRESS	1921.6 PSIA
DISCH TEMP	126.29 DEG R	HOT GAS INJ PRESS	2067.8 PSIA
EXIT DENSITY	3.988 LB/FT**3	HOT GAS INJ TEMP	1899.8 DEG R
VOL FLOW	668.68 GPM	OX INJ PRESS	3383.6 PSIA
HEAD	78196. FT	OX INJ TEMP	192.3 DEG R
POWER	1532.05 HP	OX FLOW	31.355 LB/SEC
FLOW COEF	0.060	HOT GAS FLOW	10.938 LB/SEC
HEAD COEF	0.5398	AREA RATIO	400.
		THROAT DIA	2.570 INCH
		NOX EXIT DIA	51.500 INCH

PUMP SPECIFIC SPEED	
FUEL 1 STAGE	513.1
FUEL 2 STAGE	514.2
LOX 1 STAGE	983.3
LOX 2 STAGE	0.0
FUEL BOOST	2045.4
LOX BOOST	1992.8

TABLE A-6 (Continued)

ASE OFF DESIGN DECK - CYCLE NO. 104. 8 REVISED

THRUST = 20000. MR = 6.000 PC = 1921.6

OXIDIZER BOOST PUMP			***FIRST STAGE LOX PUMP***		
DIAMETER	4.532	INCH	DIAMETER	3.055	INCH
FLOW	36.384	LB/SEC	FLOW	36.384	LB/SEC
SPEED	5081.	RPM	SPEED	55000.	RPM
EFF	0.648		EFF	0.625	
INLET PRESS	19.06	PSIA	INLET PRESS	71.28	PSIA
DISCH PRESS	83.38	PSIA	DISCH PRESS	4000.44	PSIA
DISCH TEMP	166.39	DEG R	DISCH TEMP	192.28	DEG R
EXIT DENSITY	70.500	LB/FT**3	EXIT DENSITY	70.012	LB/FT**3
VOL FLOW	231.64	GPM	VOL FLOW	231.65	GPM
HEAD	131.	FT	HEAD	8068.	FT
POWER	13.41	HP	POWER	653.37	HP
FLOW COEF	0.125		FLOW COEF	0.091	
HEAD COEF	0.4180		HEAD COEF	0.4820	
NPSP AVAIL	0.979	PSI	NPSP AVAIL	52.808	PSI
NPSP REQ	0.896	PSI	NPSP REQ	35.772	PSI
NPSH AVAIL	2.00	FT	NPSH AVAIL	107.86	FT
NPSH REQ	1.83	FT	NPSH REQ	73.07	FT
SUCT SPEC SPEED	33034.		SUCT SPEC SPEED	33492.	
SECOND STAGE LOX PUMP					
DIAMETER	0.0	INCH			
FLOW	*****	LB/SEC	*** PREBURNER ***		
SPEED	55000.	RPM	MIXTURE RATIO	0.921	
EFF	0.0		TEMPERATURE	2052.	DEG R
INLET PRESS	4000.44	PSIA	PRESS	3275.	PSIA
DISCH PRESS	4000.44	PSIA	FUEL FLOW	5.317	LB/SEC
DISCH TEMP	192.28	DEG R	OXIDIZER FLOW	4.896	LB/SEC
EXIT DENSITY	70.012	LB/FT**3	GAMMA	1.348	
VOL FLOW	0.0	GPM	CP	1.975	BTU/LB/R
HEAD	0.	FT	GAS CONSTANT	397.0	FT.LB/LBR
POWER	0.0	HP	FUEL PARASIT	0.120	
FLOW COEF	0.0				
HEAD COEF	0.0				
**** FUEL TURBINE ****			*** LOX TURBINE ***		
FLOW	7.095	LB/SEC	FLOW	3.118	LB/SEC
NO.STAGES	1.000		NO.STAGES	1.000	
PRESS RATIO T/S	1.537		PRESS RATIO T/S	1.482	
INLET TEMP	2051.561	DEG R	INLET TEMP	2051.561	DEG R
POWER	3006.481	HP	POWER	892.270	HP
INLET PRESS	3242.399	PSIA	INLET PRESS	3226.018	PSIA
EFF	0.704		EFF	0.517	
EXIT TEMP	1899.784	DEG R	EXIT TEMP	1949.067	DEG R
U/C	0.405		U/C	0.246	
PERC ADMISSION	0.516		PERC ADMISSION	0.242	
MEAN WHEEL SPEED	1870.	FT/SEC	MEAN WHEEL SPEED	1092.	FT/SEC
BLADE HEIGHT	0.30	INCH	BLADE HEIGHT	0.30	INCH
VANE ANGLE	15.40	DEG	VANE ANGLE	15.00	DEG
MEAN DIAM	4.605	INCH	MEAN DIAM	4.545	INCH

TABLE A-6 (Continued)

ASE OFF DESIGN DECK - CYCLE NO. 104.8 REVISED

THRUST = 20000. MR = 6.000 PC = 1921.6

VALVES	INLET PRESS (PSIA)	DP (PSI)	DP/P1	AREA (IN**2)
FUEL VALVE	4395.7	4.40	0.0010	2.1687
PREBURNER OXIDIZER VALVE	4000.4	440.15	0.1100	0.0417
MAIN OXIDIZER VALVE	4000.4	616.83	0.1542	0.2257
GOX CONTROL VALVE	0.0	0.0	0.0	0.0

INJECTORS	INLET PRESS (PSIA)	DP (PSI)	DP/P2	AREA (IN**2)
PREBURNER FUEL INJECTOR	3434.2	158.19	0.0483	0.6004
PREBURNER OXIDIZER INJECTOR	3558.4	283.28	0.0865	0.0520
OXIDIZER MAIN INJECTOR	3383.6	1462.03	0.7608	0.1466
HOT GAS INJECTOR	2067.8	146.20	0.0761	2.0952

TANK PRESSURANT

OX FLOW	0.134 LB/SEC
OX TEMP	400. DEG R
OX DELIV PRESS	3991.4PSIA
FUEL FLOW	0.034 LB/SEC
FUEL TEMP	474. DEG R
FUEL DELIV PRESS	3434.2PSIA

TABLE A-7

ASE OFF DESIGN DECK - CYCLE NO. 104.8 PAGE 1

THRUST = 20000. MR = 6.500 PC = 1902.0

INLET CONDITIONS		
FUEL TEMP	38.3	DEG R
FUEL PRESS	19.9	PSIA
OX TEMP	166.0	DEG R
OX PRESS	19.1	PSIA

PERFORMANCE		
THRUST	20000.	LB FORCE
IMPULSE	469.400	SEC
MIXTURE RATIO	6.500	
CHAMBER PRESS	1902.0	PSIA
FUEL FLOW	5.681	LB/SEC
OX FLOW	36.927	LB/SEC

*** FUEL BOOST PUMP ***		
DIAMETER	3.966	INCH
FLOW	5.715	LB/SEC
SPEED	20825.	RPM
EFF	0.650	
INLET PRESS	19.93	PSIA
DISCH PRESS	68.65	PSIA
DISCH TEMP	39.07	DEG R
EXIT DENSITY	4.344	LB/FT**3
VOL FLOW	590.32	GPM
HEAD	1614.	FT
POWER	25.81	HP
FLOW COEF	0.139	
HEAD COEF	0.3993	
NPSP AVAIL	0.453	PSI
NPSP REQ	0.273	PSI
NPSH AVAIL	15.00	FT
NPSH REQ	9.03	FT
SUCT SPEC SPEED	34404.	

FIRST STAGE FUEL PUMP		
DIAMETER	5.276	INCH
FLOW	5.715	LB/SEC
SPEED	92646.	RPM
EFF	0.560	
INLET PRESS	63.69	PSIA
DISCH PRESS	2263.46	PSIA
DISCH TEMP	82.73	DEG R
EXIT DENSITY	4.070	LB/FT**3
VOL FLOW	590.53	GPM
HEAD	76579.	FT
POWER	1420.74	HP
FLOW COEF	0.064	
HEAD COEF	0.5409	
NPSP AVAIL	41.781	PSI
NPSP REQ	31.467	PSI
NPSH AVAIL	1385.00	FT
NPSH REQ	1043.13	FT
SUCT SPEC SPEED	12262.	

SECOND STAGE FUEL PUMP		
DIAMETER	5.317	INCH
FLOW	5.715	LB/SEC
SPEED	92646.	RPM
EFF	0.563	
INLET PRESS	2245.71	PSIA
DISCH PRESS	4459.94	PSIA
DISCH TEMP	127.76	DEG R
EXIT DENSITY	3.984	LB/FT**3
VOL FLOW	630.36	GPM
HEAD	79282.	FT
POWER	1462.82	HP
FLOW COEF	0.056	
HEAD COEF	0.5514	

*** THRUST CHAMBER ***		
COOL IN PRESS	4206.3	PSIA
COOL PRESS LOSS	848.3	PSID
COOL TEMP RISE	349.6	DEG R
COOL DISCH TEMP	472.3	DEG R
COOL FLOW	5.033	LB/SEC
CHAMBR PRESS	1902.0	PSIA
HOT GAS INJ PRESS	2042.2	PSIA
HOT GAS INJ TEMP	1982.7	DEG R
OX INJ PRESS	3430.5	PSIA
OX INJ TEMP	190.3	DEG R
OX FLOW	32.065	LB/SEC
HOT GAS FLOW	10.543	LB/SEC
AREA RATIO	400.	
THROAT DIA	2.570	INCH
NOX EXIT DIA	51.500	INCH

PUMP SPECIFIC SPEED	
FUEL 1 STAGE	489.1
FUEL 2 STAGE	492.3
LOX 1 STAGE	1023.8
LOX 2 STAGE	0.0
FUEL BOOST	1986.6
LOX BOOST	2080.9

TABLE A-7 (Continued)

ASE OFF DESIGN DECK - CYCLE NO. 104.8 PAGE 2

THRUST = 20000. MR = 6.500 PC = 1902.0

OXIDIZER BOOST PUMP			***FIRST STAGE LOX PUMP***		
DIAMETER	4.532	INCH	DIAMETER	3.055	INCH
FLOW	37.061	LB/SEC	FLOW	37.061	LB/SEC
SPEED	4929.	RPM	SPEED	53351.	RPM
EFF	0.640		EFF	0.624	
INLET PRESS	19.06	PSIA	INLET PRESS	65.53	PSIA
DISCH PRESS	78.08	PSIA	DISCH PRESS	3685.71	PSIA
DISCH TEMP	166.37	DEG R	DISCH TEMP	190.26	DEG R
EXIT DENSITY	70.499	LB/FT**3	EXIT DENSITY	70.033	LB/FT**3
VOL FLOW	235.95	GPM	VOL FLOW	235.96	GPM
HEAD	121.	FT	HEAD	7432.	FT
POWER	12.70	HP	POWER	802.28	HP
FLOW COEF	0.131		FLOW COEF	0.096	
HEAD COEF	0.4076		HEAD COEF	0.4719	
NPSP AVAIL	0.979	PSI	NPSP AVAIL	47.078	PSI
NPSP REQ	0.978	PSI	NPSP REQ	37.214	PSI
NPSH AVAIL	2.00	FT	NPSH AVAIL	96.16	FT
NPSH REQ	2.00	FT	NPSH REQ	76.01	FT
SUCT SPEC SPEED	31096.		SUCT SPEC SPEED	31831.	
SECOND STAGE LOX PUMP					
DIAMETER	0.0	INCH			
FLOW	0.0	LB/SEC	*** PREBURNER ***		
SPEED	53351.	RPM	MIXTURE RATIO	0.973	
EFF	0.0		TEMPERATURE	2134.	DEG R
INLET PRESS	3685.71	PSIA	PRESS	3203.	PSIA
DISCH PRESS	3685.71	PSIA	FUEL FLOW	4.999	LB/SEC
DISCH TEMP	190.26	DEG R	OXIDIZER FLOW	4.862	LB/SEC
EXIT DENSITY	70.033	LB/FT**3	GAMMA	1.344	
VOL FLOW	0.0	GPM	CP	1.945	BTU/LB/R
HEAD	0.	FT	GAS CONSTANT	387.2	FT.LB/LBR
POWER	0.0	HP	FUEL PARASIT	0.120	
FLOW COEF	0.0				
HEAD COEF	0.0				
**** FUEL TURBINE ****			*** LOX TURBINE ***		
FLOW	6.850	LB/SEC	FLOW	3.011	LB/SEC
NO.STAGES	1.000		NO.STAGES	1.000	
PRESS RATIO T/S	1.522		PRESS RATIO T/S	1.468	
INLET TEMP	2133.819	DEG R	INLET TEMP	2133.819	DEG R
POWER	2882.268	HP	POWER	841.121	HP
INLET PRESS	3171.090	PSIA	INLET PRESS	3155.069	PSIA
EFF	0.704		EFF	0.509	
EXIT TEMP	1982.678	DEG R	EXIT TEMP	2032.225	DEG R
U/C	0.405		U/C	0.240	
PERC ADMISSION	0.516		PERC ADMISSION	0.242	
MEAN WHEEL SPEED	1863.	FT/SEC	MEAN WHEEL SPEED	1059.	FT/SEC
BLADE HEIGHT	0.30	INCH	BLADE HEIGHT	0.30	INCH
VANE ANGLE	15.40	DEG	VANE ANGLE	15.00	DEG
MEAN DIAM	4.605	INCH	MEAN DIAM	4.545	INCH

TABLE A-7 (Continued)

ASE OFF DESIGN DECK - CYCLE NO. 104.8 PAGE 3

THRUST = 20000. MR = 6.500 PC = 1902.0

VALVES	INLET PRESS (PSIA)	DP (PSI)	DP/P1	AREA (IN**2)
FUEL VALVE	4459.9	253.60	0.0569	0.2690
PREBURNER OXIDIZER VALVE	3685.7	204.74	0.0555	0.0607
MAIN OXIDIZER VALVE	3685.7	255.18	0.0692	0.3588
GOX CONTROL VALVE	0.0	0.0	0.0	0.0

INJECTORS	INLET PRESS (PSIA)	DP (PSI)	DP/P2	AREA (IN**2)
PREBURNER FUEL INJECTOR	3344.0	142.05	0.0444	0.6004
PREBURNER OXIDIZER INJECTOR	3482.4	279.29	0.0872	0.0520
OXIDIZER MAIN INJECTOR	3430.5	1528.54	0.8036	0.1466
HOT GAS INJECTOR	2042.2	140.18	0.0737	2.0952

TANK PRESSURANT

OX FLOW	0.134 LB/SEC
OX TEMP	405. DEG R
OX DELIV PRESS	3676.7PSIA
FUEL FLOW	0.034 LB/SEC
FUEL TEMP	472. DEG R
FUEL DELIV PRESS	3344.0PSIA

TABLE A-8

ASE OFF DESIGN DECK - CYCLE NO. 104. *B REVISED (RIM)* PAGE 1

THRUST = 800. MR = 3.500 PC = 79.1

INLET CONDITIONS		
FUEL TEMP	38.3	DEG R
FUEL PRESS	19.9	PSIA
OX TEMP	166.0	DEG R
OX PRESS	19.1	PSIA

PERFORMANCE		
THRUST	800.	LB FORCE
IMPULSE	455.000	SEC
MIXTURE RATIO	3.500	
CHAMBER PRESS	79.1	PSIA
FUEL FLOW	0.391	LB/SEC
OX FLOW	1.368	LB/SEC

*** FUEL BOOST PUMP ***		
DIAMETER	3.966	INCH
FLOW	0.403	LB/SEC
SPEED	3650.	RPM
EFF	0.331	
INLET PRESS	19.93	PSIA
DISCH PRESS	21.95	PSIA
DISCH TEMP	38.38	DEG R
EXIT DENSITY	4.343	LB/FT**3
VOL FLOW	41.67	GPM
HEAD	67.	FT
POWER	0.15	HP
FLOW COEF	0.056	
HEAD COEF	0.5383	
NPSP AVAIL	0.453	PSI
NPSP REQ	0.001	PSI
NPSH AVAIL	15.00	FT
NPSH REQ	0.04	FT
SUCT SPEC SPEED	13854.	

FIRST STAGE FUEL PUMP		
DIAMETER	5.276	INCH
FLOW	0.403	LB/SEC
SPEED	17593.	RPM
EFF	0.402	
INLET PRESS	21.92	PSIA
DISCH PRESS	117.06	PSIA
DISCH TEMP	41.41	DEG R
EXIT DENSITY	4.272	LB/FT**3
VOL FLOW	41.69	GPM
HEAD	3187.	FT
POWER	5.82	HP
FLOW COEF	0.024	
HEAD COEF	0.6242	
NPSP AVAIL	2.149	PSI
NPSP REQ	2.195	PSI
NPSH AVAIL	71.25	FT
NPSH REQ	72.76	FT
SUCT SPEC SPEED	4558.	

SECOND STAGE FUEL PUMP		
DIAMETER	5.317	INCH
FLOW	0.403	LB/SEC
SPEED	17593.	RPM
EFF	0.392	
INLET PRESS	116.97	PSIA
DISCH PRESS	211.77	PSIA
DISCH TEMP	44.45	DEG R
EXIT DENSITY	4.197	LB/FT**3
VOL FLOW	42.38	GPM
HEAD	3227.	FT
POWER	6.03	HP
FLOW COEF	0.020	
HEAD COEF	0.6224	

PUMP SPECIFIC SPEED	
FUEL 1 STAGE	267.8
FUEL 2 STAGE	267.5
LOX 1 STAGE	408.3
LOX 2 STAGE	******
FUEL BOOST	1007.6
LOX BOOST	760.3

*** THRUST CHAMBER ***		
COOL IN PRESS	192.7	PSIA
COOL PRESS LOSS	66.6	PSID
COOL TEMP RISE	492.0	DEG R
COOL DISCH TEMP	536.4	DEG R
COOL FLOW	0.345	LB/SEC
CHAMBR PRESS	79.1	PSIA
HOT GAS INJ PRESS	81.1	PSIA
HOT GAS INJ TEMP	518.5	DEG R
OX INJ PRESS	81.9	PSIA
OX INJ TEMP	168.7	DEG R
OX FLOW	1.368	LB/SEC
HOT GAS FLOW	0.391	LB/SEC
AREA RATIO	400.	
THROAT DIA	2.570	INCH
NOX EXIT DIA	51.500	INCH

TABLE A-8 (Continued)

ASE OFF DESIGN DECK - CYCLE NO. 104.8 REVISED (RIM) PAGE 2

THRUST = 800. MR = 3.500 PC = 79.1

OXIDIZER BOOST PUMP			***FIRST STAGE LOX PUMP***		
DIAMETER	4.532	INCH	DIAMETER	3.055	INCH
FLOW	1.458	LB/SEC	FLOW	1.458	LB/SEC
SPEED	864.	RPM	SPEED	9352.	RPM
EFF	0.190		EFF	0.285	
INLET PRESS	19.06	PSIA	INLET PRESS	21.60	PSIA
DISCH PRESS	21.62	PSIA	DISCH PRESS	161.81	PSIA
DISCH TEMP	166.08	DEG R	DISCH TEMP	168.68	DEG R
EXIT DENSITY	70.492	LB/FT**3	EXIT DENSITY	70.172	LB/FT**3
VOL FLOW	9.28	GPM	VOL FLOW	9.28	GPM
HEAD	5.	FT	HEAD	287.	FT
POWER	0.07	HP	POWER	2.67	HP
FLOW COEF	0.029		FLOW COEF	0.021	
HEAD COEF	0.5762		HEAD COEF	0.5936	
NPSP AVAIL	0.979	PSI	NPSP AVAIL	3.447	PSI
NPSP REQ	0.001	PSI	NPSP REQ	2.711	PSI
NPSH AVAIL	2.00	FT	NPSH AVAIL	7.04	FT
NPSH REQ	0.00	FT	NPSH REQ	5.54	FT
SUCT SPEC SPEED	9118.		SUCT SPEC SPEED	7890.	
SECOND STAGE LOX PUMP					
DIAMETER	0.0	INCH			
FLOW	0.000	LB/SEC	*** PREBURNER ***		
SPEED	9352.	RPM	MIXTURE RATIO	0.0	
EFF	0.0		TEMPERATURE	529.	DEG R
INLET PRESS	161.81	PSIA	PRESS	98.	PSIA
DISCH PRESS	161.81	PSIA	FUEL FLOW	0.332	LB/SEC
DISCH TEMP	168.68	DEG R	OXIDIZER FLOW	0.0	LB/SEC
EXIT DENSITY	70.172	LB/FT**3	GAMMA	1.400	
VOL FLOW	0.0	GPM	CP	3.500	BTU/LB/R
HEAD	0.	FT	GAS CONSTANT	766.4	FT.LB/LBR
POWER	0.0	HP	FUEL PARASIT	0.150	
FLOW COEF	0.0				
HEAD COEF	0.0				
**** FUEL TURBINE ****			*** LOX TURBINE ***		
FLOW	0.231	LB/SEC	FLOW	0.101	LB/SEC
NO.STAGES	1.000		NO.STAGES	1.000	
PRESS RATIO T/S	1.176		PRESS RATIO T/S	1.134	
INLET TEMP	528.883	DEG R	INLET TEMP	528.883	DEG R
POWER	11.612	HP	POWER	2.895	HP
INLET PRESS	97.330	PSIA	INLET PRESS	96.838	PSIA
EFF	0.432		EFF	0.308	
EXIT TEMP	518.538	DEG R	EXIT TEMP	523.115	DEG R
U/C	0.172		U/C	0.102	
PERC ADMISSION	0.516		PERC ADMISSION	0.242	
MEAN WHEEL SPEED	354.	FT/SEC	MEAN WHEEL SPEED	186.	FT/SEC
BLADE HEIGHT	0.30	INCH	BLADE HEIGHT	0.30	INCH
VANE ANGLE	15.40	DEG	VANE ANGLE	15.00	DEG
MEAN DIAM	4.605	INCH	MEAN DIAM	4.545	INCH

TABLE A-8 (Continued)

ASE OFF DESIGN DECK - CYCLE NO. 104.B *REVISED (RTM)* PAGE 3

THRUST = 800. MR = 3.500 PC = 79.1

VALVES	INLET PRESS (PSIA)	DP (PSI)	DP/P1	AREA (IN**2)
FUEL VALVE	211.8	19.11	0.0902	0.0674
PREBURNER OXIDIZER VALVE	161.8	0.0	0.0	0.0
MAIN OXIDIZER VALVE	161.8	79.90	0.4938	0.0273
GOX CONTROL VALVE	0.0	0.0	0.0	0.0

INJECTORS	INLET PRESS (PSIA)	DP (PSI)	DP/P2	AREA (IN**2)
PREBURNER FUEL INJECTOR	118.0	20.06	0.2047	0.6004
PREBURNER OXIDIZER INJECTOR	3558.4	0.0	0.0	0.0520
OXIDIZER MAIN INJECTOR	81.9	2.77	0.0351	0.1466
HOT GAS INJECTOR	81.1	1.97	0.0248	2.0952

TANK PRESSURANT

OX FLOW	0.090 LB/SEC
OX TEMP	277. DEG R
OX DELIV PRESS	159.8PSIA
FUEL FLOW	0.013 LB/SEC
FUEL TEMP	529. DEG R
FUEL DELIV PRESS	118.0PSIA

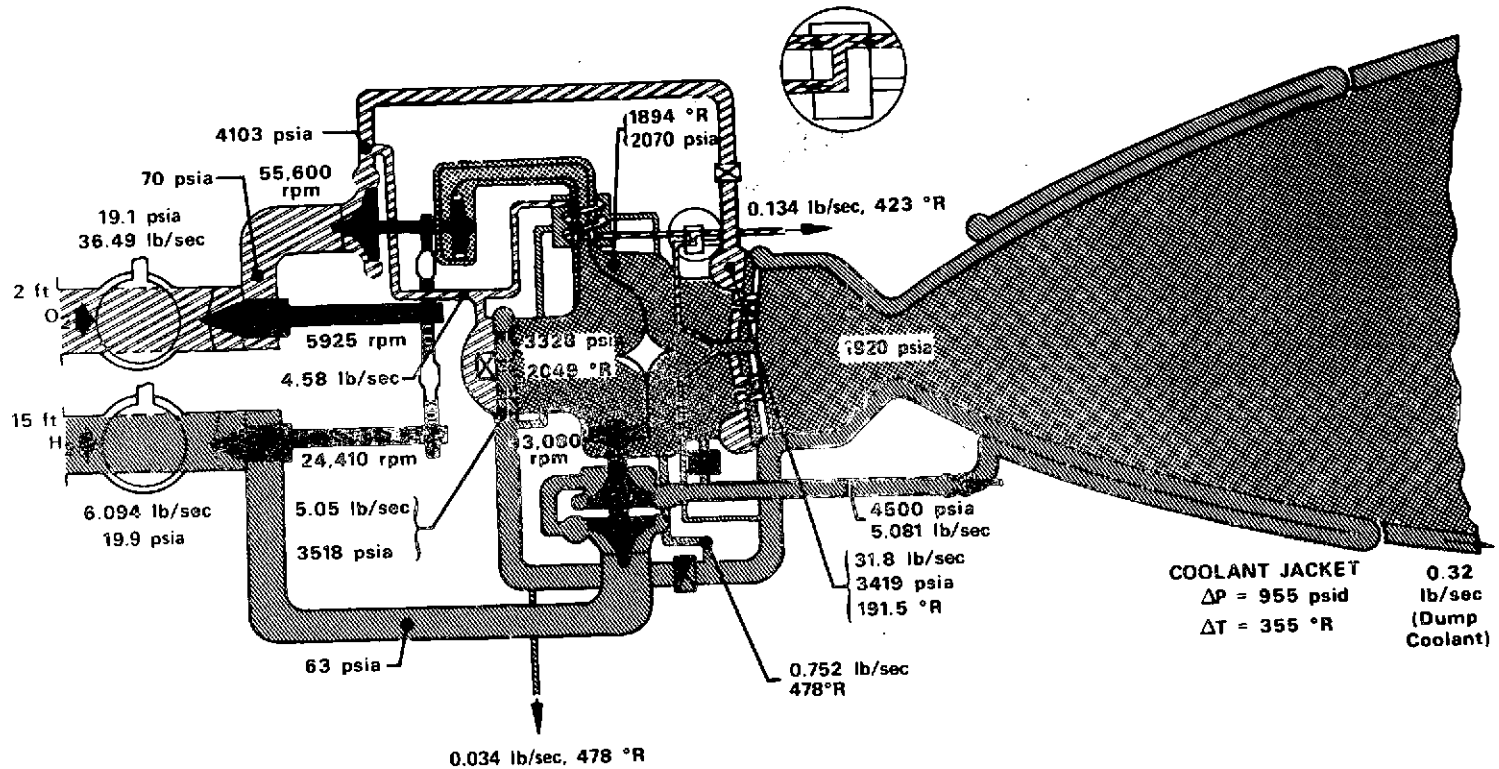

Figure A-1. Advanced Space Engine (Cycle No. 106) (Rated Thrust, Mixture Ratio = 6:1)

FD 66669F

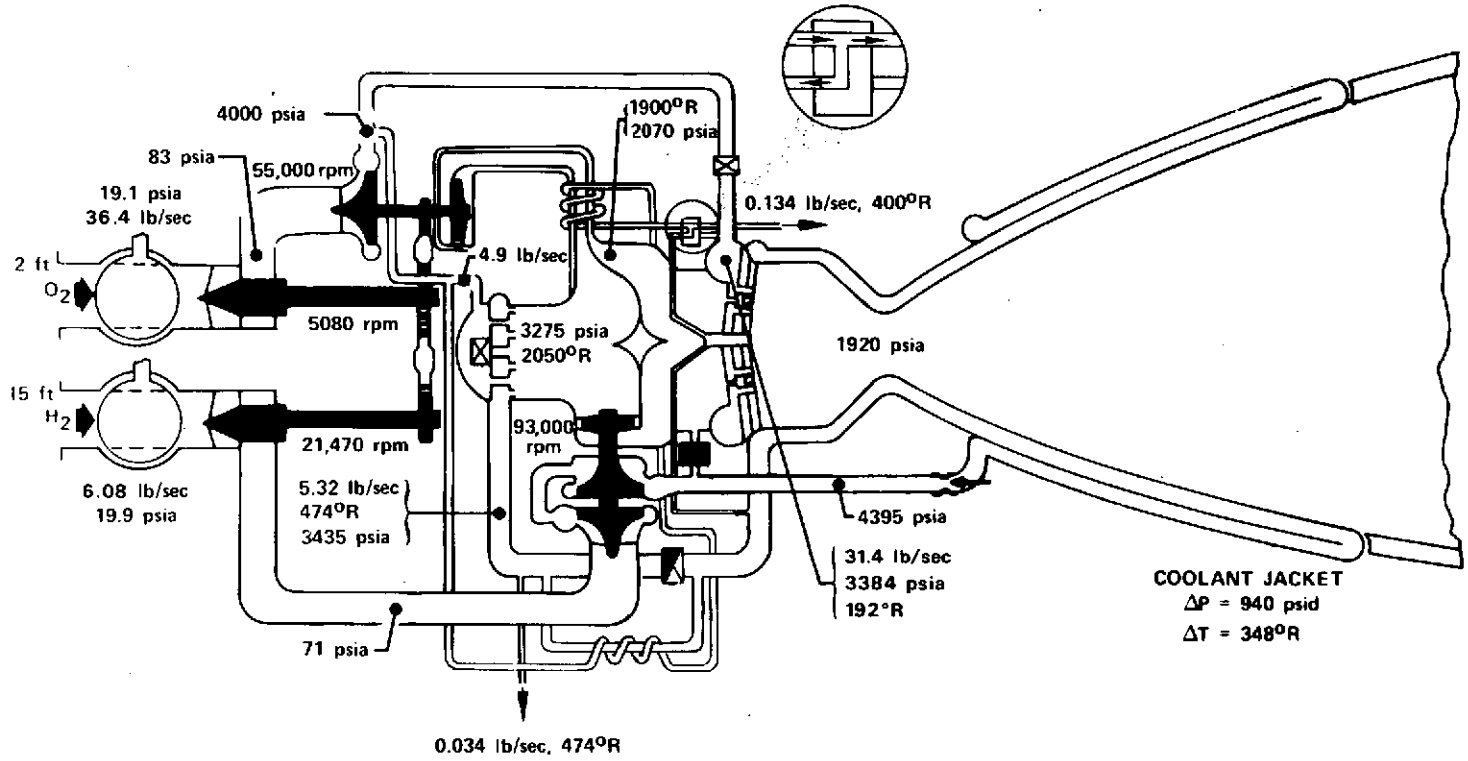

Figure A-2. Advanced Space Engine (Cycle No. 104) (Rated Thrust, Mixture Ratio = 6:1) FD 66669

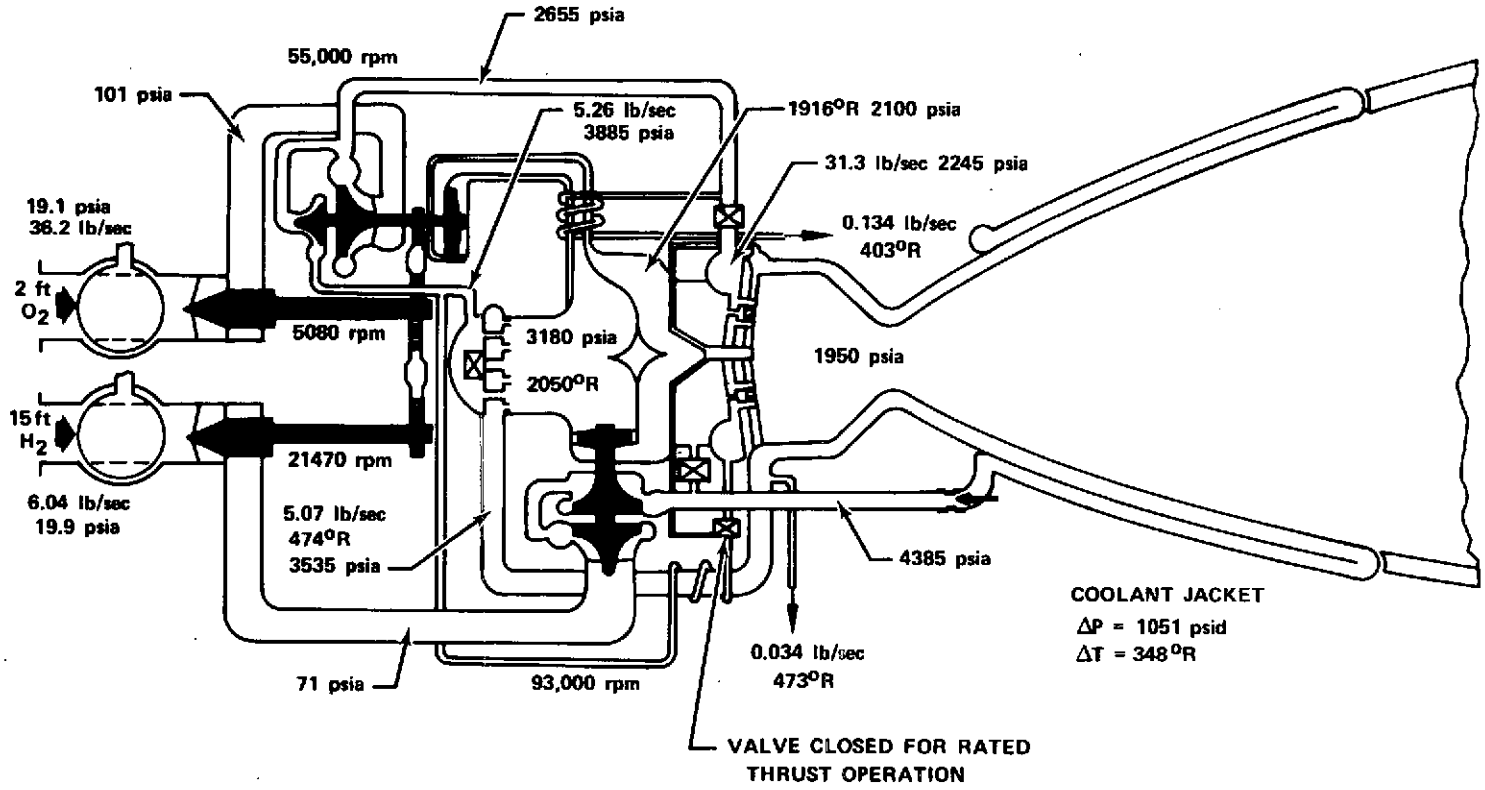

Figure A-3. Advanced Space Engine (Cycle No. 103) (Mixture Ratio = 6:1)

FD 65489

APPENDIX B
ENGINE PERFORMANCE

1. GENERAL

An in-depth point analysis was accomplished using JANNAF methodology to determine specific impulse for the 20,000-lb thrust ASE preliminary engine design at rated thrust operation for MR = 5.5:1, 6.0:1, and 6.5:1. In this Appendix, the JANNAF methodology is discussed and JANNAF predictions are compared with related test data to arrive at a "best estimate" performance level adjustment for the ASE. A list of major symbols is in paragraph 4 at the back of this Appendix.

2. JANNAF METHODOLOGY

a. Methodology

The JANNAF methodology used was essentially the same as that specified in Addendum No. 1 to CPIA Publication No. 178 and Amendment No. 1 thereto. These documents outline a procedure that permits performance to be determined without use of either the JANNAF distributed energy release (DER) program or the JANNAF real gas two-dimensional kinetics (TDK) program. The DER program was not available during the contract period of performance, and the real gas TDK program is difficult to run with a sharp cornered expansion at the throat and requires a large amount of computer time. Although this procedure was specifically written for the space shuttle main engine (SSME), it was sufficiently general so that application to the ASE was possible.

A flow diagram of the JANNAF methodology used to calculate performance is shown in figure B-1. The first step in generating overall engine performance was to define a control volume about the engine system and establish energy and flowrate balances. Figure B-2 shows schematically the control volume and the flowrate and energy changes to the system that were considered. Flowrates and energy levels were obtained from engine cycle balance and heat transfer calculations. The regenerative nozzle heat was assumed to come from the boundary layer and was added to the mainstream propellant enthalpy levels. The base enthalpy levels used for the mainstream propellants were the ones specified in the referenced procedures. These propellant base enthalpy levels were adjusted for the net change in energy determined by the energy balance for the control volume.

The JANNAF turbulent boundary layer (TBL) program was used to determine the boundary layer thrust loss, ΔF_{bl}. Wall temperature profiles used in the calculations were obtained from heat transfer analyses of the thrust chamber. Mainstream edge conditions for the boundary layer calculations were obtained using the in-house two-dimensional bell nozzle performance program run in an equilibrium mode.

Since DER is not available to establish energy release, the referenced JANNAF procedure assumes that the combustion process is vaporization limited and, as such, energy release efficiency is the same as vaporization efficiency (η_{vap}). Additionally, the procedure specifies that combustion chamber striation and oxidizer droplet characteristics be established using in-house methods and that the vaporization efficiency be determined using curves in the procedure that are a function of combustion chamber length and oxidizer droplet size. A complex

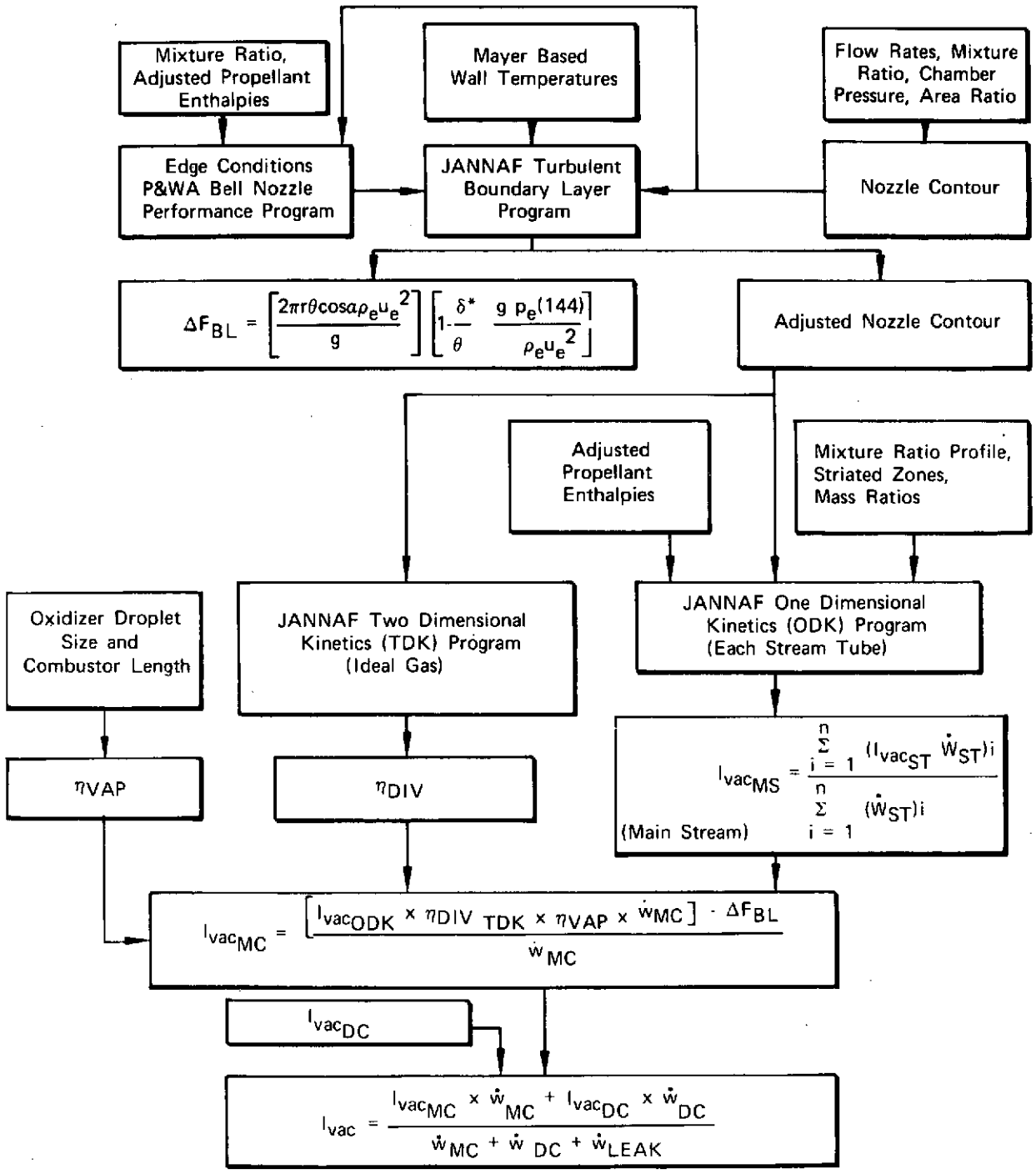

Figure B-1. JANNAF Performance Methodology Flow Chart FD 58937B

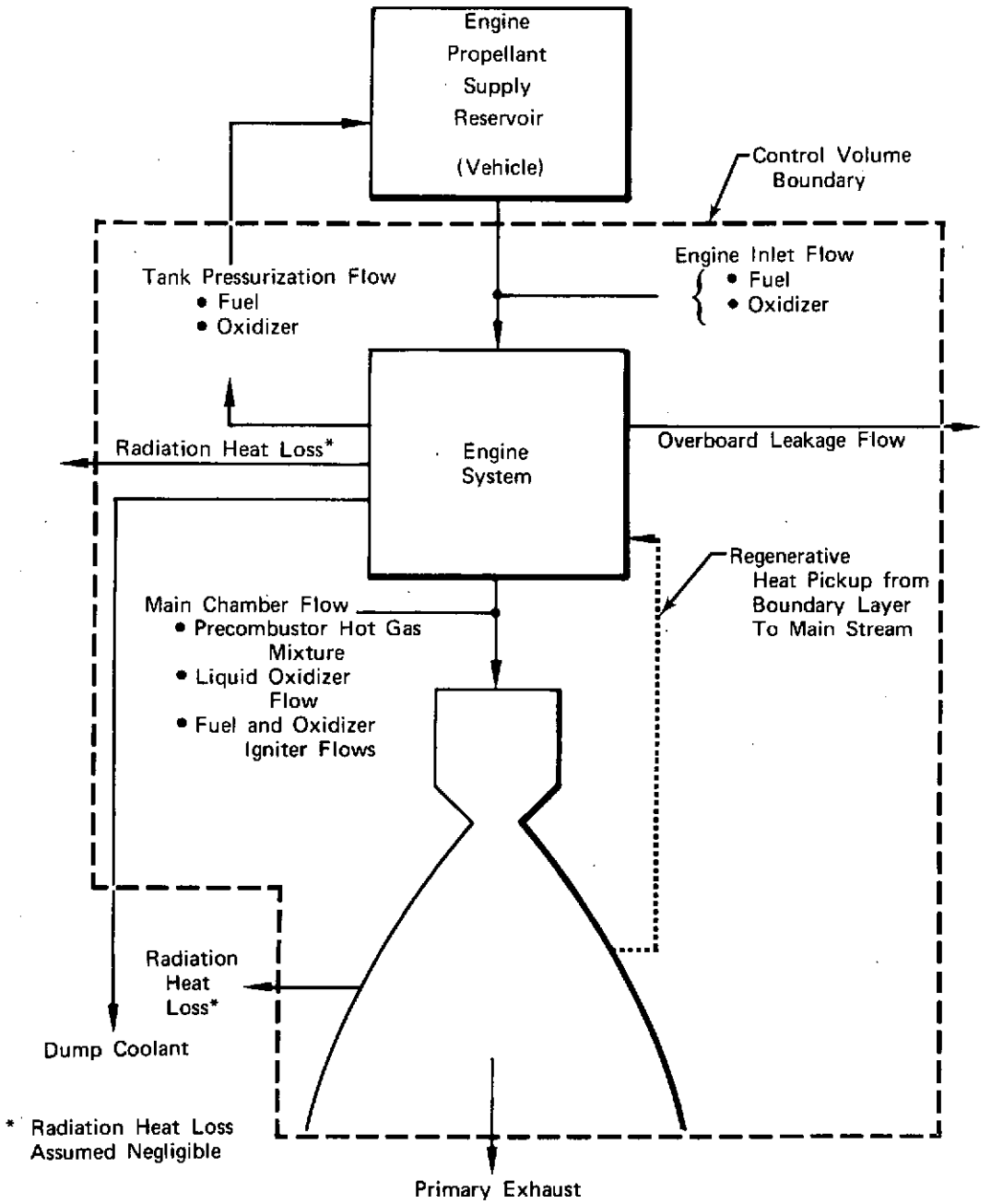

Figure B-2. Control Volume Schematic - Energy and Flow Balance FD 58938A

analysis of injection, vaporization, and mixing characteristics is required to establish these striation characteristics and oxidizer droplet size distributions. Where applicable, characteristics obtained by such an analysis during the SSME effort were used to establish striation, oxidizer droplet, and η_{vap} characteristics for the ASE. The injector was divided into three annular geometric zones. The locations of these geometric zones for the 20,000-lb thrust engine are shown in figure B-3. The mean mixture ratios of each zone were determined from an analysis of the respective engine injector element and Rigimesh flow areas. The larger middle and inner zones were then broken into three stream tubes each. The amount of mass and mean mixture ratios for these stream tubes were estimated from mass/mixture ratio distributions, determined for the SSME. The assumption that the ASE main injector has mass/mixture ratio distribution characteristics similar to the P&WA SSME should be valid, since it is similar in design and has an element density similar to the SSME design. Striation characteristics used in determining performance levels are shown in table B-1.

In the JANNAF analysis, the striation effects are evaluated by treating the variations as stream tubes of constant mixture ratio. The JANNAF one-dimensional kinetics (ODK) program was used to establish nozzle performance for each stream tube using an aerodynamic nozzle contour obtained by adjusting the metal contour for boundary layer displacement thickness. The several individual stream tube performance values were mass weighted to obtain an overall mainstream performance value. Divergent losses were obtained by running the TDK program with striated flow in an ideal gas mode.

Specific impulse of the hydrogen used for dump cooling was estimated from one-dimensional values of specific impulse for heated hydrogen ($\sim$1800°R) expanded through the small nozzles ($\epsilon = 3.5$) at the end of each of the coolant passages. As shown in figure B-1, these values were mass weighted with the specific impulse values for the main thrust chamber calculated by the above procedure to arrive at overall engine delivered specific impulse.

b. Results

Using the JANNAF methodology described above, delivered engine specific impulse values were generated for the ASE at mixture ratios of 5.5, 6.0, and 6.5. The results are summarized in table B-2. A breakdown of JANNAF I_{vac} losses for the nominal engine operating point and the idle modes are presented in table B-3.

3. "Best Estimate" Specific Impulse Values

Previous comparisons of JANNAF predictions obtained using this same methodology with test results (250,000-lb thrust XLR129 Phase I high pressure, staged combustion test data) indicated that JANNAF predictions were high by as much as 4 sec. Most of this difference appeared to be caused by using the ODK program, which could not properly account for the effects of multiple stream tubes.

"Best estimate" levels at rated thrust were obtained by adjusting the JANNAF values downward by 4 sec for the test-to-predicted-JANNAF differences. No adjustment was made to idle mode performance, since similar comparisons were not available.

GEOMETRIC ZONES USED FOR DETERMINING STRIATION CHARACTERISTICS

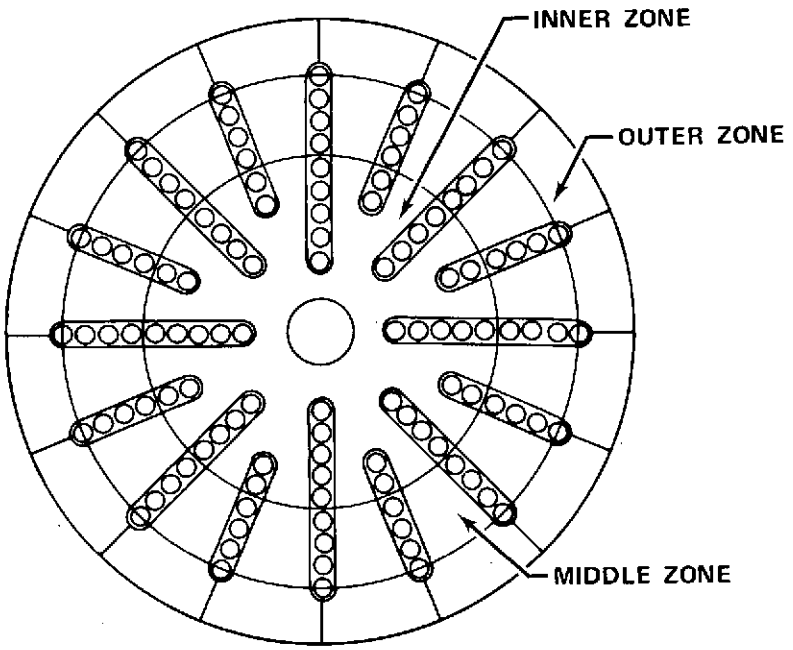

Figure B-3. Geometric Zones Used for Determining Striation Characteristics FD 72485

Table B-1. Striation Characteristics Used for JANNAF Calculations; 89-kN (20,000-lb) Thrust ASE

Overall Mixture Ratio	Zone	Stream Tube	Percent Mass*	Mixture Ratio
5.5	Inner	1	13.296	5.291
		2	13.296	5.903
		3	13.296	6.694
	Middle	1	17.145	5.267
		2	17.145	5.876
		3	17.145	6.663
	Outer	1	8.679	4.775
6.0	Inner	1	13.302	5.796
		2	13.302	6.466
		3	13.302	7.332
	Middle	1	17.152	5.769
		2	17.152	6.436
		3	17.152	7.298
	Outer	1	8.638	5.213
6.5	Inner	1	13.308	6.474
		2	13.308	7.223
		3	13.308	8.191
	Middle	1	17.158	6.444
		2	17.158	7.189
		3	17.158	8.152
	Outer	1	8.602	5.811

*Percent of total injector flowrate.

Table B-2. Summary of JANNAF Methodology Results; Advanced Space Engine (Pure Propellants)

Engine Mixture Ratio	5.5	6.0	6.5
Chamber Pressure, psia	1946	1920	1902
Area Ratio	400:1	400:1	400:1
Main Chamber Mixture Ratio	5.786	6.335	6.888
ΔFuel Enthalpy, Btu/lb H_2	+1326	+1410	+1512
Main Chamber I_{vac}, ODK, sec	491.8	489.7	485.5
ηDivergence	0.99103	0.99103	0.99103
ηVaporization	1.000	1.000	1.000
Main Chamber I_{vac}, TDK, sec	487.4	485.3	481.1
ΔF_{bl}, lb	229	220	236
Main Chamber I_{vac}, sec	478.3	475.95	471.6
Dump Coolant I_{vac}, sec	435	435	435
Overall I_{vac}, sec	477.9	475.5	471.2

Table B-2. Summary of JANNAF Methodology Results; Advanced Space Engine (Pure Propellants) (Continued)

Note: Values are for the following propellant conditions:

	Percent Mass	Enthalpy, cal/gm mole
Hydrogen	100.000	-2152.0*
Oxygen	99.398	-3086.0
Argon	0.549	-2571.0
Nitrogen	0.053	-2699.0

*This base value was adjusted by the fuel enthalpy values shown to account for enthalpy gains and losses in the system. The fuel enthalpy values were determined from a steady-state control volume (figure B-2) enthalpy balance. In accordance with JANNAF procedures, the combustion product gas boundary layer, through a series of iterative calculations, performed at numerous stations along the thrust chamber wall, provided the energy source for the fuel enthalpy increase.

Table B-3. ASE Vacuum Specific Impulse Breakdown (JANNAF Methodology)

	Rated Thrust	Pumped Idle	Tank Head Idle
Thrust, lb	20,000	800	55
Chamber Pressure, psia	1920	79	6
Engine Mixture Ratio	6.0	3.5	1.5
Chamber Mixture Ratio	6.34	3.76	1.5
I_{vac}' (Inlet Conditions) at Chamber MR, sec	485.6	475.8	420.2
Hydrogen Coolant ΔT, °R	355	499	602
$\Delta I_{vac}'$ From Regen Δh, sec	7.5	17.9	45.5
I_{vac}' (With Δh) at Chamber MR, sec	493.1	493.7	465.7
ΔI_{vac} Kinetics (ODK), sec	-1.85	-11.4	-1.15
ΔI_{vac} Divergence (TDK), sec	-4.4	-5.5	-7.2
ΔI_{vac} Boundary Layer (TBL), sec	-9.4	-25.3	-55.65
ΔI_{vac} Energy Release, sec	<-0.1	-0.2	<-0.1
ΔI_{vac} Striation, sec	-1.6	-0.8	<-0.1
ΔI_{vac} Dump Cooling, sec	-0.35	-0.25	0
I_{vac} Delivered, sec	475.5	450.2	401.7

4. LIST OF MAJOR SYMBOLS

I_{vac}'	Ideal Vacuum Specific Impulse	sec
I_{vac}	Delivered Vacuum Specific Impulse	sec
$I_{vac_{dc}}$	Dump Cooling Flow Vacuum Specific Impulse	sec
$I_{vac_{mc}}$	Main Chamber Vacuum Specific Impulse	sec
$I_{vac_{st}}$	Stream Tube Vacuum Specific Impulse	sec
$\dot{W}_{dc}$	Dump Cooling Flowrate	lb/sec
$\dot{W}_{Leak}$	Engine Leakage Flowrate	lb/sec
$\dot{W}_{mc}$	Main Chamber (Injector) Flowrate	lb/sec
$\dot{W}_{st}$	Stream Tube Flowrate	lb/sec
$\eta_c{}^*$	Characteristic Velocity Efficiency	dimensionless
η_{div}	Divergence Efficiency	dimensionless
η_{vap}	Vaporization Efficiency	dimensionless
ΔF_{bl}	Boundary Layer Thrust Loss	lb_f
$\Delta I_{vac_{kin}}$	Kinetic Vacuum Specific Impulse Loss	sec
r	Nozzle Exit Radius	ft
$\cos\alpha$	Cosine, Nozzle Divergence Angle	dimensionless
ρ_e	Density, Free Stream Edge at Nozzle Exit	lb/ft^3
u_e	Velocity, Free Stream Edge at Nozzle Exit	ft/sec
P_e	Pressure, Free Stream Edge at Nozzle Exit	lb_f/ft^2
θ	Boundary Layer Momentum Thickness	ft
δ^*	Boundary Layer Displacement Thickness	ft
g	Gravitational Constant	$\frac{lb_m\text{-ft}}{lb_f\text{-sec}^2}$

APPENDIX C
NONTUBULAR THRUST CHAMBER STRESS AND CYCLIC LIFE ANALYSIS

1. ANALYTICAL METHOD

Large thermal gradients are generated in the regeneratively cooled thrust chambers of high performance rocket engines during operation. These gradients affect the expected cyclic life of the chamber walls. Further aggravating this condition is the existence of high pressure coolant in the wall passages. Pratt & Whitney Aircraft has developed a method for analysis of nontubular thrust chambers which has been programed for a high speed digital computer. The method provides evaluation of thermal cycle life in that the thermal gradients and the coolant and chamber pressures are treated simultaneously.

The general approach in developing the mathematical model was to analyze both the hot and cold wall sections of the thrust chamber (figure C-1) with various combinations of moments (M), loads (P), and deflections (U). The unique values, M_o and P_o, for which the equilibrium boundary conditions of the two wall sections are compatible, are then determined. Once equilibrium and compatibility are obtained, operating stresses and strains are determined for the initial engine cycle. These strains are then used in calculating cyclic life through use of AMZIRC material curves provided by NASA/LeRC.

To accomplish the analysis, the hot and cold walls are treated individually as pressure loaded beams, fixed at each end, having thermal gradients in the radial direction (figure C-2). The beams have a radius of curvature (R) equal to that of the particular thrust chamber location being considered. Conditions subscripted "o" exist at the fixed end and "x" at some point along the axis of the beam (thrust chamber circumference).

For the described beam, the strain at any cross section can be defined for given values of curvature (R) and neutral axis location ($\bar{y}$), as:

$$\epsilon(y) = \frac{(y-\bar{y})}{R}$$

This expression makes the assumption that plane sections remain plane after bending. The strain distribution, coupled with the appropriate stress/strain diagram for the material (figure C-3), can be used to determine the stress variation over the cross section.

Once stress distribution is determined, both moment and axial loads at any beam cross section can be calculated. Where h is the beam thickness:

$$M_x = \int_{y=o}^{y=h} \sigma(y-\bar{y})dy$$

$$P_x = \int_{y=o}^{y=h} \sigma dy$$

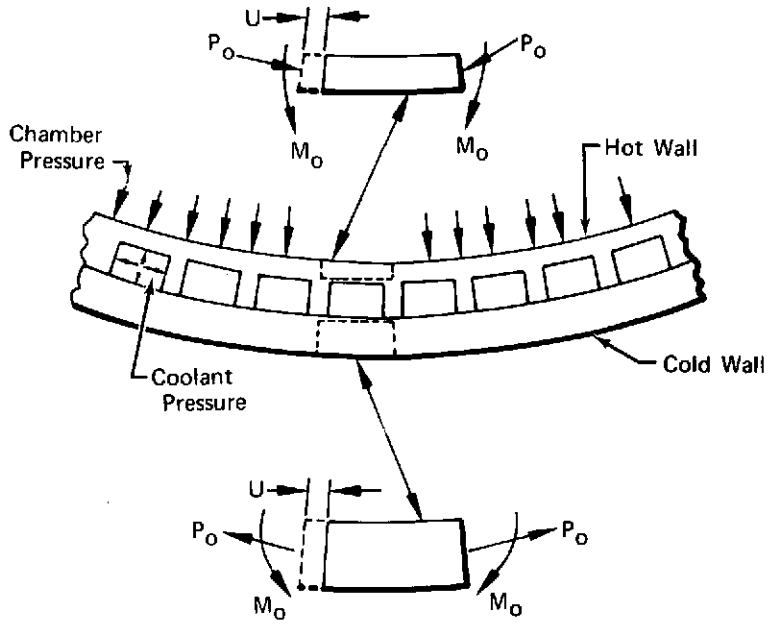

Figure C-1. Chamber Wall Free Body Diagram FD 31324A

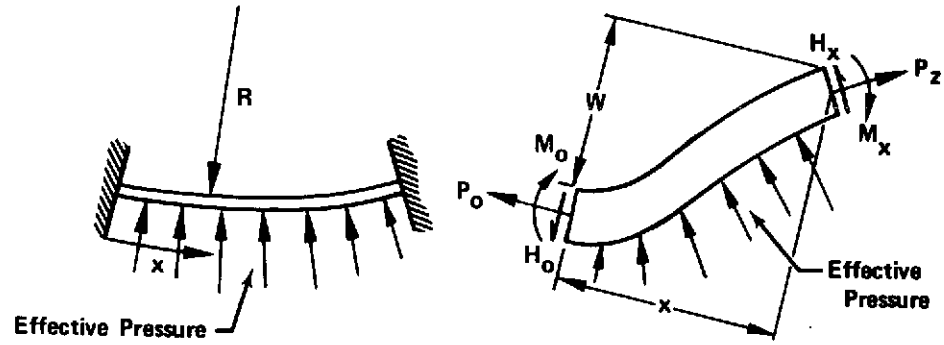

Figure C-2. Nomenclature for Equilibrium Relationship FD 31382

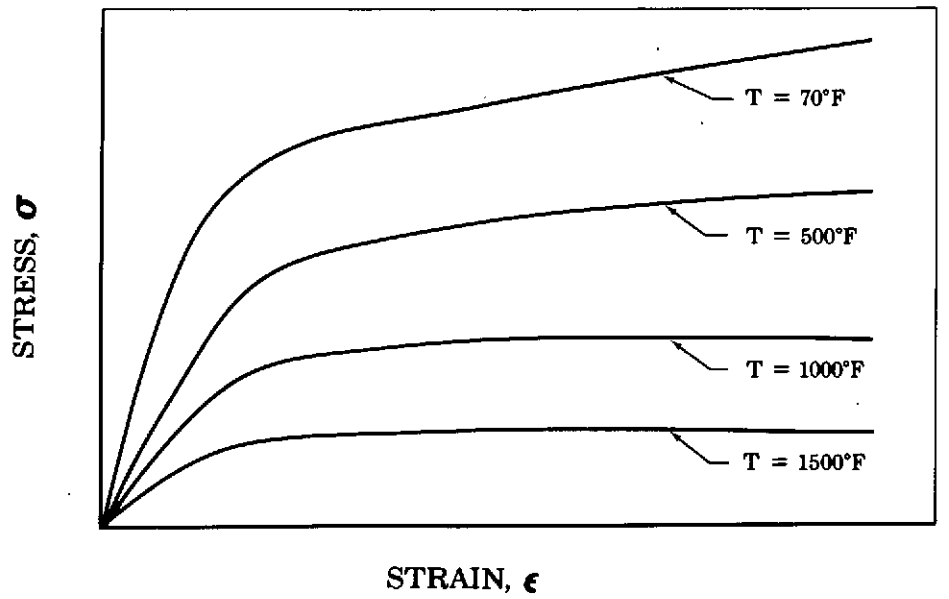

Figure C-3. Typical Stress/Strain Relationship FD 31384

Solving the above equations with various values of neutral axis location and curvature allows generation of an interaction curve (figure C-4).

This curve is used to determine deflection curvature and resultant beam neutral axes based on the moments and axial loads as calculated from the equilibrium equations below. (Note that these equations consider large deflections.)

$$M_x = f1\left(P_o,\ M_o,\ H_o,\ p,\ x,\ w,\ \frac{dw}{dx}\right)$$

$$P_x = f2\left(P_o,\ H_o,\ p,\ x,\ w,\ \frac{dw}{dx}\right)$$

$$H_x = f3\left(P_o,\ H_o,\ p,\ x,\ w,\ \frac{dw}{dx}\right)$$

$$H_o = f4\ (p)$$

The curvature and neutral axis are determined from figure 4 as functions of M_X and P_X. These parameters are used in the calculations for slope and deflection (U) as indicated below:

$$\text{Slope, } \frac{d\theta}{dx} = 1/R$$

$$\text{Deflection, } U = \int_{X=0}^{X=X} \left[(h/2 - \bar{y})\ 1/R - 1/2\left(\frac{dw}{dx}\right)^2\right] dx$$

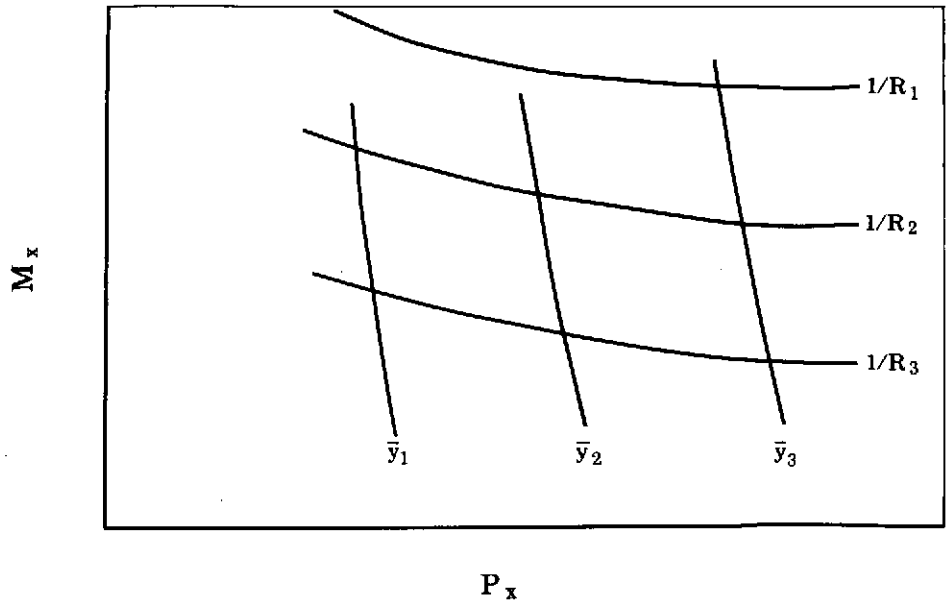

Figure C-4. Typical Relationships Between Moment, Load, Neutral Axis, and Radius of Curvature FD 31385

These results are used to construct a curve involving M_o and P_o at the beam wall vs U and θ at the middle of the beam (figure C-5). Applying the actual end conditions, $\theta = 0$, for the middle of the beam to the above graph, figure C-6 can be drawn for both hot and cold walls. Final values of M_o and P_o are found from figure C-6, where the sum of hot and cold wall loads identically equals the hoop load resulting from thrust chamber pressures. With these unique end conditions, the chamber wall circumferential strain distribution resulting from hot-to-cold wall thermal gradients and chamber thrust loading can be calculated.

The strain from hot-to-cold wall is constant since the chamber contour remains constant in the axial plane throughout the firing cycle. Thus, we can write:

$$\epsilon(y) = \text{Constant} = \alpha \Delta T(y) + \frac{\sigma(y)}{E} + \epsilon p(y)$$

where

ϵp is the plastic strain.

The stress at any location (y) through the thickness can now be determined:

$$\sigma(y) = E\,[\epsilon(y) - \epsilon p - \alpha \Delta T]$$

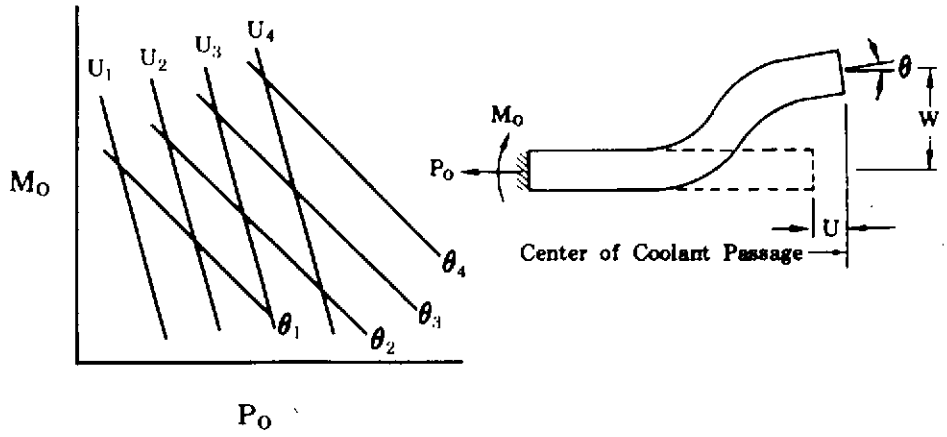

Figure C-5. Typical Relationship Between Moment, Load, Strain, and Angle FD 31356

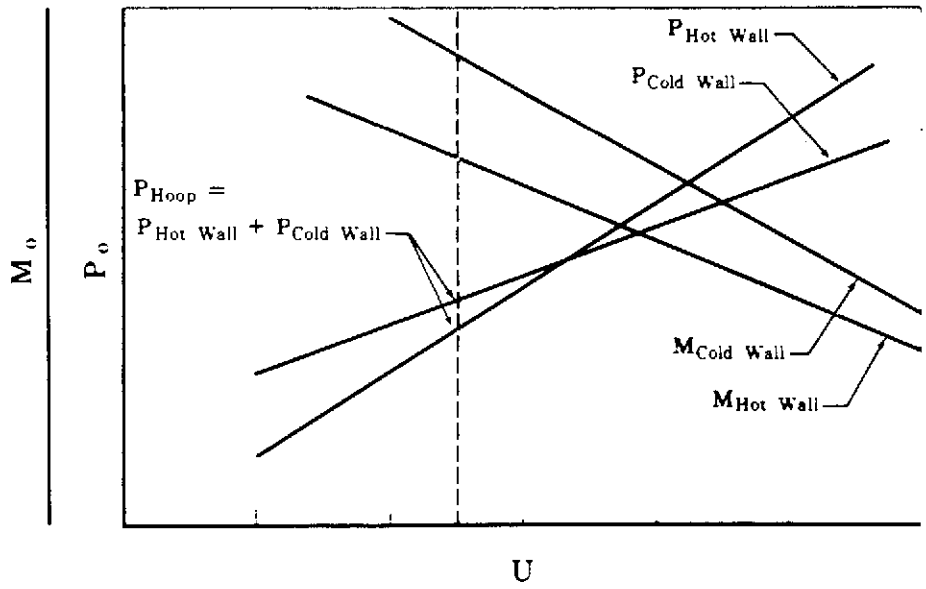

Figure C-6. Determination of M_O and P_O for Hot and Cold Walls FD 31357

The thrust load acting on the cross section allows the calculation of the constant ϵy through the use of the following equation:

$$\text{Thrust Load} = \int_{y=o}^{y=t} \sigma b \, dy$$

where b is the unit length in the X direction, or rewritten:

$$\text{Thrust Load} = \int_{y=o}^{y=t} Eb \, [\epsilon(y) - \epsilon p - \alpha \Delta T] \, dy$$

Once the constant $\epsilon(y)$ is known, the strain-from-stress

$$[\sigma(y)/E + \epsilon p \, (y)]$$

in the axial direction can be calculated from the equations above.

The strain in the radial direction is the result of the strains in the circumferential and axial directions and can be written as:

$$\epsilon y = \mu(\epsilon z + \epsilon x)$$

where ϵz, ϵy, ϵx are strains in the axial, radial, and circumferential directions and μ is Poisson's ratio. Strains in the three directions are then combined to form an equivalent total strain, ϵt, by use of the distortion energy relationship.

$$\epsilon_t = \sqrt{\frac{2}{3}} \sqrt{(\epsilon z - \epsilon y)^2 = (\epsilon y - \epsilon x)^2 + (\epsilon x - \epsilon z)^2}$$

This value is used in determining the life of the chamber from material curves such as that provided by NASA/LeRC in Contract No. NAS3-16750 in figure C-7.

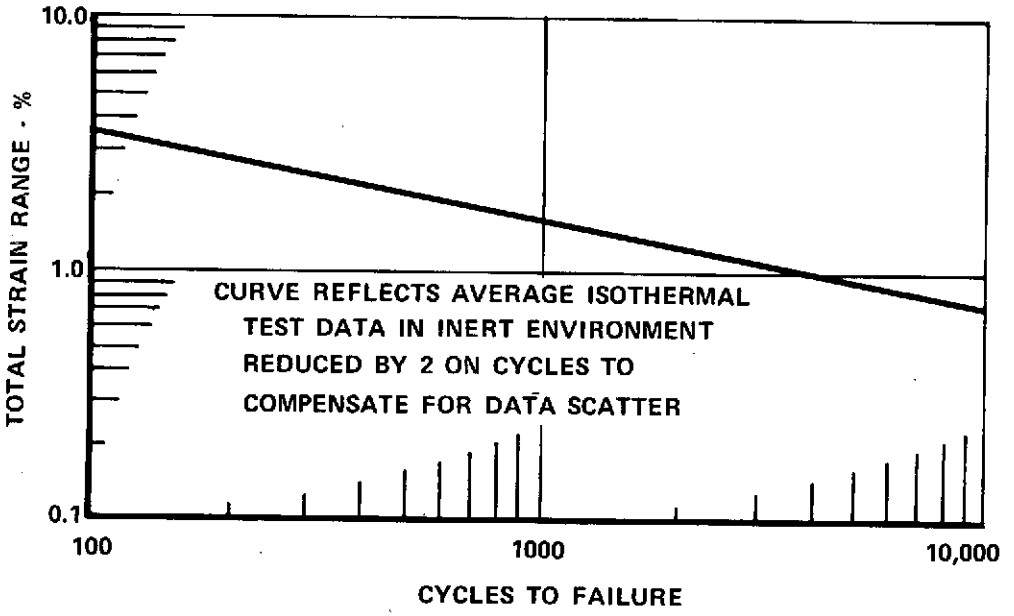

Figure C-7. Material Curve (AMZIRC -70 to 1200°F) FD 75486

APPENDIX D
THRUST CHAMBER AND NOZZLE HEAT TRANSFER ANALYSIS

1. GENERAL

The cylindrical thrust chamber and minimum surface area nozzle thrust chamber design which evolved in the ASE design study consists of three sections:

1. Regeneratively cooled nontubular chamber/nozzle section for high heat flux regions to an area ratio of 6:1

2. Regeneratively cooled tubular nozzle section from an area ratio of 6:1 to an area ratio of 100:1

3. Dump-cooled corrugated construction nozzle extension skirt from an area ratio of 100:1 to 400:1.

Heat transfer analysis of a cooled wall section requires the consideration of the heat transfer phenomena on both the combustion and coolant wall sides as well as the heat conduction within the wall. Because the combustion gas heat transfer coefficients and recovery energy are only minor functions of the chamber wall temperature, they can be independently evaluated. These factors provide the wall heat source. The cooling system thermal energy balance is completed through local evaluations of the coolant passage heat transfer.

Prior to discussing the general combustion side and individual (nontubular, tubular, corrugated) section coolant passage heat transfer analyses, several important assumptions basic to the cooling analysis are defined below:

1. The combustion-side heat transfer coefficients and recovery energy are independent of the cooling process and can be evaluated independently.

2. Radiation to the hot wall is negligible with respect to forced convection heat transfer.

3. Entrance effects on coolant heat transfer coefficients are negligible (i.e., fully developed turbulent flow regime).

4. The coolant flow is both steady and one-dimensional.

5. Heating of the coolant due to viscous dissipation is negligible.

6. Conduction within the coolant is negligible.

2. COMBUSTION SIDE THERMAL ENVIRONMENT

Thrust chamber thermal environment determination involves two strongly dependent variables:

1. Hot gas film coefficient

2. Boundary layer thermal driving potential.

The methodology which has been found to most accurately predict these variables while lending itself to rapid computer calculations is the Mayer Boundary Layer Analysis (Reference 1*), which applies to turbulent flow over an axisymmetric surface. Determination of the Mayer's Integral Film Coefficient (hot gas) is dependent on combustion product transport properties and upon the flow field definition. Combustion product transport properties in the chamber and nozzle are a function of the existing mixture ratio and a reference temperature. The temperature used was an Eckert based reference temperature, T*, (Reference 2) recommended by Mayer and defined as:

$$T^* = 0.5(T_W + T_\infty) + 0.22(T_{ADW} - T_\infty)$$

Flow field description is set by the type flow assumption and the gas specific heat ratio ($\gamma = c_p^*/c_v^*$). In the Mayer based analyses two flow types are utilized:

1. One dimensional, isentropic

2. Two dimensional, axisymmetric.

One-dimensional isentropic flow has been found to closely approximate the two-dimensional axisymmetric flow in a converging-diverging nozzle with a smooth throat contour. In engines with sharp corner expansion at the throat, however, the two-dimensional flow field varies significantly from one-dimensional predictions in a region from the throat to an area ratio of approximately 4:1. In order that the computational time might be held to a minimum through use of the more simple one-dimensional isentropic flow calculations, area ratios in the region from the throat to $\epsilon = 4{:}1$ are theoretically adjusted to provide two-dimensional flow field Mach number predictions from one-dimensional relationships. Flow field definition groundrules are presented below by thrust chamber/nozzle section:

Chamber:

Flow - One-dimensional based on injector flowrates

γ - Based on injector mixture ratio and chamber static temperature and pressure.

Nozzle: $(1 < \epsilon \leq 4.0)$

Flow - Two-dimensional axisymmetric approximation based on throat flowrates

γ - Based on injector mixture ratio and throat static temperature and pressure.

Nozzle: $(\epsilon > 4.0)$

Flow - One-dimensional based on injector flowrates

γ - Based on injector mixture ratio and throat static temperature and pressure.

*A reference list for Appendix D is given in paragraph 7.

Basic to the Mayer analysis is the definition of the Mayer's Integral Film Coefficient which accounts for and relates the effects of engine size, hot wall contour, and boundary layer thickness. The local film coefficient (h_s) expressed in finite difference form, based upon reference temperature transport properties and the appropriately defined flow field is:

$$h_s = \frac{0.023\ (Re)^{0.25}(Pr^*)^{-0.667}c_p^*(\mu/\mu_\infty)^{0.25}(T_\infty/T^*)\rho_\infty U_\infty}{\left[\text{Inti} + \sum_{\text{XInti}}^{s} (Re)^{1.25}(T_\infty/T^*)(\mu^{*0.25}/\mu_\infty^{1.25})\rho_\infty U_\infty \Delta s\right]^{0.2}}$$

The value of the initial integral (Inti) used in the Mayer Equation was determined semi-empirically based on the assumption that the heat transfer coefficient at the injector face is 10% higher than at the end of the cylindrical section of the combustion chamber. The initial integral value strongly influences the value of the heat transfer coefficient near the injector face, but its effect diminishes rapidly with combustion chamber length.

The second variable, the thermal driving potential, is based on the change in enthalpy across the boundary layer. The use of enthalpy (EDP) rather than temperature driving potential accounts for the recovery of both kinetic energy and chemical energy and is determined as follows:

$$h_o = (\eta_c^*)^2 (h_{o_{IDL}} - h_b) + h_b$$

$$\Delta h_k = U_\infty^2 / 2gJ$$

$$h_{ADW} = ho - (1 - Pr^{*0.33})\Delta h_k$$

$$EDP = h_{ADW} - h_w$$

Upon combining the Mayer Boundary Layer Integral film coefficient with the enthalpy driving potential, heat flux to the hot surface from the combustion gas stream can be defined on a unit basis:

$$Q/A = \frac{h_s\,(EDP)}{c_p^*}$$

The use of the Mayer Boundary Layer Analysis with enthalpy driving potential has been found to predict mixture ratio and propellant variation influences more accurately than previous temperature potential methods in test data correlations for both RL10 engines and 250,000 lb thrust combustion systems.

3. CONDUCTION

Because of the extremely high heat fluxes encountered in the combustion chamber and throat sections, a high conductivity material and small cooling

passage areas were mandatory. A machined, high copper alloy (AMZIRC) liner was used to satisfy this requirement, but such construction is excessively heavy for lower heat flux nozzle regions where regenerative cooling is desirable and tubular regenerative construction was assumed for such regions.

Conduction through the nontubular copper liner and through the tubular hot walls is governed by the relationship

$$Q/A = (T_{w_i} - T_{w_j})\, K_w/\delta$$

Employing the previously developed combustion side heat transfer analysis, the above conduction relationship, the convective analysis discussed below, and a selected passage geometry, a two-dimensional finite element conduction heat transfer analysis was performed to determine the wall temperature distribution through several critical stations along the nontubular liner length. To conserve computational time and cost, intermediate station heat transfer characteristics were determined by a one-dimensional thermal analysis to which a two-dimensional fin-effect correction factor calculated from wall temperature distribution and geometry was applied.

Tubular heat exchanger conduction analysis is governed by the same basic relationships as the nontubular heat exchanger. The two-dimensional analysis necessary for the nontubular section, however, was replaced by a thick walled cylinder analysis. Studies have shown this to be a satisfactory substitution which readily lends itself to low time computer solutions.

4. COOLANT SIDE HEAT TRANSFER

Evaluation techniques for coolant side convective heat transfer coefficients in both tubular and nontubular sections are essentially the same. Heat transfer to the coolant on a unit basis is governed by the relationship

$$Q/A = (T_w - T_b)\, h_c A$$

where A is the area associated with each surface nodal element defined in the two-dimensional thermal conduction analysis.

The smooth passage convective film coefficient (h_c) was based on the general relationship shown below where the constants C_1 and C_2 are functions of the coolant local temperature and pressure levels as reported by Taylor (Reference 3).

$$h_c = C_1 \left[\left(\frac{W_c}{A} \right)^{0.8} \left(\frac{1}{DH} \right)^{0.2} \right] \left[\left(\frac{c_p}{\mu} \right)_f^{0.4} (K_f)^{0.6} \left(\frac{\rho_f}{\rho_b} \right)^{0.8} \left[1 + \frac{C_2 \mu_w \rho_b}{\mu_b \rho_w} \right] \right]$$

This relationship required modifications for both passage surface roughness and curvature effects. Surface roughness (ϵ) which inreases the effective value of film coefficient is significant in nontubular liners, in which 64 μ in. roughness can be expected from the standard machining operations which generate the

required small passages. Dipprey and Sabersky (Reference 4) have studied roughness effects and, through the Stanton number (ST), developed a roughness driven frictional characteristic from which film coefficient can be determined. The Relationship constants were slightly modified for hydrogen as recommended in Reference 5 to yield:

$$ST = \frac{f/2}{0.92 + \sqrt{f/2}\,[4.7\,(\epsilon^*)^{0.2}\,(Pr_b)^{0.44} - A(\epsilon^*)]}$$

where:

$$\epsilon^* = Re_b \sqrt{f/2}\,(\epsilon/DH)$$

$$A(\epsilon^*) = \sqrt{2/f} + 2.5 \ln (2\epsilon/DH) + 3.75$$

The term ϵ in the equations is the measured passage surface roughness. The isothermal friction factor was obtained by performing iterative calculations for the function shown in figure D-1. The dimensionless terms ϵ^* and $A(\epsilon^*)$ are used to correlate the friction factor data.

From the above equations, a Stanton number was calculated for both the smooth tube and actual rough tube conditions. The ratio of the smooth to rough Stanton number (ℝ) was then applied directly to the smooth passage film coefficient yielding the desired roughness enhanced film coefficient.

$$h_{c_{rough}} = h_{c_{smooth}}\ (ℝ)$$

The second film coefficient enhancing factor is that associated with coolant turning which creates a pressure gradient within the coolant passages due to centrifugal effects and sets up a secondary flow field within the coolant. This results in an increased coolant film coefficient in the nozzle throat region. The basis for evaluating curvature enhancement is reported in Reference 2; the friction factor is related to the curvature influence through the Dean number De, where:

$$De = \frac{1}{2} R_e \left(\frac{R_t}{R_s}\right)^{1/2}$$

The friction factor of a curved passage is thus defined as:

$$(f)_{curved} = y\,(De)^x\,(f)_{straight}$$

where y and x are functions of the Dean number. Through the Reynolds analogy the fluid friction factor can then be applied as a ratio (ℂ) directly to either the smooth or rough passage film coefficients as required.

$$(h_c)_{curved} = (h_c)_{smooth}\ (ℂ)$$

$$(h_c)_{curved} = (h_c)_{rough}\ (ℂ)$$

Considering all of the above then, the local coolant film coefficient at any location within the passage was determined as:

$$(h_c) = (h_c)_{smooth} (\text{R}) (\text{C})$$

5. DUMP COOLED NOZZLE EXTENSION

Analysis for the corrugated heat exchanger is similar to that for the nontubular design. A two-dimensional critical station thermal analysis supplemented with corrected one-dimensional intermediate station analysis is performed to obtain the wall temperature distributions. Convective heat transfer discussions for the hot gas and coolant sides as discussed above are directly applicable.

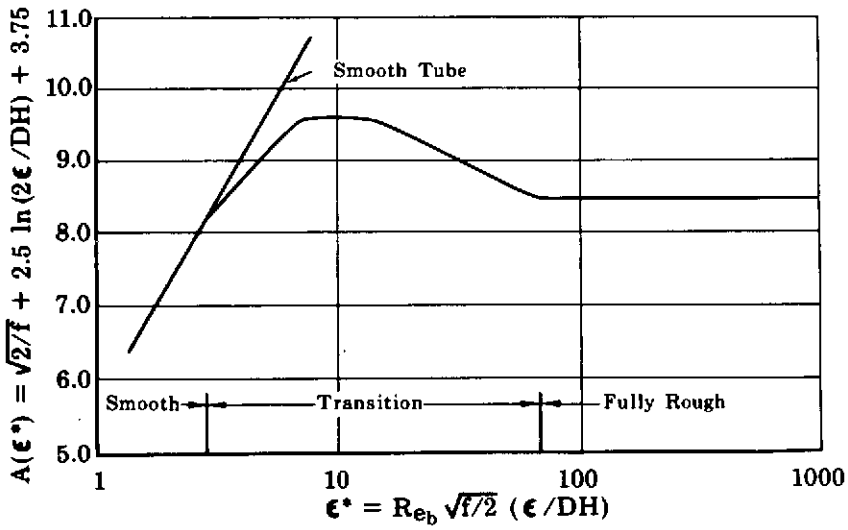

Figure D-1. Friction Similarity Function for Close-Packed Sand Grain Roughness FD 23422

6. LIST OF MAJOR SYMBOLS

A	Area	ft^2
c_p	Specific Heat at Constant Pressure	$Btu/lb_m-°R$
D_e	Dean Number	d'less
DH	Hydraulic Diameter	in.
EDP	Enthalpy Driving Potential	Btu/lb_m
f	Fanning Friction Factor	d'less
g	Gravitation Constant	$lb_m\ ft/lb_f\ sec^2$
h	Film Coefficient; Enthalpy	$Btu/hr-ft^2-°R$; Btu/lb_m

Inti	Initial Value of Mayer Integral	in.
J	Mechanical Equivalent of Heat (778.161)	ft-lb_f/Btu
K	Thermal Conductivity	Btu/hr-ft-°R
Pr	Prandtl Number	d'less
Q	Heat Transfer Rate	Btu/sec
Re	Reynolds Number	d'less
R	Radius	in.
s	Length Along Contour	in.
ST	Stanton Number	d'less
T	Temperature	°R
U	Velocity	ft/sec
W	Flowrate	lb_m/sec
XInti	Axial Length Associated With Inti	in.
μ	Viscosity	lb_m/ft-sec
ρ	Density	lb_m/ft^3
η_c^*	Combustion Efficiency	d'less
γ	Specific Heat Ratio	d'less
δ	Wall Thickness	ft
ϵ	Nozzle Area Ratio; Surface Roughness	d'less; in.

SUBSCRIPTS/SUPERSCRIPTS

ADW	Adiabatic Wall
b	Bulk
c	Coolant Side
f	Film
i	Nodal Station Designation
IDL	Ideal Condition

j	Nodal Station Designation
k	Kinetic
o	Stagnation Values
s	Combustion Side Surface
t	Tube
w	Wall
∞	Free Stream
*	Reference Temperature

7. REFERENCES

1. Mayer, E., "Analysis of Convective Heat Transfer in Rocket Nozzles," ARS Journal, 31 July 1961, 911-917.

2. "Investigation of Cooling Problems at High Chamber Pressure, Final Report," Rocketdyne Report R-6529, 15 September 1966.

3. Taylor, Maynard F., NASA TN D-4332, "Correlation of Local Heat-Transfer Coefficients for Single-Phase Turbulent Flow of Hydrogen in Tubes With Temperature Ratios to 23," January 1968.

4. Dipprey, D. F. and R. H. Sabersky, JPL Technical Report No. 32-269, "Heat and Momentum Transfer in Smooth and Rough Tubes at Various Prandtl Numbers," 6 June 1962.

5. "Investigation of Cooling Problems at High Chamber Pressures - Final Report," Rocketdyne Report R-6529, Contract NAS8-20225, 15 September 1966.

APPENDIX E
SYMBOLS AND ABBREVIATIONS

ac	Alternating Current
AEB	Advanced Engine, Bell
AFRPL	Air Force Rocket Propulsion Laboratory
AEDC	Arnold Engineering Development Center
AISI	American Iron and Steel Institute
AMS	Aerospace Material Specification
ASE	Advanced Space Engine
BEP	Best Efficiency Point
Btu	British Thermal Unit
CDR	Critical Design Review
CG	Center of Gravity
$\mathrm{C_L}$	Centerline
CPIA	Chemical Propulsion Information Agency
cm	Centimeter
CPU	Central Processing Unit
dc	Direct Current
DDT&E	Design, Develop, Test and Evaluate
deg	degree
DVS	Design Verification Specification
ECDA	Engine Control Development Area
ECU	Electronic or Engine Control (Command) Unit
EOS	Earth-to-Orbit Shuttle
ERP	Engine Reference Plane
°F	Degrees Fahrenheit
FCE	Flight Certified Engine

FFC	Final Flight Certification
FMEA	Failure Mode and Effects Analysis
FRDC	Florida Research and Development Center
ft	Foot
FY	Fiscal Year
GFP	Government Furnished Property
GHe	Gaseous Helium
GH_2	Gaseous Hydrogen
GN_2	Gaseous Nitrogen
GO_2, GOX	Gaseous Oxygen
GSE	Ground Support Equipment
gpm	Gallons Per Minute
H_2	Hydrogen
HEX	Heat Exchanger
HPFP	High Pressure Fuel Pump
HPOP	High Pressure Oxidizer Pump
hr	Hour
Hz	Hertz
ICD	Interface Control Document
ID	Inside Diameter
IDR	Initial Design Review
in.	Inch
k	kilo (One-Thousand)
kg	Kilogram
ksi	Pounds per Square Inch (Thousands)
°K	Degrees Kelvin

L	Length
lb_m	Pounds Mass
lb_f	Pounds Force
LCF	Low Cycle Fatigue
L/D	Length-to-Diameter Ratio
LeRC	Lewis Research Center
LH_2	Liquid Hydrogen
LLT	Long Lead Time
LO_2, LOX	Liquid Oxygen
LN_2	Liquid Nitrogen
LPFP	Low Pressure Fuel Pump
LPOP	Low Pressure Oxidizer Pump
m	Meter
mm	Millimeter
MCOV	Main Oxidizer Valve
M	Mega (One-Million)
MFV	Main Fuel Valve
min	Minute
MR	Mixture Ratio
MSA	Minimum Surface Area
MSFC	George C. Marshall Space Flight Center
MoS_2	Molybdenum Disulphide
N	Newton
NASA	National Aeronautics and Space Administration
NA	Not Applicable
NPSH	Net Positive Suction Head

NPSP	Net Positive Suction Pressure
O_2	Oxygen
O&FS	Operations and Flight Support
OD	Outside Diameter
OFS	Mixture Ratio Schedule
OOS	Orbit-to-Orbit Shuttle
P	Pressure
POV	Preburner Oxidizer Valve
PDR	Preliminary Design Review
PFC	Preliminary Flight Certification
PFRT	Preliminary Flight Rating Test
PI	Pumped Idle
PR	Pressure Ratio
psia	Pounds per Square Inch, Absolute
psid	Pounds per Square Inch, Differential
PU	Propellant Utilization
P&WA	Pratt & Whitney Aircraft
QT	Qualification Test
°R	Degrees Rankine
R	Radius
rad	Radian
sccs	Standard Cubic Centimeters per Second
scfm	Standard Cubic Feet per Minute
s, sec	Second
SMD	Sauter Mean Diameter
SP	Start Permission

SR	Shutdown Request
SSME	Space Shuttle Main Engine
STE	Special Test Equipment
STS	Space Transportation System
Td, Ts	Refer to NASA DR MF003M
T	Temperature
THI	Tank Head Idle
TLS	Throttle Lever Schedule
TPA	Turbopump Assembly
T/S	Total/Static Pressure Ratio
TSH	Thermodynamic Suppression Head
WBS	Work Breakdown Structure
v	Volt
vs	Versus
w	Watt
W	Weight
$\dot{W}$	Weight Flowrate

REFERENCES

1. Final Report - Orbit-to-Orbit Shuttle Engine Design Study, Pratt & Whitney Aircraft, AFRPL-TR-72-27, Contract F04611-71-C-0039, July 1972.

2. Final Report - Orbit-to-Orbit Shuttle Engine Design Study, Aerojet Liquid Rocket Company, AFRPL-TR-72-45, Contract F04611-71-C-0040, May 1972.

3. Engine System Studies Final Report - O_2/H_2 Advanced Maneuvering Propulsion Technology Program, Rocketdyne, AFRPL-TR-72-4, Contract F04611-67-C-0116, January 1972.

4. Baseline Tug Definition Document, Revision A, NASA/MSFC, Preliminary Design Office Program Development, 26 June 1972.

5. NASA/LeRC Letter, D. D. Scheer to J. P. B. Cuffe, P&WA/FRDC, dated 21 August 1972.

6. U.S. Navy Contract No. USN, MA-4489.

7. Flow Regimes in Curved Subsonic Diffusers, ASME Paper 61-WA-191, August 1961.

8. Liquid Rocket Engine Turbopump Gears, NASA Monograph, April 1972.

9. Final Report, Design, Fabricate, and Test Breadboard Liquid Hydrogen Pump, Pratt & Whitney Aircraft PWA FR-2184, Contract NAS8-11714, August 1967.

10. Final Report for the Period 26 June 1961 to 26 June 1962 on the High Pressure Rocket Engine Feasibility Program, Pratt & Whitney Aircraft, PWA FR-467, Contract AF04(611)-7435, September 1962.

11. Kah, C.L.C. and G.D. Lewis, High Pressure Rocket Engine Feasibility Program, Final Report, Pratt & Whitney Aircraft PWA FR-1171, Contract AF04(611)-7435, December 1964.

12. Design, Fabricate, and Test Breadboard Liquid Hydrogen Pump - Interim Report June 1964 through June 1965, Pratt & Whitney Aircraft PWA FR-1461, Contract NAS8-11714, July 1965.

13. Atherton, R.R., et al., Air Force Reusable Rocket Engine Program - XLR129-P-1, Final Report, Volumes I, II, and III, Pratt & Whitney Aircraft PWA FR-3832, Contract F04611-68-C-0002, AFRPL-TR-71-1, January 1971.

14. Zweifel, O., "Optimum Blade Pitch for Turbo-Machines with Special Reference to Blades of Great Curvature," The Engineer's Digest, November and December, 1946.

15. Large Hydrogen Pump Technology, June 1964 through June 1965, Pratt & Whitney Aircraft, PWA FR-1477, July 1965.

16. Space Shuttle Main Engine Definition (Phase B) Engine Design Definition Report, Volumes I through VI, Pratt & Whitney Aircraft PWA FR-4249, Contract NAS8-26186, April 1971.

17. Final Report - Properties of Materials in High Pressure Hydrogen at Cryogenic, Room and Elevated Temperatures, Pratt & Whitney Aircraft, PWA FR-5768, Contract NAS8-26191, July 1973.

18. Large Oxygen Pump Technology, July 1965 through April 1966, Pratt & Whitney Aircraft, PWA FR-1886, May 1966.

19. Mayer, E., "Analysis of Convective Heat Transfer in Rocket Nozzles," ARS Journal, 31 July 1961, pp 911-917.

20. Taylor, M. F., Correlation of Local Heat-Transfer Coefficients for Single-Phase Turbulent Flow of Hydrogen in Tubes With Temperature Ratios to 23, NASA TND-4332, January 1968.

21. Dipprey, D. F. and R. H. Sabersky, Heat and Momentum Transfer in Smooth and Rough Tubes at Various Prandtl Numbers, JPL Technical Report No. 32-269, 6 June 1962.

22. Investigation of Cooling Problems at High Chamber Pressure, Final Report, Rocketdyne Report R-6527, 15 September 1966.

23. Final Report - Advanced Engine Design Study, Bell (AEB) June 1967 to July 1967, Volumes I and II, Pratt & Whitney Aircraft, PWA FR-2372, Contract NAS8-11427, July 1967.

24. Components Design Handbook, Air Force Reusable Rocket Program, Book 4, Experimental Results, Pratt & Whitney Aircraft, PWA FR-2661, Contract F04611-68-C-0002, December 1967, pp VII 36-111.